Novel Rotaxanes for the Enantioselective Binding of Chiral Anions

Charles E. Gell

This thesis is submitted for the degree of Doctor of Philosophy

June 2019

Department of Chemistry

Declaration

This thesis has not been submitted in support of an application for another degree at this or any other university. It is the result of my own work and includes nothing that is the outcome of work done in collaboration except where specifically indicated. Many of the ideas in this thesis were the product of discussion with my supervisor Dr. Nicholas Evans.

Charles E. Gell MChem

Lancaster University, UK

Acknowledgements

Firstly, I would like to state that completing this PhD, like all PhDs, has been rather challenging and whilst I have done my best to manage, I have at times become somewhat depressed. I would like to offer an extra special thanks to Dominic, James, Jimmy and Suzy, who have helped me pull through the really difficult times.

I would like to express my appreciation for my supervisor Dr. Nick Evans (despite the fact I am still bitter that he did not offer me a coffee during my interview). I would also like to express my thanks to my second supervisor Dr. Mike Coogan, who would sign the risk assessments I did not want Nick to see and my panel members Dr. Susannah Coote and Dr. Nick Fletcher. Thanks, must also be given to summer student Tim who did some of the groundwork for this thesis, as well as MChem students Emily and Chris who made my last months in the lab more enjoyable.

I would like to express my gratitude to JSPS (Japan Society for the Promotion of Science) for funding my time working with Dr. Stephen Lyth (I^2CNER, Kyushu University). Special thanks should be given to Albert, Thomas, Jose, Aline, George, Vlad, George and Fong for helping me to settle in and making me feel welcome.

I'd also like to thank Tom, Izzy, James, Liz, Craig (non-boring), James, Miles, Patch, Betty, Josh and Henry for making my time in Lancaster bearable. Finally, thanks to Pete, James, Holly, Bryony and Ishmael who read my, often illegible, hand written notes back to me whilst I typed them up.

Abstract

This thesis reports upon investigations towards the synthesis and study of enantiopure interlocked molecules for the application of enantioselective recognition of chiral guest species.

Chapter One introduces the field of enantioselective recognition of chiral guest species and the synthesis of interlocked molecules. The review focuses upon enantioselective recognition of chiral anions, before taking an overview of the strategies employed to synthesise rotaxanes. The chapter concludes with how chirality can be introduced into rotaxanes and applications where the chirality of such rotaxanes has been explored.

Chapter Two charts the development and synthesis of a family of enantiopure chloride templated rotaxanes, incorporating enantiopure amino acid moieties as the chiral element. The enantioselective properties of these rotaxanes are then elucidated by NMR titrations using enantiopure chiral anions.

Chapter Three details the synthesis of a racemic chloride templated chiral rotaxane and behaviour of the diastereomers formed when the templating chloride anion is replaced with various enantiopure chiral anions. The separation of the diastereomeric salts of the rotaxane is reported.

Chapter Four investigates efforts towards a chiral sensing palladium (II) templated rotaxane. Both 3,5- and 2,6-substituted pyridine axle motifs are discussed.

Chapter Five describes the synthesis of a hydrogen bond templated chiral rotaxane. Following observation of diastereotopic effects on the axle due to the influence of the rotationally directional macrocycle, the effect of solvent, pH and presence of alkali metal cations on this expression of chirality by the rotaxane are disclosed.

Chapter Six further investigates the shuttling motion reported in Chapter Five. It commences with a short survey of developments to date regarding hydrogen bond templated rotaxanes demonstrating molecular motion and responding to changes in pH or addition of alkali metal cations.

Chapter Seven details the synthetic procedures and characterisation of compounds reported in this thesis, as well as titration protocols and x-ray crystal structures.

Glossary

°	Degree
aq	Aqueous
Ar	aromatic
Boc	*Tert*-Butyloxycarbonyl
br	Broad
C	Centigrade
Cat.	Catalytic
COSY	Correlated Spectroscopy
D	Deuterated
d	Doublet
DCC	*N*,*N*1-dicyclohexylcarbodiimide
DEPT	Distortionless enhancement by polarization transfer spectroscopy
DIPEA	Diisopropylethylamine
DMAP	4-Dimethylaminopyridine
DMF	Dimethylformamide
DMSO	Dimethyl sulfoxide
ESI	Electrospray ionisation
Et	Ethyl
FTIR	Fourier Transform Infrared
g	Gram
h	Hour
HMBC	Heteronuclear Multiple Bond Correlation Spectroscopy
HRMS	High Resolution Mass Spectrometry
HSQC	Heteronuclear Single Quantum Coherence Spectroscopy
Hz	Hertz
i	Iso
IR	Infrared
IT	Ion Trap
J	Coupling Constant
K	Kelvin, Association Constant
LRMS	Low Resolution Mass Spectrometry
M	Molar, Molecular Ion (Mass Spectrometry),
m	Multiplet, Medium, Meta
m/z	Mass/Charge (Mass Spectrometry)

Max	Maximum
Me	Methyl
min	Minute
mL	Millilitre
mmol	Millimole
mol	Mole
NMR	Nuclear Magnetic Resonance
NOESY	Nuclear Overhauser Effect Spectroscopy
o	*Ortho*
OAc	Acetate
p	Para
ppm	Parts Per Million
Pr	Propyl
q	Quartet
R	Alkyl or Aryl group
ROESY	Rotating Frame Nuclear Overhauser Effect Spectroscopy
RT	Room Temperature
s	Singlet, Strong
sept	Septet
t	Triplet, Tertiary
TBTA	Tris[(1-benzyl-1H-1,2,3-triazol-4-yl)methyl] amine
tert	Tertiary
THF	Tetrahydrofuran
TLC	Thin Layer Chromatography
TOCSY	Total Correlated Spectroscopy
ToF	Time of Flight
w	Weak
δ	Chemical Shift
Δ	Heat
υ_{max}	Wavenumbers, cm^{-1}

Chapter 1

Introduction

1.1 Importance of Chiral Recognition

Chiral molecules and ions are found throughout the natural world. Amino acids, sugars and hydroxy-carboxylic acids all contain chiral centres and in biological systems are generally found in their enantiopure form (L for amino acids and D for sugars). As all biological macromolecules, such as proteins, carbohydrates and DNA are all made from these chiral building blocks, they too are intrinsically chiral. This is of importance because drug molecules that contain chiral centres, will be operating in a chiral environment. As each of the enantiomers will interact differently in a chiral environment it can result in one enantiomer being the most effective and the other enantiomer having effects that range from being a less potent drug to being toxic. Due to the differing effects between enantiomers, there is a considerable drive towards enantiopure drugs.[1]

The archetypal and best known example of this is thalidomide and the teratogenic effects of one of the enantiomers (Fig. **1.1**).[2] Further examples include naproxen, where the *S* enantiomer is more active as an analgesic than the *R* enantiomer and the proton pump inhibitor omeprazole where the *S* enantiomer is more effective and sold separately as Nexium/esomeprazole.

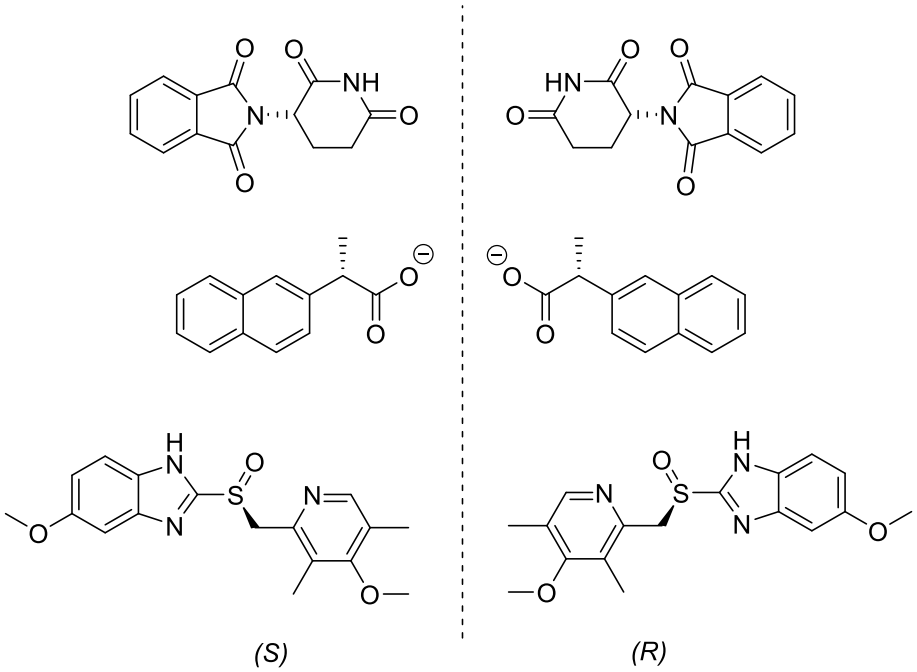

Figure 1.1 – Examples of drugs where different enantiomers have different effects (top to bottom – thalidomide, naproxen and omeprazole)

1.2 Theory of Chiral Recognition

Enantioselective recognition works on the principle that diastereoisomers, unlike enantiomers, have different physical properties as they are not mirror images of one another. Therefore, a host guest complex made with an enantiopure host can be used to distinguish between enantiomers of a chiral guest species. It is of critical importance that the binding site on the host is chiral as otherwise the host is unable to differentiate between the two enantiomers. The effect has been rationalised for tetrahedral chiral centres by use of a three-point binding model.[3] This model theorises that for enantioselective recognition the host and guest must have a minimum of three attractive points of interaction, where at least one site is stereo-chemically dependent.

This means that in one host guest complex [H.G_1] (Fig. **1.2**, left) the guest can interact with three sites on the host and in the second [H.G_2] (Fig. **1.2**, right) where it can only interact with two sites irrespective of the orientation of the guest. This results in [G_1] being bound more strongly

to the host than [G_2]. In the original model all three of these interactions were envisaged to be attractive.[3] Later models built on this theory, accepting that up to two of the three interactions could be repulsive, instead of attractive, provided that the remaining interactions are sufficiently strong to allow the host and guest to bind. [4]

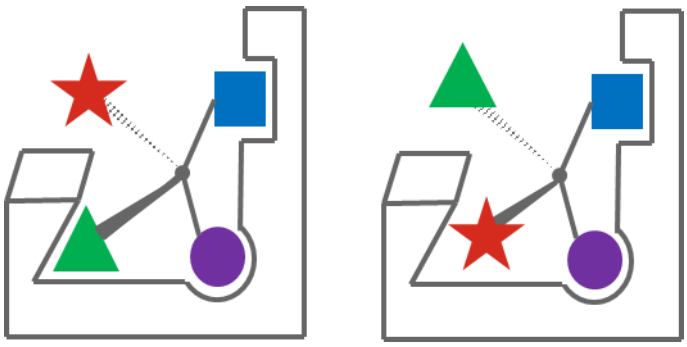

Figure 1.2 – Representation of the three point binding model, on the left all three sites on the guest [G_1] can interact with all three sites on the guest, on the right only two sites on the guest [G_2] can interact with the host resulting in weaker binding

Whilst the three-point model provides geometric criteria for the biding site of the host to allow for enantioselectivity, it does not give any indication of the intramolecular interactions required to for a host to bind a guest. Chemists have a variety of intermolecular interactions to ensure strong binding, which are chosen to complement the guest. For an ionic guest it is typical to use a host possessing the opposite charge, to deploy strong electrostatic attraction between the host and guest. However, such interactions are non-directional. More directional and hence selective attractive interactions can include hydrogen bonds, ion dipole interactions, π-π stacking interactions and σ hole interactions. In addition to this, steric hindrance is often used as a very strong short-range repulsive interaction, as it can be used to physically block one enantiomer from fitting in the binding site of an enantiopure chiral host.

1.3 Examples of Chiral Ion Recognition

The first enantioselective host for ions initially targeted chiral cations and were developed in the 1970's by Donald Cram and co-workers, where the enatioselctivity of chiral binaphthyl crown ethers towards chiral ammonium salts were reported.[5,6] In his first paper, Cram prepared enantiopure samples of ***(R,R)*-1.1** and ***(S,S)*-1.1** binapthyl crown ether and used these as hosts to extract chiral α-phenylethylammonium hexafluorophosphate salts into $CDCl_3$ from D_2O, with host **(*S,S*)-1.1** reporting an enatioselctivity of K_R/K_S = 2. In later work Cram and co-workers set about improving the enantioselectivity of the binapthyl crown ether, by varying the substitution of the binaphthyl moieties.[6] The highest enantioselectivity was reported for tetra-methyl host ***(R,R)*-1.2** and ***(S,S)*-1.2** that could achieve a more impressive selectivity of K_R/K_S = 31 of protonated methyl ester of *R*-phenylglycine in $CDCl_3$.

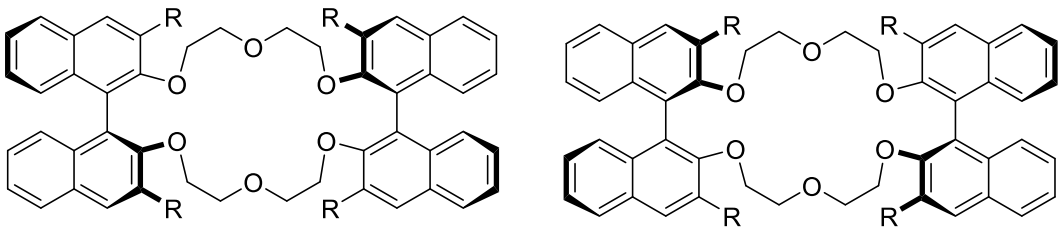

Figure 1.3 - Cram's enantioselective crown ethers 1.1 (R = H) and 1.2 (R = Me)

Receptors for chiral anions were investigated after receptors for chiral cations, possibly as anions are considered more difficult guest to bind than cations; owing to their larger more charge disperse and more directional nature when compared to cations.[7] Using macrocycles similar to Cram's chiral crown ethers, Gotor and co-workers developed a family of oxoazomacrocycles and azamacrocycles using a *trans*-cyclohexane 1,2-diamine moiety as the chiral reporter functionality, which can behave as an enantioselective receptor in water. These systems use a combination of hydrogen bonding and electrostatic attraction caused by protonated amines to bind guest species.[8–10] For example, chiral oxoazomacrocycles ***(R,R)*-1.3**

and ***(S,S,S,S)*-1.4** in multi-protonated states demonstrated enantioselectivities in aqueous NMe_4Cl (0.1 mol dm^{-3}) towards a variety of *N*-acetylated amino acids and chiral carboxylate anions. The highest reported selectivity for tetra protonated ***(R,R)*-1.3** was towards *N*-acetylated-aspartic acid, with a reported enantioselectivity of K_D/K_L = 3.5; ***(S,S,S,S)*-1.4** performed marginally more poorly with enantioselectivity of K_D/K_L = 3.0 being reported for the tris protonated form, with D and L tartrate. [8]

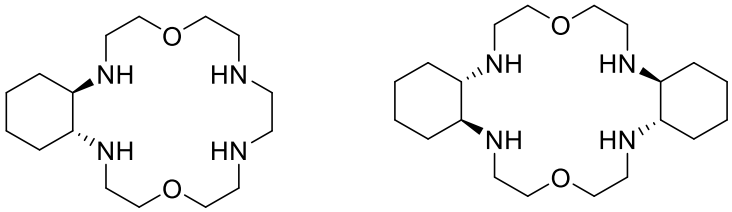

(***R*,*R*)-1.3** (***S*,*S*,*S*,*S*)-1.4**

Figure 1.4 - Gotor's enantioselective oxoazomacrocycles 1.3 and 1.4

Subsequently azamacrocycles with much higher enantioselectivities were reported. Tetra protonated macrocycle ***(R,R,R,R)*-1.5**, demonstrating a large difference in binding constants between *N*-Ac-glutamate with the D enantiomer with an enantioselectivity of K_D/K_L = 93 in aqueous NMe_4Cl (0.1 M^{-1}).[9] In a later work the more rigid pyridine containing macrocycle ***(R,R,R,R)*-1.6** was found to have a lower, but still considerable level of enantioselectivity of K_S/K_R = 12 at pH 10 towards *R* and *S* malate, dropping to lower enantioselectivities in more acidic conditions.[10]

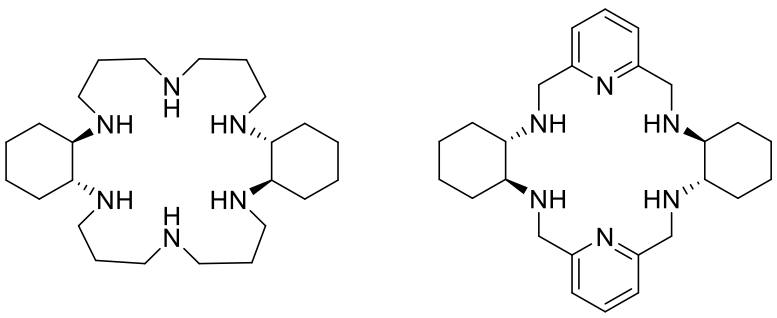

***(R,R,R,R)*-1.5** ***(R,R,R,R)*-1.6**

Figure 1.5 - Gotor and co-workers' enantioselective macrocycles 1.5 and 1.6

Kilburn and co-workers reported upon several enantioselective macrocycles, which use a number of inwards facing hydrogen bonds to bind the guest species. The receptor was made in two forms, a neutral receptor using a pair of thiourea groups ***(S,S,S,S)*-1.7** and one that has additional charge assisted binding through a pair of positively charged guanidinium groups, ***(S,S,S,S)*-1.8**. With the exception of the urea/thiourea groups both macrocycles are identical rigid structures with carboxypyridines at the four corners, creating a chiral pocket that has multiple inward facing hydrogen bonds.[11,12]

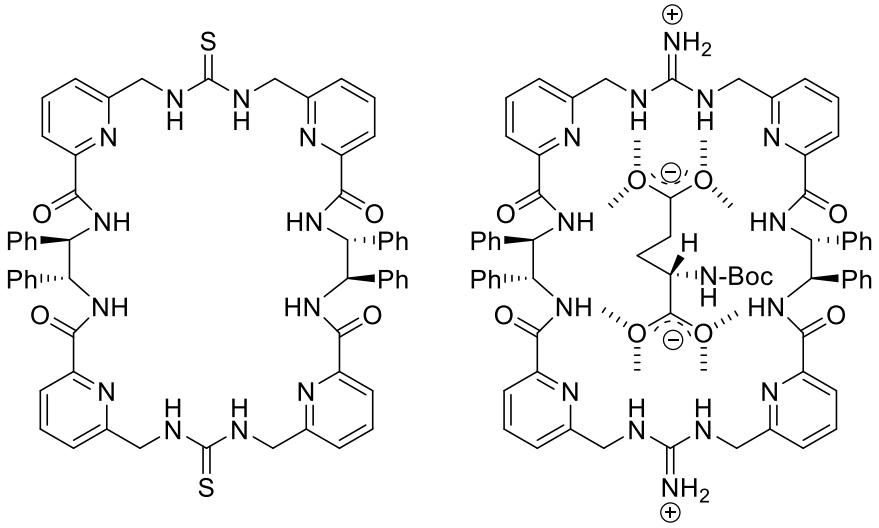

***(S,S,S,S)*-1.7** ***(S,S,S,S)*-1.8**

Figure 1.6 - Kilburn and co-workers' enantioselective thiourea and guanidinium macrocycles 1.7 and 1.8, macrocycle x is complexed to *N*-Boc-L-glutamate

The thiourea macrocycle ***(S,S,S,S)*-1.7** exhibits unusual binding properties towards *N*-Boc-glutamate in CD_3CN. The L-enantiomer is bound strongly ($K_{1:1}$ = 2.83 x 10^4 M^{-1}) in a typical 1:1 (host:guest) fashion, whilst the D-enantiomer binds to the macrocycle in a 1:2 (host:guest) fashion. The 1:2 complex is far more stable ($K_{1:2}$ = 4.92 x 10^4 M^{-1}) than the 1:1 complex ($K_{1:1}$ = 38 M^{-1}), this is attributed to the D-enantiomer not fitting into the binding cavity. If only the 1:1 binding events for D and L *N*-Boc-glutamate are considered, ***(S,S,S,S)*-1.7** demonstrates an enantioselectivity of in excess K_L/K_D = 700.[11]

The guanidinium macrocycle ***(S,S,S,S)*-1.8** demonstrates stronger binding towards *N*-boc-glutamate than ***(S,S,S,S)*-1.7** in 1:1 DMSO:H_2O, due to the two positively charged guanidinium groups. ***(S,S,S,S)*-1.8** shows 1:1 and 1:2 (host:guest) binding behaviour to the *N*-boc-L-glutamate ($K_{1:1}$ = 3.8 x 10^4 M^{-1}, $K_{1:2}$ = 5.3 x 10^3 M^{-1}) and *N*-Boc-D-glutamate($K_{1:1}$ = 2.9 x 10^4 M^{-1}, $K_{1:2}$ = 1.4 x 10^3 M^{-1}). The 1:1 binding event shows little enatioselctivity with $K_{L(1:1)}/K_{D(1:1)}$ = 1.3, although the 1:2 binding event shows enatioselctivity of $K_{L(1:1)}/K_{D(1:1)}$ = 3.8.

Chiral anion receptors have also been developed based upon 'calixarene like' macrocycle motifs. Lee and co-workers have investigated a chiral 'basket' calix[4]pyrrole receptor **1.9**.[13] In this receptor the chirality is derived from a 1,1'-bi-2-napthol group, found in the 'handle' of the 'basket'. The receptor demonstrates enantioselectivity of K_R/K_S = 10 towards *(S)*-2-phenylbutyrate, in CD_3CN. Whilst both enantiomers are capable of hydrogen bond interaction between the carboxylate of the guest and the NH groups of the pyrrole; only *(S)*-2-phenylbutyrate is able to form a π-π stacking interaction between the pyrrole of the host and the phenyl group on the guest. This result in *(S)*-2-phenylbutyrate binding more strongly to the guest species.

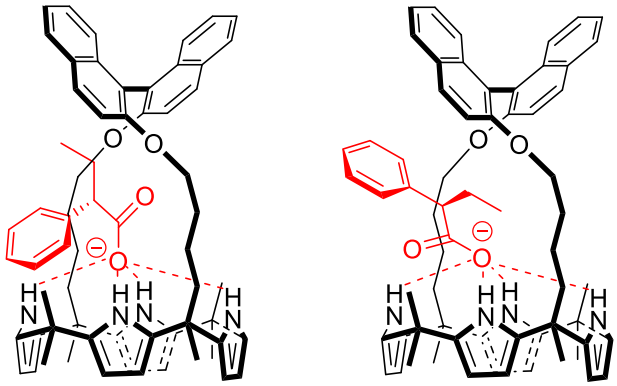

***(S)*-1.9** ***(S)*-1.9**

Figure 1.7 - Lee and co-workers' enantioselective calix-pyrrole 1.9 binding to (*S*)-2-phenylbutyrate (left) and (*R*)-2-phenylbutyrate (right)

Other 'calixarene like' motifs have been investigated such as chiral ureidothiacalix[4]arene **1.10**, developed by Lhoták and co-workers, which showed an enatioselctivity of K_D/K_L = 3.1, towards serine in D_6-DMSO.[14] A very recent example of a chiral receptor based upon bamburisil **1.11** was developed by Sokolov and Šindelář, which demonstrated an enatioselctivity of K_R/K_S = 3.2 towards methoxy mandelate salts in D_6-DMSO.[15]

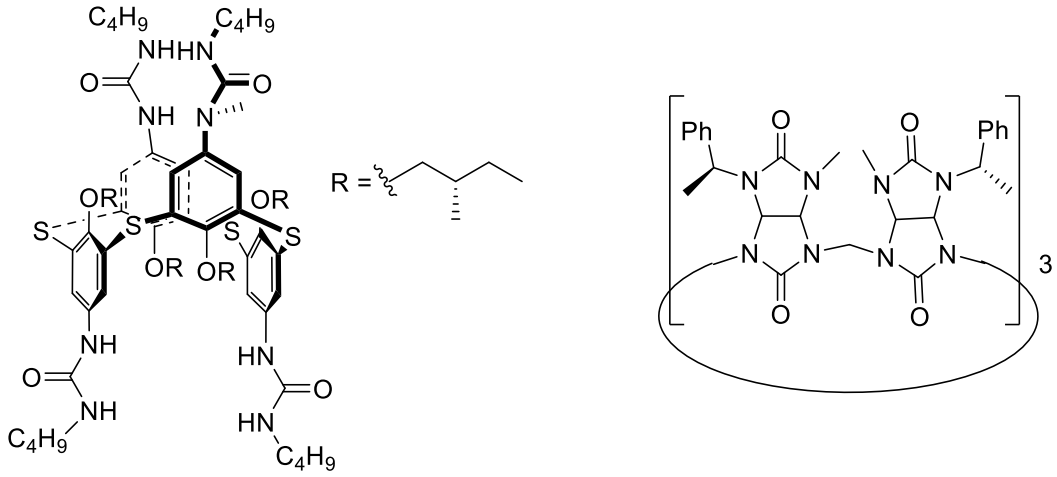

1.10 **1.11**

Figure 1.8 - Lhoták and co-workers' enantioselective calixarene 1.10 (left), Sokolov and Šindelář's enantioselective bambusuril 1.11 (right)

Whilst macrocyclic hosts are typically favoured due to their pre-organised structure, which reduces the entropic cost of binding a guest species, acyclic receptors have also been studied. Jurczak and c-workers have reported several multiple hydrogen bond donating linear compounds, by coupling sugars and amino acids to a rigid back bone, resulting in a relatively quick and straightforward synthesis.[16–20]

Jurckzak and co-workers initial receptors (representative example **1.12**), were based upon various ester protected L-valine and L-phenylalanine moieties coupled to a central benzene-1,2-diamine unit. These examples showed relatively little enantioselectivity towards mandelates in 199:1 DMSO:H_2O (K_s/K_R = 0.94-1.01) or N-acetyl-phenylalanine anions in MeCN (K_D/K_L = 0.92-1.09).[16]

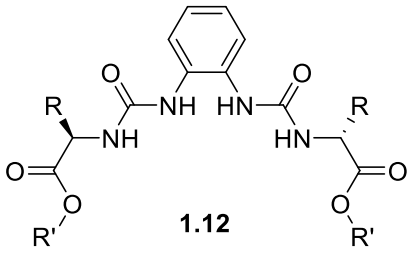

Figure 1.9 - Jurczak's amino acid based receptor 1.12 (R = ^{i}Pr, CH_2Ph, R'= Me, ^{i}Pr, ^{t}Bu)

A family of similar receptors based upon deoxyglucose instead of an amino acid yielded better results. Receptor **1.13** (R = Me) showed modest enantioselectivites towards Boc protected amino acids (in DMSO-0.5% H_2O), with enatioselectivity of K_D/K_L = 2.57 for the enantiomers of *N*-Boc-tryptophan[17,18] Later work improved the enantioselectivity by varying the substituents (R = Me, 1-napthyl) and using sugars as the chiral component to form receptors **1.13** and **1.14**. Receptor **1.13** offered a higher enantioselectivity K_R/K_S = 4.14 for the enantiomers of 3-phenylacetate.[19]

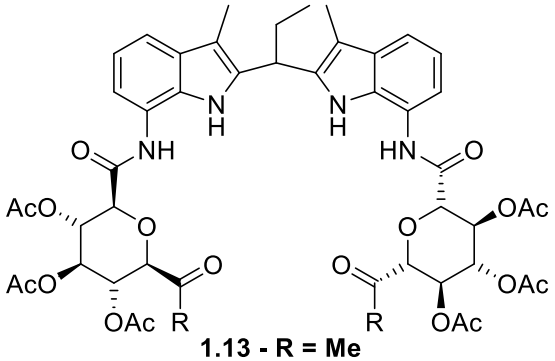

Figure 1.10 - Jurczak's enantioselective deoxyglucose based receptor 1.13 (R = Me) and 1.14 (R = 1-napthyl)

Tucker and co-workers have also investigated acyclic compounds as chiral anion receptors, by appending chiral urea groups to ferrocene as with receptors ***(S)*-1.14** and ***(S)*-1.15**.[21,22] Receptor ***(S)*-1.14** showed a small enantioselectivity towards *(R)*-2-phenybutyrate in DMSO (K_R/K_S = 1.24), using UV-Vis spectroscopy. However, the receptor was unable to differentiate between enantiomers by cyclic voltammetry as was initially planned.[21] Receptor ***(S)*-1.15**, reported in a

follow up paper, showed slightly higher enantioselectivity (K_R/K_S = 1.41) in DMSO towards (*R*)-2-hydroxyphenylacetic acid, possibly due to the enhanced hydrogen bonding from the urea caused by the electron withdrawing nitrobenzene.[22]

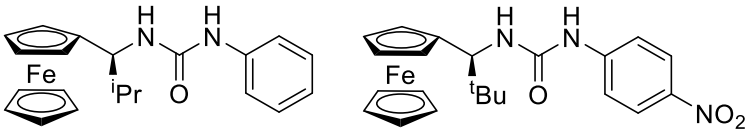

1.14 **1.15**

Figure 1.11 - Tucker and co-workers' enantioselective receptors 1.14 (left) 1.15 (right)

More recently Beer and co-workers have investigated a family of chiral (*S*)-binapthyl receptors (**1.16**, **1.17** and **1.18**), with either hydrogen bonding, halogen bonding or chalcogen bonding for differentiation between enantiomers and geometric isomers of dianions. Hydrogen bonding receptor **1.16** and halogen bonding receptor **1.17** demonstrated enantioselectivites of K_{SS}/K_{RR} = 1.6 and K_{RR}/K_{SS} = 1.8 respectively, for the *S,S* and *R,R* enantiomers of tartrate in 85:15 D_6-acetone:D_2O in a 1:1 (host:guest) binding model. Whilst chalcogen receptor **1.18** demonstrated little enatioselctivity, the authors believed this to be due to the less directional nature of charcologen bonding, allowing the resulting host-guest complex to adopt several different conformations .[23]

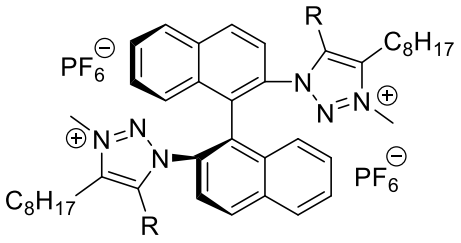

1.16 - R = H, 1.17 - R = I, 1.18 - R= SeMe

Figure 1.12 - Beer and co-workers' receptors 1.16 (R= H), 1.17 (R = I), 1.18 (R= SeMe)

A common route for the development of enantioselective chiral anion sensors is to derivatise natural products, for example cholic acid as developed by Davis and co-workers. The most successful receptors developed using this motif contained both carbamate and guanidinium

groups appended to a cholic acid molecule (receptors **1.19** and **1.20**. Initial investigations with receptor **1.19** demonstrated an enantioselectivity of 10:1 towards *N*-acetyl-L-phenylalanine in $CDCl_3$, similar results were reported for a number of amino acids.[24] Receptor **1.19** was later modified to include a lipophilic hydrocarbon tail resulting in functional receptor **1.20**, which was used in membrane experiments to separate enantiomers with a high turnover rate and enantioselectivity.[25]

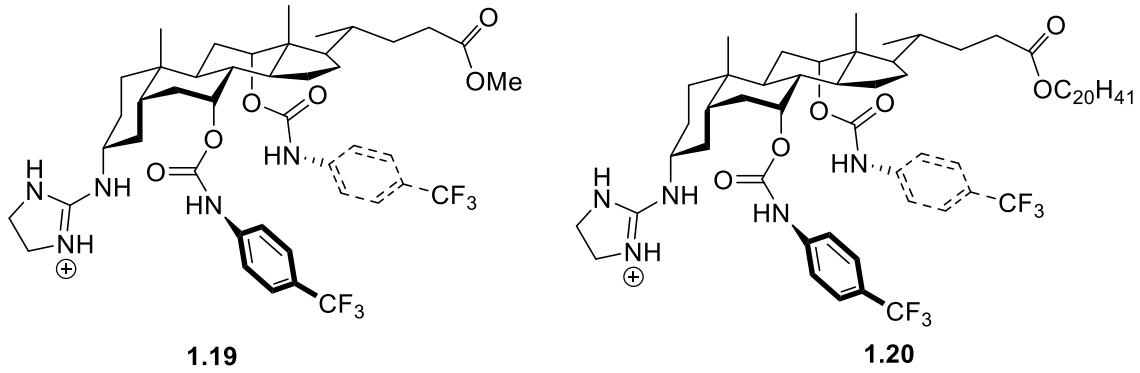

Figure 1.13 - Davis' enantioselective cholic acid based receptors 1.19 (left) and 1.20 (right)

Further examples of anion receptors from derivatives of naturally occurring compounds can be seen by the modification of naturally occurring macrocyclic molecules, taking advantage of their more rigid and pre-organised nature. Starnes and co-workers' porphyrin receptors ***(S)*-1.21** and ***(R)*-1.21**, are one example of this, having been prepared from a zinc containing porphyrin with an appended enantiopure chiral hydrogen bonding component. These receptors showed enantioselectivities of K_S/K_R =3.1, K_R/K_S = 3.1 for ***(S)*-1.21** and ***(R)*-1.21** respectively, towards TBA mandelate salts in CH_2Cl_2.[26]

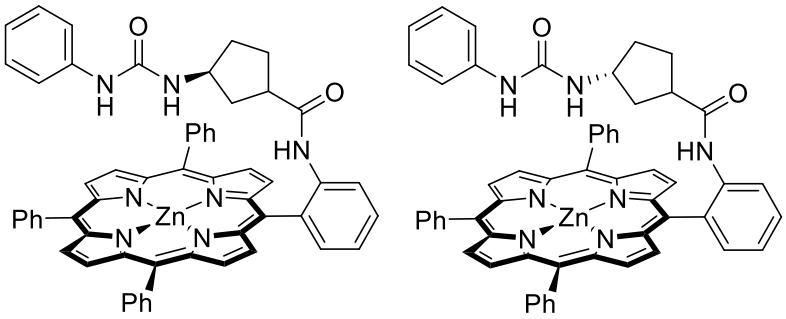

***(S)*-1.21** ***(R)*-1.21**

Figure 1.14 Starnes and co-workers' enantioselective zinc porphyrin based receptors (*S*)-1.21 and (*R*)-1.21.

Sessler and co-workers have has also studied cyclic chiral anion receptors based upon sapphryin macrocycles. Receptor **1.22** is based upon two sapphryin macrocycles together, using a chiral bis-amine to form a rigid dimer. Receptor **1.22** showed selectivity towards *N*-Cbz-glutamate in 95:5 CH_2Cl_2:MeOH (K_D/K_L =4.3).[27]

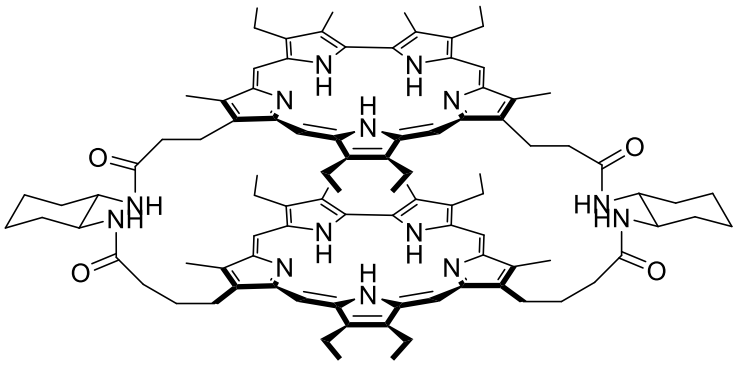

1.22

Figure 1.15 - Sessler's sapphryin dimer receptor 1.22

A variety of both macrocyclic and acyclic enantioselective receptors have been reported and studied, as illustrated by the examples discussed above. Typically the enantioselectivities of these receptors are not particularly high and are generally less than $K_{favoured}/K_{disfavoured} < 10$. A trend can be observed from these systems, that receptors that are more well defined in 3D

space, more rigid and therefore pre-organised receptors, typically the macrocyclic receptors, are often those that offer the highest enantioselectivities. From this we can conclude that molecules that offer greater control over the 3D space around the binding site of the host species, such as rotaxanes and other interlocked molecules, may offer an opportunity for the development of receptors with higher enantioselectivities.

1.4 Synthesis of Rotaxanes

Rotaxanes are 3D interlocked molecules comprising of one or more macrocyclic rings threaded upon an axle, where each end of the axle has a bulky stopper group preventing the macrocycle from dethreading (Fig. **1.16**). The unique 3D structure of rotaxanes leads to the formation of a region where the ring and the axle are in close proximity, which may be designed to selectively accommodate any one of a variety of guests.[28]

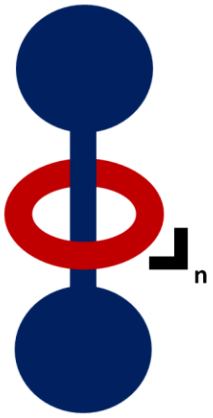

Figure 1.16 - schematic representation of a [n+1] rotaxane, where n is the number of macrocycles threaded upon the axle.

The first rotaxane synthesis was reported by Harrison and Harrison in 1967. The macrocycle was attached to Merrifield resin and then was treated 70 times with a mixture of two stoppered half axles, so that at least some of the axle would thread through the fixed macrocycle and form a rotaxane attached to the resin, achieving yields of 6%.[29]

The four principle techniques used to create rotaxanes are (Fig. **1.17**):

1) Slipping – Where the macrocycle is caused to expand, generally by heating, and forced over the stopper groups.[30]

2) Clipping- Where the macrocycle precursor is held close to the axle and a linking piece is used in a ring closing reaction to link the two ends of the macrocycle together.[31]

3) Stoppering – Where the axle is threaded through the axle and the axle then has stoppers attached, to prevent the axle dethreading.[32]

4) Snapping – Where two parts of the axle are brought together and are attached inside of the macrocycle.[29,33]

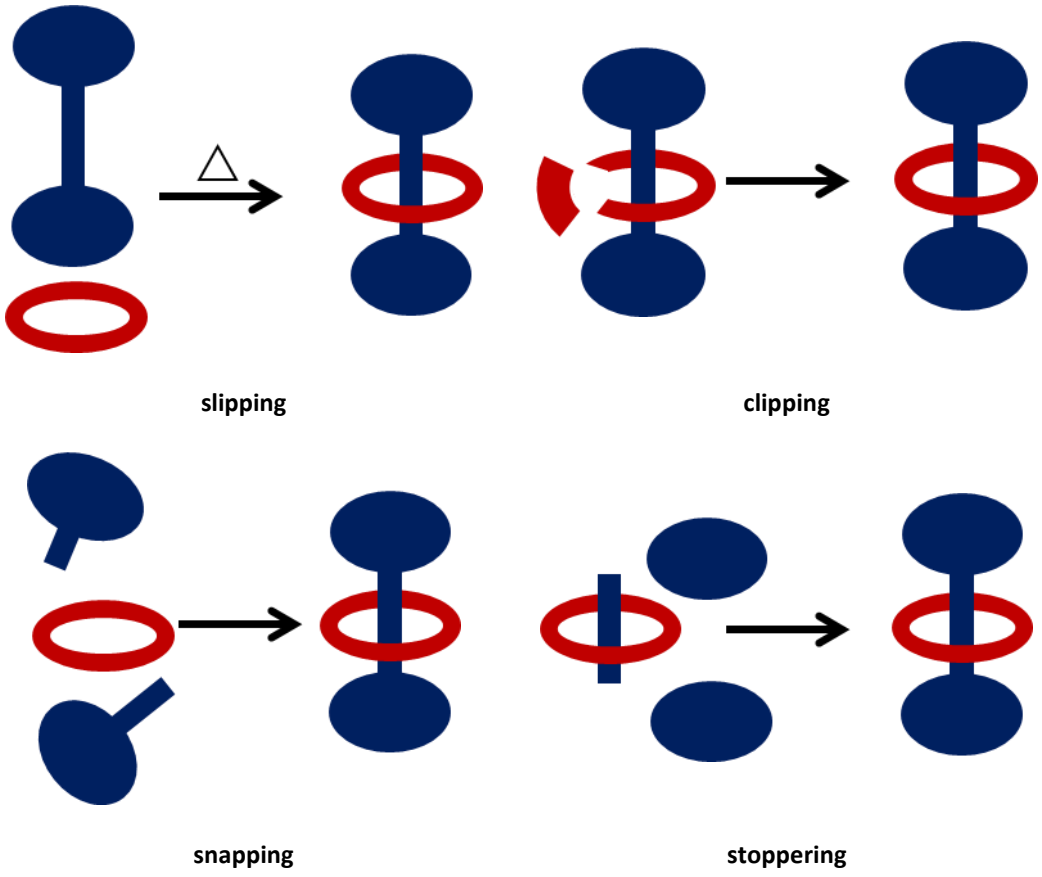

Figure 1.17 - General synthetic routes used to produce rotaxanes

These techniques are used to form the mechanical bonds that permanently hold the rotaxane together. However, to synthesise rotaxanes in high yields, rather than using a statistical approach, it is necessary to use a template to bring the non-interlocked components together.

The use of passive metals as templates was the first technique developed to prepare rotaxanes in synthetically useful yields. This method used a metal to hold the components of the rotaxane

together, whilst the rotaxane is formed. The first example of this technique was for catenanes and was developed by Sauvage to prepare [2] catenane, where a tetrahedral copper (I) cation is used to hold the non-interlocked components together.[34] The use of a passive metal as a template was then applied to rotaxanes by Gibson and co-workers to prepare rotaxane **1.23**. In this synthesis a tetrahedral copper (I) cation was used to bind to two 1,10-phenathroline groups that were strategically placed upon the macrocyclic and axle components, forming a pseudorotaxane. The pseudorotaxane was then stoppered and the templating metal removed to produce rotaxane **1.23** (Fig. **1.18**).[35] A similar rotaxane was developed by Sauvage and co-workers, although this rotaxane used porphyrin groups as stoppers.[36]

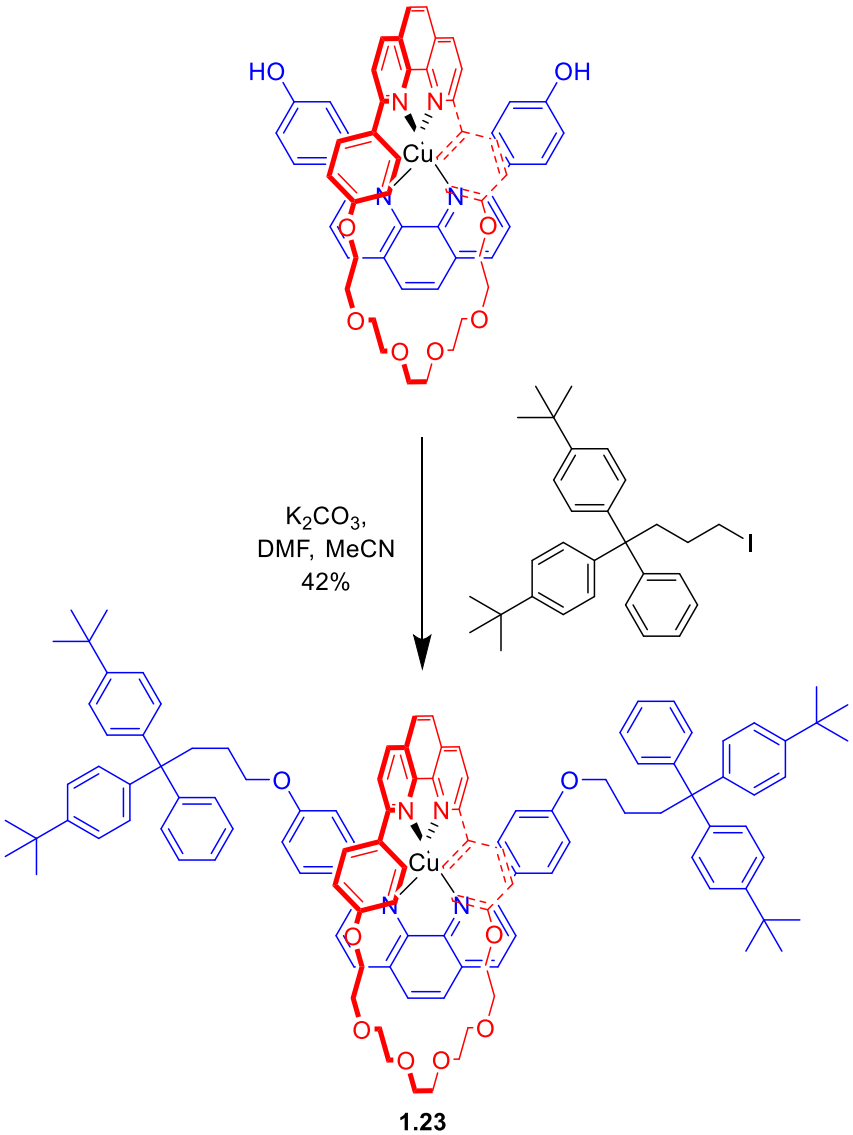

Figure 1.18 – Synthesis of Gibson's copper (I) templated rotaxane 1.23

Square planar palladium (II) cations have also been used as passive metal templates. In these systems the palladium (II) is typically bound in a 3 + 1 coordination to the two components.[37,38] Leigh and co-workers have used this technique to form rotaxane **1.24** in 77% yield. This was achieved through utilisation of a palladium (II) cation to hold macrocycle precursor, containing a tridentate pyridine-2,6-dicarboxamide ligand, together with an axle containing a monodentate pyridine ligand. The rotaxane was then formed by ring closing metathesis of the macrocycle precursor, followed by hydrogenation to afford rotaxane **1.24**.[39]

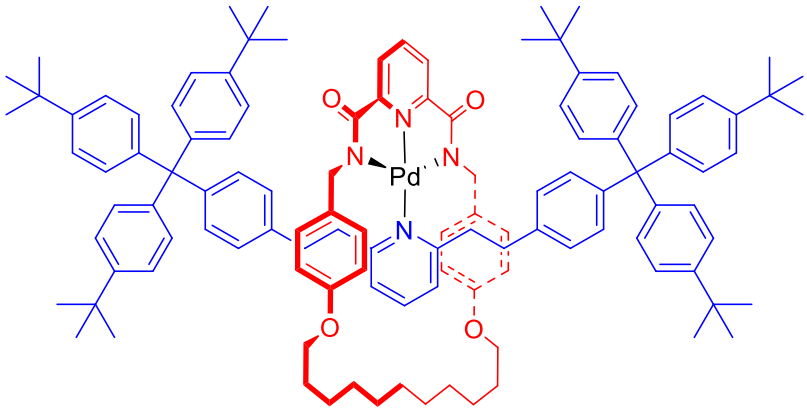

1.24

Figure 1.19 - Leigh's Palladium (II) templated rotaxane 1.24

Whilst in passive metal templated synthesis the metal is simply used to hold the precursor complex together, in the more recently developed active metal template synthesis the metal has two roles: first to hold the precursor complex together and second to act as a catalyst for the covalent bond forming reaction that leads to rotaxane or catenane formation.[40,41] The first synthesis (Fig. **1.20**), reported be Leigh and co-workers, was based upon using copper (I) as the template and as catalyst for the CuAAC 'copper click' reaction, forming rotaxane **1.25**. Yields of 94% were reported with use of stoichiometric amounts of copper (I) and 92% with 20 mol% of copper (I).[42]

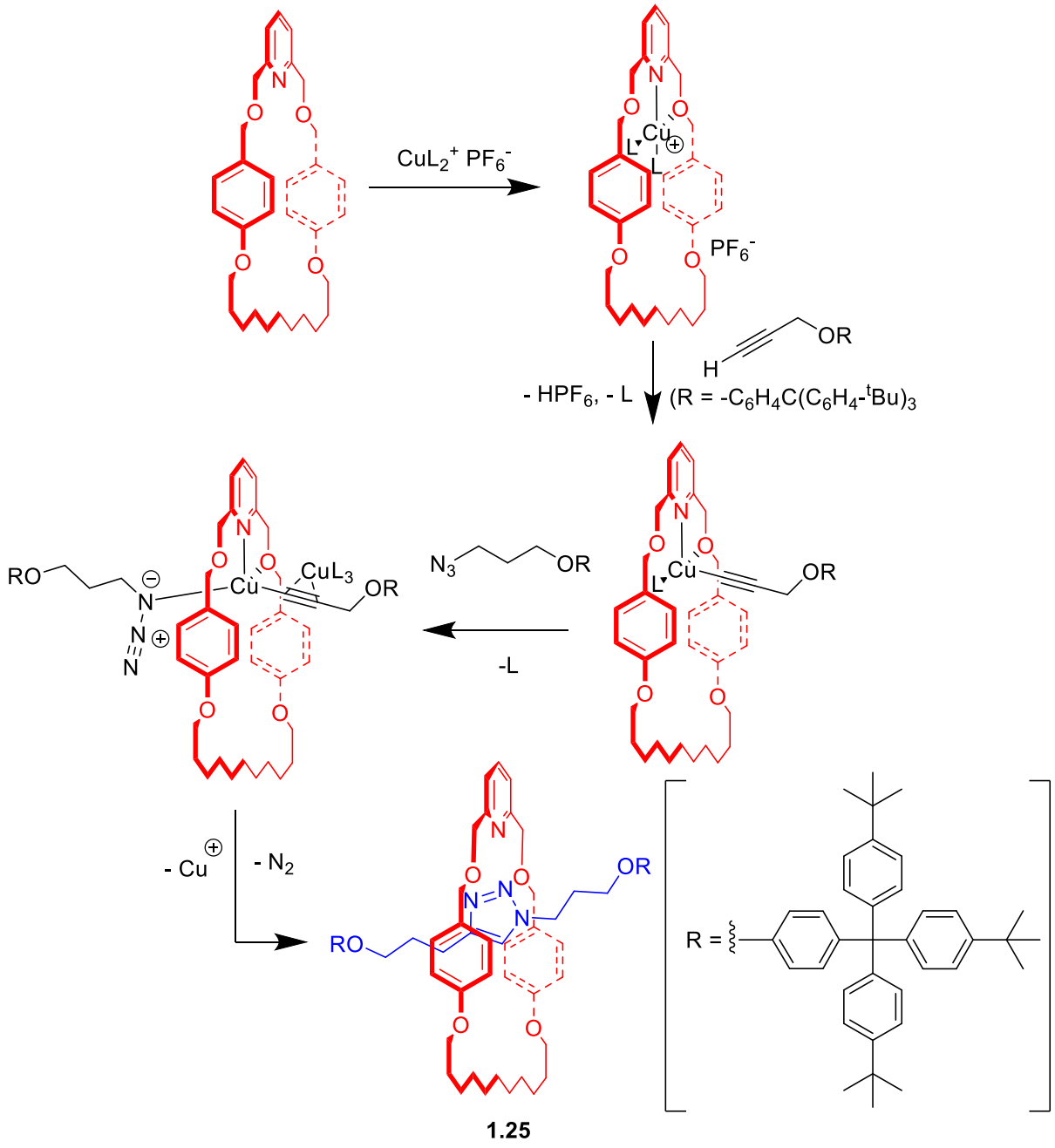

Figure 1.20 - Leigh and co-workers' Copper (I) active metal templated rotaxane 1.25

Active metal templated rotaxanes are not just limited to rotaxanes templated by copper (I) cations, Leigh and co-workers have shown that palladium (II) may also be used. In this example palladium (II) chloride was bound to pyridine containing macrocycle and two equivalents of the alkyne axle activated with copper (I) iodide were added, which bound to the palladium (II). The palladium (II) was then used as a catalyst for a Sonogashira alkyne coupling (Fig. **1.21**), to form

rotaxane **1.26** in yields of 61% and 90% for a stoichiometric amount and 5 mol % of palladium catalyst respectively.[43]

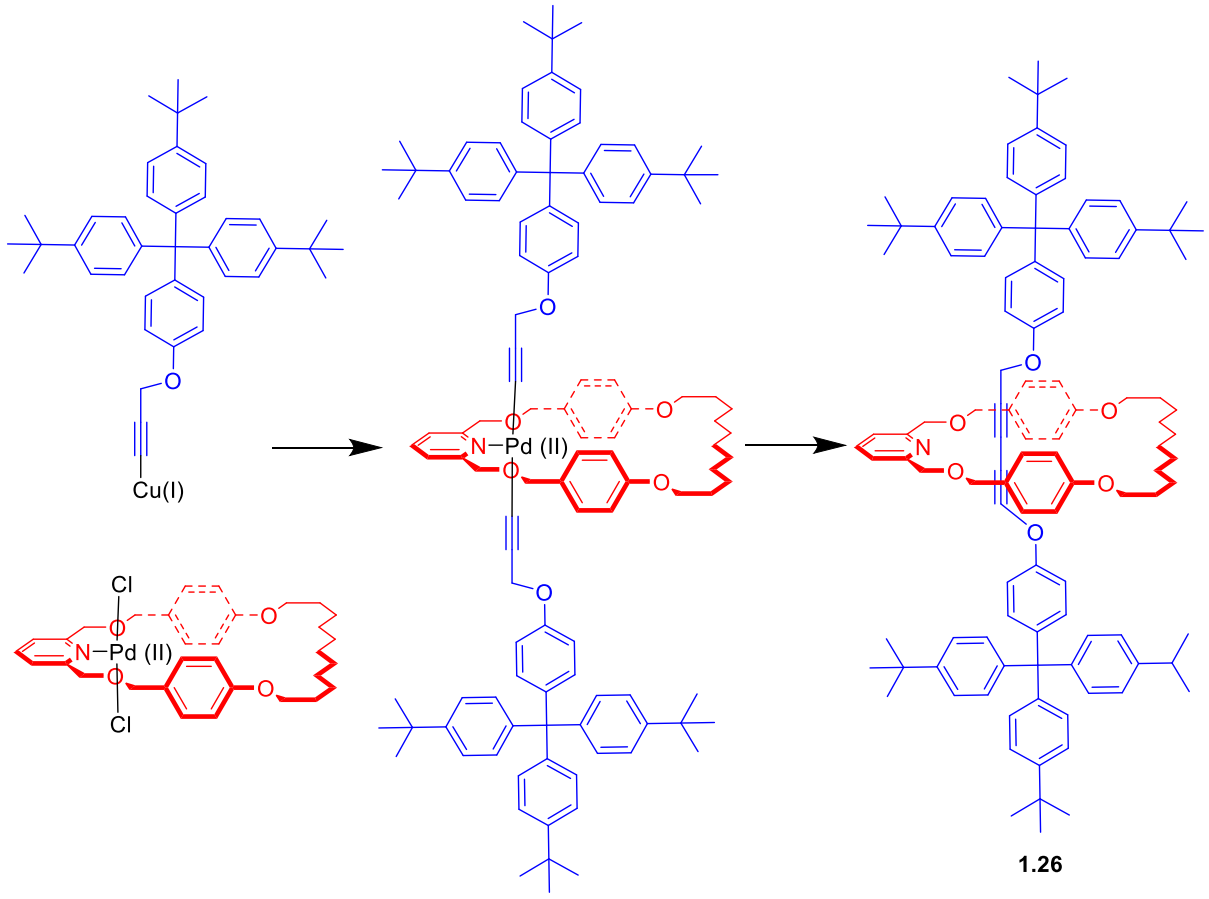

Figure 1.21 – Active metal templated synthesis of rotaxane 1.26.

Anions may also be used as templates for rotaxanes, as their geometries can be exploited in much the same way as transition metal templates. However, instead of electron donating ligands that can bind to a positively charged substrate, anion templated rotaxanes must instead use components that contain hydrogen or halogen bond donor species to bind the anion.

The first anion templated rotaxane **1.27** was developed in 1999 by Vögtle and co-workers, using a phenoxide anion attached to an axle half, acting as both the templating anion, binding within the tetra amide cavity of the macrocycle. The phenoxide anion then attacks the benzylic bromide in a nucleophilic attack to form rotaxane **1.27** in a 95% yield (Fig. **1.22**).[33]

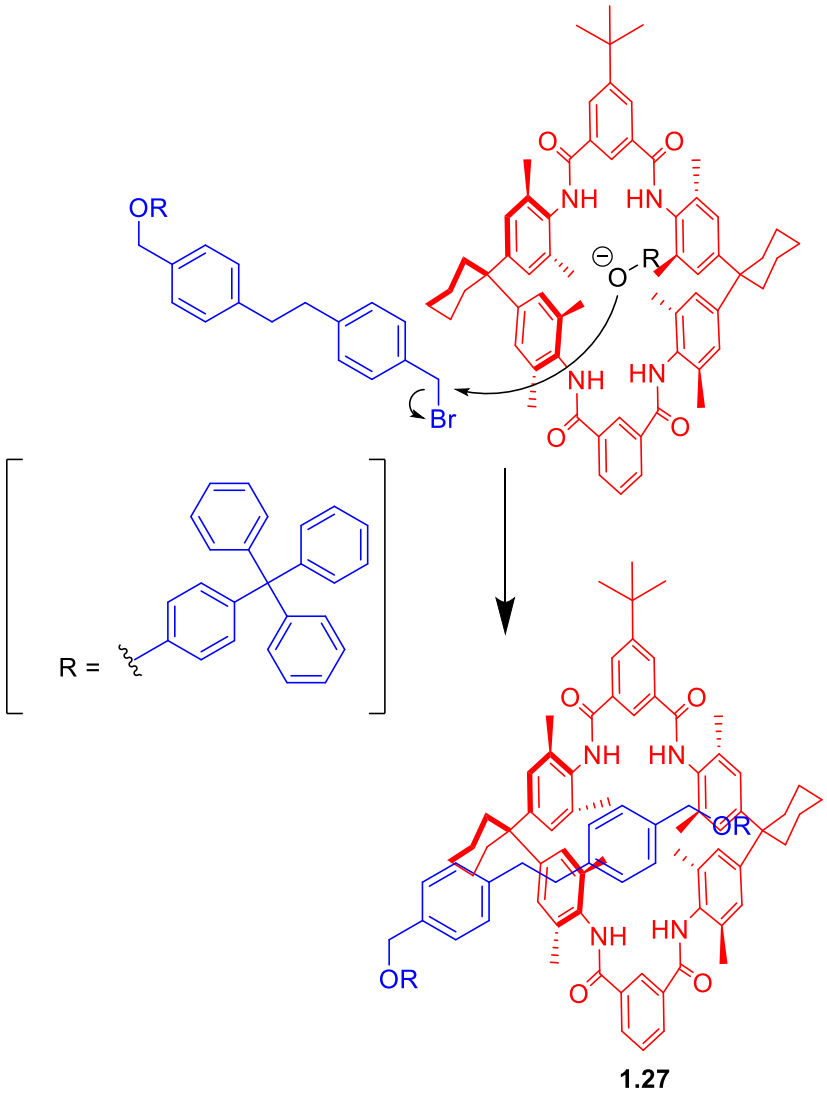

Figure 1.22 - Phenoxide anion templated synthesis of rotaxane 1.27

Later work by Schalley and co-workers again uses a phenoxide anion templated synthesis. A bis-amine axle containing a phenoxide anion is added to the same macrocycle used in rotaxane **1.28** (Fig. **1.23**), the phenoxide may then bind to either isophthalamide moiety on the macrocycle. This forms a pseudorotaxane, which may then be stoppered using two equivalents of an acid chloride stopper to form rotaxane **1.28** in 25 % yield.[44,45]

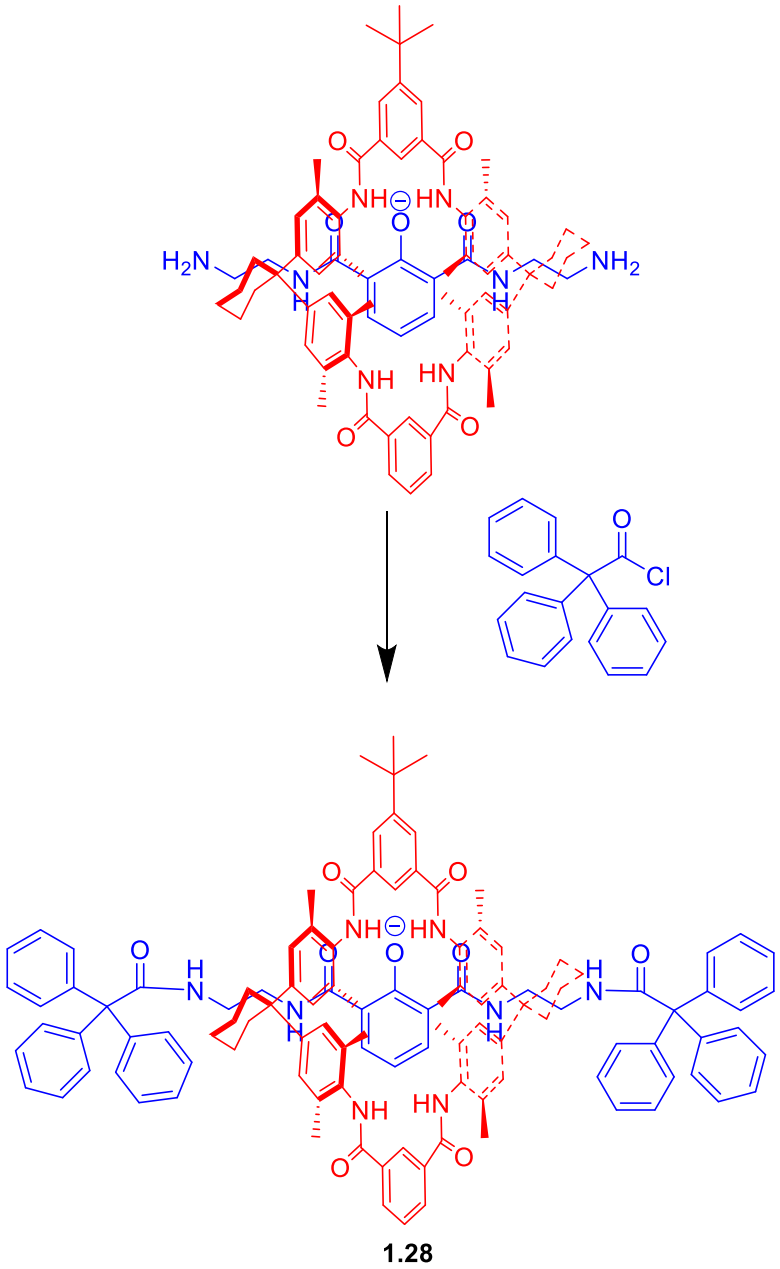

Figure 1.23 - Synthesis of phenoxide templated rotaxane 1.28

Anion templated rotaxanes have been extensively studied by Beer and co-workers.[46] In many of these systems, a chloride anion binds to a tetrahedral tetra-amide pocket created between an isophthalamide group on the macrocycle precursor and *N*-methyl-3,5-pyridine dicarboxamide group on the axle (Fig. **1.24**), bringing the two components of the rotaxane together. In the first of these systems, the macrocycle precursor is clipped shut around the axle using a ring closing metathesis reaction, catalysed by Grubbs' catalyst, forming rotaxane **1.29** in a 47% yield. The

chloride anion in this system is of critical importance as no rotaxane **1.29** could be formed by using the bromide, iodide or hexafluorophosphate salts of the axle component.[47]

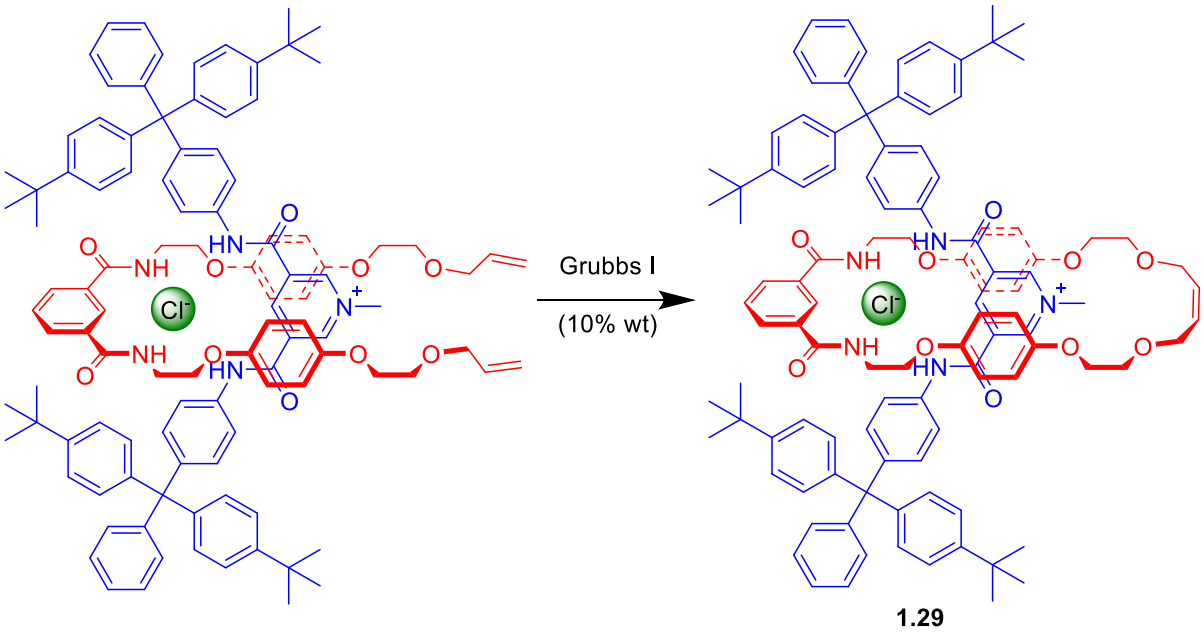

Figure 1.24 – Synthesis of Beer and co-workers' chloride templated rotaxane 1.29

A variation of this chloride templated synthesis was subsequently developed by Beer and co-workers (Fig. **1.11**), where the need for Grubbs' catalyst, which is intolerant to certain functional groups, was removed. This was achieved by using a bis-amine as the macrocycle precursor. This bis-amine could then be clipped onto the same axle as was used in rotaxane **1.29**, using isophthaloyl chloride to form rotaxane **1.30** in yields of up to 60 % (Fig. **1.11**).[48,49]

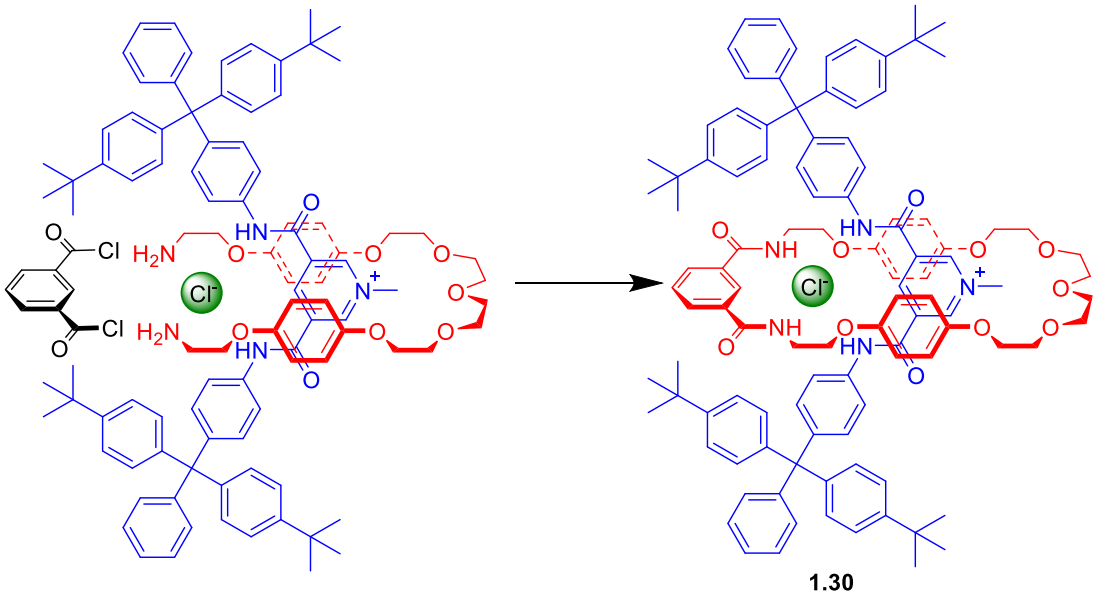

Figure 1.25 – Synthesis of chloride templated rotaxane 1.30

Nitrite anions may also be used as an anion template, having been used by Beer for the lanthanide containing rotaxanes **1.31-La^{3+}** and **1.31-Eu^{3+}**. Where the nitrite anion is used to coordinate to both the lanthanide on the macrocycle and two hydrogen bonding amines on the axle, the rotaxane could then be clipped shut using a CuAAC reaction. Rotaxanes **1.31-La^{3+}** and **1.31-Eu^{3+}**were isolated in yields of 51% and 45% respectively.[50] Other anions such as sulfate and nitrate have also been studied.[51,52]

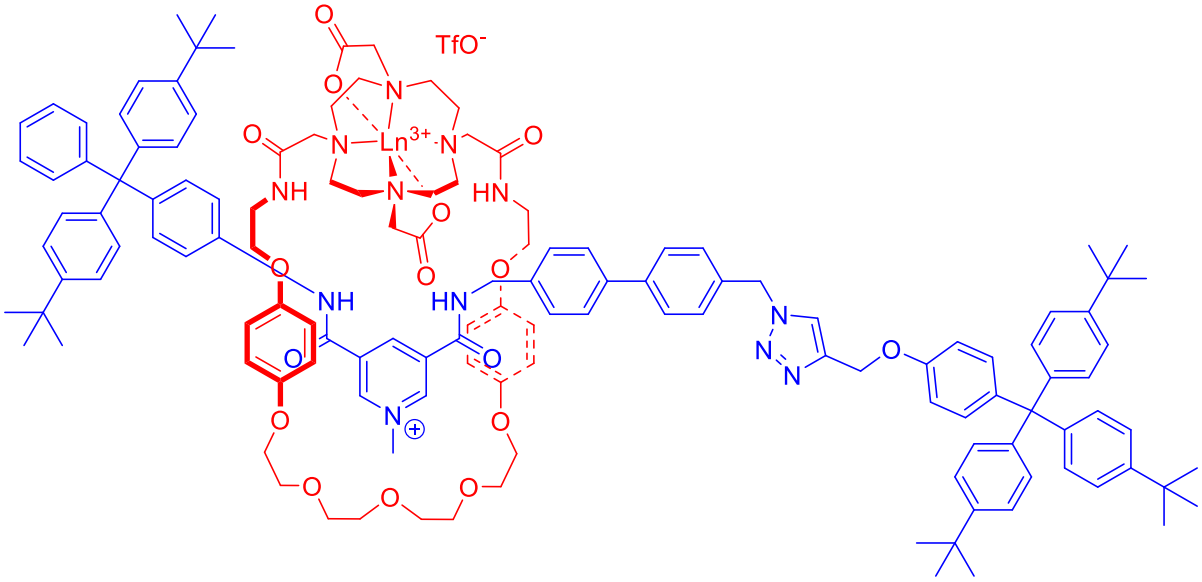

Figure 1.26 - Beer and co-workers' nitrite templated rotaxanes 1.31-La^{3+} and 1.31-Eu^{3+}.

One of the most widely explored rotaxane templating methods is hydrogen bond templated synthesis using protonated ammonium motifs. Unlike the methods discussed so far this templating method often does not use an auxiliary component, such as a metal or anion, to bring the components of the rotaxane together. Instead the macrocyclic and axle components are designed so that hydrogen bonding interactions between the components cause them to self-assemble.

One of the most explored motifs, particularly for use in rotaxane based molecular machines is the use of a secondary ammonium cation. Stoddart as well as other groups have developed many rotaxanes using this motif.[53–57] In this example by Stoddart and co-workers, rotaxane **1.32** is formed by a hydrogen bond donating secondary ammonium cation binding to a hydrogen bond accepting crown ether ring (Fig. **1.27**). The resulting pseudorotaxane was then stoppered using 3,5-di-*tert*-butylbenzyl bromide in a high pressure nucleophilic substitution reaction forming rotaxane **1.32** in 66% yield.

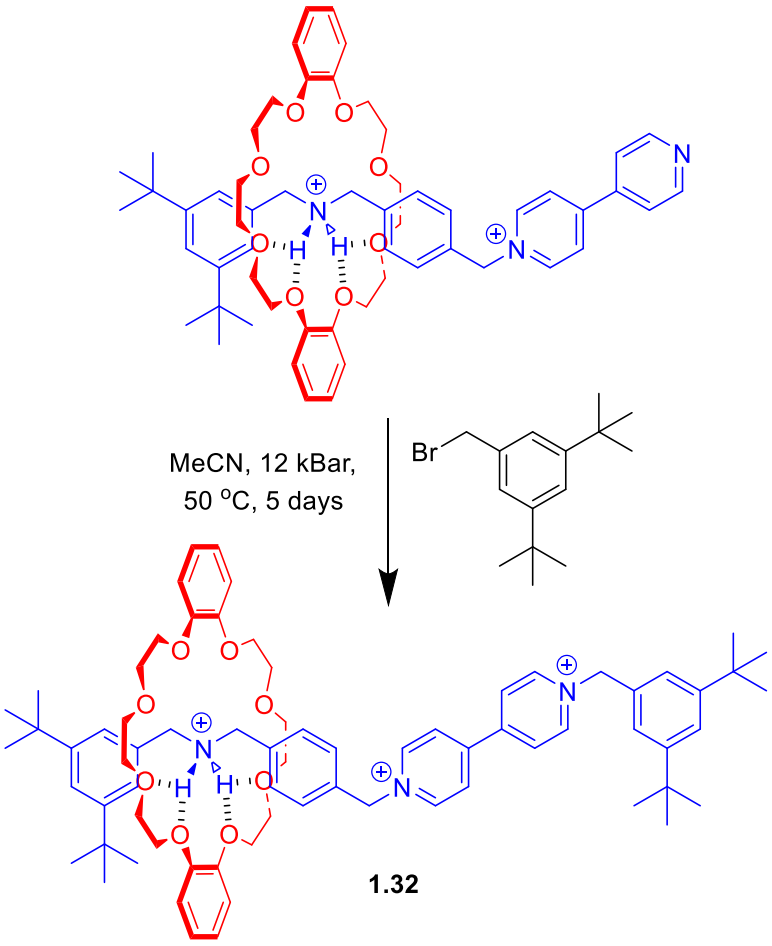

Figure 1.27 - Synthesis of Stoddart and co-workers' secondary ammonium, hydrogen bond templated rotaxane 1.32

The other major motif explored for hydrogen bond templated rotaxanes, is using a macrocycle with one or more isophthalamide groups as hydrogen bond donors and carbonyls or other electron rich oxygen atoms on the axle as hydrogen bond acceptors. Leigh and co-workers developed hydrogen bond templated rotaxane **1.33** using a motif with two isophthalamide groups on the macrocycle (Fig. **1.28**).[58] The macrocycle can be formed from commercially available materials isophthaloyl chloride and *p*-xylylenediamine. The resulting two isopthalamide groups formed from the reaction between these two components, template to the 1,4-carbonyl motif on the axle resulting in formation of rotaxane **1.33** in 62 % yield. Rotaxanes using this macrocycle and axle motif have been used for a variety of molecular machines and catalysis applications.[59,60]

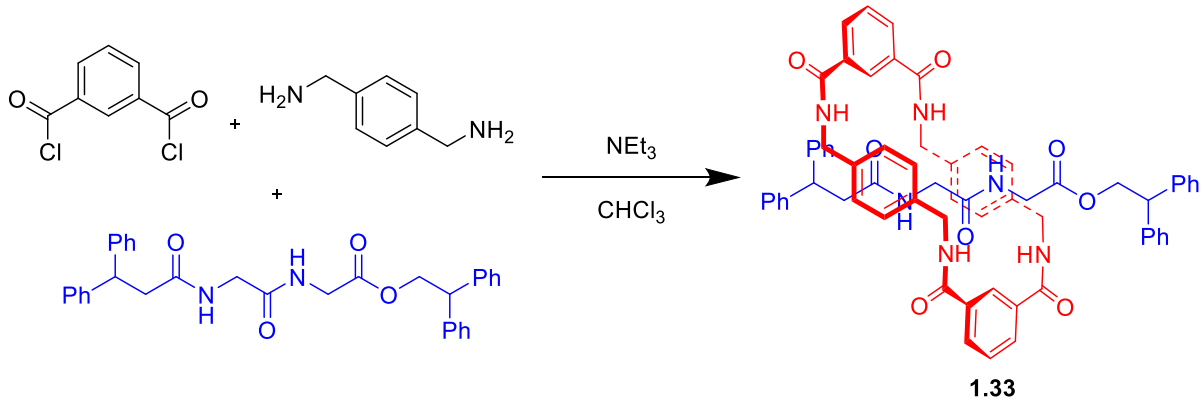

Figure 1.28 - Leigh and co-workers hydrogen bond templated rotaxane 1.33

1.5 Rotaxanes as hosts for anions

Rotaxanes with unusual 3D interlocked structures, a high degree of rigidity and the potential for a pocket to exist within their structure shielded from solvent, have been proved to be excellent hosts for simple anions. Beer and co-workers have demonstrated that many of their anion templated rotaxanes can exhibit selectivity towards anions. The first such example is rotaxane **1.29**, reported in 2002.[47] Rotaxane **1.29** consists of an axle containing a pyridinium cation, which resides with the macrocyclic ring and four hydrogen bond donating amides, strategically positioned so that they face into the macrocycle cavity.

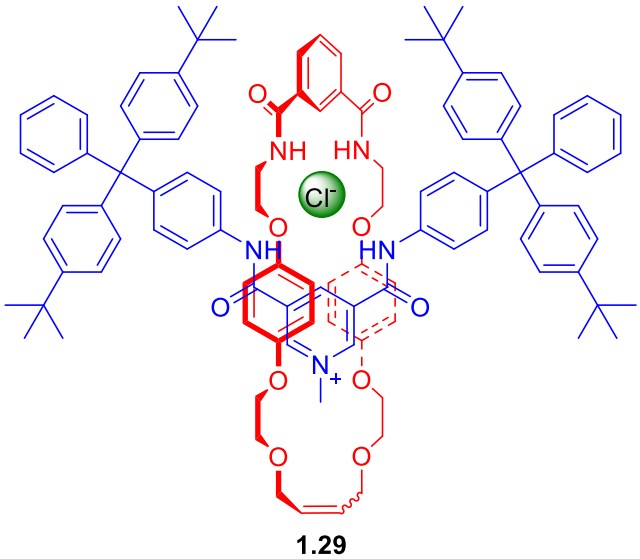

Figure 1.29 - Beer's first chloride sensing rotaxane 1.29

Rotaxane **1.29** favours chloride anions over oxo-anions (1:1 $CDCl_3$:MeOD) (Table 1), whereas the axle alone favours oxo-anions. The selectivity of rotaxane **1.29** towards chloride anions is attributed to chloride being the only anion capable of sitting within the rotaxane cavity, as the cavity was templated by a chloride anion it is the perfect size to fit a chloride anion inside. Other anions must instead reside on the periphery of the rotaxane cavity.

Table 1.1– Association Constants of Rotaxane 1.29, 1:1 MeOD:$CDCl_3$

Anion	K_a Axle [M^{-1}]	K_a Rotaxane [M^{-1}]
Cl^-	125	1130
$H_2PO_4^-$	260	300
AcO^-	22,000	100

In later work the isopthalamide moiety of the macrocycle was modified to enhance the hydrogen bond donating ability of the isophthalamide amides, with the introduction of a variety of electron withdrawing groups to form rotaxanes **1.29**, **1.29a** and **1.29b** (-H, $-NO_2$ and -I respectively).[61] The rotaxanes were titrated with TBA salts of various anions in 45:45:10 $CDCl_3$:MeOD:D_2O. Whilst the electron withdrawing groups did achieve their aim of enhancing the binding ability of these rotaxanes, this did not increase the selectivity of the rotaxanes towards chloride anions.

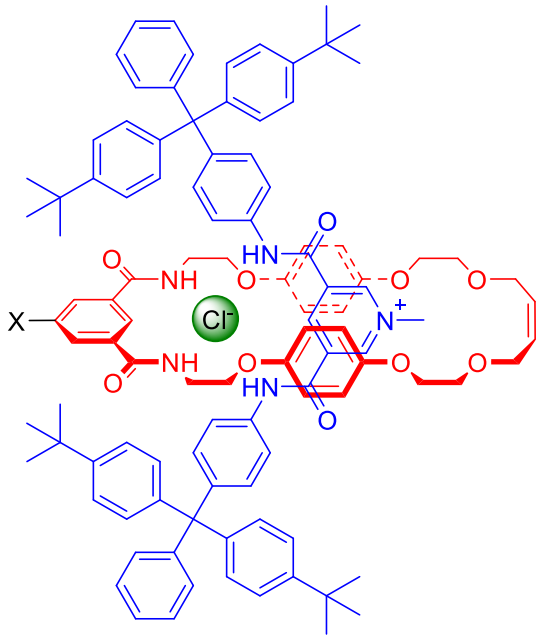

1.29 X = H
1.29a X = NO_2
1.29b X = I

Figure 1.30 - Beer's chloride sensing rotaxane with electron withdrawing groups 1.29 (X = -H), 1.29a (X = -NO_2), 1.29b (X = -I)

Table 1.2 - Association Constants of Receptor 1.29, 1.29a, 129b

Anion	K_a [M^{-1}]		
	1.29	**1.29a**	**1.29b**
Cl^-	1130	4500	4500
$H_2PO_4^-$	300	1500	1800
AcO^-	100	725	930

Sensors for fluoride have been investigated by Lin and Raju, who have reported a palladium templated rotaxane **1.34** for the sensing of fluoride anions.[62] Whilst it is stated that the receptor strongly binds fluoride anions (K_a = 2.65 x 10^4 M^{-1}) in d^6–DMSO, the binding constants of other anions that were tested were not alluded to. Although it is stated that fluoride was the only guest that caused rotaxane to give a spectroscopic response.

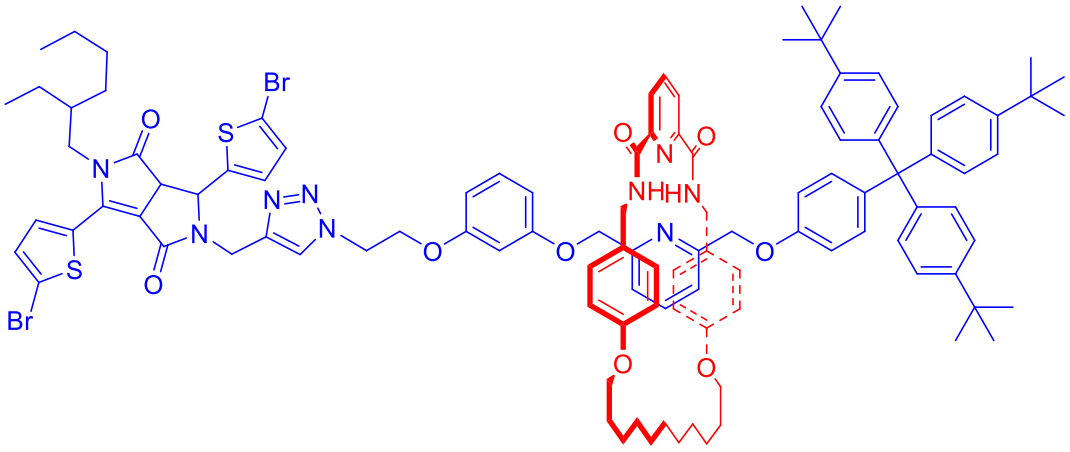

1.34

Figure 1.31 - Lin and Raju's fluoride sensing rotaxane 1.34

Beer and co-workers have also developed fluoride anion sensing rotaxanes **1.31-Ln^{3+}**and **1.31-Eu^{3+}**, which include a lanthanide metal cation within the macrocycle, as a reporting group.[50,63] Lanthanide complexes are known for their luminescent properties and are widely used for imaging, sensing and assays.[64–66] Rotaxane **1.31-Eu^{3+}** was found to have a strong preference for fluoride anions (K_a = 2.42 x 10^5 M^{-1}, 99:1 acetone:H_2O). Nitrate (K_a = 4.33 x 10^3 M^{-1}) and acetate (K_a = 2.42 x 10^4 M^{-1}) were found to bind more weakly and chloride anions were not detected to be bound to rotaxane **1.31-Eu^{3+}** at all. It was postulated that fluoride anion was bound particularly strongly due to the anion being capable of directly complexing with the metal centre and organic components of rotaxane **1.31-Eu^{3+}**, whilst other anions are thought to be complexing to the organic components.

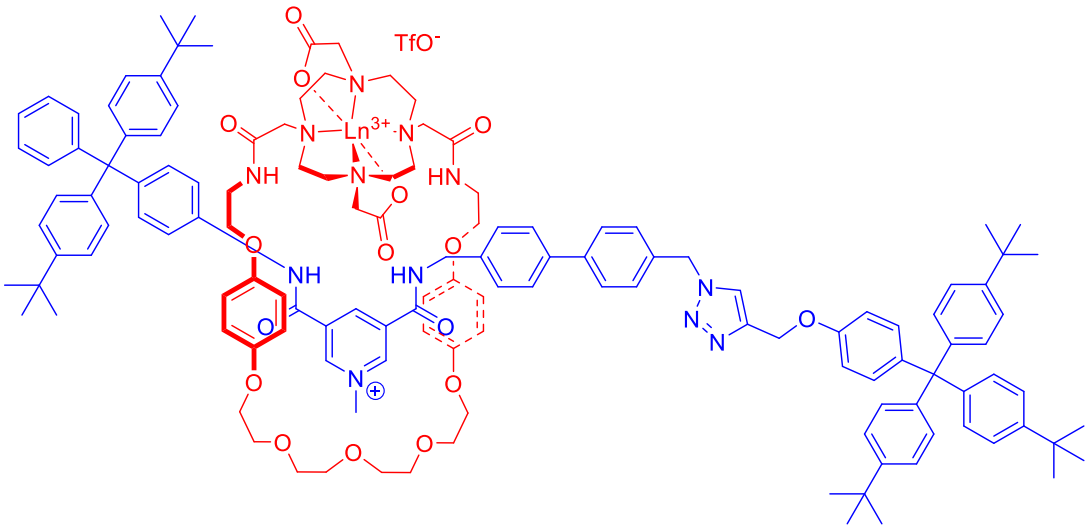

Figure 1.32 - Beer and co-workers fluoride sensing rotaxane 1.31-La^{3+} and 1.31-Eu^{3+}.

Rotaxanes have also been reported as hosts for anions with more complicated geometries, such as Beer and co-workers' [3] rotaxanes **1.35** and **1.36**, for the selective binding of sulfate anions.[67,68] Rotaxanes **1.35** and **1.36** consist of two isophthalamide macrocycles threaded upon axles, containing ferrocene and naphthalene reporter groups.

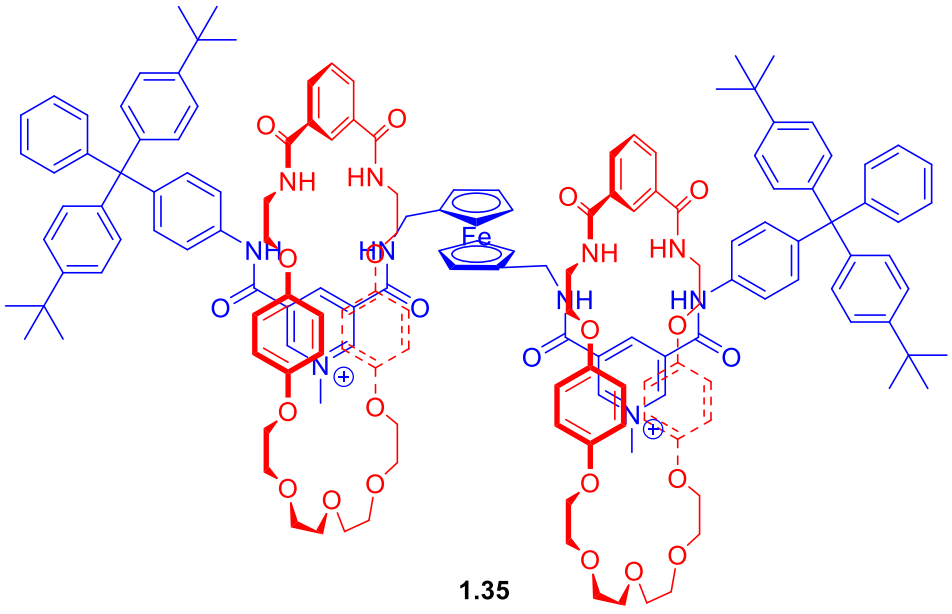

1.35

Figure 1.33 - Sulfate sensing ferrocene [3] rotaxane 1.35

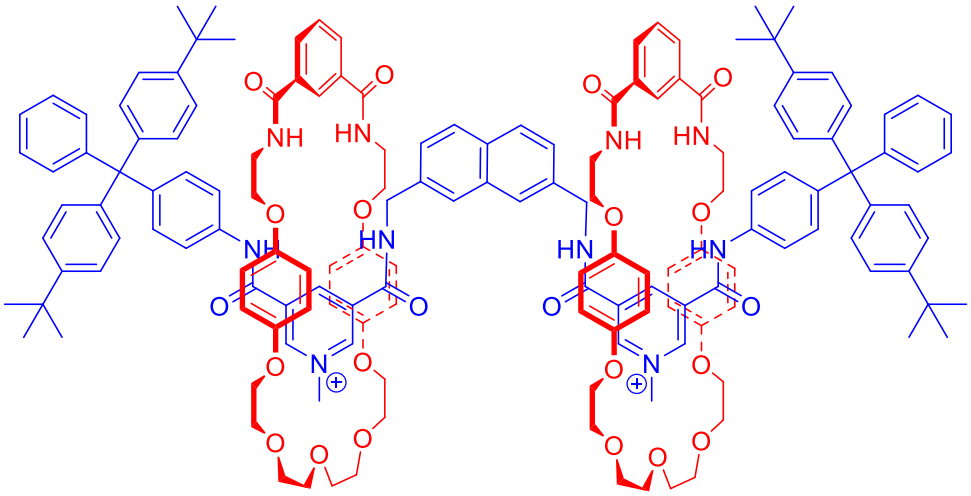

1.36

Figure 1.34 - Sulfate sensing naphthalene [3] rotaxane 1.36

Ferrocene containing rotaxane **1.35** displayed a high binding constant for sulfate anions (K_1 >10^4 M^{-1}) by ^{1}H NMR titration in a highly competitive solvent system (45:45:10 $CDCl_3$:CD_3OD:D_2O). The binding event from the sulfate is unusual in that the rotaxane is thought to fold back on top of itself, to create a sandwich for the sulphate anion to sit in Rotaxane **1.35** also demonstrated a lower binding affinity chloride anions (K_1 = 1.7 x 10^3 M^{-1}, K_2 = 2.0 x 10^2 M^{-1}), the second chloride is believed to be bound weaker due to electrostatic repulsion from the first chloride anion.

A similar rotaxane was also developed containing a UV-Vis active naphthalene group instead of a ferrocene group. Rotaxane **1.36** reported similar binding strengths for both sulfate anions (K_1 >10^4 M^{-1}) and chloride anions (K_1 = 3.0 x 10^3 M^{-1}, K_2 = 1.2 x 10^2 M^{-1}) when compared to **1.35**, albeit in 1:1 $CDCl_3$:CD_3OD, a less competitive solvent mixture. Unusually for a chloride templated rotaxane, rotaxane **1.36** demonstrated a preference for bromide anions (K_1 = 3.7 x 10^3 M^{-1}, K_2 = 2.7 x 10^2 M^{-1}) over chloride anions.

Beer and Marti-Centelles have also studied rotaxane **1.37** that can preferentially bind nitrate over other oxo anions as determined by ^{1}H NMR titrations.[69] Nitrate was found to bind more strongly than all other oxo-anions, but not as strongly as bromide or iodide. It was postulated that this is due to the large gap between the axle hydrogen bond donating triazolium groups,

providing a cavity that was the ideal size and geometry for a nitrate anion, whilst larger oxoanions would fail to fit within the cavity, or have an incorrect geometry.

Table 1.3 – Binding constants of rotaxane 1.37 with various anions

Anion	K [M^{-1}] (45:45:10 $CDCl_3$:CD_3OD:D_2O)
Cl^-	1070
Br^-	1360
I^-	820
NO_3^-	1010
HPO_4^-	-
AcO^-	-
HCO_3^-	110

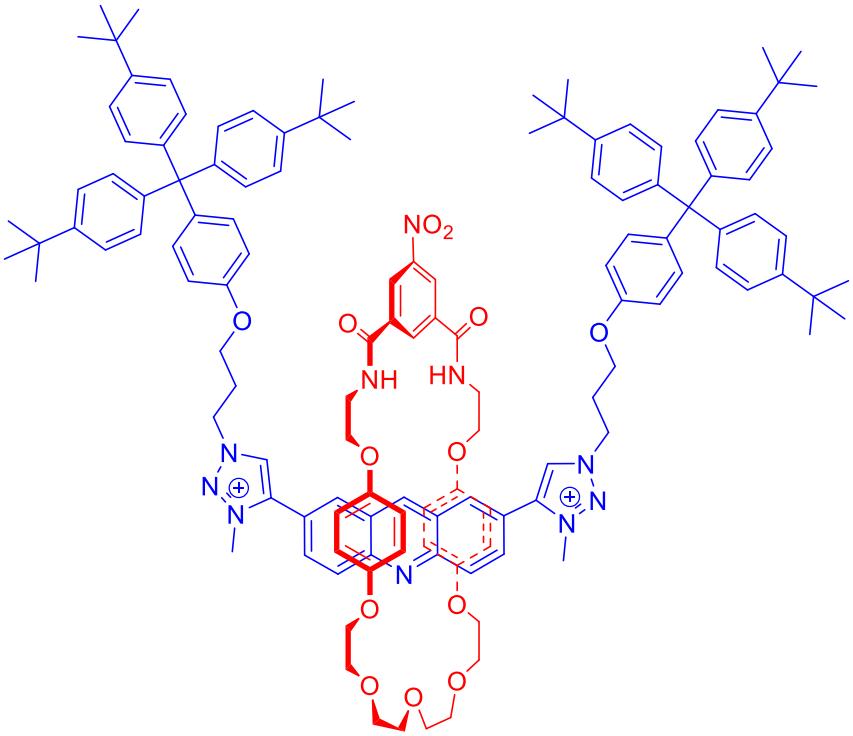

1.37

Figure 1.35 -Beer and Marti-Centelles nitrate sensing rotaxane 1.37

A more recent example of chloride sensing rotaxane is Goldup and co-workers' sensing rotaxane **1.38**, containing a naphthylamide UV-Vis reporter unit.[70] This rotaxane demonstrated a selectivity towards chloride (Table **1.4**) over other anions. The authors believe that the selectivity towards chloride anions is due to the crowded environment around the urea group, which is of sufficient size for a chloride anion but too small for any larger anion.

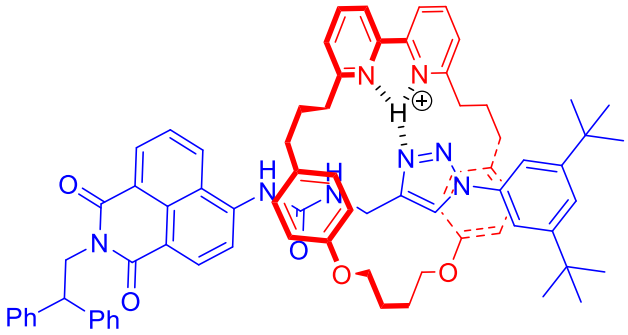

Figure 1.36 - Goldup and co-workers chloride sensing rotaxane 1.38

Table 1.4 – Binding constants of rotaxane 1.38 with TBA salts of various anions determined by ^{1}H NMR titrations (1:1 $CDCl_3$:CD_3CN)

Anion	Binding Constants (mol^{-1} dm^3) Rotaxane **1.38-HBF_4**
Cl^-	>10,000 / 28,000*
Br^-	4700
I^-	600
HSO_4^-	2300
TsO^-	1500
MsO^-	2600

* determined by UV-Vis spectroscopy

1.6 Chiral Rotaxanes and Chiral Rotaxanes as Hosts for Chiral Molecules

Rotaxanes may be chiral by inclusion of a classical chiral element (such as a chiral centre, axis or plane) or by the use of directional components, so-called mechanical chirality.

Planar mechanical chirality in rotaxanes is where the axle and macrocycle are rotationally asymmetric, but do not necessarily have any chiral components themselves. To visualise this the axle component can be considered as an arrow (Fig. **1.37,** grey arrow) and the macrocycle as a series of arrows, spinning around in a circle (Fig. **1.37**, multicoloured arrow). When the axle passes through the macrocycle it defines the direction of the clockwise or anti-clockwise 'spin' of the macrocycle, resulting in a pair of enantiomers.

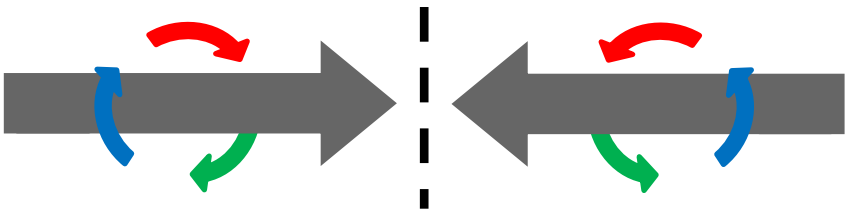

Figure 1.37 – A representation of a mechanically chiral rotaxane

Rotaxanes synthesised with chiral pool materials have been studied be both Takata and Leigh groups and used as catalysts for asymmetric synthesis.[71,72] Takata and co-workers' rotaxanes ***(R)*-1.39** and ***(R)*-1.40**, include an enantiopure chiral binapthyl group built either into the macrocycle in ***(R)*-1.39** and axle in ***(R)*-1.40**.[71] Rotaxanes ***(R)*-1.39** and ***(R)*-1.40** are formed by cation templated synthesis high yields of 71% and 75% respectively.

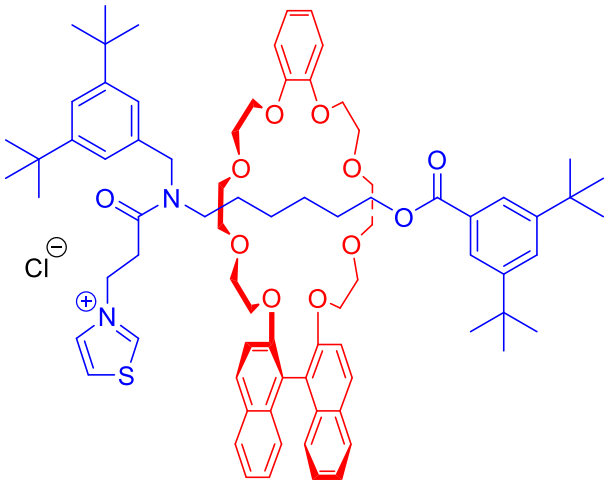

1.39

Figure 1.38 - Takata and co-workers binaphthyl rotaxane *(R)*- 1.39

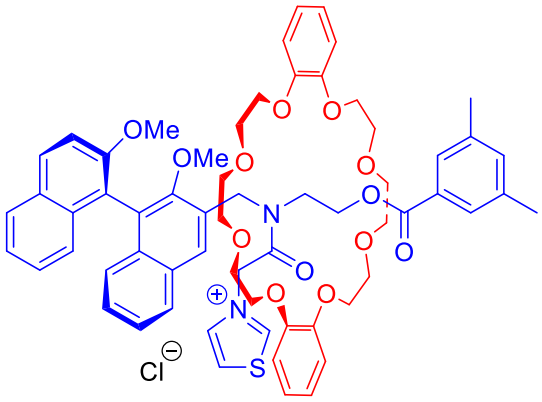

1.40

Figure 1.39 - Takata and co-workers binaphthyl rotaxane *(R)*-1.40

Rotaxanes ***(R)*-1.39** and ***(R)*-1.39** were then used to catalyse a benzoin condensation reaction, that would result in a racemate without an enantioselective catalyst (Fig. **1.40**). Addition of catalytic amounts rotaxane ***(R)*-1.39** resulted in an enantiomeric excess of 32 % ee for the *R* enantiomer (when R = H) and 25 % ee for the *S* enantiomer (R = Me), when rotaxane ***(R)*-1.39** is used instead.

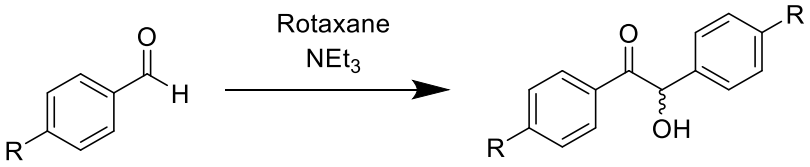

Figure 1.40 – Benzoin condensation reaction catalysed by *(R)*-1.39 and *(R)*-1.40 (R = H, Me)

Leigh and co-workers' catalytic rotaxane ***(R)*-1.41** possess chirality through incorporating a D-phenylalanine into the axle. Rotaxane ***(R)*-1.41** was formed via hydrogen bond templated synthesis, using a CuAAC "copper click" reaction to stopper the rotaxane in a yield of 35%.

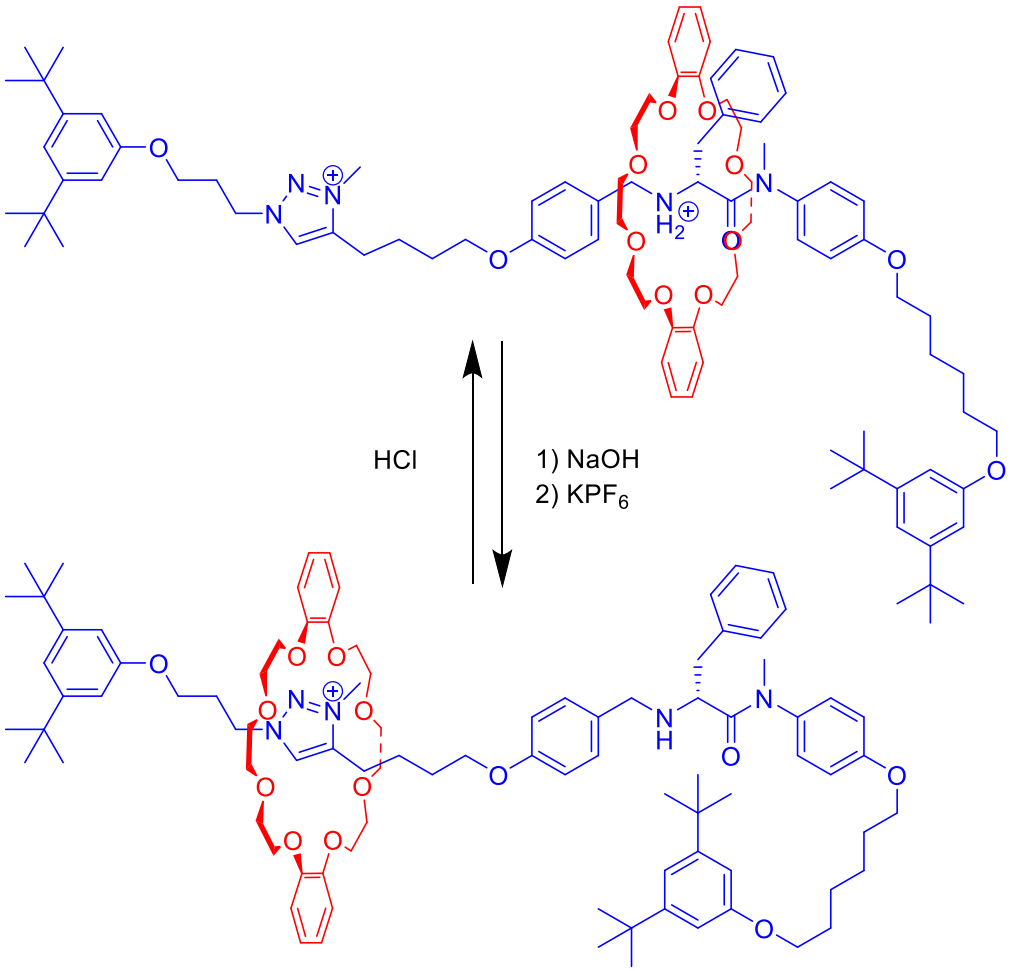

Figure 1.41 – Leigh and co-workers chiral rotaxane *(R)*-1.41

Rotaxane ***(R)*-1.41** was then used as switchable catalyst for the amine catalysed Michael addition of crotonaldehyde derivatives to 1,3-diphenyl-1,3-propanedione (Fig. **1.42**). Under acidic conditions the rotaxane was catalytically inactive, as the macrocycle resided over the catalytic

amine centre. When deprotonated, the amine was exposed and the rotaxane could catalyse the reaction, in enantiomeric ratios of up to 92:8 (*R*:*S*).

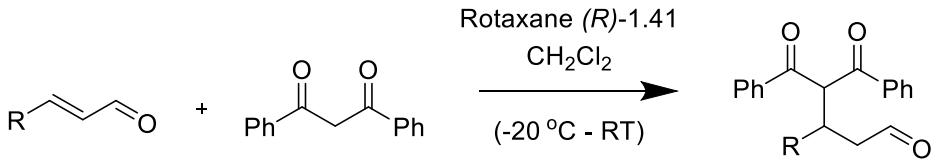

Figure 1.42 - Michael addition catalysed by rotaxane *(R)*-1.41 (R = Me, Et, ^{n}Pr, Ph)

A more recent development is hydrogen bond templated catalytic rotaxane **(*S*)-1.42** (Fig. **1.18**), synthesised by the Leigh group.[59] Rotaxane **(*S*)-1.42** uses a less conventional form of chirality called mechanical point chirality. The chirality in this rotaxane derives from the macrocycle being trapped on one end of the symmetric axle, by the bulky tolyl group causing the axle to become asymmetric and creating a chiral centre (marked with a *, Fig. **1.43**).

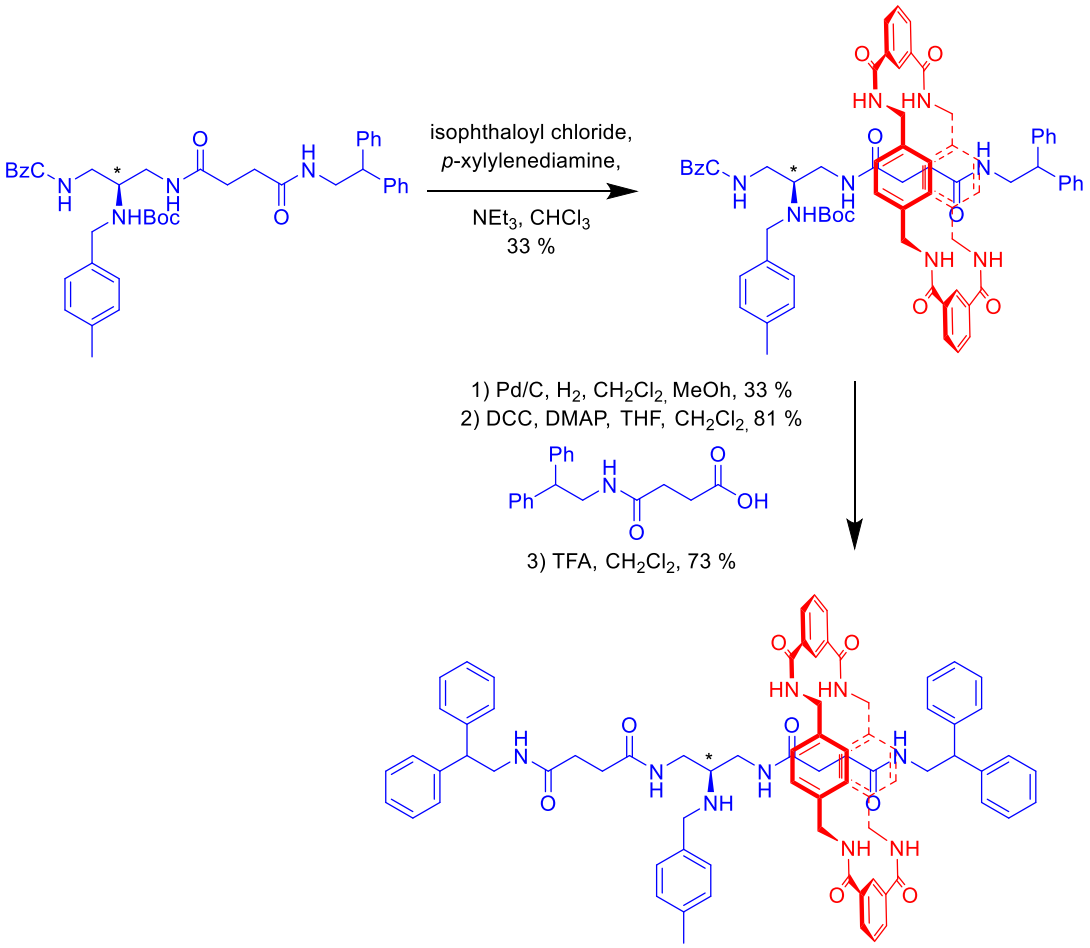

Figure 1.43 – Synthesis of Leigh and co-workers point chiral catalytic rotaxane *(S)*-1.42

Rotaxane **(*S*)-1.42** was then used to catalyse the α-amination of various aldehydes with dibenzylazodicarboxylate (Fig. **1.19**), in enantiomeric ratios of up to 71:29 (*S*:*R*). No enantioselctivity was detected when the achiral axle of rotaxane **(*S*)-1.42** was used.

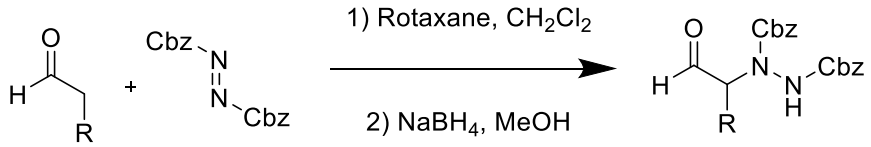

Figure 1.44 – α-amination of aldehydes catalysed by rotaxane (*S*)-1.42 (R = Me, Et, ^{i}Pr)

Whilst incorporation of an enantiopure material into a rotaxane is typically the preferred method of synthesising chiral rotaxanes, as with careful synthesis a single enantiomer of the target rotaxane can be prepared. An alternative approach is to make the rotaxane mechanically chiral, where the chirality comes from the relative directions of the interlocked components.

However, this has the issue that without any stereocontrol the rotaxane will end up as a racemate. There are many examples in the literature of a pair of mechanically chiral rotaxanes having been synthesised as a racemate and then separated by chiral HPLC.[73–76] However, until recently there has been no way of separating the enantiomers on a synthetically useful scale.

Bordoli and Goldup have looked to solve this problem by synthesising diastereotopic mechanically chiral rotaxanes, that contain both a mechanical chiral element and a more traditional point chiral element.[77] A mixture of diastereomers of mechanically chiral rotaxanes **(D,*R*$_m$)-1.43** and ***(*D,*S*$_m$)*-1.43** (Fig. **1.45**), were prepared using an active metal templated synthesis, with a chiral sugar derivative as the point chiral element. The diastereomers were then separating out using flash chromatography, before the chiral sugar was replaced with an achiral amine component, yielding enantiopure samples of **(*R*$_m$)-1.44** and ***(S*$_m$)*-1.44** deriving their chirality solely from the mechanical chirality.

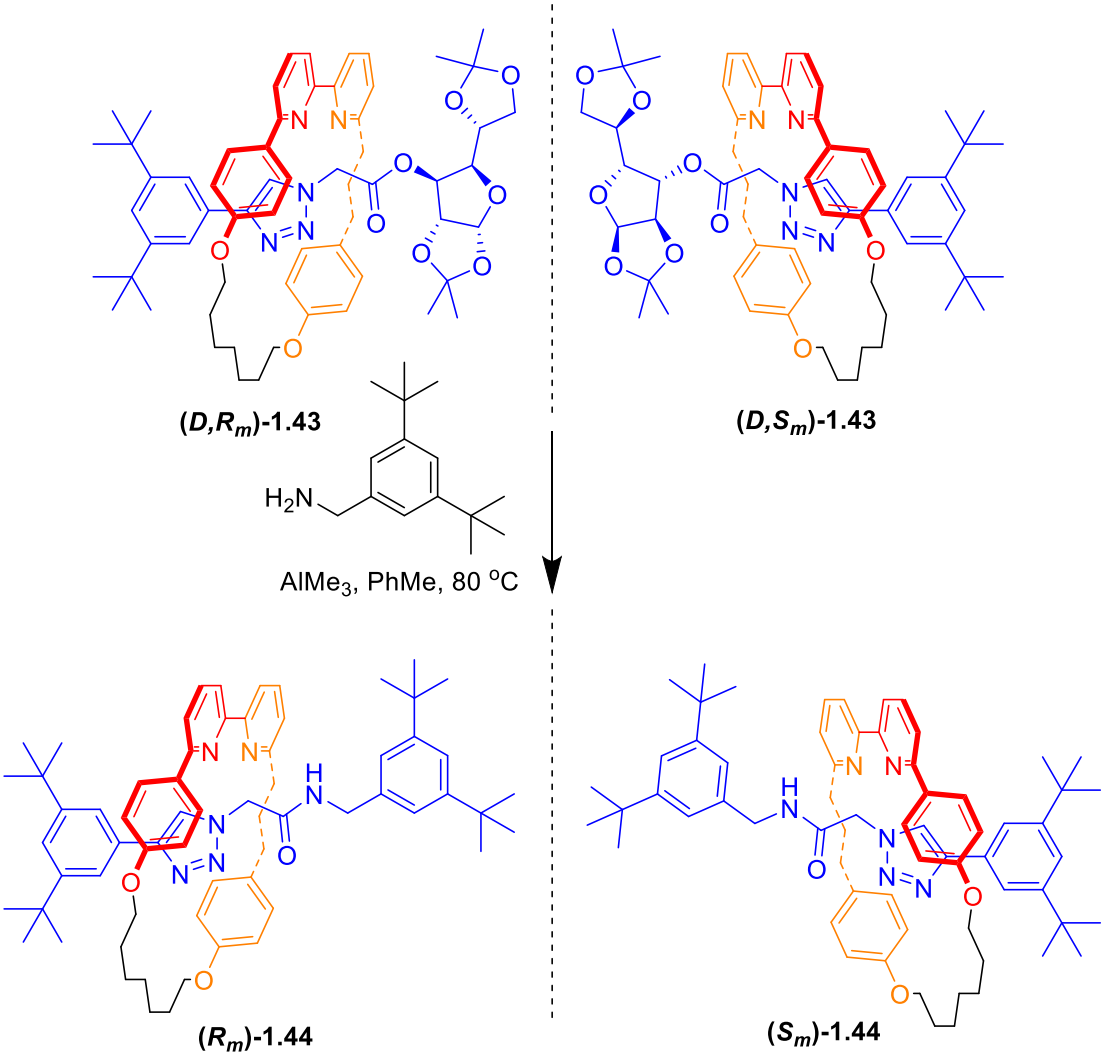

Figure 1.45 – Goldups and Bordoli's mechanically chiral rotaxanes *(*D,R_m*)*-1.43 and *(R_m)*-1.44 (left) and *(*D,S_m*)*-1.43, *(S_m)*-1.44 (right)

As this thesis was being prepared for submission, Goldup and co-workers published the diastereoselective synthesis of mechanically chiral rotaxanes, diastereo ratios of up to 98:2 (*S*,S_{mp}:*S*,R_{mp}) were achieved with rotaxane **(*S*,S_{mp})-1.45**.[78] The rotaxanes in this study were synthesised by placement of traditional enantiopure chiral point groups on the axle component. When the rotaxane is formed the point chiral group has a diastereotopic interaction with the macrocyclic component, resulting in preferential formation of one diastereomer over another. Rotaxane **(*S*,S_{mp})-1.45** was then turned into purely mechanically chiral rotaxane **(S_{mp})-1.46** (Fig. **1.46**), by destruction of the point chiral group. This was achieved by using LiHDMS to

deprotonate the chiral centre, which is alpha to a carbonyl group and then add a second benzyl group, resulting in a purely mechanically chiral rotaxane **(*S*$_{mp}$)-1.46**.

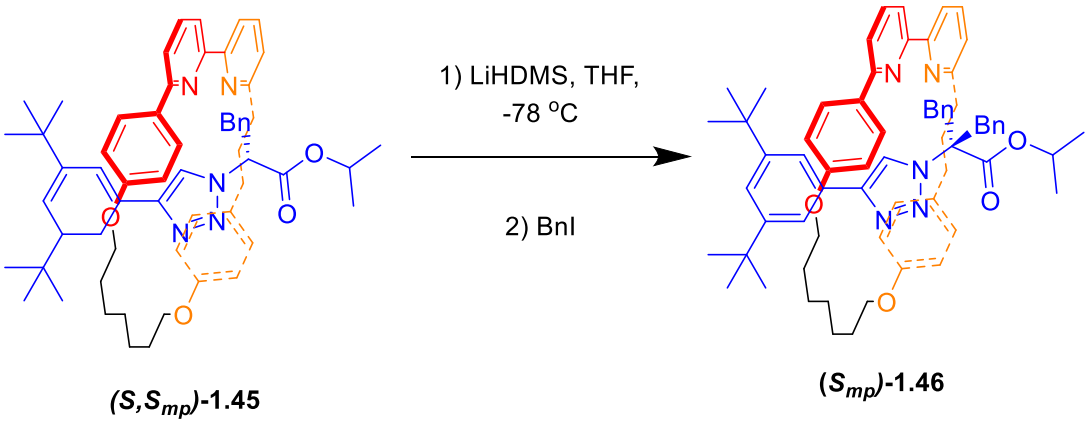

Figure 1.46 – Goldup and co-workers' diastereotopic rotaxane (*S*,*S*)-1.45 and transformation into enantiopure mechanically chiral rotaxane (*S*)-1.46

Mechanically chiral rotaxanes have also been used to bind neutral chiral guest species. Kameta and co-workers' have developed mechanically chiral rotaxane **1.47**, which may display enatioselctivity towards the D- and L-phenylalaninol.[79] However, this cannot be confirmed as the authors were unable to separate the enantiomers of rotaxane **1.47**. When the authors titrated the racemate of rotaxane **1.47** in $CDCl_3$, upon addition of either D- and L-phenylalaninol they observed that only a proportion of the signals in the ^{1}H NMR of rotaxane **1.47** would shift, indicating binding of the host. The remaining proportion of the signals would not change despite addition of excess host species, this suggests that rotaxane **1.47** may demonstrate enantioselective behaviour.

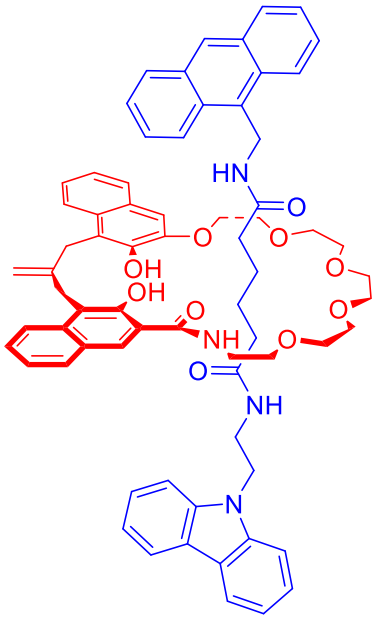

Figure 1.47 - Kameta and co-workers mechanically chiral rotaxane (*S*)-1.47.

Hirose and co-workers have reported the isolation of a single enantiomer of mechanically chiral rotaxane **1.48** and investigated its' enantioselective behaviour towards chiral ammonium salts.[80] Rotaxane **1.48** was prepared by forming a point chiral pre-rotaxane as a racemate, then separating the enantiomers by preparative chiral HPLC. A single enantiomer of the pre-rotaxane was then subject to aminolysis to form rotaxane **1.48** in 84% yield (Fig. **148**), the exact stereochemistry of rotaxane **1.48** could not be determined. The enatioselctivity of rotaxane **1.48** was determined by ^{1}H NMR titration with (*R)* and (*S)* 2-phenylglycinol in $CDCL_3$, where it demonstrated a slight enatioselctivity for (*R)*-phenylglycinol (K_R/K_S = 1.48). However, rotaxane **1.48** shows a very weak affinity to both guest species (K_R = 125 mol^{-1} dm^{-3} and K_S = 84.7 mol^{-1} dm^{-3}), even in non-competitive $CDCl_3$.

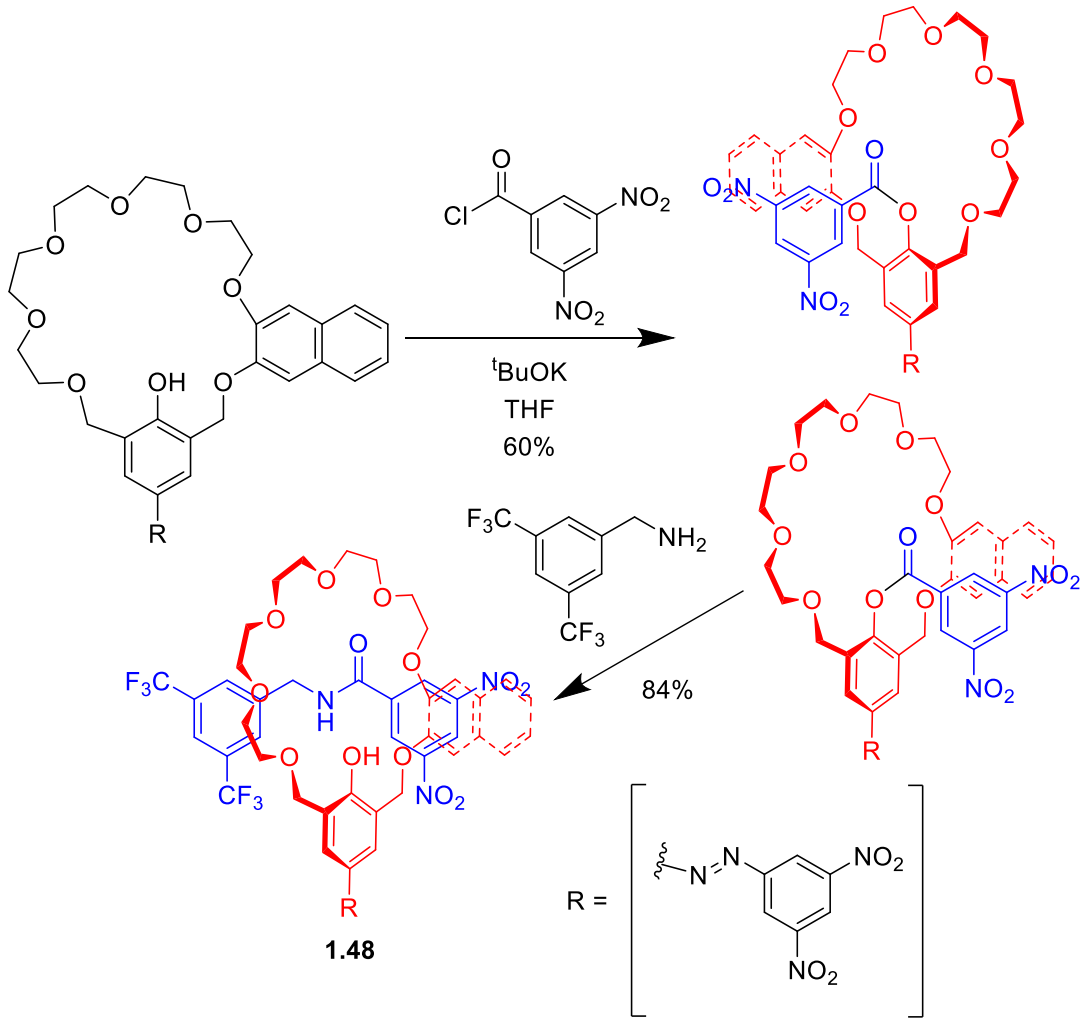

Figure 1.48 – Syntheses of Hirose and co-workers mechanically chiral rotaxane 1.48

1.7 Conclusion

A variety of chiral acyclic and macrocyclic molecules have been used as enantioselective receptors for chiral anion recognition. The enantioselectivity of these receptors is not particularly high, indicating that the field is an obvious target for further research.

Interlocked molecules, including rotaxanes, may be prepared in high yield through template synthesis. Examples of rotaxanes have been used as selective receptors for achiral anions. Meanwhile chiral rotaxanes have also been prepared, and on occasion used in asymmetric synthesis. It was therefore proposed at the outset of this work that well-designed rotaxanes could be prepared that act as enantioselective receptors for anions. Work towards achieving this aim forms the focus of this thesis.

1.8 References

[1] B. Singh Sekhon, *J. Mod. Med. Chem.*, 2013, **1**, 10-36.

[2] S. W. Smith, *Toxicol. Sci.*, 2009, **110**, 4–30.

[3] L. H. Easson and E. Stedman, *Biochem. J.*, 1933, **27**, 1257–66.

[4] V. A. Davankov, *Chirality*, 1997, **9**, 99–102.

[5] E. B. Kyba, K. Koga, L. R. Sousa, M. G. Siegel and D. J. Cram, *J. Am. Chem. Soc.*, 1973, **95**, 2692–2693.

[6] S. C. Peacock, L. A. Domeier, F. C. A. Gaeta, R. C. Helgeson, J. M. Timko and D. J. Cram, *J. Am. Chem. Soc.*, 1978, **100**, 8190–8202.

[7] P. D. Beer and P. A. Gale, *Angew. Chem. Int. Ed.*, 2001, **40**, 486–516.

[8] I. Alfonso, F. Rebolledo and V. Gotor, *Chem. - A Eur. J.*, 2000, **6**, 3331–3338.

[9] I. Alfonso, B. Dietrich, F. Rebolledo, V. Gotor and J.-M. Lehn, *Helv. Chim. Acta*, 2001, **84**, 280–295.

[10] A. González-Álvarez, I. Alfonso, P. Díaz, E. García-España and V. Gotor, *Chem. Commun.*, 2006, 1227-1229.

[11] S. Rossi, G. M. Kyne, D. L. Turner, N. J. Wells and J. D. Kilburn, *Angew. Chemie Int. Ed.*, 2002, **41**, 4233–4236.

[12] S. Bartoli, T. Mahmood, A. Malik, S. Dixon and J. D. Kilburn, *Org. Biomol. Chem.*, 2008, **6**, 2340-2345.

[13] H. Miyaji, S.-J. Hong, S.-D. Jeong, D.-W. Yoon, H.-K. Na, J. Hong, S. Ham, J. L. Sessler and C.-H. Lee, *Angew. Chem. Int. Ed.*, 2007, **46**, 2508–2511.

[14] M. Mačková, J. Mikšátko, J. Budka, V. Eigner, P. Cuřínová and P. Lhoták, *New J. Chem.*, 2015, **39**, 1382–1389.

[15] J. Sokolov and V. Šindelář, *Chem. Eur. J.*, 2018, **24**, 15482-15485.

[16] F. Ulatowski and J. Jurczak, *Tetrahedron: Asymmetry*, 2014, **25**, 962–968.

[17] P. Hamankiewicz, J. M. Granda and J. Jurczak, *Tetrahedron Lett.*, 2013, **54**, 5608–5611.

[18] J. M. Granda and J. Jurczak, *Org. Lett.*, 2013, **15**, 4730–4733.

[19] J. M. Granda and J. Jurczak, *Chem Eur. J.*, 2015, **21**, 16585–16592.

[20] D. Lichosyt, S. Wasiłek and J. Jurczak, *J. Org. Chem.*, 2016, **81**, 7342–7348.

[21] P. Laurent, H. Miyaji, S.R. Collinson, I. Prokeš, C. J. Moodyand J. H. R. Tucker and A. M. Z. Slawin, *Org. Lett*, 2002, **4**, 4037-4040.

[22] Y. Willener, K. M. Joly, C. J. Moody and J. H. R. Tucker, *J. Org. Chem.*, 2008, **73**, 1225-1233.

[23] J. Y. C. Lim, I. Marques, V. Félix and P. D. Beer, *Chem. Commun.*, 2018, **54**, 10851–10854.

[24] L. J. Lawless, A. G. Blackburn, A. J. Ayling, M. N. Pérez-Payán and A. P. Davis, *J. Chem. Soc. Perkin Trans. 1*, 2001, 1329–1341.

[25] B. Baragaña, A. G. Blackburn, P. Breccia, A. P. Davis, J. de Mendoza, J. M. Padrón-Carrillo, P. Prados, J. Riedner and J. G. de Vries, *Chem. Eur. J.*, 2002, **8**, 2931-2936.

[26] V. Nandipati, K. Akinapelli, L. Koya and S. D. Starnes, *Tetrahedron Lett.*, 2014, **55**, 985–991.

[27] J. L. Sessler, A. Andrievsky, V. Král and V. Lynch, *J. Am. Chem. Soc.*, 1997, **119**, 9385-9392.

[28] J. A. Wisner, P. D. Beer, M. G. B. Drew and M. R. Sambrook, *J. Am. Chem. Soc,* 2002, **124**, 12469-12476.
[29] I. T. Harrison and S. Harrison, *J. Am. Chem. Soc.*, 1967, **89**, 5723–5724.
[30] M. Asakawa, P. R. Ashton, R. Ballardini, V. Balzani, M. Bělohradský, M.T, Gandolfi, O. Kocian, L. Prodi, F. M, Raymo, J. F. Stoddart and M. Venturi, *J. Am. Chem. Soc.*, 1997, **119**, 302-310.
[31] P. R. Ashton, M. R. Johnston, J. F. Stoddart, M. S. Tolley and J. W. Wheeler, *J. Chem. Soc. Chem. Commun.*, 1992, 1128-1131.
[32] R. Isnin and A. E. Kaifer, *J. Am. Chem. Soc.*, 1991, **113**, 8188–8190.
[33] G. M. Hübner, J. Gläser, C. Seel and F. Vögtle, *Angew. Chem. Int. Ed.*, 1999, **38**, 383–386.
[34] J. P. Sauvage, *Acc. Chem. Res.*, 1990, **23**, 319–327.
[35] C. Wu, P. R. Lecavalier, Y. X. Shen and H. W. Gibson, *Chem. Mater.*, 1991, **3**, 569–572.
[36] J.-C. Chambron, V. Heitz and J.-P. Sauvage, *J. Chem. Soc. Chem. Commun.*, 1992, 1131-1133.
[37] C. Hamann, J.-M. Kern and J.-P. Sauvage, *Dalt. Trans.*, 2003, 3770-3775.
[38] Y. Furusho, T. Matsuyama, T. Takata, T. Moriuchi and T. Hirao, *Tet. Lett.*, 2004, **45**, 9593–9597.
[39] A.-M. Fuller, D. A. Leigh, P. J. Lusby, I. D. H. Oswald, S. Parsons and D. B. Walker, *Angew. Chem. Int. Ed.*, 2004, **43**, 3914–3918.
[40] J. D. Crowley, S. M. Goldup, A.-L. Lee, D. A. Leigh and R. T. McBurney, *Chem. Soc. Rev.*, 2009, **38**, 1530-1541.
[41] J. E. M. Lewis, P. D. Beer, S. J. Loeb and S. M. Goldup, *Chem. Soc. Rev.*, 2017, **46**, 2577–2591.
[42] V. Aucagne, K. D. Hänni, D. A. Leigh, P. J. Lusby and D. B. Walker, *J. Am. Chem. Soc.*, 2006, **128**, 2186-2187.
[43] J. Berná, J. D. Crowley, S. M. Goldup, K. D. Hänni, A.-L. Lee and D. A. Leigh, *Angew. Chem. Int. Ed.*, 2007, **46**, 5709–5713.
[44] P. Ghosh, O. Mermagen and C. A. Schalley, *Chem. Commun.*, 2002, 2628–2629.
[45] C. A. Schalley, G. Silva, C. F. Nising and P. Linnartz, *Helv. Chim. Acta*, 2002, **85**, 1578–1596.
[46] G. T. Spence and P. D. Beer, *Acc. Chem. Res.*, 2013, **46**, 571–586.
[47] J. A. Wisner, P. D. Beer, M. G. B. Drew and M. R. Sambrook, *J. Am. Chem. Soc.*, 2002, **124**, 12469-12476.
[48] L. M. Hancock and P. D. Beer, *Chem. Eur. J.*, 2009, **15**, 42–44.
[49] L. M. Hancock, L. C. Gilday, S. Carvalho, P. J. Costa, V. Félix, C. J. Serpell, N. L. Kilah and P. D. Beer, *Chem. Eur. J.*, 2010, **16**, 13082–13094.
[50] M. J. Langton, O. A. Blackburn, T. Lang, S. Faulkner, P. D. Beer, M. J. Langton, O. A. Blackburn, T. Lang, S. Faulkner and P. D. Beer, *Angew. Chem. Int. Ed*, 2014, **53**, 11463–11466.
[51] B. Huang, S. M. Santos, V. Felix and P. D. Beer, *Chem. Commun.*, 2008, 4610-4612.
[52] M. J. Langton, L. C. Duckworth and P. D. Beer, *Chem. Commun.*, 2013, **49**, 8608-8610.
[53] A. Makarem, R. Berg, F. Rominger and B. F. Straub, *Angew. Chem. Int. Ed.*, 2015, **54**, 7431–7435.
[54] M.-V. Martínez-Díaz, N. Spencer and J. F. Stoddart, *Angew. Chem. Int. Ed. English*, 1997, **36**, 1904–1907.

[55] F. Coutrot and E. Busseron, *Chem. Eur. J.*, 2008, **14**, 4784–4787.
[56] D. A. Leigh and A. R. Thomson, *Tetrahedron*, 2008, **64**, 8411–8416.
[57] C. M. Álvarez, H. Barbero and D. Miguel, *European J. Org. Chem.*, 2015, **2015**, 6631–6640.
[58] D. A. Leigh, A. Murphy, J. P. Smart and A. M. Z. Slawin, *Angew. Chem. Int. Ed. English*, 1997, **36**, 728–732.
[59] Y. Cakmak, S. Erbas-Cakmak and D. A. Leigh, *J. Am. Chem. Soc.*, 2016, **138**, 1749–1751.
[60] C. M. Keaveney and D. A. Leigh, *Angew. Chem. Int. Ed.*, 2004, **43**, 1222–1224.
[61] M. R. Sambrook, P. D. Beer, M. D. Lankshear, R. F. Ludlow and J. A. Wisner, *Org. Biomol. Chem.*, 2006, **4**, 1529-1538.
[62] M. V. R. Raju and H.-C. Lin, *Org. Lett.*, 2013, **15**, 1274–1277.
[63] F. Zapata, O. A. Blackburn, M. J. Langton, S. Faulkner and P. D. Beer, *Chem. Commun.*, 2013, **49**, 8157.
[64] C. Allain, P. D. Beer, S. Faulkner, M. W. Jones, A. M. Kenwright, N. L. Kilah, R. C. Knighton, T. J. Sørensen and M. Tropiano, *Chem. Sci*, 2013, **4**, 489.
[65] C. Allain and S. Faulkner, *Future Med. Chem.*, 2010, **2**, 339–350.
[66] S. Faulkner, L. S. Natrajan, W. S. Perry and D. Sykes, *Dalt. Trans.*, 2009, 3890-3899.
[67] N. H. Evans, C. J. Serpell and P. D. Beer, *Chem. Commun.*, 2011, **47**, 8775-8777.
[68] M. J. Langton and P. D. Beer, *Chem. Eur. J.*, 2012, **18**, 14406–14412.
[69] V. Martí-Centelles and P. D. Beer, *Chem. Eur. J.*, 2015, **21**, 9397–9404.
[70] M. Denis, L. Qin, P. Turner, K. A. Jolliffe and S. M. Goldup, *Angew. Chem. Int. Ed.*, 2018, **57**, 5315–5319.
[71] Y. Tachibana, N. Kihara and T. Takata, *J. Am. Chem. Soc.*, 2004, **126**, 3438-3439.
[72] V. Blanco, D. A. Leigh, V. Marcos, J. A. Morales-Serna and A. L. Nussbaumer, *J. Am. Chem. Soc.*, 2014, **136**, 4905–4908.
[73] C. A. Schalley, K. Beizai and F. Vögtle, *Acc. Chem. Res*., 2001, **34**, 465-576.
[74] R. Schmieder, G. Hübner, C. Seel and F. Vögtle, *Angew. Chem. Int. Ed.*, 1999, **38**, 3528–3530.
[75] P. E. Glen, J. A. T. O'Neill and A.-L. Lee, *Tetrahedron*, 2013, **69**, 57–68.
[76] C. Yamamoto, Y. Okamoto, T. Schmidt, R. Jäger and F. Vögtle, *J. Am. Chem. Soc.*, 1997, **119**, 10547-10548.
[77] R. J. Bordoli and S. M. Goldup, *J. Am. Chem. Soc.*, 2014, **136**, 4817–4820.
[78] M. Jinks, A. de Juan, M. Denis, C. Fletcher, M. Galli, E. Jamieson, F. Modicome, Z. Zhang and S. M. Goldup, *Angew. Chem. Int. Ed.*, 2018, **57**, 14806-14810.
[79] N. Kameta, Y. Nagawa, M. Karikomi and K. Hiratani, *Chem. Commun.*, 2006, 3714-3716.
[80] K. Hirose, M. Ukimi, S. Ueda, C. Onoda, R. Kano, K. Tsuda, Y. Hinohara, Y. Tobe, K. Hirose, M. Ukimi, S. Ueda, C. Onoda, R. Kano, K. Tsuda, Y. Hinohara and Y. Tobe, *Symmetry*, 2018, **10**, 20.

Chapter 2: Investigations into a Family of Enantiopure Chloride Templated Rotaxanes for the Enantioselective Binding of Chiral Anions

2.1. Introduction

2.1.1. Chapter Aims

Chloride templated rotaxanes have been widely developed by the Beer group for the binding and sensing of a variety of anions.[1–3] These systems generally favour halides over other anions, due to the geometrically complementary tetra-amide cavity created by the templating chloride anion. However, these rotaxanes have been shown to bind oxoanions in highly competitive solvent mixtures, with the oxoanions binding at the periphery of the rotaxane cavity. It is hypothesised that the introduction of enantiopure chiral groups in close proximity to the rotaxane cavity may result in a rotaxane that is capable of enantioselective recognition of chiral oxoanions.

The aim of this chapter is to synthesise and elucidate the enantioselective properties of a family of enantiopure chloride templated rotaxanes, with enantiopure amino acid moieties located on the axle, either side of the of tetra-amide cavity of the rotaxane. As such this will require meeting the following objectives:

1) Synthesis of an achiral prototype rotaxane **2.1** (Fig. **2.1**), containing the achiral amino acid glycine, to establish a practical synthetic route.
2) Use the synthetic route developed for prototype rotaxane **2.1** to synthesise a family of enantiopure chiral rotaxanes **2.1**, **2.2**, and **2.3** (Fig. **2.1**), containing L-alanine, L-valine and L-phenylalanine moieties respectively.
3) Exchange the templating chloride anion of glycine **2.1**, L-alanine **2.2**, L-valine **2.3**, and L-phenylalanine **2.4** rotaxanes for a non-coordinating hexafluorophosphate anion, to act as hosts for chiral guest species.
4) Elucidate the enantioselective behaviours of rotaxanes **2.2**, **2.3**, and **2.4** (Fig. **2.1**), using NMR titrations with the prepared enantiopure TBA salts.

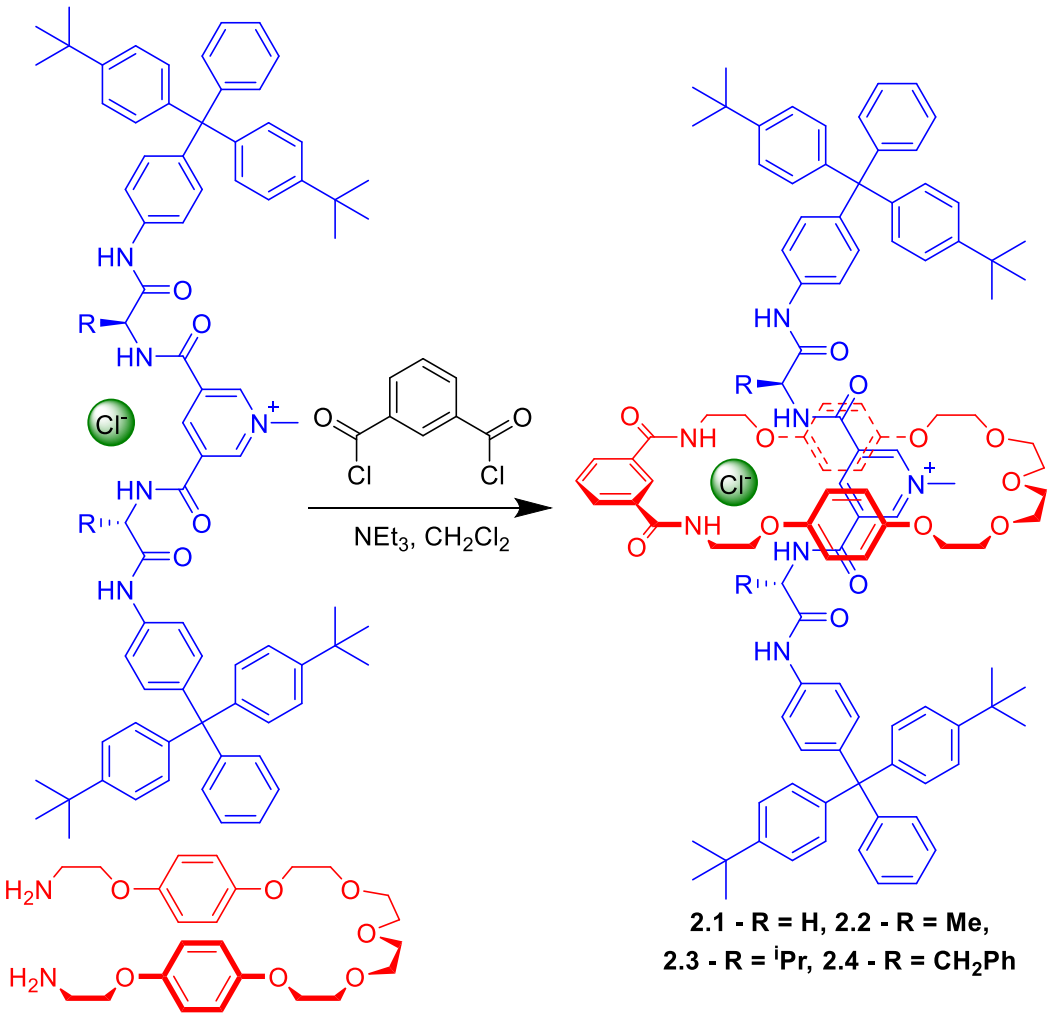

Figure 2.1 – Proposed synthesis of the chloride templated rotaxanes that will be developed in this chapter (2.1 – R = H, 2.2 – R = Me, 2.3 – R = ^{i}Pr, 2.4 – R= CH_2Ph)

2.1.2. Background

We and others propose that chiral catenanes and rotaxanes may prove to be excellent enantioselective hosts for chiral guests, due to the 3D structures of such interlocked molecules in comparison to simpler macrocyclic and acyclic hosts.[4–6] Several systems have been developed contemporaneously with the rotaxanes developed in this chapter. One such example is Niemeyer and co-workers calcium templated catenane **2.5** (Fig **2.2**).[7] The incorporation of two 1,1'-binaphthyl-phosophates into the catenane, provides for a source of chirality and a binding site for cationic guests once the templating calcium cation is removed.

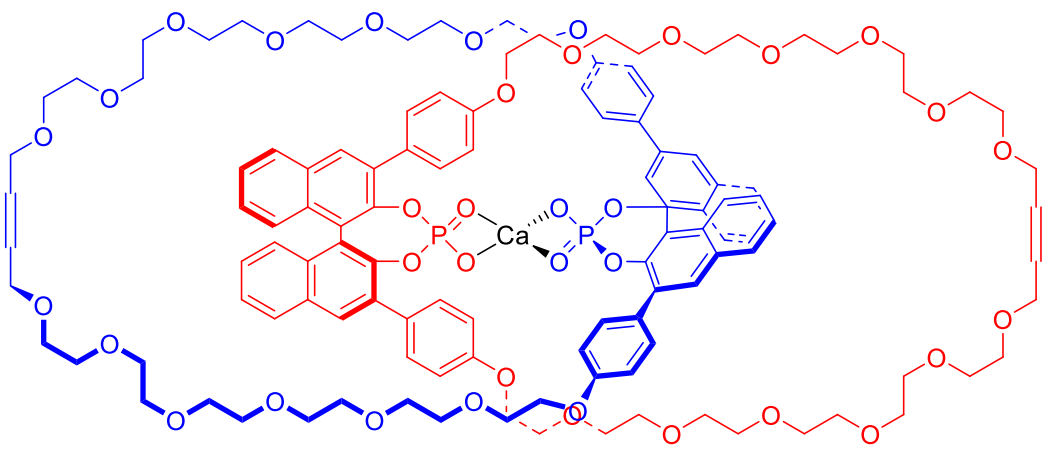

Figure 2.2 - Niemeyer and co-workers calcium templated chiral sensing catenane 2.5

Niemeyer and co-workers then compared the enantioselective properties of the TBA salts of the non-interlocked macrocycle of the catenane as the mono-anion and the catenane as a di-anion by ^{1}H NMR titration (D_6-DMSO, Table **2.1**).The titrations show that whilst neither the catenane (K_{fav}/K_{disfav} = 1.4-1.6) and the non-interlocked macrocycle (K_{fav}/K_{disfav} 1.0-1.3) have particularly high enantioselectivities, the interlocked catenane has higher enantioselectivity than the non-interlocked macrocycle.

Table 2.1 –Binding constants and enantioselectivities of catenane 2.5 versus non-interlocked macrocycle (298 K, D_6-DMSO)

	Macrocycle		Catenane **2.5**	
Binding mode (host:guest)	2:1		1:1	
Diamine (di-hydrochloride salt)	K_a [mol^{-1} dm^3]	K_{fav}/K_{disfav}	K_a [mol^{-1} dm^3]	K_{fav}/K_{disfav}
L-Lys-OMe	630 ± 20	1.1	4100 ± 610	1.4
D-Lys-OMe	700 ± 30		5700 ± 730	
L-Arg-OMe	570 ± 25	1.3	5550 ± 320	1.5
D-Arg-OMe	770 ± 35		8200 ± 610	
S,S-1,2-diaminocyclohexane	870 ± 170	1.0	15800 ± 2900	1.6
R,R-1,2-diaminocyclohexane	840 ± 100		10050 ± 1300	

In a detailed study, Beer and co-workers reported upon a range of chiral [2]rotaxanes for enantioselective anion recognition (Fig **2.3**).[8] Amongst these rotaxanes **2.6** and **2.7** were

prepared in 48% and 30% yields respectively by copper (I) active templated synthesis. Both rotaxanes **2.6** and **2.7** incorporated *(S)*-BINOL groups into the macrocycle to act as the component that allows for enantioselective discrimination between compounds, with rotaxane **2.6** having two additional chiral groups on the axle derived form *(S)*-serine.

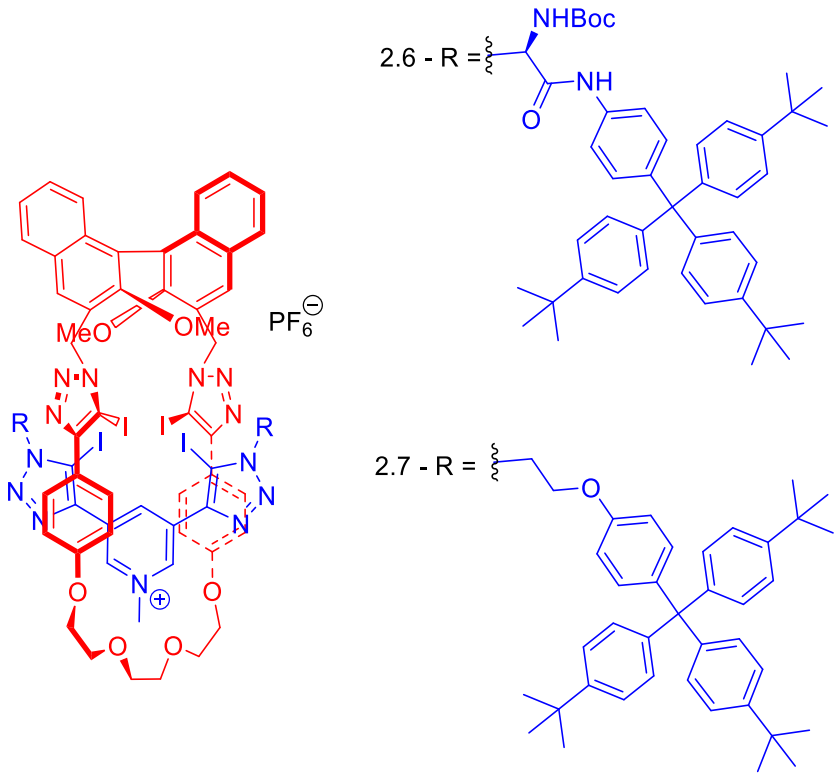

Figure 2.3 - Beer and co-workers halogen bonding enantioselective [2] rotaxanes 2.6 and 2.7

^{1}H NMR titrations with a variety of chiral TBA salts (Table **2.2**) revealed that rotaxanes **2.6** and **2.7** exhibit good enantioselectivities ($K_{fav/disfav}$) of up to 2.93:1 for *N*-Boc-proline (98:2 D_6-acetone:D_2O) and 3.45:1 for *N*-Boc-leucine (99:1 D_6-acetone:D_2O) respectively. It was found that although rotaxane **2.6** bound anions more strongly, rotaxane **2.7** is more enantioselective. The study also investigated a version of rotaxane **2.6** without the *S*-BINOL group on the macrocyclic component with the same chiral anions, although this had no enantioselectivity ($K_{fav/disfav} \leq 1.2$), suggesting that the enantiodiscrimination in rotaxanes **2.6** and **2.7** primarily comes from the *S*-BINOL of the macrocyclic component.

Table 2.2 – Enantioselctivities and binding constants (K, mol^{-1} dm^{-3}) of rotaxanes 2.6 and 2.7 (98:2 D_6-acetone:D_2O)

	Rotaxane **2.6**			Rotaxane **2.7**		
chiral anion	K_S	K_R	$K_{fav/disfav}$	K_S	K_R	$K_{fav/disfav}$
N-Boc-leucine	2500	1500	1.62	140	470	3.45
N-Boc-tryptophan	5000	2900	1.73	470	760	1.61
N-Boc-proline	4300	1465	2.93	1700	2600	1.51
BINOL-PO_4	550	1200	2.13	350	630	1.79

Subsequently, Beer and co-workers reported a chloride anion, halogen bonding [3]rotaxane **2.8**, synthesised in 37% yield (Fig. **2.4**).[9] [3]Rotaxane **2.8** was designed to bind di-carboxylates between the two interlocked cavities, with a BINOL unit included in the centre of the axle to provide enantioselectivity. [3]Rotaxane **2.8** shows stereoselectivity for TBA *R* and *S* glutamate, with binding constants of K_S = 35,000 ± 2000 and K_R =6220 ± 70 in 60:39:1 $CHCl_3$:MeOH:H_2O, equating to an enatioselctivity of $K_{fav/disfav}$ = 5.66.

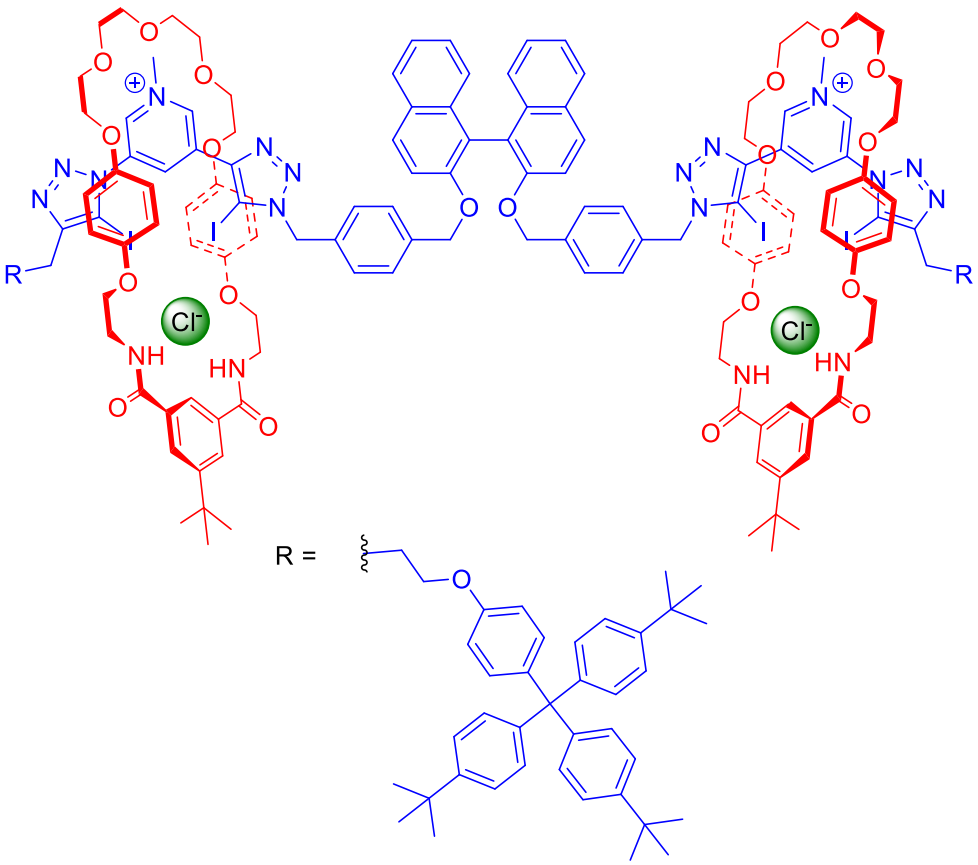

Figure 2.4 - Beer and co-workers enantioselective [3]rotaxane 2.8

In this chapter a family of *hydrogen* bonding enantioselective rotaxanes will be prepared with chiral groups either side of the macrocycle binding site, different from the halogen bonding rotaxanes so far discussed, using a variation of the chloride templated rotaxane synthesis reported by Hancock and Beer (Fig. **2.5**).[2] The synthesis of rotaxane **2.9** utilises three key interactions between the macrocycle precursor **2.10** and axle **2.11**:

- A hydrogen bond templating interaction between the electron deficient methyl protons of axle **2.11** pyridinium group and the polyether oxygens of macrocycle precursor **2.10** (Fig. **2.5**, a).
- A π-π stacking effect from the hydroquinone groups of macrocycle precursor **2.10** to the electron deficient pyridinium of axle **2.11** (Fig. **2.5**, a).
- The final and most important interaction is the chloride templating interaction between macrocycle precursor **2.10**, where a single amine has coupled to the isophthaloyl

chloride and the axle amides (Fig. **2.5**, b). This is the main interaction that brings the rotaxane together (Fig. **2.5**, c).

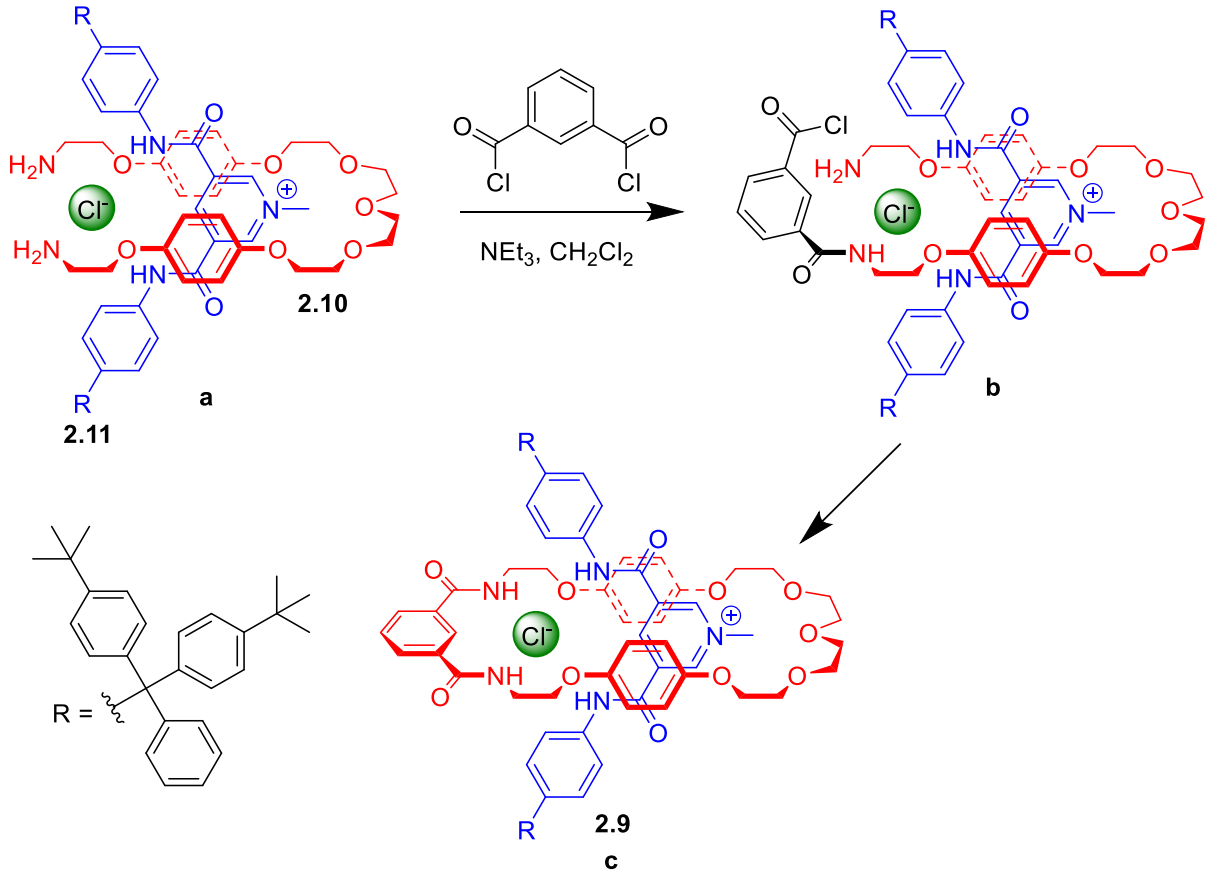

Figure 2.2 – Chloride templated rotaxane 2.9 synthesised by Hancock and Beer

2.2. Macrocycle Precursor Synthesis

Synthesis began with the preparation of macrocycle precursor **2.10**. The established literature procedure for the synthesis of this compound (Fig. **2.6**) required a step that had a difficult and time consuming synthesis and purification.[2,10,11] This step is the double deprotonation and mono-functionalisation of hydroquinone with potassium hydroxide and bromoacetonitrile, to form compound **2.12** on a roughly 5-10 g scale. This step requires the rigorous exclusion of oxygen and purification requires a long and difficult column to remove any oxidation products formed during the reaction. To avoid this a new route was investigated.

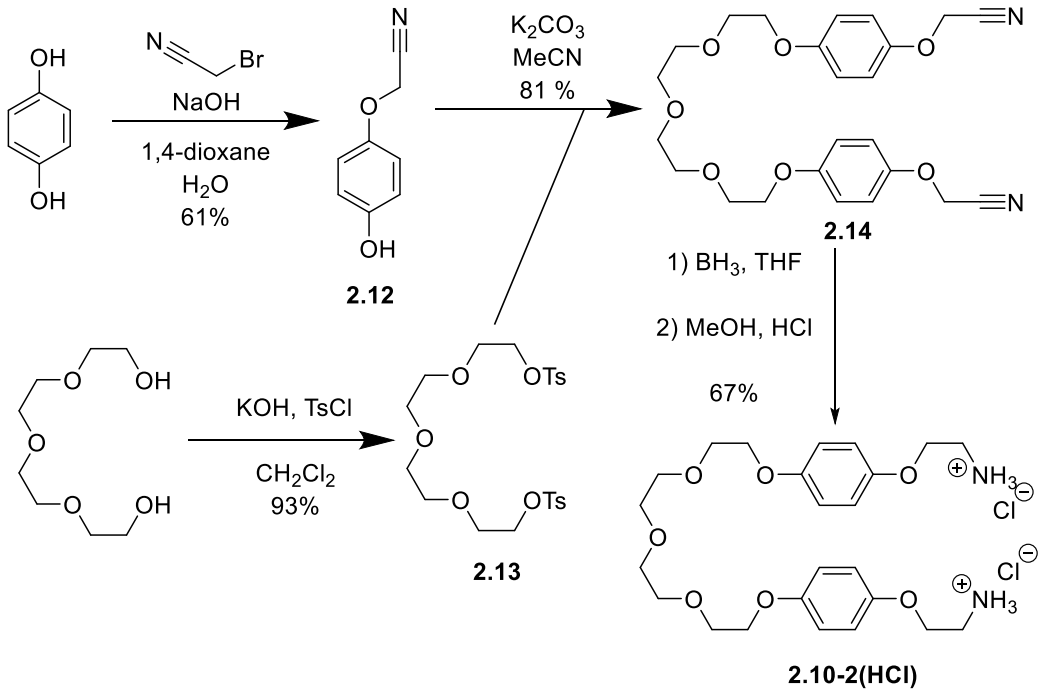

Figure 2.6 – Literature synthesis of macrocycle precursor 2.10

Throughout the work recorded in this thesis, compounds were typically analysed by ^{1}H and ^{13}C NMR spectroscopy and mass spectrometry, and where novel IR spectroscopy. In addition, for enantiopure compounds optical rotations were recorded.

2.2.1. New Synthetic Route

The new route (Fig. **2.7**) began with the reduction of the commercially available monofunctionalised hydroquinone (4-hydroxyphenoxy)acetic acid using borane in THF. After quenching excess borane, the material was purified using an aqueous work up and column chromatography to afford compound **2.15** in 77% yield. Compound **2.15** was then coupled to bromoacetonitrile by refluxing in MeCN in the presence of K_2CO_3. The compound was purified by column chromatography to yield compound **2.16** in 87% yield. Compound **2.16** was then activated with tosyl chloride in the presence of DMAP and NEt_3 in CH_2Cl_2 to give compound **2.17** in 84% yield. It was then attempted to couple two equivalents of **2.17** together using diethylene glycol and NaH in THF to form compound **2.14**. However, this reaction was unsuccessful on multiple occasions, with the majority of the recovered material being starting material **2.17**. Had

the reaction been successful the bis-nitrile **2.14**, would have been reduced with borane in THF, then isolated as the bis-hydrochloride salt of **2.10-2(HCl)** before being deprotonated with aqueous 10% NaOH in a biphasic mixture of water and CH_2Cl_2 to form macrocycle precursor **2.10**.

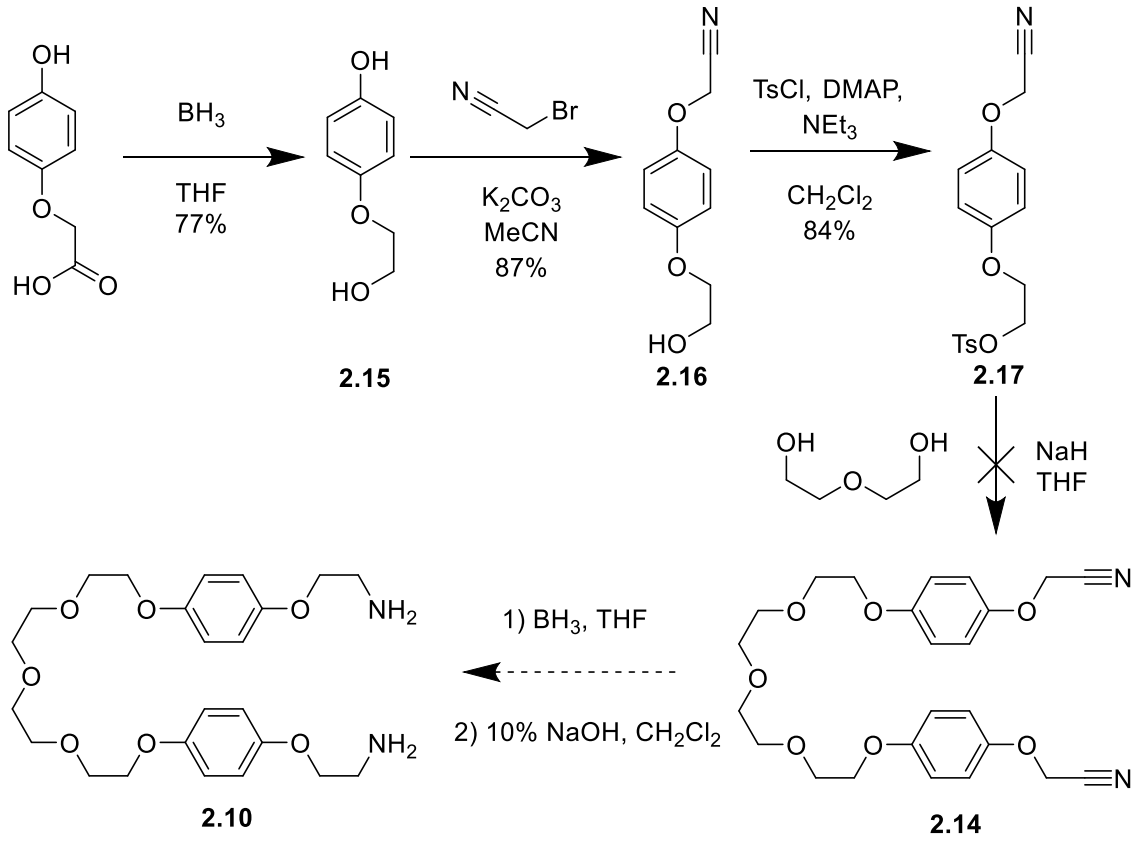

Figure 2.7 – Attempted new route to macrocycle precursor 2.10

2.2.2. Established Synthetic Route

As the alternative synthetic route was unsuccessful, it was decided to revert to the established literature procedure (Fig. **2.8**) for the synthesis of the macrocycle precursor **2.10**.[2,10,11] This began with the mono-functionalisation of hydroquinone with bromoacetonitrile in the presence of sodium hydroxide in a water and dioxane mixture. After stirring the reaction mixture for 30 minutes, the solution was acidified, then the product was extracted with CH_2Cl_2. and purified using column chromatography, isolating compound **2.12** in 69% yield. Two equivalents of compound **2.12** were then coupled together using di-tosylate **2.13**, supplied by Dr. Nicholas Evans, by refluxing in MeCN in the presence of K_2CO_3. The crude product was recrystallised in

EtOAc/hexane to afford pure **2.14** in 41% yield. Compound **2.14** was then treated with a BH_3.THF complex. After quenching excess borane, the mixture was acidified and the solvent removed. The resulting solid was suspended between 10% NaOH (aq) and CH_2Cl_2, the organic layer separated, dried and solvent removed to yield bis-amine **2.10** in a 91% yield.

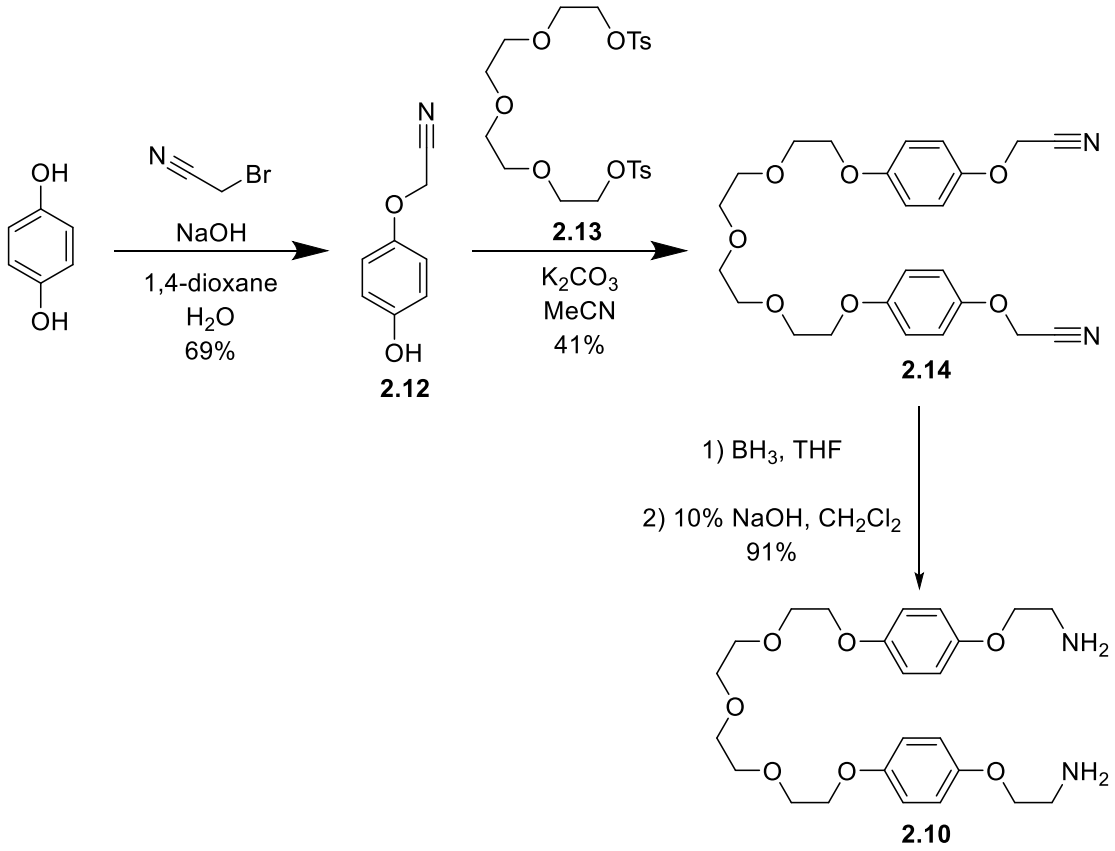

Figure 2.8 – Synthesis of macrocycle precursor 2.10

2.2.3. Macrocycle synthesis

For later comparison with the rotaxanes prepared in this project and to ease NMR assignments a small portion of macrocycle precursor **2.10** was used to synthesise macrocycle **2.18**, using an established templation strategy.[10]

Pyridinium template **2.19** was prepared in two steps from a literature procedure (Fig. **2.9**).[12] Pyridine-3,5-dicarboxylic acid was refluxed in $SOCl_2$ with a catalytic amount of DMF for one hour. The $SOCl_2$ was removed and the resulting solid was dissolved in CH_2Cl_2, NEt_3 was added followed by n-hexylamine. The mixture was stirred for one hour and was purified using an aqueous work

up to afford hexyl thread **2.20** in 85% yield. Hexyl thread **2.20** was then dissolved in $CHCl_3$, followed by the addition of MeI. The solution was refluxed for 16 h and the solvent removed. The resulting solid was dissolved in $CHCl_3$ then washed repeatedly with 1 mol dm^{-3} $NH_4Cl_{(aq)}$ to afford pyridinium template **2.19** in 95% yield.

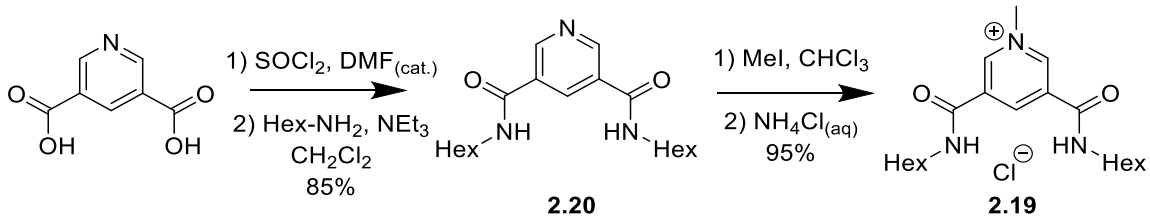

Figure 2.9 – Synthesis of pyridinium template 2.19

A stoichiometric amount of pyridinium template **2.19** was then added to macrocycle precursor **2.10** in CH_2Cl_2 and stirred for 30 minutes. NEt_3 was added followed by the dropwise addition of isophthaloyl chloride in CH_2Cl_2. The mixture was stirred for 1 h, then purified by an aqueous work up, followed by column chromatography and finally trituration with ice cold MeOH, to afford macrocycle **2.18** in 16% yield.

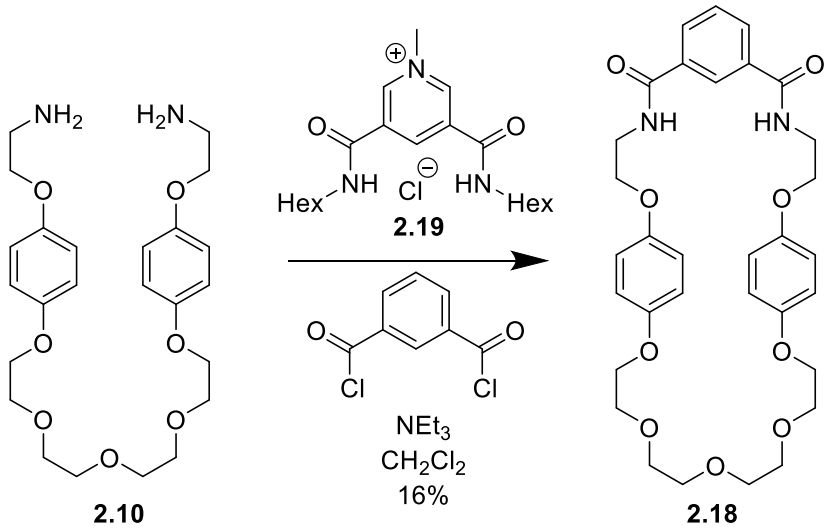

Figure 2.10 – Synthesis of macrocycle 2.18

2.3. Amino Acid Containing Axle Synthesis

Following the synthesis of macrocycle precursor **2.10** the synthesis of the four amino acid containing axles was embarked upon. The four amino acids chosen were glycine, L-alanine, L-valine and L-phenylalanine to synthesise axles **2.21**, **2.22**, **2.23** and **2.24** (Fig. **2.11**). Glycine was chosen as an achiral prototype, to be used to develop the synthetic route that was employed to synthesise all four axles. Once glycine axle **2.21** was prepared the synthesis of L-alanine axle **2.22**, L-valine axle **2.23** and L-phenylalanine axle **2.24** were investigated. These amino acids were chosen as they contain no reactive functional groups on the side chain, that may complicate the synthesis of the relevant axle and it was hypothesised that the steric bulk of side chains of these amino acids will provide the enantiodiscrimination required. In addition, it was hypothesised that the aromatic groups of L-phenylalanine may assist the binding of guest species with aromatic groups, through π-π stacking.

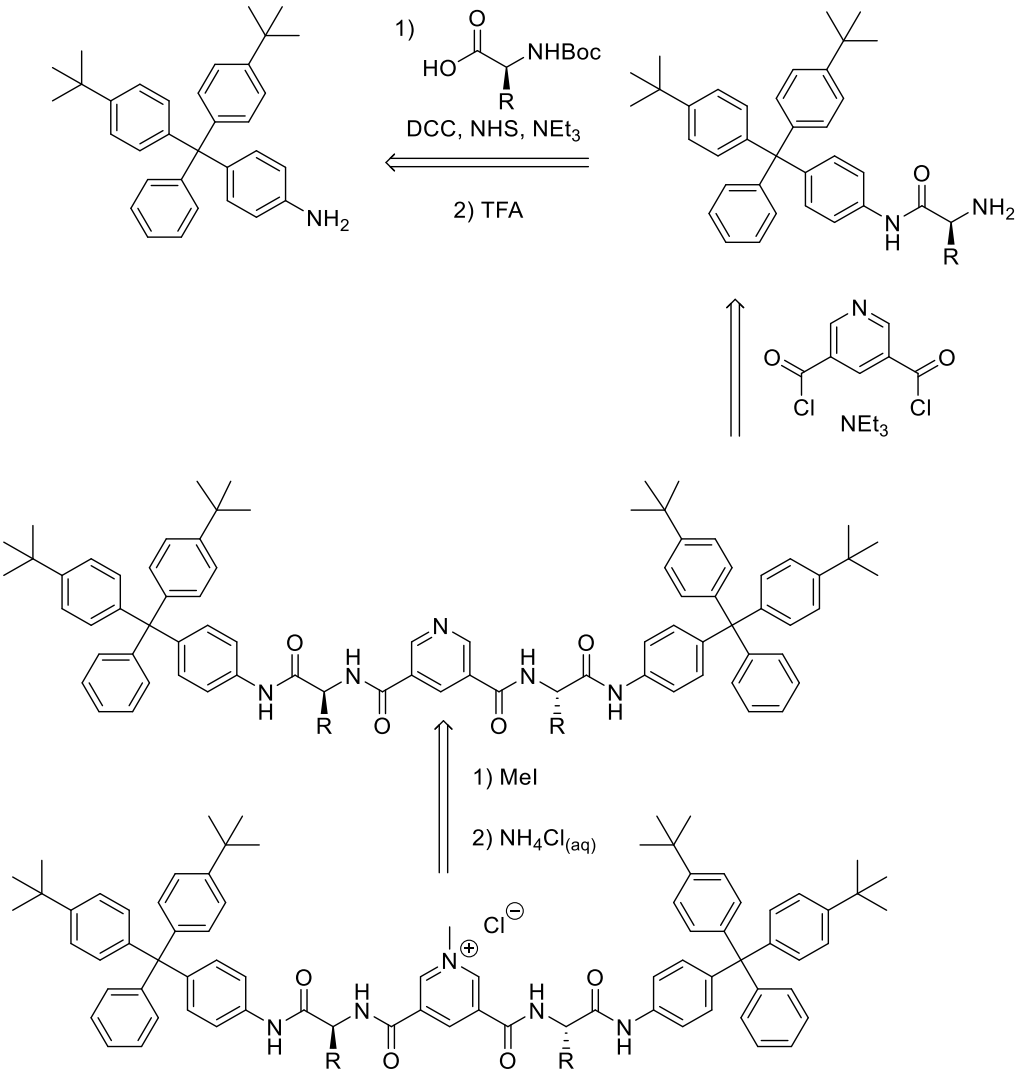

Figure 2.11 – Retrosynthesis of the axles for the rotaxanes in this chapter (2.21 – R = H, 2.22 – R = Me, 2.23– R = ^{i}Pr, 2.24 – R= CH_2Ph)

2.3.1. Synthesis of Stopper 2.25

Synthesis of glycine axle **2.21** began with the preparation in bulk of stopper **2.25** (Fig. **2.12**) to be used as a starting material for all the chloride templated rotaxanes in this thesis, following a literature procedure.[1] 4-Bromo-*tert*-butylbenzene in THF was added dropwise to Mg turnings covered in THF with catalytic I_2. The mixture was stirred for one hour and then methyl benzoate in THF was added dropwise. The solution was stirred for a further hour, then acidified with 10% $HCl_{(aq)}$ and extracted with petrol 40-60. The solvent was removed and the resulting solid was recrystalised from MeOH to afford compound **2.26** in 83% yield. Compound **2.26** was then refluxed for 16 h in acetyl chloride, excess acetyl chloride was removed and the resulting solid

was heated to 110 °C for 48 h in aniline under a flow of N_2 gas. The solution was acidified with $HCl_{(aq)}$ and the resulting precipitate was collected by filtration, then washed with saturated $Na_2CO_{3(aq)}$ and water. The resulting precipitate was filtered through a plug of silica then recrystalised from toluene/hexane to afford compound **2.25** in 49% yield.

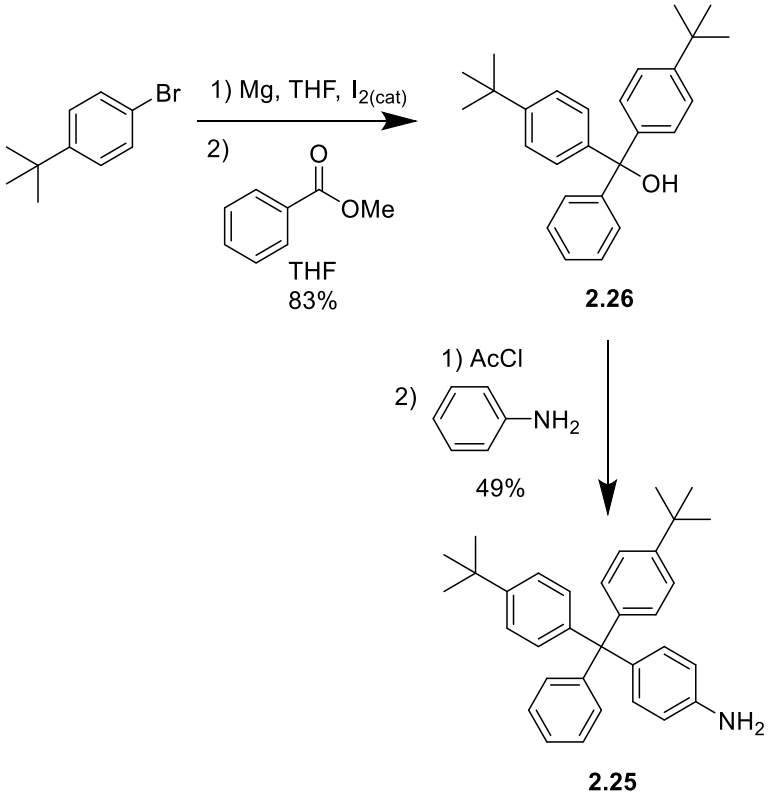

Figure 2.12 – Synthesis of stopper 2.25

2.3.2. Synthesis of Prototype Glycine Containing Axle

Prototype glycine axle **2.21** was synthesised in four steps (Fig. **2.13**), starting with stopper **2.25**. Bulky amine stopper **2.25** was coupled with *N*-Boc-glycine using DCC and *N*-hydroxysuccinimide. After aqueous workup and column chromatography, compound **2.27** was isolated in 79% yield. The Boc protecting group of compound **2.27** was removed by dissolving compound **2.27** in CH_2Cl_2, followed by the addition of TFA. The solution was stirred for 1 h and then amine **2.28** was extracted using an aqueous work-up in 95% yield.

Pyridine-3,5-dicarboxylic acid was refluxed for 1 h in $SOCl_2$ with a catalytic amount of DMF, excess $SOCl_2$ was removed and the resulting acid chloride was dissolved in CH_2Cl_2. NEt_3 followed by amine **2.28** were added and the solution was stirred for 1h. The solution was purified using an aqueous work up followed by column chromatography to afford compound **2.29** in 52% yield. Compound **2.29** was then dissolved in a mixture of $CHCl_3$ and MeI then heated to 45 °C for 16 h. Excess MeI and the solvent were removed, the residue dissolved in $CHCl_3$ and washed repeatedly with 1 mol dm^{-3} $NH_4Cl_{(aq)}$ to produce compound **2.21** as the chloride salt in 62% yield.

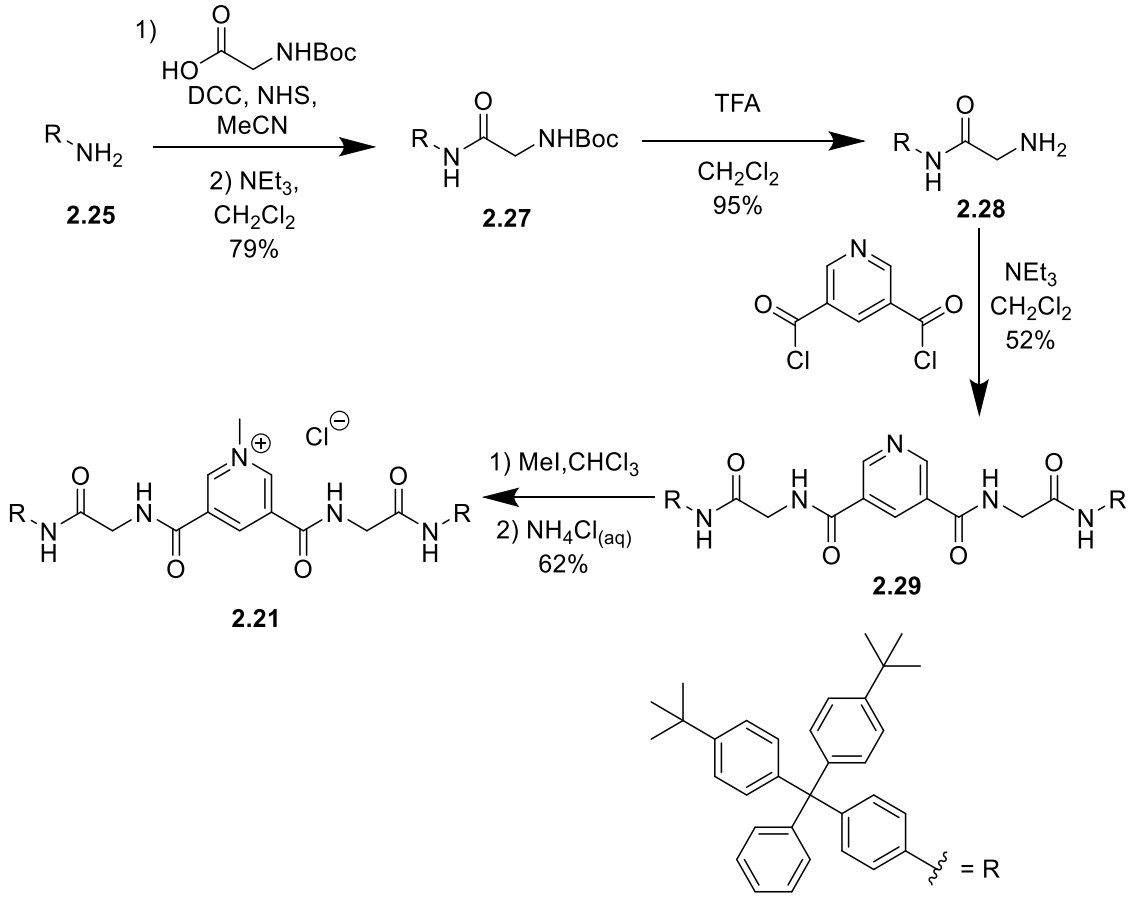

Figure 2.13 – Synthesis of glycine axle 2.21

Glycine axle **2.21** was reported by Beer and co-workers during the development of this project, using a broadly similar method to what has been reported.[13]

2.3.3. Synthesis of Chiral Amino Acid Containing Axles

L-Alanine axle **2.22** and L-phenylalanine axle **2.24** was prepared using the same method developed for glycine axle **2.21** (Fig. **2.14**). An attempt was also made to prepare L-valine axle **2.23**. Amine stopper **2.25** was coupled with the appropriate *N*-Boc protected enantiopure amino acid in a DCC and NHS mediated coupling, compounds **2.30**, **2.31** and **2.32** were then purified using an aqueous work up followed by column chromatography. Whilst the coupling worked well when using L-alanine and L-phenylalanine, the reaction was problematic for L-valine as the yield was poor. The low yield of the L-valine coupling was attributed to the bulky iso-propyl group of the L-valine preventing coupling with bulky stopper **25**. Several further attempts were made to increase the yield of L-valine compound **2.31**, by increasing reaction times and the number of equivalents of coupling reagents and *N*-Boc-valine. However, these were all unsuccessful, therefore it was decided not to proceed with the synthesis of L-valine axle **2.31**. The Boc protecting group of L-alanine compound **2.30** and L-phenylalanine compound **2.32** were then cleaved by TFA in CH_2Cl_2 in good yield to form amines **2.33** and **2.34**.

Pyridine-3,5-dicarboxylic acid and a catalytic amount of DMF were then refluxed for 1 h in $SOCl_2$. Excess $SOCl_2$ was then removed and the resulting acid chloride was dissolved in CH_2Cl_2 with NEt_3 and with either amine **2.33** or **2.34**. The solution was stirred for 1 h and then purified using an aqueous work up followed by column chromatography to afford both compound **2.35** and **2.36** in 75% yield. Compounds **2.35** and **2.36** were then heated to 45 ^oC in MeI and $CHCl_3$. The $CHCl_3$ and excess MeI were removed and residues were dissolved in $CHCl_3$ and then washed with 1 mol dm^{-3} to afford L-alanine axle **2.22** and L-phenylalanine axle **2.24** in 92% and 99% yield respectively.

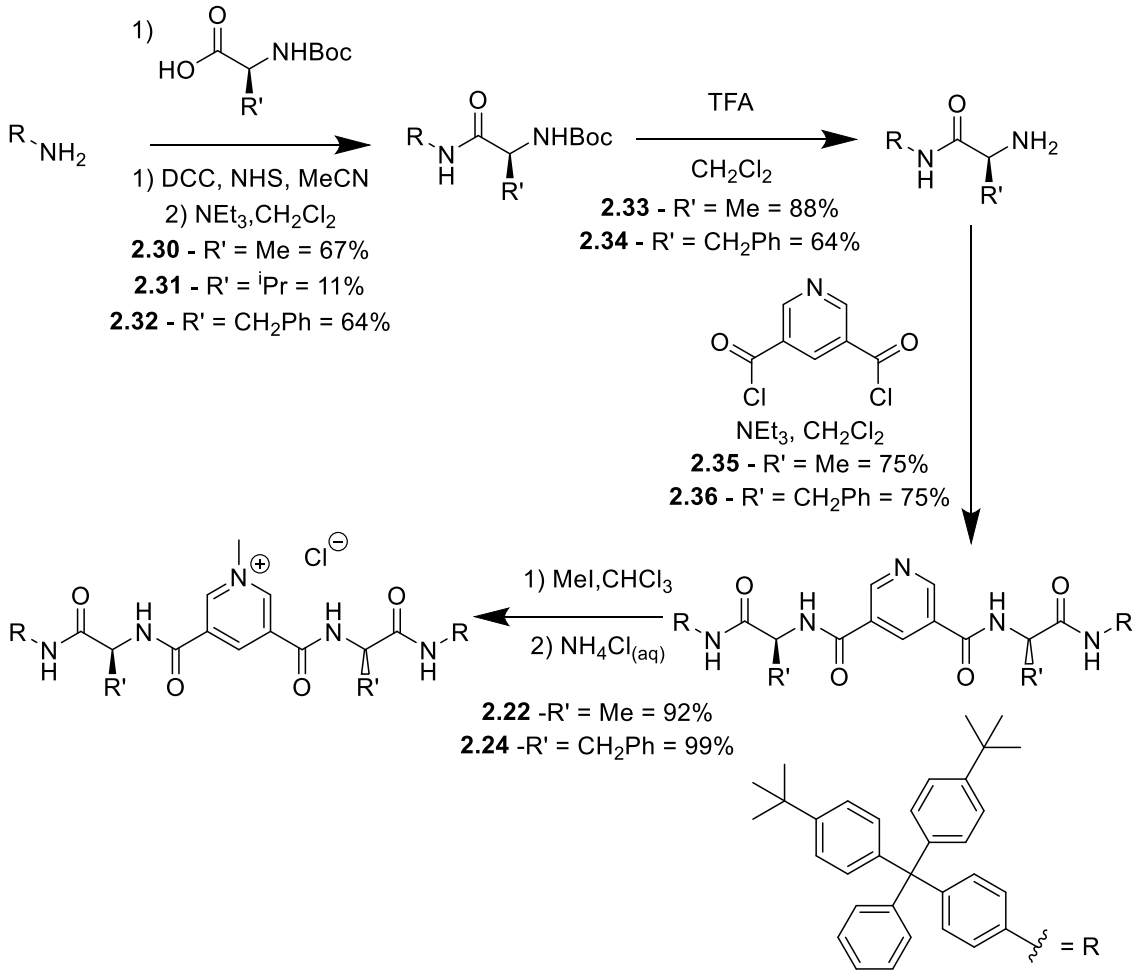

Figure 2.14 – Synthesis of L-alanine axle 2.22, L-phenylalanine axle 2.24 and attempted synthesis of L-valine axle 2.23

2.4. Amino Acid Containing Rotaxane Synthesis

2.4.1. Synthesis and Purification

Glycine rotaxane **2.1**, L-alanine rotaxane **2.2** and L-phenylalanine rotaxane **2.4** were prepared as follows (Fig. **2.15**).[2] Macrocycle precursor **2.10** and the relevant axle were dissolved in dry CH_2Cl_2 and stirred for 30 minutes, then NEt_3 was added followed by the dropwise addition of isophthaloyl chloride in CH_2Cl_2. The solution was stirred for 1 h then submitted to an aqueous work up. Several techniques were then attempted to separate the rotaxane from the impurities that were not soluble in water.

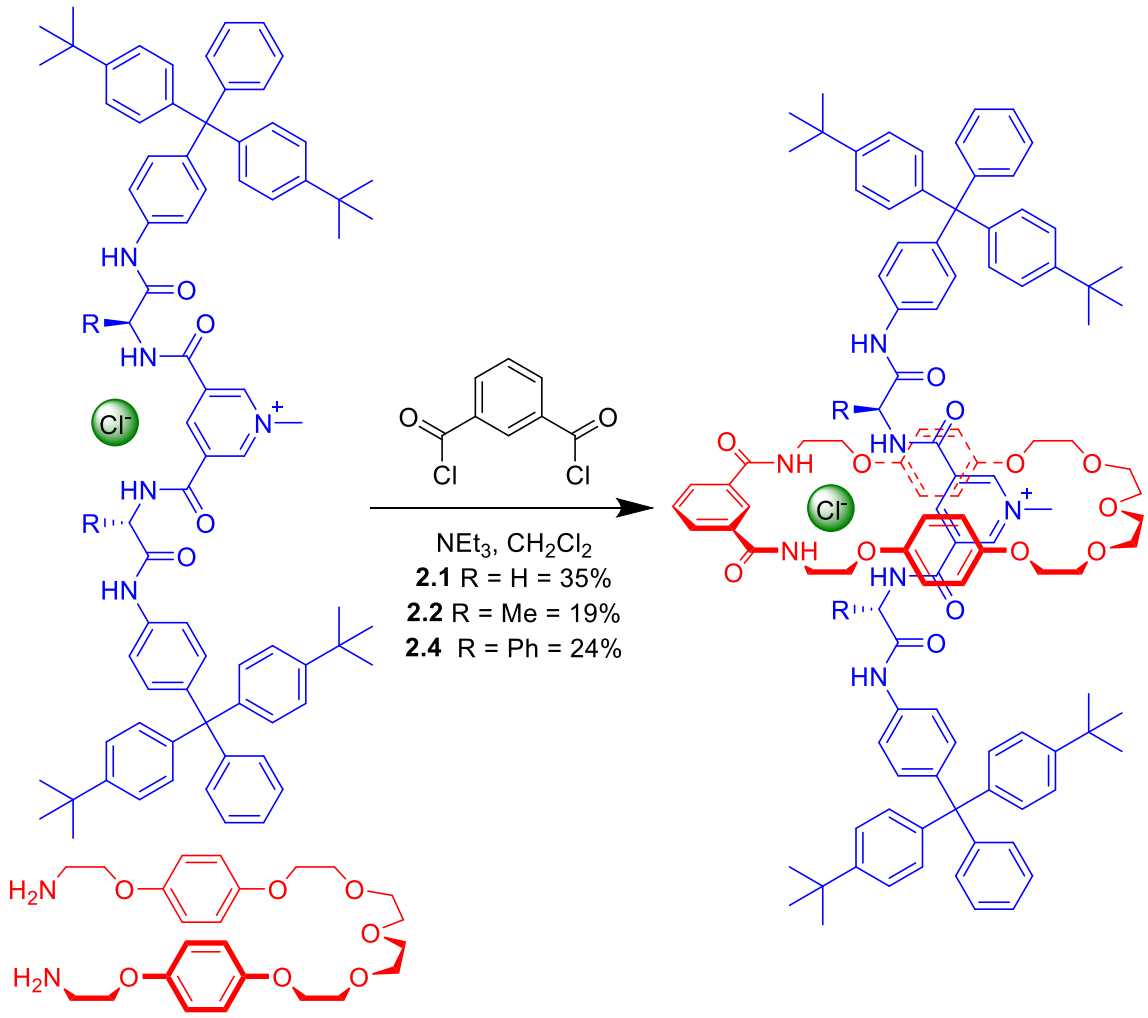

Figure 2.15 – Synthesis of rotaxanes 2.1 (R = H), 2.2 (R = Me)and 2.4 (R = CH_2Ph)

The majority of the impurities contaminating rotaxanes **2.1**, **2.2** and **2.4** could be removed using a standard silica column chromatography, using 96:4 CH_2Cl_2:MeOH solvent mixture as eluent. However, what was suspected to be a macrocyclic impurity proved extremely difficult to remove, (peaks corresponding to free macrocycle **2.18** were found in the NMR spectra) despite attempts to purify all three of the rotaxanes by preparative TLC and column chromatography using a variety of eluents and attempts to recrystallise rotaxane **2.1**, **2.2** and **2.4** from various solvent systems. Repeated use of these techniques rapidly reduced the amount of material to unusable amounts and resulted in the three rotaxanes being synthesised multiple times.

It is thought that rotaxanes **2.1**, **2.2** and **2.4** synthesised in this chapter and the suspected macrocyclic impurity have similar polarities, so are difficult to separate by standard methods,

indeed rotaxanes **2.1**, **2.2** and **2.4** appeared clean by analytical TLC. Instead an alternative strategy was pursued for glycine rotaxane **2.1** and L-phenylalanine rotaxane **2.4**. These rotaxanes were purified by first removing any impurities that could be removed whilst the rotaxane was the chlorides salt, by flash chromatography, then altering the polarity of the rotaxane by exchanging the templating chloride anion for another anion. The rotaxane may then be purified by further flash chromatography, as the impurity and rotaxane would no longer have the same polarity. This method was not used on L-alanine rotaxane **2.2**, due to a lack of time and it was anticipated that L-alanine rotaxane **2.2** would have a lower enantioselctivity than L-phenylalanine rotaxane **2.4**.

Further batches of rotaxane **2.1** and **2.4** was prepared and submitted to an aqueous work up. The compounds were then passed through a plug of silica as the chloride salt, to remove any ionic and polymeric impurities, then the templating chloride anion was exchanged for a sulfate anion. The sulfate salts of rotaxanes **2.1** and **2.4** were then loaded on to a plug of silica, where the sulfate salt of rotaxanes **2.1** and **2.4** stuck to the top. The plug of silica was washed through to remove any non-ionic impurities, as well as any rotaxane **2.1** or **2.4** that remained as the chloride salt. Once the non-ionic impurities had been removed rotaxanes **2.1** and **2.4** were removed from the plug of silica through the addition of ammonium chloride, which exchanged rotaxanes **2.1** and **2.4** to the chloride salt, which reduced the polarity of rotaxanes **2.1** and **2.4**. The eluent was removed and rotaxanes **2.1** and **2.4** were dissolved in CH_2Cl_2 then washed with 1 mol dm^{-3} NH_4Cl and water to ensure isolation as the chloride salt. The solvent was removed to yield rotaxanes **2.1** and **2.4** in 23% and 13% yield respectively.

As approximately half of the total amount of rotaxanes **2.1** and **2.4** were washed off with the non-ionic impurities, the process was repeated from exchanging the rotaxanes **2.1** and **2.4** to the sulfate salt onwards to yield a further 12% of rotaxane **2.1** and 12% of rotaxane **2.4**. Giving combined yields of 11% of rotaxane **2.1** and 24% of rotaxane **2.4**.

Rotaxanes **2.1** and **2.4** were characterised by ^{1}H and ^{13}C NMR spectroscopy, mass spectrometry, IR spectroscopy, an optical rotation was measured of rotaxane **2.4** and a crystal structure was obtained of rotaxane **2.1**. In addition, an impure sample of L-alanine rotaxane **2.2**, which was not purified using the ion exchange method, was synthesised in an estimated maximum possible yield of 19%. L-Alanine rotaxane **2.2** was characterised by ^{1}H NMR spectroscopy and mass spectrometry.

2.4.2. Characterisation of Glycine Rotaxane 2.1

The ^{1}H NMR spectrum of glycine rotaxane **2.1** (Fig. **2.16**) shows perturbations in the chemical shift of multiple protons when compared to the ^{1}H NMR spectra of axle **2.21** and macrocycle **2.18**. Axle protons 20 and 21 are observed to shift upfield due to the shielding effects of the macrocycle cavity. Macrocycle proton d is observed to shift downfield, due to this proton hydrogen bonding to the templating chloride anion. In addition, macrocycle hydroquinone protons i and j have split and shifted upfield, due to a π-π stacking interaction between the electron rich hydroquinone aromatic system and the electron deficient pyridinium system of the axle.

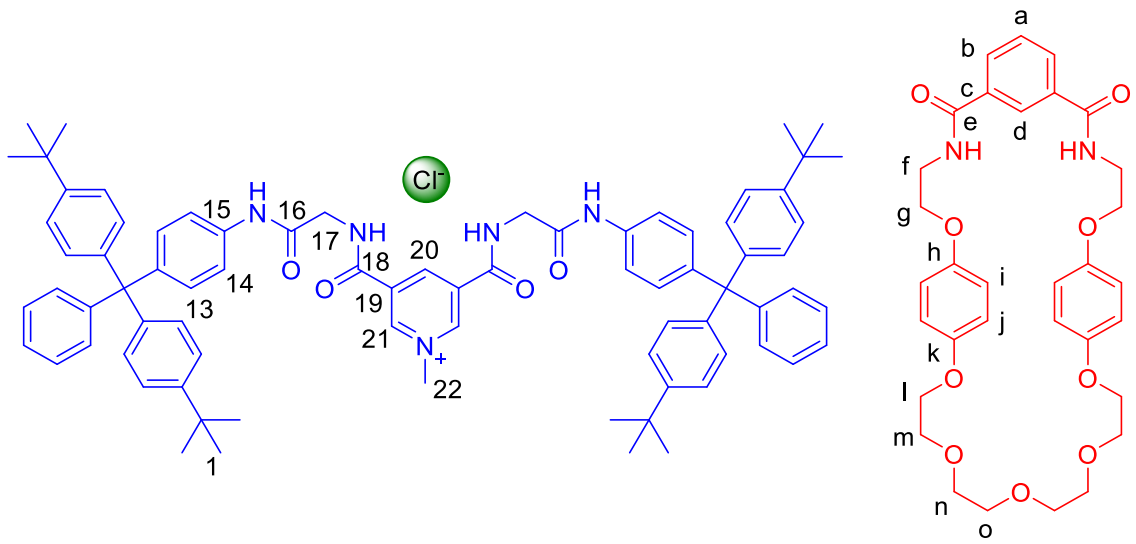

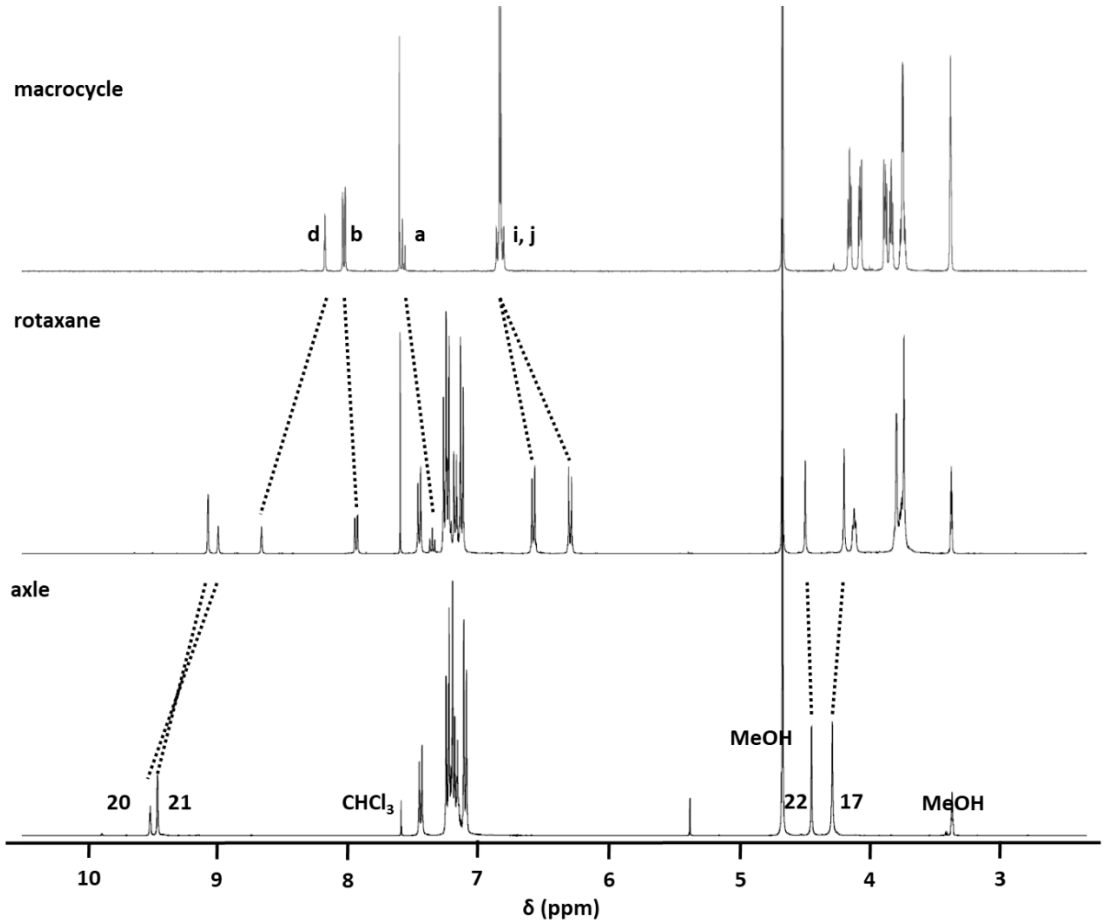

Figure 2.16 – ^{1}H NMR spectra of axle 2.21, rotaxane 2.1, and macrocycle 2.18 (400 MHz, 298 K, 1:1 $CDCl_3$:CD_3OD)

The crystal structure of rotaxane **2.1** (Fig. **2.17**), confirms what was observed in the ^{1}H NMR spectrum, with the macrocyclic component residing over the pyridinium unit of the axle. In addition, it can be seen that the four amides are arranged in a tetrahedral arrangement around the templating chloride anion, as is typical for chloride templated rotaxanes.

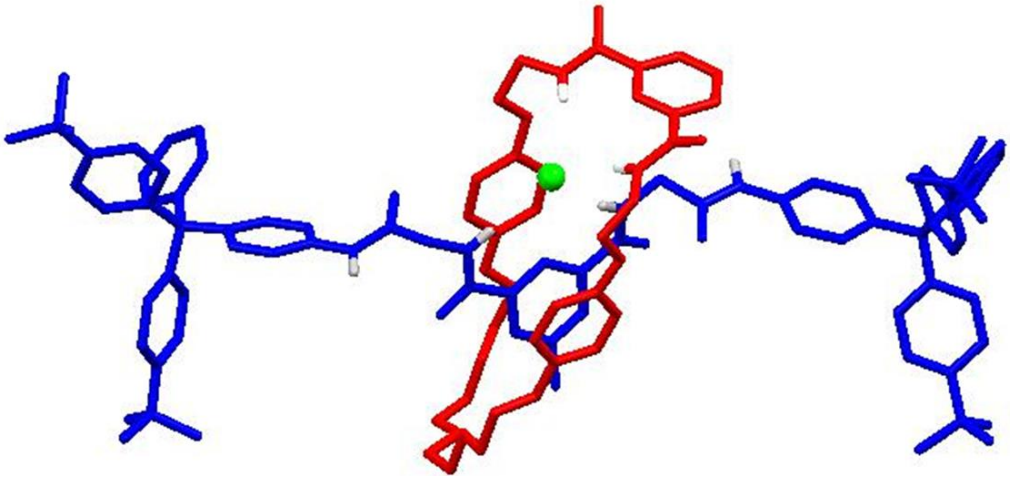

Figure 2.17 – X-ray crystal structure of glycine rotaxane 2.1 (Obtained by N. Halcovitch, solvent and non-amide protons omitted for clarity)

2.4.3. Characterisation of L-alanine rotaxane 2.2

The ^{1}H NMR spectrum (Fig. **2.18**) of the contaminated L-alanine rotaxane **2.2** can only be compared to that of macrocycle **2.18** in D_6-acetone as axle **2.22** forms a gel in this solvent. Evidence that the axle had threaded through the macrocycle, is similar to glycine rotaxane **2.1.** Proton c can be observed to shift upfield, due to it hydrogen bonding to the chloride anion and protons i and j are observed to have split and shifted upfield, due to a π-π stacking interaction with the pyridinium moiety of the axle. In addition, these peaks have developed a splitting pattern a triplet of doublets at 6.2 ppm and a heavily distorted doublet of doublets at 6.6 ppm, other peaks also possess multiplicities that are unexpected. This effect is not seen in the ^{1}H NMR spectrum of glycine rotaxane **2.1** (Fig. **2.13**), suggesting that this effect is due to the addition of the methyl group of the L-alanine moiety. One possible cause of this effect may be that the methyl group is causing a steric clash with the macrocycle, causing a twisting of the macrocycle. Alternatively the macrocycle may be rapidly shuttling along the macrocycle in both glycine rotaxane **2.1** and L-alanine rotaxane **2.2**, but in glycine rotaxane **2.1** this happens rapidly relative to the ^{1}H NMR timescale so averages out. In L-alanine rotaxane **2.2** the methyl substituent may be providing a barrier to shuttling, slowing down this movement, so that it can be observed by

^{1}H NMR spectroscopy. Alternatively, this effect may be due to the change in solvent used during acquisition of the NMR spectra.

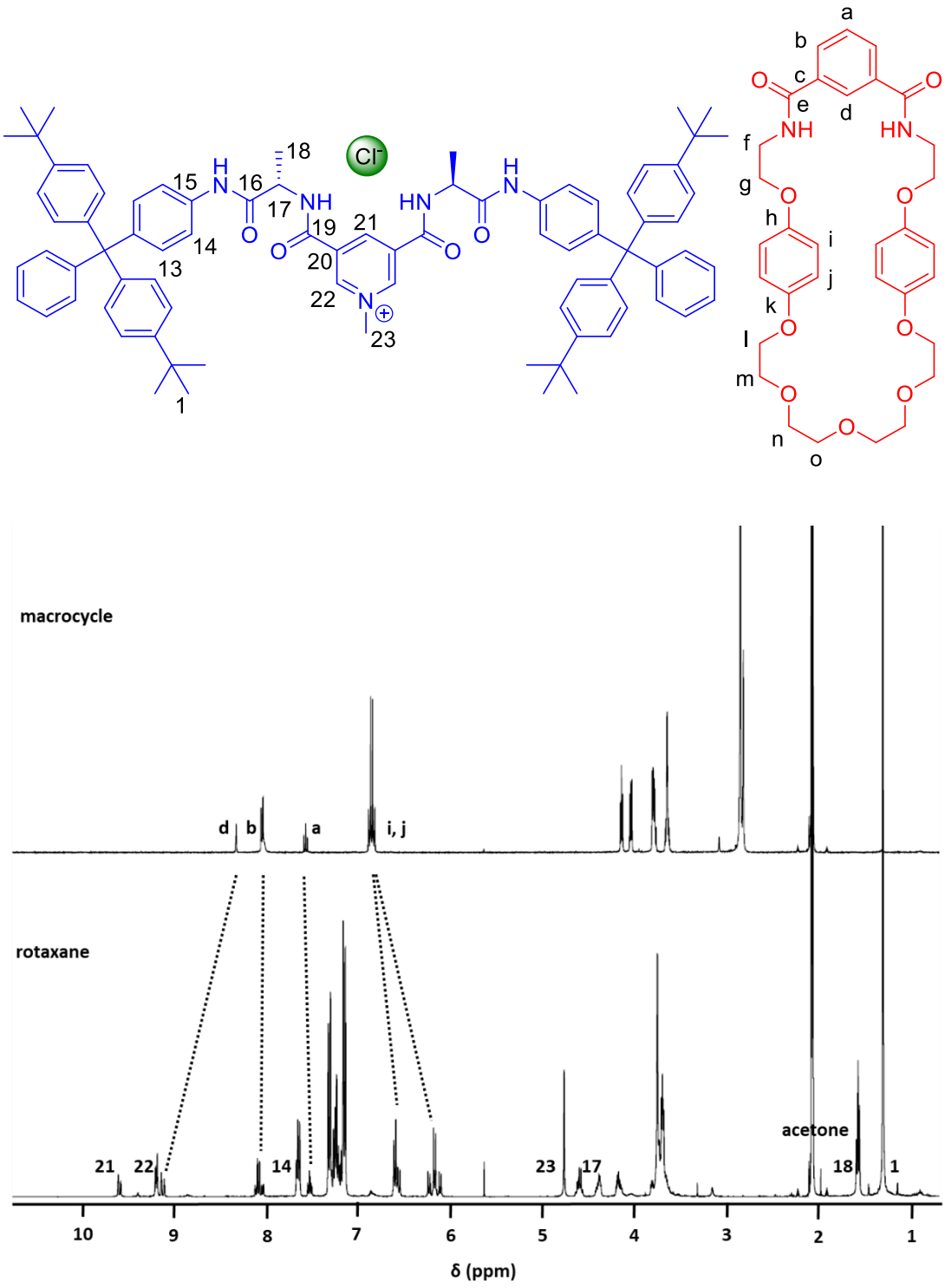

Figure 2.18 – ^{1}H NMR spectra of macrocycle 2.18 and L-alanine rotaxane 2.2, with some macrocyclic impurities. (400 MHz, 298 K, D_6-acetone)

2.4.4. Characterisation of L-phenylalanine rotaxane 2.4

Evidence of L-phenylalanine rotaxane **2.4** formation is seen through perturbations of a number of peaks in the ^{1}H NMR spectrum, relative to axle **2.24** and macrocycle **2.18** (Fig. **2.19**). Axle protons 24 and 26, corresponding to the protons of the pyridinium moiety, are observed to shift downfield in the rotaxane, due to the shielding effect of the macrocycle cavity. In addition, macrocycle proton d is observed to shift upfield, due to this proton hydrogen bonding to the templating chloride anion. Macrocycle protons i and j also split and shift upfield, due to a π-π stacking interaction between the electron rich hydroquinone units of the macrocycle and electron deficient pyridinium moiety of the axle. In addition, multiple protons on the axle and macrocycle are observed to have multiplicities that were unexpected, in a similar to L-alanine rotaxane **2.2**. This is most noticeable in the coupling of macrocycle protons i and j, which are not doublets as would be expected, but instead are split into what initially appears as a pair of heavily roofed doublets of doublets. A further example can be seen where macrocycle protons 26 has split into a doublet, when a singlet would be expected. This is thought to be either due to the macrocycle twisting around the axle, resulting in peaks that should be identical to be inequivalent, or due to the macrocycle shuttling along the axle slowly on the ^{1}H NMR timescale, resulting in the appearance of new peaks.

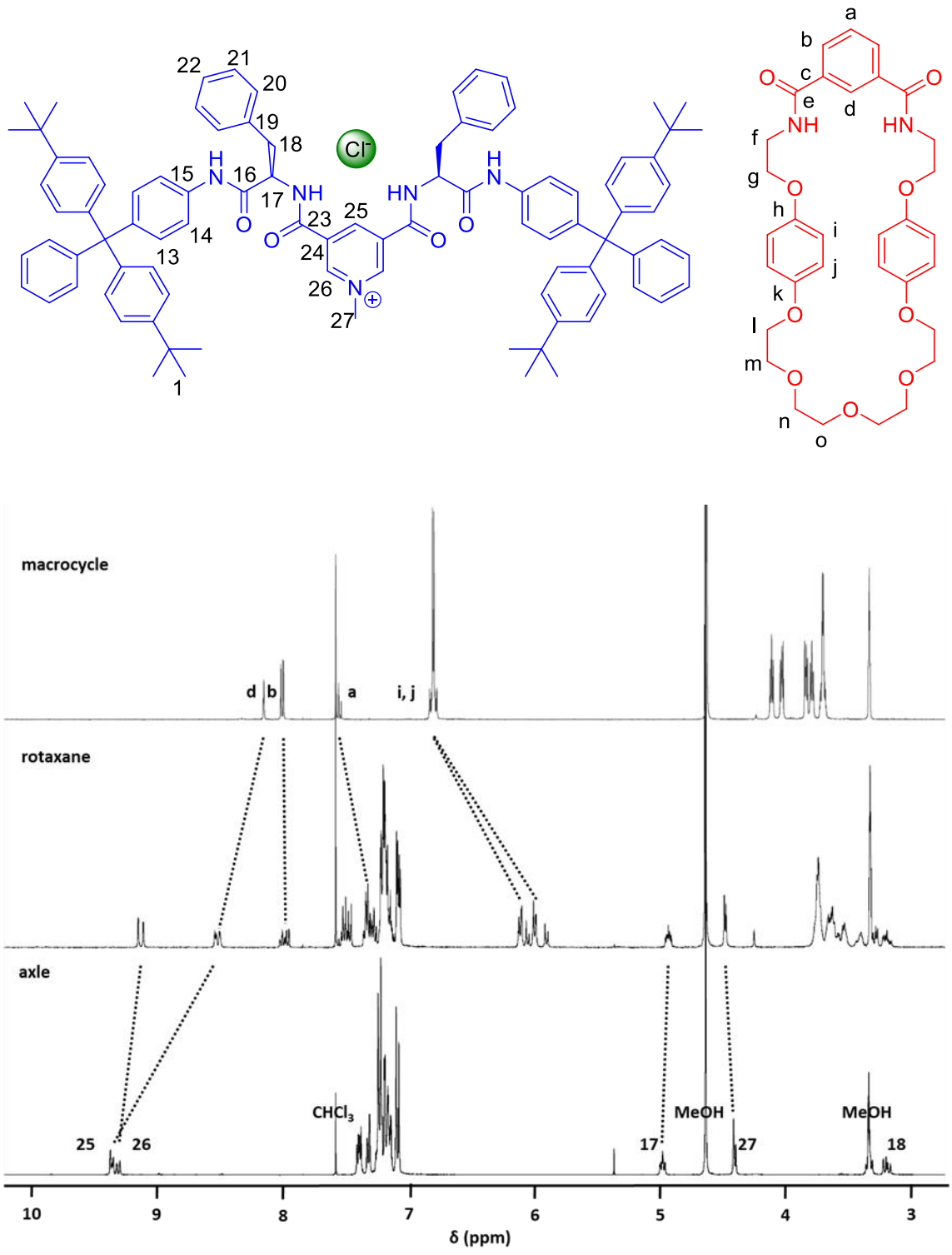

Figure 2.19 – ^{1}H NMR spectra of L-phenylalanine axle 2.4, L-phenylalanine rotaxane 2.24, and macrocycle 2.18 (400 MHz, 298 K, 1:1 $CDCl_3$:CD_3OD)

2.5. Investigations of the Enantioselectivity of Rotaxanes using NMR Titrations

2.5.1. Preparation of Hexafluorophosphate Salts of Rotaxanes 2.1, 2.4 and Axle 2.24

To study the anion binding properties of rotaxanes **2.1**, **2.4** and axle **2.24** it was necessary to exchange the templating chloride anion for a non-competitive hexafluorophosphate anion. This was done in near quantitative yields by repeated washing of rotaxanes **2.1**, **2.4** and axle **2.24** in CH_2Cl_2 with aqueous solutions of NH_4PF_6.[2]

2.5.2. Preparation of *R* and *S* TBA Mandelate Salts

Salts of enantiopure chiral anions with a non-competitive cation were also required. TBA was chosen as an appropriate non-competitive cation. TBA *R* and *S* mandelate (**2.37** and **2.38**) were prepared by deprotonating the appropriate enantiomer of mandelic acid with TBA hydroxide in MeOH.[14]

2.5.3. General Procedure for Titrations

The enantioselective properties of rotaxanes **2.1.PF$_6$**, **2.4.PF$_6$** and axle **2.24 PF$_6$** towards the enantiomers of TBA mandelate were investigated by a series of ^{1}H NMR titration experiments in 1:1 $CDCl_3$:CD_3OD. The binding of anions was observed to be fast on the NMR time scale therefore it was possible to track the change in chemical shift of peaks on the rotaxane or axle at each number of equivalents of TBA mandelate. Due to the use of protic CD_3OD it was not possible to track amide protons, as these had exchanged for deuterium.

Titration curves were plotted by measuring the change of chemical shift of peaks that were observed to have a large perturbation in their chemical shift (e.g. protons d and 21 of glycine rotaxane **2.1.PF$_6$** (Fig. **2.20**)), as a function of the equivalents of anion added to the respective rotaxane or axle. Curves were fitted by WinEQNMR using a 1:1 binding model.

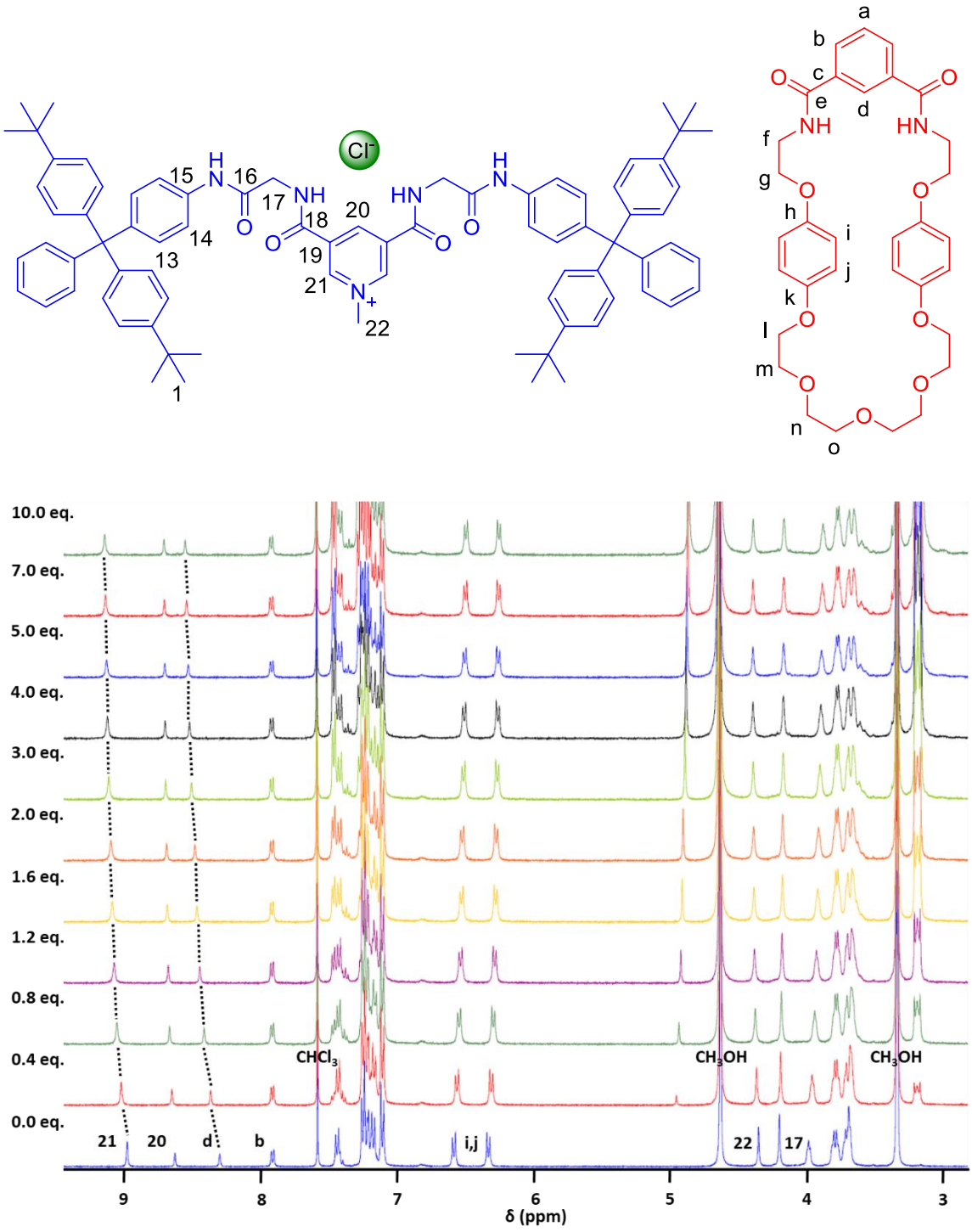

Figure 2.20 – ^{1}H NMR of glycine rotaxane 2.1.PF$_6$ with various amounts of TBA *S*-Mandelate (400 MHz, 298 K, 1:1 CD$_3$OD:CDCl$_3$)

2.5.4. Glycine Rotaxane 2.1-PF_6 Titrations

A pair of initial quantitative titrations were carried out with achiral glycine rotaxane **2.1-PF_6** (Fig. **2.21**) and the *R* and *S* enantiomers of the prepared TBA mandelate. This was to verify the method used for the titration, as both enantiomers of TBA mandelate should have the same binding constant, as glycine rotaxane **2.1-PF_6** lacks any chiral groups so should be incapable of enantioselectivity.

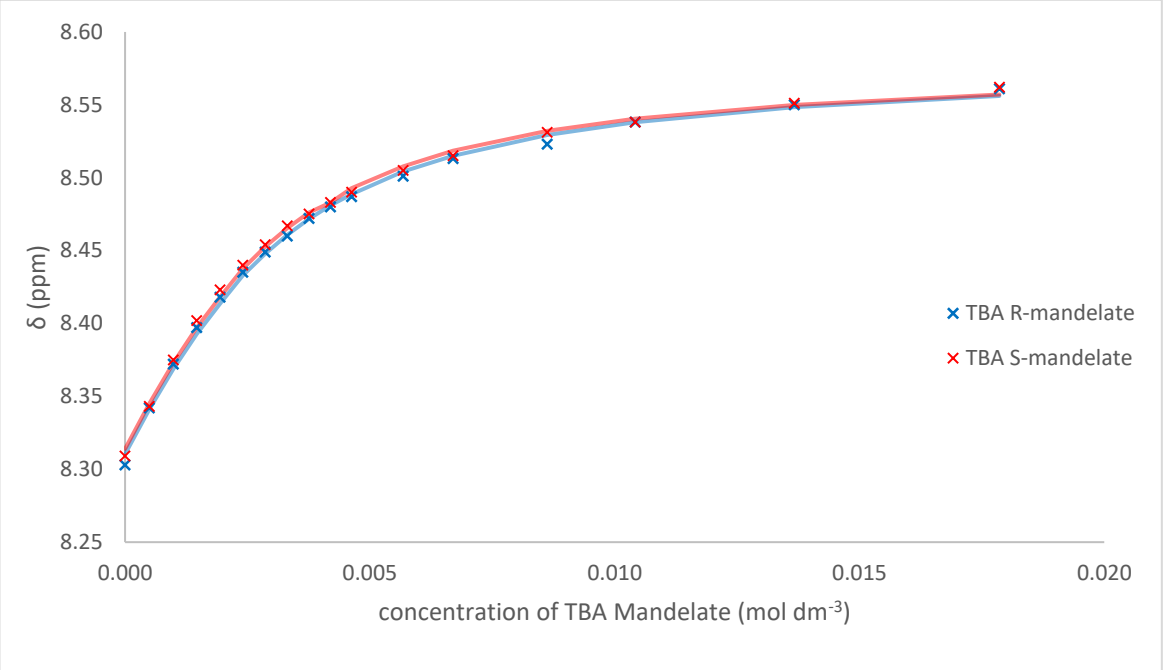

Figure 2.21 – Chemical shift perturbation of glycine rotaxane 2.1-PF_6 with *R* and *S* TBA Mandelate (^{1}H NMR, 1:1 $CDCl_3$:CD_3OD, 298 K, 2.5 mmol dm^{-3}) tracking proton d, crosses represent experimental data points, continuous lines represent calculated curves.

Binding constants of K_R = 680 ± 40 mol^{-1} dm^3 and K_S = 630 ± 40 mol^{-1} dm^3 were calculated by WinEQNMR for the enantiomers of TBA mandelate with glycine rotaxane **2.4** using proton d and K_R = 650 ± 40 mol^{-1} dm^3 and K_S = 690 ± 10 mol^{-1} dm^3 using proton 21 (Fig. **2.20**).[15] The ratio of association constants K_{fav}/K_{disfav} < 1.1 for the glycine rotaxane **2.1.PF_6**, implies that if K_{fav}/K_{disfav} > 1.1 for either of the phenylalanine axle or rotaxane then this would indicate enantioselective anion binding.

2.5.5. Phenylalanine Rotaxane and Axle titrations with *R* and *S* TBA Mandelate

Quantitative titrations were then carried out on chiral L-phenylalanine rotaxane **2.4-PF$_6$** and L-phenylalanine axle **2.24-PF$_6$** with the *R* and *S* enantiomers of TBA mandelate, to determine if either rotaxane **2.4-PF$_6$** or axle **2.24-PF$_6$** possesses enantioselectivity towards either enantiomer. The binding curves for rotaxane **2.4-PF$_6$** (Fig. **2.22**) and axle **2.24-PF$_6$** (Fig. **2.23**) are shown below, along with the binding constant (Table **2.3**)

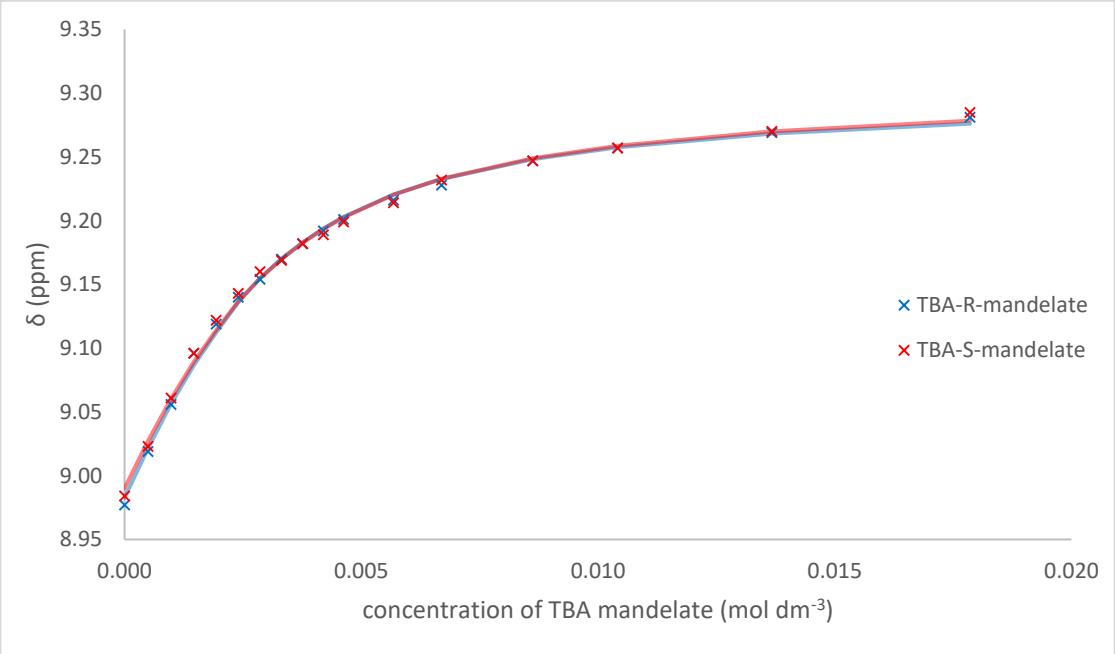

Figure 2.22 – Chemical shift perturbation of phenylalanine rotaxane 2.4-PF$_6$ with *R* and *S* TBA Mandelate (^{1}H NMR, 1:1 $CDCl_3$:CD_3OD, 298 K, 2.5 mmol dm^{-3}) tracking proton 26, crosses represent experimental data points, continuous lines represent calculated curves.

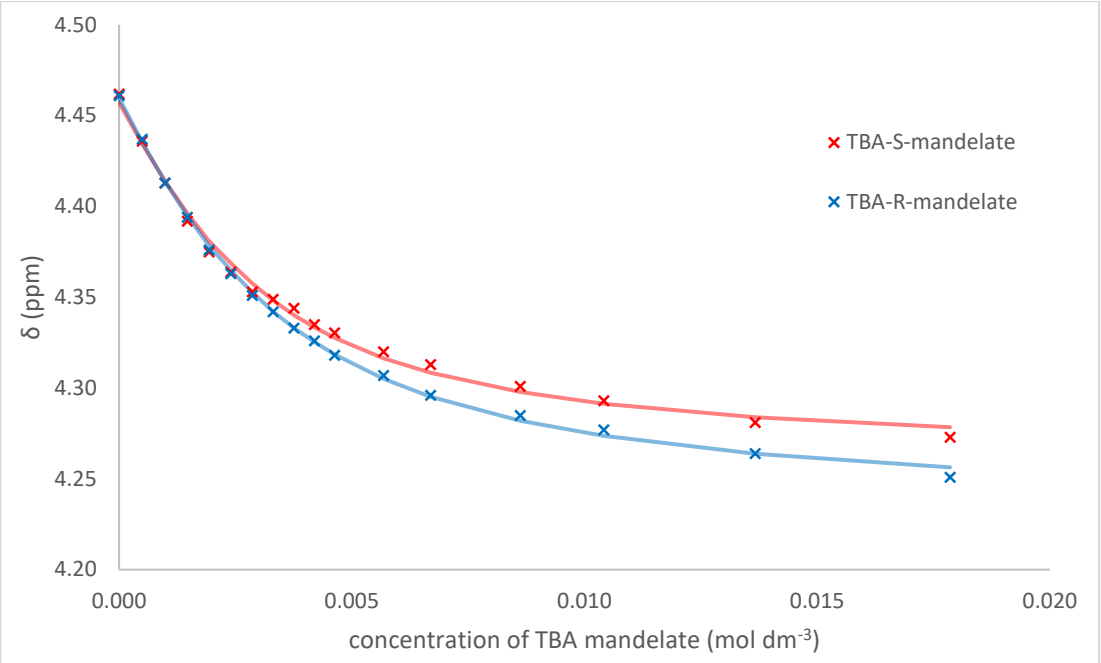

Figure 2.23 – Chemical shift perturbation of phenylalanine axle 2.24-PF_6 with *R* and *S* TBA Mandelate (^{1}H NMR, 1:1 $CDCl_3$:CD_3OD, 298 K, 2.5 mmol dm^{-3}) tracking proton 27, crosses represent experimental data points, continuous lines represent calculated curves.

Table 2.3 – Binding constants, K (mol^{-1} dm^3) of rotaxane 2.4-PF_6 and axle 2.24-PF_6 with TBA *R* and *S* mandelate (1:1 $CDCl_3$:CD_3OD, 2.5 ×10^{-3} mol dm^{-3}, 400 MHz, error ≤ 10%, *error <= 15%)

	L-phenylalanine rotaxane **2.4-PF_6**		L-phenylalanine axle **2.24-PF_6**
Proton Measured	26	b	27
R-mandelate	750	750*	511
S-mandelate	680	780*	630
Enantioselectivity (K_{fav}/K_{disfav})	1.1	1.0	1.2

The calculated binding constants show that both L-phenylalanine rotaxane **2.4-PF$_6$** and axle **2.24-PF$_6$** have enantioselectivities (K_{fav}/K_{disfac}) of 1.2 or less. This suggests that rotaxane **2.4-PF$_6$** and axle **2.24-PF$_6$** have little, if any, enantioselectivity for the enantiomers of TBA mandelate.

Initially it was suspected that the TBA mandelate salts had racemised, producing the similar binding constants for both enantiomers. However, this was dismissed when the optical rotations of *R* and *S* TBA mandelate were confirmed to be similar to literature values (Table **2.4**), suggesting that neither enantiomer had racemised.[14] This indicated that the lack of enantioselectivity towards the enantiomers of TBA mandelate was likely due to the L-phenylalanine rotaxane **2.4-PF$_6$** and axle **2.24-PF$_6$**. However, the lack of enantioselectivity for the enantiomers of TBA mandelate, does not necessarily mean that L-phenylalanine rotaxane **2.4-PF$_6$** would not be enantioselective for other chiral anions or in other solvent systems. However, there was insufficient time to complete these investigations.

Table 2.4 – Observed and literature values of $[\alpha]_D$ for *R* and *S* mandelate (variations in $[\alpha]_D$ are attributed to temperature difference during measurement)

	Observed $[\alpha]_D^{25}$	**Literature $[\alpha]_D^{20}$**
TBA *S*-mandelate	+47.0	+40.58
TBA *R*-mandelate	-52.0	-39.28

It is also noted, that Beer and co-workers observed low levels of enantioselectivity (K_{fav}/K_{disfav} = 1.2, TBA BINOL-PO_4 in 98:2 D_6-acetone:D_2O) with a chiral halogen bonding [2]rotaxane, which only possessed stereogenic centres on the axle.[9] It is therefore possible that to achieve enantiodiscrimination, chiral groups may be required on the macrocycle component, as demonstrated by Beer and co-workers (see above).

2.6. Conclusions

In this chapter the synthesis of four hydrogen bonding amino acid containing chloride templated rotaxanes for the enantioselective binding of chiral anions were investigated (Fig. **2.24**). The four rotaxanes contained either a glycine (rotaxane **2.1**), L-alanine (rotaxane **2.2**), L-valine (rotaxane **2.3**) or L-phenylalanine moiety (rotaxane **2.4**) (Fig. **2.24**). Three novel rotaxanes (**2.1**, **2.2** and **2.4**) were synthesised in 35%, 19% (estimated maximum) and 24% yield respectively. It was found that the steric bulk of the isopropyl group of L-valine made it difficult to prepare precursor compounds in acceptable yields and was therefore not pursued. Of the three rotaxanes synthesised only useful amounts of glycine rotaxane **2.1** and L-phenylalanine rotaxane **2.4** were produced.

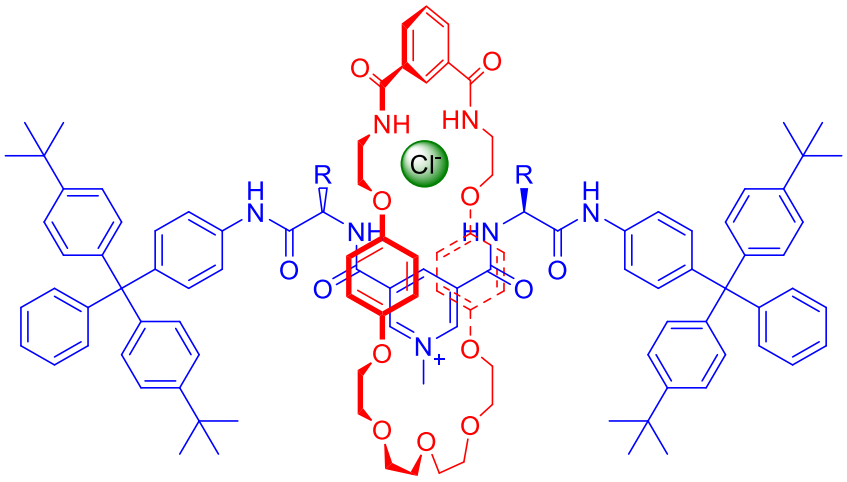

Figure 2.24 – Chloride templated rotaxanes that were investigated in this chapter (2.1 – R = H, 2.2 – R = Me, 2.3 – R = ^{i}Pr, 2.4 – R= CH_2Ph)

Glycine rotaxane **2.1,** L-phenylalanine rotaxane **2.4** and L-phenylalanine axle **2.24** were then exchanged to the hexafluorophosphate salts and titrated with enantiopure *R* and *S* TBA mandelate, which was followed by ^{1}H NMR spectroscopy. As expected glycine rotaxane **2.1** had no enantioselectivity for either enantiomer, suggesting that the method used for the titration could be used to detect if chiral L-phenylalanine rotaxane **2.4** or axle **2.24** could demonstrate enantioselective behaviour. Unfortunately L-phenylalanine rotaxane **2.4** and axle **2.24**

demonstrated enantioselectivities (K_{fav}/K_{disfav}) of 1.1 and 1.2 respectively, suggesting that neither compounds can be considered enantioselective for the enantiomers of *R* and *S* mandelate.

The most logical future work on this project should first investigate the synthesis and purification of useful amounts of pure L-alanine rotaxane **2.2**, as well as the synthesis of analogous rotaxanes containing other amino acid moieties. However, from the literature precedent[16] and the results in this chapter a more effective option may be to introduce a chiral element into the macrocyclic element of the rotaxane. The rotaxanes synthesised in this chapter as well as any future rotaxanes developed, should then be titrated with both enantiomers of a variety of enantiopure anions, to determine if these rotaxanes have enantioselectivity towards other anions.

2.7. References

[1] J.A. Wisner, P.D. Beer, M.G.B. Drew and M.R. Sambrook, *J. Am. Chem. Soc.*, 2002, **42**, 12469-12476.

[2] L. M. Hancock and P. D. Beer, *Chem. - A Eur. J.*, 2009, **15**, 42–44.

[3] M. J. Langton and P. D. Beer, *Acc. Chem. Res.*, 2014, **47**, 1935–1949.

[4] V. A. Davankov, *Chirality*, 1997, **9**, 99–102.

[5] N. H. Evans, *Chem. Eur. J.*, 2018, **24**, 3101–3112.

[6] E. M. G. Jamieson, F. Modicom and S. M. Goldup, *Chem. Soc. Rev.*, 2018, **47**, 5266-5311.

[7] R. Mitra, M. Thiele, F. Octa-Smolin, M. C. Letzel and J. Niemeyer, *Chem. Commun. Chem. Commun*, 2016, **52**, 5977–5980.

[8] J. Y. C. Lim, I. Marques, V. Félix and P. D. Beer, *J. Am. Chem. Soc.*, 2017, **139**, 12228–12239.

[9] J. Y. C. Lim, I. Marques, V. Félix and P. D. Beer, *Angew. Chemie Int. Ed.*, 2018, **57**, 584–588.

[10] L.M. Hancock, DPhil Thesis, Anion-Templated Synthesis of Functional Interlocked Architectures, 2011.

[11] K.-Y. Ng, V. Felix, S. M. Santos, N. H. Rees and P. D. Beer, *Chem. Commun.*, 2008, **0**, 1281.

[12] F. Rob, H. J. Van Ramesdonk, W. Van Gerresheim, P. Bosma, J. J. Scheele and J. W. Verhoeven, *J. Am. Chem. Soc.*, 1984, **106**, 3826–3832.

[13] L. C. Gilday, N. G. White and P. D. Beer, *Supramol. Chem.*, 2016, **28**, 62–83.

[14] C. R. Allen, P. L. Richard, A. J. Ward, L. G. A. van de Water, A. F. Masters and T. Maschmeyer, *Tetrahedron Lett.*, 2006, **47**, 7367–7370.

[15] M.J. Hynes, *J. Chem. Soc., Dalton Trans.,* 1993, 311-312.

[16] J. Y. C. Lim, I. Marques, V. Félix and P. D. Beer, *J. Am. Chem. Soc.*, 2017, **139**, 12228–12239.

Chapter 3

Investigations into the Synthesis and Separation of Chloride Templated Mechanically Chiral Interlocked Molecules

3.1. Introduction

3.1.1. Mechanical Chirality in Interlocked Molecules

Interlocked molecules may be chiral through the incorporation of classically chiral elements, such as a tetrahedral carbon atom with four inequivalent substituents (like the rotaxanes developed in Chapter Two). Mechanically interlocked molecules may also be chiral by virtue of another, less explored type of chirality, namely *mechanical chirality*.

Mechanical chirality in rotaxanes and catenanes arises from the interlocked components possessing directionality. In rotaxanes this is achieved by making the two ends of the axle component inequivalent giving the axle a direction (represented by the grey arrow Fig. **3.1**). In addition, the macrocyclic component is rotationally asymmetric, *i.e.* the macrocycle has either a clockwise or anti-clockwise direction depending on whether it is viewed from above or below a plane. This is similar to how a spinning wheel can be observed to be rotating clockwise or anti-clockwise direction depending on the view of the observer. (The observed direction of the macrocycle can be represented by a set of coloured arrows in a cycle Fig. **3.1**)

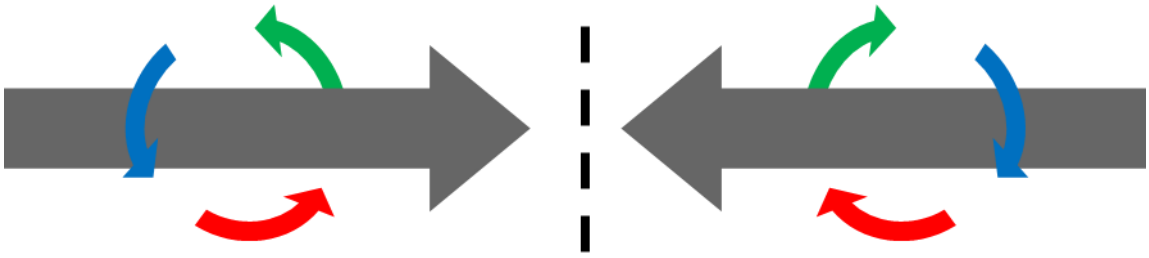

Figure 3.1 – A schematic of a pair of enantiomers of a mechanically chiral rotaxane. The axle component is represented by the grey arrow and the macrocycle component is represented by the coloured arrows.

Individually the macrocyclic and axle components are achiral. However, when the two components are combined the result is a chiral molecule. This is because, when the axle is passed through the rotationally asymmetric macrocycle, the direction of the macrocycle is defined by whichever face of the plane of the macrocycle the axle has passed through. If the axle has passed through the clockwise face of the plane one enantiomer has formed and a second enantiomer is formed when the axle has passed through the anticlockwise face.

Mechanically chiral catenanes may be thought of in an analogous manner. However, instead of the axle a second rotationally asymmetric macrocycle is used (represent by the grey arrow in Fig. **3.2**). Like the axle this second macrocycle is still used to define the direction of the original macrocycle (represented by the multi-coloured arrows in Fig. **3.2**). As the first macrocycle can have a clockwise or anticlockwise direction, relative to the second macrocycle, resulting in a pair of enantiomers.

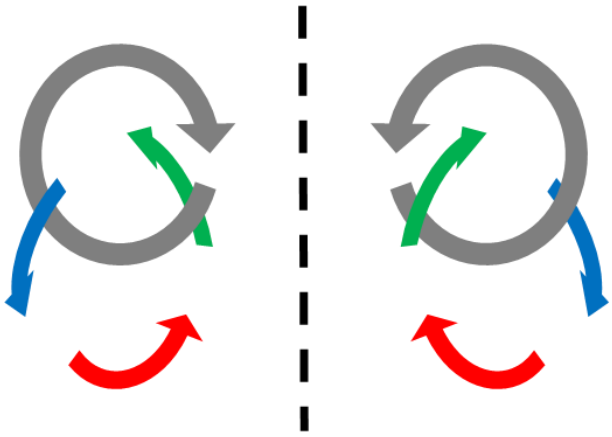

Figure 3.2 – A schematic of a pair of enantiomers of a mechanically chiral catenane. The first macrocycle component is represented by the coloured arrows and the second component is represented by the grey arrow.

Mechanically chiral rotaxanes and catenanes have previously been synthesised by a number of groups.[1–5] However, there are few literature examples of mechanically chiral interlocked molecules where one enantiomer has been formed in an enantiomeric excess or examples where the enantiomers of the interlocked molecule have been separated; a key feature if the

chiral properties of these rotaxanes is to be exploited. As far as we were aware at the start of this work, the highest published enantiomeric excess achieved in the stereoselective synthesis of a mechanically chiral rotaxane was only 4.4% for a rotaxane by Takata and co-workers, using an ammonium templated synthesis that is stoppered with achiral phosphine catalysed esterification.[5]

More recent work by Bordoli and Goldup have demonstrated that it is possible to achieve enantiopure samples of mechanically chiral rotaxanes, without using chiral HPLC, by separation of diastereomeric rotaxanes, that subsequently have the chiral derivatising agent removed. This was achieved by using a CuAAC (copper click) active metal templated synthesis to bring together and couple axle the component, macrocycle and enantiopure chiral stopper together to form a pair of rotaxanes as a 1:1 mixture of diastereomers (Fig. **3.3**). These diastereomers could be separated by column chromatography, the chiral stopper exchanged with an achiral stopper, revealing enantiopure samples of a mechanically chiral rotaxane.[2]

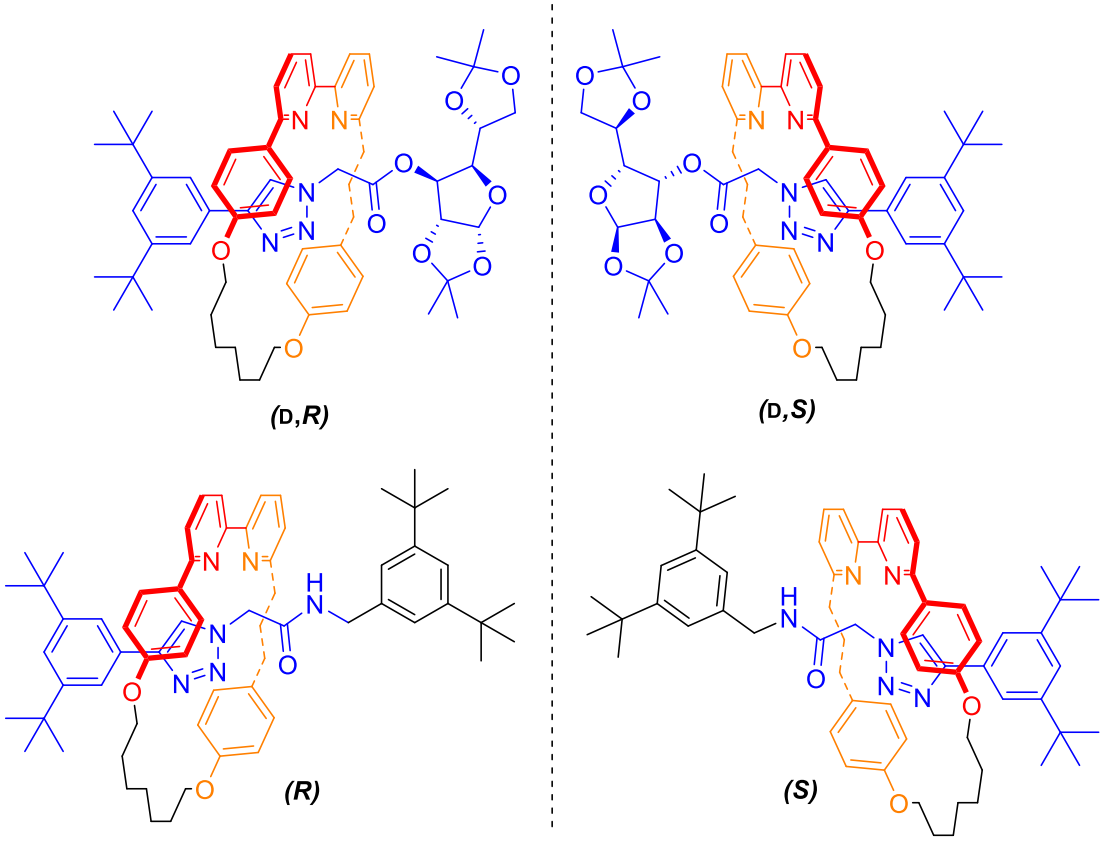

Figure 3.3- Both diastereomers and enantiomers of Goldup and Bordoli's mechanically chiral rotaxanes

3.1.2. Chapter Aims

In this chapter we are targeting the synthesis and resolution of a mechanically chiral rotaxane and catenane on the preparative scale without the use of a covalently attached enantiopure chiral auxiliary. If sufficient quantities of enantiopure rotaxane and/or catenane are accessed, NMR titrations will be undertaken to ascertain their enatioselctivity towards chiral anions.

The strategy to be pursued is illustrated in full for rotaxane **3.1** (Fig. **3.4**) below. Rotaxane **3.1** will be prepared by the same chloride templated rotaxane synthesis used in Chapter 2, but using an asymmetric axle **3.2** and asymmetric macrocycle precursor **3.3**. The resulting racemate will then be exchanged for an enantiopure chiral counter anion, to form a diastereomeric salt. It is anticipated that either column chromatography or crystallisation will allow for separation of the

diastereomers. Exchanging back to an achiral counter anion will reveal samples of the mechanically chiral rotaxane.

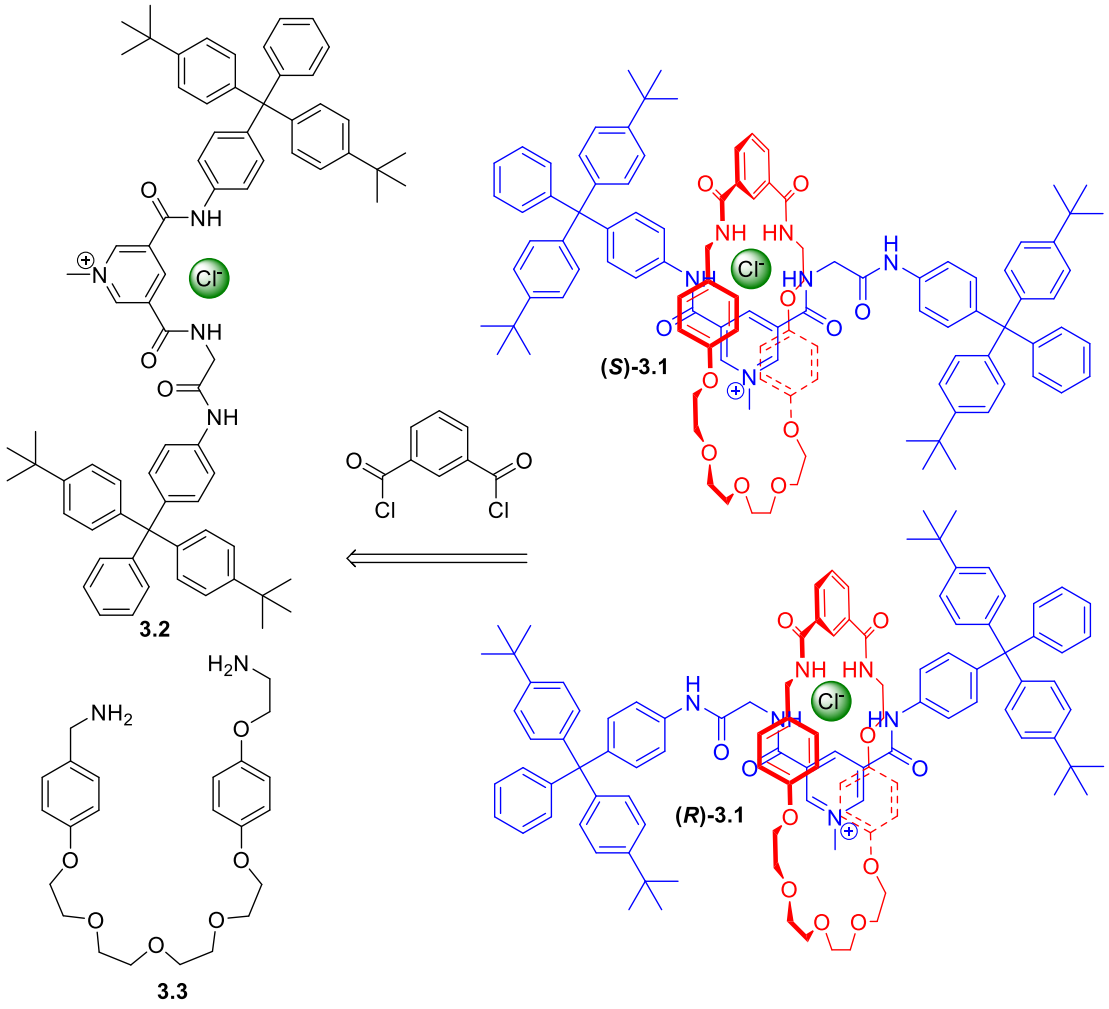

Figure 3.4 – Proposed chloride templated synthesis of rotaxane 3.1

An equivalent strategy will be used to prepare the catenane **3.4**. This will involve using an adaption of the rotaxane template strategy first developed by Beer *et al*.[6,7]

3.2. Precursor Synthesis

3.2.1. Axle Synthesis

The first attempt to synthesise axle **3.2** is shown in Fig. **3.5**. 3,5-Pyridinedicarboxylic acid was doubly esterified by refluxing overnight in MeOH with concentrated sulfuric acid. After extraction of the basified reaction mixture,, the product, di-ester **3.5** was isolated in 75% yield.[8] Di-ester **3.5** was then stirred with 1.1 equivalents of potassium hydroxide in MeOH overnight.

After work up mono-ester **3.6** was isolated by vacuum filtration in 72% yield.[8] The carboxylic acid of mono-ester **3.6** was then activated with oxalyl chloride and reacted with glycine methyl ester hydrochloride and NEt_3 in CH_2Cl_2. After stirring for three hours the reaction mixture was submitted to an aqueous work up, followed by column chromatography. Compound **3.7** was isolated in 33% yield, which while disappointing (in hindsight the hygroscopic glycine methyl ester hydrochloride may have been wet), sufficient material was in hand to continue the next step of the synthesis.

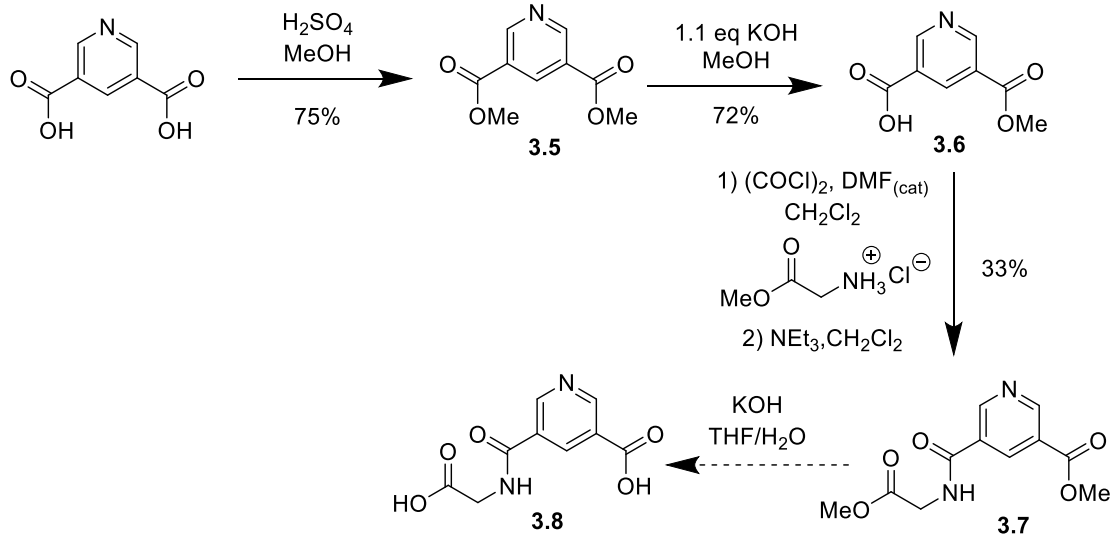

Figure 3.5 – First attempt at the synthesis of axle 3.3

Compound **3.7** and KOH were then dissolved in a THF and water, then stirred overnight. The solution was neutralised with 10% citric acid and extraction of the product attempted with CH_2Cl_2. However, no product was found in the organic phase. It is hypothesised that compound **3.8** is water soluble owing to the three ionisable sites present in the molecule. An attempt was made to precipitate out compound **3.8** by adding ammonium chloride. However, this was unsuccessful and therefore a new route was needed (Fig. **3.6**)

A more successful route was then developed, following a literature procedure for the first two steps (Fig. **3.6**).[9] Mono-ester **3.6** was activated with oxalyl chloride, was reacted with stopper **2.25** (Chapter 2) and triethylamine. The product was purified by an aqueous work up and then column chromatography to yield compound **3.9** in 57% yield. The protecting methyl ester group

on compound **3.9** was then removed by hydrolysis with potassium hydroxide in THF. The mixture was carefully acidified, and the compound **3.10** extracted, being isolated in 84% yield. The carboxylic acid group of compound **3.10** was then activated with oxalyl chloride and then coupled to glycine-amine stopper **2.28** (Chapter 2) in the presence of NEt_3. The crude mixture was then submitted to an aqueous work up followed by column chromatography to afford compound **3.11** in 46% yield. Methylation of compound **3.11** using MeI, was then followed by anion exchange by repeated washing of a chloroform solution of the methyl iodide salt with 1 mol dm^{-3} ammonium chloride, axle **3.2** was isolated in 96% yield.

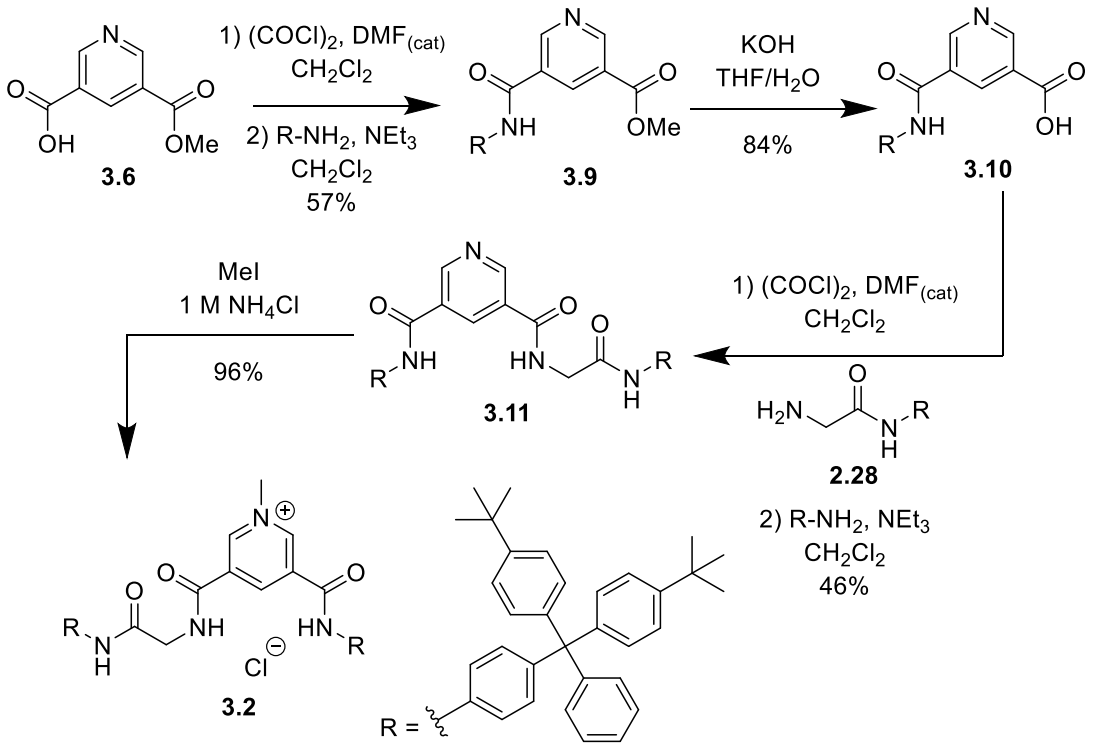

Figure 3.6 – Synthesis of the chloride salt of axle 3.2

3.2.2. Macrocycle Precursor Synthesis

Novel macrocycle precursor, bis-amine **3.3**, was prepared in a high yielding five step procedure (Fig. **3.7**). Monotosylate **3.12** was prepared in 80% yield by reacting a large excess of tetraethylene glycol with tosyl chloride.[10] Mono-tosylate **3.12** was then dissolved in MeCN and refluxed for 48 hours with 4-cyanophenol in the presence of potassium carbonate. Excess potassium carbonate was removed by filtration and the solvent removed. The resulting solid

was dissolved in CH_2Cl_2 and subject to an aqueous work up to afford compound **3.13** in 93% yield. Compound **3.13**, tosyl chloride, NEt_3, and catalytic DMAP were then dissolved in CH_2Cl_2 and stirred overnight. The solution was subject to an aqueous work up to afford tosylate **3.14** in 97% yield. Tosylate **3.14** was then refluxed with previously prepared compound **2.12** (Chapter 2) in MeCN in the presence of K_2CO_3 overnight. The excess K_2CO_3 was removed by filtration and the solvent was removed to afford a brown oil. The oil was then dissolved in CH_2Cl_2 and purified by dissolving the oil in Et_2O and removing any precipitate by filtration. The filtrate was collected, and the solvent removed to afford bis-nitrile **3.15** in 94% yield. Bis-amine **3.3** was produced by reducing bis-nitrile **3.15** with borane in THF. After quenching excess borane and work up the amine was isolated in 92% yield.

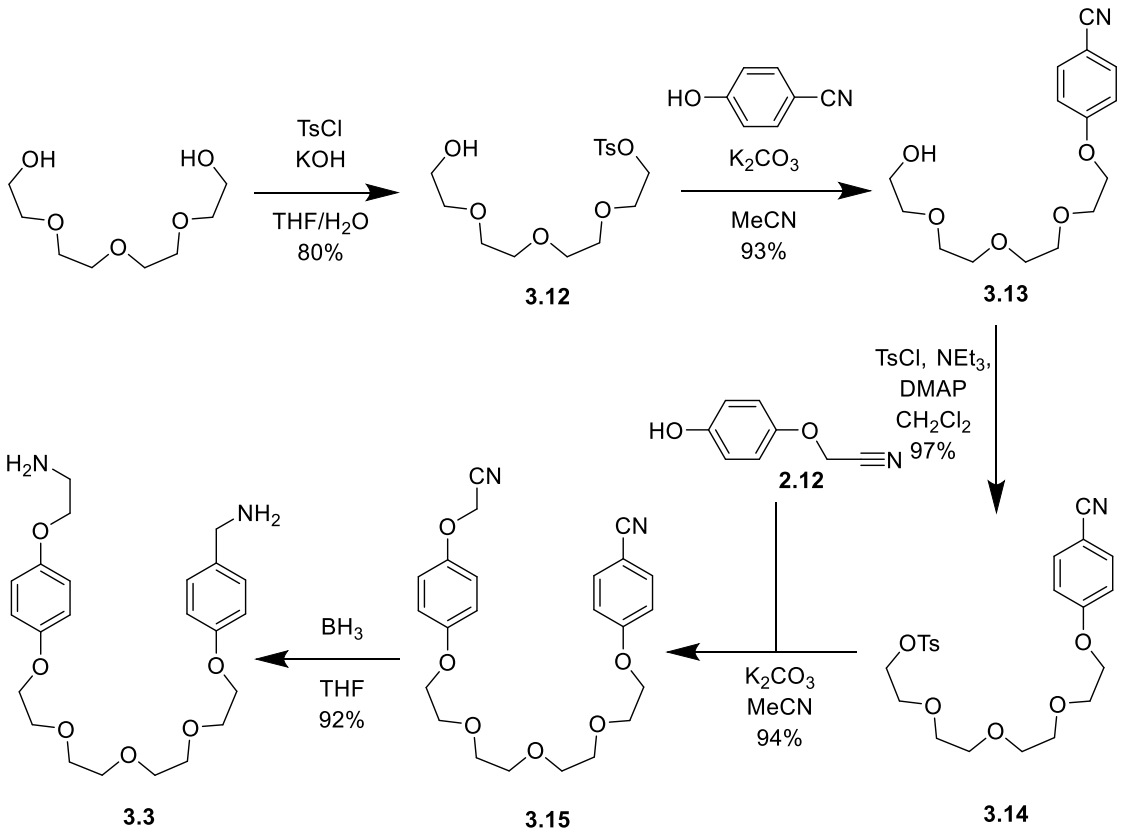

Figure 3.7 – Synthesis of macrocycle precursor bis amine 3.3

To aid subsequent characterisation a portion of bis-amine **3.3** was reacted on to form macrocycle **3.16** (Fig. **3.8**). Bis-amine **3.3** was dissolved in CH_2Cl_2 with pyridinium chloride template **2.19** (Chapter 2), then stirred for 30 minutes. NEt_3 was added, followed by the

dropwise addition of isophthaloyl chloride in CH_2Cl_2. The solution was stirred for a further hour, then purified using an aqueous work up, followed by column chromatography and trituration with MeOH, to afford macrocycle **3.16** in 30% yield.

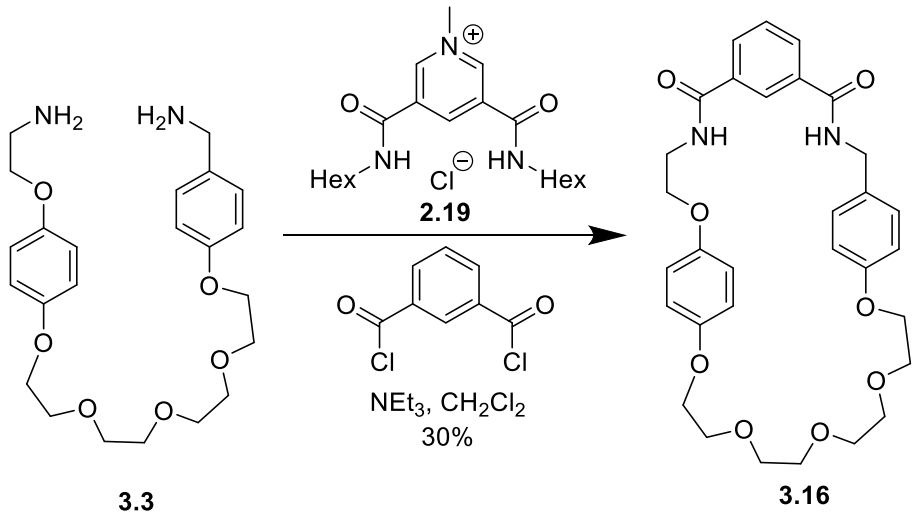

Figure 3.8 – Synthesis of asymmetric macrocycle 3.16

3.3. Synthesis and Investigations into Separating the Enantiomers of Rotaxane 3.1

3.3.1. Synthesis of the Enantiomers of Rotaxane 3.1

Rotaxane **3.1** was synthesised by using a method analogous to a chloride templated synthetic method developed by Beer *et al* (Fig. **3.9**).[6] Axle **3.2** and macrocycle precursor **3.3** were dissolved in CH_2Cl_2, NEt_3 was added followed by the dropwise addition of isophthaloyl chloride. The reaction was stirred for one hour, then submitted to an aqueous work up. Numerous attempts were made to purify rotaxane **3.1**, various solvent eluents were tried using both flash column chromatography and prep TLC. However, as with the chloride templated rotaxanes **2.1** and **2.4** (Chapter 2), residual macrocyclic impurities still contaminated the rotaxane. The most successful technique for purifying rotaxane **3.1** was the same used to purify the chloride templated rotaxanes **2.1** and **2.4** (Chapter 2). The majority of the impurities contaminating rotaxane **3.1**, were removed by column chromatography, the fractions containing rotaxane **3.1** were then combined and the solvent removed.

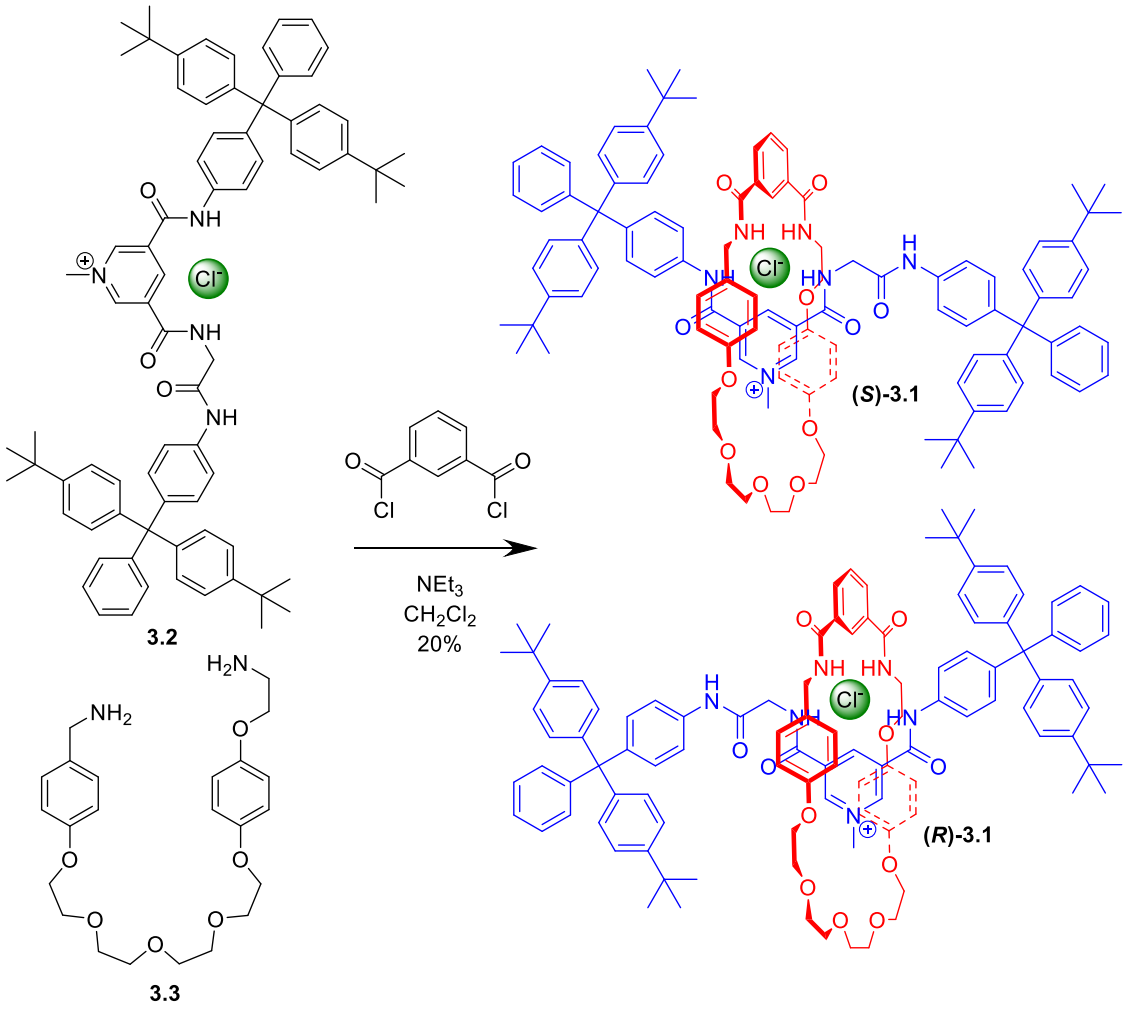

Figure 3.9 – Synthesis of both enantiomers of rotaxane 3.1

The residue containing rotaxane **3.1** was then dissolved in CH_2Cl_2 and washed multiple times with $(NH_4)_2SO_{4(aq)}$. The sulfate salt of rotaxane **3.1**, contaminated with residual macrocyclic impurities was then loaded onto a plug of silica and washed with 94:6 CH_2Cl_2:MeOH, any rotaxane **3.1** that had not exchange to the sulfate salt was also flushed off and collected. Once all macrocyclic impurities had been removed the portion of rotaxane **3.1** that remained as the sulfate salt was flushed off with a solution of NH_4Cl in 85:15 CH_2Cl_2. The solvent was removed and the solid was dissolved in CH_2Cl_2, the solution was washed with 1 mol dm^{-3} NH_4Cl, then the organic layer was collected and the solvent removed, to produce the racemate of rotaxane **3.1** in 15% yield. The procedure was repeated on the portion of rotaxane **3.1** that did not exchange to the sulfate salt, to produce a further amount of rotaxane **3.1**, with a combined yield of 20%.

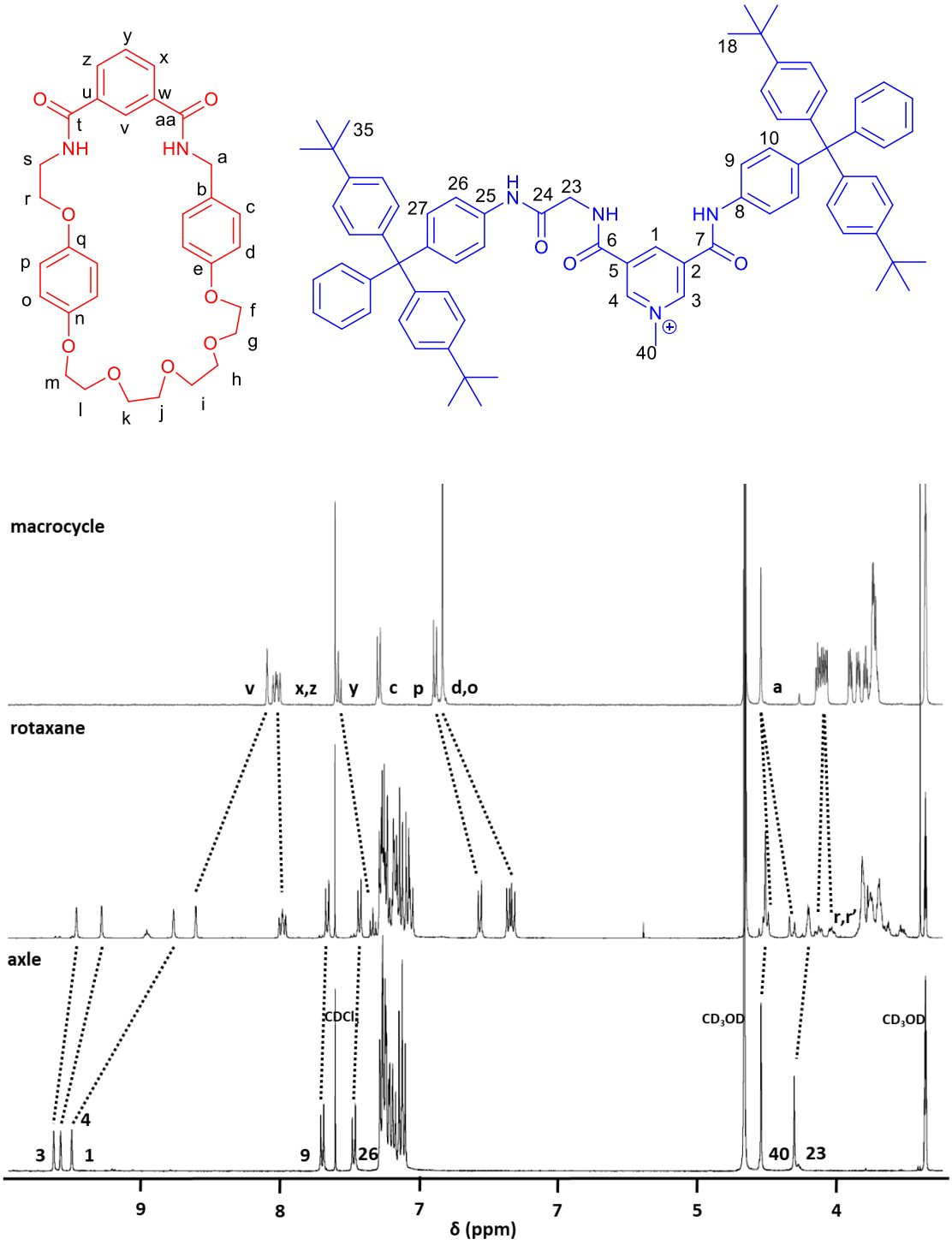

Figure 3.10 – ^{1}H NMR of rotaxane 3.1, axle 3.2 and macrocycle 3.16 (400 MHz, 298 K, 1:1 $CDCl_3$:CD_3OD, assigned with assistance from Dr Geoffrey Akien)

Rotaxane **3.1** was characterised by NMR and IR spectroscopies and mass spectrometry. The molecular ion for the rotaxane at 1661.8743 Da ($[M]^+$ predicted at 1161.8775) was identifiable in the mass spectrum. Inspection of the ^{1}H NMR spectrum (Fig. **3.10**) also provides evidence for

the sucessful formation of interlocked rotaxane **3.1**. Significant changes in the chemical shift of the protons of rotaxane **3.1** were observed, when compared to axle **3.2** and macrocycle **3.16**. Macrocycle protons d, o and p can be observed to have shifted upfield, attributed to π-π stacking between electron rich π systems on the macrocycle and electron difficient pyridinium group on the axle. In addition, protons 1,3 and 4 can be observed to have shifted upfield, indicating that these protons now reside within the macrocycle cavity and participiate in the π-π stacking. This effect is more pronounced on protons 4 than 3, suggesting that the macrocycle may reside slightly less over protons 3, owing to their close proximity to the bulky axle stopper groups.

In addition macrocycle -CH_2- protons a and r are observed to demonstrate diasterotopic behaviour, thought to be due to the rigidity of the macrocycle preventing the rotation of the –CH_2- groups. This causes the individual protons of a and r to observed different parts of the axle, resulting in the protons becoming diasterotopic.

A ^{1}H ROESY was taken of rotaxane **3.1** (Fig. **3.11**), this showed that the positon of the macrocycle on the axle was similar to that of other chloide templated macrocycles. A cross peak can be seen between macrocycle protons f-m, corresponding to the polyether -OCH_2- groups and axle protons 40 (Fig. **3.11** – 4). In addition a cross peak can be seen between macrocycle proton v and axle proton 1 (Fig. **3.11** – 1)., as well as cross peaks between macrocycle protons c,d,p and o with axle protons 3 and 4 (Fig. **3.11** – 2) and o,p with 40 (Fig. **3.11** – 3).These cross peaks suggests that the macrocycle is residing over the pyridium moeity on the axle and not over the glycine moeity, as is typical with chloride templated rotaxanes with this motif.

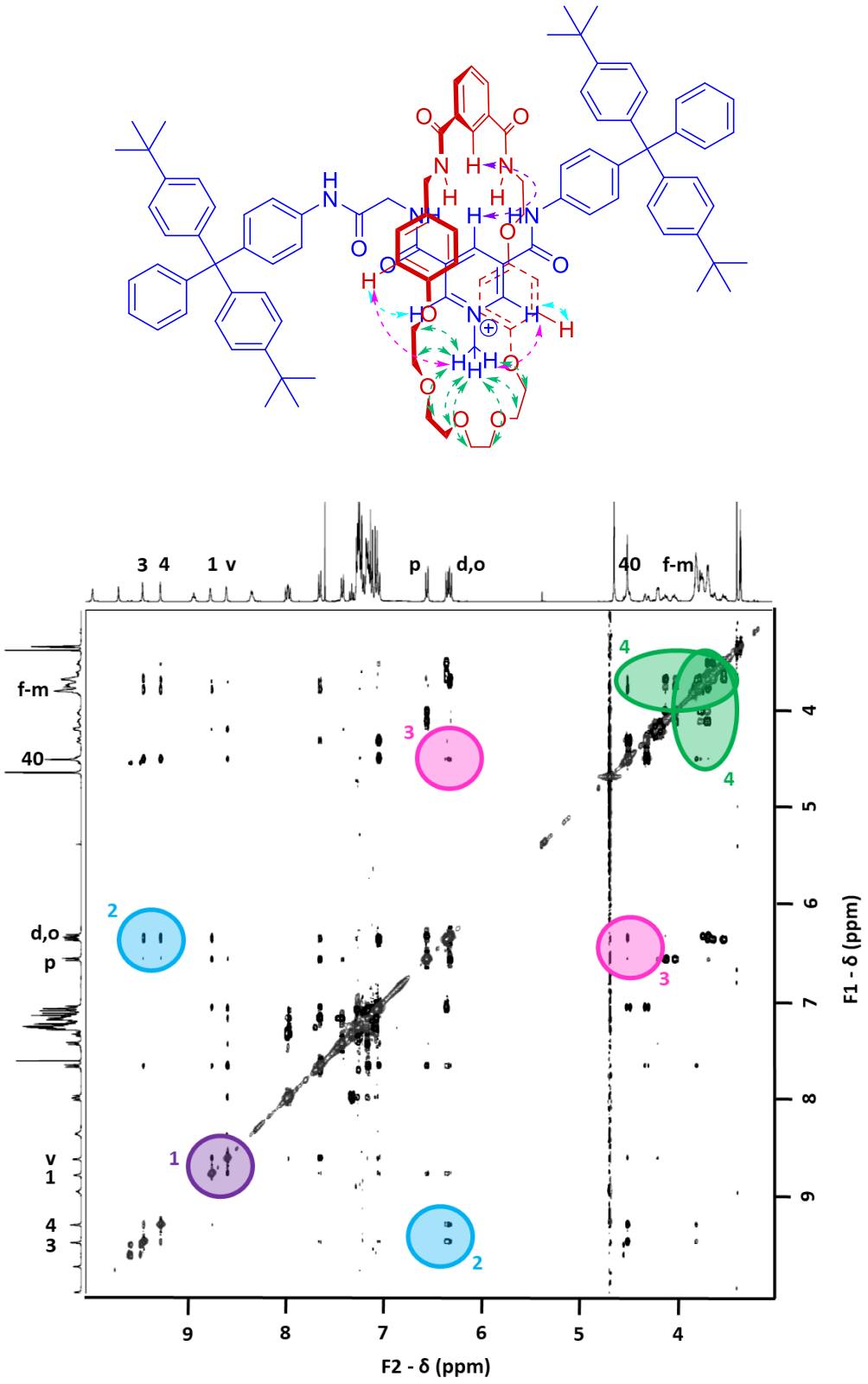

Figure 3.12 – ^{1}H ROESY NMR of rotaxane 3.1 (400 MHz, 298 K, 1:1 $CDCl_3$:CD_3OD, chloride counter anion omitted from structure for clarity, arrow colour corresponds to the highlighted cross peak of the same colour)

3.3.2. Investigating the Separation of the Enantiomers of Rotaxane 3.1

With rotaxane **3.1** isolated as a racemate, attempts to separate the enantiomers of rotaxane **3.1** could proceed. First, the chloride anion was exchanged to three different enantiopure anions, O'O'dibenzoyl-L-tartrate (rotaxane **3.1-b**), L-tartrate (rotaxane **3.1-c**) and (*1R*)-(-)-10 camphorsulfonate (rotaxane **3.1-d**) salts. This was accomplished by washing samples of rotaxane **3.1** in CH_2Cl_2 repeatedly with 0.2 mol dm^{-3} aqueous solutions of the respective enantiopure anions, then with deionised water. The exchange was verified by checking integrations in ^1H NMR spectra (Fig. **3.13**).

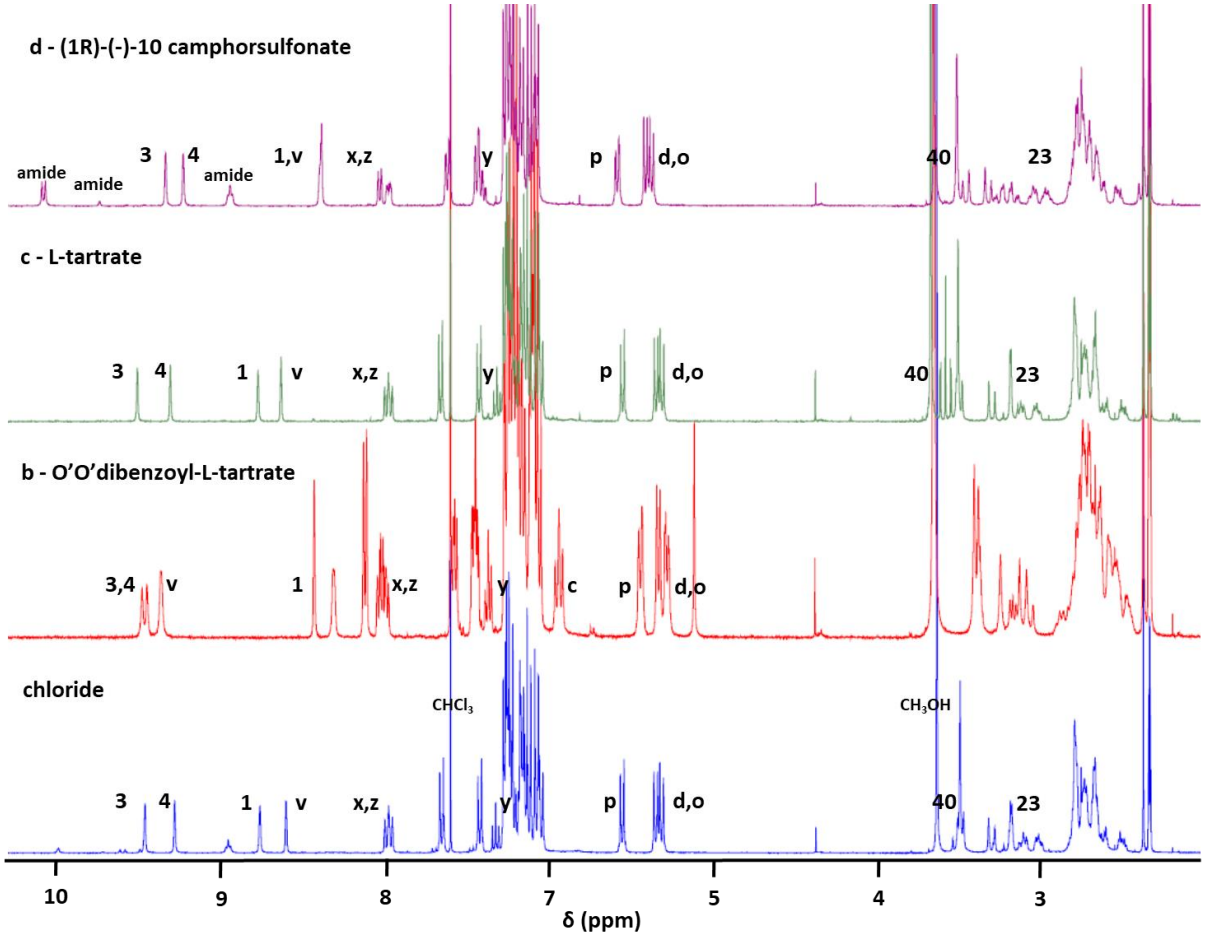

Figure 3.13 – ^1H NMR spectra of rotaxane 3.1, 3.1-b, 3.1-c, 3.1-d (400 MHz, 298 K, 1:1 $CDCl_3$:CD_3OD)

The ^1H NMR spectrum of rotaxanes **3.1-b** and **3.1-d**, indicated that these rotaxanes had changed anions, as there were significant perturbations in chemical shifts of the peaks, when compared

to rotaxane **3.1-a**. In addition amide peaks were seen to appear in rotaxane **3.1-d**. However, the ^{1}H NMR spectrum of rotaxane **3.1-c**, was near identical to rotaxane **3.1**, suggesting that rotaxane **3.1-c** is actually just the chloride salt.

To determine if the rotaxanes could be separated by silica gel chromatography, analytical TLCs of the three salts of rotaxane **3.1** (**3.1-b**, **3.1-c**, **3.1-d**) and the chloride salt rotaxane **3.1**, were run in various solvent eluents. The most promising mixture in the TLC analysis was 94:6 MeCN:MeOH with rotaxane **3.1-d**, as three spots could be observed on the TLC plate; these spots were attributed to the chloride salt, and one for each diastereomer. The R_f of **3.1-c**, was consistently the same as rotaxane **3.1**, this provides further evidence that rotaxane **3.1-c** is in fact the chloride salt.

Samples of rotaxane **3.1-b** and **3.1-d** were dissolved in various non-chlorinated solvents and attempts were made to separate the diastereotopic salts by crystallisation. A sample of rotaxane **3.1-d** was loaded on to a preparative TLC plate and run multiple times with 94:6 MeCN:MeOH, where three spots were observed. The material was recovered from the preparative TLC plate and the presence of rotaxane was confirmed by ^{1}H NMR spectroscopy. The samples were then washed with 1 mol dm^{-3} NH_4Cl followed by water. The optical rotations of the samples were then measured. The middle and lower bands were observed to have optical rotations of α_D = -7.5 and α_D = +7.5 (0.3 c, 3 mg ml^{-1}) respectively. As these optical rotations are of opposite sign and equal magnitude and were obtained from different bands on the preparative TLC, this strongly suggests that the enantiomers of rotaxane **3.1** have been separated. If appropriate chiral HPLC columns were available verification of the enantiopurity could be achieved.

The top band of the preparative TLC was also observed to have a negative optical rotation. This implies that there is a non-racemic mixture of the two positively charged rotaxane **3.1** enantiomeric components, This may be due to the (1*R*)-(-)-10 camphorsulfonate binding more strongly to one enantiomer of rotaxane **3.1**, this suggests that the rotaxane does demonstrate enantioselectivity.

3.4. Investigating the Synthesis and Separation of the Enantiomers of a Chloride Templated Mechanically Chiral Catenane

The terphenyl stoppers of the rotaxanes so far studied, are likely to interfere with the crystal packing of the interlocked molecule when attempting to grow single crystals. Lacking these groups analogous catenanes could therefore be grown as crystals more readily. As a mechanically chiral catenane can be prepared from the macrocycle precursor **3.3**, which was already in hand, a proof of principle synthesis of mechanically chiral catenane **3.4** was embarked upon (Fig. **3.14**).

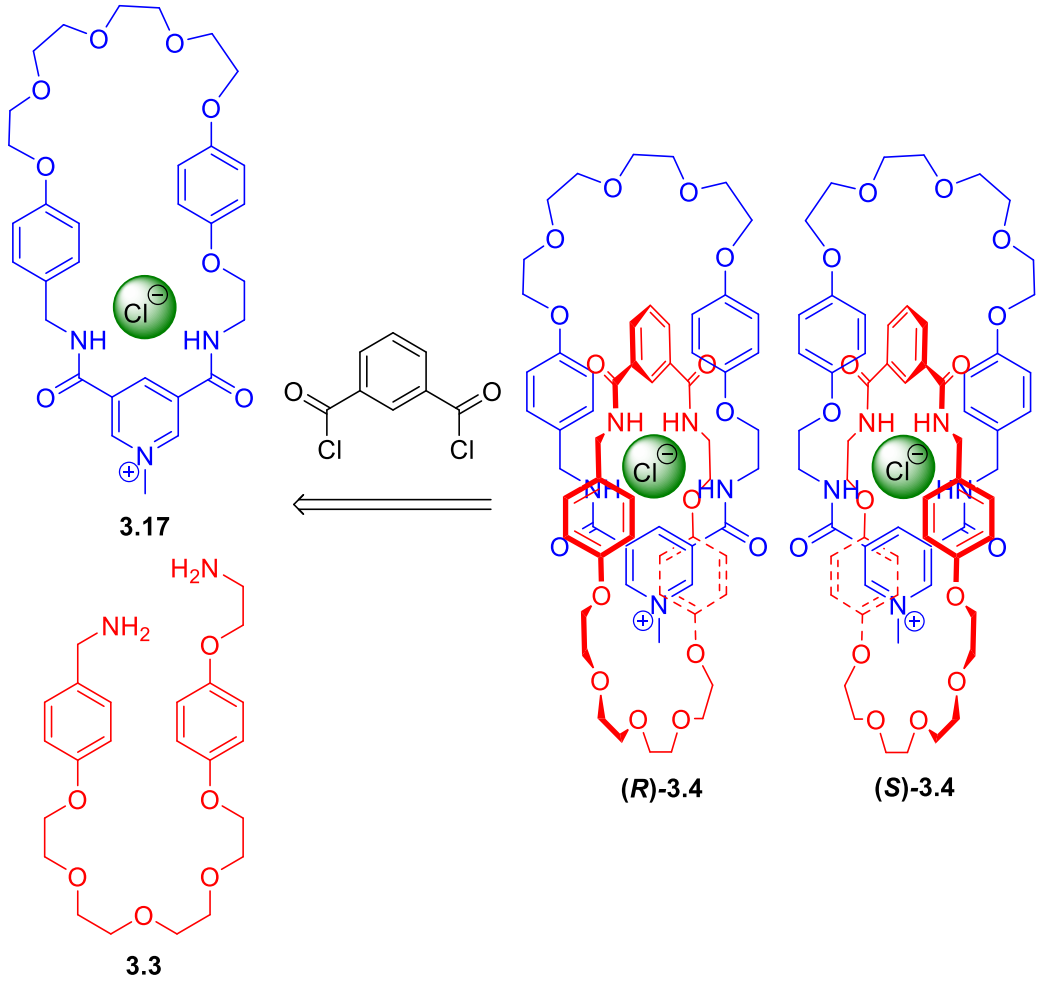

Figure 3.14 – Proposed synthesis of mechanically chiral catenane 3.4

3.4.1. Precursor Synthesis

With macrocycle precursor bis-amine **3.3** in hand, the only other precursor required was pyridinium macrocycle **3.17**. This was preparable in two step steps from bis-amine **3.3** following a procedure analogous to that used to prepare macrocycle **3.16** (Fig. **3.15**). Pyridine-3,5-dicarbonyl dichloride was prepared by refluxing pyridine-3-5-dicarboxylic acid in $SOCl_2$ with catalytic DMF. The excess $SOCl_2$ was removed and the residue dissolved in CH_2Cl_2, then added in a dropwise manner to a solution of bis-amine **3.3**, templating hexyl thread **2.19** (Chapter 2) and NEt_3 in CH_2Cl_2. The solution was purified using an aqueous work up and then flash column chromatography. It was found that pyridyl macrocycle **3.18** was contaminated by small amounts of hexyl thread **2.19**, so was purified again using flash column chromatography which removed more but not all of the hexyl thread, yielding pyridyl macrocycle **3.18** in a maximum possible yield of 28%. Pyridyl macrocycle **3.18** was then submitted to standard methylation conditions (MeI in $CHCl_3$ heated to 45 ^oC) to afford pyridinium macrocycle **3.17** as the iodide salt in quantitative yield, still containing small amounts of hexyl thread **2.19**. Pyridinium macrocycle **3.17** was not exchanged to the chloride salt, as literature precedent showed that this was unnecessary.[7]

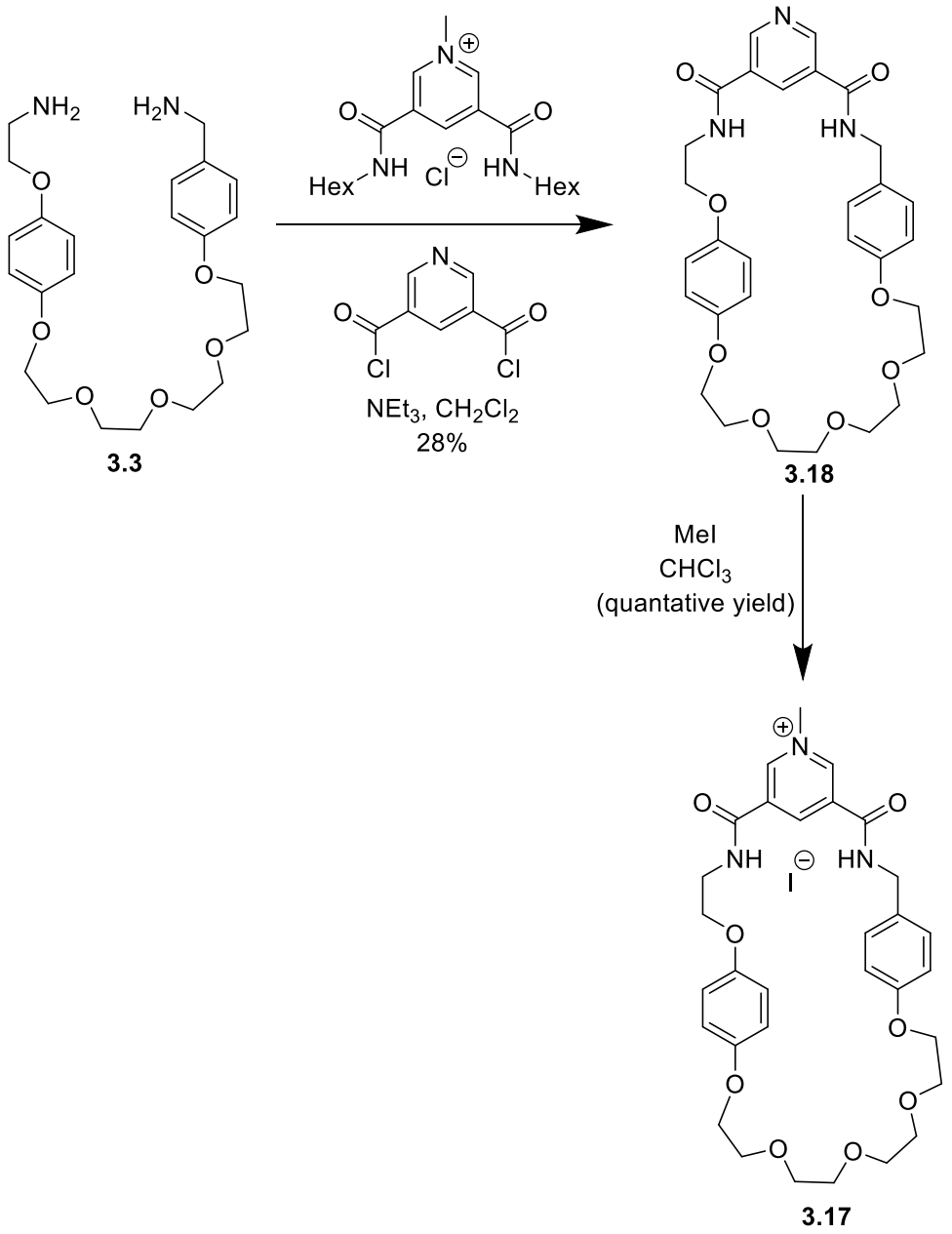

Figure 3.15 - Synthesis of pyridinium iodide macrocycle 3.17

3.4.2. Synthesis of a Chloride Templated Mechanically Chiral Catenane

Catenane **3.4** were prepared using a chloride templated clipping synthesis, in a similar manner to rotaxane **3.1**. Literature precedent suggests that despite iodide being the counter-anion of pyridinium macrocycle **3.17**, a chloride templated clipping synthesis is still possible; as the amide formation produces chloride anions, which may then act as a template allowing catenane formation.[7]

Pyridinium macrocycle **3.17** was combined with bis-amine **3.3** in CH_2Cl_2, NEt_3 was added followed by the dropwise addition of isophthaloyl chloride in CH_2Cl_2 (Fig. **3.16**). The solution was stirred for one hour, then submitted to an aqueous work up. The majority of the impurities were removed by silica flash column chromatography and the material further purified by preparative TLC, catenane **3.4** with some impurities was isolated in a maximum possible 10% yield. The compound was characterised by ^{1}H NMR spectroscopy and mass spectrometry, where the molecular ion was found at 1144.5128 Da ($[M]^+$ predicted at 1144.5125 Da).

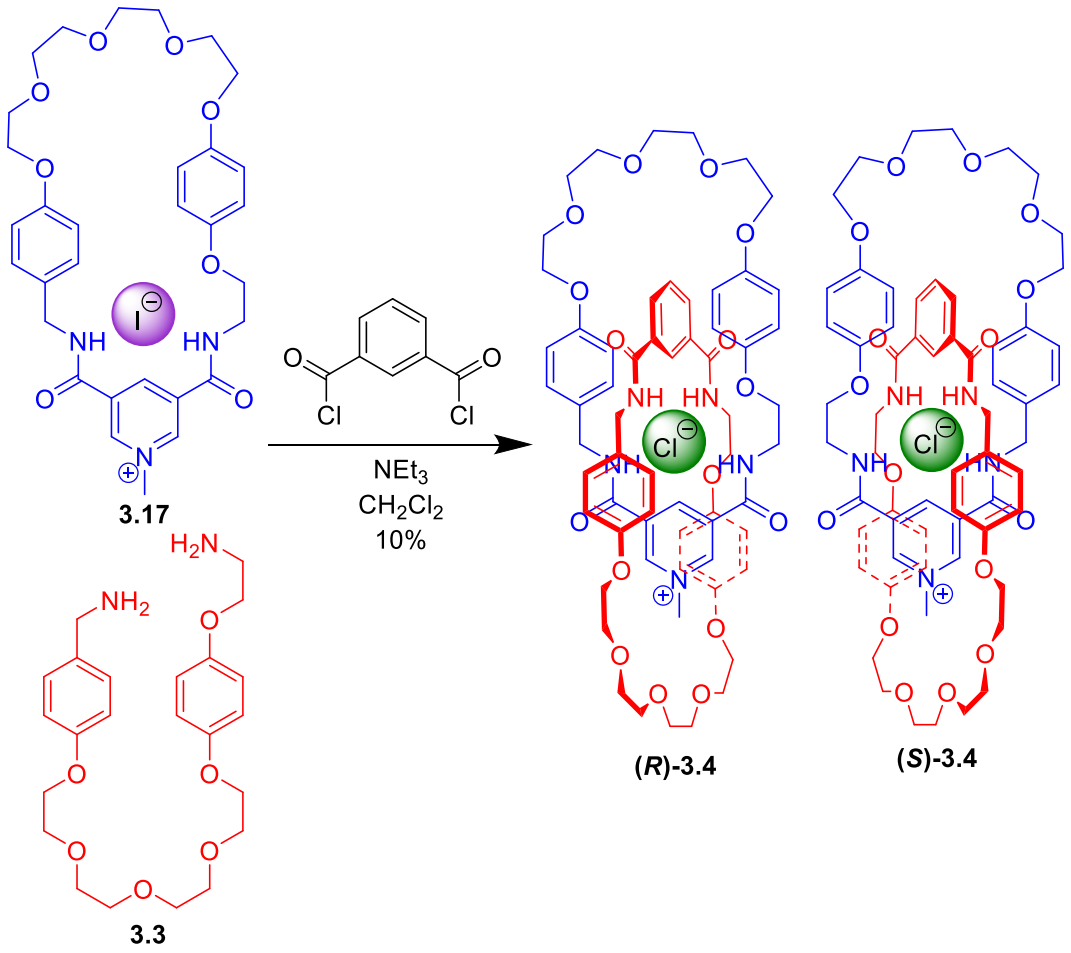

Figure 3.16 – Synthesis of mechanically chiral catenane 3.4

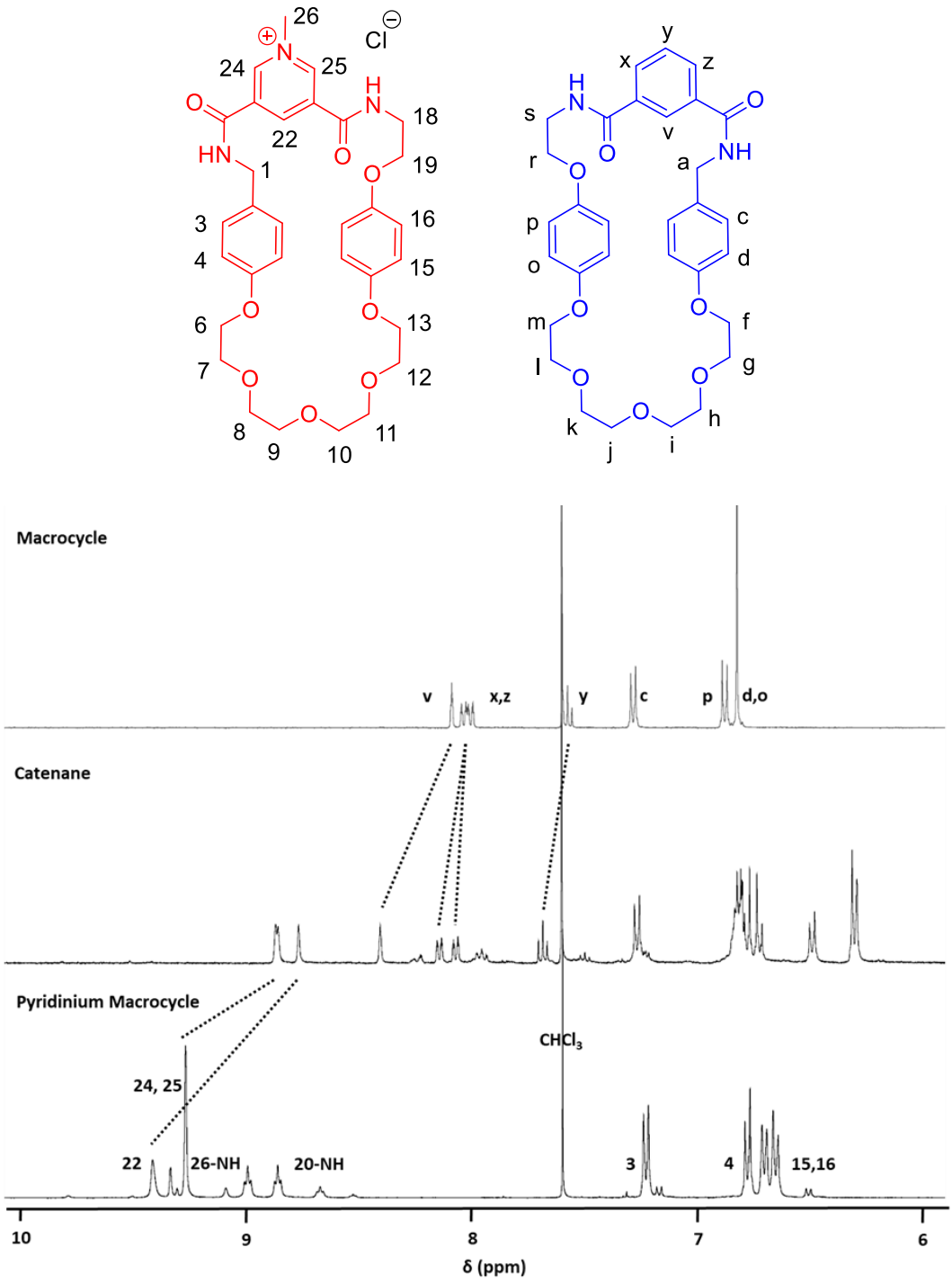

Figure 3.17 – ^{1}H NMR of macrocycle 3.16, catenane 3.4, and pyridinium macrocycle 3.17 (400 MHz, 298 K, 1:1 $CDCl_3$:CD_3OD)

Only peaks corresponding to the pyridinium and isopthalamide motifs of catenane **3.4** were able to be assigned due to the lack of material preventing a full analysis of the sample. ^{1}H NMR evidence (Fig. **3.17**) showed perturbations in all the aromatic proton peaks and integration of these peaks was consistent with formation of catenane **3.4**. A downfield shift of proton v from

neutral macrocycle **3.16** to catenane **3.4** is suggestive of hydrogen bonding between proton c and the templating chloride anion. The upfield shift of pyridinium peaks 22, 24 and 25 of pyridinium macrocycle **3.17** are attributed to the shielding effect due to presence of these compounds within the cavity of the macrocycle. Modest downfield shifts of isophthalamide protons x, y and z can also be observed.

3.4.3. Attempts to separate the enantiomers of catenane 3.4

With the 20 mg of impure catenane **3.4** available, only one attempt to separate the enantiomers of catenane **3.4** was possible. It was decided to attempt the separation of the two enantiomers by exchanging the chloride anion of catenane **3.4** for an enantiopure (1*R*)-(+)-10-camphorsulfonate, then attempt to recrystallise.

The chloride salt enantiomers of catenane **3.4** were dissolved in CH_2Cl_2, then washed with 8 × 1 mol dm^{-3} ammonium (1*R*)-(+)-10-camphorsulfonate and then with water. The solvent was removed and attempts were made to re-crystallise the resulting diastereomers from non-chlorinated solvents, to prevent exchange back to the chloride salt.

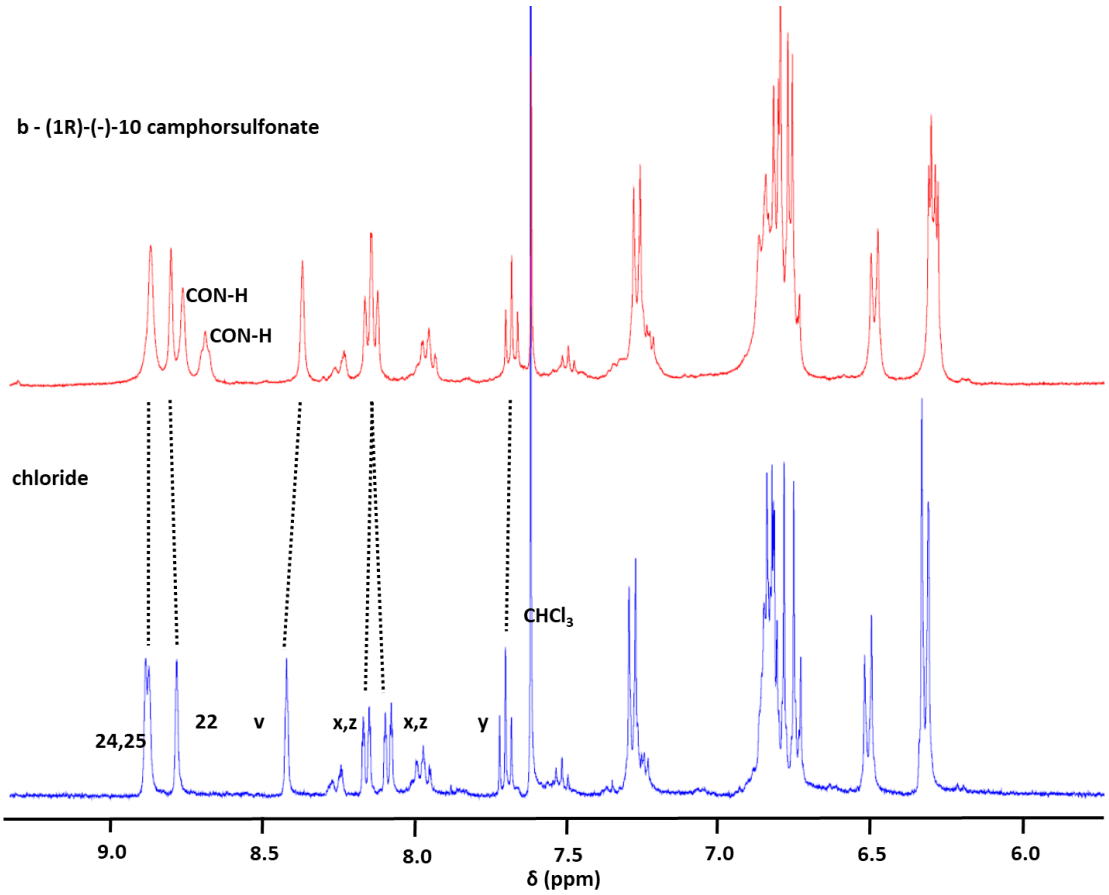

Figure 3.18 – ^{1}H NMR spectra of catenane 3.4 and 3.4-b (400 MHz, 298 K, 1:1 $CDCl_3$:CD_3OD)

The ^{1}H NMR spectra (Fig. **3.18**) showed changes in the chemical shifts and broadening of some of the previously identified peaks, indicating a change in the structure of catenane **3.4-b** when compared to catenane **3.4**. Protons x and z are observed to coalesce into a single peak and amide peaks are also observed. In addition new peaks are observed at a lower chemical shift, attributed to the protons of the camphorsulfonate anion, confirming that a change of anion has occurred.

Unfortunately, no useable crystals for x-ray structural determination have been produced so far. In the future, if more material is produced, it may be more effective to take a similar approach used to isolate the enantiomers of rotaxane **3.1**; where the templating chloride of catenane **3.4** is exchanged for an enantiopure chiral anion and then separated by chromatographic methods.

3.5. Conclusion

The synthesis of both a mechanically chiral rotaxane and catenane have both been achieved by chloride anion templation. Pure rotaxane **3.1** was synthesised in 20 % yield, using the same technique to purify chloride template rotaxanes **2.1** and **2.4** from Chapter 2, where the rotaxane was purified via the sulfate salt. Portions of rotaxane **3.1** were then taken and the templating chloride anion of rotaxane **3.1** was then exchanged for enantiopure (-)-O'O'dibenzoyl-L-tartrate (rotaxane **3.1-b**) and (*1R*)-(-)-10 camphorsulfonate anions (rotaxane **3.1-d**).

Investigations were then made to separate the enantiomers of rotaxanes **3.1-b** and **3.1-d** by chromatography. Initial screening was done by silica TLC, it was found that the (*1R*)-(-)-10 camphorsulfonate salt of rotaxane **3.1** (**3.1-d**) could be separated using 94:6 MeCN:MeOH. This solvent mixture was then successfully used to separate a larger amount of rotaxane **3.1-d** by silica preparative TLC. The two clean diastereomers of rotaxane **3.1-d** were exchanged back to the chloride salt, where the separation of the enantiomers of rotaxane **3.1-d** were confirmed by analysing the optical rotation of the two enantiomers, which were found to be α_D = -7.5 and α_D = +7.5. The opposite sign and same magnitude strongly suggests that the enantiomers were separated pure.

Future work on this project should focus on preparing more of rotaxane **3.1** and attempting to separate the enantiomers using on a larger scale. Once this is complete the chirality of the two enantiomers of rotaxane **3.1** should be probed using NMR titrations with a chiral anion to determine the enantioselectivity of the two enantiomers.

In addition, a proof of principle synthesis of mechanically chiral catenane **3.4** was attempted. Precursor compound pyridinium macrocycle **3.17** were obtained. Pyridinium macrocycle **3.17** was then used to successfully synthesise mechanically chiral catenane **3.4**, unfortunately catenane **3.4** was still contaminated with some impurities The templating chloride anion of catenane3.4 was exchanged to the (*1R*)-(-)-10 camphorsulfonate anion and attempts were made

to separate the enantiomers by crystallisation, although attempts to crystallise the enantiomers have so far been unsuccessful.

Future work on this project should be focused on synthesising a useful amount of catenane **3.4** and ensuring that it has been separated from any impurities. Once this has been completed further attempts should be made to separate the two enantiomers.

3.6. References

[1] N. Kameta, Y. Nagawa, M. Karikomi and K. Hiratani, *Chem. Commun.*, 2006, 3714-3716.
[2] R. J. Bordoli and S. M. Goldup, *J. Am. Chem. Soc.*, 2014, **136**, 4817–4820.
[3] D. K. Mitchell and J.-P. Sauvage, *Angew. Chemie Int. Ed. Engl.*, 1988, **27**, 930–931.
[4] C. Yamamoto, Y. Okamoto, T. Schmidt, R. Jäger, F. Vögtle, *J. Am. Chem. Soc.*, 1997, **119**, 10547-10548.
[5] Y. Makita, N. Kihara, N. Nakakoji, T. Takata, S. Inagaki, C. Yamamoto and Y. Okamoto, *Chem. Lett.*, 2007, **36**, 162–163.
[6] L. M. Hancock and P. D. Beer, *Chem. Eur. J.*, 2009, **15**, 42–44.
[7] L. M. Hancock, L. C. Gilday, N. L. Kilah, C. J. Serpell and P. D. Beer, *Chem. Commun.*, 2011, **47**, 1725–1727.
[8] K.N, Broadus, S.R. Kass, *J. Am. Chem. Soc.*, 2000, **122**, 9014-9018.
[9] L. M. Hancock and P. D. Beer, *Chem. Commun.*, 2011, **47**, 6012.
[10]K. D. Park, R. Liu and H. Kohn, *Chem. Biol.*, 2009, **16**, 763–772

Chapter 4

Investigations towards a Palladium Templated Enantioselective Rotaxane

4.1. Introduction

4.1.1. Palladium Templated Rotaxanes

Palladium templated pseudorotaxanes were first reported by Sauvage and co-workers in 2003 (Pseudorotaxane **4.1**, Fig **4.1**). These so-called '3+1' systems threaded a 2,6-pyridine thread through a tridentate terpyridyl macrocycle.[1]

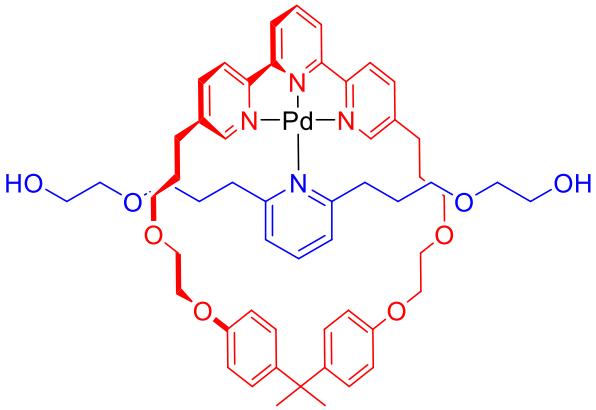

4.1

Figure 4.1 - Sauvage's 3+1 palladium (II) templated pseudorotaxane 4.1

Shortly afterwards Leigh and co-workers disclosed the results of investigations into the preparation of a fully interlocked Pd(II) templated rotaxanes.[2] The Pd(II) cation was able to template the synthesis of rotaxane **4.2** by clipping shut a tridentate 2,6-dicaroxyamido pyridine ligand around a 2,6-alkylether substituted pyridine axle in a high yield of 77%.

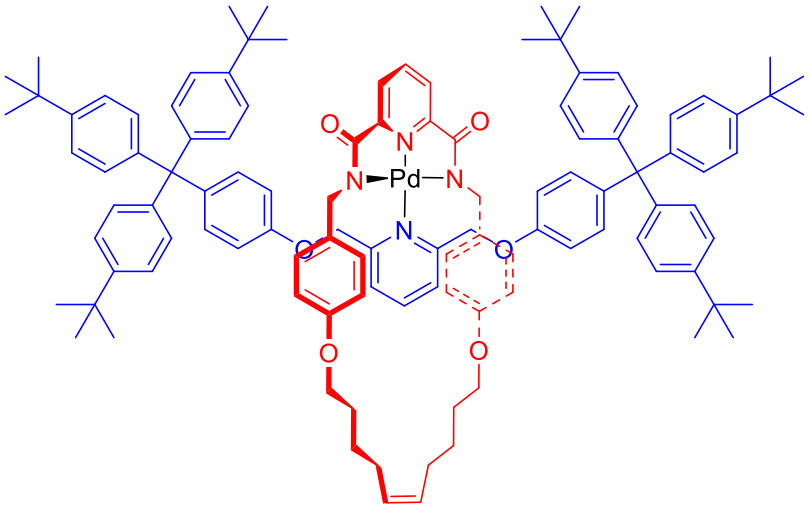

4.2

Figure 4.2 - Leigh's 2,6 pyridine axle palladium templated rotaxane 4.2

However, interlocked rotaxane was not observed when using a 3,5-substituted axle component. Crystal structures of failed rotaxane **4.3** revealed that in both cases the '3,5-axle' resides exclusively on one face of the macrocycle. Similar results were reported contemporaneously by Takata and co-workers.[3]

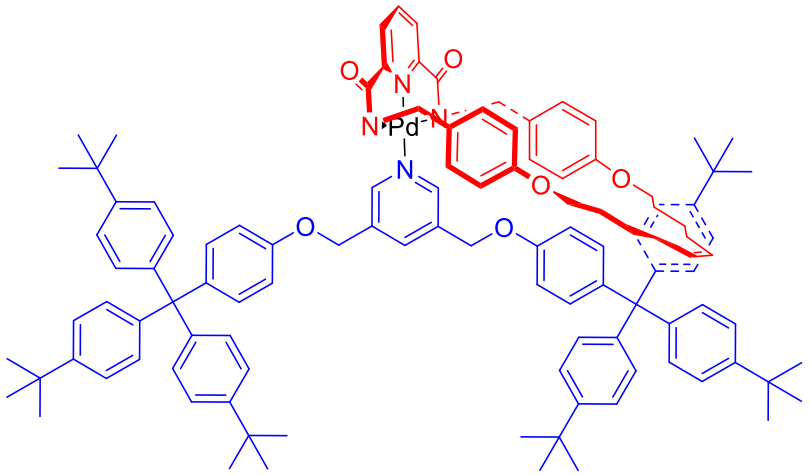

4.3

Figure 4.3 - Result of Leigh's unsuccessful 2,6-pyridine axle palladium templated rotaxane 4.3 synthesis

The authors attributed these results to the strained and crowded geometry around the palladium (II) caused by the 2,6-pyridine axle in failed rotaxane **4.3**. This geometry meant that

when the macrocycle was clipped shut, it was only possible to close the macrocycle around the axle, allowing rotaxane formation to occur; whilst the less strained and less crowded 3,5 pyridine axle, had sufficient space for the macrocycle to form on top of the axle. After this, to our knowledge, rotaxanes and catenanes using a palladium (II) templated motif with a pyridine acting as the only axle ligand have all used an axle with a 2,6 substituted pyridine axle.[4–8]

4.1.2. Chapter Aims

In this chapter, the first aim is to prove that a Pd(II) templated rotaxane may be synthesised using a 3,5-substituted pyridine axle component. To avoid the 'perching' issue previously observed, a small macrocycle will be used. It is anticipated that the rigidity of a small macrocycle will force the 3,5-substituted pyridine component to thread through, that upon stoppering will form a fully interlocked rotaxane **4.4**.

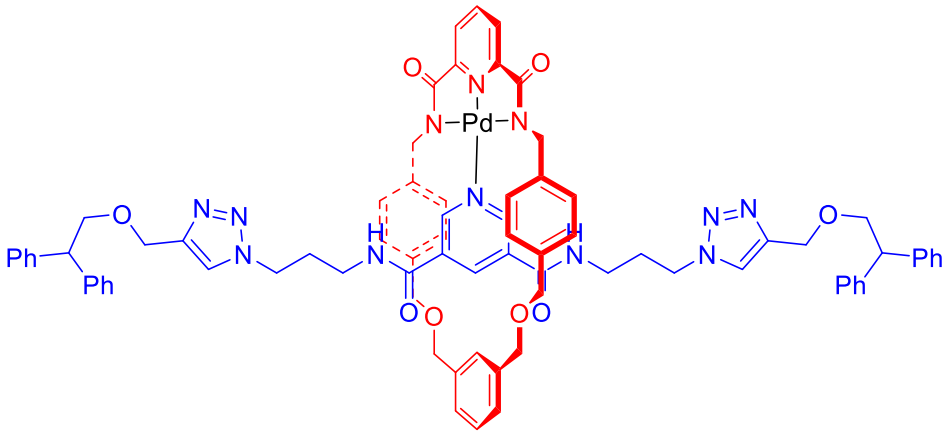

4.4

Figure 4.4 - Structure of proposed achiral prototype rotaxane 4.4

Once the synthetic route to the prototype rotaxane **4.4** has been proved, chiral rotaxane **4.5** capable of enantioselective recognition will be prepared (Fig. **4.5**). Chiral aromatic carboxylate anions may then be bound through hydrogen bonding to a urea functionality appended to the macrocycle and π-π stacking with a chiral benzyl substituent on the axle component.

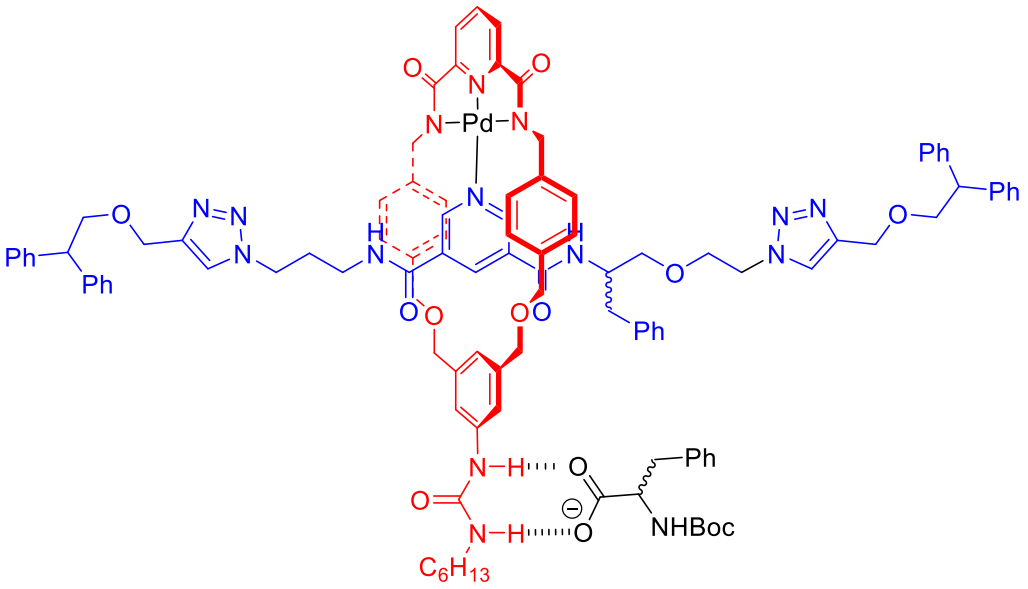

Figure 4.5 – Structure of proposed enantioselective rotaxane 4.5 binding to a chiral carboxylate aromatic anion

4.2. Investigations Towards a Pd(II) Templated Rotaxane Incorporating a 3,5-Pyridyl Axle

4.2.1. Synthesis of Rotaxane Precursors

To prepare rotaxane **4.4**, macrocycle **4.6**, stopper **4.7** and pyridiyl bis azide **4.8** were required (Fig. **4.6** and **4.7**). Pyridine bis-azide **4.8** was already available (supplied by Dr. Nicholas Evans).[9] Therefore, synthesis focused upon preparing macrocycle **4.6** and stopper **4.7**.

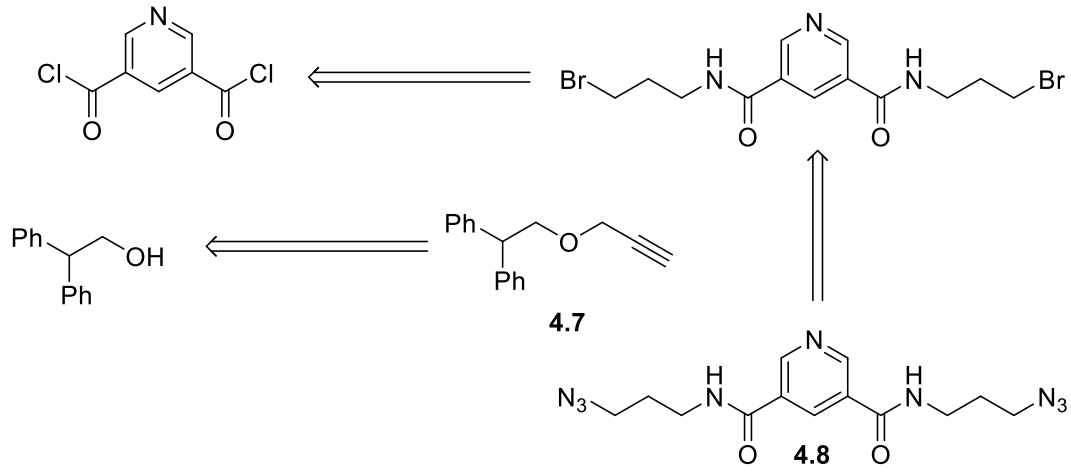

Figure 4.6 – Retrosynthesis of stopper 4.7 and pyridyl bis azide 4.8

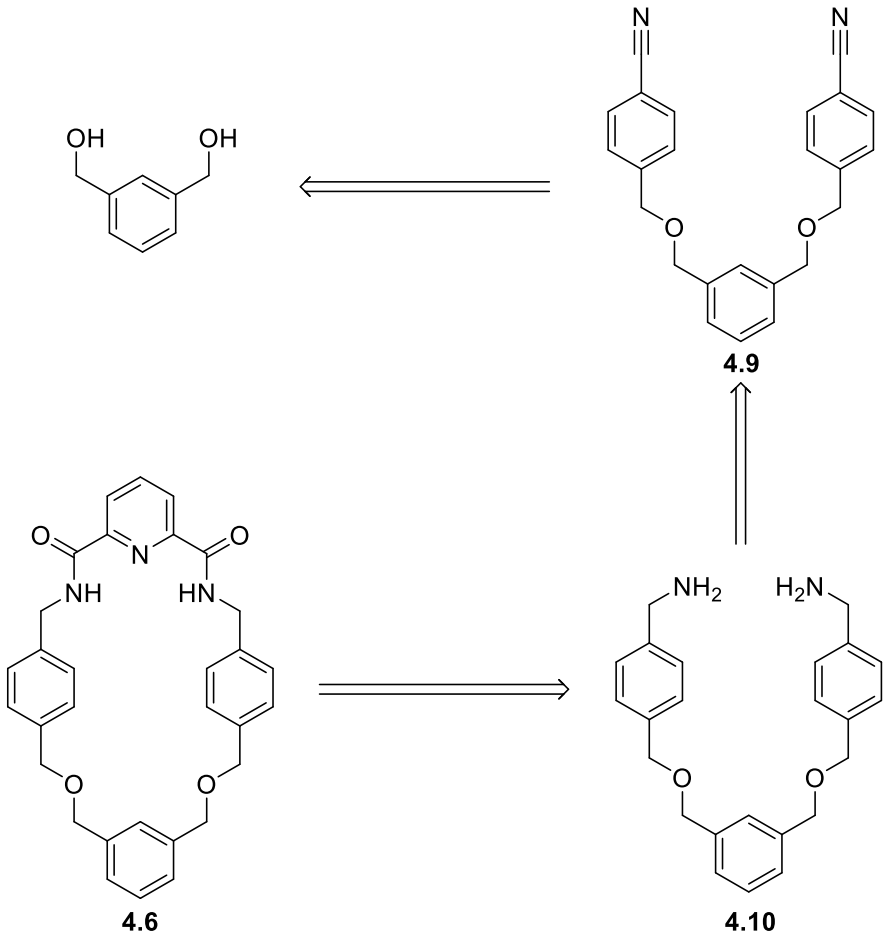

Figure 4.7 – Retrosynthesis of macrocycle 4.6

Macrocycle **4.6** was prepared in three steps (Fig **4.8**), 1,3-(benzene-diyl)dimethanol was doubly deprotonated with excess sodium hydride in THF, followed by the addition of 2.2 equivalents of 4-(bromomethyl)benzonitrile. After aqueous work up and column chromatography bis-nitrile **4.9** was afforded in 78% yield. The resulting bis-nitrile **4.9** was then reduced using borane in THF to give bis-amine **4.10** in 85% yield. Macrocycle **4.6** was prepared by a reaction of bis amine **4.10** and 2,6-pyridine dicarbonyl dichloride (prepared by refluxing 2,6-pyridinedcaboxylic acid in $SOCl_2$) under high dilution conditions. After aqueous work up and flash column chromatography macrocycle **4.6** was isolated in 21% yield. In addition to full characterisation by NMR and IR spectroscopy and mass spectrometry, single crystals of macrocycle **4.6** were grown from MeCN solution, that proved suitable for x-ray structure determination (Fig. **4.9** carried out by Dr. Michael Coogan).

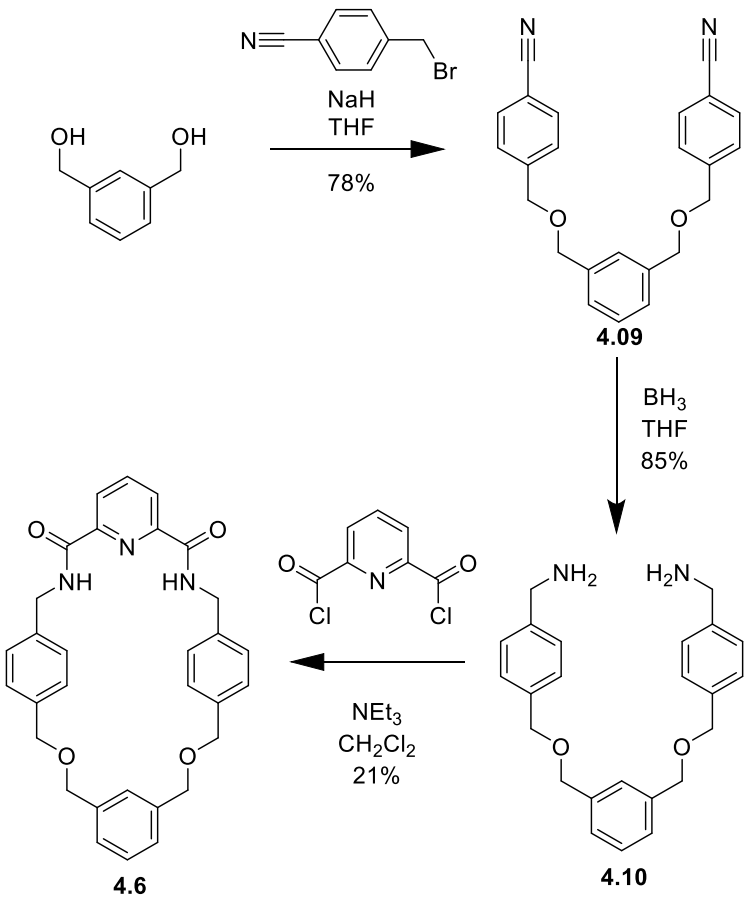

Figure 4.78 – Synthesis of macrocycle 4.6

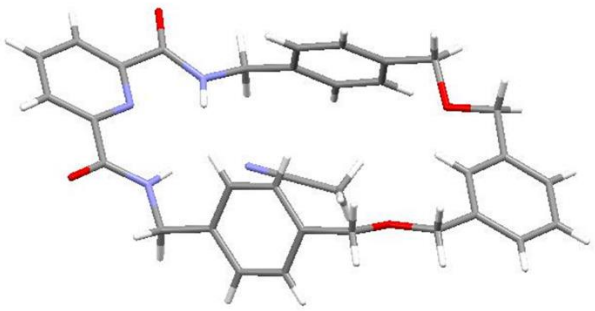

Figure 4.9 – X-ray diffraction structure of macrocycle 4.6

The x-ray crystal structure of macrocycle **4.6** reveals the amides are arranged in a syn conformation, which is consistent with the pyridyl lone pair interacting with both amide N-H protons. The amide N-H protons also interact with the lone pair of an MeCN molecule, which sits within the macrocycle cavity.

Alkyne stopper **4.7** was produced in a single step (Fig **4.10**), by deprotonating 2,2-diphenylethanol in THF with excess sodium hydride. Excess propargyl bromide was added and the reaction allowed to stir for 24 hours, the mixture was quenched with water and extracted with diethyl ether. The material was purified by column chromatography producing alkyne **4.7** in 77% yield.[10]

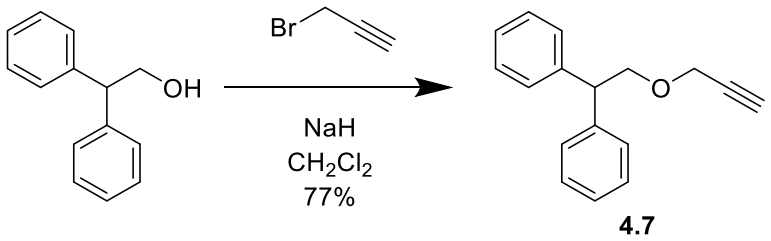

Figure 4.10 – Synthesis of stopper 4.7

4.2.2. Attempted Rotaxane Synthesis

With all necessary precursors in hand, synthesis of the Pd (II) templated rotaxane **4.4** could be attempted (Fig. **4.11**). In a manner analogous to Leigh's 2004 paper, macrocycle **4.6** was exposed to a stoichiometric amount of $Pd(OAc)_2$ in a 1:1 mixture of MeCN:CH_2Cl_2, to allow for metalation of the macrocycle.[2] After 1 h the solvent was removed *in vacuo*, and the resulting residue was dissolved in neat CH_2Cl_2. Bis-azide thread **4.8** was added and the solution was stirred for a further hour. The solvent was removed *in vacuo* to analyse pseudorotaxane **4.11** by ^{1}H NMR spectroscopy.

Stopper groups were then appended to pseudorotaxane **4.11** using a CuAAC 'copper click' reaction. Two equivalents of stopper **4.7**, DIPEA and catalytic amounts of $Cu(NCMe)_4BF_4$ and TBTA, were then added to pseudorotaxane **4.10** in CH_2Cl_2 and the mixture was stirred overnight.

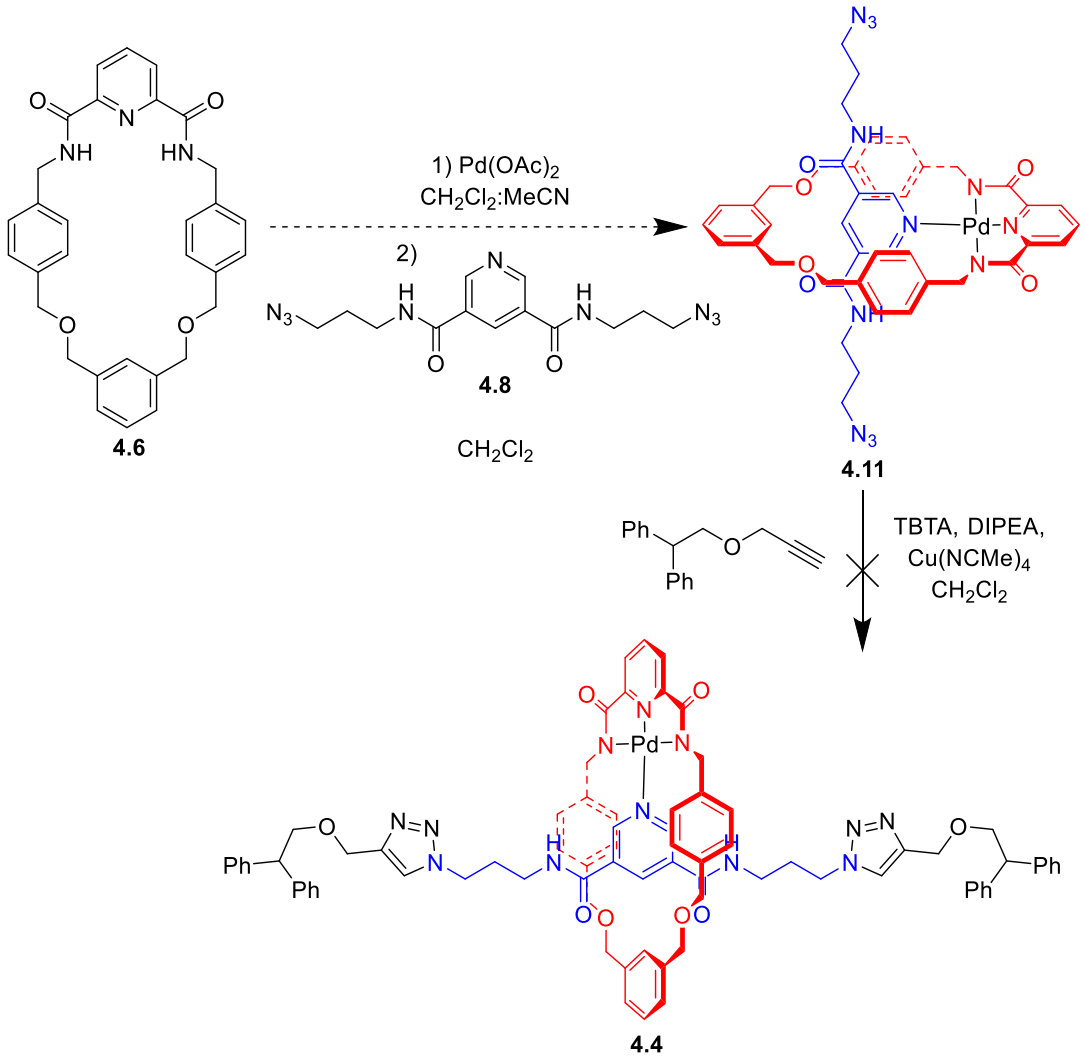

Figure 4.11 – Attempted synthesis of Rotaxane 4.4

Attempts were made to purify the rotaxane by silica column chromatography. However, each time a column was run the material was always contaminated with what was suspected to be free macrocycle and axle impurities. In addition, in the ^{1}H NMR spectrum the signals associated with the axle protons appeared more than once, suggesting that the axle was no longer symmetric. This was easiest to observe in the ^{1}H NMR spectra of macrocycle-pyridine thread complex **4.11**.

Inspection of the ^{1}H NMR spectrum (Fig. **4.12**) of the macrocycle Pd thread complex **4.11** provides some indication of what may be occurring. Resonances for thread protons 3, 4, 4-NH, and 6 have split and appear twice in the ^{1}H NMR spectrum, indicating that the two halves of the

thread are experiencing inequivalent environments. Considering that no rotaxane could be isolated after the subsequent 'click' reaction, it is proposed that the axle is not threaded through the macrocycle (which would give a symmetric ^{1}H NMR spectrum) and is instead perched on the axle.

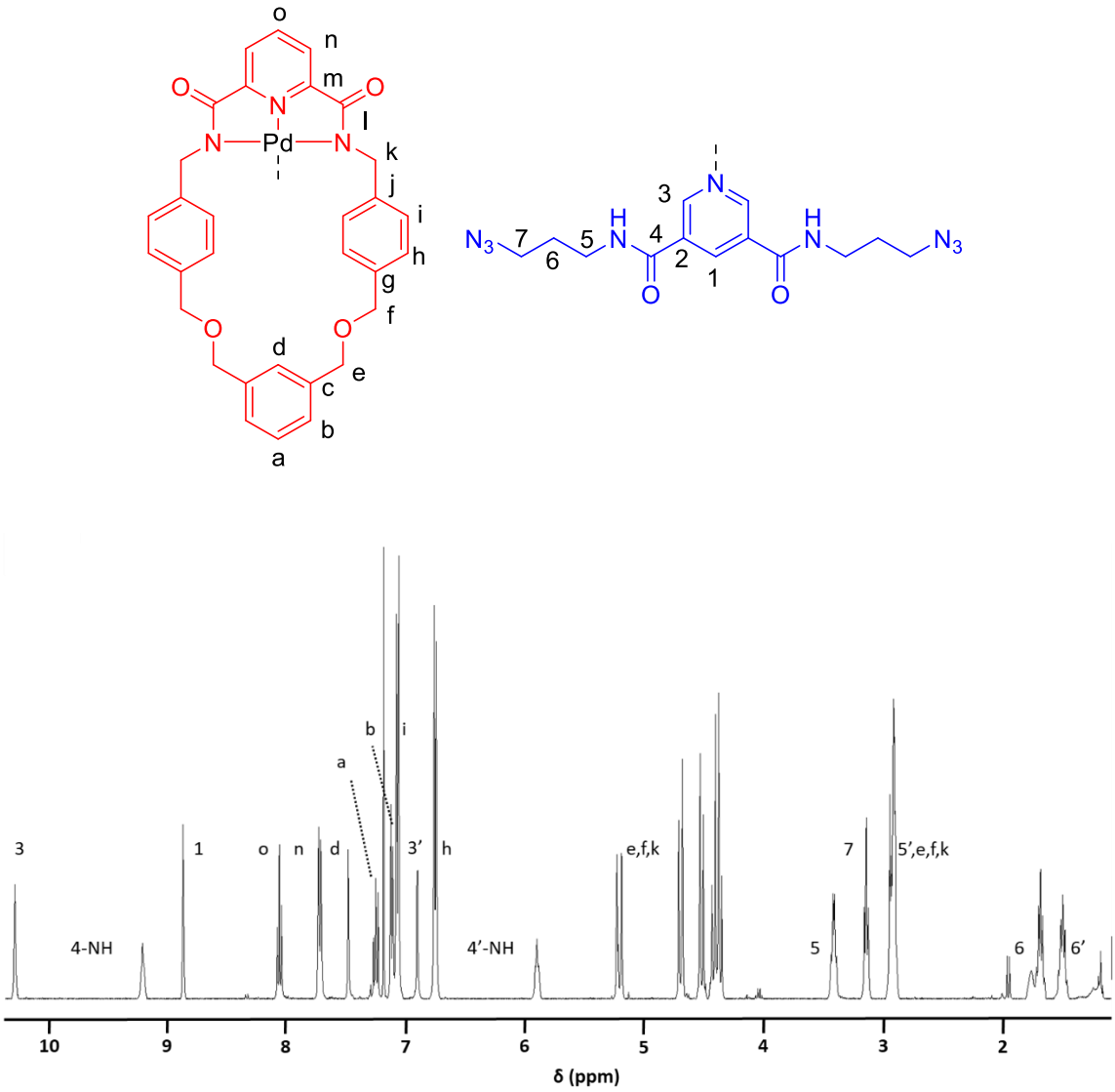

Figure 4.12 – ^{1}H NMR spectrum of macrocycle-pyridine thread complex 4.11 ($CDCl_3$, 400 MHz, 298 K)

It was proposed that the apparent failure of the axle to thread through the metallated macrocycle might be resolved by removing the 1,3-substituted benzene moiety from the

macrocycle and replacing it with a more flexible, less sterically demanding polyether chain. Hence attention turned to preparing such a macrocycle.

4.3. Further Studies Using a More Flexible Macrocycle

4.3.1. Macrocycle Synthesis

Macrocycle **4.12** was synthesised in three steps (Fig. **4.13**), following a literature procedure.[11] Diethylene glycol was doubly deprotonated with excess sodium hydride in THF, followed by the addition of 2.2 equivalents of 4-(bromomethyl)benzonitrile, the material was then purified using an aqueous work up followed by column chromatography to give bis-nitrile **4.13** in 92% yield. Bis-nitrile **4.13** was then reduced with borane in THF, then submitted to an aqueous work up followed by column chromatography to produce bis-amine **4.14** in 46% yield. Macrocycle **4.12** was prepared by a reaction of 2,6-pyridine dicarbonyl dichloride (prepared by refluxing 2,6-pyridinedcaboxylic acid in $SOCl_2$) and bis-amine **4.14** under high dilution conditions. After aqueous work up and flash column chromatography macrocycle **4.12** was isolated in 14% yield. The isolated yield of macrocycle is even lower than for the preparation of macrocycle **4.4**, possibly due to greater competition from oligomerisation reactions in this case. However, enough macrocycle was isolated to not require further optimisation of this reaction.

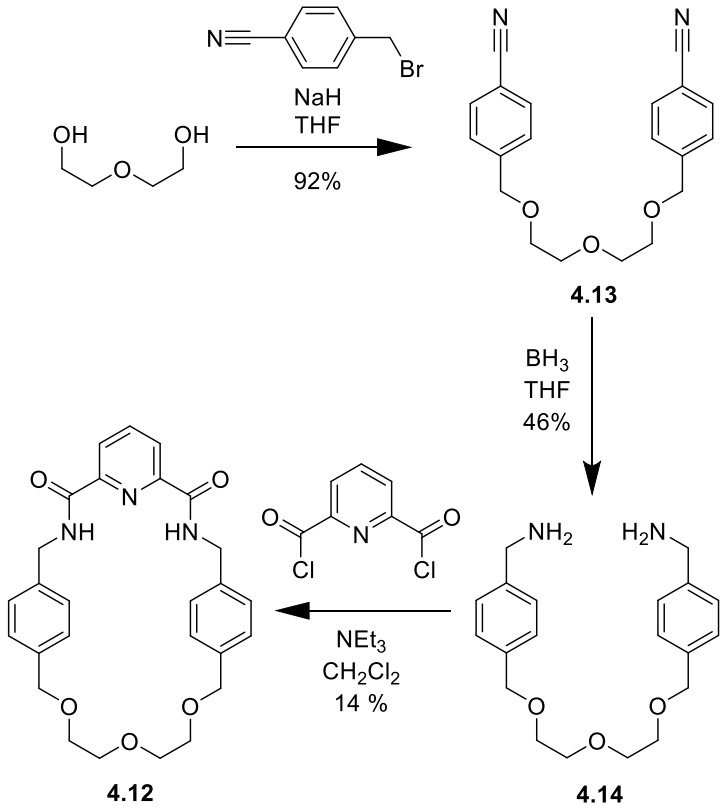

Figure 4.13 – Synthesis of Macrocycle 4.12

4.3.2. Attempted Synthesis of a Rotaxane Containing Polyether Macrocycle

With all macrocycle in hand, the synthesis of Pd (II) templated rotaxane **4.15** could attempted (Fig. **4.14**). Again in an analogous manner to the previous attempt to synthesise rotaxane **4.4** and Leigh's 2004 paper, macrocycle **4.12** was combined with a stoichiometric amount of $Pd(OAc)_2$ in a 1:1 mixture of $MeCN:CH_2Cl_2$, to metalate the macrocycle. After 1 h the solvent was removed *in vacuo*, and the resulting residue was dissolved in CH_2Cl_2. Bis-azide thread **4.8** was added and the solution was stirred for a further hour. The solvent was removed *in vacuo* and pseudorotaxane **4.16** was analysed by ^1H NMR spectroscopy.

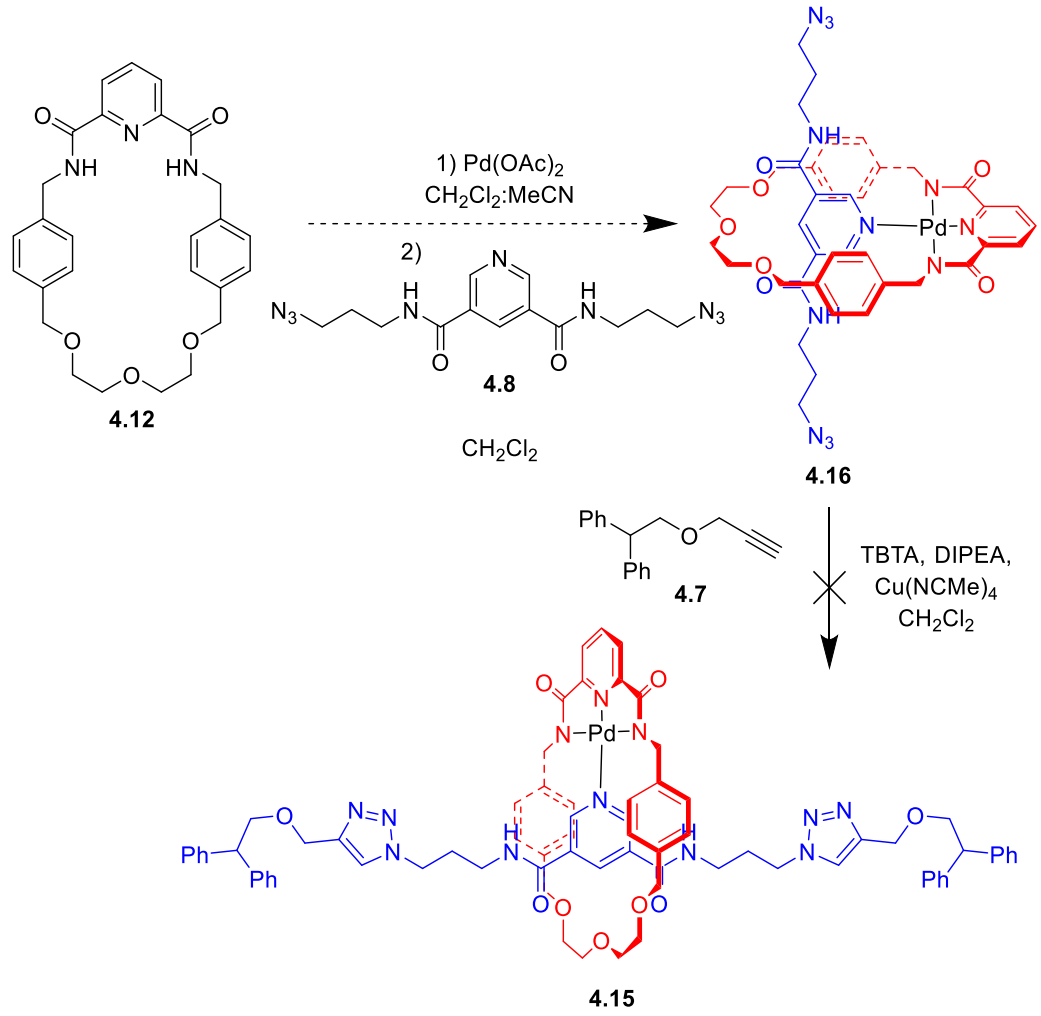

Figure 4.14 – Attempted Synthesis of Rotaxane 4.15

Pseudo rotaxane **4.16** was stoppered using a CuAAC 'copper click' reaction in CH_2Cl_2, alkyne stopper **4.7**, DIPEA and catalytic amounts of $Cu(MeCN)_4BF_4$ and TBTA were added and the mixture was allowed to stir overnight. The solvent was removed *in vacuo* and purification was unsuccessfully attempted by flash chromatography. Again, considering no rotaxane **4.15** was isolated and that ^{1}H NMR spectroscopy of the pseudorotaxane **4.16** suggested that the macrocycle was again perched on top of the axle component (Fig. **4.15**), as the ^{1}H NMR spectrum was again showing the presence asymmetric axle proton peaks. This is easiest to observe in protons 3, 3' and 6, 6', although no peak upfield of proton e integrates to more than two protons, indicating that these are split too.

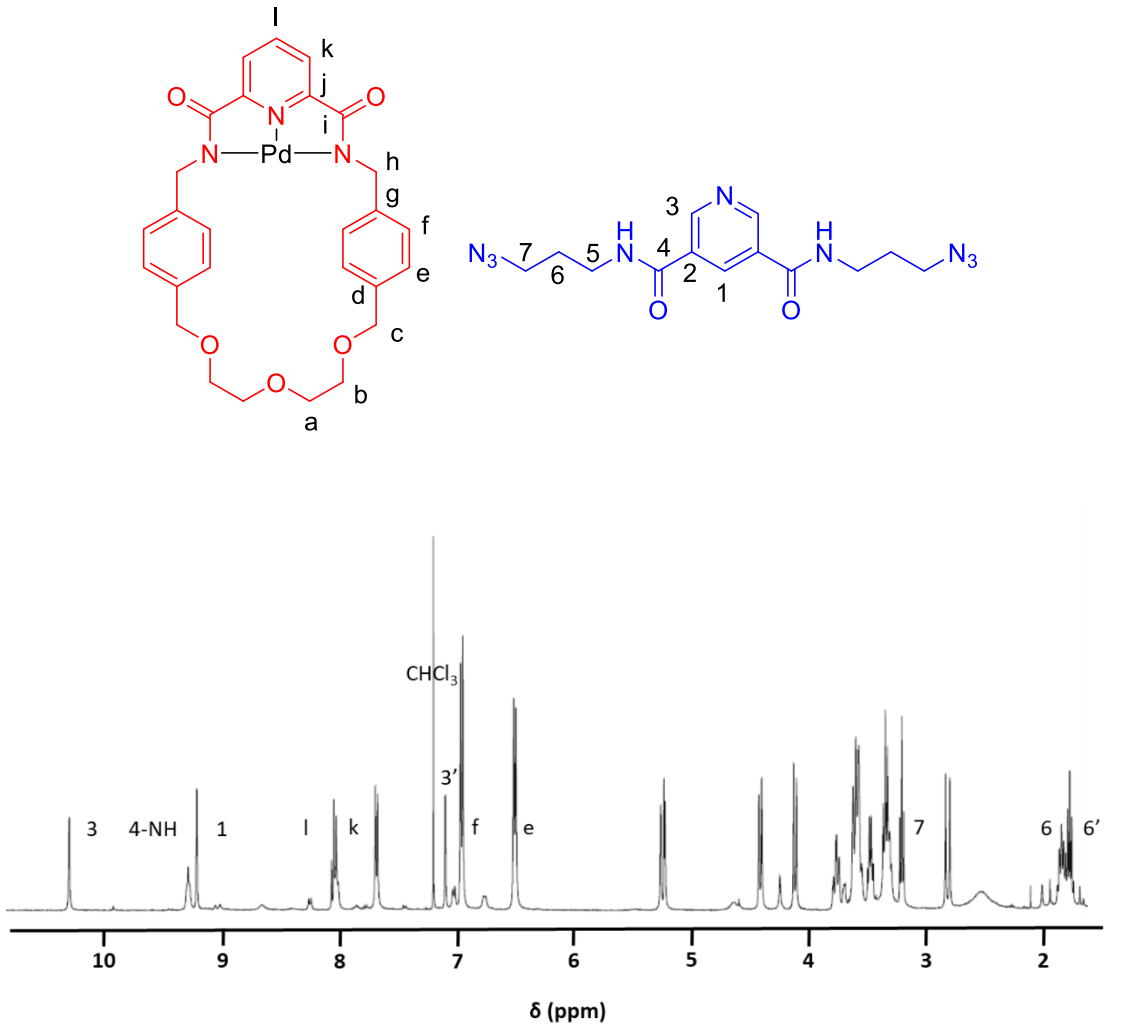

Figure 4.15– ^{1}H NMR spectra of Macrocycle-pyridine complex 4.16 ($CDCl_3$, 400 MHz, 298 K)

4.3.3. Attempted Pseudorotaxane Synthesis

To determine whether the failure to synthesise rotaxanes **4.4** and **4.15** was due to the macrocycle perching on top of the axle components, Pd adducts with macrocycles **4.6** and **4.12** and hexyl thread **2.20** (Chapter 2) were prepared, and growth of single crystals attempted.

As it was suspected that neither rotaxane could be synthesised, as it was thought the macrocycle was perching on top of the axle component, adducts **4.17** and **4.18** were synthesised (Fig. **4.16**), in order to grow crystal structures. Indeed, a crystal structure of adduct **4.18** was grown (Fig **4.17**).

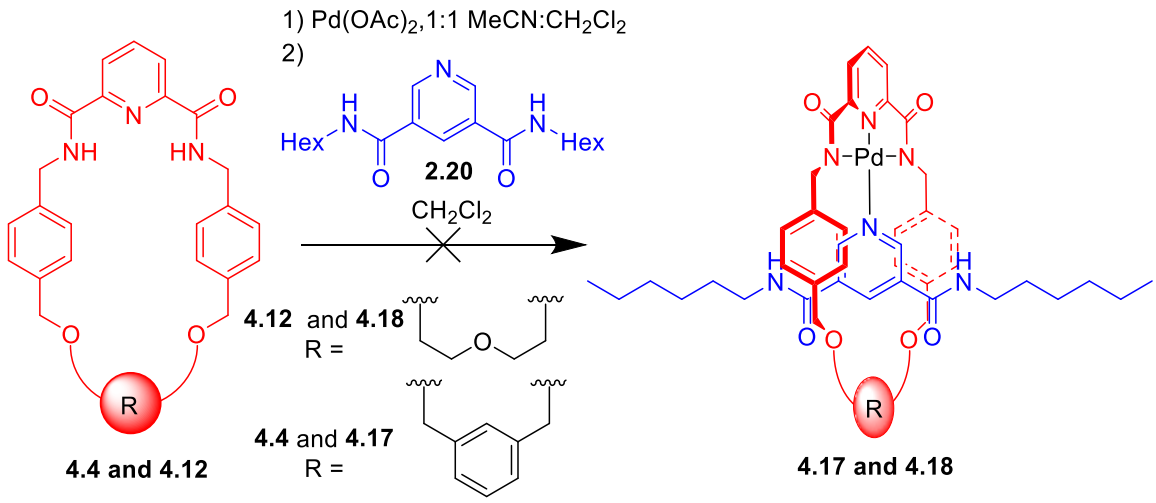

Figure 4.16 – Attempted synthesis of pseudorotaxanes 4.17 and 4.18

Using thread **2.20** (Chapter 2), adducts **4.17** and **4.18** were prepared (Fig. **4.16**). The appropriate macrocycle (**4.4** or **4.12**), was dissolved in a 1:1 mixture of MeCN and CH_2Cl_2 and a stoichiometric amount of palladium (II) acetate was added. The mixture was stirred for one hour, then the solvent was removed *in vacuo*. The palladium complexed macrocycle was dissolved in CH_2Cl_2 and pyridine thread **2.20** (Chapter 2) was added, the mixture was stirred for a further hour and the solvent was removed *in vacuo* to produce what was thought to be pseudorotaxanes **4.17** and **4.18** in quantitative yields. These adducts were then used to grow crystals suitable for x-ray structural determination.

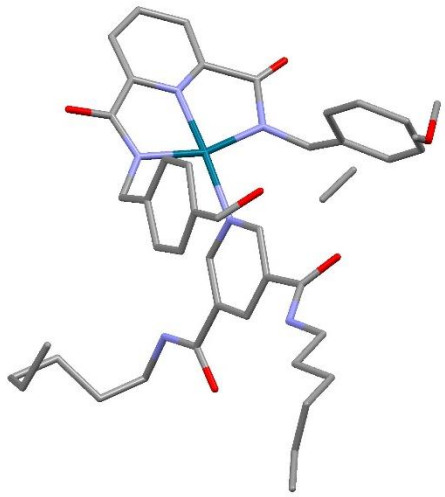

Figure 4.17 – X-ray crystal structure of failed pseudorotaxane 4.17

Single crystals of **4.17** were obtained from slow evaporation of a chloroform solution.From this a partial x-ray crystal structure was attained (Fig. **4.17**). The partial crystal structure revealed that the thread was not passing through the cavity of the macrocycle, instead the macrocycle was perching on top of the axle. This perching is consistent with the ^{1}H NMR evidence obtained of the attempts to make rotaxane **4.4** and **4.15** (Fig. **4.15**).

4.4. Preparation of Pyridine complexes

It appeared that a rotaxane using a 3,5-bisamide pyridyl axle could not be formed using the small macrocycles **4.6** and **4.12**, metallated with Pd(II). However, it was hoped that it would still be possible to prepare a rotaxane using a small macrocycle, and a 2,6-pyridyl thread. In first instance, it was decided to verify that pyridine itself could reside within the macrocycle cavity while coordinated to the Pd bound by the tridentate pyridyl-bisamide motif of the macrocycle.

Complexes **4.19** and **4.20** were prepared by simply adding (approximately) one equivalent of pyridine to a dichloromethane solution of the metallated macrocycle, stirring for one hour, and then removing the solvent *in vacuo* (Fig. **4.18**).

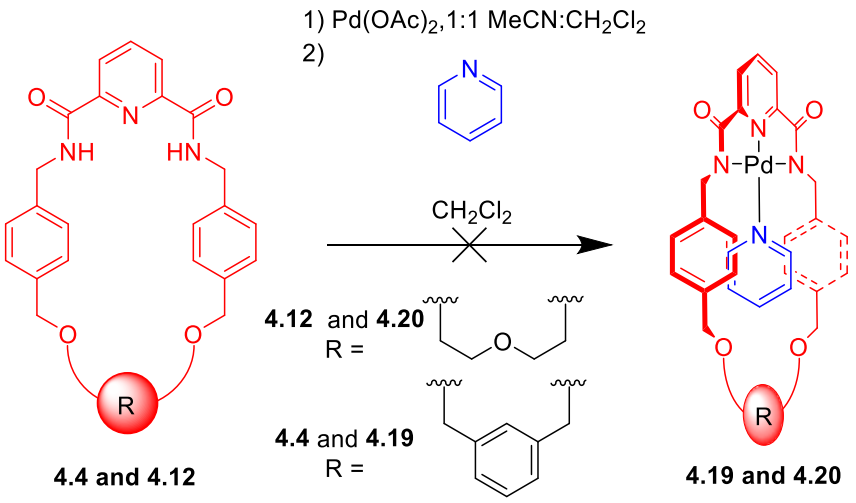

Figure 4.18 – Synthesis of macrocycle-pyridine complexes 4.19 and 4.20

The ^{1}H NMR spectra of palladium complex **4.20** was examined (Fig. **4.19**). Initial observations showed an upfield shift of macrocycle protons d and e, indicating that these protons may be shifted upfield due to the presence of pyridine in the cavity of the macrocycle. However, previous work indicated that this upfield shift may be a false positive. Instead attention was focused upon the pyridine group, to determine if protons that should be identical have split. It was found that protons 1 and 2 on the complexed pyridine molecule had indeed split, indicating that the pyridine may not be sitting in the macrocycle cavity, but instead may be resting to the side.

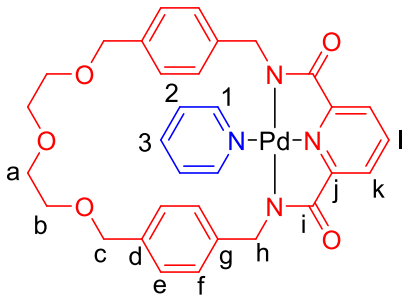

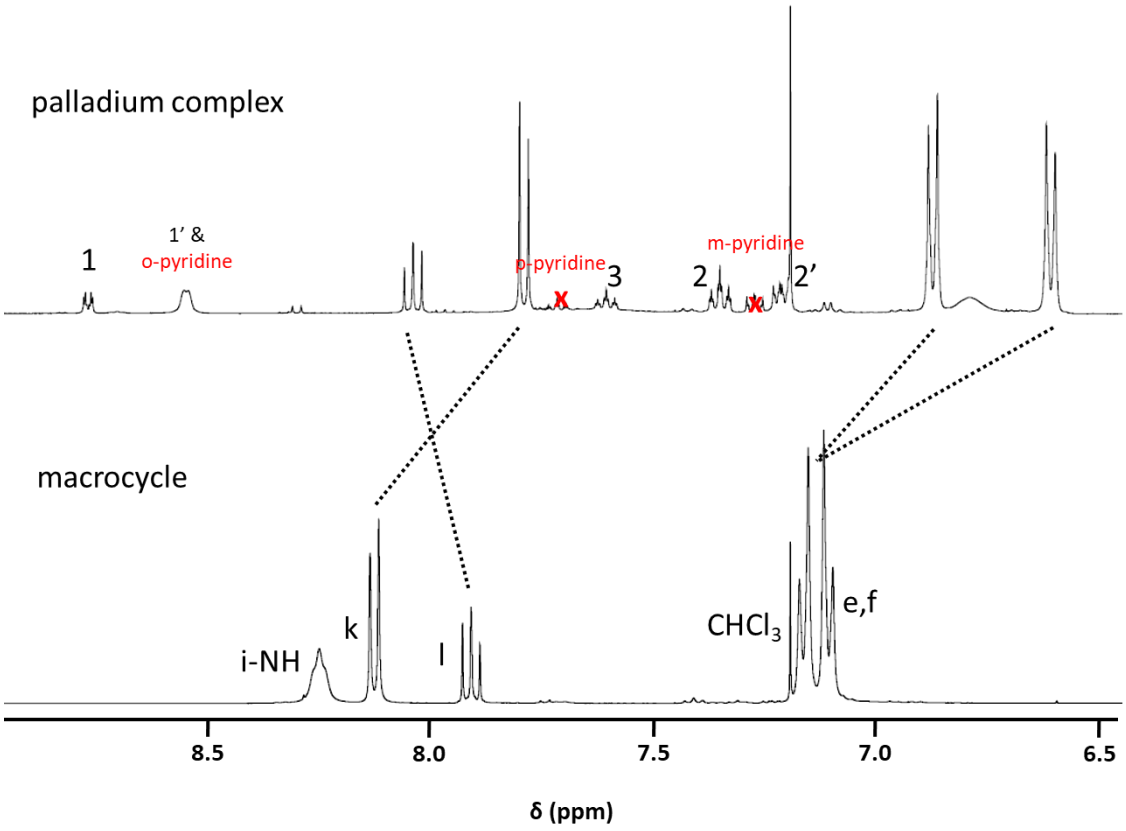

Figure 4.19 – ^{1}H NMR spectra of macrocycle 4.12 and palladium complex 4.20, contaminated with pyridine (shown in red) (400 MHz, 298 K, $CDCl_3$, spectra assigned with assistance from ^{1}H COSY)

Using palladium pyridine complexes **4.19** and **4.20** to test if the macrocycle can accommodate the palladium (II) and pyridine group, fails to consider that the structure of the macrocycle is not flat, but bends after the amide bonds. This bending can be seen in the single crystal x-ray structures of the analogous macrocycle **4.6** (Fig. **4.9**) and failed pseudorotaxane **4.17** (Fig. **4.17**). In addition, the pyridine in this molecule cannot be considered a thread, as it does not have any side chains. This lack of thread structure may make it more favourable for the pyridine not to sit within the ring, but instead go with the shape of the macrocycle and the square planar geometry of the palladium (II). Addition of a thread like structure at the 2 and 6 positions on the pyridine may force the interlocked structure to thread, as otherwise they will sterically clash with the structure of the macrocycle.

Attempts were made to determine the structure of complexes **4.19** and **4.20** using single crystal x-ray diffraction. A single crystal of complex **4.20** could be grown, unfortunately they were unsuitable for x-ray diffraction.

4.5. Investigations into a 2,6-pseudorotaxane

At this stage, a more careful search of the literature revealed that a 2,6-substituted pyridyl fragment could thread through the Pd metallated macrocycle **4.12**, and that a fully interlocked rotaxane could be prepared and isolated.[12] To confirm this pseudorotaxane **4.21** was investigated. Thread **4.22** of pseudorotaxane **4.21** also incorporates two symmetric $-CF_3$ groups, to make it easier determine if pseudorotaxane **4.21** was de-symmetrising, as the ^{19}F NMR spectrum should only show one peak if the thread is residing within the macrocycle, or two peaks if instead the macrocycle is perching on top of the thread.

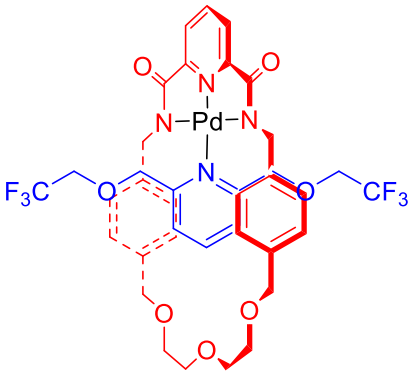

Figure 4.20 - Structure of proposed pseudorotaxane 4.21

4.5.1. Thread and Pseudorotaxane Synthesis

2,6-Subsitiuted thread **4.22** was synthesised in two steps (Fig **4.21**). 2,2,2-Trifluoroethanol was activated, using tosyl chloride, NEt_3 and catalytic DMAP in CH_2Cl_2. Following an aqueous work up tosylate **4.23** was obtained in 87% yield.[13] 2,6-Pyridinedimethanol was then dissolved in THF and deprotonated with NaH, followed by the addition of compound **4.23**, the mixture was stirred overnight then purified by aqueous work up and silica column chromatography producing thread **4.22** in 21% yield.

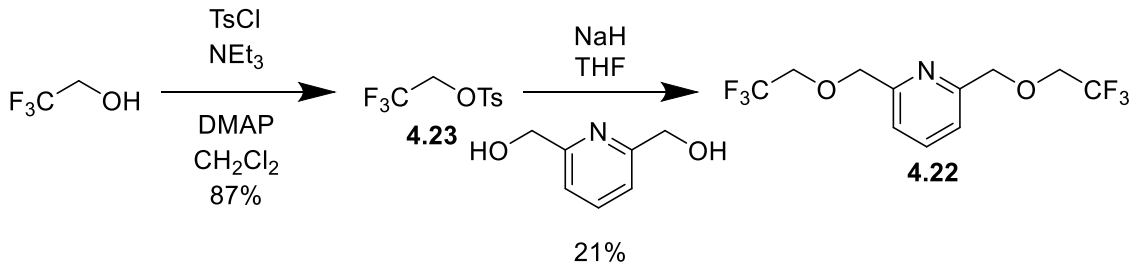

Figure 4.21 - Synthesis of 2,6 pyridine substituted thread 4.22

Pseudorotaxane **4.21** was then prepared by simply adding one equivalent of thread **4.22** to a CH_2Cl_2 solution of the metallated macrocycle **4.12**, stirring for one hour, and then removing the solvent *in vacuo*. The majority of the impurities were then removed by column chromatography (Fig. **4.22**).

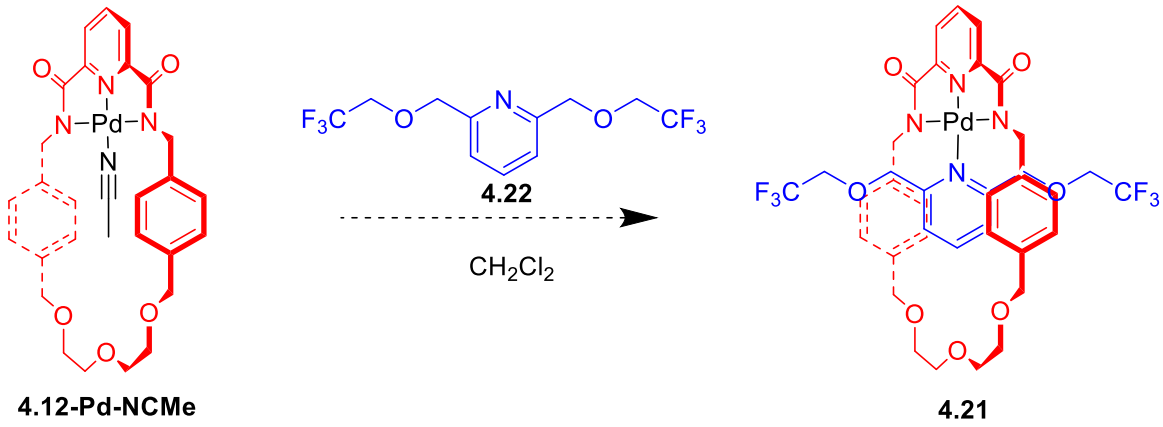

Figure 4.21 – Attempted synthesis of pseudorotaxane 4.21

4.5.2. NMR investigations

Pseudorotaxane **4.21** was then investigated by ^{19}F NMR. The ^{19}F NMR spectrum (Fig. **4.23**) showed four different $-CF_3$ environments, a peak at -74.1 ppm, attributed to uncoordinated thread **4.22**, a large peak at -73.4 ppm and two peaks of equal integration at -72.9 and -74.0 ppm. The large peak at -73.4 ppm was attributed to the thread passing through the macrocycle and the two $-CF_3$ groups of the thread residing in a symmetric environment. Whilst the two smaller peaks at -72.9 and -74.0 ppm were attributed to a smaller proportion of the thread where the macrocycle was resting on top. This result provided preliminary evidence that a Pd

(II) templated rotaxane could indeed be synthesised using macrocycle **4.12** and a 2,6-substituted pyridyl thread.

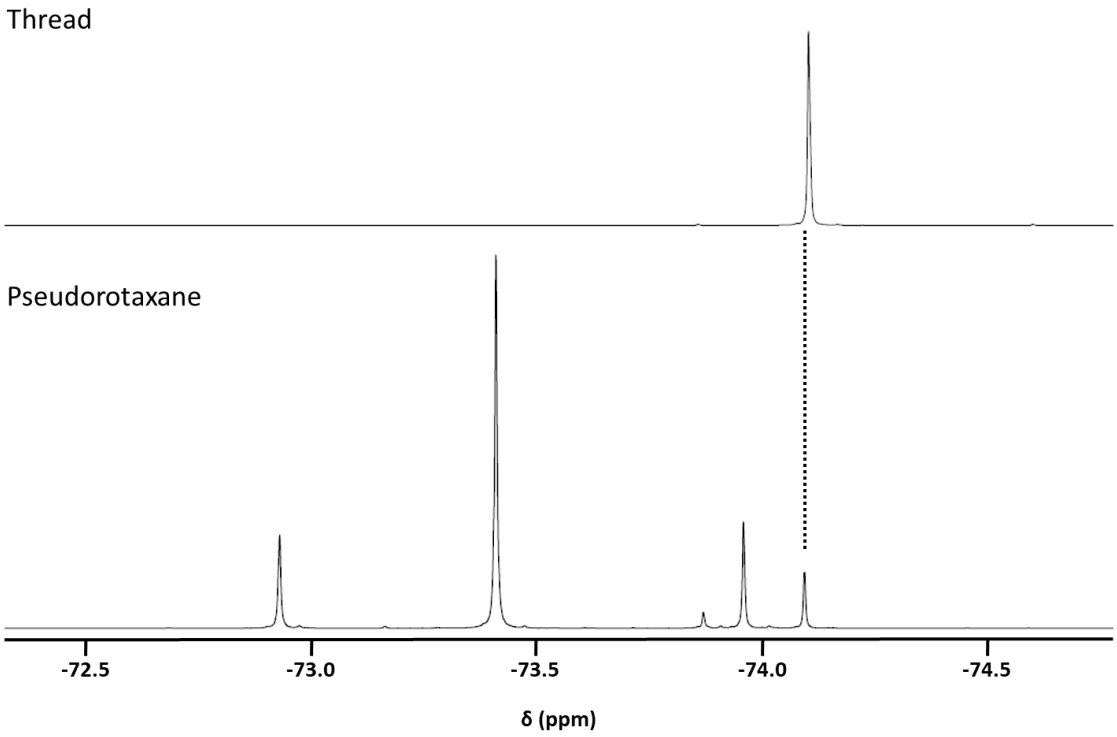

Figure 4.23 – ^{19}F {^{1}H} NMR spectrum of pseudorotaxane 4.21 and thread 4.22 (376 MHz, 298 K, $CDCl_3$)

4.6. A 2,6 Pyridine Templated Rotaxane

Following the literature precedent that a Pd (II) templated rotaxane with macrocycle **4.12** and a 2,6-pyridine containing axle could be formed, as well as the promising result in the synthesis of pseudorotaxane **4.21**; the decision was taken to attempt the synthesis of rotaxane **4.24** (Fig. **4.24**), using a 2,6-pyridyl thread component and a CuAAC click reaction.[12]

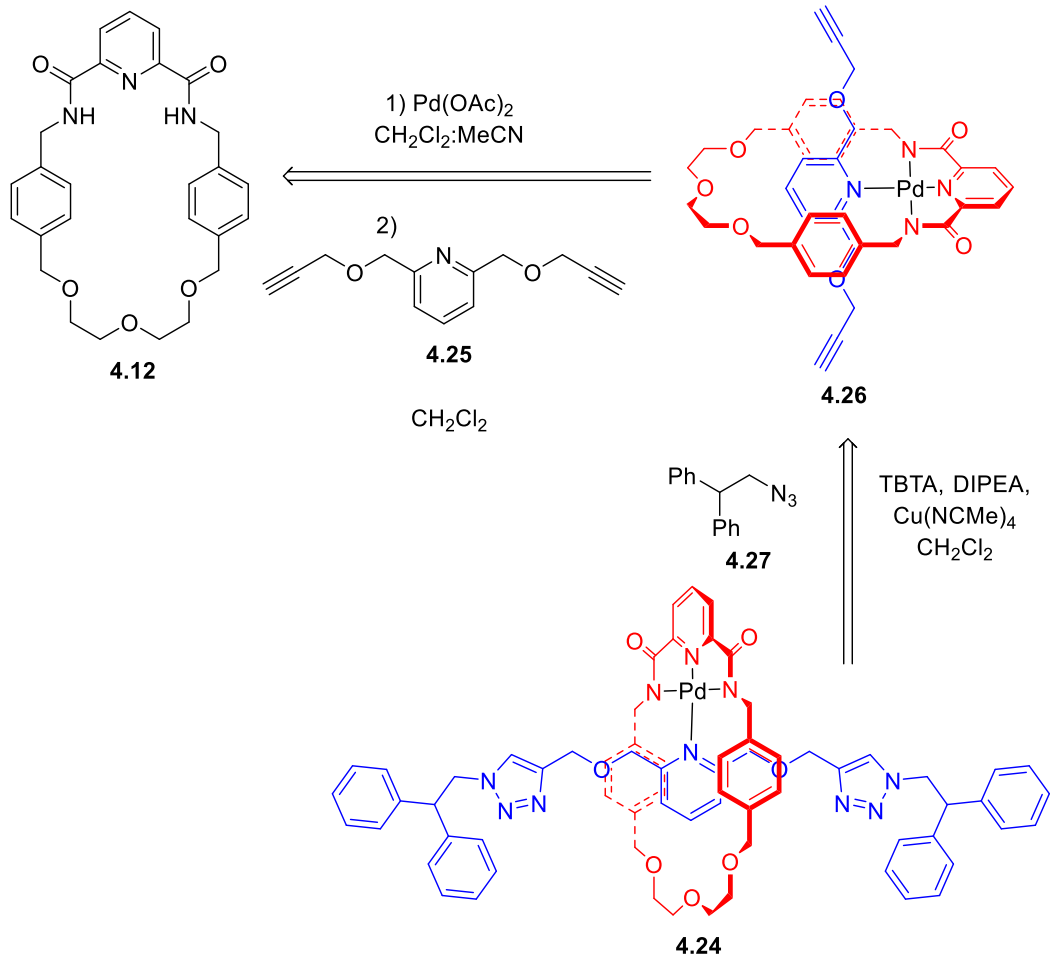

Figure 4.24 – Retrosynthetic analysis of rotaxane 4.24

4.6.1. Axle Component Synthesis

As macrocycle **4.12** had already been synthesised, the only components that needed to be prepared were alkyne thread **4.25** and azide stopper **4.27**. Alkyne thread **4.25** was prepared in a single step (Fig. **4.25**). Pyridine-2,6-dimethanol was doubly deprotonated with excess NaH in THF. Excess propargyl bromide was added and the solution was allowed to stir overnight. The compound was purified using an aqueous work up and column chromatography, producing alkyne axle **4.25** in 77% yield.[14]

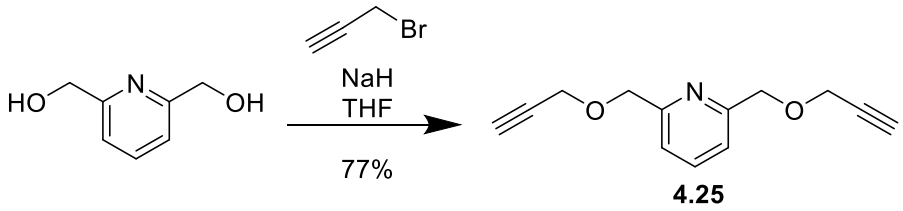

Figure 4.25 – Synthesis of alkyne thread 4.25

Azide stopper **4.27** was synthesised in two steps (Fig. **4.26**). 2,2-Diphenlyethanol, methanesulfonyl chloride and NEt_3 were dissolved in ice cold CH_2Cl_2. The solution was stirred for ten minutes then purified using an aqueous work up, producing compound **4.28** in 86% yield.[15] Compound **4.28** was immediately taken on and dissolved in DMF, excess sodium azide was added and the solution was heated to 80 ^oC for 72 hours. The resulting azide was extracted with CH_2Cl_2, and after solvent removal isolated in a maximum yield of 65%. The material contained small quantities of impurities, which were attempted to remove by silica gel column chromatography. However, this led to degradation of the desired azide product. Close inspection of the ^1H NMR spectrum revealed the principle contaminant to be 1,1-diphenylethene. This implies azide **4.27** is rather unstable with respect to the elimination of toxic HN_3 (Fig. **4.27**). **It is therefore recommended that this synthesis is not re-attempted and certainly that no attempt should be made to purify the material on silica.**

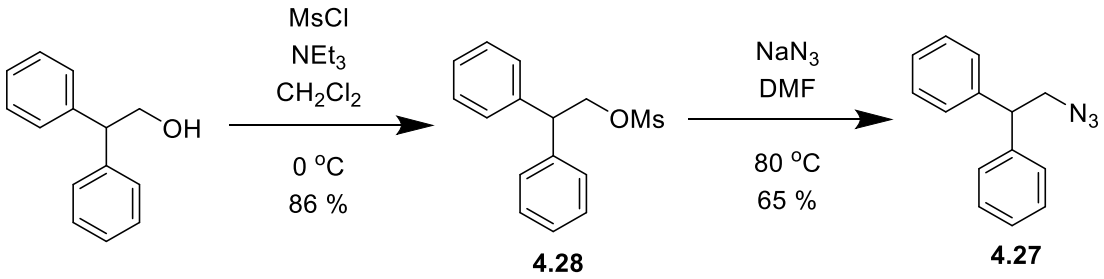

Figure 4.26 – Synthesis of azide stopper 4.27

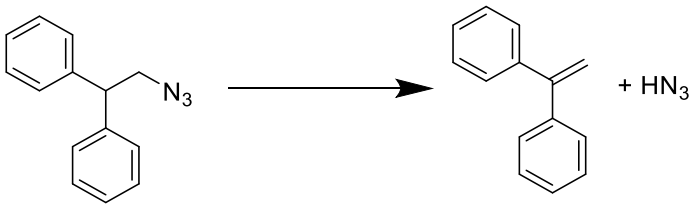

4.27

Figure 4.27 – Anticipated degredation of azide stopper 4.27

4.6.2. Attempted Rotaxane Synthesis

With macrocycle **4.12**, alkyne thread **4.25** and azide **4.27** prepared synthesis of rotaxane **4.24** could begin (Fig. **4.28**). Macrocycle **4.12** and a stoichiometric amount of palladium (II) acetate were dissolved in a 1:1 mixture of MeCN and CH_2Cl_2, then stirred for one hour, after which the solvent was removed. The mixture was dissolved in CH_2Cl_2, then alkyne thread **4.25** was added and the solution was stirred for one hour. After an hour azide stopper **4.27**, DIPEA and 10 mol% of $Cu(MeCN)_4BF_4$ and TBTA were added. The solution was stirred overnight then the solvent was removed.

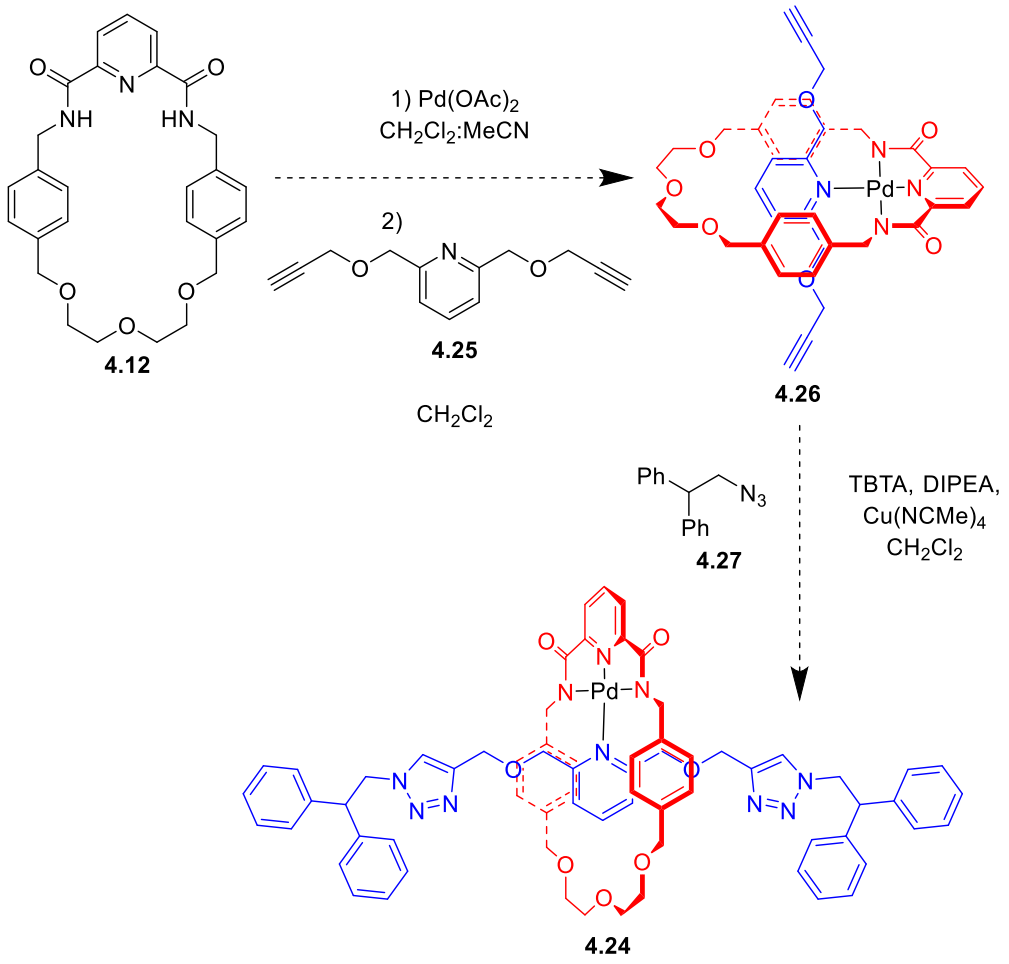

Figure 4.28 – Attempted synthesis of rotaxane 4.24

Attempts were made to purify the material by flash column chromatography then by preparative TLC. However, rotaxane **4.24** could not be isolated pure. After both flash column chromatography and preparative TLC, impurities could still be detected by ^{1}H NMR spectroscopy and by TLC. The TLC revealed that there were still three spots, what was thought to be rotaxane **4.24** and a spot that had a higher $\underline{R_f}$ and a spot that had a lower R_f. The ^{1}H NMR spectra (Fig. **4.29**) were difficult to interpret, with all three spectra containing many peaks. However, in all three ^{1}H NMR spectra protons e and f could be tentatively assigned, as having moved upfield, suggesting the axle is passing through the metallated macrocycle. It was only in the post-preparative TLC spectra that pyridine peaks l,k,1 and 2 could be assigned, no other peaks could be reasonably assigned with the data available. Considering the large number of peaks in the spectra, it is possible to suggest that the rotaxane has not formed and a non-threaded complex

of the metallated macrocycle and stoppered axle is decomposing. Alternatively, the rotaxane may have formed but is decomposing on silica during purification. Following the repeated attempted purification there was little material left and this was used to unsuccessfully grow crystals for x-ray diffraction.

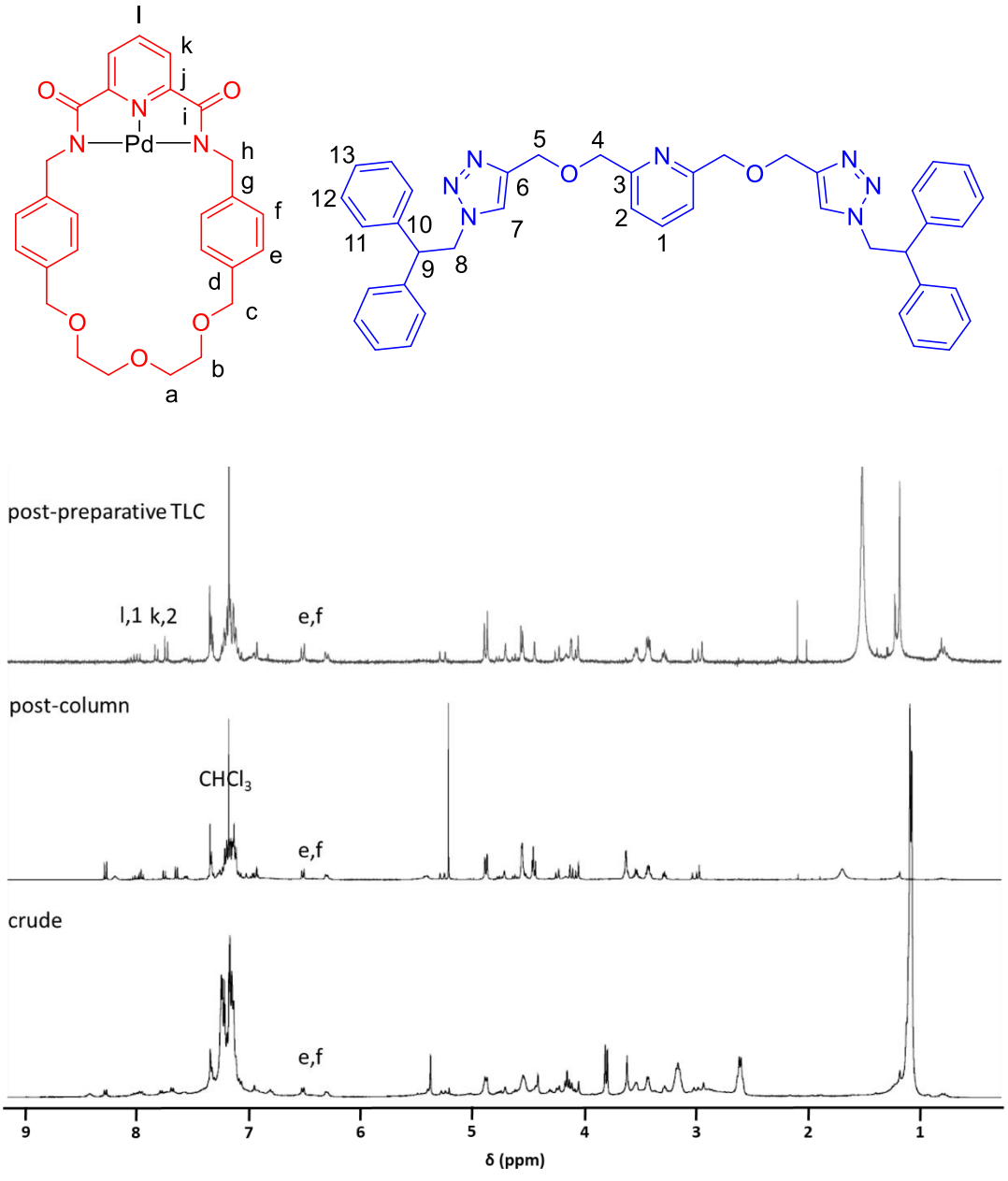

Figure 4.29 – ^{1}H NMR of samples of what was thought to be rotaxane 4.24 at various stages of purification (400 MHz, 298 K, $CDCl_3$)

The possible failure to form rotaxane **4.24** may be due to the flexibility of thread **4.25**, as rotaxane **4.29** using macrocycle **4.12** as the macrocyclic component used a far more rigid axle

component around the central pyridine of the axle.[12] The thread used in rotaxane **4.29** has two alkynes either side of the pyridine, whilst the target rotaxane **4.24** has flexible sp^3 hybridised groups which can bend. This may mean it is preferable for the axle groups to bend away from the macrocycle rather than thread.

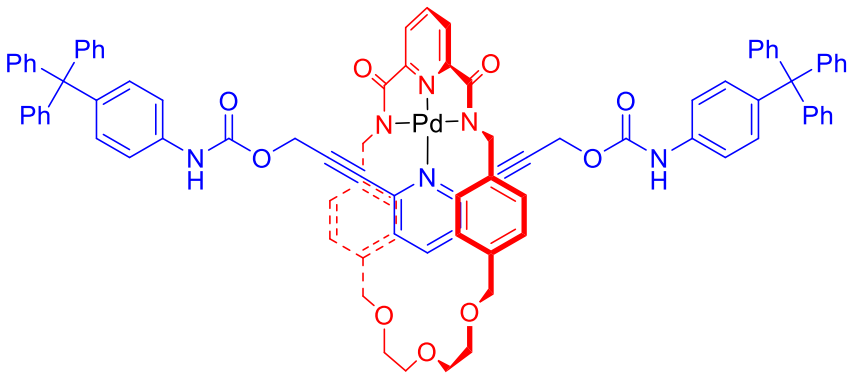

4.29

Figure 4.30 - Chiu and co-workers 2,6-pyridine axle containing Pd(II) templated rotaxane 4.29

4.7. Conclusions and Future Work

A novel small pyridyl macrocycle was prepared. While it could be successfully metallated with Pd(II) and a complex formed with a 3,5-pyridyl bis-azide thread, no rotaxane was isolated after an attempted CuAAC "click" reaction. After further studies with **4.12** and an analogous polyether macrocycle, the conclusion was reached that failure to isolate rotaxanes was due to the perching of the 3,5-pyridine axle component.

Inspired by literature precedent, attention turned to using a 2,6-pyridyl axle component. A ^{19}F NMR study with a fluorinated non-stoppered axle component gave indications that threading through the polyether macrocycle was possible. However, it was not possible to isolate pure rotaxane, when fully interlocked structure formation was attempted.

However, rather than continuing with this work, attention turned towards study of a different rotaxane system for which more promising results had been achieved at Lancaster**.**

4.8. References

[1] C. Hamann, J.-M. Kern and J.-P. Sauvage, *Dalt. Trans.*, 2003, 3770-3375.

[2] A.-M. Fuller, D. A. Leigh, P. J. Lusby, I. D. H. Oswald, S. Parsons and D. B. Walker, *Angew. Chem. Int. Ed.*, 2004, **43**, 3914–3918.

[3] Y. Furusho, T. Matsuyama, T. Takata, T. Moriuchi and T. Hirao, *Tetrahedron Lett.*, 2004, **45**, 9593–9597.

[4] D. A. Leigh, P. J. Lusby, A. M. Z. Slawin and D. B. Walker, *Chem. Commun.*, 2005, 4919-2921.

[5] A.-M. L. Fuller, D. A. Leigh and P. J. Lusby, *Angew. Chem. Int. Ed.*, 2007, **46**, 5015–5019.

[6] A.-M. L. Fuller, D. A. Leigh and P. J. Lusby, *J. Am. Chem. Soc.*, 2010, **132**, 4954–4959.

[7] G. De Bo, J. De Winter, P. Gerbaux and C.-A. Fustin, *Angew. Chem. Int. Ed.*, 2011, **50**, 9093–9096.

[8] C. Browne, T. K. Ronson and J. R. Nitschke, *Angew. Chem. Int. Ed*, 2014, **53**, 10701–10705.

[9] F. Zapata, O. A. Blackburn, M. J. Langton, S. Faulkner and P. D. Beer, *Chem. Commun.*, 2013, **49**, 8157-8159.

[10] N. H. Evans, C. E. Gell and M. J. G. Peach, *Org. Biomol. Chem.*, 2016, **14**, 7972–7981.

[11] A. Vidonne and D. Philp, *Tetrahedron*, 2008, **64**, 8464–8475.

[12] W.-C. Hung, L.-Y. Wang, C.-C. Lai, Y.-H. Liu, S.-M. Peng and S.-H. Chiu, *Tetrahedron Lett.*, 2009, **50**, 267–270.

[13] T. M. Gøgsig, L. S. Søbjerg, A. T. Lindhardt, K. L. Jensen and T. Skrydstrup, *J. Org. Chem.*, 2008, **73**, 3404–3410.

[14] B. Lewandowski and S. Jarosz, *Org. Lett.*, 2010, **12**, 2532–2535.

[15] M.P. Stracke, G. Ebeling, R. Cataluña and J. Dupont, *Energy Fuels,* 2007, **3** 1695-1698.

Chapter 5

A Hydrogen Bond Templated Mechanically Chiral Rotaxane

5.1. Introduction

5.1.1. Hydrogen Bond Templated Rotaxanes

As already discussed in Chapter One and Chapter Three, rotaxanes may be prepared by hydrogen bond templation in the absence of a discrete anion (or cation).[1–3] Strategically placed hydrogen bond donor and acceptor groups on the relevant precursors can allow for the generation of rotaxanes rapidly and in good yield.

In this chapter, experimental studies will turn to using a neutral hydrogen bond templating methodology developed within the Evans group.[4–6]

In this templating method pre-organised inward facing amide groups on the macrocycle can hydrogen bond to the lone pairs of an amide carbonyl on the axle (Fig. **5.1**) . This is supplemented with further hydrogen bonds between the lone pairs of the polyether oxygens situated on the macrocycle and the amide proton on the axle. This supplementary interaction is critical for the rotaxane to form.[4,5,7]

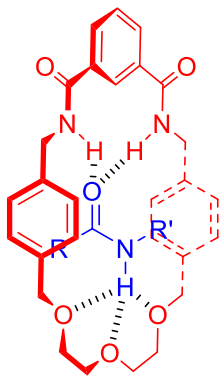

Figure 5.1 – Hydrogen bond templated rotaxane motif

As discussed in chapter 3, mechanical chirality in rotaxanes does not derive from a classical chiral element such as a chiral centre, axis or plane. Instead the chirality is derived from the combination of a non-rotationally symmetric macrocycle and axle.

5.1.2. Chapter Aims

The motif proposed for the rotaxanes synthesised in this chapter, is based upon analogous rotaxane **5.1** (Fig. **5.2**), previously synthesised by the Evans group.[5] Rotaxane **5.1** already has an a directional axle, as the two ends of the axle are inequivalent. All that is required to make the rotaxane mechanically chiral is therefore to include a rotationally asymmetric macrocycle. Macrocycle **5.2** was designed to replace the macrocycle used in rotaxane **5.1** to form both enantiomers of mechanically chiral rotaxane **5.3** (Fig. **5.3**).

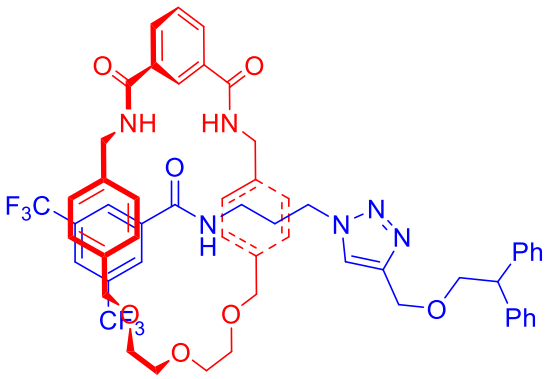

5.1

Figure 5.2 - Hydrogen bond templated rotaxane 5.1 previously developed by the Evans group

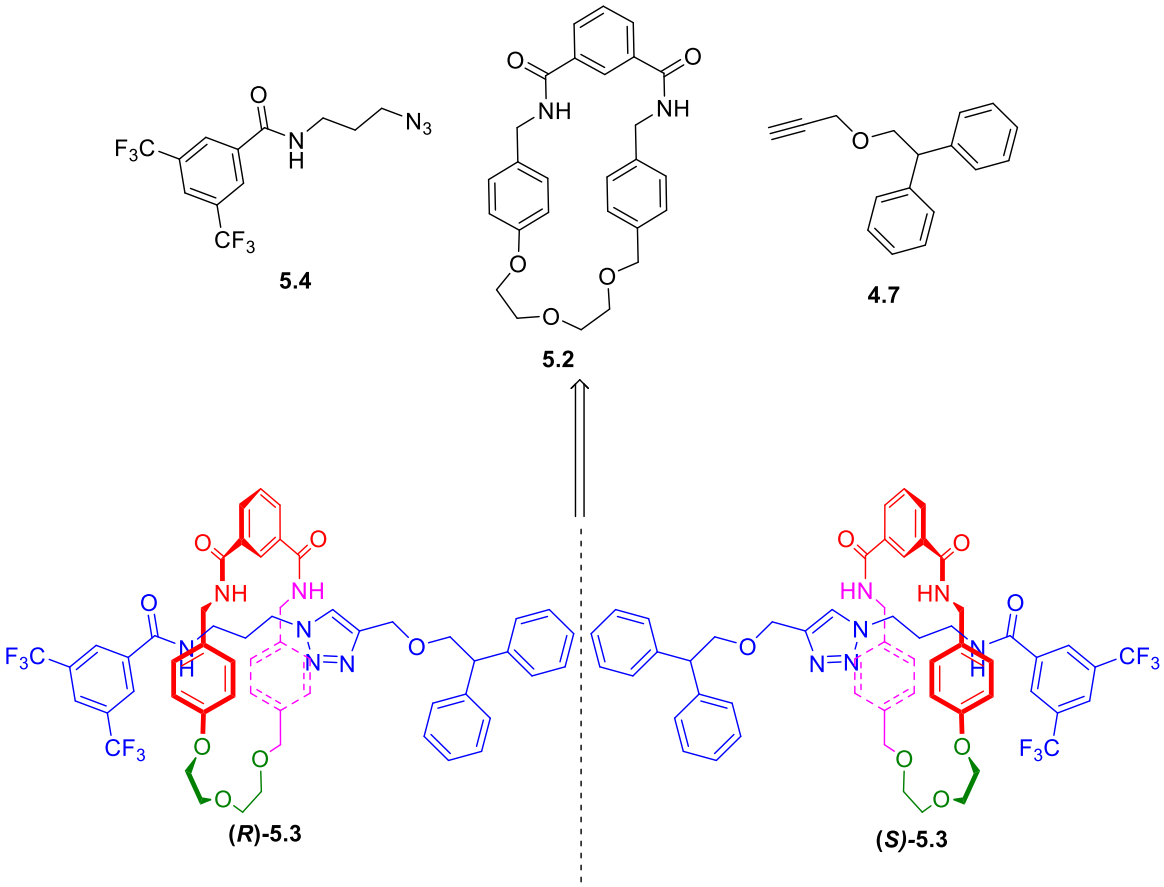

Figure 5.3 - Retrosynthesis of both enantiomers of rotaxane 5.3

The objectives of this study are:

1) Prepare components of rotaxane **5.3** including macrocycle **5.2**
2) Prepare, isolate and characterise rotaxane **5.3**
3) Attempt to separate the enantiomers of rotaxane **5.3**

Initial studies towards this macrocycle and rotaxane were undertaken by Timur Mcardle-Ismaguilov. Preliminary evidence of rotaxane formation was obtained, but the species was not isolated pure. Several steps of the macrocycle synthesis were also unoptimised.

5.2 Synthesis of Rotaxane and Rotaxane Components

5.2.1. Axle Component Synthesis

With alkyne stopper **4.7** already in hand (see Chapter Four), attention turned to the preparation of azide **5.4** by a short two step procedure (Fig. **5.4**).[5] 3-bromopropylamine hydrobromide and 3,5-bis(trifluoromethyl)benzoyl chloride were reacted together in the presence of excess triethylamine. Following aqueous work-up bromo-amide **5.5** was isolated pure in 96% yield. In the second step, **5.5** was submitted to a nucleophilic substitution reaction by use of 3 eq of NaN_3. After extraction, **5.4** was isolated pure in 94% yield.

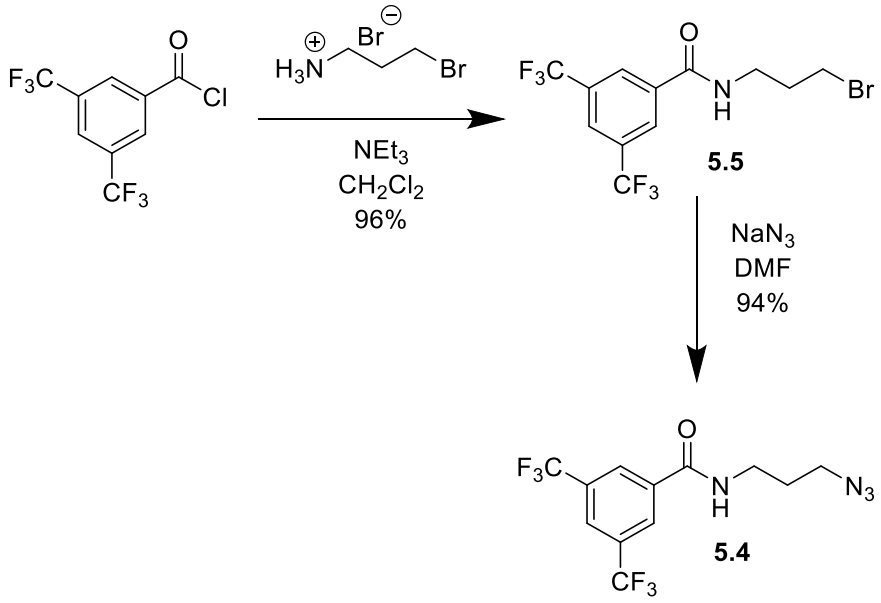

Figure 5.4 – **Synthesis of azide thread 5.4**

5.2.2. Macrocycle Synthesis

Macrocycle **5.2** has already been synthesised by Timur Mcardle-Ismaguilov, using an adapted version of reactions used to make macrocycle **3.16** (Chapter 3). This synthesis was repeated, looking to optimise low yielding steps in the synthesis (Fig. **5.5**).

Asymmetric macrocycle **5.2** was synthesised in five steps. A large excess of diethylene glycol was reacted with tosyl chloride and sodium hydroxide in a THF and water mixture. Following extraction with CH_2Cl_2 mono-tosylate **5.6** was isolated in 86% yield. Mono-tosylate **5.6** was then

refluxed in MeCN with 1.5 equivalents of 4-cyanophenol in the presence of K_2CO_3. The mixture was purified using a basic aqueous work up to yield mono-nitrile **5.7** in 82% yield. Mono-nitrile **5.7** was then deprotonated with NaH in THF, the resulting alkoxide was then stirred with 4-(bromomethyl)benzonitrile. The solution was quenched with water and the crude product purified by silica column chromatography to produce bis-nitrile **5.8** in 85% yield. Bis-nitrile **5.8** was then reduced by refluxing in THF in the presence of borane in THF. Resulting bis-amine **5.9** was purified using an aqueous work up, producing bis-amine **5.9** in 67% yield. Bis-amine **5.9**, pyridinium chloride **2.19** (Chapter 2) and NEt_3 were then dissolved in CH_2Cl_2 and to this was slowly added a solution of isophthaloyl chloride in CH_2Cl_2 under pseudo-high dilution conditions. After an aqueous work up, the crude product was purified by silica gel column chromatography and trituration with EtOAc to produce pure macrocycle **5.2** in 26% yield.

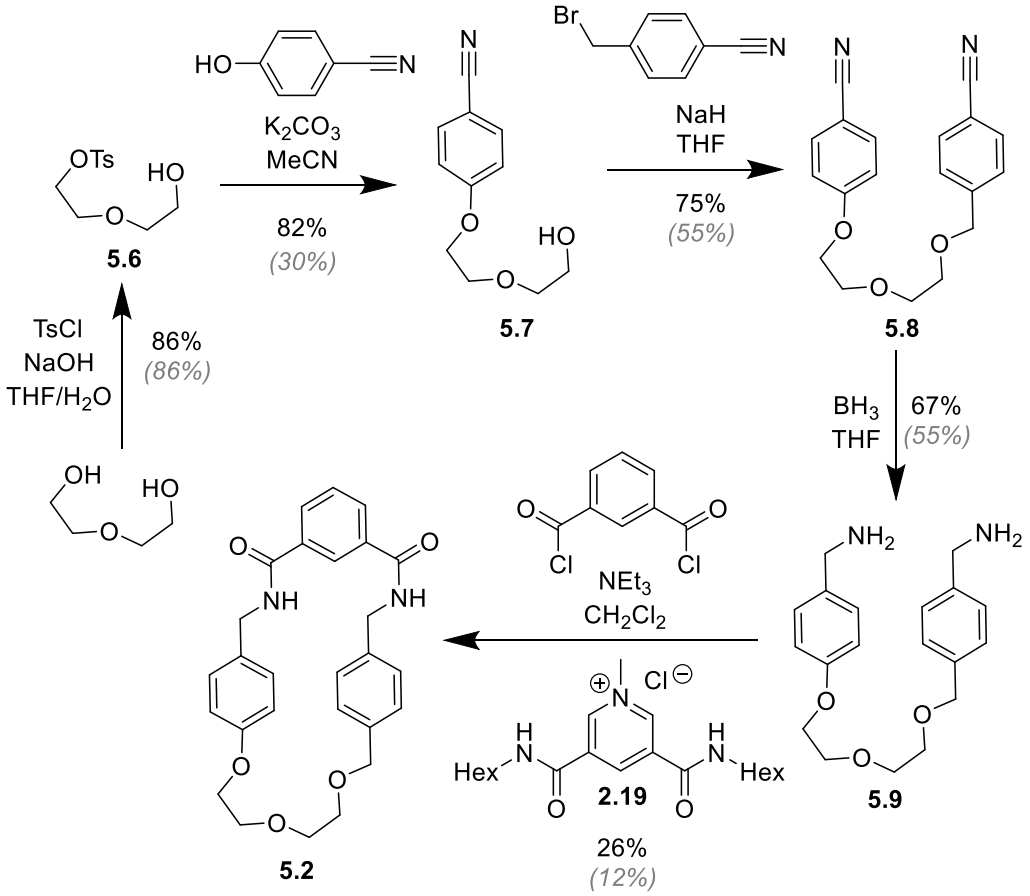

Figure 5.5 - Synthesis of macrocycle 5.2, yields of previous unoptimised attempts are shown in brackets

All of the yields after optimisation were either the same or higher than previously recorded (Fig. **5.4**). The first significant increase in yield, was achieved in the synthesis of mono-nitrile **5.7** from 30% to 82%. This was attributed to purifying compound **5.7** using only a basic work up to remove excess cyanophenol and not an aqueous work up followed by column chromatography; it is thought that compound **5.7** has a tendency to stick on to the silica used to purify it during column chromatography. The small increases in yield of bis-nitrile **5.8** and bis-amine **5.9** are attributed to using larger quantities of starting materials, which minimised incidental losses.

The second major increase in yield is seen in the synthesis of macrocycle **5.2**, where the yield more than doubled, from 12% to 26%. This was attributed to two key changes:

- Use of a template and high dilution conditions, rather than using only a template, thus minimizing polymerization reactions.
- Macrocycle **5.2** was purified by using column chromatography followed by trituration with EtOAc. Previously the macrocycle was purified by two chromatographic columns. It is believed that macrocycle **5.2** sticks to the silica during column chromatography, even when highly polar solvent mixes are used, significantly reducing the yield.

5.2.3. Rotaxane Synthesis and Characterisation

Rotaxane **5.2** was synthesised by dissolving one equivalents of axle **5.4** and suspending macrocycle **5.5** in CH_2Cl_2 (Fig. **5.6**), the solution was briefly heated to reflux, to maximise the amount of macrocycle **5.2** that was dissolved, then allowed to cool and stirred for 30 minutes. Alkyne stopper **4.7** (Chapter 4), DIPEA and catalytic amounts of $Cu(NCMe)_4BF_4$ and TBTA were then added, to stopper the axle using a CuAAc reaction (copper 'click' reaction). The solution was stirred for an hour then purified by an aqueous work up followed by careful column chromatography, to isolate rotaxane **5.3** as a racemate in 34% yield.

The synthesis was repeated using the same procedure except one and a half equivalents of alkyne stopper **4.7** and thread **5.4**, which increased the yield of rotaxane **5.3** to 44% and gave a yield of unthreaded axle **5.10** of 50%.

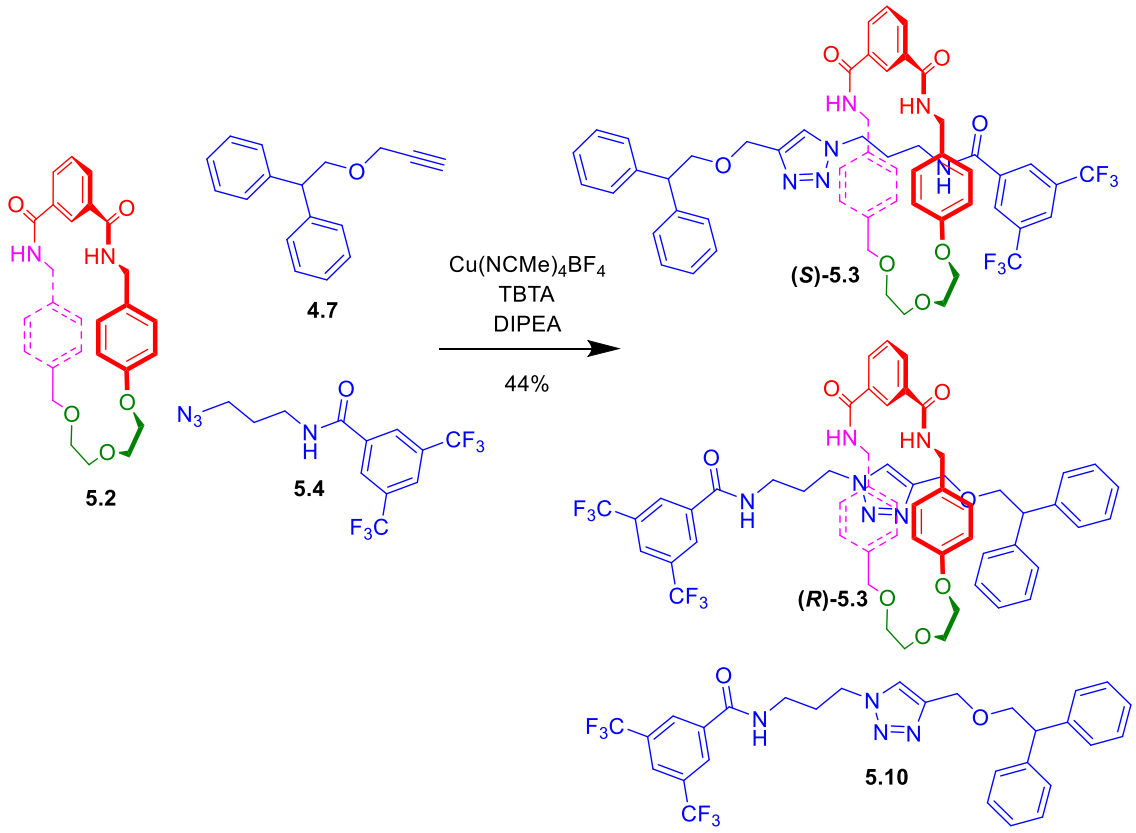

Figure 5.6 – Synthesis of mechanically chiral rotaxane 5.3 and unthreaded axle 5.10

Rotaxane **5.3** was characterised by NMR and IR spectroscopy and HR mass spectrometry. Comparison of the ^{1}H NMR spectra of the rotaxane and non-interlocked axle component **5.10** provides evidence for interlocked structure formation and that the macrocycle resided over the templating amide group (Fig. **5.7**). The amide F-NH, axle aromatic CH group D, axle CH_2 groups G and H can be observed to shift upfield, in the ^{1}H NMR spectra of rotaxane **5.3** when compared to axle **5.10**. This is indicative of the shielding effect from the components residing within the macrocycle cavity. Macrocycle **5.2** was not compared to rotaxane **5.3** owing to the poor solubility of the macrocycle in $CDCl_3$.

Axle protons G have also split, indicating that the two protons on CH_2 groups have become diastereotopic. This is thought to be due to axle protons G experiencing the rotational

asymmetry of the macrocycle, resulting in the protons becoming non-equivalant and splitting. This splitting of protons G is not seen in analogous achiral rotaxane **5.1**, demonstrating that this effect is caused by the chirality of the molecule.[5]

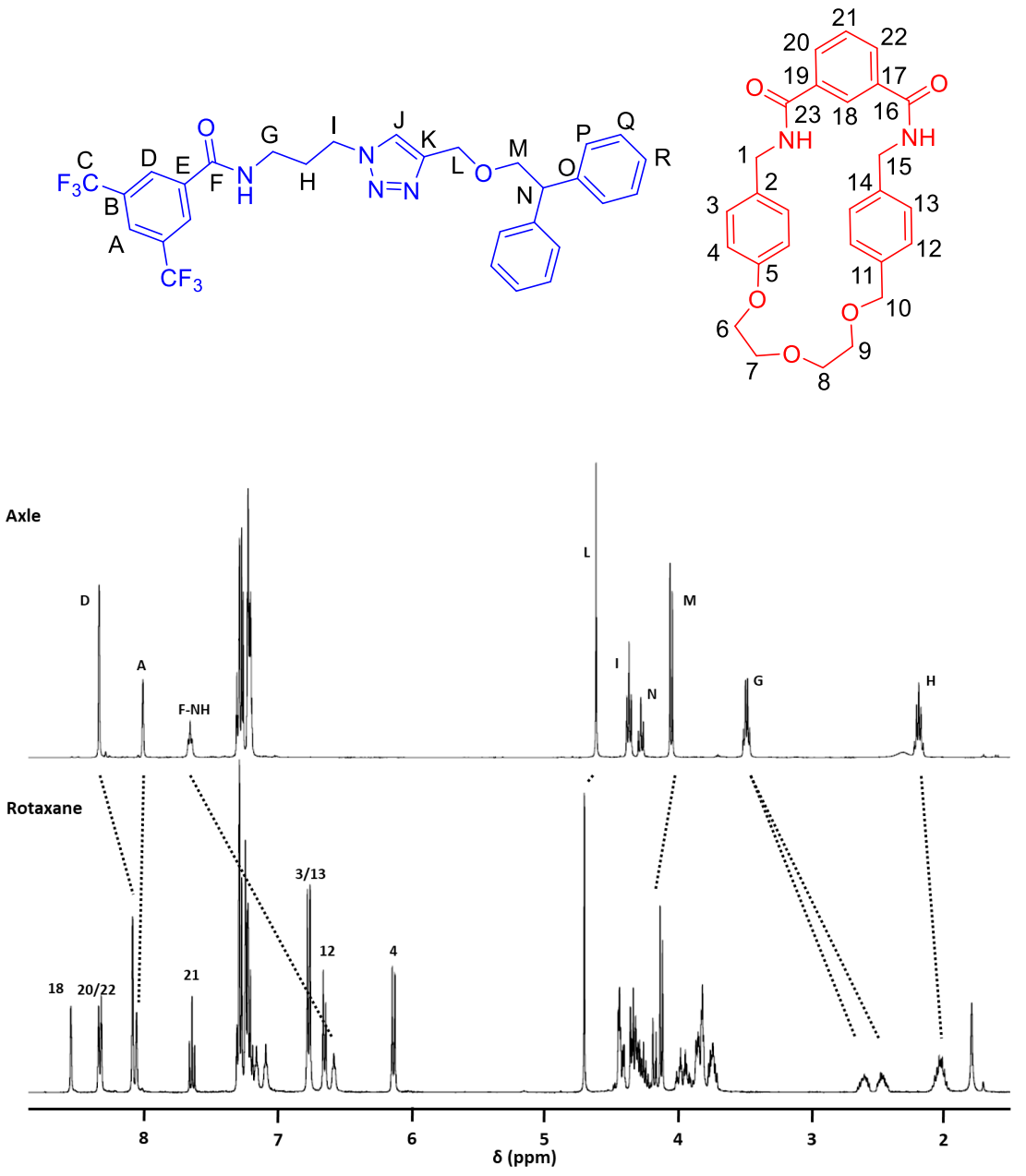

Figure 5.7 – ^{1}H NMR of rotaxane 5.3 as a racemate and axle 5.10 (400 MHz, 298 K, $CDCl_3$)

The diastereotopic nature of protons G is confirmed by the ^{1}H-^{13}C HSQC NMR spectrum (Fig. **5.8**). The two peaks at 2.45 and 2.59 ppm couple to a single carbon resonance at 38.3 ppm.

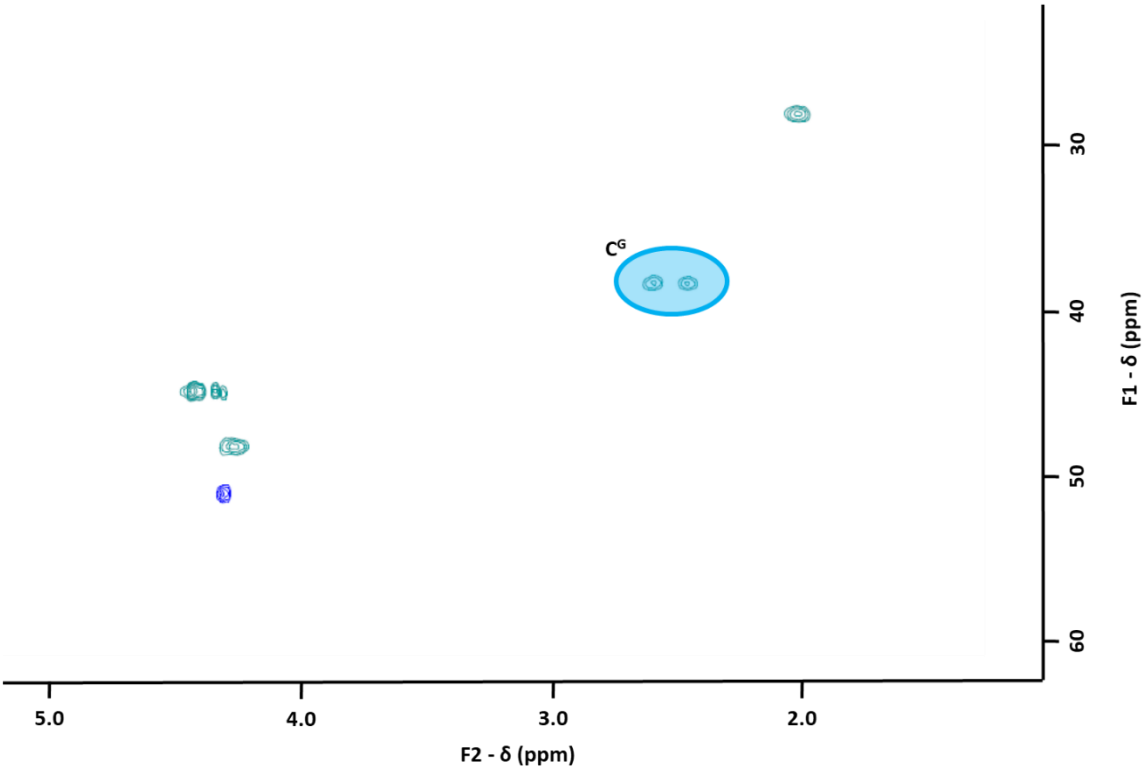

Figure 5.8 – Partial ^{1}H – ^{13}C HSQC of rotaxane 5.3 ($CDCl_3$, 298K)

5.2.4. Separation of Enantiomers by Chiral HPLC

Samples of rotaxane **5.3** were submitted to analytical chiral HPLC, to see whether the enantiomers of rotaxane **5.3** could be separated on a chiral stationary phase. Chiral HPLC was carried out with assistance from Dr. David Rochester.

Samples were analysed on a CHIRALPAK AD-H 4.66 mm × 250 mm column with at a concentration of ≈ 1 × 10^{-4} mol cm^{-3} in 9:1 hexane:IPA and an injection volume of 2 µL. Reasonable separation was achieved in a solution of 4:1 hexane:IPA at a flow rate of 1.5 mL min^{-1} (Fig. **5.9**, Table **5.1**). However, baseline separation of the peaks attributed to the rotaxane was not achievable. Integration of the two peaks at 28 and 32 min, reveals a ratio of 48:52 of material between the two peaks. This non-50:50 ratio is attributed to the lack of baseline separation between the two peaks and is unlikely to be due to any enantiomeric excess. From this data we can conclude that the enantiomers of rotaxane **5.3** were formed as a racemate, which is to be expected in a synthesis that does not have any stereocontrol.

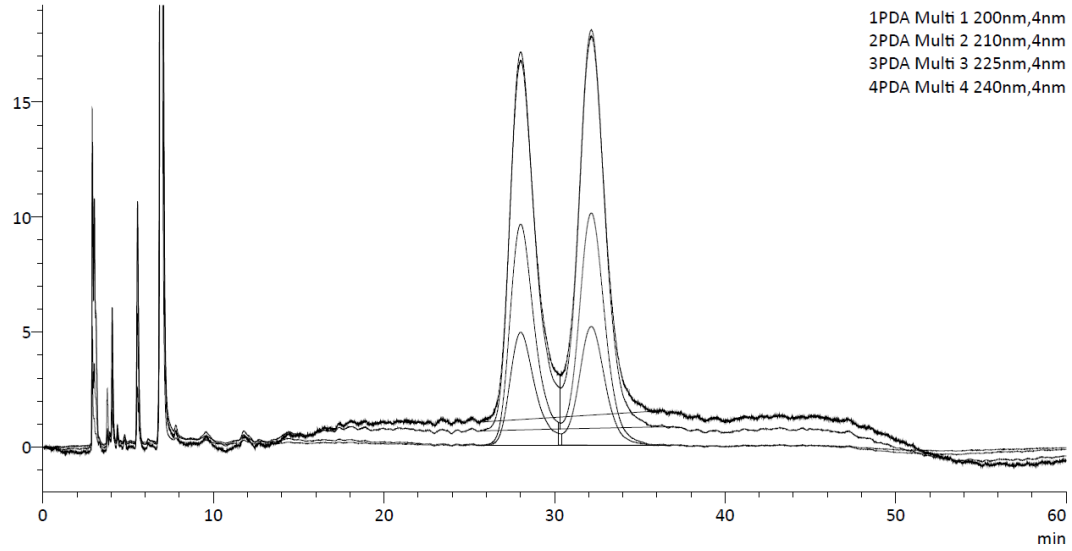

Figure 5.9 – Chromatogram of rotaxane 5.3 (CHIRALPAK AD-H 4.6 mm × 250 mm, 4:1 hexane IPA, 1.5 ml min^{-1})

Table 5.1 – Integration of chromatogram peaks at 240 nm

Peak	Retention Time (min)	Area	Area %
1	28.028	516298	47.493
2	32.163	570811	52.507
Total		1087109	100.000

Investigations were made to increase the separation between the peaks through use of a reduced injection volume. However, this was unsuccessful owing to background noise making it impossible to determine if separation of then peaks had occurred. In addition, attempts to separate the two enantiomers using different stationary phases (CHIRALPAK OJ-H and CHIRALPAK OD-H), were undertaken but also proved unsuccessful.

5.3. Investigating the Chiral Properties of Rotaxane 5.3

Considering the interesting observation of the splitting of protons G in the ^{1}H NMR of rotaxane **5.3** (Fig. **5.9**), attention turned to investigating whether it was possible to modulate the expression of chirality by varying conditions and/or applying a stimulus that could affect the co-conformation of the rotaxane.[8]

5.3.1. Investigating the Expression of Chirality in Different Solvents

The initial NMR studies of rotaxane **5.3** in $CDCl_3$ suggested that the chirality of the molecule is expressed only in the sites where the axle is sheathed in the macrocycle. It was postulated that varying the solvent, whilst maintaining the same concentration of rotaxane **5.3,** may alter the expression of chirality within the rotaxane. To study this ^{1}H, ^{1}H-^{1}H COSY and ^{1}H-^{13}C HSQC NMR spectra were taken of rotaxane **5.3** in number of deuterated solvents (Fig. **5.10**)

A non-competitive solvent, such as $CDCl_3$, (Fig. **5.9**) has been shown to keep the macrocycle in close proximity to the templating amide group. It was thought that more competitive hydrogen bonding solvents, such as D_6-DMSO, D_6-acetone, CD_3OD or CD_3CN may weaken the templating interaction by interfering with the templating hydrogen bonds. The weakening of the templating bonds on rotaxane **5.3** would permit the macrocycle to move more freely along the axle.

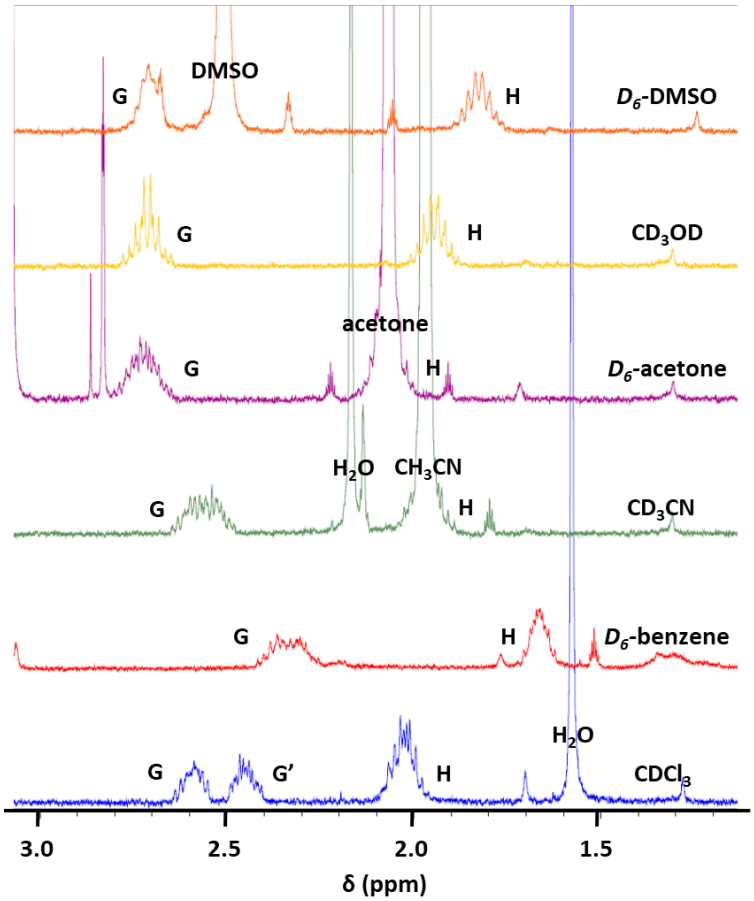

Figure 5.10 – ^{1}H NMR of rotaxane 5.3 in various deuterated solvents (400 MHz, 298 K)

The ^{1}H NMR spectra of rotaxane **5.3** in various solvents (Fig. **5.10**) show that different solvents alter the expression of chirality within the molecule. Diastereotopic protons G are observed to alter their coupling patterns and coalesce into a single and narrower peak in all solvents, when compared to $CDCl_3$. The multiplicity of the peak G also can be observed to become more like a triplet of doublets, that would be expected from a CH_2 group sandwiched between a CH_2 and an amide NH. The changes in protons G suggest that in solvents other than $CDCl_3$ the chirality of the molecule is expressed less through proton G suggesting that the macrocycle is free to shuttle more freely when the hydrogen bonding interaction is weakened by competitive hydrogen bonding solvents.

To determine what solvent parameters affect the expression of chirality within the molecule, using the peak widths at the baseline of the ^{1}H NMR of protons G as a proxy, then comparing

these figures to the Gutmann acceptor and donor numbers (AN and DN), the relative permittivity of the solvent (ε) and the dipole moment of the solvent (μ).

Table 5.2 – Solvent effect parameter and rotaxane 5.3 protons G and H peak width[9,10]

Solvent	Acceptor Number	Donor Number	Relative Permittivity	Dipole Moment (debye)	Proton G Peak Width
	AN	DN	ε	μ	(ppm)
$CDCl_3$	23.1	0	4.7	1.10	0.247
D$_6$-benzene	8.2	0.1	2.3	0.00	0.189
CD_3CN	18.9	14.1	36.0	3.44	0.179
D$_6$-acetone	12.5	17.0	20.7	2.88	0.155
CD_3OD	41.3	19.0	32.6	1.71	0.145
D$_6$-DMSO	19.3	29.8	46.7	3.90	0.093

A pattern can be observed when the shape of peaks attributed to protons G are compared to the Gutmann donor number of the solvent, a measure of the nucleophilicity, hydrogen bond accepting ability or Lewis basicity of the solvent. The width of the peak attributed to proton G decreases as the Gutmann donor number increases. Indeed, the correlation between the donor number of solvent and the width of peak attributed to proton G forms an apparent linear relationship (Fig. **5.11**, particularly when *D*$_6$-benzene is ignored, as it is the only solvent that does not have any lone pairs of electrons to disrupt hydrogen bonding with. This suggests the most important solvent parameter for this effect is the ability of the solvent to accept hydrogen bonds from the macrocycle and axle components from the amide N-H groups of rotaxane **5.3**.

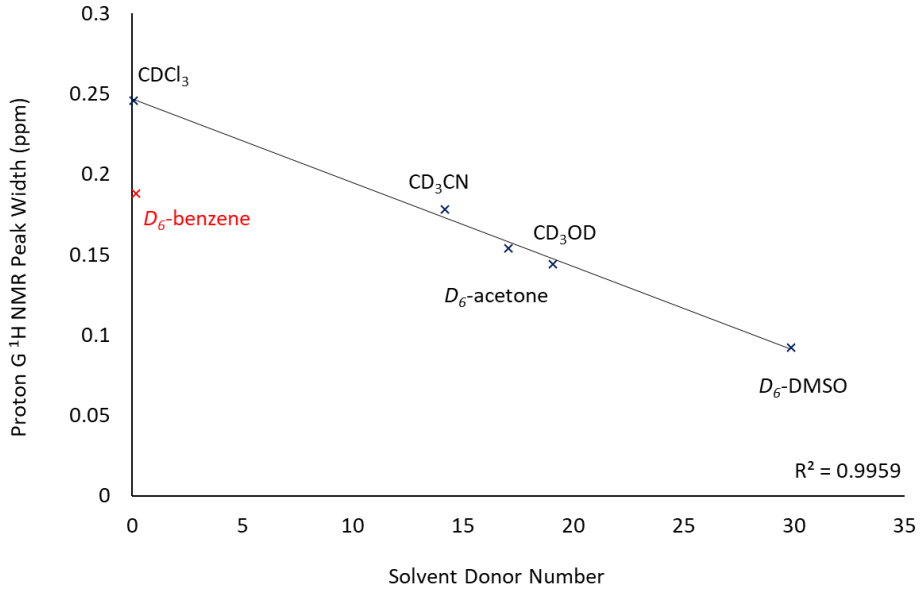

Figure 5.11 – Comparing the solvent donor number of various NMR solvents with the ^{1}H NMR peak width of proton G on rotaxane 5.3 (D_6-benzene is excluded from the trendline)

5.3.2. Investigating the Expression of Chirality using NMR Titrations

Literature precedent suggests that shuttling of the macrocycle along the axle in rotaxane **5.3** may be controlled by varying the pH or addition of alkali metal cations, which would alter the appearance of protons G and G' in the ^{1}H NMR spectrum. To determine if this is the case, NMR titrations were carried out. [11,12]

5.3.2.1. Investigating the Effect of pH on the Expression of Chirality

Addition of TFA to rotaxane **5.3** was expected to result in protonation of the triazole moiety. The protonated triazole may then be stabilised through electron donation from the electron rich polyether groups, that will hydrogen bond to the proton and π-π stacking from the electron rich aromatic groups, this may result in either a shuttling or pirouetting of the macrocycle, inducing a conformational change within rotaxane **5.3** (Fig. **5.12**). If movement of the macrocycle occurs, this may change the expression of chirality within the rotaxane.

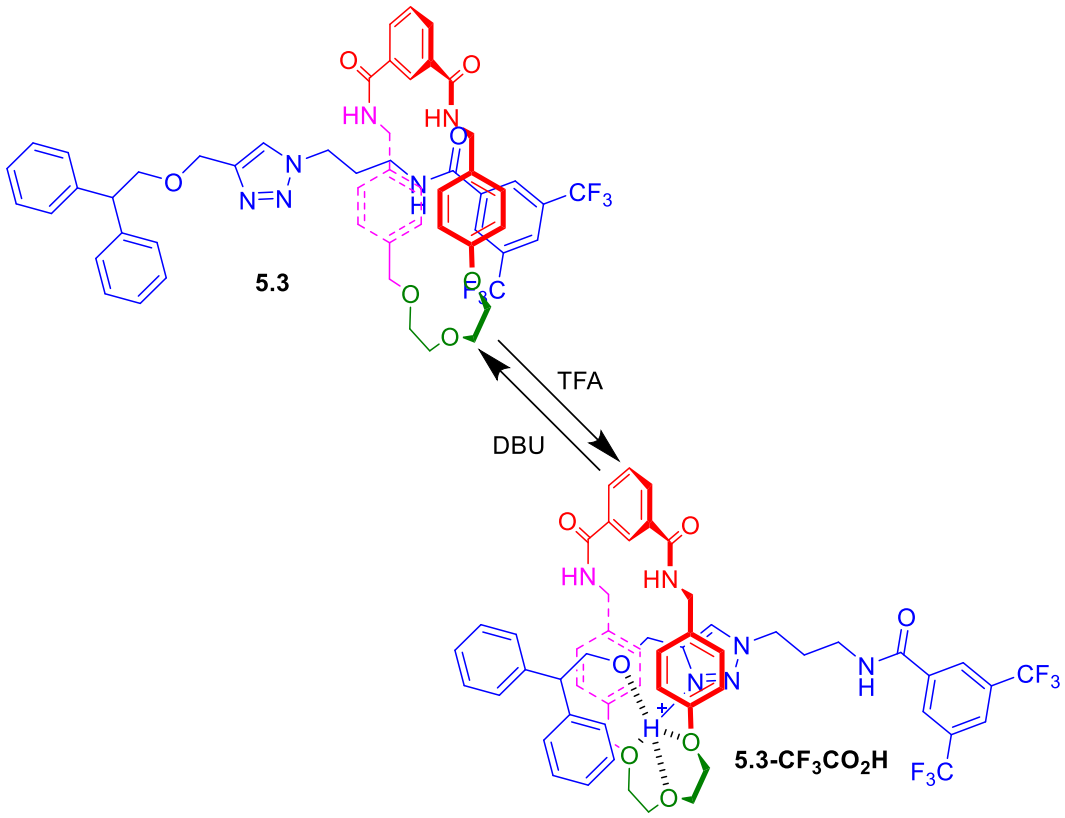

Figure 5.12 – A possible conformational change in rotaxane 5.3 caused by addition of TFA

To establish whether protonation of the triazole induces a change in the expression of chirality within the molecule ^{1}H NMR titrations were carried out on rotaxane **5.3** in $CDCl_3$ (Fig. **5.13**), where aliquots of TFA, dissolved in $CDCl_3$ were added to rotaxane **5.3**. The titration shows that as more TFA is added a downfield shift of triazole proton J can be observed, indicative of protonation of the triazole group. In addition, macrocycle aromatic protons 18, 20 and 22 can be observed to shift upfield, indicative of a change in hydrogen bonding of the amide groups on the macrocycle. Axle protons L and H are observed to shift upfield and proton G is observed to shift downfield. This suggests that protons L and H are now within the macrocycle cavity and proton G is no longer within the macrocycle cavity.

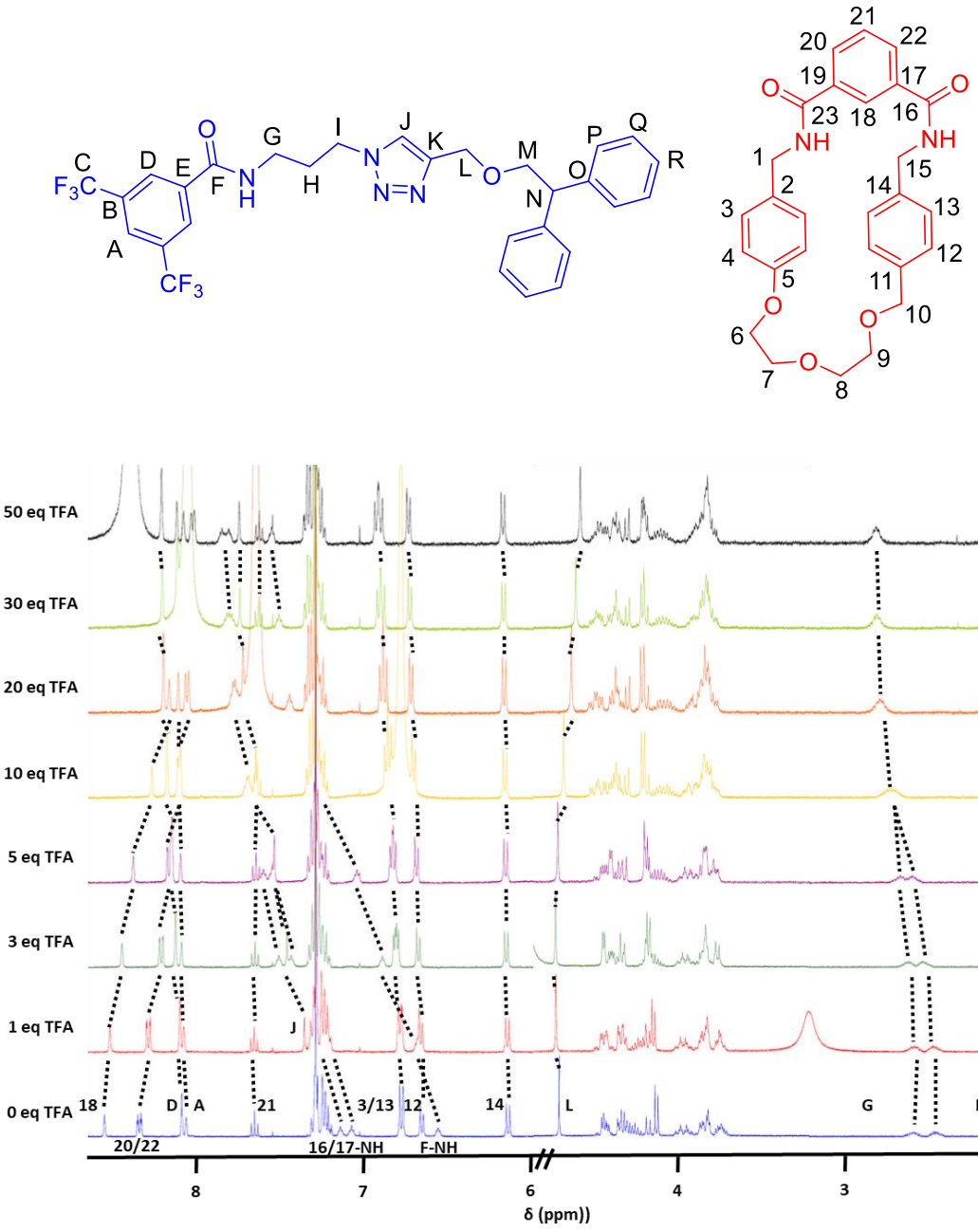

Figure 5.13 – Titration of rotaxane 5.3 with TFA ($CDCl_3$, 400 MHz, 298 K)

The two peaks of proton G, which appears to no longer reside within the macrocycle cavity, can be observed to coalesce and form a single peak that becomes narrower as more TFA is added. This suggests that the expression of chirality within the molecule has changed, as proton G is experiencing the chirality of the molecule less, as there are fewer observable interactions between protons G suggesting that they are no longer diastereotopic.

5.3.2.2. Investigating the Effect of Li^+ on the Expression of Chirality

Following successful demonstration of the modulation of the expression of chirality caused by variation of pH, attention turned towards adding Li^+ to rotaxane **5.3**. This is because the metal cation can bind to both the triazole group, the macrocycle polyether groups and axle amide carbonyl (Fig. **5.14**), resulting in a change in conformation of rotaxane **5.3**, resulting in a change of expression of the chirality of the molecule. To investigate this a ^1H NMR titration was carried out where a solution of $LiPF_6$ in CD_3CN was gradually added to a solution of rotaxane **5.3** in CD_3CN (Fig. **5.15**).

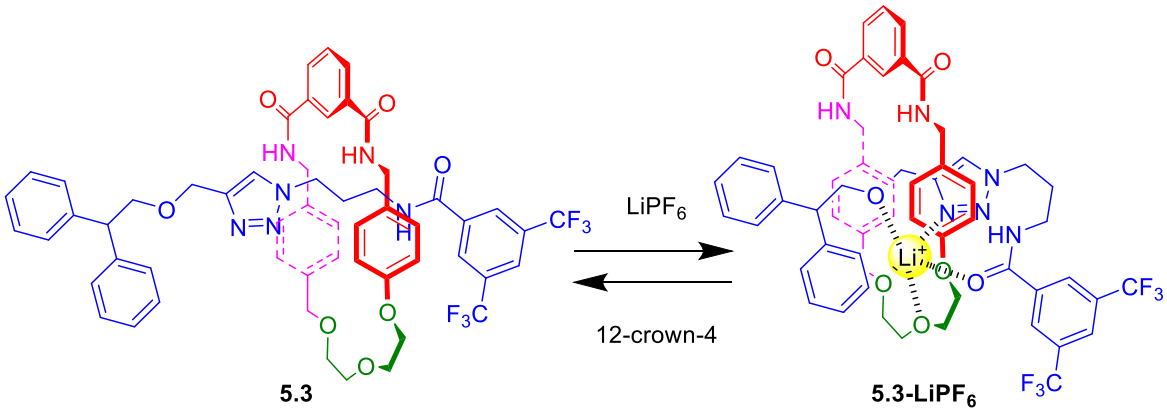

Figure 5.14 – Possible conformational change of rotaxane 5.3 upon addition of $LiPF_6$

The titration undertaken (Fig. **5.15**), shows that as more $LiPF_6$ is added a downfield shift of triazole proton J can be observed, indicative of loss of electron density in the triazole group from a charge dipole interaction with the Li^+ cation. In addition, internal macrocycle aromatic proton 18 can be observed to shift upfield, indicative of a change in hydrogen bonding of the amide groups on the macrocycle. Axle protons G are observed to shift downfield and proton L is observed to shift upfield. This suggests that protons G are now outside the macrocycle cavity and that protons L are now within the macrocycle cavity. A significant narrowing of the peak attributed to protons G can be observed, reflecting a reduction in the diastereotopic nature of the two protons.

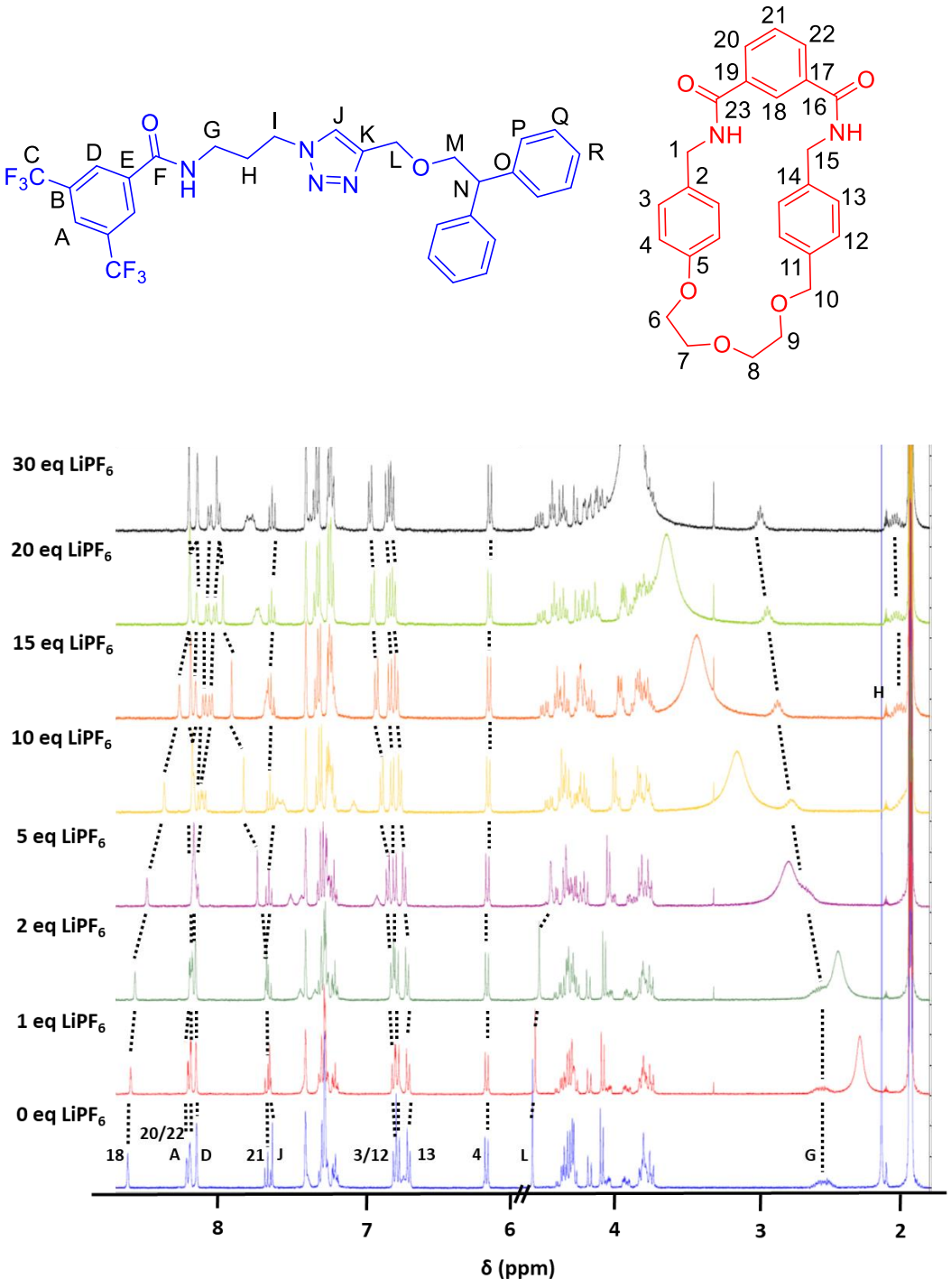

Figure 5.15 – Titration of rotaxane 5.3 with $LiPF_6$ (CD_3CN, 400 MHz, 298 K)

5.4. Investigating the Separation of the Enantiomers of Rotaxane 5.3

Following the synthesis of rotaxane **5.3** as a racemate, investigations were undertaken to separate the enantiomers of rotaxane **5.3**. Inspiration was taken from the promising results in Chapter 3, where diastereotopic salts of rotaxane with an enantiopure anion were separated

by chromatography. As rotaxane **5.3** is neutral, it proved necessary to methylate the triazole group to form a cationic rotaxane.

Rotaxane **5.3** was methylated by refluxing in iodomethane for 48 h. The excess iodomethane was removed *in vacuo* to afford rotaxane **5.11** in a quantitative yield as the iodide salt (Fig. **5.16**).

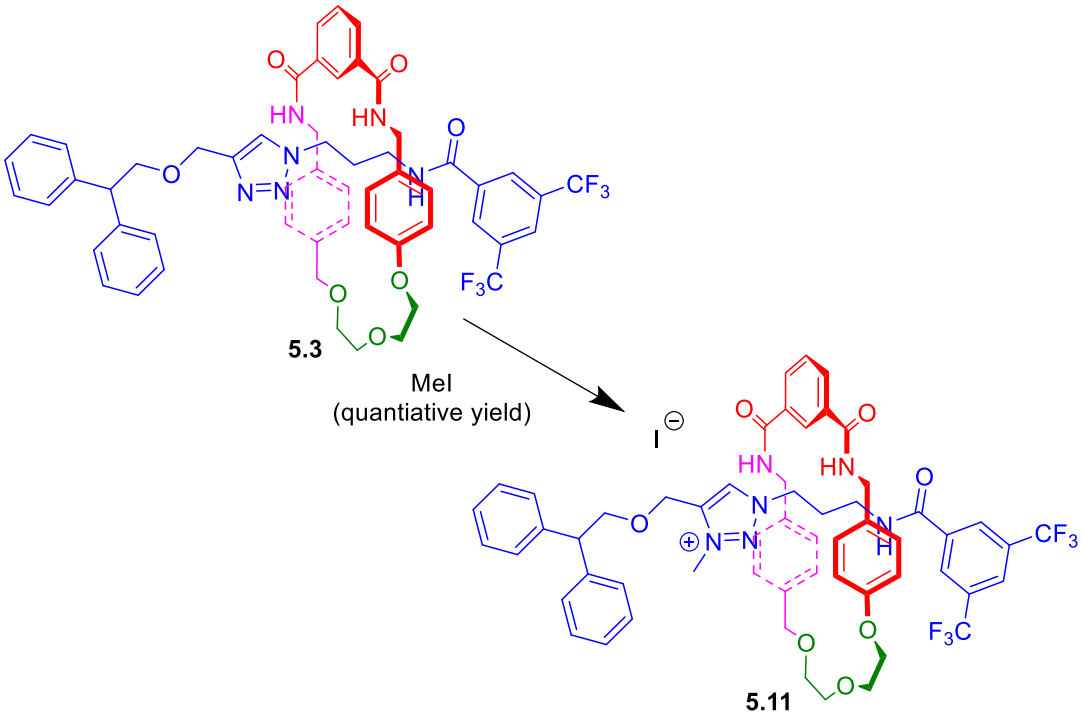

Figure 5.16 – Synthesis of methylated rotaxane 5.11

Methylated rotaxane **5.11** was characterised by NMR and IR spectroscopy and HR mass spectrometry. When the ^{1}H NMR spectra of methylated rotaxane **5.11** was compared to neutral rotaxane **5.3** perturbations in the ^{1}H NMR spectrum could be observed (Fig. **5.17**). A peak attributed to proton S appears, due to the methylation of the triazole, in addition triazole proton J shifts upfield, consistent with the triazole becoming positively charged. Shifts in other areas of the rotaxane are indicative that the macrocycle has moved to cover the methylated triazole in preference to the amide group on the axle. Proton G can be observed to become narrower and has shifted downfield and proton H can be observed to become broader and has shifted upfield. This indicates that proton G is no longer within the macrocycle and proton H now resides within the macrocycle. In addition, protons 3 and 13 can be observed to split, suggesting a π-π stacking

interaction between the electron deficient methylated triazole and relatively electron rich macrocycle aromatic groups. Finally, axle protons D can be observed to shift upfield, indicating that chemical shift of these protons is no longer affected by the macrocycle.

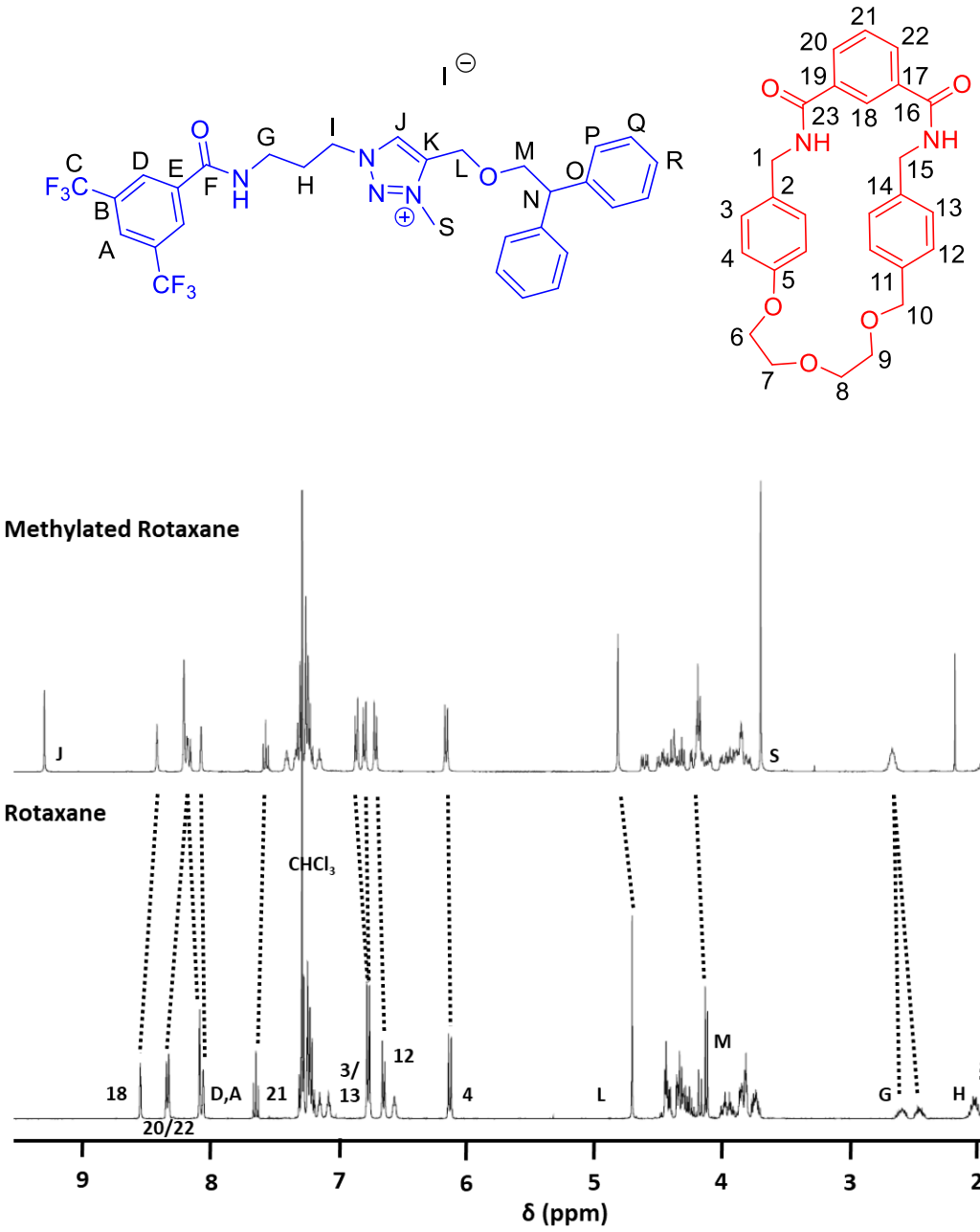

Figure 5.17 – ^{1}H NMR of methylated rotaxane 5.11 and neutral rotaxane 5.3 ($CDCl_3$, 400 MHz, 298 K)

Portions of the iodide salt of rotaxane **5.11** were then dissolved in CH_2Cl_2 and washed (8 × 5 mL) with 0.2 mol dm^{-3} solutions of various salts of enantiopure chiral anions to form rotaxane **5.11-**

b (-)-O'O'dibenzoyl-L-tartrate, rotaxane **5.11-c** L-tartrate, and rotaxane **5.11-d** (*1R*)-(-)-10 camphorsulfonate. Inspection of the ^{1}H NMR spectra (Fig. **5.18**) suggested that the iodide anion was successfully exchanged to the relevant anion for rotaxanes **5.11-b** and **5.11-d**. However, as for mechanically chiral rotaxane **3.1** (Chapter 3) rotaxane **5.11** would not exchange to L-tartrate anion (rotaxane **5.11-c**).

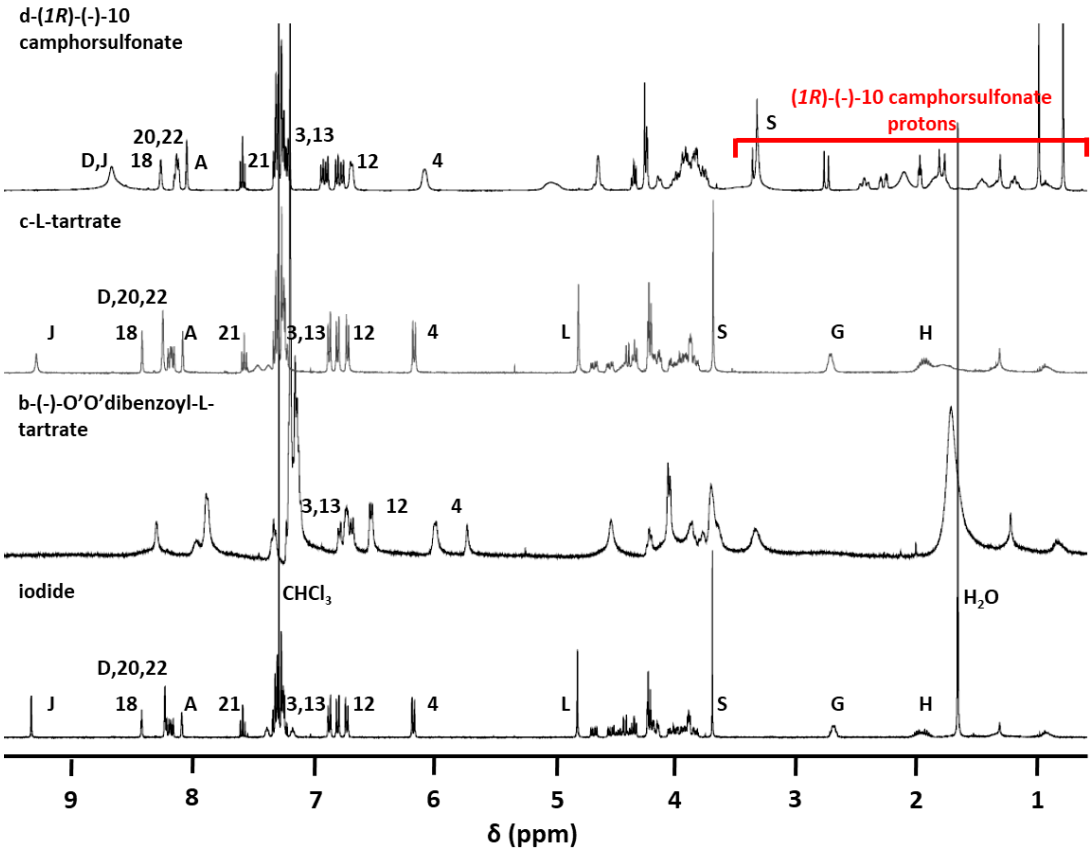

Figure 5.18 - ^{1}H NMR of rotaxanes 5.11, 5.11-b, 5.11-c, 5.11-d (400 MHz, 298 K, $CDCl_3$)

Investigations were then made into separating the enantiomers of rotaxanes **5.11-b** and **5.11-d**. Separation of the diastereomeric rotaxane salts was not possible by column chromatography or preparative TLC as it was found that the material stuck to the silica and could not be removed even with highly polar eluents. Attempts were then made to separate the diastereomers of the rotaxanes by slow crystal growth. No crystals suitable for x-ray diffraction structural determination were grown, despite repeated attempts with a variety of solvent systems.

5.5. Conclusion

Mechanically chiral rotaxane **5.3** was successfully synthesised as in 44% yield, as a racemate. Rotaxane **5.3** was characterised by NMR and IR spectroscopy and HR mass spectrometry. Analytical chiral HPLC was carried out, with baseline separation of the two enantiomer peaks almost achieved.

Attention on (neutral) rotaxane **5.3** focused on the expression of chirality as reported by the appearance of the two protons (G) on the carbon adjacent to the axle amide. First solvent was varied. Solvents that were poor electron donors resulted in the macrocycle residing at the templating axle amide, resulting in diastereotopic behaviour of protons G. Solvents that were good electron donors interfered with the inter-component hydrogen bonding, and so the macrocycle moved freely along the axle, and only a single peak was observed for proton environment G. Subsequently, it was found that addition of TFA or $LiPF_6$ caused a shuttling of the macrocycle along the axle resulting in a change in the expression of chirality.

The rotaxane was then methylated in quantitative yield to form rotaxane **5.11**. It was observed that methylation did appear to induce motion of the macrocycle ring – with a loss in diastereotopic behaviour of protons G. The achiral iodide counter anion was exchanged for several enantiopure chiral anions to form diastereomeric salts. Attempts were made to separate the enantiomers, although this were unsuccessful.

Considering the difficulty in separating the enantiomers of rotaxanes **5.11-b** and **5.11-d**, attention instead turned to further investigating the shuttling behaviour of such rotaxane systems, as described in Chapter 6.

5.6. References

[1] W. L. Mock and J. Pierpont, *J. Chem. Soc. Chem. Commun.*, 1990, 1509-1511.
[2] M.-V. Martínez-Díaz, N. Spencer and J. F. Stoddart, *Angew. Chemie Int. Ed. English*, 1997, **36**, 1904–1907.
[3] C. M. Keaveney and D. A. Leigh, *Angew. Chemie Int. Ed.*, 2004, **43**, 1222–1224.
[4] N. H. Evans and G. R. Akien, *Supramol. Chem.*, 2018, **30**, 158–164.
[5] B. E. Fletcher, M. J. G. Peach and N. H. Evans, *Org. Biomol. Chem.*, 2017, **15**, 2797–2803.
[6] N.H. Evans, C. E. Gell and M. J. G. Peach, *Org. Biomol. Chem.*, 2016, **14**, 7972–7981.
[7] A. Vidonne, T. Kosikova and D. Philp, *Chem. Sci.*, 2016, **7**, 2592-2603
[8] G. Bottari, D. A. Leigh and E. M. Pé Rez, *J. Am. Chem. Soc.*, 2003, **125**, 13360–13361.
[9] G. Wypych, *Handbook of solvents 1st Edition*, ChemTec, Toronto, 2001.
[10] U. Mayer, V. Gutmann and W. Gerger, *Monatshefte ffir Chemie*, 1975, **106**, 1235–1257.
[11] W. Zhou, J. Li, X. He, C. Li, J. Lv, Y. Li, S. Wang, H. Liu and D. Zhu, *Chem. - A Eur. J.*, 2008, **14**, 754–763.
[12] Zheng, W. Zhou, J. Lv, X. Yin, Y. Li, H. Liu and Y. Li, *Chem. - A Eur. J.*, 2009, **15**, 13253–13262.

Chapter 6

Further Investigation into Hydrogen Bond Templated Rotaxanes for Use as Molecular Machines

6.1. Introduction

6.1.1. Chapter Aims

The aim of this chapter is to develop a hydrogen bond rotaxane, using a similar motif to mechanically chiral hydrogen bond templated rotaxane **5.3** in Chapter 5, and demonstrate that the macrocycle of the rotaxane can shuttle along the axle, in response to external stimuli.

The rotaxane described in Chapter 5, has the potential to act as a molecular switch, as the axle possesses two stations where the macrocycle can reside. The first station is the templating amide moiety, where the macrocycle will reside when the rotaxane is not exposed to stimuli. The second station is a 1,2,3-triazole, formed by a Huisgen 1,3-dipolar cycloaddition ("Cu click reaction") used to stopper the rotaxane.

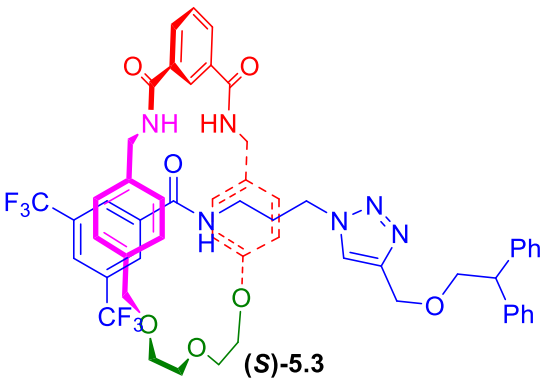

(*S*)-5.3

Figure 6.1 - Mechanically chiral rotaxane *(S)*-5.3 developed in chapter 5

The rotaxanes developed in this chapter will have several modifications made to the structure. For ease of synthesis and analysis a symmetric macrocycle will be used. Furthermore, the axle will be made more rigid, to ensure what we observe is a translational shuttling of the macrocycle and not a conformational change in the rotaxane. The shuttling behaviour of the rotaxane will then be tested by qualitative NMR titrations with the addition of acid or alkali metal cation.

6.1.2. A Short Review of Hydrogen Bond Templated Rotaxanes as Molecular Machines

The following literature review will focus upon illustrative examples of hydrogen bond templated rotaxanes, where molecular motion is induced by variation in pH or addition and removal of alkali metal cations.

Rotaxanes are perhaps most famous for their use as molecular machines, a molecule that can provide a useful work in response to a stimuli, especially since the awarding of the 2016 Nobel Prize in Chemistry.[1,2] This ability of rotaxanes to act as molecular machines arises due to the lack of a covalent link between the macrocycle and axle. In appropriately designed systems this allows the macrocycle to shuttle along and to pirouette around the axle. Such motions have been triggered by a variety of stimuli including; heat, light, electrochemical or chemical reduction/oxidation, change of solvent, addition of cations, addition of anions, addition of neutral molecules and change of pH.[3–8]

These controlled molecular motions are not just a chemical curiosity, they have been exploited by chemists to make functional molecular machines. An example of this is a shuttling rotaxane in Stoddart and Heath's 160 KB binary computer, where an electrochemical oxidation causes the macrocycle to shuttle between the ground state (0 or off) site to the excited state (1 or on).[9] The Leigh group have also developed rotaxanes, that when excited by light undergo a change in conformation of the axle component, inducing a shuttling motion that moves a liquid droplet up an incline.[10] The same group have also constructed rotaxanes that can prepare peptide sequences in a predefined order, as the macrocycle shuttles along the axle.[11]

6.1.2.1. Shuttling Induced by a Change of pH

Protonation or deprotonation often causes changes in the hydrogen bonding and electrostatic interactions within a molecule. In interlocked molecules, such as rotaxanes, these changes of intramolecular interactions can be used to move the components relative to one another,

thereby creating a molecular machine. Hydrogen bond templated rotaxanes that shuttle due to change in pH have been studied since the 1990's and generally come in two types.

The first type consists of rotaxanes using either a polyether macrocycle or any macrocycle that has oxygen atoms symmetrically arranged (e.g. crown ethers, cururbiturils). Typically, in such rotaxanes, under acidic conditions the macrocycle resides at a protonated secondary ammonium cation, while under basic conditions the macrocycle resides at a permanent positive charge (Fig. **6.2**).

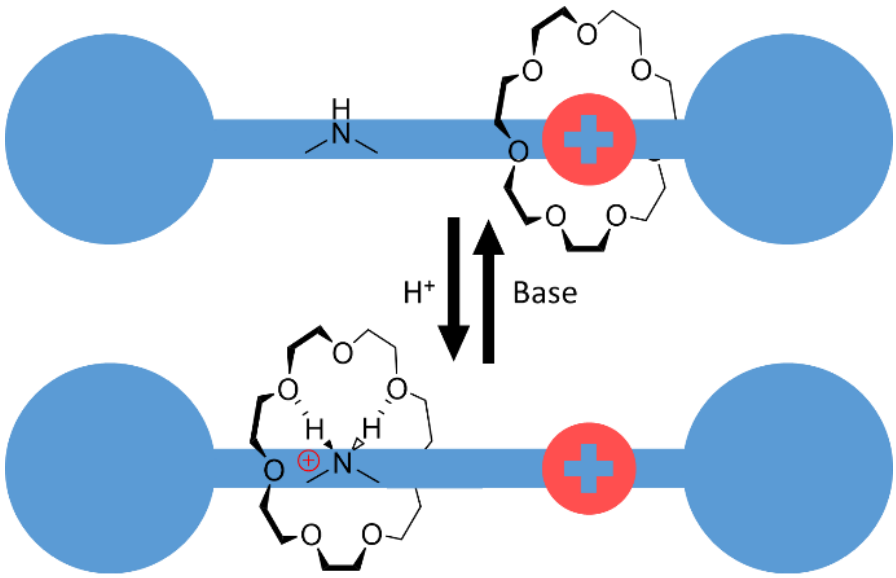

Figure 6.2 – A typical shuttling motif of a polyether based rotaxane shuttle triggered by pH change.

The second type consist of a macrocycle with two or four hydrogen bonding benzylic amides, or less frequently amines. Typically, these rotaxanes have macrocycles containing one or two isophthalamide moieties, that bind a carbonyl group on the axle, acting as one shuttling site and the template for the rotaxane. The macrocycle then moves to a second site upon an axle group protonating or deprotonating due to a change of pH (Fig. **6.3**). These rotaxanes can be used to stabilise a negative charge through hydrogen bond donation or have additional groups as part of the macrocycle (e.g. a polyether chain), that can stabilise a positive charge.

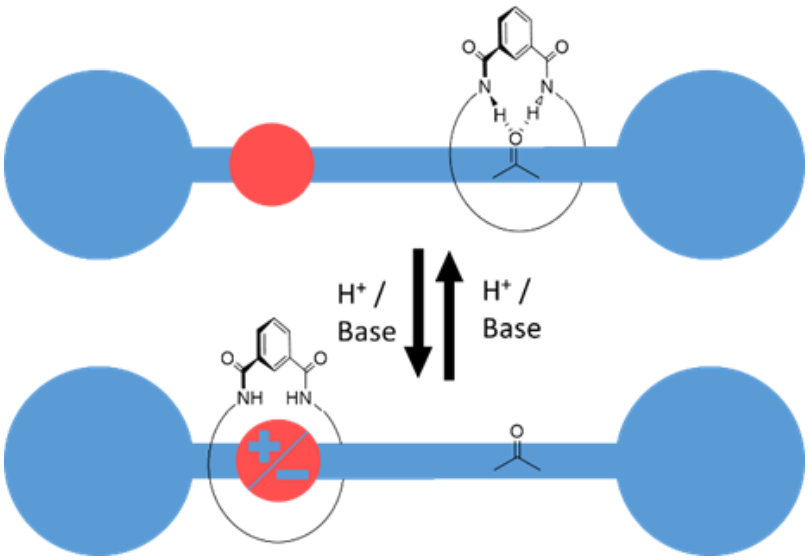

Figure 6.3 – A typical shuttling motif of an isophthalamide-carbonyl based rotaxane shuttle triggered by pH change.

6.1.2.1.1. Cucurubituril Based pH Dependent Shuttling Rotaxanes

Mock in 1990 first demonstrated that pH can be used to control the position of a macrocycle on an axle, using a cucurubit[6]uril based pseudorotaxane **6.1** in water (Fig. **6.4**).[12] At high pH the macrocycle sits above the primary and secondary ammonium cations, to stabilise them through charge dipole and hydrogen bonding interactions. At lower pH the aniline, which has a lower pK_a, is also protonated causing the macrocycle to shuttle. This shuttling occurs as the hexa-methylene spacer between the anilinium ion and the secondary amine, is a similar length to the inside of the macrocycle. This causes the macrocycle to bind the ammonium cations separated by a hexa-methylene chain more strongly (K = 2.8 × 10^6) than the ammonium cations separated by the shorter tetra-methylene chain (K = 2.7 × 10^5), leading to shuttling of the macrocycle. In addition, the formation of pseudorotaxane **6.1** could argued be to a second form of molecular machine behaviour, as at very high pH only the neutral free thread and macrocycle are found and upon protonation the pseudorotaxane forms.

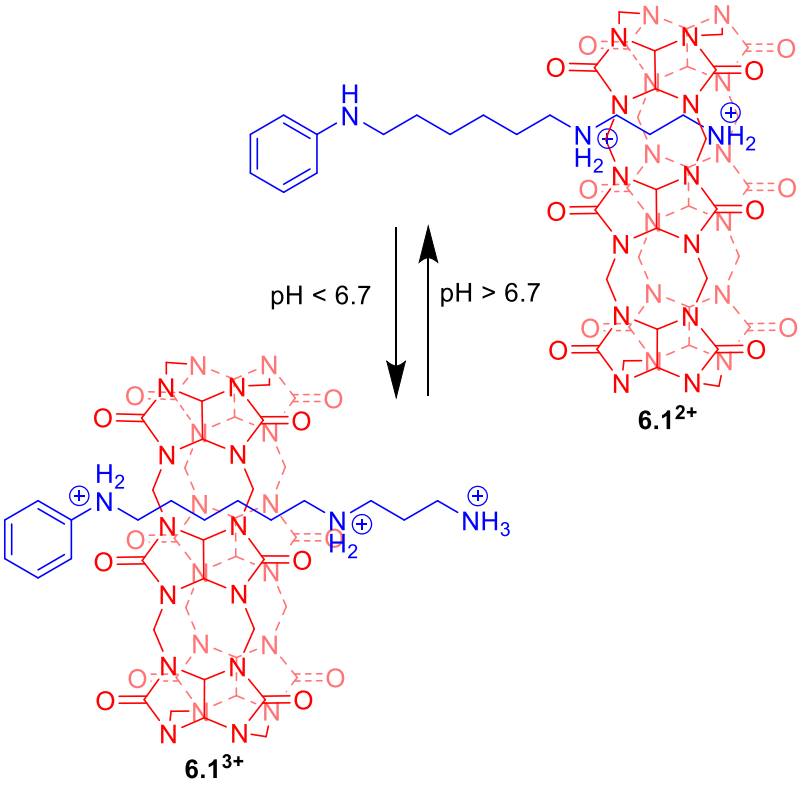

Figure 6.4 - Mock's cucurbit[6]uril pH shuttling pseudorotaxane 6.1

There are other examples of this type of system, notably by Kim. However, these are all pseudorotaxanes.[13] Tuncel and co-workers have developed this system into true rotaxanes having developed [3]rotaxane **6.2**, using a secondary ammonium cation on the axle to act as a template.[14,15] [3]Rotaxane **6.2** has been shown to shuttle in water (Fig. **6.5**), under basic conditions the macrocycles of [3]rotaxane cover the hydrophobic spacer chain, when protonated with hydrochloric acid and heated the macrocycles move to bind the protonated amines. This process can then be reversed without heating by adding sodium hydroxide.

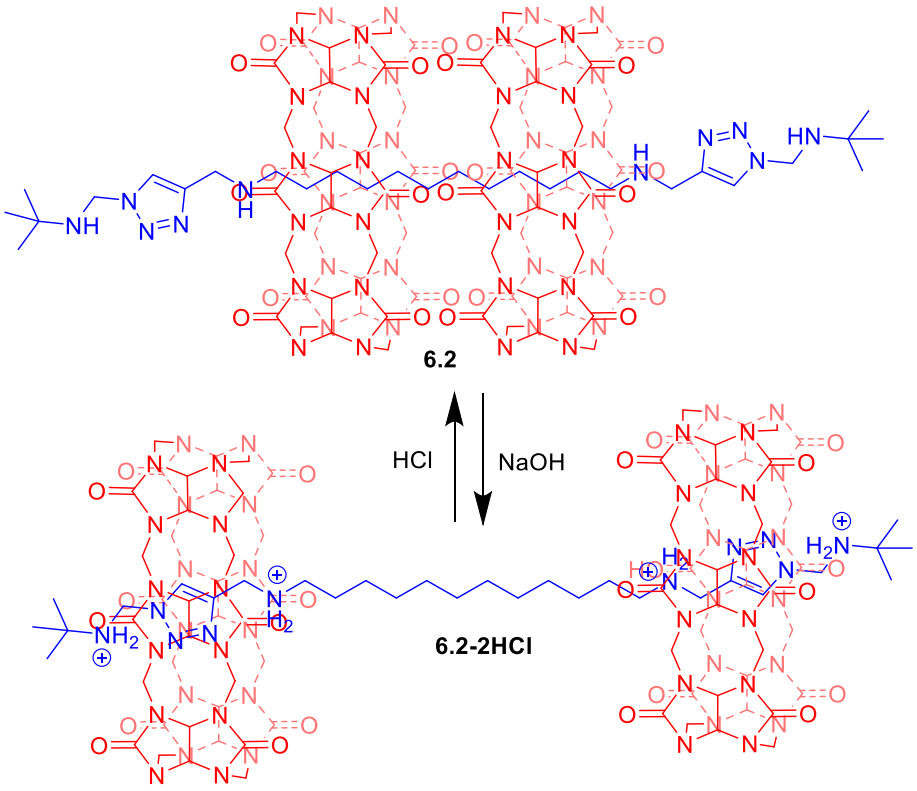

Figure 6.5 – Tuncel's cucurbit[6]uril pH shuttling [3]rotaxane 6.2

The insolubility of cucurbitrils in solvents other than acidic water and difficulties faced introducing functional groups to these molecules, limits their usefulness as macrocycles in rotaxane based molecular machines.[16,17] Instead chemists have developed rotaxane based molecular machines that use macrocycles that are easier to functionalise, such as crown ethers.

6.1.2.1.2. Crown Ether Based pH Dependent Shuttling Rotaxanes

Perhaps the most well explored rotaxanes that undergo shuttling induced by pH change, are those that use a crown ether as the macrocycle. Stoddart and co-workers developed shuttling rotaxane **6.3** containing a dibenzo-24-crown-8 macrocycle, that was synthesised, using a secondary ammonium cation acting as a template in the axle precursor (Fig. **6.6**).[18] In rotaxane **6.3** the secondary ammonium cation acted as the acidic station, and upon addition of DIPEA in D_{10}-diethyl ether the ammonium cation is deprotonated causing the macrocycle changed shape and shuttle to the bipyridinium station. This is to stabilise the π-deficient system with π-π

stacking from the electron rich catechol moieties. The process was then reversed by the addition of TFA, protonating the amine, causing the macrocycle to shuttle back to the ammonium cation.

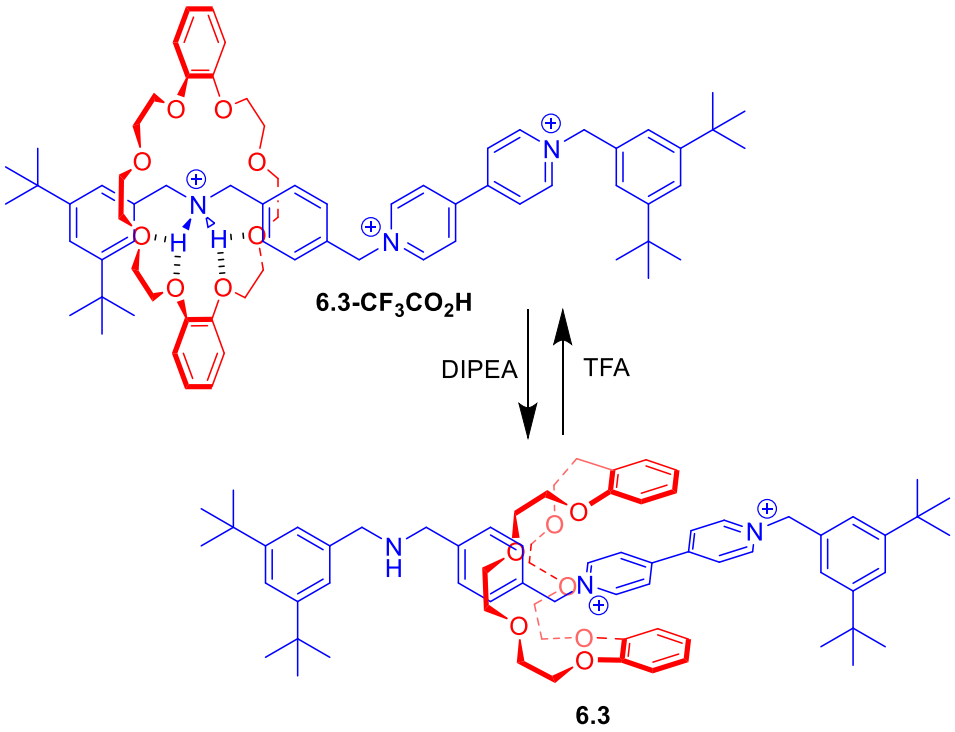

Figure 6.6 – Stoddart's crown ether rotaxane 6.3

There have been multiple iterations of this systems for example by Leigh, Loeb, and Takata, all using an ammonium cation as the template and acidic site and an electron deficient π system as the basic site.[19–21] However, Coutrot's 1-methyl-1,2,3-triazolium containing rotaxane **6.4** (Fig. **6.7**) is a key development in this class of rotaxanes, as it uses a CuAAC click reaction to link the two axle halves in high yield (72%). The resulting triazole can then be chemoselectively methylated in quantitative yield, to provide the second station.[22] This design of rotaxane shuttle has been further developed by Lützen, Tian, Álvarez and Liu to make multiple shuttle rotaxanes that report the location of the macrocycle by the incorporation of sensing functionality into the rotaxane structure.[23–26]

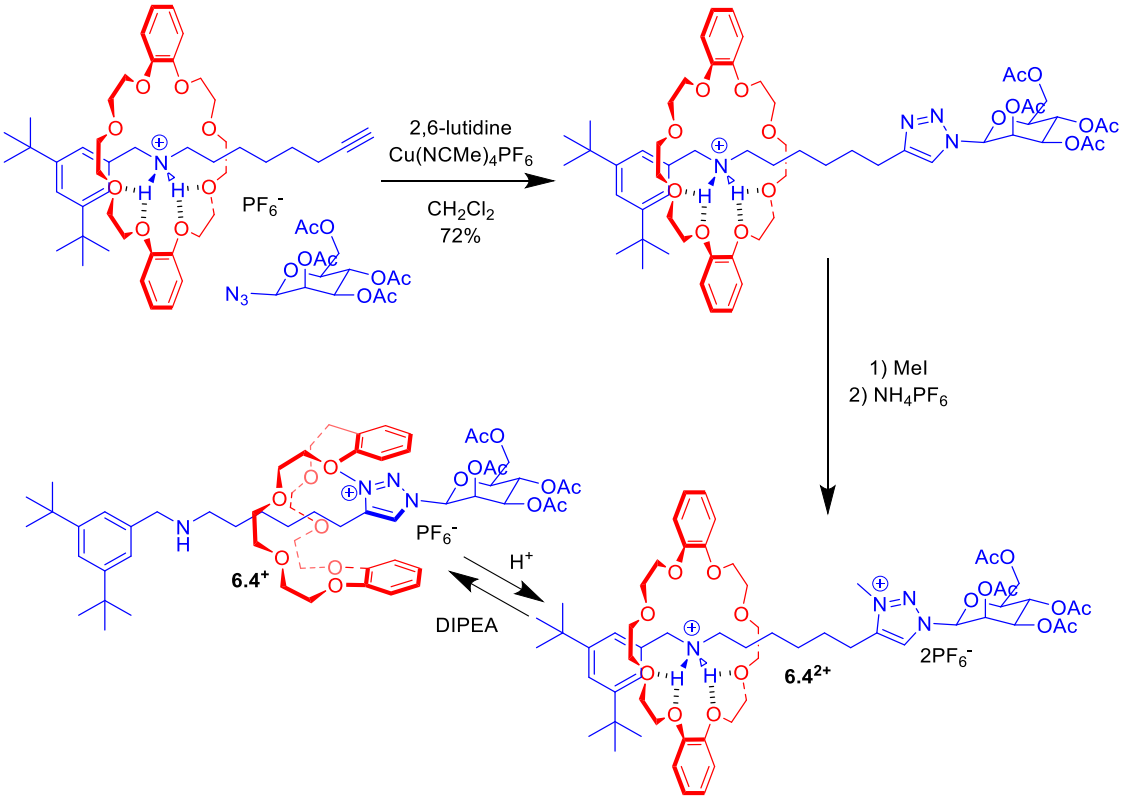

Figure 6.7 –Synthesis of Coutrot's triazolium rotaxane 6.4

A particularly attractive example was prepared by Chen and co-worker, a [2]rotaxane based pulley **6.5**, using three linked dibenzo-24-crown-8 rings, shaped like a pulley and a flexible axle that runs through them like a rope. The axle contains three sets of alternating pH sensitive secondary ammonium groups and 1-methyl-1,2,3-triazolium groups, making the two ends of the axle inequivalent. (Fig. **6.8**) Under acidic conditions the three ammonium groups bind to the crown ether rings, but under basic conditions the axle shuttles along three triazoium units bind to the crown ether rings. This causes the entire axle to move, in doing so the changes the length of the two ends of the stopper that protrude from the macrocycles, acting like a pulley.[27]

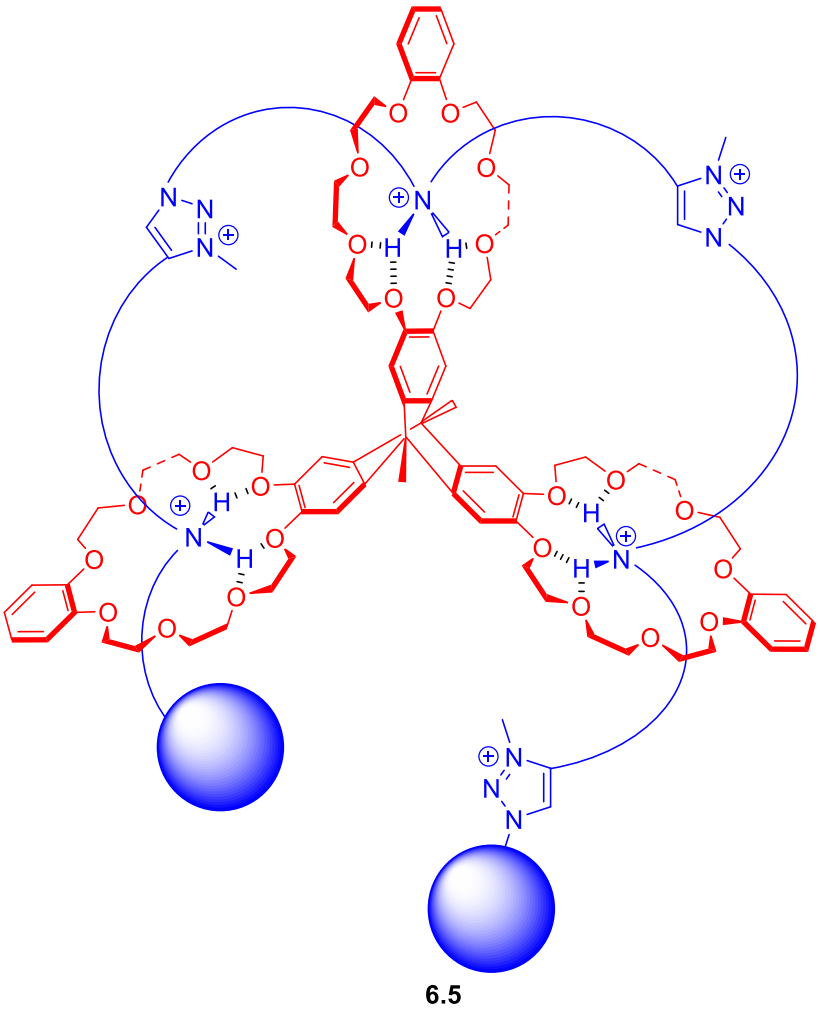

6.5

Figure 6.8- Schematic of Chen's [2]rotaxane 6.5 based pulley

Whilst rotaxanes that use crown ethers as the macrocycle are the most studied components of hydrogen bond templated molecular machines, owing to their versatility and commercial availability, they can only be used to bind to positive charges. This limits crown ether based macrocycles to only being used in systems where a neutral molecule is protonated. An alternative motif is required for negative charges.

6.1.2.1.3. Isophthalamide Based pH Dependent Shuttling Rotaxanes

Isophthalamide rotaxanes offer greater flexibility than crown ether rotaxanes, as they can act as shuttles, by either the deprotonation or protonation of the axle component, depending on the presence of additional functionality on the macrocycle. Rotaxane **6.6** (Fig. **6.9**), developed by the Leigh group is an example of such an isophthalamide based system. The rotaxane was

synthesised by using a hydrogen bond templated clipping method, where two isophthalamide units on the macrocycle hydrogen bond to a succinamide unit on the axle.[28]

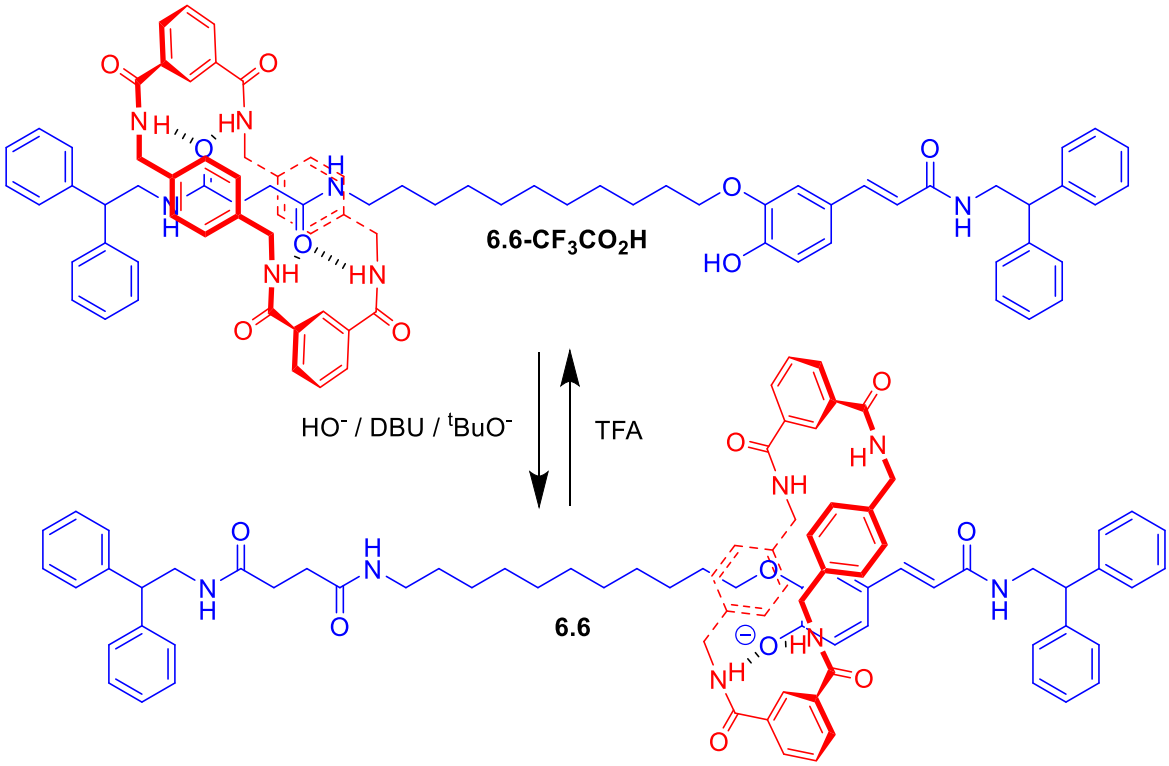

Figure 6.9 – Leigh's isophthalamide based anion recognising molecular machine 6.6

In neutral and acidic conditions the macrocycle sits over the succinamide group, so both macrocycle isopthtalamides can hydrogen bond to the carbonyl groups. Under basic conditions, the macrocycle moves to stabilise the phenolate anion, through hydrogen bonding. Surprisingly, the base induced shuttling only works in polar solvents (DMF, MeOH and MeCN) and not in less polar solvents ($CDCl_3$ and CH_2Cl_2). It is postulated that this is because when the macrocycle shuttles, only one of the isophthalamides can hydrogen bond to the axle as the phenolate can only accommodate one of them, the second is left exposed. Polar solvents stabilise the second isophthalamide and succinamide unit by hydrogen bonding, whilst non-polar solvents are unable to do so.

Li and co-workers have subsequently developed a dual responsive rotaxane molecular machine **6.7** (Fig. **6.10**), using an isophthalamide-polyether based macrocycle, synthesised using an ammonium cation as a template.[29]

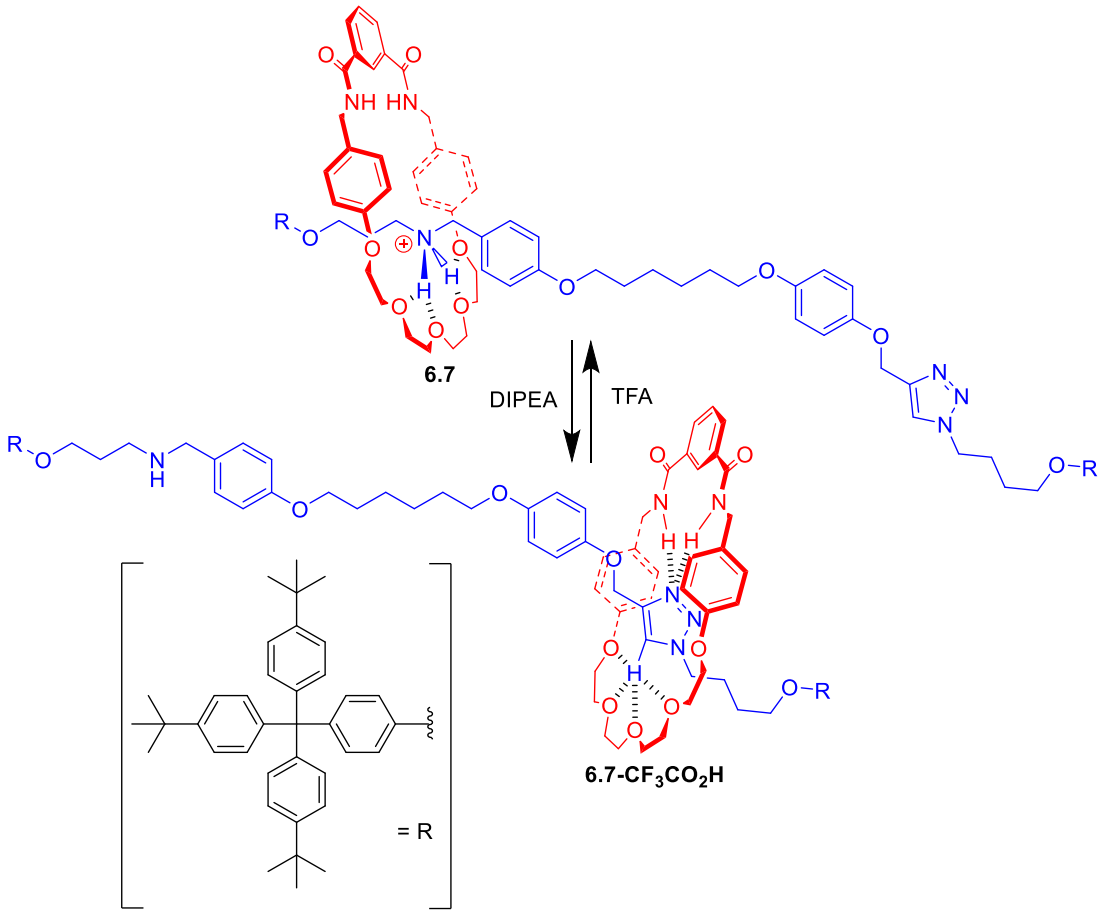

Figure 6.10 – Li's polyether-isopthalamide molecular machine 6.7

Under acidic conditions the macrocycle resides over the secondary ammonium cation, where the hydrogen bond accepting polyether groups bind to the ammonium cation. When the complex is neutralised the macrocycle then moves to the triazole, the authors propose this is due to the hydrogen bond interaction between the triazole proton and macrocycle polyethers, as well as the triazole lone pair and isophthalamide amide protons. The motion can be reversed by addition of TFA. Rotaxane **6.7** is a dual-responsive shuttle, as the addition of a chloride anion in the deprotonated state, causes the macrocycle to pirouette around the triazole, so that all three protons capable of hydrogen bonding can bind to the chloride anion.

Li and co-workers have also reported rotaxane **6.8** (Fig. **6.11**) that used a slight variation of the isophthalamide macrocycle motif, using a pyridine-2,6-diyldimethanamine instead of an isopthalamide, which has a similar geometry.[30]

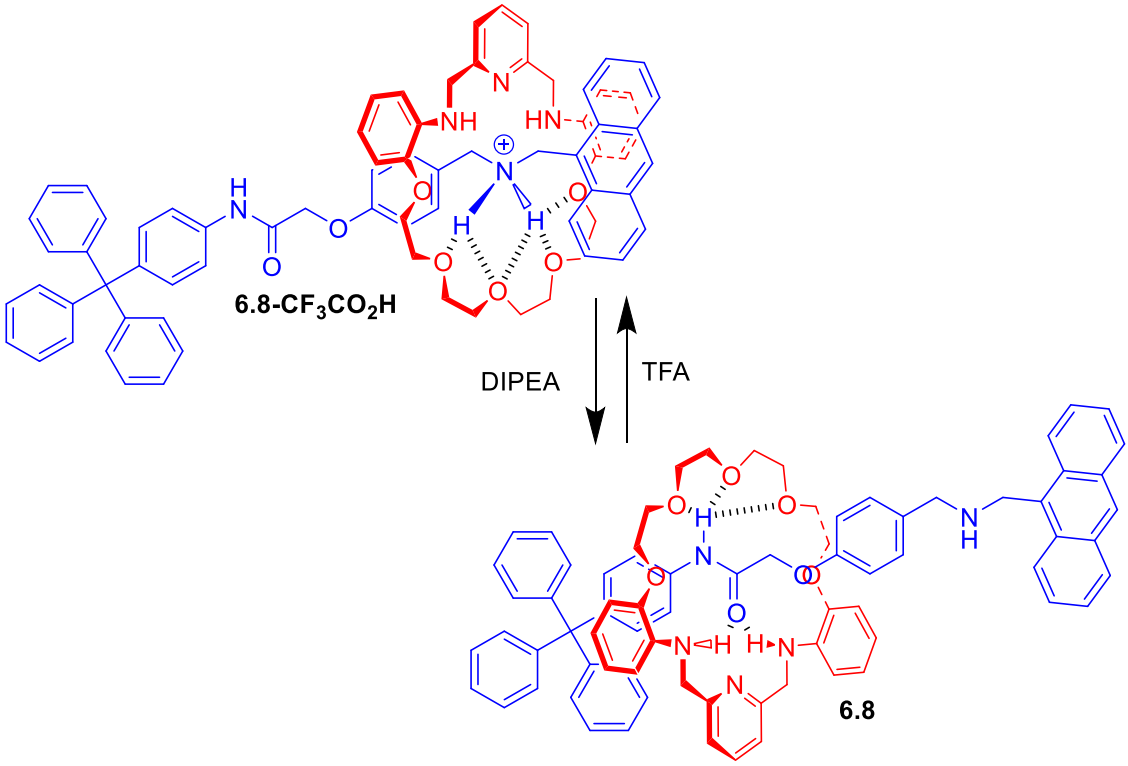

Figure 6.11 – Li's pyridine-2,6-diyldimethanamine -isopthalamide molecular machine 6.10

Upon addition of a base the macrocycle shuttles to the amide group on the axle, where the anilines can hydrogen bond to the amide carbonyl and the polyether system can hydrogen bond to the N-H proton of the amide. The shuttling can then be reversed by addition of TFA, which protonates the secondary amine of the axle, over the macrocycles less basic aniline and pyridine units. As discussed later in this review, the shuttling of the neutral rotaxane can also be triggered by the addition of metal cations.

6.1.2.1.4. pH Dependent Shuttling Rotaxanes Synthesised Using an Amide N-H to Pyridine Hydrogen Bond

There is one family of rotaxanes that do not fall into either of the two categories described so far, rotaxanes **6.9** and **6.10** developed by Lüning and co-workers (Fig. **6.12**). These use a hydrogen bond between an inwards facing pyridine on the macrocycle, to an amide proton on the axle, the rotaxanes were then stoppered using a click reaction.[31,32] Rotaxanes **6.9** and **6.10**

were synthesised in low yields of 3 % and 7 % respectively, offering an explanation as to why this motif may not be better explored.

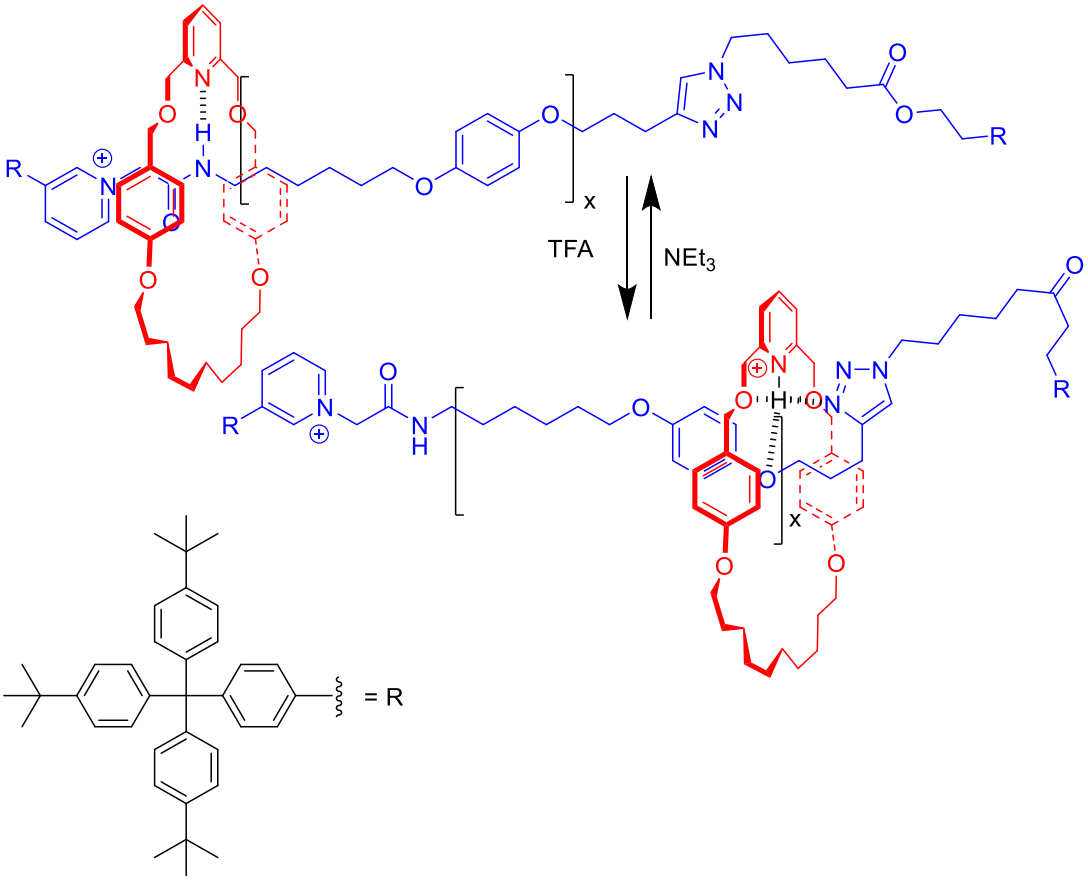

Figure 6.12 – Lüning's shuttling rotaxanes 6.9 (x=1) and 6.11 (x=2)

Shuttling in rotaxanes **6.9** and **6.10** is triggered by the protonation of the macrocycles pyridine moiety, this causes an electrostatic repulsion, forcing the macrocycle to shuttle. The protonated macrocycle is then stabilised through the hydroquinone oxygen and triazole lone pairs accepting the hydrogen bond. This system is rather unusual, as typically the axle is altered by the change in pH and not the macrocycle. The process is reversed by deprotonation of the axle, causing the macrocycle to revert to the initial pyridine-amide proton hydrogen bond.

6.1.2.2. Shuttling Induced by Alkali Metal Cations

Rotaxane based molecular machines that undergo motion due to the addition and removal of alkali metal cations are less common than rotaxanes that undergo motion due to a change in pH. However, alkali metal triggered systems typically share features with those that are

triggered by protonation of the molecule, for the interactions that will stabilise a positively charged proton will generally stabilise a positively charged alkali metal cation. These rotaxanes generally contain a macrocycle with a polyether chain or some other arrangement of Lewis basic donor groups. There are typically two sites on the axle, a site that has no groups capable of donating electrons to the alkali metal cation, but can interact with the macrocycle and a site on the axle that is not capable of interacting with the macrocycle, but can donate electron density to the metal cation (Fig. **6.13**). Systems have also been designed to cause the macrocycle to pirouette based upon similar principles. Alkali metal cations are attractive as a stimuli for the induction of molecular motion, as they are readily available, and in the cases of Na^+ and K^+, are relatively non-toxic and environmentally benign.

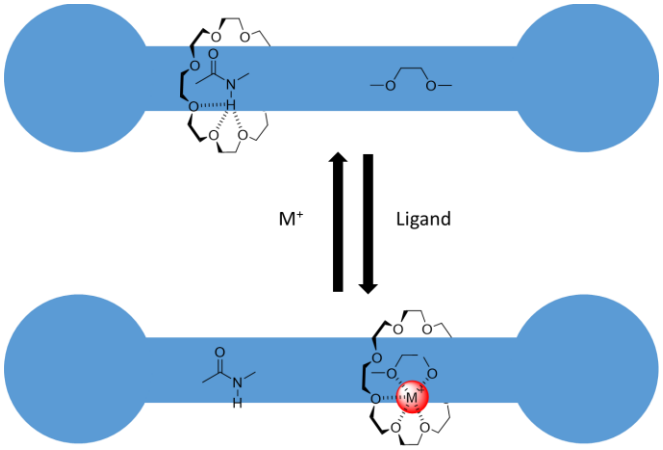

Figure 6.13 – Schematic of alkali metal induced molecular motion

Although not a hydrogen bond templated system, the first example of an alkali metal cation driven molecular machine, was Stoddart and Sanders' metastable [2]pseudorotaxane **6.11** (Fig. **6.14**). Pseudorotaxane **6.11** is considered to be metastable as heating pseudorotaxane **6.11** in solution will cause the macrocycle to slip over the stopper groups.[33,34] The rotaxane was templated using a technique developed by Sanders, using Li^+ enhanced π-π stacking between an electron deficient groups on the axle and electron rich 1,5-dioxynapthlanene polyether rings, as well as Li^+ charge dipole interactions.

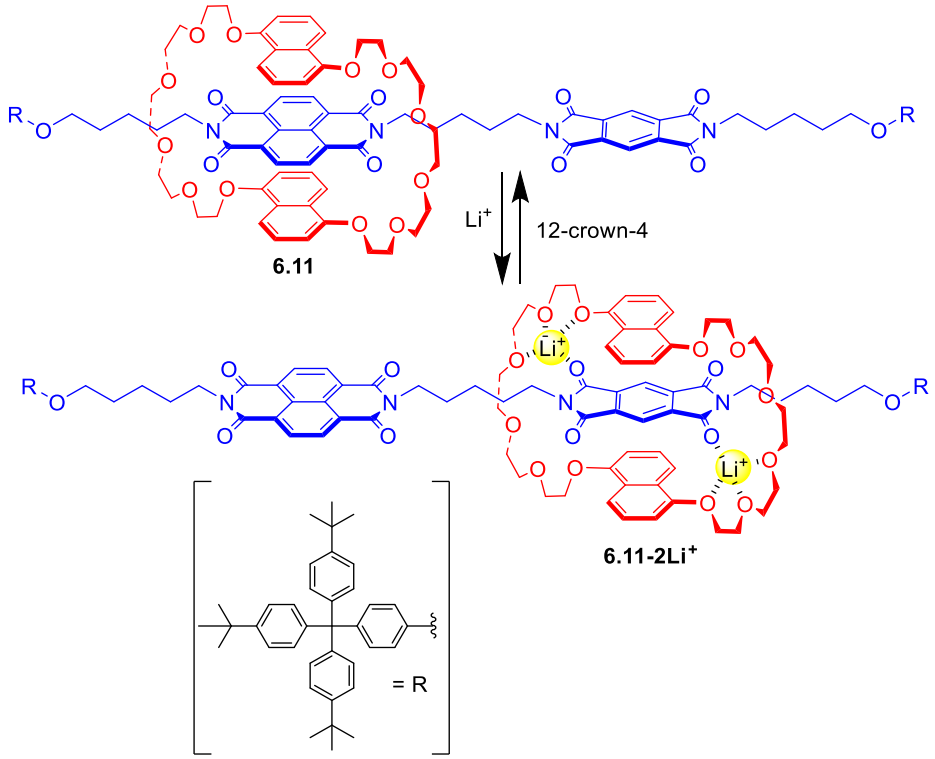

Figure 6.14 – Stoddart and Sanders' Li^+ Shuttling Pseudorotaxane

Without any Li^+ present, the macrocycle sits over the larger electron deficient π-system. When Li^+ is added, the macrocycle shuttles to the smaller π-deficient system to accommodate both the Li^+ and an element of π-π stacking. The process can then be reversed by addition of 12-crown-4, which removes the Li^+.

Chiu later developed a Na^+ templated rotaxane **6.12** that shuttles in the presence of K^+ cations (Fig. **6.15**). The system uses a crown ether macrocycle and an axle containing polyether groups to bind to a templating Na^+ cation. When the templating Na^+ is removed, the macrocycle resides over the carbamate, stabilised by hydrogen bonding to it. However, shuttling could not be controlled by the addition of Na^+, as Na^+ can bind to both carbamate and polyether sites on the axle, causing the macrocycle to rapidly and uncontrollably shuttle between the two sites. Addition of K^+ can be used to control shuttling between the two sites, as the larger and more charge diffuse K^+ can only bind to the polyether site on the axle. When K^+ is added, the macrocycle shuttles to the polyether chain, then addition of [2.2.2]cryptand removes the K^+ and causes it to shuttle back.[35]

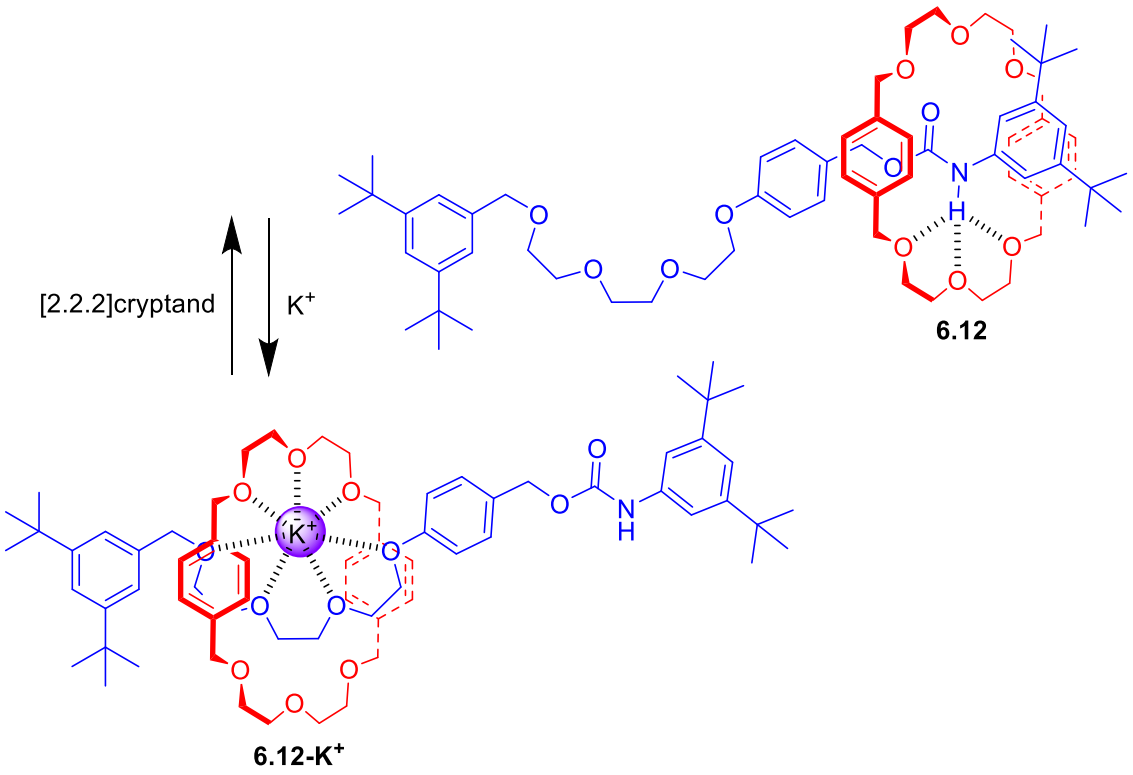

Figure 6.15 – Chiu's Na^+ templated K^+ triggered shuttling rotaxane 6.12.

There are very few examples of hydrogen bond templated rotaxanes that undergo large amplitude motion due to the addition of alkali metal cations. The first was rotaxane **6.8** developed by Li and discussed earlier in the review as a pH triggered shuttling rotaxane. Motion in rotaxane **6.8** can also be induced by the addition of the alkali metal cation Li^+ and the transition metal cation Zn^{2+} (Fig. **6.16**).[30]

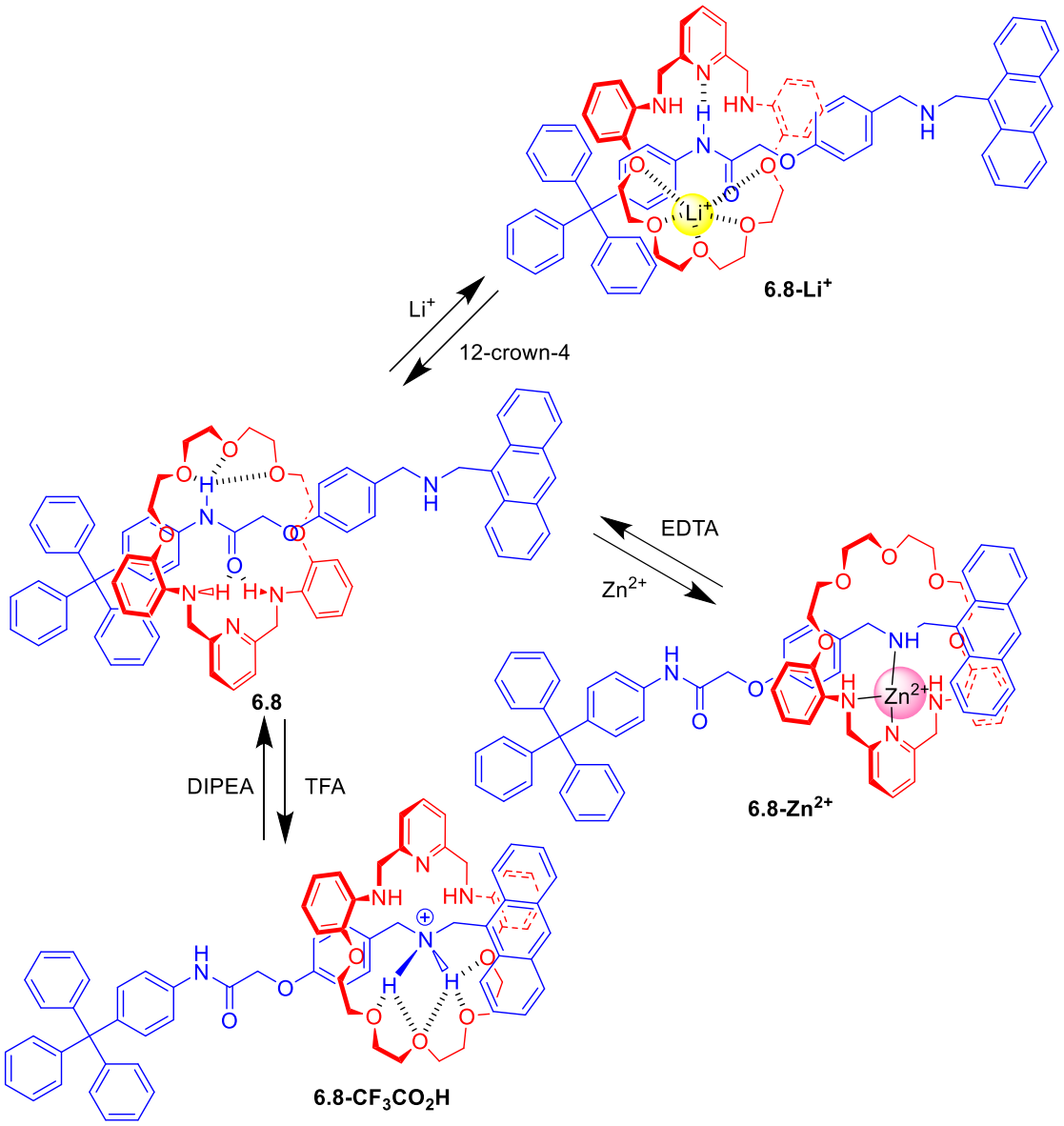

Figure 6.16 – Li's Li^+, Zn^{2+} and pH shuttling rotaxane 6.12

The addition of Li^+ to the neutral rotaxane **6.8**, causes a pirouetting motion around the amide, as the Li^+ has a charge dipole interaction with both the macrocycle polyethers and amide carbonyl, additionally the amide can hydrogen bond to the pyridine. Removal of the Li^+ ion with 12-crown-4 results in the macrocycle pirouetting back to its original position. Whereas addition of Zn^{2+} triggers shuttling to the axle amine, which is revered upon chelation of the Zn^{2+} with EDTA.

The difference in behaviour between Li^+ and H^+ is attributed to the axle secondary amine having a higher p*K*a than the macrocycle pyridine. Upon addition of a single equivalent of acid the

secondary amine on the axle is protonated, forcing the macrocycle to shuttle, in order to bind to the ammonium group. Whilst Li^+ is not forced to bind to the secondary amine, so the preferred interaction is for the Li^+ to bind polyethers and carbonyl, through a charge dipole interaction. A supplementary interaction with the pyridine binding the amide proton can also be seen. The difference in behaviour between Li^+ and Zn^{2+} is attributed to the Zn^{2+} being unable to fit in the polyether cavity, so instead has to bind to the amines and pyridine.

A further example of a hydrogen bond templated rotaxane that can act as a molecular machines, is Beer's pyridine-*N*-oxide rotaxane **6.13** (Fig **6.17**).[36] This was templated using both a hydrogen bond templated synthesis and Na^+ cation templated synthesis. Without a metal cation template, the rotaxane was only isolated in 10% yield. The use of the Na^+ cation allowed for the rotaxane to form in a much higher yield of 50%. In uncomplexed rotaxane **6.13**, the pyridine-*N*-oxide hydrogen bonds to the isophthalamide moiety on the macrocycle. Addition of the alkali metal cation Na^+ or alkali-earth cation Ba^{2+} caused the macrocycle to pirouette, so that the calixarene unit and pyridine-*N*-oxide, can both stabilise the cation through a charge dipole interaction. For the Ba^{2+} complex this could be reversed by precipitating the cation out with TBA sulfate, causing the macrocycle to return to its original position.

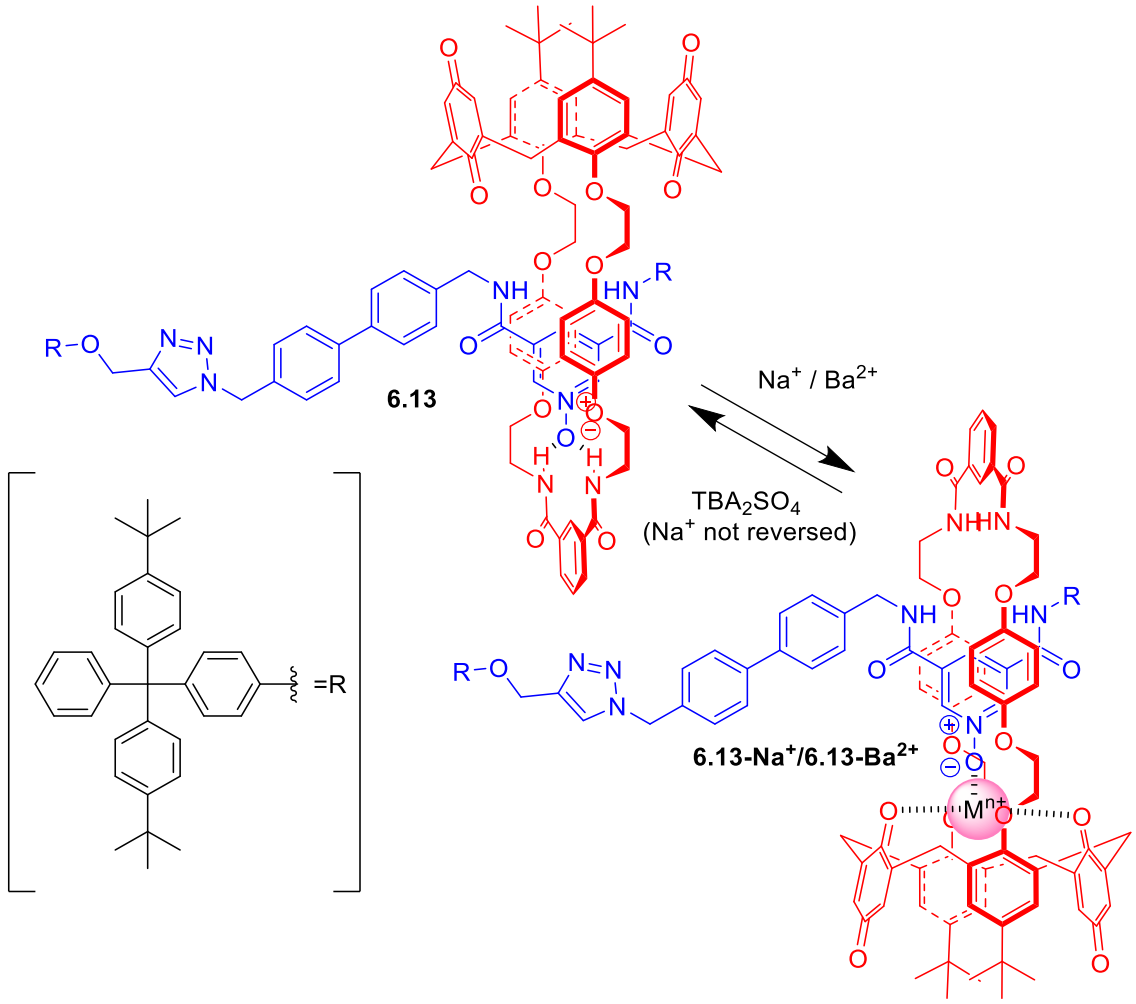

Figure 6.17 – Beer's Pirouetting Pyridine-*N*-oxide Na^+ and Ba^+ triggered rotaxane 6.13

6.1.2.3. Conclusions

Shuttling caused by the variation of the pH of has been relatively well explored using crown ether based macrocycles and has been developed into sophisticated functional architectures. However, systems using isophthalamide macrocycles have not been investigated in the same depth, as they are not commercially available. Most research on these systems has been limited to rotaxanes templated using a primary ammonium cation and shuttling induced by protonation of a neutral molecule. This offers considerable scope for further research into rotaxanes triggered by deprotonation of a neutral molecule and shuttling induced by protonation of groups other than a secondary amine, such as a 1,2,3-triazole that can easily be incorporated into these systems.

There are only a handful of examples of rotaxane based molecular machines triggered by the addition of alkali metal cations and even fewer based on hydrogen bond templated rotaxanes. These hydrogen bond templated rotaxanes, so far have only demonstrated pirouetting motions. Future research should investigate the development of a hydrogen bond templated rotaxane that can shuttle upon addition of an alkali metal, as it is clear that this is a significant gap within the literature.

6.2. Investigation into a 2,3,4,5,6-Pentafluorobenzamide Based Rotaxane

Taking inspiration from the mechanically chiral rotaxane developed in the previous chapter and rotaxane **5.1** (Chapter 5), previously developed by the Evans group, a novel hydrogen bond templated rotaxane **6.14** was designed.[37] The rotaxane will still use the same hydrogen bond templating motif and synthesis using a Cu click reaction to stopper the rotaxane. However, the proposed rotaxane will have several key changes made from both rotaxane **5.1** and mechanically chiral rotaxane **5.3** (Chapter 5) to promote shuttling behaviour and to attempt to increase the yield of rotaxane formations (Fig. **6.18**):

- Addition of an aromatic spacer group on the axle, instead of an alkyl chain (magneta, Fig. **6.18**).
- A change of stopper from a 3,5-bis(trifluoromethyl)benzamide to a 2,3,4,5,6-pentafluorobenzamide (blue, Fig. **6.18**).
- Placing the alkyne unit on the axle component and the azide on the stopper component (black/green, Fig. **6.18**).

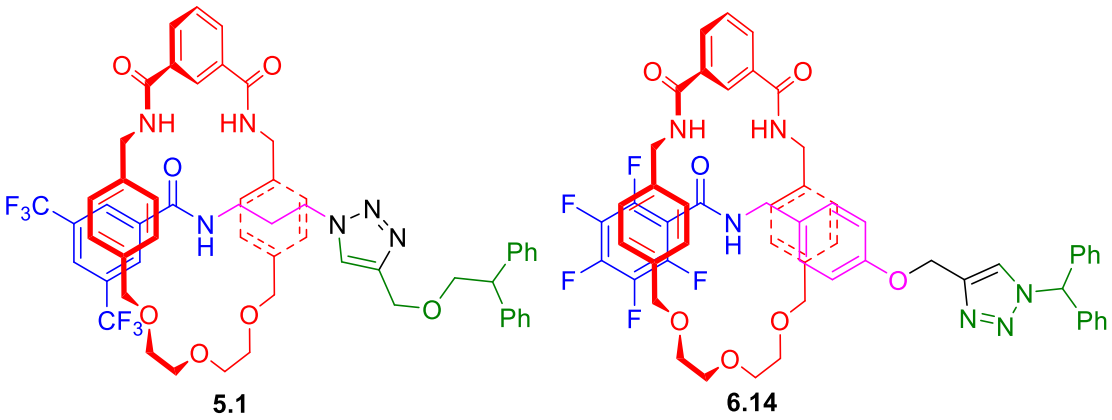

Figure 6.18 – Evans' rotaxane 5.1 (left) and target rotaxane 6.14 (right) (red – macrocycle, blue –stopper, magenta – spacer, triazole and stopper - black and green)

The replacement of the propylene spacer group for an aromatic spacer group (blue Fig. **6.18**) increases the rigidity of the axle, so that when stimuli is applied the only option is for the macrocycle to shuttle along the axle. If the axle is flexible like in rotaxane **5.1** it may be preferable for the rotaxane to undergo a conformational change, preventing rotaxane **6.14** from acting as a molecular shuttle.

Replacing the stopper group has been changed from a 3,5-bis(trifluoromethyl)benzamide to a 2,3,4,5,6-pentafluorobenzamide (blue Fig. **6.18**), is anticipated to increase the yield of rotaxane formation. It is believed that the more strongly withdrawing electronic effects of the pentafluorobenzamide over the a 3,5-bis(trifluoromethyl)benzamide will increase the yield of the rotaxane, as the more strongly electron withdrawing substituent will reduce the electron density on the axle amide NH, thereby increasing the NH proton acidity. This will strengthen the hydrogen bonding between the axle amide NH and the polyether groups on the macrocycle, thereby providing a stronger thermodynamic driving force for the threading.

Whilst the pentafluorobenzamide is smaller than the 3,5-bis(trifluoromethyl)benzamide, there is evidence that it will be equally effective as a stopper group. Work done by Mahan and Dennis demonstrates that rotaxanes do not necessarily need sterically bulky stopper groups, but can instead be stoppered through electrostatic repulsion between the stopper and the macrocycle.[38]

It was shown that stoppers containing multiple fluorine atoms, with their high electronegativity and high electron density will repel macrocycles containing polyether groups. As the electron rich electronegative oxygen atoms are repelled by the electron rich fluorine atoms, preventing the macrocycle from dethreading.

Finally, the switch to a 2,3,4,5,6-pentafluorobenzamide on the axle component necessitates consideration as to where the azide group, required to attach the stopper using a Cu click reaction, should go (black and green Fig. **6.18**). As attempting to attach an azide group to a molecule containing a fluorinated electron deficient aromatic system, may result in nucleophilic aromatic substitution occurring. This will result in the formation of a potentially explosive poly-azide compound (Fig. **6.19**).[39] To remove this hazard, it was decided that the thread component should be the alkyne component and the stopper should be the azide component.

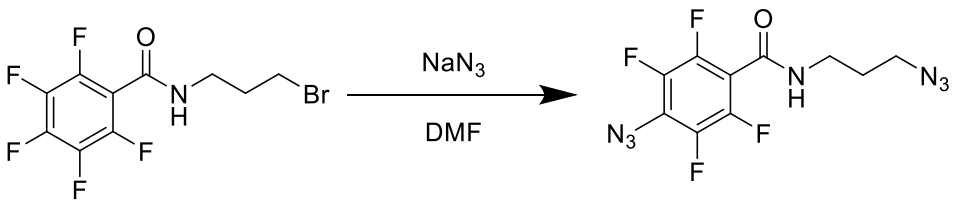

Figure 6.19 - Potential reaction of a 2,3,4,5,6-pentafluorobenzamide motif with sodium azide

6.2.1. Macrocycle Synthesis

Synthesis of rotaxane began with the synthesis of macrocycle **6.15**, following a literature procedure (Fig. **6.20**).[37,40] Bis-amine **4.14**, previously prepared in chapter 4, was combined with a stoichiometric amount of pyridinium chloride template **2.19** in CH_2Cl_2, NEt_3 followed by isophthaloyl chloride in CH_2Cl_2 was added dropwise, the mixture was then stirred for one hour and purified by silica column chromatography, producing macrocycle **6.15** in 16% yield.

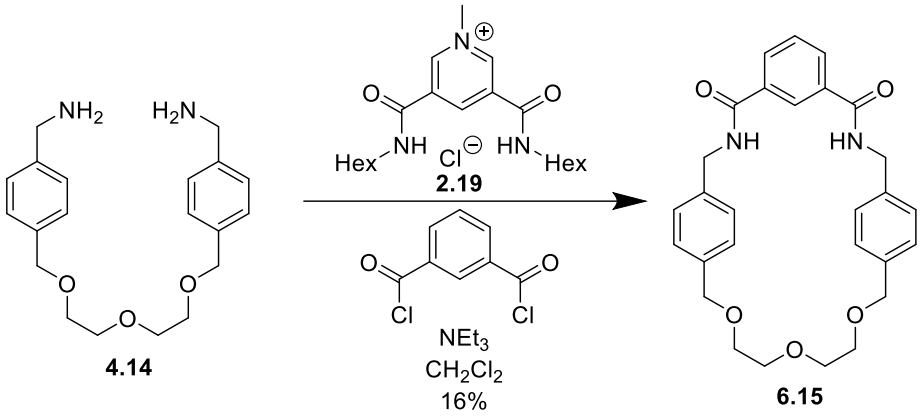

Figure 6.20– Synthesis of macrocycle 6.15

6.2.2. Pseudorotaxane Studies

With macrocycle **6.15** in hand, a preliminary check was carried out to verify whether or not the pentafluorobenzamide would act as a stopper. An experiment undertaken by Philp *et al* provided a basis for testing this. An equimolar amount of macrocycle **6.15** and benzanilide, acting as an axle, were combined in 0.5 mL $CDCl_3$, the ^1H NMR of the individual benzanilide and macrocycle **6.15** were compared to the mixture (Fig. **6.21**).[40]

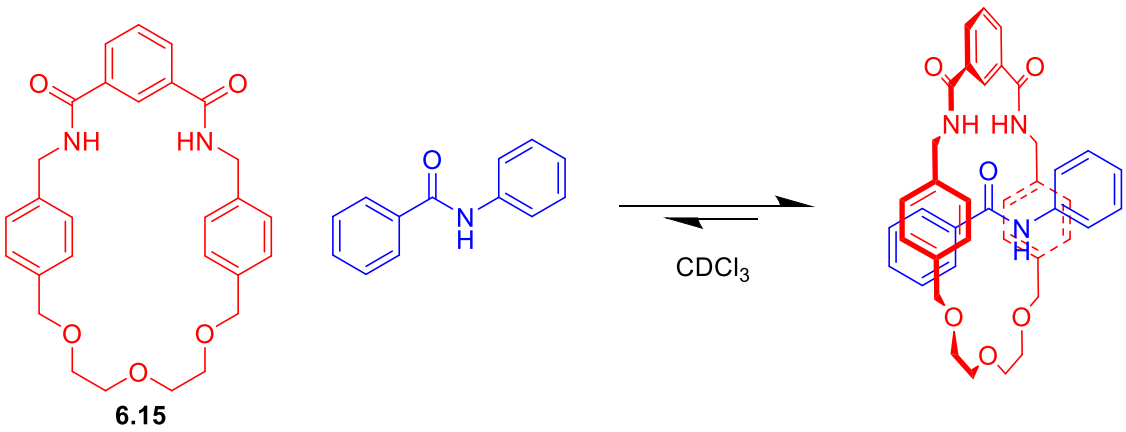

Figure 6.21 – Threading of benzanilide through macrocycle 6.15[DPH1]

The ^1H NMR spectrum (Fig. **6.22**) of the equimolar mixture of macrocycle **6.15** and benzanilide shows significant shifts of signals, compared to the corresponding signals of the individual components, this is indicative of a benzanilide threading through macrocycle **6.15**. Broadening of the peaks were observed, indicating that there is an exchanging equilibrium between the

threaded state and unbound macrocycle **6.15** and benzanilide. If the benzanilide had not thread through the macrocycle, little to no change in chemical shift would be observed.

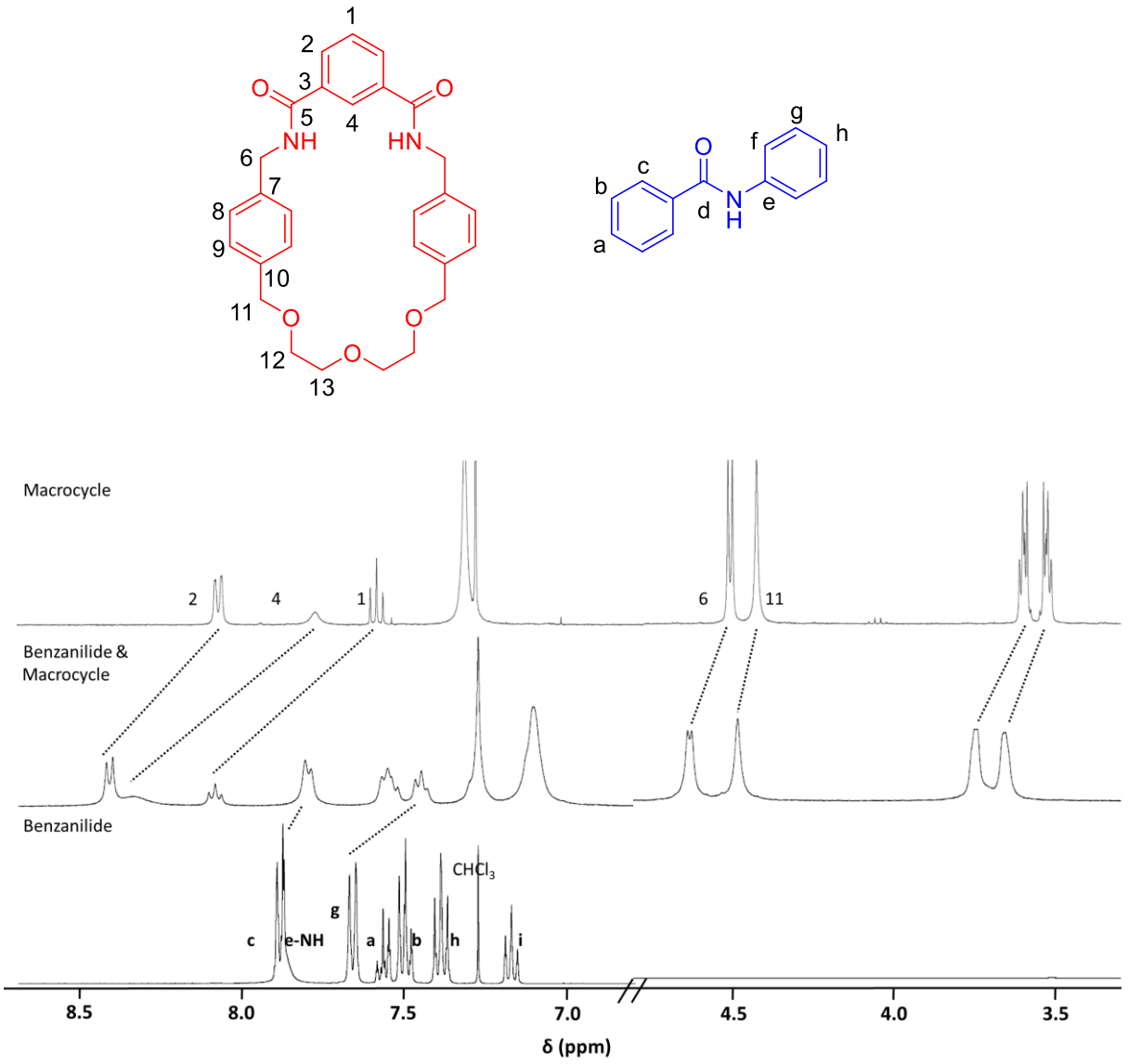

Figure 6.22 – ^{1}H NMR spectra (400 MHz, 298 K, $CDCl_3$, 8.4 mmol cm^{-3}, 3.0-5.0 ppm and 6.5-9.0 ppm) of macrocycle 6.15 benzanilide and an equimolar mixture of benzanilide and macrocycle 6.15.

To test if a pentafluorobenzene moiety can act as a stopper, a modified version of this test was carried out (Fig. **6.23**). Axle **6.16** was designed to act as an analogue for the axle used in rotaxane **6.14**, containing an already proven stopper, a pentafluorobenzene stopper and a templating amide group. If the pentafluorobenzene may act as a stopper group, then when axle **6.16** is

combined with macrocycle **6.15** then no change in the ^{1}H NMR chemical shift of the components compared to the components alone would be observed. If the stoppers can prevent threading, as they cannot fit through the macrocycle, then logically they must be capable of preventing the macrocycle from dethreading.

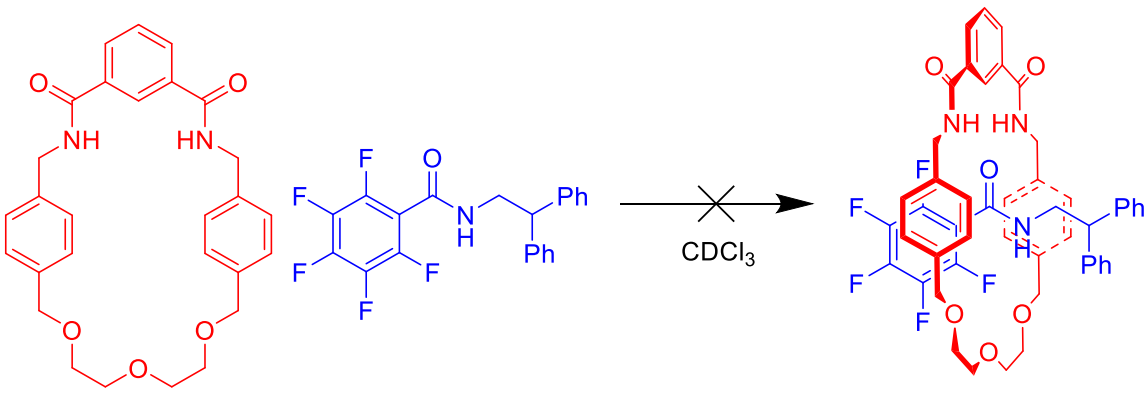

Figure 6.23 – Failed threading of axle 6.16 through macrocycle 6.15

Before the test was carried out, axle **6.16** was synthesised in a single step (Fig. **6.24**). To 2,2-diphenylethylamine in CH_2Cl_2, triethylamine, then 1.2 equivalents of 2,3,4,5,6-pentafluorobenzoyl chloride were added. Axle **6.16** was purified using an aqueous work up and was isolated in 97% yield. An equimolar amount of macrocycle **6.15** and axle **6.16** were then combined in 0.5 mL of $CDCl_3$, the ^{1}H NMR spectra was compared to the individual components.

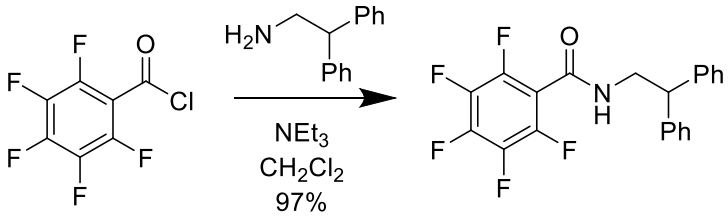

Figure 6.24 – Synthesis of axle 6.16

The ^{1}H NMR spectra (Fig. **6.25**) of the equimolar mixture of macrocycle **6.15** and axle **6.16** was taken and shows minimal changes in the chemical shifts of the signals from the corresponding signals of the individual components. This indicates that axle **6.16** is not threading through macrocycle **6.15**. To confirm this a DOSY (Diffusion Ordered SpectrocopY) was obtained of the

equimolar mixture of macrocycle **6.15** and axle **6.16**, from this the rates of diffusion were measured (400 MHz, 298 K, $CDCl_3$, 8.4 mmol cm^{-3}) Diffusion constants of resonances arising from macrocycle **6.15** and axle **6.16**. The diffusion constant of macrocycle **6.15** and macrocycle **6.16** were between 7.93×10^{-10} m^2s^{-1} and 8.30×10^{-10} m^2s^{-1} ($\pm 3.31 \times 10^{-12}$ m^2s^{-1}) and 9.99×10^{-10} m^2s^{-1} and between 10.1×10^{-10} m^2s^{-1} ($\pm 4.69 \times 10^{-12}$ m^2s^{-1}) respectively. As the macrocycle and axle diffuse at different rates, it is highly unlikely that they are interacting. From these two pieces of evidence axle **6.16** does not thread through macrocycle **6.15**. Therefore, the pentafluorobenzene stopper was determined to be able to act as a stopper for rotaxanes containing macrocycle **6.15**.

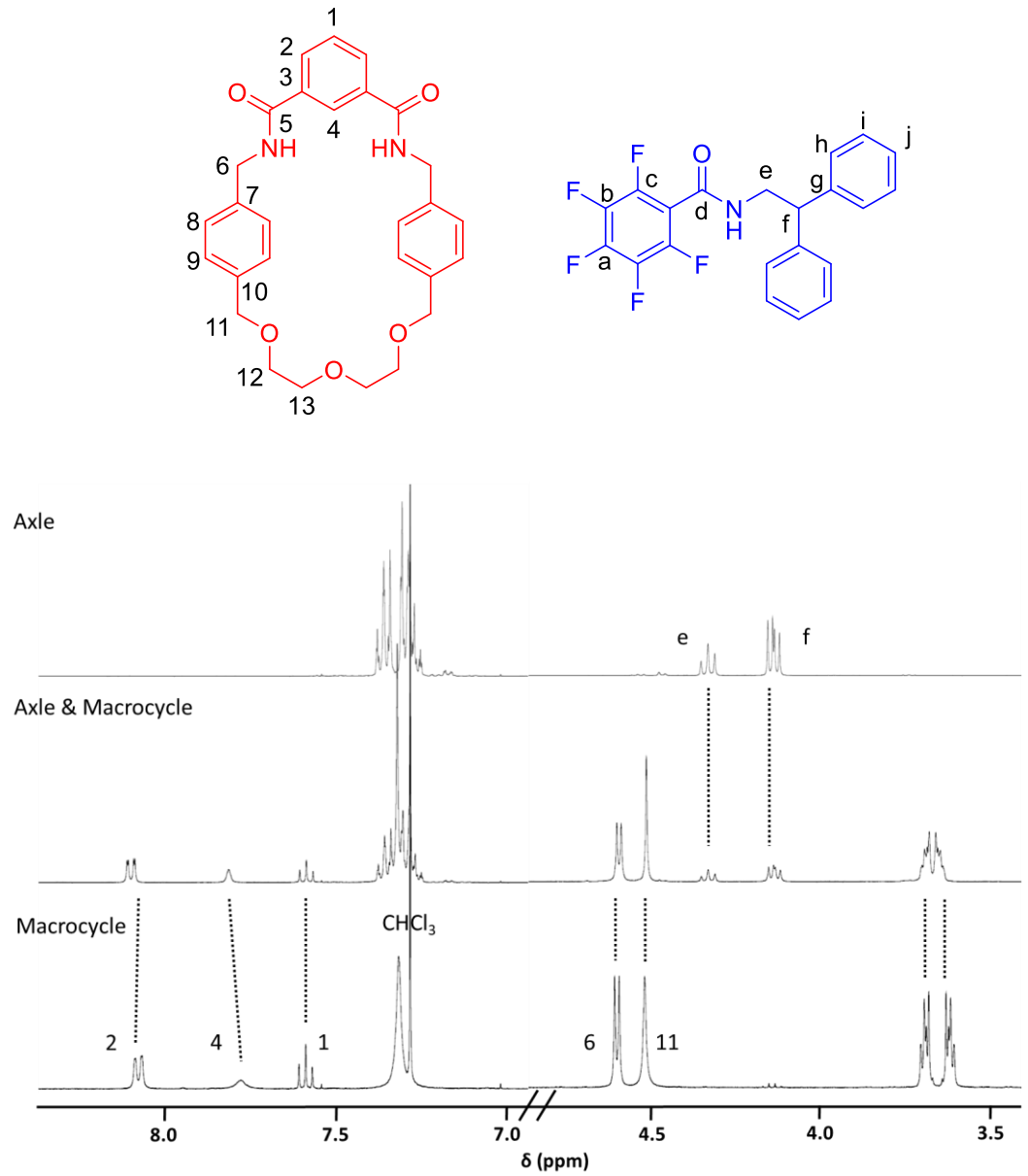

Figure 6.25 – ^{1}H NMR spectra (400 MHz, 298 K, $CDCl_3$, 8.4 mmol cm^{-3}) of macrocycle 6.15, axle 6.16 and an equimolar mixture of the axle and macrocycle.

6.2.3. Axle Component Synthesis

Next the three step synthesis of the rotaxane axle component **6.17** began by following a modified literature procedure to produce amine **6.18**.[41] Excess 4-cyanophenol was refluxed in MeCN with propargyl bromide (80% in toluene) in the presence of K_2CO_3 for 16 hours. After a basic work up nitrile **6.19** was produced in 88% yield. Nitrile **6.19** was then reduced with $LiAlH_4$

in THF and then purified using silica column chromatography, giving a 54% yield of amine **6.18**. An excess of amine **6.18** was then added to a mixture of 2,3,4,5,6-pentafluorbenzoyl chloride and NEt_3 in CH_2Cl_2, an aqueous work up was undertaken to produce thread **6.17** in 70% yield.

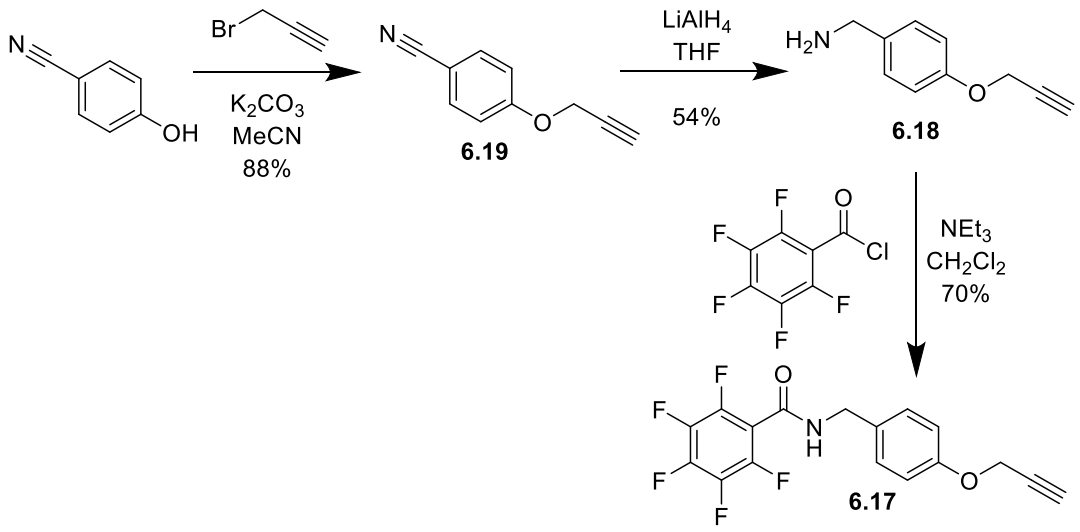

Figure 6.26 – Synthesis of thread 6.17

Finally azide stopper **6.20** was prepared in a single step, following a literature procedure (Fig. **6.27**).[42] Bromodiphenylmethane and 3 equivalents of sodium azide were heated to 80 °C in DMF for 3 days. After dilution with water and extraction with EtOAc, azide **6.20** was isolated in 62% yield.

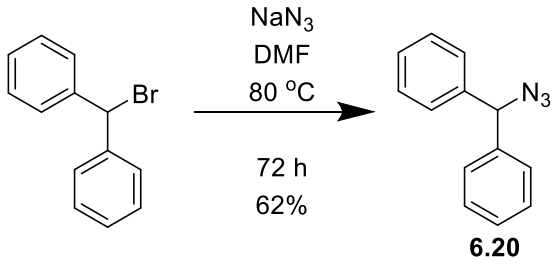

Figure 6.27 – Synthesis of stopper 6.20

6.2.4. Attempted Synthesis of 2,3,4,5,6-Pentafluorobenzamide Rotaxane

With macrocycle **6.15**, thread **6.17** and stopper **6.20** in hand a Cu click reaction was used in an attempt to form rotaxane **6.14** (Fig. **6.28**). Equimolar amounts of macrocycle **6.15** and thread

6.17 were stirred in dry CH_2Cl_2 for one hour. DIPEA, azide stopper **6.20** and catalytic amounts of TBTA and $Cu(MeCN)_4BF_4$ were added. The reaction was left to stir for 16 h. After aqueous work up the crude product was analysed by ^1H and ^{19}F NMR spectroscopy and was found to contain no rotaxane, only free macrocycle and axle. The reaction was then repeated with five equivalents of axle and stopper to one equivalent of macrocycle, similarly no rotaxane was detected.

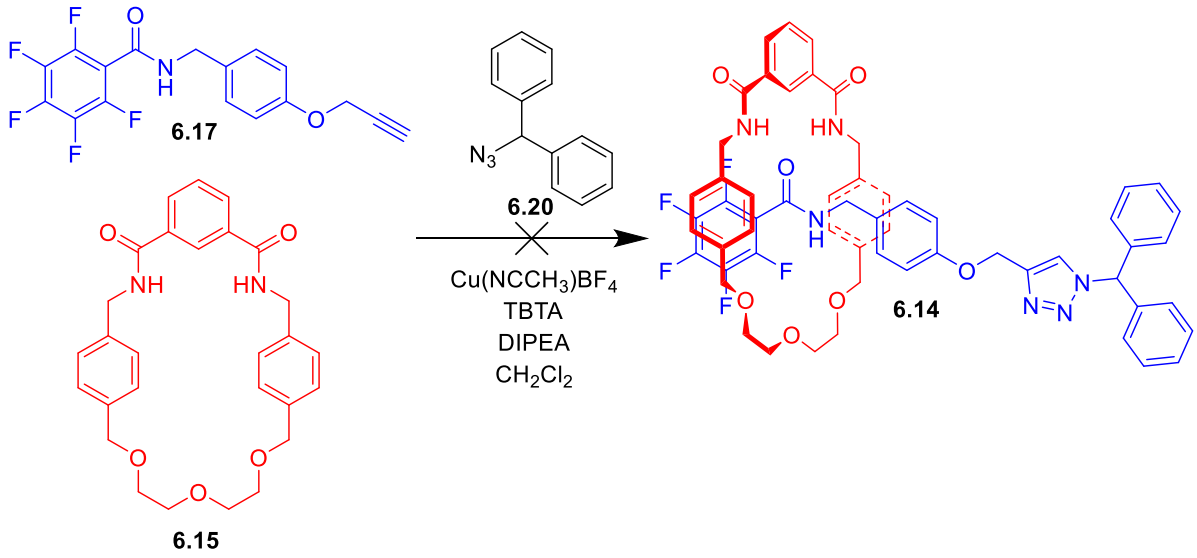

Figure 6.28 – Attempted Synthesis of Rotaxane 6.14

To investigate if thread **6.17** was capable of threading through macrocycle **6.15** an equimolar amount of the two components were dissolved in $CDCl_3$. The ^1H NMR spectra of the mixture was then compared to the components individually (Fig. **6.29**). When comparing the ^1H NMR spectra, it is immediately obvious that there is no change in chemical shift of any of the peaks in the mixture, when compared to the individual components. The lack of change in chemical shift, suggests that the macrocycle **6.15** and thread **6.17** do not interact. As a threading event would be indicated by an upfield shift of axle protons residing within the macrocycle and downfield shift of some macrocycle peak.

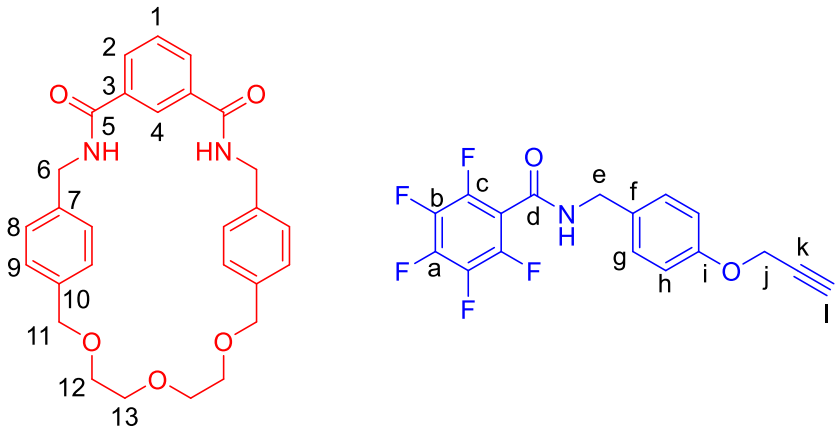

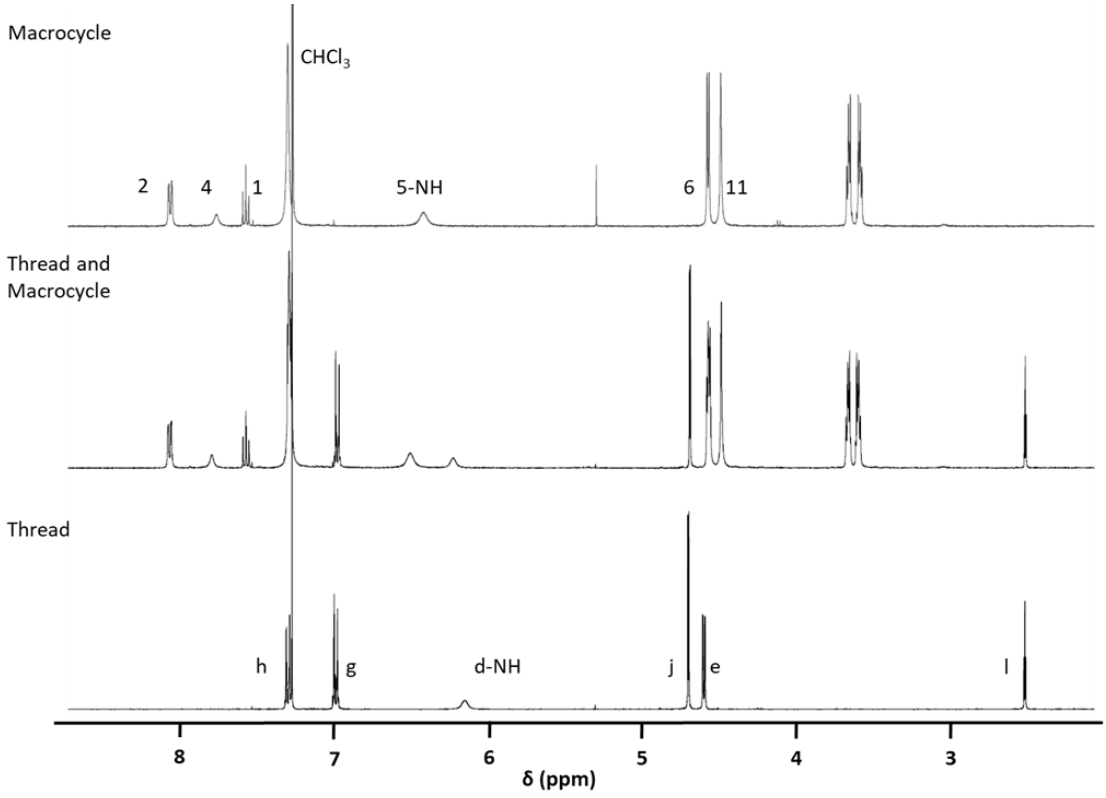

Figure 6.29 – ^{1}H NMR spectra of the attempted threading of thread 6.17 through macrocycle 6.15 (400 MHz, 298 K, $CDCl_3$)

Attention thus turned to explaining why thread **6.17** had failed to thread through macrocycle **6.15**. Of the new components to this system it was unlikely to be due to the aromatic spacer between the amide and the alkyne, as it has been demonstrated that the *N*-benzylbenzamide as well as larger groups could fit through.[40] Instead it may be due to the electrostatic or steric

repulsion of the fluorine atoms, particularly those at the 2 and 6 position, on the pentafluorobenzamide being too strong and preventing the macrocycle approaching the templating amide, preventing threading from occurring.

Alternatively the failure of thread **6.17** to pass through macrocycle **6.15** may be due to electron withdrawing effect of the pentafluorobenzene stopper on the amide group. Whilst the electron withdrawing effect of this group does strengthen the hydrogen bonds between the axle amide proton and the polyether oxygen on the axle, it may also weaken the hydrogen bonds between the macrocycle amide protons and the axle carbonyl. As the electron density on the axle carbonyl will also be reduced by the electron withdrawing inductive effects of the pentafluroro benzene moiety, this will reduce the electron density available on the carbonyl for hydrogen bonding, thereby weakening the hydrogen bonds between the axle and macrocycle. To investigate this, it was proposed that molecular modelling of the threading event may be of assistance.

6.3. Computational Modelling

Molecular modelling *in silico* of the threading event was undertaken to quickly and cheaply answer two questions:

1) What functional groups could be placed on the benzamide moiety to assist with the threading event and maximise the yield of rotaxane formation?
2) Why did thread **6.17** fail to thread through macrocycle **6.15**?

6.3.1. Preliminary Modelling

Preliminary modelling of the threading event was undertaken on a limited 'rough' model and compares the distances of the hydrogen bonds between the thread amide carbonyl and the 'macrocycle' amide N-Hs (Fig. **6.30**). To minimise time, the majority of the axle and macrocycle were removed. To model the use of different functional groups on the stopper, substituents

were then varied at the para position (R_1), meta positions (R_2) and ortho positions (R_3). *N,N*-dimethylisophthalamide was then used to simulate the macrocycle.

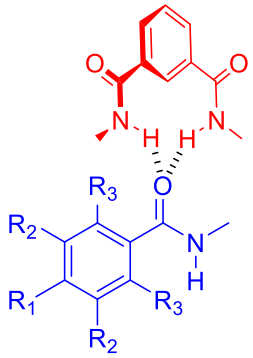

Figure 6.30 – **Components and intermolecular interactions modelled between macrocycle and axle proxies *N,N*-dimethylisophthalamide and *N*-methylbenzamide**

Modelling calculations were carried out using Gaussian 09, B3LYP functional, with a 6-31G* basis set for all atoms and $CHCl_3$ solvent effects were modelled using the standard Gaussian 09 parameters for cavity and solvent.[37,43,44] An isolated *N*-methylbenzamide was modelled first, followed by complexation to a *N,N*-dimethylisophthalamide, with amides *syn* relative to one another.

The strength of the intermolecular interaction between the components was judged by comparing bond lengths between the *N,N*-dimethylisophthalamide amide protons (H^a) and *N*-methylbenzamide amide carbonyl (O^t), results are shown in Table **6.1**.

Table 6.1 – H^a-O^t bond lengths from computational modelling

Compound Number	Functional Groups			H-O (Å)		
	R_1	R_2	R_3	1	2	Average
6.21	H	H	H	2.055	2.184	2.120
6.22	F	F	F	2.163	2.451	2.307
6.23	H	CF_3	H	2.156	2.497	2.327
6.24	OMe	OMe	H	2.074	2.161	2.118

Results (Table **6.1**) showed that the compound **6.24** had the shortest bonds between protons H^m and carbonyl oxygen O^t and therefore should have stronger hydrogen bonds. Indicating that the complex formed between these two components would be strongest and of the components tested would result in the highest yields of rotaxane produced. Synthesis on a eudesmic acid containing rotaxane (Table **x**, $R_1 = R_2 = OMe$, $R_3 = H$) began immediately following these results.

Whilst this model expediently provided sufficient information to proceed with synthesis, it does suffer from multiple flaws. Primarily the models fails to include the interaction between the amide N-H on the thread and the polyether oxygen atoms on the macrocycle. This may give erroneous results as more electron withdrawing groups on the aromatic system are likely to strengthen this bond, whilst electron donating groups are likely to weaken this bond. This is due to a more electron deficient amide N-H being a better hydrogen bond donor.

The model also does also not take into account of steric influences of the rest of the molecule, or the rigid nature of the macrocycle and the size of the macrocycles cavity. In addition the modelling was done in $CHCl_3$ instead of a solvent that would typically be used to synthesise a rotaxane (e.g. CH_2Cl_2). Because of this, the model is not capable of answering why thread **6.17** failed to thread through macrocycle **6.15**. To solve this a more comprehensive model is required.

6.3.2. Comprehensive Modelling

To resolve the issues of the previous modelling, a new more representative model was investigated. The new model would look at the threading event of appropriate molecules, similar to alkyne thread **6.17**, through macrocycle **6.15** (Fig. **6.31**). This new model resolves the flaws in the previous model, by modelling all three of the hydrogen bonding interactions between the macrocycle and axle, considers steric effects caused by the components, includes the effects of the rigidity of the macrocycle and uses a solvent that is appropriate for the subsequent stoppering click reaction.

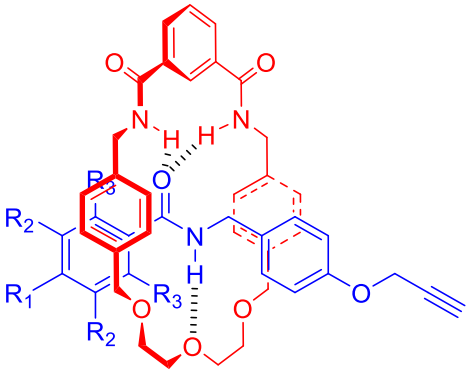

Figure 6.31 – General structure of pseudorotaxanes 6.35 to 6.39

Modelling calculations were carried out using the same parameters as before. Using Gaussian 09, a B3LYP functional, with a 6-31G* basis set for all atoms and CH_2Cl_2 solvent effects were modelled using the standard Gaussian 09 parameters for solvent and cavity.[43] Isolated macrocycle **6.15** was modelled first, followed by pseudorotaxane formation with alkyne threads **6.38,** which used an unfunctionalized benzamide moiety. To model the use of different functional groups on the stopper, substituents were then varied at the para position (R_1), meta positions (R_2) and ortho positions (R_3).

Each model then adds different substituents to the 2,3,4,5 and 6 position on the aromatic ring of the benzamide moiety, representing potentially suitable components. Separately, uncomplexed alkynes were modelled using the same parameters.

Pseudorotaxanes **6.35** to **6.39** were compared by calculating the ΔG of threading, which was calculated by taking the difference between the ΔG of pseudorotaxane and the ΔG of free macrocycle and ΔG of free alkyne. The resulting value of $\Delta G_{threading}$ will correspond to the strength of the interactions between the macrocycle **6.15** and the appropriate alkyne threads. The more negative the value of the energy, the stronger the interaction between macrocycle **6.15** and the appropriate alkyne thread, providing a guide as to which axles will form a pseudorotaxane and which axle will produce a pseudorotaxane in the highest yield.

Table 6.2 – Calculated $\Delta G_{threading}$ of modelled pseudorotaxanes 6.35 to 6.39 in CH_2Cl_2

Compound	Functional Groups			Rotaxane	Axle	Macrocycle	$\Delta G_{threading}$	
Number	R_1	R_2	R_3	Ha	Ha	Ha	Ha	KJ mol^{-1}
6.35	H	$-CF_3$	H	-3106.76923766	-1536.05393310	-1570.68524538	-0.03005918	-78.92
6.36	OMe	OMe	OMe	-2776.24883892	-1205.53601424	-1570.68524538	-0.02757930	-72.41
6.37	F	F	H	-2730.37672640	-1159.66600881	-1570.68524538	-0.02547221	-66.88
6.38	H	H	H	-2432.69255229	-861.98205637	-1570.68524538	-0.02525054	-66.30
6.39	F	F	F	-2928.81584314	-1358.10653707	-1570.68524538	-0.02406069	-63.17

The results from table **6.2** indicate that of the systems modelled pseudorotaxane **6.35** is the most stable, unlike in the previous model where the analogue was found to be least stable. Indicating that the previous models lack of consideration to thread amide N-H to polyether O hydrogen bonds has a considerable effect.

From the modelling undertaken, it seems that there is no discernible pattern between the substituents electron donating and electron withdrawing effects and $\Delta G_{threading}$, only that a pseudorotaxane with a stronger withdrawing or donating effect has a higher $\Delta G_{threading}$ (The pentafluorobenzene pseudorotaxane **6.39,** is an exception that will be discussed later). This may be due to electron withdrawing groups weakening the macrocycle amide N-H to thread amide carbonyl hydrogen bonds, but strengthening the thread amide N-H to macrocycle polyether hydrogen bonds and electron donating groups doing the reverse. To explore this further more modelling is required with a greater variety of substituents, in addition use of a mixture of electron withdrawing groups and electron donating groups may be of interest.

Using this computational model, alongside the empirically gained knowledge, may provide an explanation as to why rotaxane **6.14** did not form. Whilst the models indicate that pseudorotaxane **6.39** should still form based on the negative value of $\Delta G_{threading}$, the 3D model

has suggested that there may be a steric clash between the fluorine atoms at the 2 and 6 positions and macrocycle (Fig. **6.32** and **6.33**). As in the modelling the macrocyclic component and axle component are 'forced' together clues for this steric clash must be deduced from deformations of the components of pseudorotaxane **6.39**, when compared to the other pseudorotaxanes, using 3,4,5-trifluorobenzene pseudorotaxane **6.37** as a representative example.

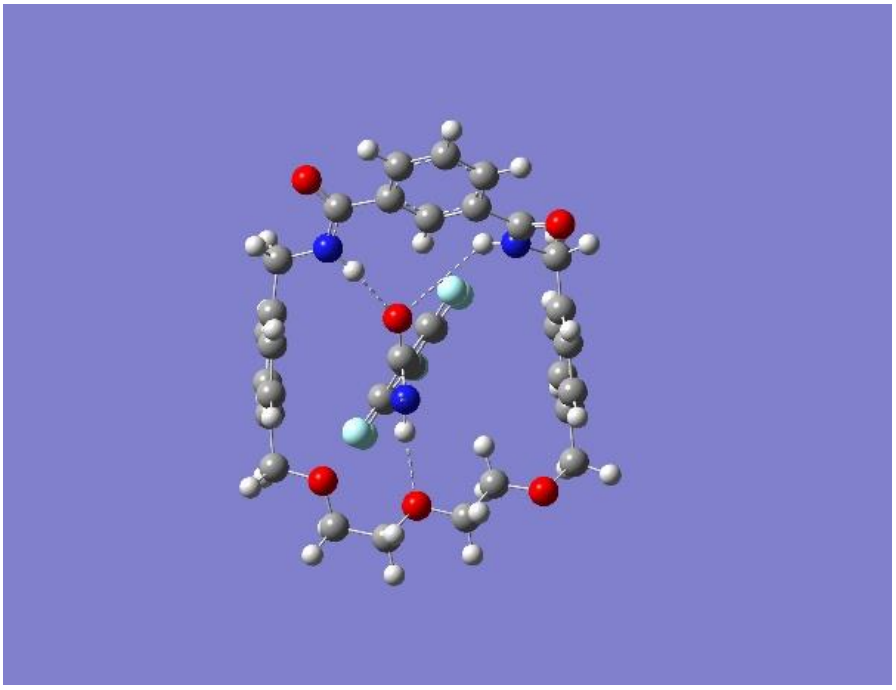

Figure 6.32 – Computational model of pseudorotaxane 6.39 with a 2,3,4,5,6-pentafluorobenzene stopper (axle atoms after the amide were deleted for clarity).

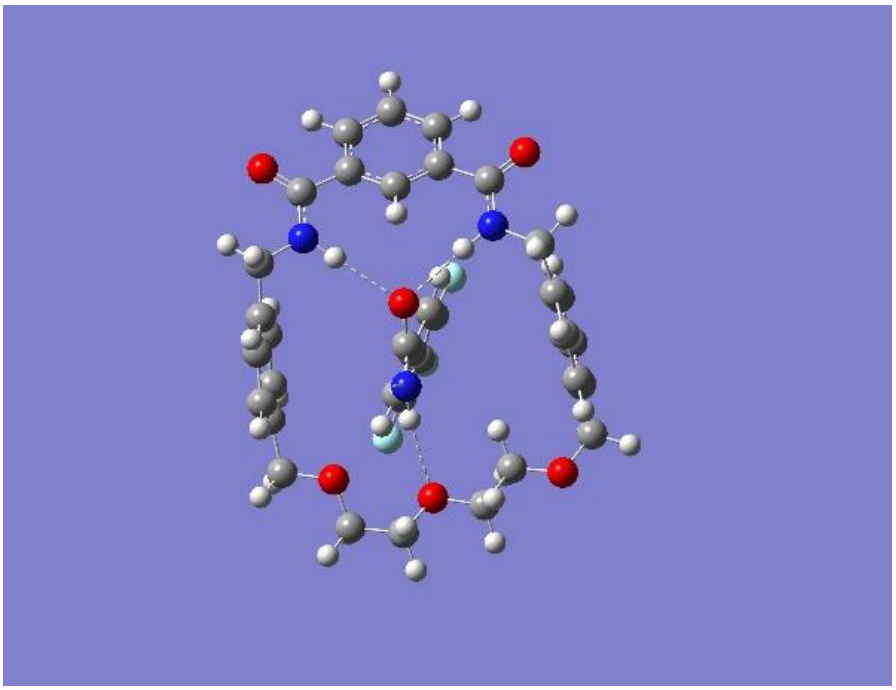

Figure 6.33 – Computational model of pseudorotaxane 6.37 with a 3,4,5-trifluorobenzene stopper, representative of pseudorotaxanes 6.35-6.38 (axle atoms after the amide were deleted for clarity).

The computational model of pseudorotaxane **6.39** shows a deformation of the isopthalamide groups, as in pseudorotaxane **6.39** the isopthalamide faces away from the stopper group (Fig. **6.32**). However, in the other pseudorotaxanes the isopthalamide group faces towards the stopper (Fig. **6.33**). This results in a change of the dihedral angle in the model between the axle carbonyl and the aromatic system, 36.8 ° in pseudorotaxane **6.39** versus 22.2 ° in pseudorotaxane **6.37** and approximately 22 ° in all of the other rotaxanes modelled. This increase in dihedral angle is to avoid the macrocycle proton ortho to both isopthalamide amides from sterically clashing with the stopper group. This increase in dihedral angle is disfavoured, as it results in poorer overlap between the π orbitals of the aromatic system and π orbitals of the amide, reducing resonance stabilisation of the molecule. These deformations of pseudorotaxane **6.39** suggests that a steric clash is the main reason that pseudorotaxane **6.39** and therefore rotaxane **6.14** cannot be formed.

6.4. Synthesis of a Eudesmic Acid Stoppered Hydrogen Bond Templated Rotaxane

6.4.1. Pseudorotaxane Studies

Initial computer modelling indicated that of the systems investigated, a eudesmic acid derived axle precursor was most likely to produce a rotaxane. However, before embarking on the relevant synthesis, a quick threading experiment was undertaken. This was done following the same method that was used for 2,3,4,5,6-pentafluorobenzene axle **6.16**.

First axle **6.40**, an analogue of thread used in pseudorotaxane **6.36**, was synthesised in a single step (Fig. **6.34**). Eudesmic acid was refluxed in thionyl chloride with a catalytic amount of DMF for 1 h, excess thionyl chloride was then removed. The resulting solid was dissolved in CH_2Cl_2 then excess NEt_3 and 2,2-diphenylethylamine were added. The mixture was subject to an aqueous work up producing thread **6.40** in 96% yield.

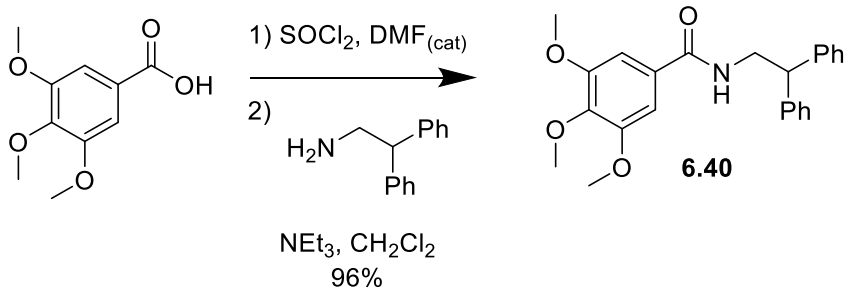

Figure 6.34 – Synthesis of axle 6.40

With macrocycle **6.15** and thread **6.40** in hand an equimolar amount of both components were then combined in 0.5 mL of $CDCl_3$ (Fig. **6.35**), the ^1H NMR spectra were compared to the individual components (Fig. **6.36**).

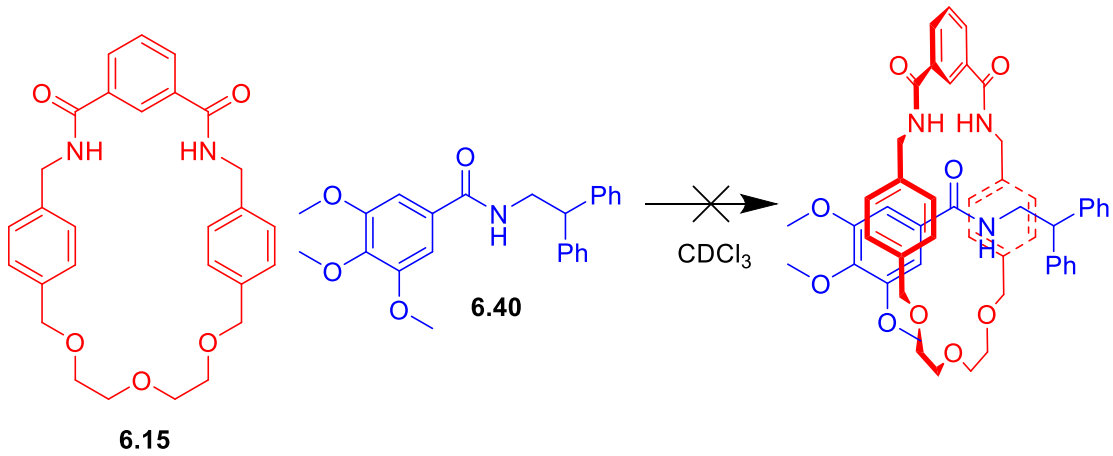

Figure 6.35 – Failed threading of axle 6.15 through macrocycle 6.40

Inspection of the ^{1}H NMR spectra (Fig. **6.36**) of the equimolar mixture of macrocycle **6.15** and axle **6.40**, reveal negligible change in the chemical shifts of the signals when compared to the corresponding signals of the individual components. This suggests that axle **6.40** is not threading through macrocycle **6.15**. A DOSY (Diffusion Ordered SpectrocopY) of the equimolar mixture of macrocycle **6.15** and axle **6.40** was obtained to confirm this and measure the rates of diffusion (400 MHz, 298 K, $CDCl_3$, 8.4 mmol cm^{-3}). The diffusion constant of axle **6.40** was determined to be between 9.99 × 10^{-10} m^{2}s^{-1} and 10.1 × 10^{-10} m^{2}s^{-1} (± 4.69 × 10^{-12} m^{2}s^{-1}) the macrocycle **6.15**between 7.93 × 10^{-10} m^{2}s^{-1} and 8.30 × 10^{-10} m^{2}s^{-1} (± 3.31 × 10^{-12} m^{2}s^{-1}). As axle **6.40** and macrocycle **6.15** diffuse at different rates, it is highly unlikely that they are interacting. From these two pieces of evidence it is inferred that axle **6.40** does not thread through macrocycle **6.15**. Therefore the 3,4,5-trimethoxy benzene group was determined to be able to act as a stopper for rotaxanes containing macrocycle **6.15**.

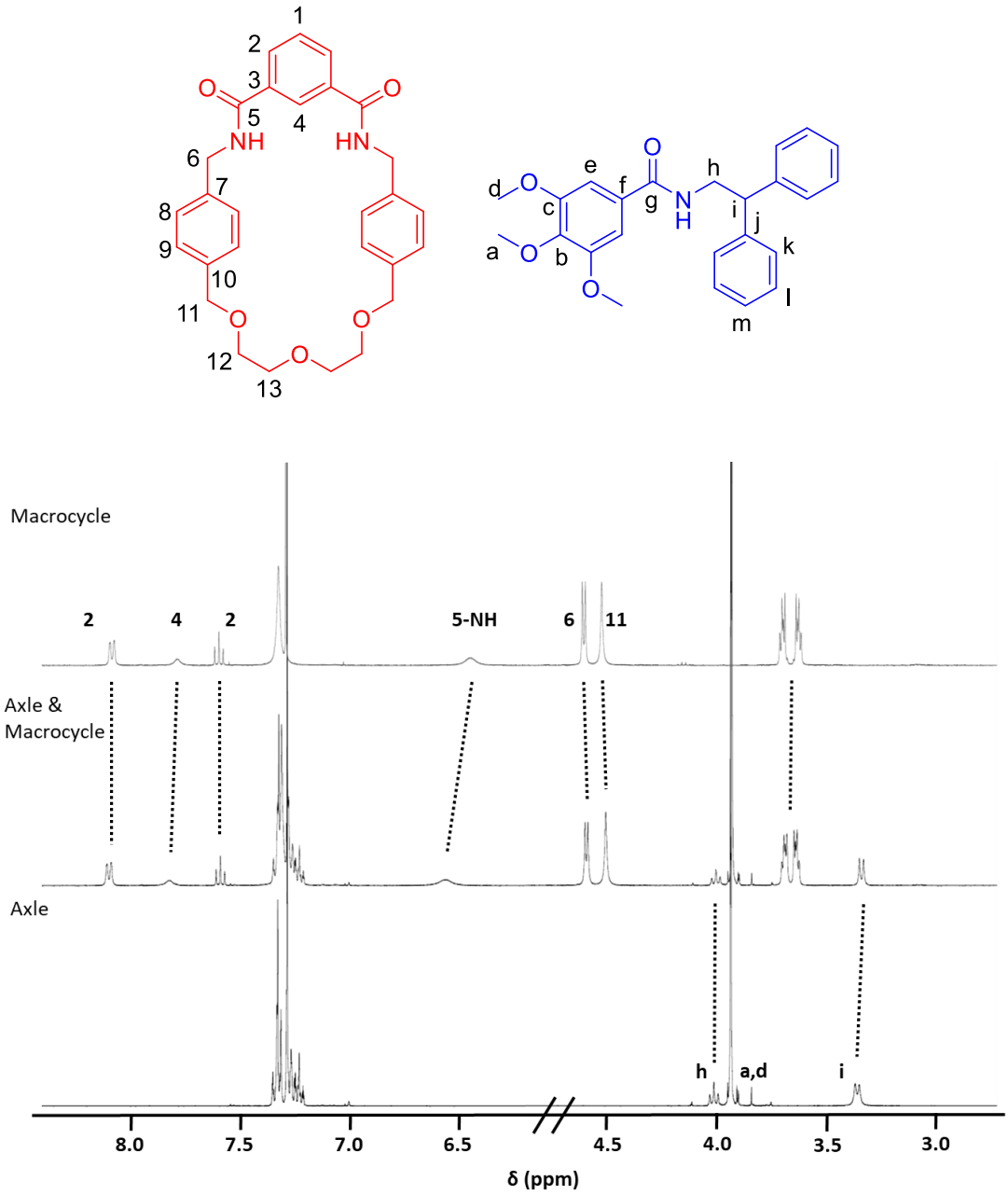

Figure 6.36 – ^{1}H NMR spectra (400 MHz, 298 K, $CDCl_3$, 8.4 mmol cm^{-3}, 3.5-5.0 ppm and 7-8.5 ppm) of macrocycle 6.15, axle 6.40 and an equimolar mixture of the axle and macrocycle.

6.4.2. Eudesmic Acid Rotaxane Synthesis

With the macrocycle **6.15** and azide stopper **6.20** already in hand, the only component required to synthesise rotaxane **6.41** was thread **6.42**. The synthesis of thread **6.42** (Fig. **6.37**), started from a stock of pre-prepared amine **6.18**. Eudesmic acid was refluxed in $SOCl_2$ with a catalytic amount of DMF for one hour, Excess $SOCl_2$ was removed and the resulting acid chloride was

dissolved in CH_2Cl_2. NEt_3 was added followed by amine **6.18**, the resulting amide was purified by an aqueous work up followed by and column chromatography to afford thread **6.42** in 94 % yield.

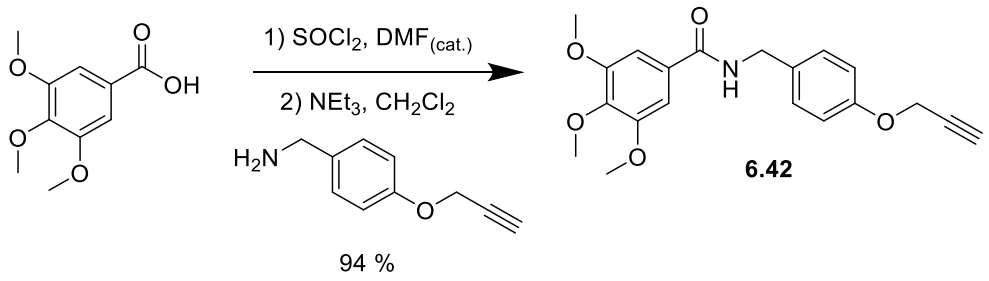

Figure 6.37 – Synthesis of alkyne thread 6.42

A Cu click reaction was used in an attempt to form rotaxane **6.41** (Fig. **6.38**). In the initial attempt, a single equivalent of macrocycle **6.15** and 1.25 equivalents of thread **6.42** were stirred in CH_2Cl_2 for 1 h. DIPEA, azide stopper **6.20**, catalytic TBTA and catalytic $Cu(MeCN)_4BF_4$ were added and the reaction was left for 16 h. The solution was isolated by an aqueous work up and column chromatography in a low 14% yield.

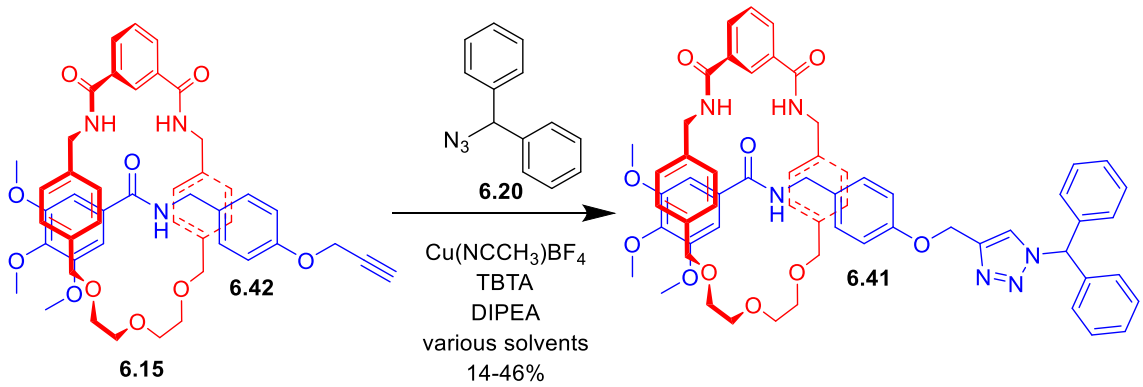

Figure 6.38 – Synthesis of rotaxane 6.41

Table 6.3 – Conditions and yields of rotaxane 6.41 formation

Attempt No.	Axle Eq.	Toluene:CH_2Cl_2 Ratio	Solvent Vol.	Macrocycle concentration	Yield	Notes
			(cm^{-3})	(nmol cm^{-3})		
1	1.25	0:1	5	8.42	14%	
2	5.8	0:1	5	12.6	15%	
3	5.8	1:0	5	8.42	16%	
4	5.8	5:2	7	6.01	29%	
5	5.8	3:2	5	12.6	29%	Refluxed 1 h in toluene
6	5.8	2:1	6	25.3	46%	Refluxed 1h in toluene and more concentrated

A further five attempts were made to synthesise rotaxane **6.41** (Table **6.3**)**,** varying the solvent, equivalents of axle and method used during pseudorotaxane formation. After the pseudorotaxane was formed the procedure was broadly identical.

The second attempt increased the number of equivalents of axle used, However, this had a negligible effect on increasing the overall yield only increasing by 1%. It was proposed that the low yield may be due to CH_2Cl_2 binding inside of the cavity of macrocycle **6.15**, hydrogen bonding to the isopthalamide moiety and altering the equilibrium between pseudorotaxane and unthreaded axle and macrocycle. Therefore in the third attempt toluene was used as the solvent. Unfortunately, the components were sparingly soluble in toluene, possibly preventing pseudorotaxane formations. The mixture was briefly heated and both macrocycle **6.15** and thread **6.41** dissolved, although on cooling precipitated out. This again had a negligible effect on the yield, only increasing by a further 1%.

The low yield from attempt 3 was attributed to the poor solubility of the components in toluene. An alternative approach was then taken for attempts 4 and 5, macrocycle **6.15** and thread **6.42** were suspended in toluene, 5 mL and 3 mL respectively. The toluene solution was heated until all of the solids had dissolved, the solution was then allowed to cool to room temperature and

CH_2Cl_2 was added until any solids formed during cooling were dissolved. Once this was complete the reaction was carried out as before, producing rotaxane **6.41** in both cases in 29% yield, over double the yield of attempt 1.

It is believed that the use of a mixed solvent, increased the yield, as it provided as non-polar and non-competitive a solvent mixture as was possible, whilst maintaining the solubility of the components. The same yield for both attempts 4 and 5, is attributed to variations in the solvent mixture and techniques used. As attempt 4 used a less polar solvent mixture, but attempt 5 used less solvent albeit more polar and was refluxed for one hour. It is likely that these two effects cancelled out, as higher concentrations typically favour pseudorotaxane formation, whilst more polar solvent mixes will disfavour pseudorotaxane formation.

Using the data gathered from the previous attempts a final attempt was made to generate a larger amount of material for further study. It was decided that the best approach would be to continue to use the ratio of 1:5.8 macrocycle **6.15** to thread **6.42**, dissolve the material in the minimum of hot toluene (4 mL), then reflux the mixture for one hour, followed by the slow addition of CH_2Cl_2 (2 mL). In this case the larger amount of material used made it far easier to obtain as concentrated a solution and as non-polar a solvent mixture as possible. In this attempt rotaxane **6.40** was obtained in 46% yield, more than three times the yield of the first attempt. Now with a useable amount of material the shuttling properties of rotaxane **6.41** could be elucidated.

Rotaxane **6.41** was characterised by ^{1}H and ^{13}C NMR spectroscopy and HR mass spectrometry. The ^{1}H NMR spectrum of rotaxane **6.41**, compared to those of macrocycle **6.15** and axle **6.43** (a by-product of the synthesis of rotaxane **6.41**) is shown in Fig. **6.39**. Axle protons e that reside within the macrocycle cavity are observed to shift upfield, due to the shielding effect of the macrocycle. Methyl ether protons a and b are observed to have to split and have a different chemical shift, attributed to an interaction with the macrocycle. Macrocycle protons 5 appear to have become diastereotopic, this is due to the rigidity of the macrocycle preventing rotation

of the respective carbon atoms and different groups placed either side of the macrocycle; a similar effect is observed with macrocycle proton 8.

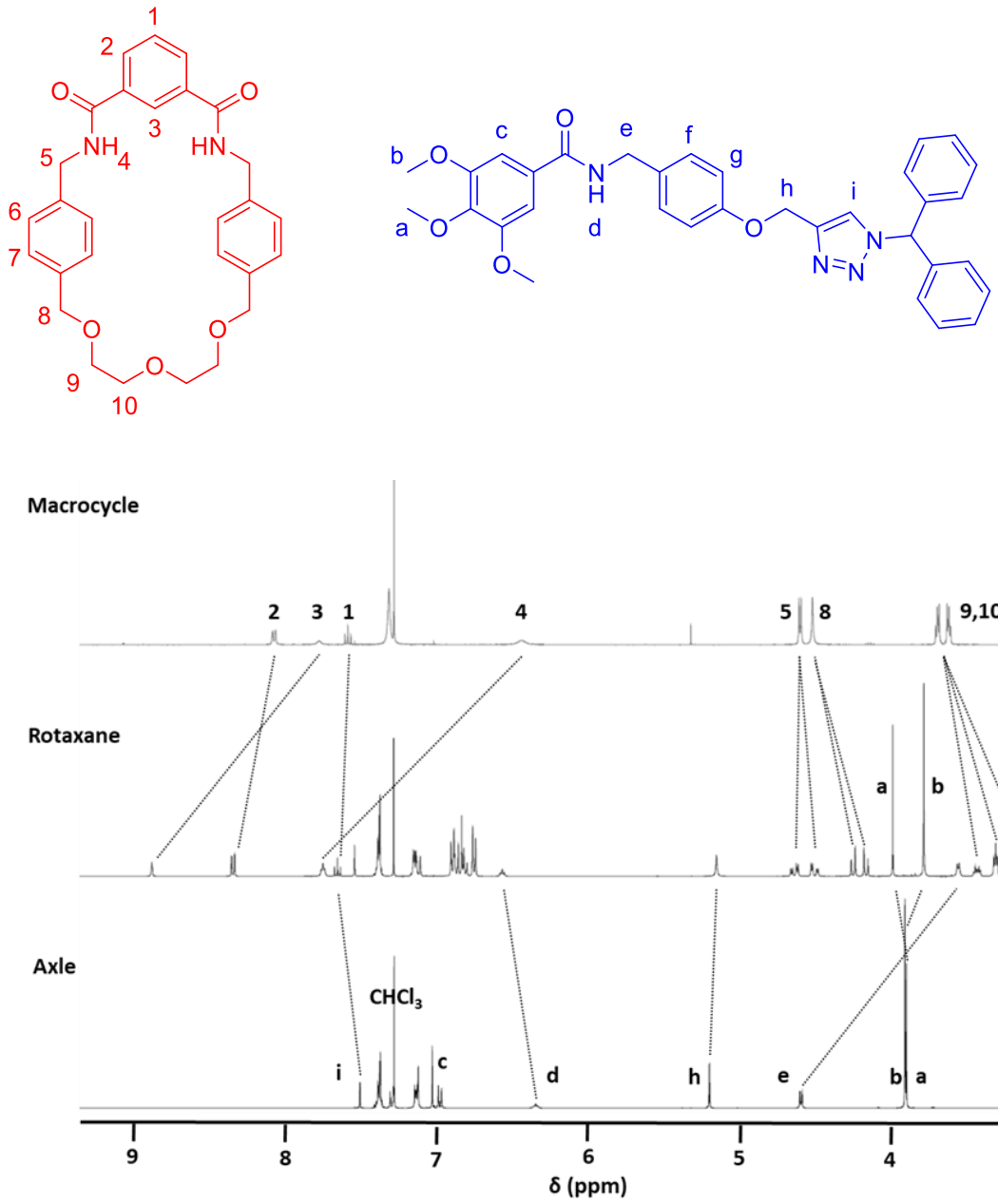

Figure 6.39 – ^{1}H NMR of macrocycle 6.15, rotaxane 6.41 and axle 6.43 ($CDCl_3$, 400 MHz, 298 K.)

6.5. Investigations Into pH Induced Motion

After the successful synthesis of rotaxane **6.41**, focus was turned to the potential pH induced shuttling behaviour. In the beginning of this chapter it was suggested that a shuttling motion may be induced by the protonation of the triazole moiety, which would create a positively charged station that the polyether oxygen atoms may coordinate to and would be aided by π-π stacking from the electron rich macrocycle aromatic groups (Fig. **6.40**).

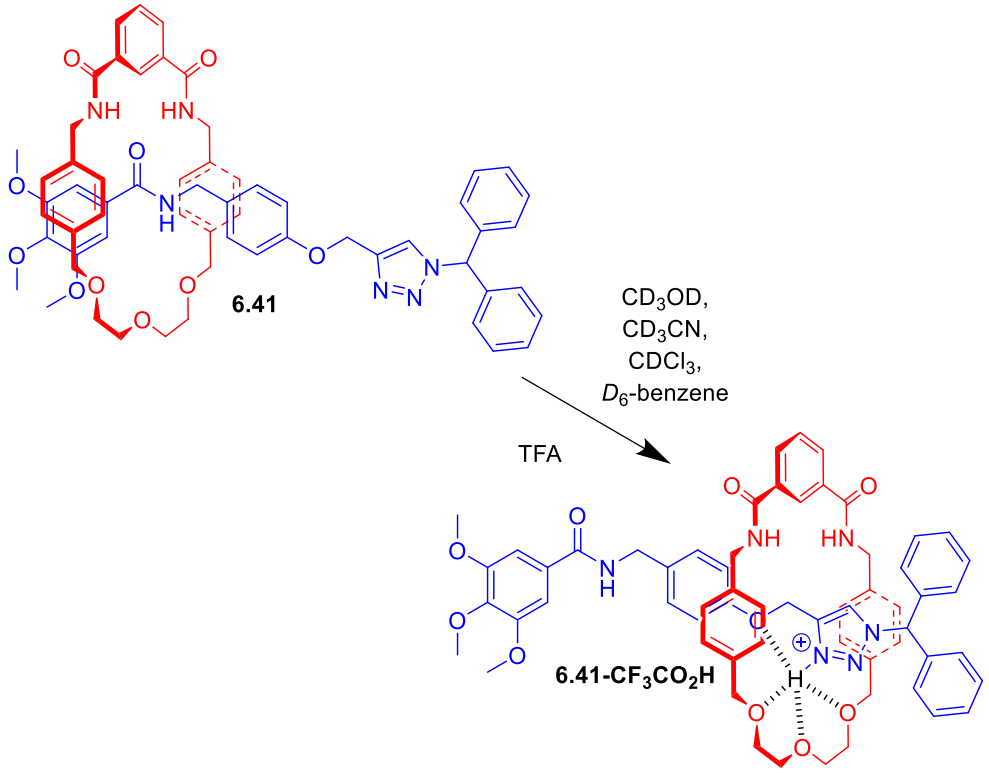

Figure 6.40- Expected shuttling movement of rotaxane 6.41 following addition of TFA

To determine the capacity of rotaxane **6.40** to undergo such shuttling molecular motion a ^{1}H NMR titration was carried out where a solution of TFA in $CDCl_3$ was gradually added to a solution of rotaxane **6.41** in $CDCl_3$. Addition of TFA caused chemical shift changes in a number of protons of rotaxane **4.41** (Fig. **6.41**).

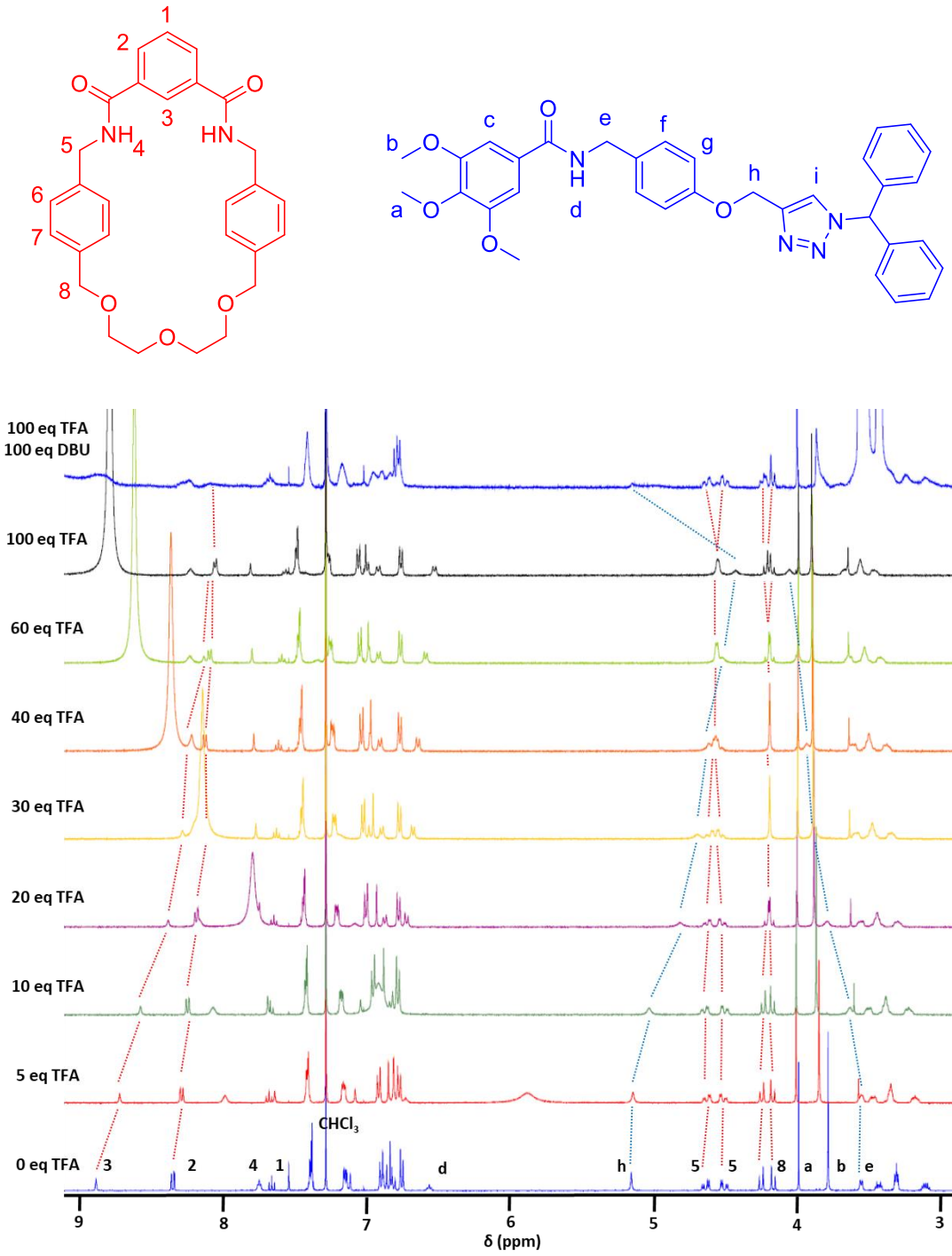

Figure 6.41 – ^{1}H NMR in $CDCl_3$ of rotaxane 6.41 with various equivalents of TFA and DBU (400 MHz, 298 K.)

Little movement was observed in the ^{1}H NMR spectra before 5 equivalents of TFA were added. However, at higher numbers of equivalents of TFA more pronounced changes in chemical shift were observed. Notably an upfield shift in axle proton h and a downfield shift in proton e, indicating that proton h was being shielded by the macrocycle and proton were being deshielded

through no longer being shielded by the macrocycle. Macrocycle isopthalamide protons 2 and 3 show a steady upfield shift, internal macrocycle proton 3 due to no longer participating in a hydrogen bonding with the axle carbonyl. In addition, the diastereotopic protons 5 are witnessed to coalesce into a single peak at 60 equivalents of TFA before separating into new diastereotopic peaks at higher equivalents of TFA; a similar effect is observed with diastereotopic protons 8. This is believed to be due to a dynamic behaviour, where the macrocycle is shuttling between the two sites, until at higher equivalents of TFA it is observed to favour the protonated triazolium over the axle amide. Addition of DBU reversed this motion, where shifted peaks were observed to return to their original chemical shifts. This indicates that the motion is due to addition of TFA and not a concentration or ionic strength effect. The titration was repeated with the axle alone and it was found that addition of TFA resulted in little change in the ^{1}H NMR spectra of axle **6.43**.

Initial results in $CDCl_3$ indicated a large number of equivalents of TFA were required to induce movement. This js thought to be due to the strength of the templating hydrogen bonds, holding the macrocycle in place and preventing it from moving along the axle. It was though the use of a more competitive solvent would weaken these hydrogen bonds, allowing the macrocycle to shuttle more easily. The ^{1}H NMR titrations with TFA were repeated in CD_3OD and CD_3CN. However, no perturbation in resonances was observed in CD_3OD and only a small amount of perturbation of the resonances was observed of movement in CD_3CN, both of those were less promising than titration done in $CDCl_3$.

Using the trend observed in amount of movement ($CD_3OD < CD_3CN < CDCl_3$), it was concluded that the disappointing results in $CDCl_3$ were not due to the strength of the templating hydrogen bonds. As the solvents most capable of disrupting the templating hydrogen bonding between the macrocycle and axle in ^{1}H NMR titrations demonstrated the least movement. Instead it was thought that the lack of movement may be due to how the solvent affects the protonated triazolium moiety. In solvents with a lone pair of electrons such as the three solvents tested so

far, the protonated species can be stabilised through the solvent acting as a hydrogen bond acceptor. This effect would prevent the polyether oxygen atoms from coordinating to the protonated species. To resolve this issue D_6-benzene was chosen as the solvent for the next TFA titration (Fig. **6.42**), as it does not have a lone pair of electrons, so is least able to stabilise the triazolium moiety.

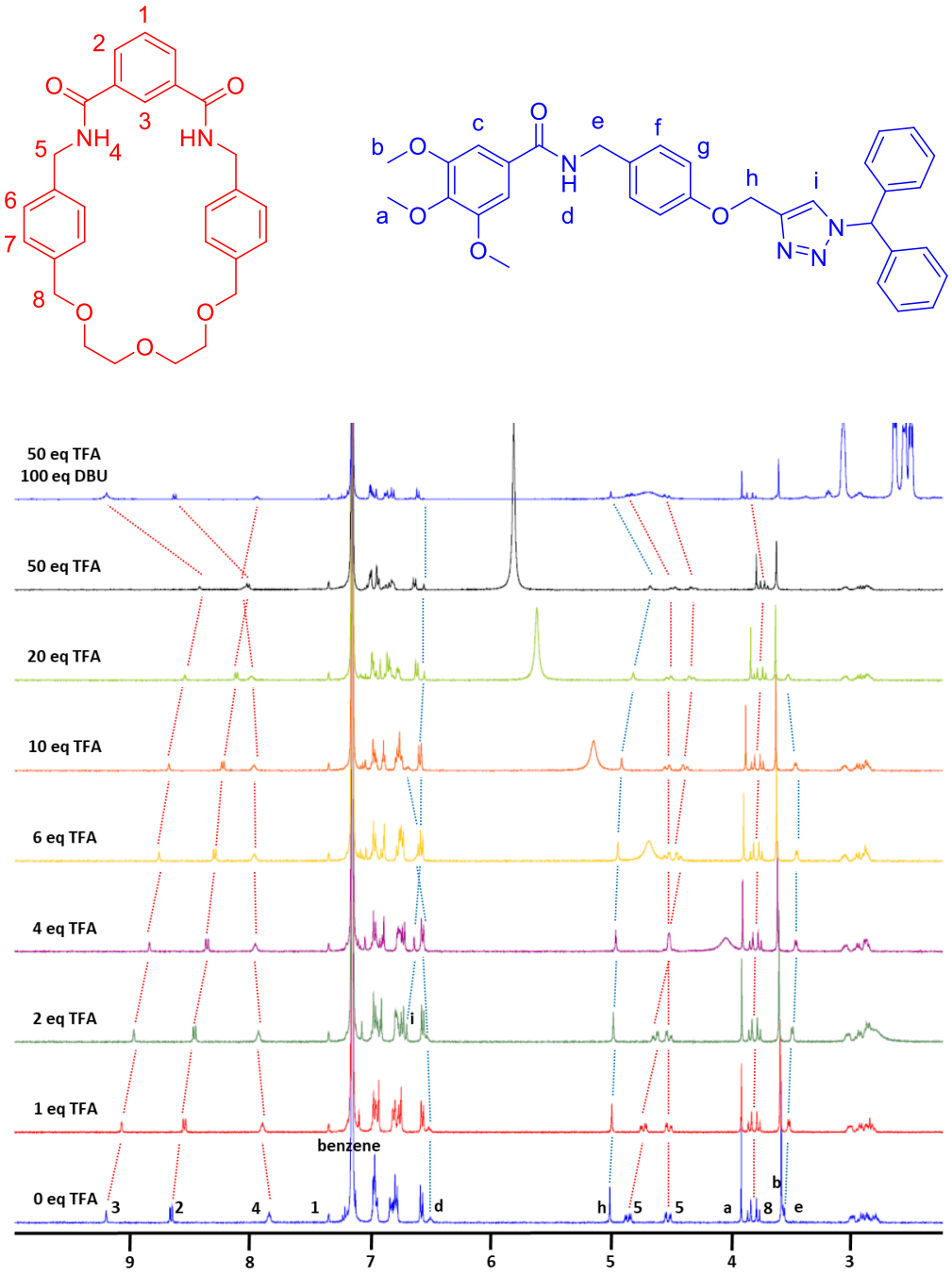

Figure 6.42 – ^{1}H NMR in D_6-Benzene of rotaxane 6.41 with various equivalents of TFA and DBU (400 MHz, 298 K)

Upon addition of small amounts of TFA in D_6-benzene to rotaxane **6.41** several peaks are observed to alter their chemical shift. Unlike in $CDCl_3$ lower numbers of equivalents of TFA were required to induce movement, indeed only four equivalents of TFA were required to reach the point where macrocyclic diastereotopic protons 5 coalesced, compared to 60 equivalents in $CDCl_3$ and 6 equivalents of TFA before the peaks had separated again. An upfield shift was also observed for macrocycle isopthalamide protons 2 and 3. Proton h was observed to shift downfield, despite being next to the protonated site, due to a shielding effect caused by the macrocycle covering proton h. Finally all peaks returned to their original positions after 100 equivalents of DBU were added, suggesting that the motion was due to protonation of the molecule and not the ionic strength of the solution.

As shuttling behaviour of rotaxane **6.41** occurred upon addition of a lower number of equivalents of TFA in C_6D_6 than in $CDCl_3$, suggesting that shuttling is more favourable in less polar and containing no hydrogen bond accepting groups.

6.6. Alkali Metal Induced Shuttling

Following the successful demonstration of shuttling behaviour caused by variation of pH, literature precedent suggests that these systems will demonstrate shuttling behaviour, as the metal cation will bind to both the macrocycle polyether groups and triazolium group (Fig. **6.43**). To determine the capacity of rotaxane **6.41** to undergo such shuttling molecular motion a ^1H NMR titration was carried out where a solution of $LiPF_6$ and $NaPF_6$ in CD_3CN was gradually added to a solution of rotaxane **6.41** in CD_3CN.

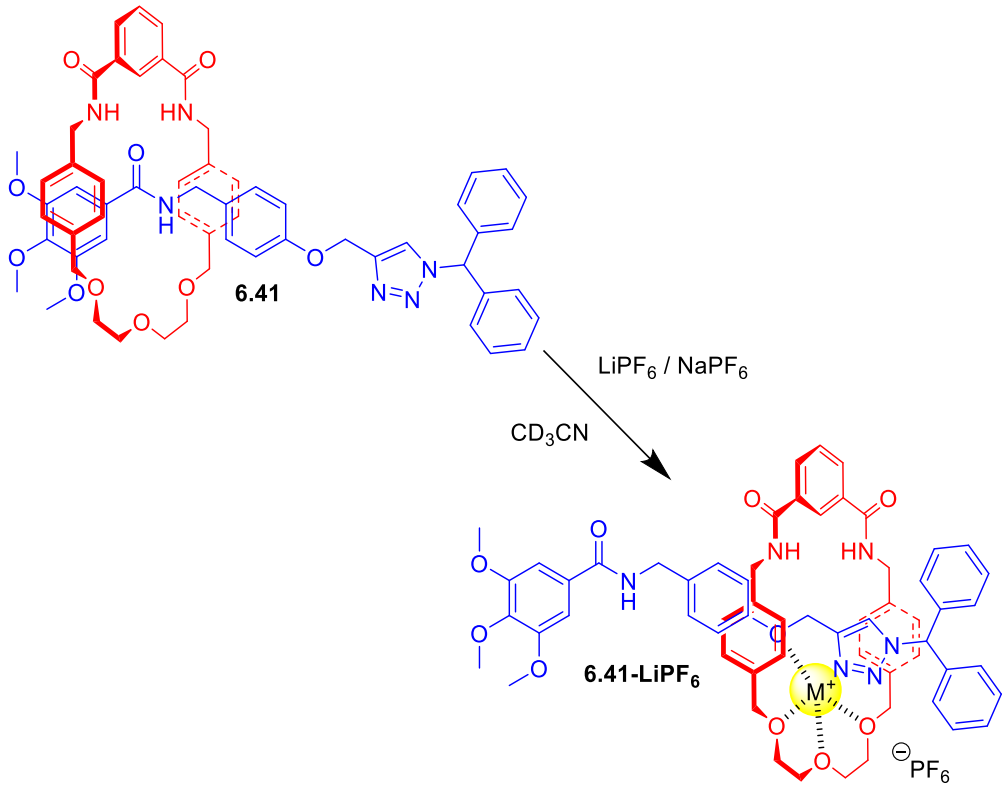

Figure 6.43- Expected shuttling movement of rotaxane 6.41 with alkali metal cations

Addition of $LiPF_6$ caused chemical shift changes in a number of protons on rotaxane **6.41** (Fig. **6.44**). Change of chemical shift was observed after a single equivalent of $LiPF_6$ was added. Diastereotopic macrocycle protons 5 were observed to coalesce after four equivalents of $LiPF_6$ were added and then separated upon addition of more $LiPF_6$. A similar effect was seen on proton 8. This suggests that the macrocycle was rapidly shuttling between the two sites, before settling above the triazole. In addition, axle proton e was observed to shift upfield, due to no longer being subject to the shielding effect of the macrocycle and axle proton h was observed to shift downfield, due to the shielding effect of the macrocycle. The change in chemical shift was partially reversed by addition of 12-crown-4. However, it was not fully reversed, possibly due to rotaxane **6.41** competitively binding the Li^+ cation.

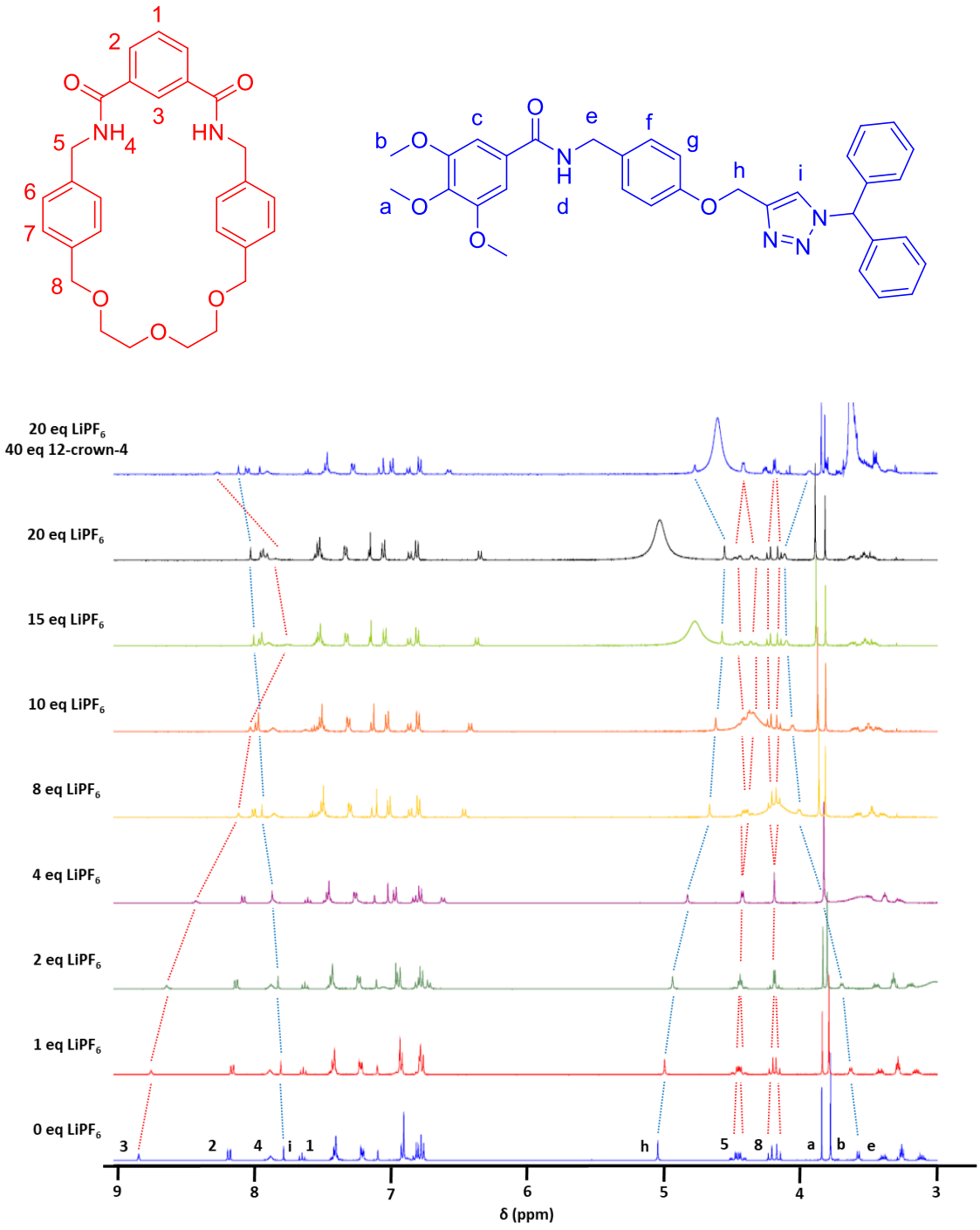

Figure 6.44– ^{1}H NMR in D_6-CD_3CN of rotaxane 6.41 with various equivalents of $LiPF_6$ and 12-crown-4 (400 MHz, 298 K)

A titration was also carried out using $NaPF_6$. However, no changes in the chemical shift of the components was observed, inferring that the Na^+ cation is unable to bind to rotaxane **6.41**. This may be due to the increased size of the Na^+ cation over Li^+ cation.

6.7. Conclusions and Future Work

Novel hydrogen bond templated rotaxane **6.41** has been prepared in 46% yield after extensive optimisation and with design informed by computational modelling. While pentafluoro rotaxane **6.14** could not be prepared, believed to be due to steric clash from the studies reported here, in the future it would be interesting to see if it can act as a stopper for rotaxanes involving this size macrocycle – but this would require the stopper to be further from the macrocycle binding site.

Rotaxane **6.44** based on pseudorotaxane **6.35**, containing a 3,5-bis(trifluoromethyl) benzene moiety (Fig. **6.55**) was also synthesised by Christopher Bithell[45] using the synthetic method developed in this thesis. This rotaxane was synthesised in 70% yield, using the optimised conditions reported in this Chapter. Whilst limited, this data provides tentative evidence that the modelling undertaken provides a useful guide for synthesis of this type of hydrogen bond templated rotaxanes. To evaluate this more fully in future, it would be prudent to attempt to synthesise all of the pseudorototaxane **6.35** to **6.39** under identical conditions and compare yields.

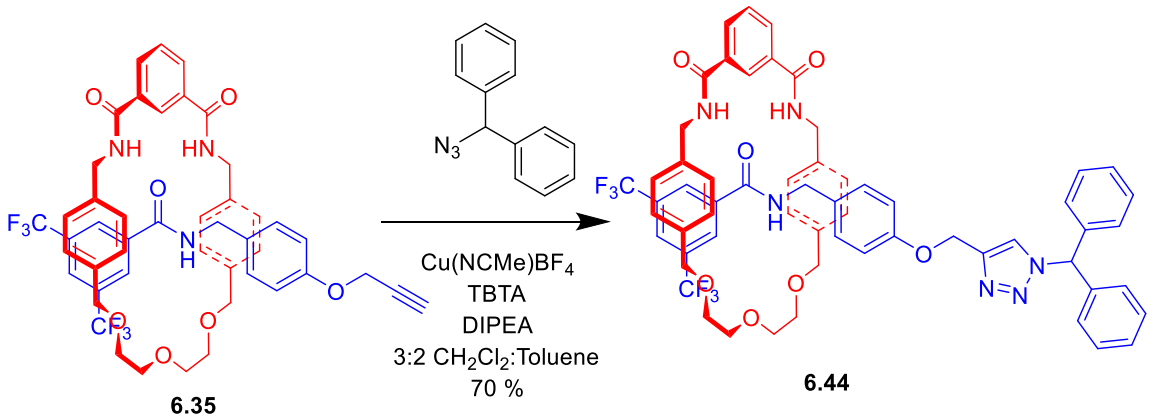

Figure 6.55 – Synthesis of rotaxane 6.44 by Christopher Bithell

Pleasingly, rotaxane **6.41** was shown to undergo molecular motion in $CDCl_3$ and C_6D_6 upon addition of TFA, it was found that molecular motion due to the change of pH proceeds better in non-polar solvents than polar solvents. It was also found that rotaxane **6.41** could undergo

molecular motion in CD_3CN in and CD_3CN upon addition of $LiPF_6$, but not $NaPF_6$, thought to be due to the increased size of the Na^+ cation. In future it may be of interest to investigate alkali earth metal cations, particularly Mg^{2+} and Be^{2+}, due to their smaller size relative to alkali metals.

6.8. References

7. R. Ballardini, V. Balzani, A. Credi, M. T. Gandolfi and M. Venturi, *Acc. Chem. Res.*, 2001, **34**, 445-455.
8. J. F. Stoddart, *Angew. Chemie Int. Ed.*, 2017, **56**, 11094–11125.
9. V. Balzani, A. Credi and M. Venturi, *Chem. Soc. Rev.*, 2009, **38**, 1542.
10. S. Erbas-Cakmak, D. A. Leigh, C. T. McTernan and A. L. Nussbaumer, *Chem. Rev.*, 2015, **115**, 10081–10206.
11. A. C. Fahrenbach, C. J. Bruns, H. Li, A. Trabolsi, A. Coskun and J. F. Stoddart, *Acc. Chem. Res.*, 2014, **47**, 482–493.
12. H. Fujita, T. Ooya, M. Kurisawa, H. Mori, M. Terano and N. Yui, *Macromol. Rapid Commun.*, 1996, **17**, 509–515.
13. A. Sørensen, S. S. Andersen, A. H. Flood and J. O. Jeppesen, *Chem. Commun.*, 2013, **49**, 5936.
14. N. H. Evans and G. R. Akien, *Supramol. Chem.*, 2018, **30**, 158–164.
15. J. E. Green, J. Wook Choi, A. Boukai, Y. Bunimovich, E. Johnston-Halperin, E. DeIonno, Y. Luo, B. A. Sheriff, K. Xu, Y. Shik Shin, H.-R. Tseng, J. F. Stoddart and J. R. Heath, *Nature*, 2007, **445**, 414–417.
16. J. Berná, D. A. Leigh, M. Lubomska, S. M. Mendoza, E. M. Pérez, P. Rudolf, G. Teobaldi and F. Zerbetto, *Nat. Mater.*, 2005, **4**, 704–710.
17. G. De Bo, M. A. Y. Gall, M. O. Kitching, S. Kuschel, D. A. Leigh, D. J. Tetlow and J. W. Ward, *J. Am. Chem. Soc.*, 2017, **139**, 10875–10879.
18. W. L. Mock and J. Pierpont, *J. Chem. Soc. Chem. Commun.*, 1990, 1509-1511.
19. J. Wook Lee, K. Kim and K. Kim, *Chem. Commun.*, 2001, 1042–1043.
20. D. Tuncel, N. Cindir and Ü. Koldemir, *J. Incl. Phenom. Macrocycl. Chem.*, 2006, **55**, 373–380.
21. D. Tuncel, Ö. Özsar, H. B. Tiftik and B. Salih, *Chem. Commun.*, 2007, 1369–1371.
22. J. W.Lee, S. Samal, N. Selvapalam, and H. J.J. Kim and K. Kim, *Acc. Chem. Res.*, 2003, **36**, 621-630.
23. K. Kim, N. Selvapalam, Y. H. Ko, K. M. Park, D. Kim and J. Kim, *Chem. Soc. Rev.*, 2007, **36**, 267–279.
24. M.-V. Martínez-Díaz, N. Spencer and J. F. Stoddart, *Angew. Chemie Int. Ed. English*, 1997, **36**, 1904–1907.
25. D. A. Leigh and A. R. Thomson, *Tetrahedron*, 2008, **64**, 8411–8416.
26. S. J. Loeb and J. A. Wisner, *Chem. Commun.*, 1998, 2757–2758.
27. S. Suzuki, K. Nakazono and T. Takata, *Org. Lett.*, 2010, **12**, 712–715.
28. F. Coutrot and E. Busseron, *Chem. - A Eur. J.*, 2008, **14**, 4784–4787.
29. M. Berg, S. Nozinovic, M. Engeser and A. Lützen, *European J. Org. Chem.*, 2015, **2015**, 5966–5978.
30. H. Zhang, B. Zhou, H. Li, D.-H. Qu and H. Tian, *J. Org. Chem.*, 2013, **78**, 2091–2098.
31. C. M. Álvarez, H. Barbero and D. Miguel, *European J. Org. Chem.*, 2015, **2015**, 6631–6640.
32. W. Yang, Y. Li, J. Zhang, N. Chen, S. Chen, H. Liu and Y. Li, *Small*, 2012, **8**, 2602–2607.

33. Z. Meng and C.-F. Chen, *Chem. Commun.*, 2015, **51**, 8241–8244.
34. C. M. Keaveney and D. A. Leigh, *Angew. Chemie Int. Ed.*, 2004, **43**, 1222–1224.
35. H. Zheng, W. Zhou, J. Lv, X. Yin, Y. Li, H. Liu and Y. Li, *Chem. - A Eur. J.*, 2009, **15**, 13253–13262.
36. W. Zhou, J. Li, X. He, C. Li, J. Lv, Y. Li, S. Wang, H. Liu and D. Zhu, *Chem. - A Eur. J.*, 2008, **14**, 754–763.
37. B. Hesseler, M. Zindler, R. Herges and U. Lüning, *European J. Org. Chem.*, 2014, **2014**, 3885–3901.
38. O. Beyer, B. Hesseler and U. Lüning, *Synthesis (Stuttg).*, 2015, **47**, 2485–2495.
39. S.A Vignon, T. Jarrosson, T. Iijima, H.R. Tseng, J.K.M. Sanders and J.F. Stoddart, *J. Am. Chem. Soc.*, **126**, 9884-9885.
40. G. Kaiser, T. Jarrosson, S. Otto, Y.-F. Ng, A. D. Bond and J. K. M. Sanders, *Angew. Chemie Int. Ed.*, 2004, **43**, 1959–1962.
41. K.-D. Wu, Y.-H. Lin, C.-C. Lai and S.-H. Chiu, *Org. Lett.*, 2014, **16**, 1068–1071.
42. L. M. Hancock and P. D. Beer, *Chem. Commun.*, 2011, **47**, 6012.
43. B. E. Fletcher, M. J. G. Peach and N. H. Evans, *Org. Biomol. Chem.*, 2017, **15**, 2797–2803.
44. E. J. M. and and J. A. Dennis, *Org. Lett*., 2006, **8**, 5085-5088.
45. K. A. H. Chehade and H. P. Spielmann, *J. Org. Chem*., 2000, **65**, 4949-4953.
46. A. Vidonne and D. Philp, *Tetrahedron*, 2008, **64**, 8464–8475.
47. R. Sekiya, Y. Uemura, H. Murakami and T. Haino, *Angew. Chemie Int. Ed.*, 2014, **53**, 5619–5623.
48. E. Schreiner, T. Wilcke and T. Müller, *Synlett*, 2015, **27**, 379–382.
49. G. E. S. M. J. Frisch, G. W. Trucks, H. B. Schlegel, V. B. M. A. Robb, J. R. Cheeseman, G. Scalmani, M. C. B. Mennucci, G. A. Petersson, H. Nakatsuji, G. Z. X. Li, H. P. Hratchian, A. F. Izmaylov, J. Bloino, R. F. J. L. Sonnenberg, M. Hada, M. Ehara, K. Toyota, O. K. J. Hasegawa, M. Ishida, T. Nakajima, Y. Honda, J. E. P. H. Nakai, T. Vreven, J. A. Montgomery, Jr., E. B. F. Ogliaro, M. Bearpark, J. J. Heyd, J. N. K. N. Kudin, V. N. Staroverov, R. Kobayashi, S. S. I. K. Raghavachari, A. Rendell, J. C. Burant, M. K. J. Tomasi, M. Cossi, N. Rega, J. M. Millam, J. J. J. E. Knox, J. B. Cross, V. Bakken, C. Adamo, A. J. A. R. Gomperts, R. E. Stratmann, O. Yazyev, R. L. M. R. Cammi, C. Pomelli, J. W. Ochterski, P. S. K. Morokuma, V. G. Zakrzewski, G. A. Voth, Ö. F. J. J. Dannenberg, S. Dapprich, A. D. Daniels and J. C. and D. J. F. J. B. Foresman, J. V. Ortiz, Gaussian, Inc., Wallingford CT, 2009.
50. N. H. Evans, C. E. Gell and M. J. G. Peach, *Org. Biomol. Chem.*, 2016, **14**, 7972–7981.
51. C. Bithell, *MChem thesis*, Lancaster University, 2018.

Chapter 7

Experimental

7.1. Instrument Methods

NMR spectra were recorded on a Bruker Ultrashield 400 Plus spectrometer or a Bruker 300 spectrometer at 298 K. ^{1}H and $^{13}C\{^{1}H\}$ spectra were assigned using a combination of ^{1}H, $^{13}C\{^{1}H\}$, ^{13}C DEPT 135, ^{1}H-^{1}H COSY, ^{1}H-^{13}C HMBC and ^{1}H-^{13}C HSQC. Protons and other magnetically active nuclei are labelled according to their nearest carbon atom, each unique carbon atom is identified by a number or letter shown on the structure included for each compound. Compounds where multiple active nuclei share a peak are denoted by commas between the identifying symbol and where a peak can be attributed to two or more possible nuclei are denoted with forward slashes between the identifying symbol. If an assignment is repeated due to a diastereotopic effect or other desymmeterisation of the molecule the second peak is denoted with an apostrophe.

Mass spectra were acquired by the mass spectrometry service at Lancaster University on a Shimadzu LCMS-IT-ToF instrument. Melting points were recorded on a Gallenkamp capillary melting point apparatus and are uncorrected. Infrared spectra were recorded on an Agilent Technologies Cary 630 FTIR spectrometer.

7.2. Solvents and Reagents

All commercially sourced solvents and reagents were used without further purification. Where dry solvents and reagents were used, they were purchased dry and stored under an inert atmosphere. $Cu(NCMe)_4BF_4$ was stored in a desiccator over P_2O_5. In all cases deionised water was used.

Analytical TLC was used to monitor the progress of column chromatography and were typically examined under short wavelength (λ = 254 nm) UV light, as were all prep-TLC plates. On the occasion that the molecule lacked a suitable fluorophore, potassium permanganate or aqueous acidic ammonium molybdate stain were used to develop the analytical TLC plates

7.3. Synthetic Procedures and Characterisation

7.3.1. Experimental for Chapter 2

Compound **2.13** was kindly supplied by Dr. Nicholas Evans.

2.1 Glycine rotaxane chloride salt

To glycine axle **2.21** (300 mg, 0.351 mmol) and bis-amine **2.10** (233 mg, 0.502 mmol) in dry CH_2Cl_2 (20 mL), NEt_3 (0.0.12 mL, 89 mg, 0.879 mmol) was added, followed by a dropwise addition of isophthaloyl chloride (122 mg, 0.602 mmol) in CH_2Cl_2 (10 mL). The solution was stirred for 1 h then washed with 10% HCl (20 mL) and water (2 × 20 mL), dried with $MgSO_4$ and the solvent removed *in vacuo*. The residue was purified via flash column chromatography (silica, 95:5 CH_2Cl_2:MeOH) to afford a yellow solid with some macrocyclic impurities (438 mg).

The impure rotaxane was dissolved in $CHCl_3$ (50 mL) then washed with 0.2 mol dm^{-3} $(NH_4)_2SO_4$ (8 × 50 mL), then dried with $MgSO_4$. The solvent was removed *in vacuo* and the residue was loaded onto a plug of silica and washed with 95:5 CH_2Cl_2:MeOH, the solution was set aside for later use. The rotaxane was then flushed off the silica using 85:15 (CH_2Cl_2:MeOH) saturated with NH_4Cl and the solvent removed *in vacuo*. The residue was dissolved in CH_2Cl_2 (30 mL) and washed with 1 mol dm^{-3} NH_4Cl (20 mL) and water, then dried with $MgSO_4$ to afford rotaxane **2.1** (103 mg, 23 %) The solvent was then removed *in vacuo* from the wash solution to afford impure rotaxane **2.1** (94 mg), the exchange to the sulfate salt and subsequent column chromatography was repeated on the impure material to afford further rotaxane **6.1** (55 mg, 12 %, combined yield 35 %).

Mp: >230 °C, (dec.).

^{1}H NMR (400 MHz, 1:1 $CDCl_3$:MeOD) δ: 8.97 (d, 2H, ^4J = 1.2 Hz, $C^{21}H$), 8.89 (s, 1H, $C^{20}H$), 8.56 (s, 1H, C^dH), 7.83 (dd, 2H, ^3J = 7.8 Hz, ^4J = 1.7 Hz, C^bH), 7.35 (d, 4H, ^3J = 8.7 Hz, $C^{14}H$), 7.24 (t, 1H, ^3J = 7.8 Hz, C^aH), 6.98-7.17 (m, 30H, ArH), 6.47 (d, 4H, ^3J = 9.0 Hz, $C^{i/j}H$), 6.18 (d, 4H, ^3J = 9.0 Hz, $C^{i/j}H$),

4.37 (s, 3H, $C^{22}H$), 4.07 (s, 4H, $C^{17}H$), 3.99 (t, 4H, ^{3}J = 5.8 Hz, $C^{g}H$), 3.58-3.69 (m, 20H, OCH_2, $C^{f}H$), 1.19 (s, 36H, $C^{1}H$).

$^{13}C\{^{1}H\}$ NMR (100 MHz, 1:1 $CDCl_3$:MeOD) δ: 168.2 (C^{e}), 166.6 (C^{16}), 160.9 (C^{18}), 153.2 ($C^{h/k}$), 152.0 ($C^{h/k}$), 148.4 (C^{3}), 147.1 (ArC), 145.8 (C^{21}), 143.8, 143.3 (2 × ArC), 139.2 (C^{20}), 135.6, 134.0, 132.6, 131.5 (4 × ArC), 131.1 (C^{b}), 130.9 (C^{c}), 130.6 (ArC), 128.9 (C^{a}), 127.2, 125.6 (2 × ArC), 124.8 (C^{d}), 124.1, 118.7 (C^{14}), 115.1 ($C^{i/j}$), 114.8 ($C^{i/j}$), 70.5, 70.0, 68.0 (4 × OCH_2, overlap at 70.5), 66.2 (C^{g}), 63.7 (C^{11}), 49.1 (C^{22}), 43.7 (C^{17}), 40.3 (C^{f}), 34.1 (C^{2}), 31.0 (C^{1}).

HRMS (ESI): *m/z*: 1748.9085 $[M]^+$, $C_{110}H_{122}N_7O_{13v}$requires 1748.9095.

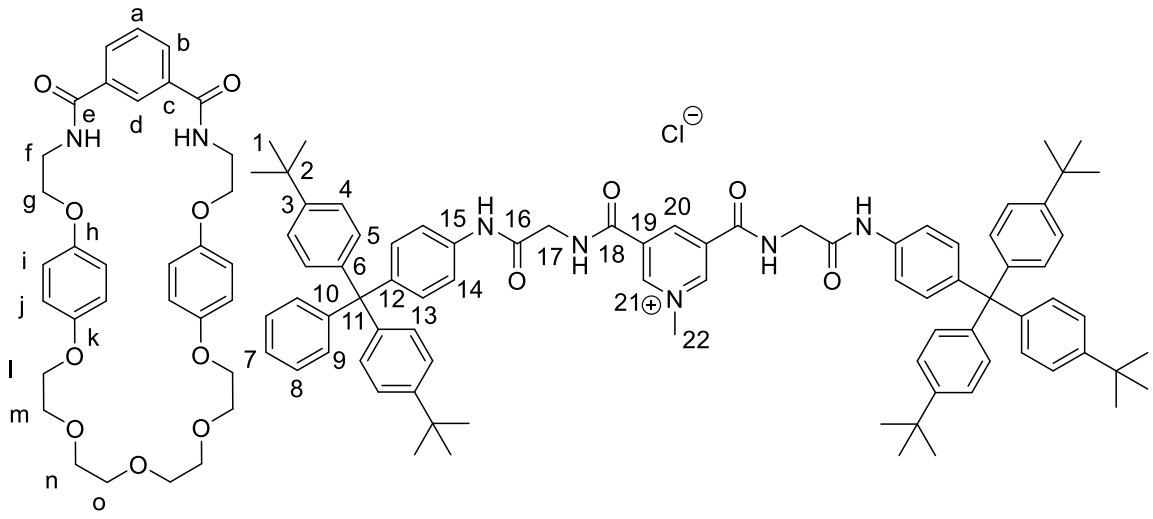

2.1-PF_6 Glycine rotaxane hexafluorophosphate salt

Glycine rotaxane chloride **2.1** (55 mg, 0.031 mmol) in CH_2Cl_2 was washed with 0.1 mol dm^{-3} NH_4PF_6 (8 × 10 mL) then water (2 × 10 mL). The solvent was removed *in vacuo* to afford a yellow solid (53 mg, 89 %).

^{1}H NMR (400 MHz, 1:1 $CDCl_3$:MeOD) δ: 8.87 (d, 2H, ^{4}J = 1.5 Hz, $C^{21}H$), 8.51 (s, 1H, $C^{20}H$), 8.19 (s, 1H, $C^{d}H$), 7.82 (dd, 2H, ^{3}J = 7.8 Hz, ^{4}J = 1.7 Hz, $C^{b}H$), 7.34 (d, 4H, ^{3}J = 7.3 Hz, $C^{14}H$), 7.31 (t, 1H, ^{3}J = 7.8 Hz, $C^{a}H$), 6.98-7.17 (m, 30H, ArH), 6.49 (d, 4H, ^{3}J = 9.0 Hz, $C^{i/j}H$), 6.24 (d, 4H, ^{3}J = 9.0 Hz, $C^{i/j}H$), 4.23 (s, 3H, $C^{22}H$), 4.11 (s, 4H, $C^{17}H$), 3.89 (t, 4H, ^{3}J = 4.8 Hz, $C^{g}H$), 3.56-3.73 (m, 20H, OCH_2, $C^{f}H$), 1.19 (s, 36H, $C^{1}H$).

$^{13}C\{^{1}H\}$ NMR(100 MHz, 1:1 $CDCl_3$:MeOD) δ: 168.5 (C^{e}), 166.7 (C^{16}), 160.9 (C^{18}), 153.1 ($C^{h/k}$), 152.0 ($C^{h/k}$), 148.4 (C^{3}), 147.1 (ArC), 145.7 (C^{21}), 143.7, 143.4 (2 × ArC), 140.9 (C^{20}), 135.5, 134.5 (2 × ArC), 132.8 (C^{19}), 131.5 (ArC), 130.9 (C^{c}), 130.7 (ArC), 130.6 (C^{b}), 128.9 (C^{a}), 127.2, 125.7 (2 × ArC), 124.9 (C^{d}), 124.1 (ArC), 118.6 (C^{14}), 115.4 ($C^{i/j}$), 114.9 ($C^{i/j}$), 70.6, 70.5, 70.0, 67.9 (4 × OCH_2), 66.6 (C^{g}), 63.7 (C^{11}), 49.0 (C^{22}), 43.7 (C^{17}), 38.8 (C^{f}), 34.1 (C^{2}), 31.0 (C^{1}).

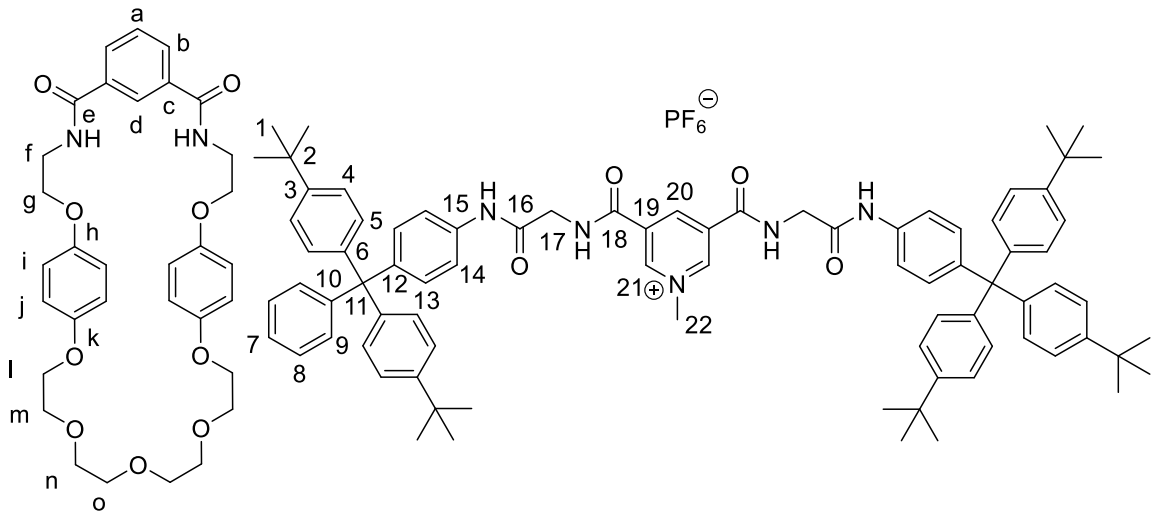

2.2 L-alanine rotaxane chloride salt

Pyridinium axle **2.22** (135 mg, 0.111 mmol) was dissolved in dry CH_2Cl_2 (25 mL) to which bis amine **2.10** (62 mg, 0.111 mmol) was added and the reaction allowed to stir for 30 minutes, at RT under Ar. NEt_3 (9.6 mg, 0.013 mL, 0.095 mmol) was added, followed by the dropwise addition of isophthaloyl chloride (31 mg, 0.111 mmol) in dry CH_2Cl_2 (10 mL). The solution was allowed to stir for 1 h, at RT under Ar. The reaction mixture was washed with 10% $HCl_{(aq)}$ (2 × 25 mL) and then water (2 × 25 mL). The organic layer was dried with $MgSO_4$ and the solvent removed *in vacuo* to yield a yellow solid. The yellow solid was purified by column chromatography (silica, 95:5 CH_2Cl_2:MeOH) to yield the product, a yellow solid, contaminated with non-interlocked macrocycle. The material was then dissolved in CH_2Cl_2 and washed with $NH_4PF_{6(aq)}$ (0.1 M, 5 × 10 mL) and the solvent removed *in vacuo* to leave a yellow solid. The yellow solid was twice purified by column chromatography (silica 97:3 CH_2Cl_2:MeOH) (silica 66:30:4 CH_2Cl_2:acetone:MeOH) to yield the product as a yellow solid contaminated with macrocyclic impurities (40 mg, 19%).

^{1}H NMR (400 MHz, D_6-acetone) δ: 9.95 (d, 1H, ^3J = 8.5 Hz, $C^{20}H$), 9.19 (d, 2H, ^3J = 8.5 Hz), 9.14 (s, 0.5H, $C^{d}H$), 9.11 (s, 0.5 H, $C^{d'}H$), 8.11 (dt, 0.5H, ^3J = 7.7 Hz, ^4J = 1.5 Hz $C^{b}H$), 8.08 (dd, ^3J = 7.8 Hz, ^4J = 1.5 Hz, $C^{b'}H$), 8.04 (dt, 0.5H, ^3J = 7.7 Hz, ^4J = 1.5 Hz $C^{b}H$), 7.63-7.68 (m, 4H, $C^{14}H$), 7.53 (td, 1H, ^3J = 7.8 Hz, ^4J =3.0 Hz), 7.12-7.34 (m, 34H, ArH), 6.60 (d, 3H, ^3J = 9.1 Hz, $C^{i/j}$), 6.56 (d, 1H, ^3J = 9.1 Hz, $C^{i/j}$), 6.23 (d, 1H, ^3J = 9.1 Hz, $C^{i/j}$), 6.23 (d, 1H, ^3J = 9.1 Hz, $C^{i/j}$), 6.18 (d, 2H, ^3J = 9.1 Hz, $C^{i/j}$), 6.11 (d, 1H, ^3J = 9.1 Hz, $C^{i/j}$), 4.76 (s, 3H, $C^{23}H$), 4.60 (quintet, 2H, ^3J = 7.7 Hz, $C^{17}H$), 4.35-4.43 (m, 2H, $C^{g}H$), 4.20 (m, 2H, $C^{g'}H$), 3.60-3.83 (m, 18H, OCH_2, $C^{f}H$), 1.57 (t, 6H, ^3J = 7.0 Hz, $C^{18}H$), 1.30 (s, 36H, $C^{1}H$).

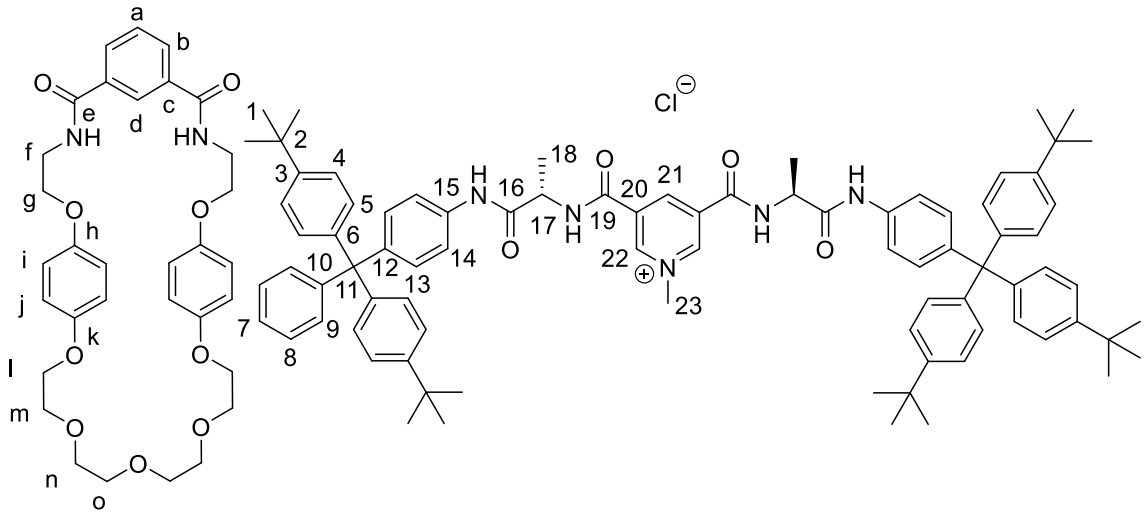

2.4 L-phenylalanine rotaxane chloride salt

To L-phenylalanine axle **2.24** (183 mg, 0.133 mmol) and bis-amine **2.10** (124 mg, 0.267 mmol) in dry CH_2Cl_2 (20 mL), NEt_3 (0.11 mL, 81 mg, 0.801 mmol) was added, followed by a dropwise addition of isophthaloyl chloride (65 mg, 0.32 mmol) in CH_2Cl_2 (10 mL). The solution was stirred for 1 h then washed with 10% HCl (20 mL) and water (2 × 20 mL), dried with $MgSO_4$ and the solvent removed *in vacuo*. The residue was purified via flash column chromatography (silica, 95:5 CH_2Cl_2:MeOH) to afford a yellow solid with some macrocyclic impurities (113 mg).

The impure rotaxane was dissolved in $CHCl_3$ (50 mL) then washed with 0.2 mol dm^{-3} $(NH_4)_2SO_4$ (8 × 50 mL), then dried with $MgSO_4$. The solvent was removed *in vacuo* and the residue was

loaded onto a plug of silica and washed with 96:4 CH_2Cl_2:MeOH, the solution was set aside for later use. The rotaxane was then flushed off the silica using 85:15 (CH_2Cl_2) saturated with NH_4Cl and the solvent removed *in vacuo*. The residue was dissolved in CH_2Cl_2 (30 mL) and washed with 1 mol dm^{-3} NH_4Cl (20 mL) and water, then dried with $MgSO_4$ to afford rotaxane **2.4** (30 mg, 13 %) The solvent was then removed *in vacuo* from the wash solution to afford impure rotaxane **2.4** (94 mg), the exchange to the sulfate salt and subsequent column chromatography was repeated on the impure material to afford further rotaxane **2.4** (24 mg, 11 %, combined yield 24 %).

Mp: >230 °C (dec.)

^{1}H NMR (400 MHz, 1:1 $CDCl_3$:MeOD) δ: 9.16 (dd, 2H, ^4J = 1.2 Hz, $C^{26}H$), 9.14 (d, 2H, ^4J = 1.4 Hz, $C^{26'}H$), 8.49-8.58 (m, 2H, $C^{d,25}H$), 8.02 (tt, 1H, ^3J = 7.7 Hz, ^4J = 1.7 Hz, C^bH), 7.98 (dd, 1H, ^3J = 7.7 Hz, ^4J = 1.7 Hz, C^bH), 7.55 (t, 1H, ^3J = 7.7 Hz, C^aH), 7.53 (d, 2H, ^3J = 9.2 Hz, $C^{14}H$), 7.49 (d, 2H, ^3J = 8.8 Hz, $C^{14'}H$), 5.07-7.38 (m, 32 H, ArH), 6.09-6.15 (m, 3H, $C^{i/j}H$), 6.06 (d, 1H, ^3J = 9.2 Hz, $C^{i/j}H$), 6.01 (d, 3H, ^3J = 9.0 Hz, $C^{i/j}H$), 5.92 (d, 1H, ^3J = 9.2 Hz, $C^{i/j}H$), 4.91-4.97 (m, 2H, $C^{17}H$), 4.50 (d, 3H, $C^{27}H$), 3.51-3.81 (m, 22H, OCH_2, C^gH), 3.40-3.47 (m, 2H, $C^{g'}H$), 3.31 (dd, 2H, ^2J = 14.0 Hz, ^3J = 5.7 Hz, $C^{18}H$), 3.22 (ddd, 2H, ^2J = 14.0 Hz, ^3J = 9.5 Hz, ^3J = 4.4 Hz $C^{18'}H$), 1.29 (s, 36 H, C^1H).

$^{13}C\{^1H\}$ NMR(100 MHz, 1:1 $CDCl_3$:MeOD) δ: 169.7, 169.5, 168.4, 168.1, 160.2, (5 × CONH) 153.1 ($C^{h/k}$), 153.0 (ArC), 151.7 ($C^{h/k}$), 149.0, 148.4 147.0 (3 × ArC), 145.1 (C^{26}), 143.7, 143.7, 143.6 (3 × ArC), 140.3 (C^{25}) 136.7, 136.7, 135.6, 132.5, 132.4, 131.6, 131.5, 130.9, 130.5, 129.1, 128.6, 127.2, 127.0, 127.0, 125.7, 124.2, (16 × ArC), 118.8 (C^{14}), 118.7 ($C^{14'}$), 114.8, 114.7, 114.5, 114.4 ($C^{i,i',j,j'}$), 70.4, 69.9, 68.1, 67.9, 66.4 (OCH_2), 63.7 (C^{11}), 56.9 (C^{17}), 49.2 (C^{27}), 39.8 (C^g), 37.2 (C^{18}), 37.2 (C^2), 31.0 (C^1).

*More ^{1}H and ^{13}C signals than would be expected are detected due to the presence of rotamers.

HRMS (ESI): *m/z*: 1929.0020 $[M]^+$, $C_{124}H_{134}N_7O_{13}$ requires 1929.0034.

$[\alpha]_D^{25}$: +5.5 (10 mg ml^{-1}, $CHCl_3$)

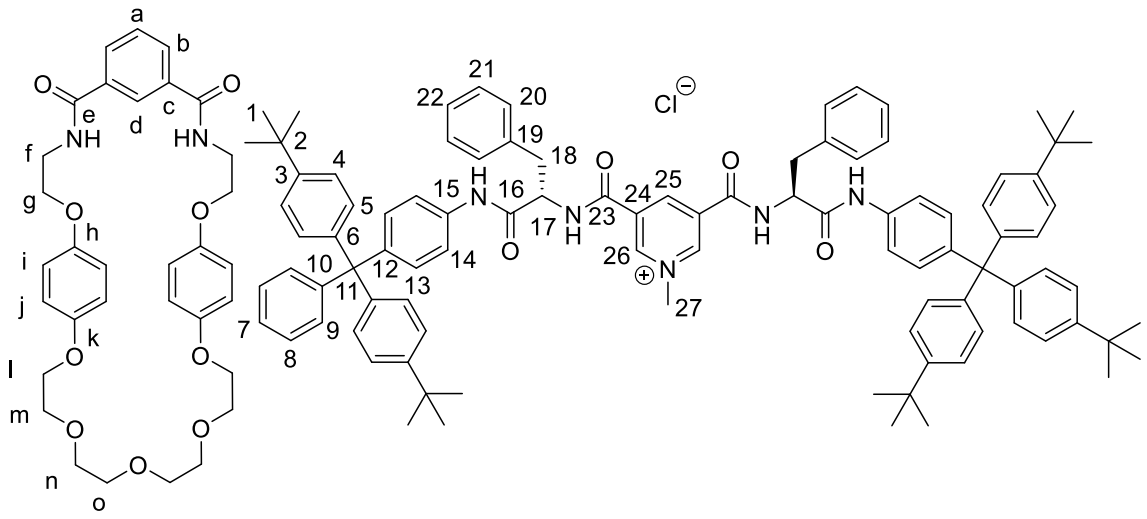

2.4-PF_6 L-Phenylalanine rotaxane hexafluorophosphate salt

Rotaxane **2.4** (22 mg, 0.0109 mmol) in CH_2Cl_2 was washed with 0.1 mol dm^{-3} NH_4PF_6 (8 × 10 mL) then water (2 × 10 mL). The solvent was removed *in vacuo* to afford a yellow solid (16 mg, 70 %).

^{1}H NMR (400 MHz, 1:1 $CDCl_3$:MeOD) δ: 8.99 (d, 1H, ^4J = 1.1 Hz, $C^{26}H$), 8.96 (d, 1H, ^4J = 1.3 Hz, $C^{26'}H$), 8.39 (s, 1H, $C^{25}H$), 8.35 (s, 0.5H, $C^{d}H$), 8.34 (s, 0.5H, $C^{d'}H$), 7.99 (ddt, 1H, ^3J = 15 Hz, ^3J = 7.8 Hz, ^4J = 1.4 Hz, $C^{b}H$), 7.95 (dd, 1H, ^3J = 7.8 Hz, ^4J = 1.7 Hz, $C^{b'}H$), 7.56 (t, 1H, ^3J = 7.8 Hz), 7.48 (d, 2H, ^3J = 8.8 Hz, $C^{14}H$), 7.45 (d, 2H, ^3J = 8.8 Hz, $C^{14'}H$), 7.07-7.39 (m, 36H, ArH), 6.22 (d, 1H, ^3J = 9.1 Hz), 6.28 (d, 2H, ^3J = 9.1 Hz), 6.12 (d, 1H, ^3J = 9.1 Hz), 6.03 (d, 3H, ^3J = 9.1 Hz), 5.92 (d, 1H, ^3J = 9.1 Hz, $C^{i, i', j, j'}H$), 4.97 (ddd, 2H, ^3J = 9.5 Hz, ^3J = 9.5 Hz, ^3J = 5.8 Hz, $C^{17}H$), 4.46 (d, 3H, ^3J = 7.6 Hz, $C^{27}H$), 3.47-3.83 (m, 22H, OCH_2, $C^{g}H$), 3.38 (obscured CD_3OH, $C^{g'}H$), 3.31 (dd, 2H, ^4J = 14.0 Hz, ^3J = 5.6 Hz, $C^{18}H$), 3.12 (ddd, 2H, ^4J = 14.0 Hz, ^3J = 9.4 Hz, ^4J = 2.8 Hz, $C^{18'}H$), 1.30 (s, 36H, $C^{1}H$).

^{19}F NMR (376 MHz, 1:1 $CDCl_3$:MeOD) δ: -73.5 (d, ^1J = 710 Hz, PF_6^-).

^{31}P NMR (162 MHz, 1:1 $CDCl_3$:MeOD) δ: -144.4 (sept, ^1J = 710 Hz, PF_6^-).

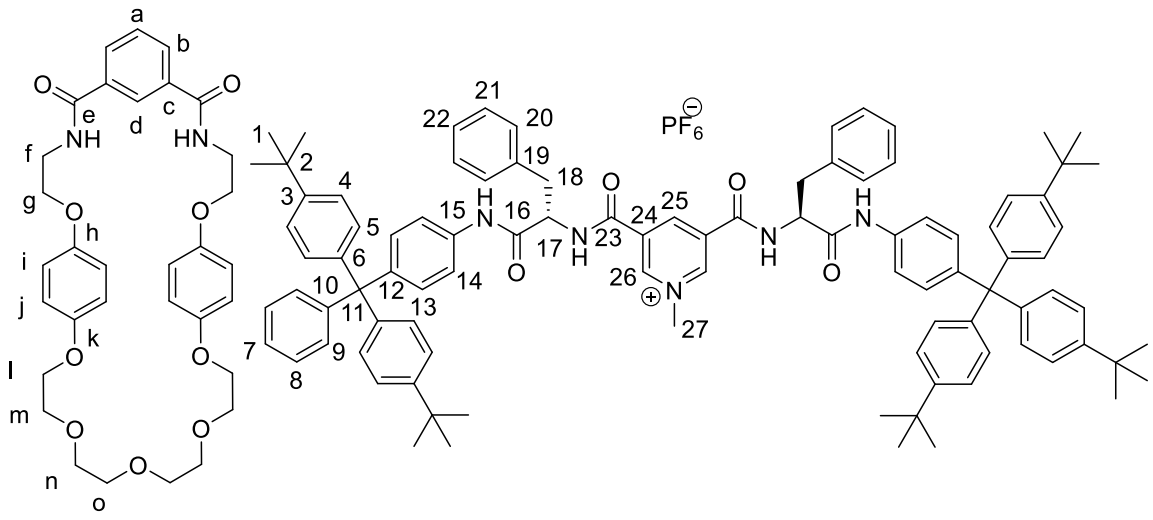

2.10 Polyether bis-amine[1]

To a solution of polyether bis-nitrile **2.14** (3.19 g, 6.98 mmol) in dry THF (10 mL), BH_3·THF (1 mol dm^{-3}, 28 mL, 28 mmol) was slowly added. The reaction mixture was heated to reflux for 6 h under an Ar atmosphere, then quenched with MeOH. Concentrated $HCl_{(aq)}$ (10 mL) was added, the mixture was allowed to stir for a further 30 minutes at RT and the solvent was then removed *in vacuo* to leave a fluffy white solid containing a large proportion of water. The white solid was then suspended in CH_2Cl_2 (200 mL) and 10% NaOH (200 mL), the biphasic mixture was stirred vigorously for 30 minutes. The organic layer was separated and washed with H_2O (2 × 100 mL) and dried over $MgSO_4$. The solvent was removed *in vacuo* to leave the product, an oily yellow solid (2.95g, 91%).

^{1}H NMR (400 MHz, $CDCl_3$) δ: 6.72-6.80 (8H, m, $C^{4,5}H$), 4.09 (4H, t, ^3J = 5.2 Hz, C^7H), 3.95 (4H, t, ^3J = 5.3 Hz, C^2H), 3.85 (4H, t, ^3J = 5.2 Hz, C^8H), 3.69-3.76 (8H, m, $C^{9,10}H$), 3.07 (4H, t, ^3J = 5.3 Hz, C^1H).

^{13}C{^{1}H} NMR(100 MHz, $CDCl_3$) δ: 153.2, 153.1 ($C^{3,6}$), 115.7, 115.4 ($C^{4,5}$), 70.8 (C^2), 70.7 ($C^{9,10}$), 69.9 (C^8), 68.1 (C^7), 41.7 (C^1).

HRMS (ESI): *m/z*: 487.2409 $[M+Na]^+$, $C_{24}H_{36}N_2O_7Na$ requires 487.2421.

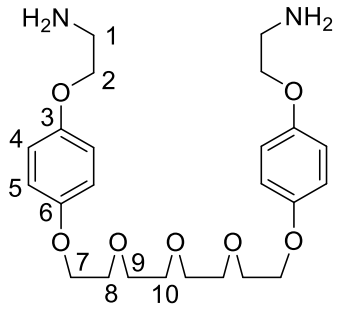

The obtained data is consistent with literature values.

2.12 2-(4-Hydroxyphenoxy)acetonitrile[2]

A solution of NaOH (4.00 g, 100 mmol) in H_2O (85 mL) and 1,4-dioxane (85 mL) was thoroughly degassed with N_2. Hydroquinone (5.51 g, 50.0 mmol) was added to the solution followed by bromoacetonitrile (6.00 g, 3.38 mL, 50.0 mmol). The reaction was stirred for 30 minutes at RT, whilst N_2 was continuously bubbled through the reaction mixture. The reaction mixture was acidified with 10% $HCl_{(aq)}$ and extracted with CH_2Cl_2 (3 × 250 mL) The organic fractions were combined and dried with $MgSO_4$ and the solvent was removed *in vacuo* to leave a brown oil. The brown oil was purified by column chromatography (silica, 98:2 CH_2Cl_2:MeOH) to give the product as a white waxy solid (5.11 g, 69%).

^{1}H NMR (400 MHz, $CDCl_3$) δ: 6.92 (2H, d, ^3J = 9.3 Hz, C^3H), 6.83 (2H, d, ^3J = 9.3 Hz, C^2H), 4.73 (2H, s, C^5H).

$^{13}C\{^1H\}$ NMR (100 MHz, $CDCl_3$) δ: 151.6 (C^4), 150.8 (C^1), 117.0 (C^3), 116.4 (C^2), 115.4 (C^6), 55.1 (C^5).

HRMS (ESI): *m/z*: 167.0815 $[M+NH_4]^+$, $C_8H_{11}N_2O_2$ requires 167.0821.

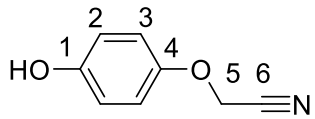

The obtained data is consistent with literature values.

2.14 2-(4-(2-Allyloxy)ethoxy)phenoxy)acetonitrile[1]

To a solution of bis-tosylate tetraethylene glycol **2.13** (8.49 g, 16.9 mmol), dissolved in dry MeCN (25 mL), K_2CO_3 (11.7 g, 84.8 mmol) and a solution of compound **2.12** (5.05 g, 33.2 mmol) dissolved in MeCN (25 mL) were added. The reaction mixture was heated to reflux for 48 h under an Ar atmosphere, then cooled to RT. The reaction mixture was filtered under suction and the solvent removed *in vacuo* to leave a sticky brown solid. The solid was dissolved in $CHCl_3$ (100 mL), dried over $MgSO_4$ and the solvent removed *in vacuo*, then recrystallized (toluene/hexane) to yield the product, a white oily solid (3.19 g, 41%).

^{1}H NMR (400 MHz, $CDCl_3$) δ: 6.89-6.96 (8H, m, $C^{4,5}H$), 4.73 (4H, s, C^2H), 4.86 (8H, t, ^3J = 4.9 Hz, $C^{7,8}H$), 3.72 (8H, m, $C^{9,10}H$).

$^{13}C\{^1H\}$ NMR (100 MHz, $CDCl_3$) δ: 154.9 (C^3), 150.8 (C^6), 116.7, 115.8 ($C^{4,5}$), 115.4 (C^1), 70.8, 70.7, 69.8, 68.0 (4 × CH_2O), 54.9 (C^2).

HRMS (ESI): *m/z*: 457.1975 $[M+H]^+$, $C_{24}H_{29}N_2O_7$ requires 457.1975.

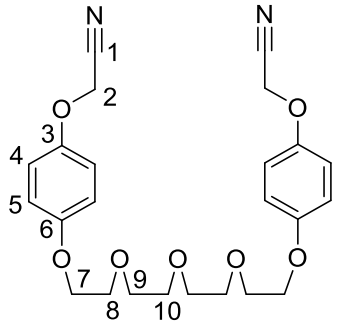

The obtained data is consistent with literature values.

2.15 4-(2-Hydroxyethoxy)phenol[3]

To a solution of (4-hydroxyphenoxy) acetic acid (2.50 g, 14.9 mmol) in dry THF (10 mL), BH_3·THF (1 mol dm^{-3}, 37 mL, 37 mmol) was added dropwise. The reaction mixture was stirred for 16 h at RT under an Ar atmosphere. The resulting solution was quenched with MeOH and then

partitioned between EtOAc and water. The organic layer was then washed with brine (50 mL), dried over $MgSO_4$ and the solvent removed *in vacuo*, leaving a colourless oil, which on standing crystallised as a white solid. The product was then purified using column chromatography (silica, 50:50 EtOAc:petrol 40-60), to give the product as a white solid (1.76g, 77%).

Mp 90-91 ^oC

^{1}H NMR (400 MHz, d_6-DMSO) δ: 8.89 (s, 1H, C^1OH), 6.75 (d, 2H, ^3J = 9.1 Hz, C^2H)**,** 6.66 (d, 2H, ^3J = 9.1 Hz, C^3H), 4.81 (t, 1H, ^3J = 5.5 Hz, C^6OH) 3.86 (t, 2H, ^3J = 5.0 Hz, C^5H) 3.67 (q, 2H, ^3J = 5.0 Hz, C^6H)**.**

$^{13}C\{^1H\}$ NMR (100 MHz, d_6-DMSO), δ: 151.9 (C^2), 151.6 (C^3), 116.1 (C^1), 115.6 (C^4), 70.4 (C^5), 60.2 (C^6).

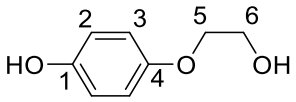

The obtained data is consistent with literature values.

2.16 (*p*-(2-Hydroxyethoxy)phenoxy)acetonitrile

Bromoacetonitrile (0.79 mL, 1.36 g, 12.1 mmol) was added to a solution of 4-(2-hydroxyethoxy) phenol **2.15** (1.70 g, 11.0 mmol) in dry MeCN (30 mL) and K_2CO_3 (1.67 g, 12.1 mmol) were added. The reaction mixture was heated to reflux for 16 h under Ar atmosphere. The brown reaction mixture was allowed to cool to RT, filtered under suction and the solvent removed *in vacuo.* The resulting solid was dissolved in CH_2Cl_2, (50 mL) and dried over $MgSO_4$. The solvent was then removed *in vacuo*, resulting in a brown oil. The oil was purified by column chromatography (silica, 99:1 CH_2Cl_2:MeOH), to yield the product, a brown oil (1.72 g, 87%).

^{1}H NMR (400 MHz, $CDCl_3$) δ: 6.92 (d, 4H, ^3J = 9.3 Hz, C^4H), 6.92 (d, 2H, ^3J = 9.3 Hz, C^5H), 4.71 (s, 2H, C^7H), 4.05 (t, 2H, ^3J = 4.6 Hz, C^2H), 3.95 (q, 2H, ^3J = 4.6 Hz, C^1H), 2.18 (s, br, 1H, C^1OH)**.**

^{13}C {^{1}H} NMR (100 MHz, $CDCl_3$), δ: 154.6 (C^6), 151.0 (C^3), 116.7 (C^4), 115.7 (C^5) 115.3 (C^8), 69.8 (C^2), 61.4 (C^1), 54.9 (C^7).

IR υ_{max}: 3403 (s, br, OH), 2932 (w, ArH), 2876 (w, CH_2), 1593, (w,), 1504 (s, Ar).

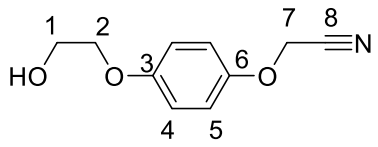

2.17 (*p*-(2-Hydroxyethoxy tosyl)phenoxy)acetonitrile

To a solution of (*p*-(2-hydroxyethoxy)phenoxy)acetonitrile **2.16** (1.67g, 9.30 mmol) in dry CH_2Cl_2 (35 mL) cooled to 0 ^{o}C, NEt_3 (1.95 mL, 1.41 g, 14.0 mmol), DMAP (cat.) and *p*-toluenesulfonyl chloride (1.95 g, 10.2 mmol) was added. The reaction was stirred for 16 hours at RT, under an Ar atmosphere. CH_2Cl_2 (25 ml) and water (25 mL) were added and then the solution was neutralised with $HCl_{(aq)}$ (1 M). The organic layer was separated, washed with water (2 × 25 mL), brine (2 × 25 mL), dried with $MgSO_4$ and the solvent was removed *in vacuo* to give the product as a brown oil (2.72 g, 84%)

^{1}H NMR (400 MHz, $CDCl_3$) δ: 7.81 (d, 2H, ^{3}J = 8.1 Hz, C^4H), 7.35 (d, 2H, ^{3}J = 8.1 Hz, C^3H), 6.90 (d, 2H, ^{3}J = 9.4 Hz, C^{10}H), 6.77 (d, 2H, ^{3}J = 9.4 Hz, C^9H), 4.70 (s, 2H, C^{12}H)**,** 4.35 (t, 2H, ^{3}J = 4.7 Hz, C^6H), 4.12 (t, 2H, ^{3}J = 4.7 Hz, C^7H), 2.45 (s, 3H, C^1H).

^{13}C{^{1}H} NMR (100 MHz, $CDCl_3$) δ: 154.0 (C^{11}), 151.2 (C^8), 145.0 (C^2), 132.9 (C^5), 129.9 (C^3), 128.0 (C^4), 116.7 (C^{10}), 115.9 (C^9), 115.3 (C^{13}), 68.1 (C^7), 66.1 (C^6), 54.8 (C^{12}), 22.7 (C^1).

IR υ_{max}: 2920 (w, ArH), 2961 (w, CH_2), 2887 (w, CH_3), 1597 (m, Ar), 1508 (s, Ar).

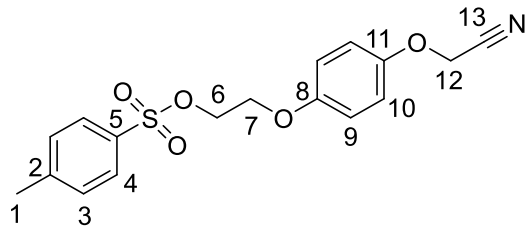

2.18 Polyether Macrocycle[4]

Pyridinium axle **2.19** (200 mg, 0.486 mmol) was dissolved in dry CH_2Cl_2 (20ml) to which bis amine **2.10** (226 mg, 0.486 mmol) was added and the mixture was stirred for 30 minutes, at RT under Ar. NEt_3 (123 mg, 0.17 mL, 1.22mmol) was added and then isophthaloyl chloride (118 mg, 0.582 mmol) in CH_2Cl_2 (10 mL) was added dropwise and the reaction was left for 1 h, at RT under Ar. The mixture was washed with 10% $HCl_{(aq)}$ (2 × 25 mL) and then water (1 × 25 mL). The organic layer was dried with $MgSO_4$ and the solvent removed *in vacuo* to yield a yellow solid. The yellow solid was purified by column chromatography (silica, 98:2 to 97:3 CH_2Cl_2:MeOH) to obtain a white solid, contaminated with small amounts of pyridinium axle **2.19**. The solid was washed with ice cold MeOH to yield the product as a white solid (46 mg, 16%).

R_f = 0.30 (98:2 CH_2Cl_2:MeOH)

^{1}H NMR (400 MHz, $CDCl_3$) δ: 7.97 (dd, 2H, ^3J = 7.7 Hz, ^4J = 1.5 Hz, C^2H), 7.90 (s, 1H, C^4H), 7.48 (t, 1H, ^3J = 7.7 Hz, C^1H), 6.66-6.75 (m, 10H, C^5NH, $C^{9,10}H$), 4.01 (t, 4H, ^3J = 9.6 Hz, C^7H), 3.96 (t, 4H, ^3J = 9.5 Hz, $C^{12}H$), 3.75-3.82 (m, 8H $C^{6,13}H$), 3.65-3.60 (8H, m, $C^{6,13}H$).

$^{13}C\{^1H\}$ NMR (100 MHz, $CDCl_3$) δ: 166.7 (C^5), 153.4, 152.6 ($C^{8,11}$), 134.6(C^5), 131.0 (C^2), 129.4 (C^1), 123.7 (C^4), 115.7, 115.4 ($C^{9/10}$), 70.8, 70.7 ($C^{14,15}$), 69.7 (C^{13}), 68.2 (C^7), 67.3 (C^{12}), 39.7 (C^6).

HRMS (ESI): *m/z*: 633.2190 $[M + K]^+$, $C_{32}H_{38}N_2O_9$ requires 633.2209.

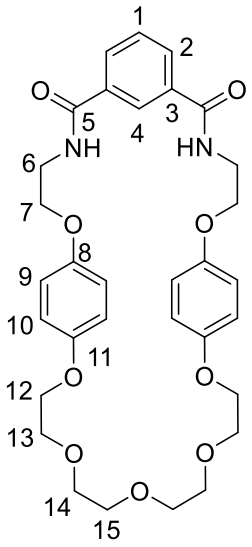

The data is consistent with literature values.

2.19 1-Methyl-(N^3, N^5-dihexyl)pyridium-3,5-dicarboxamide chloride[4]

To pyridine **2.20** (519 mg, 1.44 mmol) in $CHCl_3$ (8 mL) MeI (2 mL) was added and the solution was heated to 50 °C under Ar for 16 h. The $CHCl_3$ and excess MeI was removed *in vacuo*. The resulting solid was dissolved in CH_2Cl_2 (50 mL), washed with $NH_4Cl_{(aq)}$ (1 M, 8 × 50 mL) and then water (50 mL). The organic phase was collected and the solvent removed *in vacuo* to leave the product as a yellow solid (563 mg, 95%).

^{1}H NMR (400 MHz, $CDCl_3$) δ: 10.39 (1H, s, C^8H), 9.43 (2H, d, ^2J = 1.1 Hz, $C^{10}H$), 9.32 (2H, t, br, ^3J = 5.7 Hz, C^7NH), 4.57 (3H, s, $C^{11}H$), 3.42 (4H, td, ^3J = 7.4 Hz, ^3J = 5.7 Hz, C^6H), 1.67 (4H, quin, ^3J = 7.4 Hz, C^5H), 1.21-1.41 (12H, m, $C^{2,3,4}H$), 0.87 (6, t, ^3J = 7.3 Hz, C^1H).

^{13}C{^{1}H} NMR (100 MHz, $CDCl_3$) δ: 160.3 (C^7), 146.2 (C^{10}), 142.2 (C^8), 134.5 (C^9), 49.3 (C^{11}), 40.9 (C^6), 31.5 (1 xCH_2), 29.0 (C^5), 26.8, 22.6 (2 × CH_2), 14.1 (C^1).

HRMS (ESI): *m/z*: 348.2648 $[M]^+$, $C_{20}H_{34}N_3O_2$ requires 348.2646.

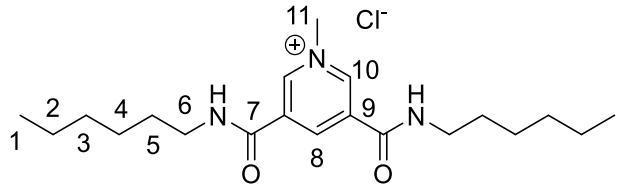

The data is consistent with literature values

2.20 N^3, N^5-Dihexylpyridine-3, 5-dicarboxamide[4]

3,5-Pyridine dicarboxylic acid (300 mg, 1.80 mmol) was dissolved in $SOCl_2$ (5 mL), DMF (cat.) was added and the solution was heated to reflux for 1 h (using a condenser fitted with a $CaCl_2$ drying tube). The excess $SOCl_2$ was removed *in vacuo* to leave a yellow solid. The bis-acyl chloride was dissolved in dry CH_2Cl_2 (25 mL) and NEt_3 (450 mg, 0.63 mL, 4.49 mmol) and hexylamine (400 mg, 0.53 mL, 3.95 mmol) were added, the reaction was stirred for 1h at RT, under an Ar atmosphere.

The mixture was washed with $HCl_{(aq)}$ (1 M, 50 mL), NaOH (1 M, 50 mL) and water (25 mL), the organic layer was dried with $MgSO_4$ and the solvent was removed *in vacuo* to leave the product as a white solid (537 mg 85%).

^{1}H NMR (400 MHz, $CDCl_3$) δ: 9.14 (2H, d, ^4J = 2.1 Hz, $C^{10}H$), 8.54 (1H, t, ^4J = 2.1 Hz, C^8H), 6.69 (2H, t, br, ^3J = 5.7 Hz, C^7NH), 3.50 (4H, td, ^3J = 7.2 Hz, ^3J = 5.7 Hz, C^6H), 1.66 (4H, quin, ^3J = 7.2 Hz, C^5H), 1.32-1.45 (12H, m, $C^{4,3,2}H$), 0.92 (6H, t, ^3J = 7.0 Hz, C^1H).

$^{13}C\{^1H\}$ NMR (100 MHz, $CDCl_3$) δ: 164.5 (C^7), 149.8 (C^{10}), 134.0 (C^8), 130.4 (C^9), 40.4 (C^6), 31.5 (1 × CH_2), 29.5 (C^5), 26.7, 22.6 (2 × CH_2), 14.0 (C^1).

HRMS (ESI): *m/z*: 356.2313 $[M+Na]^+$, $C_{19}H_{31}N_3O_2$ requires 356.2313.

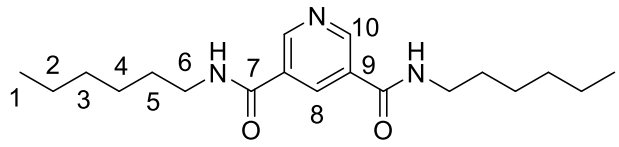

The data is consistent with literature values.

2.21 1-Methyl-(*N*^{3},*N*^{5}-((Bis(4-*tert*-butylphenyl)(phenyl)methyl)phenyl-glycine)pyridium-3,5-dicarboxamide chloride[5]

Pyridine axle **2.29** (96 mg, 0.084 mmol) was dissolved in MeI (5 mL) and heated to reflux for 16h. The excess MeI was removed *in vacuo* to yield the methylated iodide salt a yellow solid. The solid was dissolved in CH_2Cl_2 (50 mL) and washed with $NH_4Cl_{(aq)}$ (1 M, 8 × 50 mL) and the organic phase was dried with $MgSO_4$. The solvent was removed by a stream of compressed air to yield the product as yellow solid. (63 mg, 62%)

Mp: >230 °C, (dec.)

^{1}H NMR (400 MHz, 1:1 $CDCl_3$:CD_3OD) δ: 9.51 (1H, s, $C^{20}H$), 9.48 (2H, s, $C^{21}H$), 7.45 (d, 4H, ^3J = 8.8 Hz, $C^{13}H$), 7.14-7.27 (20H, m, ArH), 7.10 (8H, d, ^3J = 8.7 Hz ArH), 4.48 (3H, s, $C^{22}H$), 4.28 (4H, s, $C^{17}H$), 1.30 (36H, s, C^1H).

$^{13}C\{^{1}H\}$ NMR (100 MHz, 1:1 $CDCl_3$:CD_3OD) δ: 167.2 (C^{16}), 161.8 (C^{18}), 148.4, 147.1 (2 × ArC), 146.9 (C^{21}), 143.7, 143.4 (2 × ArC), 141.8 (C^{20}), 135.5 (ArC), 134.0 (C^{19}), 131.5, 131.0, 130.6, 127.2, 125.7, 124.1 (5 × ArC), 118.9 (C^{14}), 63.7 (C^{11}), 48.7 (C^{27}), 43.5 (C^{17}), 34.1 (C^{2}), 31.0 (C^{1}).

IR υ_{max}: 3257 (m, br, CONH), 3056 (w, N^+CH_3) 2958 (m, CH_3), 2903 (w, CH_2), 2860 (w, CH), 1670 (s, CON), 1600 (m, Ar), 1506 (m, Ar).

LRMS (ESI): *m/*z: 1154.7 $[M\text{-}Cl^-]^+$, $C_{78}H_{84}N_5O_4$ requires 1154.7

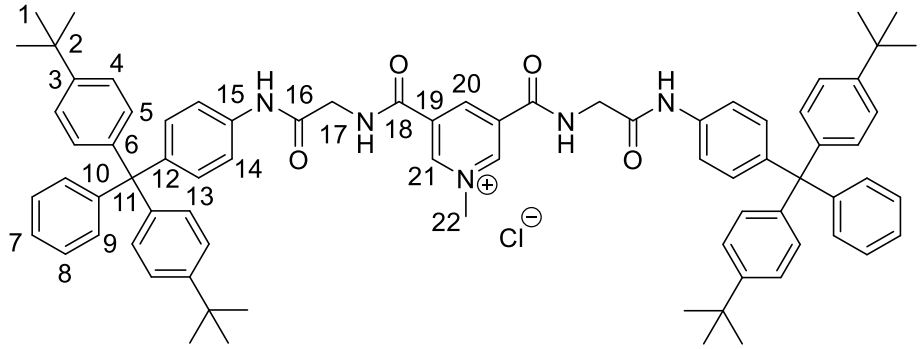

The obtained data is consistent with literature values.

2.21-PF_6 1-Methyl-(*N^3,N^5*-((Bis(4-*tert*-butylphenyl)(phenyl)methyl)phenyl-L-alanine)pyridium-3,5-dicarboxamide hexafluorophosphate

Rotaxane **2.21** (22 mg, 0.0109 mmol) in CH_2Cl_2 was washed with 0.1 mol dm^{-3} NH_4PF_6 (8 × 10 mL) then water (2 × 10 mL). The solvent was removed *in vacuo* to afford a yellow solid (16 mg, 70 %).

^{1}H NMR (400 MHz, 1:1 $CDCl_3$:MeOD) δ: 9.06 (d, 1H, $C^{25}H$), 9.01 (d, 2H, $C^{26}H$), 6.83-7.18 (m, 44H, ArH), 4.81 (t, 2H, $C^{17}H$), 4.12-4.21 (m, 3H, $C^{27}H$), 3.11 (dd, 2H, $C^{18}H$), 2.96 (dd, 2H, $C^{18'}H$), 1.12 (s, 36H, $C^{1}H$).

^{13}C NMR (100 MHz, 1:1 $CDCl_3$:MeOD) δ: 169.7 (C^{16}), 161.0 (C^{23}), 148.7 (C^{3}), 147.0 (C^{26}), 146.7, 143.7, 143.7 (3 × ArC), 141.7 (C^{25}), 136.1, 135.1 (2 × ArC), 134.0 (C^{23}), 131.5, 131.0, 130.6, 129.1, 128.3, 127.2, 127.0, 125.7, 124.1 (9 × ArC), 119.1 (C^{14}), 63.7 (C^{11}), 56.4 (C^{17}), 48.9 (C^{29}), 38.0 (C^{18}), 34.1 (C^{2}), 31.0 (C^{1}).

^{19}F NMR (376 MHz, 1:1 $CDCl_3$:MeOD) δ: -73.7 (d, ^1J = 710 Hz, PF_6^-)

^{31}P NMR (162 MHz, 1:1 $CDCl_3$:MeOD) δ: -144.7 (sept, ^1J = 710 Hz, PF_6^-)

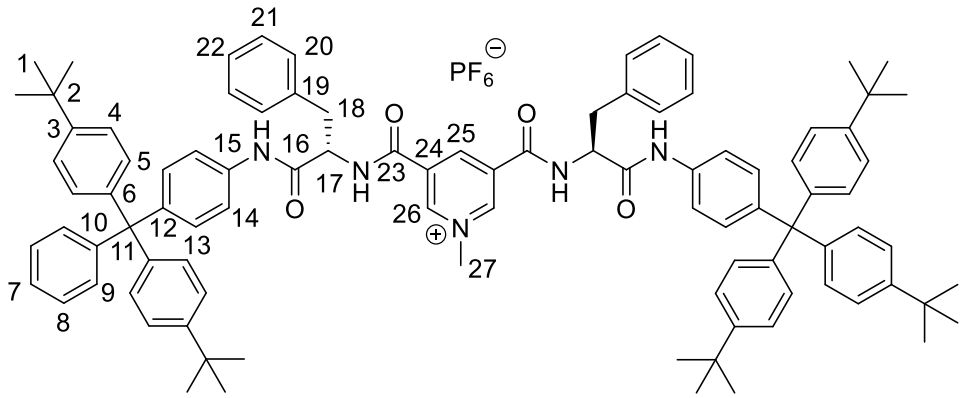

2.22 1-Methyl-(N^3,N^5-((Bis(4-*tert*-butylphenyl)(phenyl)methyl)phenyl-L-alanine)pyridium-3,5-dicarboxamide chloride

Pyridine axle **2.35** (395 mg, 0.34 mmol) was dissolved in MeI (5 mL) and heated to reflux for 16h. The excess MeI was removed *in vacuo* to yield the methylated iodide salt a yellow solid. The solid was dissolved in CH_2Cl_2 (50 mL) and washed with $NH_4Cl_{(aq)}$ (1 M, 8 × 50 mL) and water (25 mL). The organic phase was dried with $MgSO_4$ and the solvent was removed by a stream of compressed air to yield the product as a yellow solid. (378 mg, 92%)

Mp: >230 °C (dec.)

^{1}H NMR 400 MHz, d_6-DMSO) δ: 10.27 (2H, s, C^{19}NH), 9.57 (2H, s, C^{22}H), 9.49 (1H, s, C^{19}NH), 9.46 (2H, s, C^{21}H), 7.53 (4H, d, ^3J = 8.8 Hz, C^{14}H), 7.04-7.34 (26H, m, ArH), 4.68 (2H, m, ^3J = 7.0 Hz, C^{17}H), 4.44 (3H, s, C^{23}H), 1.48 (6H, d, ^3J = 7.1 Hz, C^{18}H), 1.26 (36H, s, C^{22}H).

^{13}C{^{1}H} NMR (100 MHz, d_6-DMSO) δ: 170.9(C^{19}), 161.5(C^{16}), 150.4 (C^{20}), 147.3 (C^{21}), 142.3 (C^{22}), 148.3., 144.1, 137.0, 133.0, 131.2, 130.8, 130.5, 128.1, 124.9, 119.0, (10 × ArC), 63.7 (C^{11}), 51.9 (C^{17}), 47.4 (C^{23}), 34.5 (C^2), 31.6 (C^1), 18.3 (C^{18}). (2 × ArC missing - coincidental)

IR υ_{max}: 3314 (m, br, CONH), 2960 (m, CH_3), 29110 (w, CH_2), 2868 (w, CH), 1664 (s, CON), 1601 (m, Ar), 1506 (m, Ar).

HRMS (ESI): *m/z*: 1182.6786 $[M]^+$, $C_{80}H_{88}N_5O_4$a requires 1182.6831.

$[\alpha]_D^{25}$: +41.0 (10 mg ml^{-1}, $CHCl_3$)

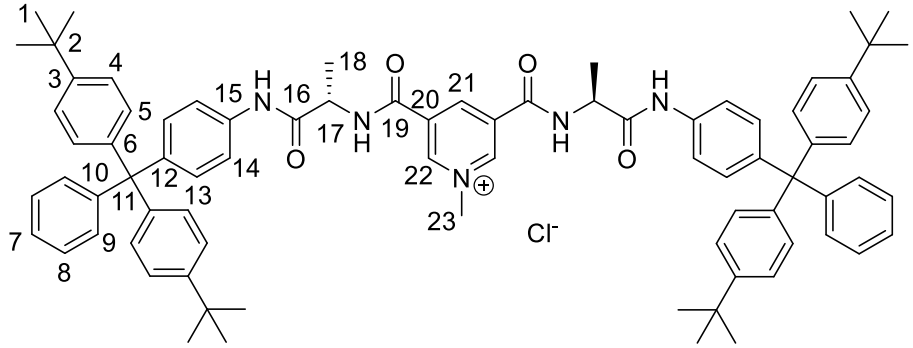

2.24 1-Methyl-(N^3,N^5-((Bis(4-*tert*-butylphenyl)(phenyl)methyl)phenyl-L-alanine)pyridium-3,5-dicarboxamide chloride

Pyridine axle **2.36** (681 mg, 0.52 mmol) was dissolved in $CHCl_3$ (8 mL) and MeI (4 mL), then heated to reflux for 16h. The excess MeI was removed *in vacuo* to yield the methylated iodide salt a yellow solid. The solid was dissolved in $CHCl_3$ (50 mL) and washed with $NH_4Cl_{(aq)}$ (1 M, 8 × 50 mL) and water (25 mL). The organic phase was dried with $MgSO_4$ and the solvent was removed by a stream of compressed air to yield the product as a yellow solid. (703 mg, 99%)

Mp: >230 °C C(dec.)

^{1}H NMR (400 MHz, 1:1 $CDCl_3$:MeOD) δ: 9.34 (d, 2H, ^3J = 9.5 Hz, $C^{26}H$), 9.30 (d, 1H, ^3J = 9.5 Hz, $C^{25}H$), 7.39 (dd, 4H, ^3J = 8.8 Hz, ^4J = 4.8 Hz, $C^{14}H$), 7.38 (d, ^3J = 7.2 Hz, 4H, ArH), 7.12-7.26 (m, 28H, ArH), 7.08 (d, 8H , ^3J = 8.7 Hz, ArH), 4.97 (ddd, 2H, ^3J = 8.4 Hz, ^3J = 6.4 Hz, ^4J = 2.2 Hz, $C^{17}H$), 4.37-4.41 (m, 4H, $C^{27}H$), 3.29-3.35 (m, 2H, $C^{18}H$, CD_3OH), 3.18 (dd, 2H, ^2J = 13.8 Hz, ^3J = 8.8 Hz, $C^{18'}H$), 1.29 (s, 36H, C^1H).

^{13}C{^{1}H} NMR (100 MHz, 1:1 $CDCl_3$:MeOD) δ: 167.9 (C^{16}), 161.0 (C^{23}), 148.4 (C^3), 147.0 (ArC), 146.7 (C^{26}), 143.7 (ArC), 141.9 (C^{25}), 136.4 (C^{19}), 135.3 (ArC), 133.9 (C^{24}), 131.5, 130.9, 130.6, 129.1, 128.4, 127.2, 126.9, 125.7, 124.1 (9 × ArC), 119.0 (C^{14}), 63.7 (C^{11}), 55.7 (C^{17}), 38.0 (C^{18}), 34.1 (C^2), 31.0 (C^1).

IR υ_{max}:3282 (m, CONH), 3054 (m, CONH), 3032 (w, ArH), 2904 (m, CH_3/CH_2), 2958 (m, CH_3/CH_2), 2868 (m, CH_3/CH_2), 1653 (s, CONH), 1597 (s, py), 1508 (s, Ar).

HRMS (ESI): *m/z*: 1334.7451 $[M]^+$ $C_{92}H_{96}N_5O_4$ requires 1334.7457.

$[\alpha]_D^{25}$: +19.5 (10 mg ml^{-1}, $CHCl_3$)

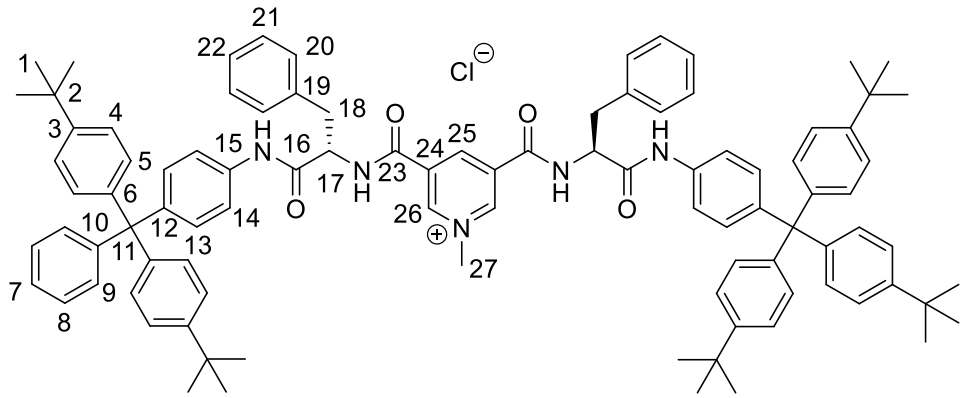

2.25 4-(Bis(4-*tert*-butylphenyl)(phenyl)methyl)aniline[6]

Alcohol **2.26** (5.00 g, 13.4 mmol) was dissolved in excess acetyl chloride (25 mL) and heated to reflux (using a condenser fitted with a $CaCl_2$ drying tube) for 16 h. Excess acetyl chloride was removed *in vacuo*, to leave a white solid. Aniline (25 mL) was added and the mixture was heated to reflux for 48 h, under an Ar atmosphere, resulting in a purple solution. The reaction mixture was allowed to cool and then poured onto 10% $HCl_{(aq)}$ (300 mL), after being stirred for 20 minutes the resulting purple precipitate was collected by vacuum filtration. The precipitate was washed with saturated K_2CO_3 (50 mL) and H_2O (2 × 50 mL), then dissolved in CH_2Cl_2, dried over $MgSO_4$ and eluted through a plug of silica to give a pale yellow solution. The solvent was removed *in vacuo*, to give a brown oil, which was recrystallized (toluene/hexane) to yield the product as an orange solid (2.92 g, 45 %).

Mp: 181-183 °C

^{1}H NMR (400 MHz, $CDCl_3$) δ: 7.04-7.26 (13H, m, ArH), 6.96 (2H, d, ^3J = 8.8 Hz, $C^{13}H$) 6.56 (2H, d, ^3J = 8.8 Hz, $C^{14}H$), 1.29 (18H, s, C^1H).

$^{13}C\{^{1}H\}$ NMR (100 MHz, $CDCl_3$) δ: 148.3, 147.6, 144.2, 143.9, 137.5, 132.1, 131.2, 130.7, 127.2, 125.6, 124.1, 114.1 (12 × ArC), 63.4 (C^{11}), 34.4 (C^{2}), 31.4 (C^{1}).

HRMS (ESI): *m/z*: 448.2984 $[M+H]^+$, $C_{33}H_{38}N$ requires 448.2999.

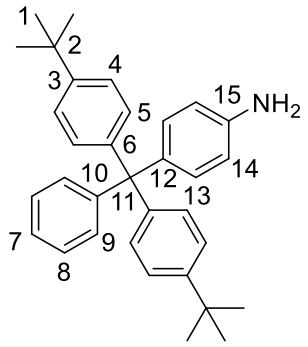

The obtained data is consistent with literature values.

2.26 Bis(4-tert-butylphenyl)(phenyl)methanol[6]

Under an Ar atmosphere, magnesium turnings (2.00 g, 82.3 mmol) were covered with dry THF (25 mL) and I_2 (cat.) was added. 1-Bromo-4-*tert*-butylbenzene (14.4 g, 11.7 mL, 67.5 mmol) in dry THF (25 mL) was added dropwise over 15 minutes, then heated until effervescence was observed, upon which the heating was removed and the reaction left to stir for 2 h at RT. Methyl benzoate (4.08 g, 3.75 mL, 32.9 mmol) dissolved in dry THF (10 mL) was then added dropwise and the reaction was then left stirring for a further 16 h, at RT under Ar. The reaction mixture was carefully neutralised with 10% $HCl_{(aq)}$ and then extracted with petrol 40-60 (3 × 100 mL). The combined organic layers were washed with H_2O (3 × 100 mL) and dried over $MgSO_4$. The solvent was removed *in vacuo* to give a yellow waxy solid, which was recrystallized from MeOH to give the product, as a white powder (10.2 g, 83%).

Mp: 110-111 °C

^{1}H NMR (400 MHz, $CDCl_3$) δ: 7.05- 7.55 (13H, m, ArH), 1.30 (18H, s, $C^{1}H$).

$^{13}C\{^{1}H\}$ NMR (100 MHz, $CDCl_3$) δ: 149.6, 144.8, 140.8, 128.5, 128.2, 127.2, 126.7, 124.6 (8 × ArC), 83.1 (C^{11}), 34.38 (C^{2}), 31.39 (C^{1}).

HRMS (ESI): *m/z*: 355.2403 $[M\text{-}OH]^+$, $C_{27}H_{31}$ requires 355.2426.

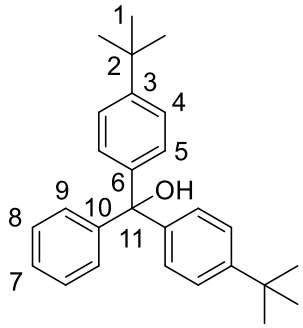

The obtained data is consistent with literature values.

2.27 *N*-Boc-(Bis(4-*tert*-butylphenyl)(phenyl)methyl)phenyl-glycine[5]

N-Boc-glycine (0.240 g, 1.40 mmol) was dissolved in dry MeCN (50 mL), to which DCC (0.35 g, 1.7 mmol) and *N*-hydroxysuccinimide (0.200 g, 1.70 mmol) were added. The reaction was stirred for 16 h at RT, under an Ar atmosphere. The reaction mixture was filtered by gravity and the solvent removed *in vacuo*, to leave a white solid. The white solid was dissolved in CH_2Cl_2 (50 mL), to which NEt_3 (0.18 g, 0.24 mL, 1.75 mmol) and amine **2.25** (0.50 g, 1.12 mmol) were added. The reaction was stirred for 24 h at RT, under an Ar atmosphere. The solution was washed with $HCl_{(aq)}$ (1 M, 2 × 25 mL) and H_2O (2 × 25 mL), then the organic layer dried over $MgSO_4$ and the solvent removed *in vacuo* to leave a foamy white solid. The white solid was purified by column chromatography (silica, 199:1 CH_2Cl_2:MeOH), with the product being isolated, as a foaming white solid (0.54 g, 79%).

Mp: 132-134 °C

^{1}H NMR (400 MHz, $CDCl_3$) δ: 8.03 (s, br, 1H, $C^{16}NH$), 7.24 (d, 2H, ^3J = 8.7 Hz, $C^{14}H$), 7.06-7.24 (m, 15H, ArH), 5.18 (s, br, 1H, $C^{18}NH$), 3.89 (d, 2H, ^3J = 6.0 Hz, $C^{17}H$), 1.47 (s, 9H, $C^{20}H$), 1.29 (s, 18H, C^1H).

$^{13}C\{^1H\}$ NMR (100 MHz, $CDCl_3$) δ: 167.6 (C^{16}), 148.5 (C^{18}), 147.1, 143.6, 135.0, 131.8, 131.1, 130.8, 130.7, 127.3, 125.8, 124.2, 118.8 (12 × ArC), 63.8 (C^{11}), 45.7 (C^{17}), 34.3 (C^2), 31.4 (C^1), 28.3 (C^{20}).

IR υ_{max}: 3310 (m, br, CONH), 2961 (m, CH_3), 2904 (w, CH_2), 2866 (w, CH), 1675 (s, CON), 1601 (m, Ar), 1506 (s, Ar).

HRMS (ESI): *m/z*: 605.3739 $[M+H]^+$, $C_{40}H_{49}N_2O_3$ requires 605.3743.

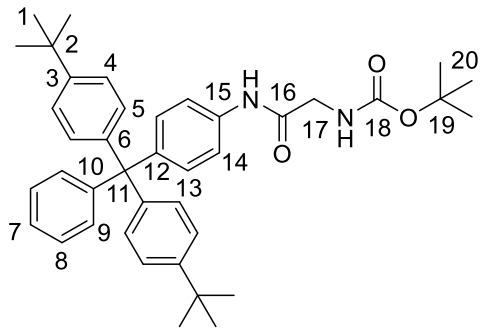

The obtained data is consistent with literature values.

2.28 *N*-(Bis(4-*tert*-butylphenyl)(phenyl)methyl)phenyl-glycine[5]

Boc protected amine **2.27** (0.26 g, 0.43 mmol) was dissolved in CH_2Cl_2 (10 mL) to which TFA (1 mL) was added, the reaction was stirred for 16 h at RT. 10% NaOH was added until the mixture reached pH 10. The mixture was further diluted with CH_2Cl_2 (10 mL), washed with water (2 × 25 mL), the organic layer was dried with K_2CO_3 and the solvent removed *in vacuo* to leave the product, a white foamy solid (0.21 g, 95%).

Mp: 128-129 °C

^{1}H NMR (400 MHz, $CDCl_3$) δ: 9.39 (s, br, 1H, $C^{16}NH$), 7.46 (d, 2H, $C^{14}H$), 7.08-7.35 (15H, m, ArH), 3.46 (2H, s, $C^{17}NH$), 1.57 (2H, s, $C^{17}H$), 1.30 (18H, s, $C^{20}H$).

^{13}C{^{1}H} NMR (100 MHz, $CDCl_3$) δ: 170.6 (C^{16}), 147.2, 143.7, 143.1, 135.2, 131.8, 131.2, 130.7, 130.7, 127.3, 125.7, 124.2 (11 × ArC), 118.3 (C^{14}), 63.8 (C^{11}), 45.1 (C^{17}), 34.3 (C^2), 31.4 (C^1).

IR υ_{max}: 3289 (m, br, CONH), 2958 (m, CH_3), 2903 (w, CH_2), 2868 (w, CH), 1675 (s, CON), 1597 (m, Ar), 1508 (s, Ar).

HRMS (ESI): *m/z*: 505.3197 $[M+H]^+$, $C_{35}H_{41}N_2O$ requires 505.3219.

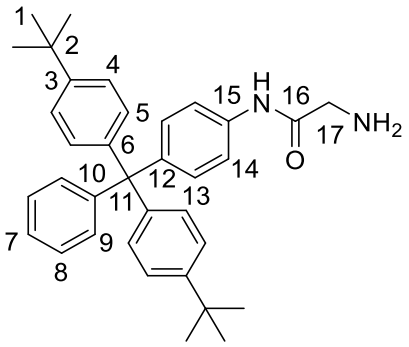

The obtained data is consistent with literature values.

2.29 N^3,N^5-((Bis(4-*tert*-butylphenyl)(phenyl)methyl)phenyl-glycine)pyridine-3,5-dicarboxamide[5]

3,5-Pyridine dicarboxylic acid (34 mg, 0.20 mmol) was dissolved in $SOCl_2$ (5 mL), DMF (cat.) was added and the solution was heated to reflux for 16 h (using a condenser fitted with a $CaCl_2$ drying tube). The excess $SOCl_2$ was removed *in vacuo* to leave a yellow solid. The bis-acyl chloride was dissolved in dry CH_2Cl_2 (25 mL), NEt_3 (66 mg, 0.1 mL, 0.654 mmol) and amine **2.27** (220 mg, 0.436 mmol) were added, the reaction was stirred for 16 h at RT, under an Ar atmosphere. The mixture was diluted with CH_2Cl_2 (25 mL) and washed with $HCl_{(aq)}$ (1 M, 50 mL) and NaOH (1 M, 50 mL), the organic layer was dried with $MgSO_4$ and the solvent was removed *in vacuo* to leave a yellow solid. The solid was purified by column chromatography (silica, 97:3 CH_2Cl_2:MeOH), to yield the product, a yellow solid (117 mg, 52%).

^{1}H NMR (400 MHz, $CDCl_3$) δ: 9.05 (2H, s, $C^{21}H$), 8.88 (s, br, 2H, CNH), 8.73 (1H, s, $C^{20}H$), 8.37 (s, br, 2H, CNH), 7.06-7.16 (34H, m, ArH), 4.10 (4H, d, ^3J = 4.6 Hz, $C^{17}H$), 1.27 (36H, s, C^1H).

^{13}C{^{1}H} NMR (100 MHz, $CDCl_3$) δ: 168.2 (C^{16}), 163.1 (C^{18}), 151.3 (C^3) 148.5, 145.3, 143.9, 143.6, 131.8, 131.1, 130.6, 127.4, 125.3, 124.3, 123.9, 118.8 (12 × ArC), 63.8 (C^{11}), 45.1 (C^{17}), 34.3 (C^2), 31.4 (C^1).

IR υ_{max}: 3278 (m, br, CONH), 2961 (m, CH_3), 2903 (w, CH_2), 2865 (w, CH), 1653 (s, CON), 1599 (m, Ar), 1506 (m, Ar).

LRMS (ESI): *m/z*: 1140.6 $[M+H]^+$, $C_{77}H_{82}N_5O_4$ requires 1140.6.

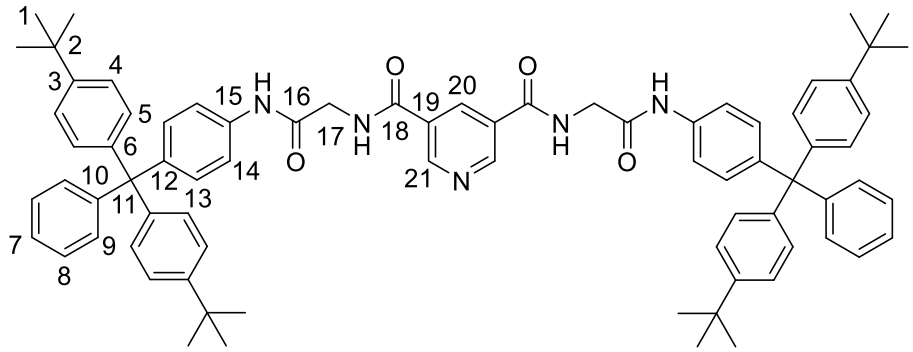

The obtained data is consistent with literature values.

2.30 *N*-Boc-(Bis(4-*tert*-butylphenyl)(phenyl)methyl)phenyl-L-alanine

N-Boc-L-alanine (0.76g, 4.01 mmol) was dissolved in dry MeCN (30 mL), to which DCC (1.15 g, 5.60 mmol) and *N*-hydroxysuccinimide (0.65 g, 5.60 mmol) were added. The reaction was stirred for 16 h at RT, under an Ar atmosphere. The reaction mixture was filtered by gravity and the solvent removed *in vacuo*, to leave a white solid. The white solid was dissolved in CH_2Cl_2 (30 mL), to which NEt_3 (0.51 g, 0.70 mL, 5.00 mmol) and amine **9** (1.22 g, 2.73 mmol) were added. The reaction was stirred for 24 h at RT, under an Ar atmosphere. The solution was washed with $HCl_{(aq)}$ (1 M, 2 × 25 mL) and H_2O (2 × 25 mL), then the organic layer dried over $MgSO_4$ and the solvent removed *in vacuo* to leave a foamy white solid. The white solid was purified by column chromatography (silica, 9:1 petrol 40-60:EtOAc), with the product being isolated, as a foaming white solid (1.10g, 67%).

R_f = 0.11 (9:1 petrol 40-60:EtOAc)

Mp: 128-129 ^oC

^{1}H NMR (400 MHz, $CDCl_3$) δ: 7.08-7.43 (17H, m, ArH), 1.48 (9H, s, $C^{21}H$), 1.44 (3H, d, ^3J = 7.1 Hz, $C^{18}H$), 1.42 (1H, q, ^3J = 7.1 Hz, $C^{17}H$), 1.32 (18H, s, C^1H).

$^{13}C\{^{1}H\}$ NMR (100 MHz, $CDCl_3$) δ: 170.6 (C^{16}), 148.5 (C^{19}), 147.1, 143.7, 143.3, 140.0, 135.4, 131.8, 131.1, 130.7, 121.7, 125.8, 124.2, 118.7 (12 × ArC), 63.8 (C^{11}), 50.8 (C^{17}), 34.3 (C^{2}), 31.4 (C^{1}), 31.2 (C^{20}), 17.5 (C^{18}).

IR υ_{max}: 3316 (m, br, CONH), 2963 (m, CH_3), 2903 (w, CH_2), 2870 (w, CH), 1672 (s, CON), 1601 (m, Ar), 1506 (s, Ar).

HRMS (ESI): *m/z*: 641.3686 $[M+Na]^+$, $C_{36}H_{43}N_2ONa$ requires 641.3714.

$[\alpha]_D^{25}$: -12.0 (10 mg ml^{-1}, $CHCl_3$)

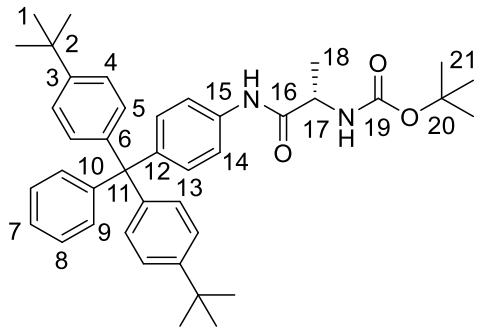

2.31 *N*-Boc-(Bis(4-*tert*-butylphenyl)(phenyl)methyl)phenyl-L-valine

N-Boc-L-valine (0.610 g, 2.8 mmol) was dissolved in dry MeCN (50 mL), to which DCC (0.70 g, 3.40 mmol) and N-hydroxysuccinimide (0.400 g, 3.40 mmol) were added. The reaction was stirred for 16 h at RT, under an Ar atmosphere. The reaction mixture was filtered by gravity and the solvent removed *in vacuo*, to leave a white solid. The white solid was dissolved in CH_2Cl_2 (50 mL), to which NEt_3 (0.36 g, 0.48 mL, 3.50 mmol) and amine **2.25** (1.00 g, 2.24 mmol) were added. The reaction was stirred for 24 h at RT, under an Ar atmosphere. The solution was washed with $HCl_{(aq)}$ (1 M, 2 × 25 mL) and H_2O (2 × 25 mL), then the organic layer dried over $MgSO_4$ and the solvent removed *in vacuo* to leave a foamy white solid. The white solid was purified by column chromatography (silica, CH_2Cl_2), to leave the product, a foamy white solid (144 mg, 11%).

Mp: 136-138 ^{o}C

^{1}H NMR (400 MHz, $CDCl_3$) δ: 8.04 (1H, br s, $C^{16}NH$), 7.31 (2H, dt, ^{3}J = 8.8 Hz, ^{4}J = 2 Hz, $C^{14}H$), 6.98-7.17 (15H, m, ArH), 5.13 (1H, d, ^{3}J = 8.6 Hz, $C^{20}NH$), 3.93 (1H, dd, ^{3}J = 8.6 Hz, ^{3}J = 6.6 Hz, $C^{17}H$), 2.15 (1H, m, $C^{18}H$), 1.36 (9H, s, ^{3}J = 8.8 Hz, $C^{22}H$), 1.21 (18H, s, $C^{1}H$), 0.93 (3H, d, ^{3}J = 6.9 Hz, $C^{19}H$), 0.89 (3H, d, ^{3}J = 6.9 Hz, $C^{19'}H$).

$^{13}C\{^{1}H\}$ NMR (100 MHz, $CDCl_3$) δ: 170.14 (C^{16}), 156.2 (C^{20}), 148.5, 147.1, 143.7, 143.55, 135.2, 131.7, 131.1, 130.68, 127.3, 127.8, 124.3, 118.9 (12 × ArC), 63.8 (C^{11}), 61.0 (C^{17}), 34.3 (C^{2}), 31.4 (C^{1}), 31.2 (C^{21}), 29.7 (C^{22}) 28.3 (C^{18}), 19.5 (C^{19}).

IR υ_{max}: 3315 (m, br, CONH), 2961 (m, CH_3), 2904 (w, CH_2), 2870 (w, CH), 1664 (s, CON), 11600 (m, Ar), 1504 (s, Ar).

HRMS (ESI): *m/z*: 647.4201 $[M+H]^+$, $C_{43}H_{55}N_2O_3$ requires 647.4213.

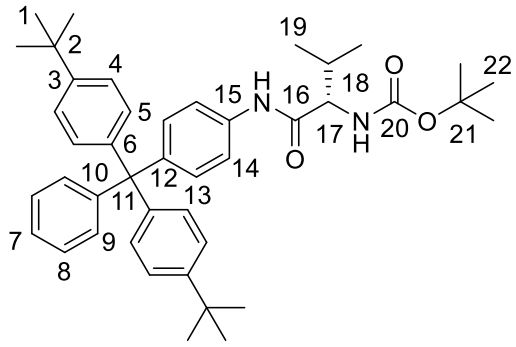

2.32 *N*-Boc-(Bis(4-*tert*-butylphenyl)(phenyl)methyl)phenyl-L-phenylalanine

N-Boc-L-phenylalanine (0.45 g, 1.68 mmol) was dissolved in dry MeCN (10 mL), to which DCC (0.49 g, 2.35 mmol) and *N*-hydroxysuccinimide (0.27 g, 2.35 mmol) were added. The reaction was stirred for 1 h at RT, under an Ar atmosphere. The precipitate was removed by gravity filtration and the solvent of the filtrate removed *in vacuo*, to leave a white solid. The white solid was dissolved in CH_2Cl_2 (10 mL), to which NEt_3 (0.24 g, 0.33 mL, 2.35 mmol) and amine **2.25** (0.50 g, 1.12 mmol) were added. The reaction was stirred for 72 h at RT, under an Ar atmosphere. CH_2Cl_2 (25 mL) was added to the solution, which was then washed with $HCl_{(aq)}$ (1 M, 2 × 25 mL) and H_2O (2 × 25 mL). The organic layer dried over $MgSO_4$ and the solvent removed *in vacuo* to

leave a foamy white solid. The white solid was purified by column chromatography (silica, 96:4 CH_2Cl_2:EtOAc), with the product being isolated, as a foaming white solid (0.50 g, 64%).

R_f = 0.32 (96:4 CH_2Cl_2:EtOAc)

Mp: 125-127 °C

^{1}H NMR (400 MHz, $CDCl_3$) δ: 7.68 (1H, s, C^{16}NH), 7.07-7.35 (22 H, m, ArH), 4.45 (1H, d, ^3J = 7.0 Hz, C^{17}H), 3.16 (2H, d, ^3J = 7.0 Hz, C^{18}H), 1.44 (9H, s, C^{25}H), 1.32 (18H, s, C^1H).

^{13}C{^{1}H} NMR (100 MHz, $CDCl_3$) δ: 169.4 (C^{16}), 151.6 (C^{23}), 148.5, 147.1, 143.6, 136.7, 134.8, 131.7, 131.1 130.7, 129.3, 128.8, 127.3, 127.1, 125.8, 124.2, 119.0 (16 × ArC, 1 missing coincidental) 80.3 (C^{24}), 63.7 (C^{11}), 56.7 (C^{17}), 38.3 (C^{18}), 34.3 (C^2), 31.4 (C^1), 28.3 (C^{25}).

IR υ_{max}: 3301 (m, br, CONH), 3058 (m, ArH), 2961 (w, CH/CH_2), 2868 (w, CH/CH_2), 1662 (CONH), 1601(s, Ar), 1506 (s, Ar).

HRMS (ESI): 717.4013 $[M + K]^+$, $C_{47}H_{54}N_2O_3Na$ requires 717.4027.

$[\alpha]_D^{25}$: +9.5 (10 mg ml^{-1}, $CHCl_3$)

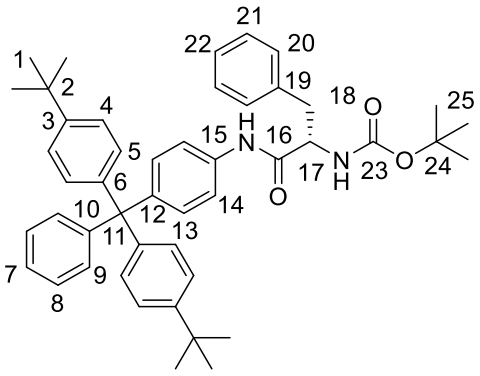

2.33 *N*-(Bis(4-*tert*-butylphenyl)(phenyl)methyl)phenyl- L-alanine

Boc protected amine **2.30** (0.72 g, 1.16 mmol) was dissolved in CH_2Cl_2 20 mL) to which TFA (2 mL) was added, the reaction was stirred for 2 h at RT. 10% NaOH was added until the mixture reached pH 10. The mixture was further diluted with CH_2Cl_2 (20 mL), washed with water (2 × 20

mL), the organic layer was dried with K_2CO_3 and the solvent removed *in vacuo* to leave the product, a white foamy solid (0.53 g, 88%).

Mp: 133-135 °C

^{1}H NMR (400 MHz, $CDCl_3$) δ: 9.41 (1H, br s, $C^{15}NH$), 7.39 (2H, d, ^3J = 8.8 Hz, $C^{14}H$), 6.98-7.17 (13H, m, ArH), 3.65 (2H,br s, $C^{17}NH$), 1.48 (9H, s, $C^{21}H$), 1.37 (1H, q, ^3J = 7.0 Hz, $C^{17}H$), 1.44 (3H, d, ^3J = 7.0 Hz, $C^{18}H$), 1.22 (18H, s, C^1H).

$^{13}C\{^1H\}$ NMR (100 MHz, $CDCl_3$) δ: 167.7 (C^{16}), 148.4, 147.2, 143.7, 143.1, 135.3, 131.8, 131.1, 130.7, 127.30, 125.7, 124.2, 118.3 (12 × ArC), 63.8 (C^{11}), 51.0 (C^{17}), 34.3 (C^2), 31.4 (C^1), 18.9 (C^{18}).

IR υ_{max}: 3301 (m, br, CONH), 2958 (m, CH_3), 2902 (w, CH), 1684 (s, CON), 1601 (m, Ar), 1588 (m, Ar), 1508 (s, Ar).

HRMS (ESI): *m/z*: 519.3357 $[M+H]^+$, $C_{36}H_{43}N_2O$ requires 519.3370.

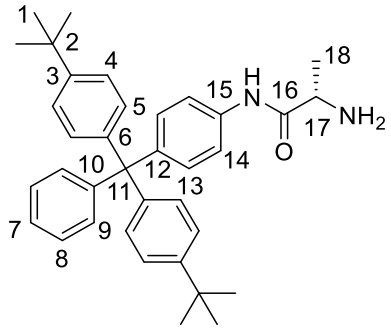

2.34 *N*-(Bis(4-*tert*-butylphenyl)(phenyl)methyl)phenyl- L-alanine

Boc protected amine **2.32** (449 mg, 0.768 mmol) was dissolved in CH_2Cl_2 (10 mL) to which TFA (1 mL) was added, the reaction was stirred for 2 h at RT. 10% NaOH was added until the mixture reached pH 10. The mixture was further diluted with CH_2Cl_2 (20 mL), washed with water (2 × 20 mL), the organic layer was dried with $MgSO_4$ and the solvent removed *in vacuo* to leave the product, a white foamy solid (329 mg, 64 %).

Mp: 114-115 °C

^{1}H NMR (400 MHz, $CDCl_3$) δ: 9.41 (s, 1H, C^{16}NH), 7.48 (dt, 2H, ^{3}J = 8.7 Hz, ^{4}J = 2.3 Hz, C^{14}H), 7.32-7.37 (m, 2H, ArH), 7.17-7.30 (m, 16 H, ArH), 7.13 (dt, 2H, ^{3}J = 8.7 Hz, ^{5}J = 2.3 Hz), 3.79 (dd, 1H, ^{3}J = 9.0 Hz, ^{3}J = 3.5 Hz, C^{17}H, 3.40 (dd, 1H, ^{2}J = 13.8 Hz, ^{3}J = 3.9 Hz, C^{18}H), 2.80 (dd, 1H, ^{2}J = 13.8 Hz, ^{3}J = 9.0 Hz, $C^{18'}$H), 1.33 (s, 18H, C^{1}H).

^{13}C{^{1}H} NMR (100 MHz, $CDCl_3$) δ: 171.9 (C^{16}), 148.5 (C^{12}), 147.1, 143.7 (2 × ArC), 143.1 (C^{15}), 137.6, 135.3, 131.8, 131.2 (4 × ArC), 130.7 (C^{13}), 129.3, 128.9, 127.3, 127.0, 125.7, 124.2 (6 × ArC), 118.4 (C^{14}), 63.8 (C^{11}), 56.8 (C^{17}), 40.6 (C^{18}), 34.3 (C^{2}), 31.4 (C^{1}).

IR υ_{max}: 3293 (m, CONH), 3054 (CONH), 3028 (ArC), 2957 (w, CH/CH_2), 2903 (w, CH/CH_2), 1685 (s, CONH), 1586 (s, Ar), 1508 (s, Ar).

HRMS (ESI): *m/z*: 595.3670 $[M+H]^+$, $C_{42}H_{46}N_2O$ requires 595.3683.

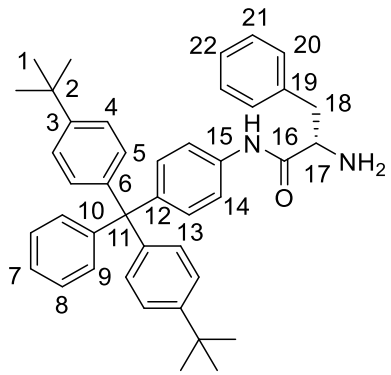

2.35 *N*^{3},*N*^{5}-((Bis(4-*tert*-butylphenyl)(phenyl)methyl)phenyl-L-alanine)pyridine-3,5-dicarboxamide

3,5-Pyridine dicarboxylic acid (76 mg, 0.46 mmol) was dissolved in $SOCl_2$ (5 mL), DMF (cat.) was added and the solution was heated to reflux for 1 h (using a condenser fitted with a $CaCl_2$ drying tube). The excess $SOCl_2$ was removed *in vacuo* to leave a yellow solid. The bis-acyl chloride was dissolved in dry CH_2Cl_2 (25 mL) and NEt_3 (152 mg, 0.21 mL, 1.51 mmol) and amine **2.33** (525 mg, 1.01 mmol) were added, the reaction was stirred for 1h at RT, under an Ar atmosphere. The mixture was diluted with CH_2Cl_2 (25 mL) and washed with $HCl_{(aq)}$ (1 M, 50 mL) and NaOH (1 M, 50 mL), the organic layer was dried with $MgSO_4$ and the solvent was removed *in vacuo* to leave

a yellow solid. The solid was purified by column chromatography (silica, 97:3 CH_2Cl_2:MeOH), to yield the product, a yellow solid (397 mg, 75%).

^{1}H NMR (400 MHz, d_6-DMSO) δ: 9.15 (2H, d, ^4J = 2.2 Hz, $C^{22}H$), 9.01 (2H, d, ^3J = 6.4 Hz, $C^{19}NH$), 8.68 (1H, t, ^4J = 2.2 Hz, $C^{21}H$), 7.51 (4H, d, ^3J = 8.8 Hz, $C^{14}H$), 7.02-7.34 (26H, m, ArH), 4.61 (2H, m, ^3J = 6.9 Hz, $C^{17}H$), 1.43 (6H, d, ^3J = 7.2 Hz, $C^{18}H$), 1.25 (36H, s, C^1H) .

^{13}C{^{1}H} NMR (100 MHz, d_6-DMSO) δ: 171.3 (C^{19}), 165.0 (C^{16}), 151.3 (C^{22}), 144.8 (C^{20}), 135.0 (C^{21}), 148.8, 147.3 142.1, 137.1, 131.1, 130.8, 130.5, 126.2, 124.9, 119.0 (12 × ArC), 63.7 (C^{11}), 50.5 (C^{17}), 34.5 (C^2), 31.6 (C^1), 18.1 (C^{18}).

IR υ_{max}: 3293 (m, br, CONH), 2958 (m, CH_3), 2901 (w, CH_2), 2868 (w, CH), 1653 (s, CON), 1638 (m, Ar), 1597 (m, Ar), 1506 (m, Ar).

HRMS (ESI): *m/z*: 1190.6456 $[M+H]^+$, $C_{79}H_{85}N_5O_4Na$ requires 1190.6494.

$[\alpha]_D^{25}$: +1.0 (10 mg ml^{-1}, $CHCl_3$)

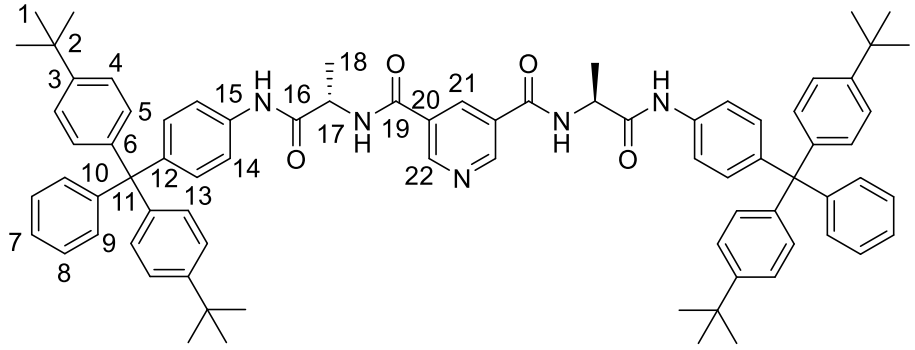

2.36 *N*^{3},*N*^{5}-((Bis(4-*tert*-butylphenyl)(phenyl)methyl)phenyl-L-alanine)pyridine-3,5-dicarboxamide

3,5-Pyridine dicarboxylic acid (65 mg, 0.387 mmol) was suspended in $SOCl_2$ (5 mL), DMF (cat.) was added and the solution was heated to reflux for 1 h (using a condenser fitted with a $CaCl_2$ drying tube). The excess $SOCl_2$ was removed *in vacuo* to leave a yellow solid. The bis-acyl chloride was dissolved in dry CH_2Cl_2 (20 mL) and NEt_3 (131 mg, 0.18 mL, 1.29 mmol) and amine **2.34** (512 mg, 0.861 mmol) were added, the reaction was stirred for 1h at RT, under an Ar atmosphere.

The mixture was diluted with CH_2Cl_2 (20 mL) and washed with $HCl_{(aq)}$ (1 M, 25 mL) and NaOH (1 M, 25 mL), the organic layer was dried with $MgSO_4$ and the solvent was removed *in vacuo* to afford a yellow solid. The solid was purified by column chromatography (silica, 99:1 CH_2Cl_2:MeOH), to yield the product, a yellow solid (383 mg, 75%).

R_f = 0.29 (99:2 CH_2Cl_2:MeOH)

Mp: >230 °C

^{1}H NMR (400 MHz, 3:1 $CDCl_3$:MeOD) δ: 9.45 (d, 2H, ^3J = 3.4 Hz, ^4J = 2.1 Hz, C^{26}NH), 8.99 (t, 2H, ^4J = 2.1 Hz, C^{26}H), 8.47 (dt, 1H, ^3J = 7.47 Hz, ^4J = 2.1 Hz, C^{25}H), 8.45 (d, br, 2H, ^3J = 8.1 Hz), 7.35 (dd, 4H, ^3J = 8.8 Hz, ^4J = 2.8 Hz, C^{14}H), 7.12-7.27 (m, 32H, ArH), 7.07 (dt, 8H, ^3J = 8.7 Hz, ^4J = 2.1 Hz, ArH), 4.91-4.98 (m, 2H, C^{17}H), 3.28 (dd, 2H, ^2J = 13.7 Hz, ^3J = 6.8 Hz, C^{18}H), 3.11 (dd, 2H, ^2J = 13.7 Hz, ^3J = 7.8 Hz, $C^{18'}$H), 1.27 (s, 36 H, C^1H).

^{13}C{^{1}H} NMR (100 MHz, 3:1 $CDCl_3$:MeOD) δ: 169.6 (C^{16}), 165.2 (C^{23}), 150.8 (C^{24}), 148.5 (C^{13}), 147.0, 143.6, 143.6, 136.4, 135.1 (5 × ArC), 134.4 (C^{24}), 131.6, 131.0, 129.5, 129.4 (4 × ArC), 129.1 (C^{25}), 128.5, 127.2, 126.9, 125.6, 124.1 (5 × ArC), 119.0 (C^{14}), 63.7 (C^{11}), 55.7 (C^{17}), 38.2 (C^{18}), 34.2 (C^2), 31.1 (C^1).

IR υ_{max}: 3304 (m, br CONH), 3055 (m, CONH), 3032 (w, ArH), 2958 (m, CH/CH_2), 2903 (m, CH/CH_2), 2868 (m, CH/CH_2), 1653 (s, CONH), 1597 (s, py) 1508 (s, Ar).

HRMS (ESI): *m/z*: 1320.7359 $[M]^+$ $C_{91}H_{94}N_5O_4$ requires 1320.7300

$[\alpha]_D^{25}$: +4.0 (10 mg ml^{-1}, $CHCl_3$)

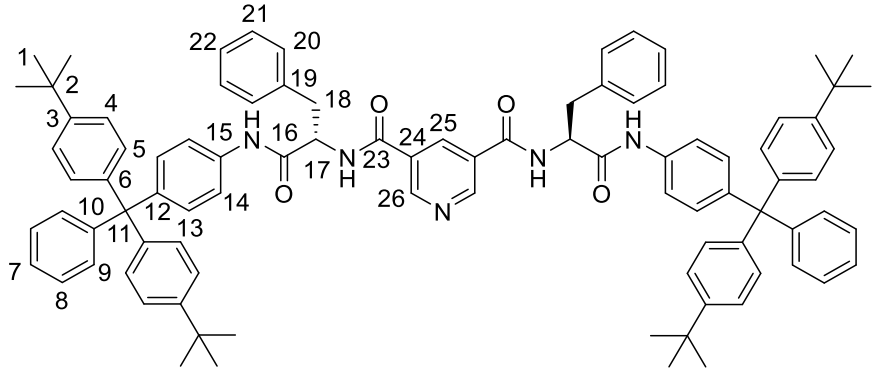

2.37 TBA *R*-mandelate[7]

To (*R*)-mandelic acid (500 mg, 3.29 mmol) in MeOH (10 mL), cooled to 0 °C, tetrabutylammonium hydroxide 1 mol dm^{-3} (3.29 mL, 3.29 mmol) was added dropwise. The solution was stirred for 1h at room temperature and the solvent removed *in vacuo*. The resulting oil was placed under high vacuum for 24 h, then dried in a desiccator at -18 °C for 7 days to afford 1.29 g of a white solid in quantitative yield.

^{1}H NMR (400 MHz, $CDCl_3$) δ: 7.57 (d, 2H, ^{3}J = 7.5 Hz, $C^{3}H$), 7.24 (t, 2H, ^{3}J = 7.5 Hz, $C^{2}H$), 7.15 (dt, 1H, ^{3}J = 7.5 Hz, ^{4}J = 1.2 Hz, $C^{1}H$), 4.85 (s, 1H, $C^{5}H$), 3.10-3.16 (m, 8H, $C^{a}H$), 1.48-1.58 (m, 8H, $C^{b}H$), 1.36 (sextet, 8H, ^{3}J = 7.3 Hz, $C^{c}H$), 0.98 (t, 12H, ^{3}J = 7.3 Hz, $C^{d}H$).

$^{13}C\{^{1}H\}$ NMR (100 MHz, $CDCl_3$) δ: 176.0 (C^{6}), 144.2 (C^{4}), 127.6 (C^{2}), 126.7 (C^{3}), 126.1 (C^{5}), 74.5 (C^{5}), 58.6 (C^{a}), 23.9 (C^{b}), 19.7 (C^{c}), 13.7 (C^{d}).

$[\alpha]_D^{25}$: -52.0 (10 mg ml^{-1}, H_2O)

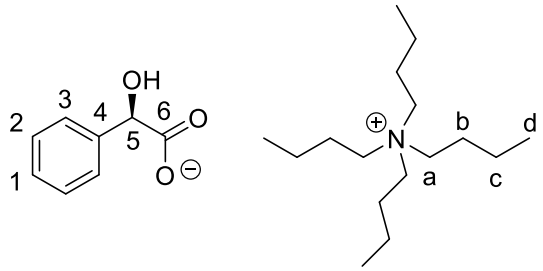

The data is consistent with literature values.

2.36 TBA *S*-mandelate[7]

To (*S*)-mandelic acid (500 mg, 3.29 mmol) in MeOH (10 mL), cooled to 0 °C, tetrabutylammonium hydroxide 1 mol dm^{-3} (3.29 mL, 3.29 mmol) was added dropwise. The solution was stirred for 1h at room temperature and the solvent removed *in vacuo*. The resulting oil was placed under high vacuum for 24 h, then dried in a desiccator at -18 °C for 7 days to afford 1.30 g of a white solid in quantitative yield.

^{1}H NMR (400 MHz, $CDCl_3$) δ: 7.59 (d, 2H, ^{3}J = 7.5 Hz, $C^{3}H$), 7.26 (t, 2H, ^{3}J = 7.5 Hz, $C^{2}H$), 7.16 (dt, 1H, ^{3}J = 7.5 Hz, ^{4}J = 1.2 Hz, $C^{1}H$), 4.85 (s, 1H, $C^{5}H$), 3.13-3.21 (m, 8H, $C^{a}H$), 1.51-1.60 (m, 8H, $C^{b}H$), 1.39 (sextet, 8H, ^{3}J = 7.3 Hz, $C^{c}H$), 0.99 (t, 12H, ^{3}J = 7.3 Hz, $C^{d}H$).

$^{13}C\{^{1}H\}$ NMR (100 MHz, $CDCl_3$) δ: 176.1 (C^{6}), 144.2 (C^{4}), 127.6 (C^{2}), 126.7 (C^{3}), 126.0 (C^{5}), 74.5 (C^{5}), 58.6 (C^{a}), 23.9 (C^{b}), 19.7 (C^{c}), 13.7 (C^{d}).

$[\alpha]_D^{25}$: +47.0 (10 mg ml^{-1}, H_2O)

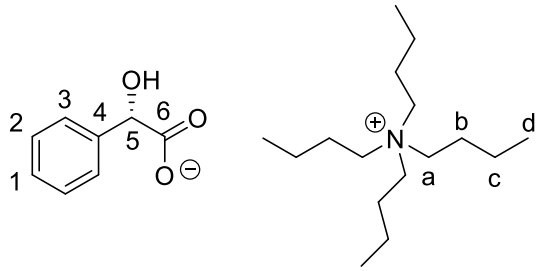

The data is consistent with literature values.

7.3.2. Experimental for Chapter 3

3.1 Mechanically Chiral Rotaxane Chloride Salt

To pyridinium axle **3.2** (250 mg, 0.22 mmol) and bis-amine **3.3** (96 mg, 0.22 mmol) in dry CH_2Cl_2 (20 mL), NEt_3 (0.09 mL, 67 mg, 0.66 mmol) was added, followed by a dropwise addition of isophthaloyl chloride (54 mg, 0.26 mmol) in CH_2Cl_2 (10 mL). The solution was stirred for 1 h then washed with 10% HCl (20 mL) and water (2 × 20 mL), dried with $MgSO_4$ and the solvent removed *in vacuo*. The residue was purified via flash column chromatography (silica, 96:4 CH_2Cl_2:MeOH) to afford a yellow solid with some macrocyclic impurities (106 mg).

The impure rotaxane was dissolved in $CHCl_3$ (20 mL) then washed with 0.2 mol dm^{-3} $(NH_4)_2SO_4$ (8 × 10 mL), then dried with $MgSO_4$. The solvent was removed *in vacuo* and the residue was loaded onto a plug of silica and washed with 96:4 CH_2Cl_2:MeOH, the solution was set aside for later use. The rotaxane was then flushed off the silica using 85:15 (CH_2Cl_2) saturated with NH_4Cl and the solvent removed *in vacuo*. The residue was dissolved in CH_2Cl_2 (30 mL) and washed with 1 mol dm^{-3} NH_4Cl (20 mL) and water, then dried with $MgSO_4$ to afford rotaxane **3.1** (57 mg, 15

%) The solvent was then removed *in vacuo* from the wash solution to afford impure rotaxane **3.1** (20 mg).

Mp = >230 °C

^{1}H NMR (400 MHz, 1:1 $CDCl_3$:CD_3OD) δ: 9.46 (s, 1H, $C^{3}H$), 9.28 (s, 1H, $C^{4}H$), 8.95 (t, br, ^{3}J = 5.7 Hz $C^{6}NH$), 8.76 (s, 1H, $C^{1}H$), 8.60 (s, 1H, $C^{v}H$), 7.99 (d, ^{3}J = 7.9 Hz $C^{z}H$), 7.96 (d, ^{3}J = 7.9 Hz $C^{z}H$), 7.65 (d, ^{3}J = 8.8 Hz $C^{9}H$), 7.42 (d, ^{3}J = 8.8 Hz $C^{26}H$), 7.33 (t, ^{3}J = 7.9 Hz $C^{y}H$), 7.02-7.29 (m, 30H, ArH), 6.55 (d, ^{3}J = 9.0 Hz $C^{p}H$), 6.35 (d, ^{3}J = 8.6 Hz $C^{d}H$), 6.31 (d, ^{3}J = 9.0 Hz $C^{o}H$), 4.50 (s, 3H, $C^{40}H$) 4.49 (d, 1H, ^{2}J = 14.9 Hz, $C^{a}H$), 4.30 (d, 1H, ^{2}J = 14.9 Hz, $C^{a'}H$), 3.99-4.30 (m, 4H, $C^{23,r}H$), 4.59-3.81 (m, 16H, OCH_2), 1.33 (s, 18H, $C^{18}H$), 1.30 (s, 18H, $C^{35}H$).

^{13}C{^{1}H} NMR (100 MHz, 1:1 $CDCl_3$:CD_3OD) δ: 168.0 (C^{t}), 167.3 (C^{aa}), 166.6 (C^{24}), 161.2 (C^{6}), 158.9 (C^{7}), 157.1 (C^{e}), 152.9 (C^{n}), 151.8 (C^{q}), 148.5 (C^{16}), 148.4 (C^{33}), 147.1 (C^{19}), 146.8 (C^{36}), 146.4 (C^{3}), 146.2 (C^{4}), 145.0 (C^{8}), 143.8 (C^{30}), 143.5 (C^{13}), 143.2 (C^{25}), 140.6 (C^{1}), 135.6 (C^{28}), 134.5 (C^{11}), 133.7 (C^{w}), 133.6 (C^{u}), 133.1 (C^{2}), 132.4 (C^{5}), 131.7 (C^{10}), 131.5 (C^{27}), 131.3 (C^{z}), 131.2 (C^{x}), 131.0 ($C^{20,37}$, coincidental), 130.6 ($C^{14,b}$, coincidental), 129.2 (C^{c}), 129.0 (C^{y}), 127.3 (C^{38}), 127.2 (C^{21}), 125.7 (C^{39}), 125.6 (C^{22}), 125.0 (C^{v}), 124.2 (C^{15}), 124.1 (C^{32}), 120.2 (C^{9}), 118.6 (C^{26}), 114.8 (C^{p}), 114.7 (C^{o}), 114.0 (C^{d}), 70.7 ($C^{i, j}$, coincidental), 70.6 (C^{h}), 70.5 (C^{k}), 70.0 (C^{l}), 70.0 (C^{g}), 67.9 (C^{f}), 67.6 (C^{m}), 65.6 (C^{r}), 63.8 (C^{12}), 63.7 (C^{29}), 48.7 (C^{40}), 43.5 (C^{23}), 43.3 (C^{a}), 40.2 (C^{s}), 34.1 (C^{34}), 34.1 (C^{17}), 31.0 (C^{35}), 31.0 (C^{18}).

*NMR assigned with assistance from Dr. Geoff Akien and NOSEY, ROESY and TOCSY experiments.

HRMS (ESI): *m/z*: 1661.8743 $[M]^+$, $C_{107}H_{117}N_6O_3$ requires 1661.8775.

IR υ_{max}: 3280 (m, CONH), 3054 (m, ArH), 2957 (m, CH_3/CH_2) , 2903 (m, CH_2/CH_3), 2868 (m, OCH_2), 1654.9 s (CONH), 1602.8 (s, py), 1533 (s, Ar), 1506 (s, Ar)

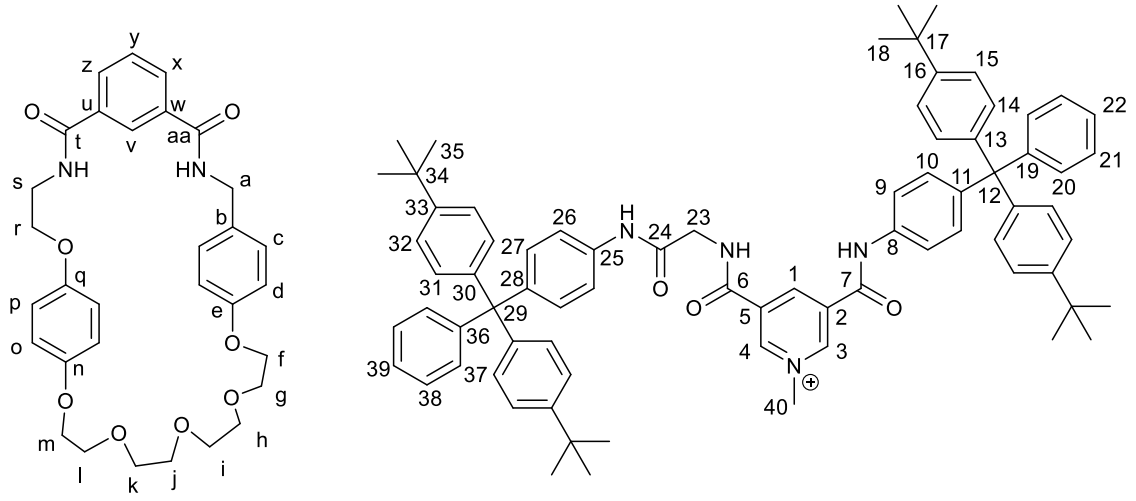

3.1-b Mechanically Chiral Rotaxane (−)-O,O'-Dibenzoyl-L-tartrate salt

Mechanically chiral rotaxane **3.** 1(12 mg, 0.007 mmol) was dissolved in CH_2Cl_2 (10 mL) and then washed with 0.1 mol dm^{-3} (−)-O,O'-Dibenzoyl-L-tartrate (8 × 5 mL), then water (10 mL). The solvent was removed *in vacuo* to afford a yellow solid (12 mg, 92 %).

^{1}H NMR (400 MHz, 1:1 $CDCl_3$:CD_3OD) δ: 9.47 (s, 2H, CNH), 9.45 (s, 2H, CNH), 9.34 (s, 2H, ArH), 8.43 (s, 2H, ArH), 8.31 (s, 2H, ArH), 8.12 (d, 4H, ^3J = 8.4 Hz, $C^{x,z}H$), 7.97-8.05 (m, 4H), 7.59 (d, 2H, 8.8 Hz, ArH), 7.57 (d, 2H, 8.8 Hz, ArH), 7.42-7.48 (m, 6H, ArH), 7.36 (t, 2H, ^3J = 7.5 Hz, $C^{y}H$), 7.04-7.28 (m, 58 H, Ar H), 6.94 (d, 4H, ^3J = 9.1 Hz $C^{c}H$), 6.44 (d, 4H, ^3J = 9.0 Hz, $C^{o/p}H$), 6.33 (d, 4H, ^3J = 8.4 Hz, $C^{d}H$), 6.28 (d, 4H, ^3J = 8.9 Hz, $C^{o/p}H$), 6.12 (s, 1H, ArH), 4.41 (s, 3H, $C^{40}H$), 4.39 (s, 3H, $C^{40}H$), 4.15 (d, 2H, ^3J = 15.9 Hz, OCH_2/NCH_2), 4.08 (d, 2H, ^3J = 15.9 Hz, OCH_2/NCH_2), 3.43-3.92 (m, 18H, CH_2), 1.32 (s, 18H, $C^{18/35}H$), 1.28 (s, 18H, $C^{18/35}H$).

*broadness of the ^{1}H thought to be due to two rotaxanes being co-ordinated to each anion, ^{13}C insufficient peaks detected due to lack of material.

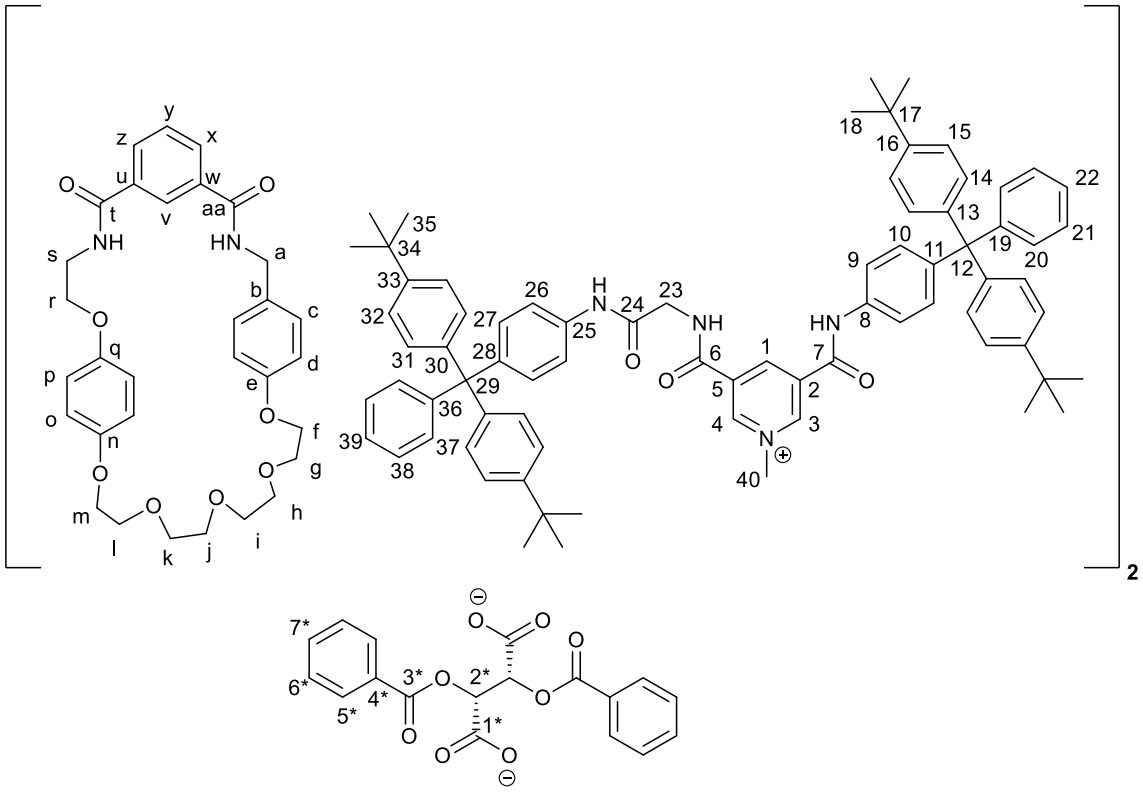

3.1-d Mechanically Chiral Rotaxane camphorsulfonate salt

Mechanically chiral rotaxane **3.1** (12 mg, 0.007 mmol) was dissolved in CH_2Cl_2 (10 mL) and then washed with 0.1 mol dm^{-3} ammonium camphorsulfonate (8 × 5 mL), then water (10 mL). The solvent was removed *in vacuo* to afford a yellow solid (12 mg, 92 %).

^{1}H NMR (400 MHz, 1:1 $CDCl_3$:CD_3OD) δ: 9.23 (s, 1H, $C^{3/4}H$), 9.13 (s, 1H, $C^{3/4}H$), 7.92 (d, 1H, ^3J = 7.8 Hz, $C^{x/z}H$), &.85-7.29 (m, 1H, $C^{x/z}H$), 7.52 (dd, 2H, ^3J = 8.7 Hz, ^4J = 1.9 Hz, $C^{9/26}H$), 7.34 (dd, 2H, ^3J = 8.7 Hz, ^4J = 1.5 Hz), 7.30 (dt, 1H, ^3J = 7.8 Hz, ^4J = 2.2 Hz, $C^{y}H$), 6.95-7.19 (m, 32 H, ArH), 6.49 (dd, 2H, ^3J = 9.0 Hz, ^4J = 1.5 Hz, $C^{o}H$), 6.31 (d, 2H, ^3J = 8.7 Hz, $C^{o}H$), 6.28 (d, 2H, ^3J = 9.0 Hz, $C^{o}H$), 4.41 (s, 3H, $C^{40}H$), 4.36 (d, 1H, ^2J = 14.8 Hz, $C^{a}H$), 4.23 (d, 1H, ^2J = 14.8 Hz, $C^{a'}H$), 4.16 (dd, 1H, ^2J = 16.2 Hz, ^4J = 1.9 Hz, NCH_2), 4.04 (d, 1H, ^2J = 16.2 Hz, NCH_2), 3.93-3.99 (m, 1H, $C^{23}H$), 3.83-3.91 (m, 1H, $C^{23}H$), 3.75-3.81 (m, 18H, OCH_2), 3.29 (d, 1H, ^2J = 14.7 $C^{4*}H$), 3.28 (2H, s, CH_2), 3.73 (d, 1H, ^2J = 14.7 Hz, $C^{4*}H$), 2.52 (t, 1 H, ^3J = 11.4 Hz), 2.21 (dt, 1H, ^2J = 17.1 Hz, ^3J = 3.8 Hz, CH), 1.94-1.98 (m, 1H, CH_2), 1.81-1.91 (m, 1H, CH), 1.73 (d, 1H, ^2J = 18.0 Hz, CH), 1.53-1.61 (m, 1H, CH), 1.23 (s, 18H, $C^{18/35}H$), 1.17-1.21 (m, 24H, $C^{18/35}H$, CH_2), 0.97 (s, 3H, $C^{9*/10*}H$), 0.73 (s, 3H, $C^{9*/10*}H$).

*Insufficient peaks detected in `^{13}C spectra due to lack of material

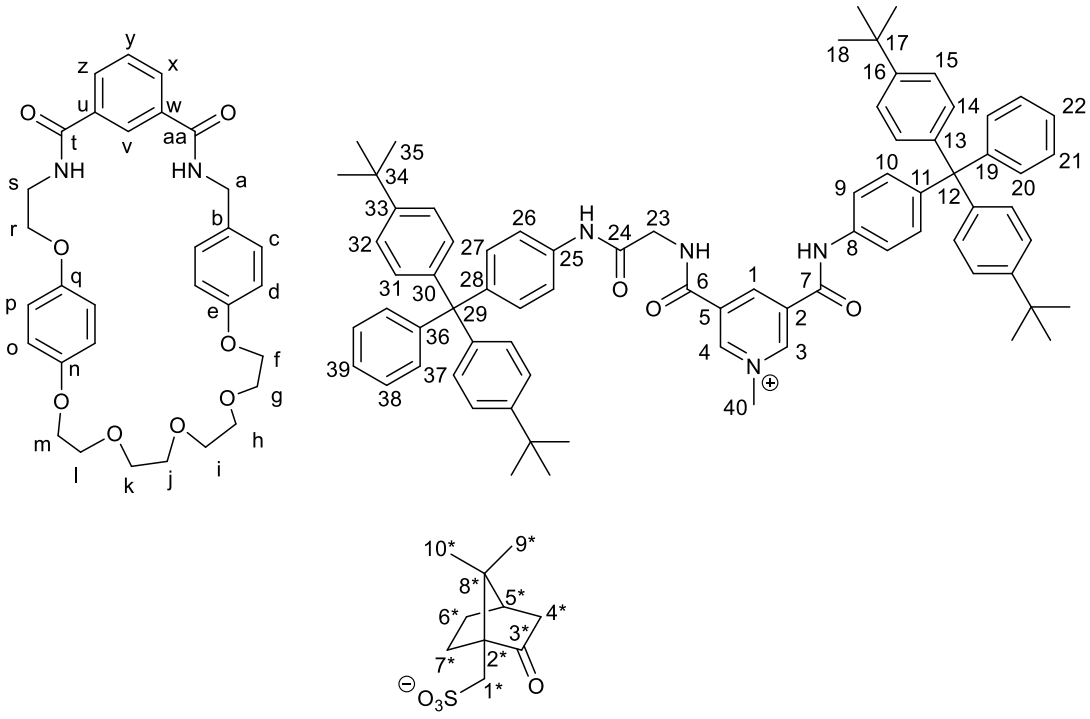

3.2 Chloride salt of *N*^{1}-Methyl *N*^{3}-((Bis(4-*tert*-butylphenyl)(phenyl)methyl)phenyl-glycine)-*N*^{5}-((Bis(4-*tert*-butylphenyl)(phenyl)methyl)phenyl pyridine-3,5-dicarboxamide

Pyridine axle **3.11** (198 mg, 0.183 mmol), was dissolved in $CHCl_3$ (3 mL) and MeI (2 mL) was added. The solution was stirred for 16 h heated to 50 ºC under Ar. The mixture was allowed to cool and the $CHCl_3$ and excess MeI were removed *in vacuo* to leave a yellow solid. The solid was redissolved in CH_2Cl_2, then washed with 1M NH_4Cl (8 × 25 mL) and water (25 mL), the solvent was removed *in vacuo* to leave the product as a yellow solid.

Mp = >230 °C

^{1}H NMR (400 MHz, d_6 - acetone) δ: 11.35 (s, 1H, C^{7}NH), 10.65 (s, 1H, C^{1}H), 10.26 (t, 1H, ^{3}J = 5.9 Hz, C^{6}NH), 9.87 (s, 1H, C^{6}NH), 9.64 (s, 1H, $C^{3/4}$H), 9.56 (s, 1H, $C^{3/4}$H), 7.99 (d, 2H, ^{3}J = 8.8 Hz, $C^{9/26}$H), 7.64 (d, 2H, ^{3}J = 8.8 Hz $C^{9/26}$H), 7.06-7.37 (m, 30H, ArH), 4.71 (s, 3H, C^{40}H), 4.22 (d, 2H, ^{3}J = 5.9 Hz, C^{23}H), 1.31 (s, 1H, $C^{18/35}$H), 1.30(s, 1H, $C^{18/35}$H).

$^{13}C\{^{1}H\}$ NMR (100 MHz, d_6 - acetone) δ: 166.7 (C^{24}), 161.3 (C^{6}), 159.3 (C^{7}), 148.4, 148.3, 147.9, 147.5 (4 × ArC), 147.3, 147.2 ($C^{3/4}$), 144.0, 144.0, 143.6, 142.2 (4 × ArC), 141.5 (C^{1}), 136.9, 136.6, 133.9, 133.1, 131.1, 131.0, 130.9, 130.8, 130.6, 130.5, 127.5, 127.4, 125.8, 125.7, 124.4, 124.3 (16 × ArC), 119.4, 118.6 ($C^{9/26}$), 63.8 , 63.7($C^{12/25}$), 48.9 (C^{40}), 44.2 (C^{23}), 34.0, 34.0 ($C^{17/34}$), 30.8 ($C^{18/35}$). (1 × CH_3 missing – coincidental).

HRMS (ESI): *m/z*: 1097.6263 $[M]^+$, $C_{75}H_{78}N_4O_3$ requires 1097.6303.

IR υ_{max}: 3179 (m, CONH), 3053 (m, CONH), 3028 (w, ArH), 2956 (m, CH_3/CH_2), 2902 (m, CH_3/CH_2), 2865 (m, CH_3/CH_2), 1678 (s, CONH), 1601 (s, py), 1508 (s, Ar).

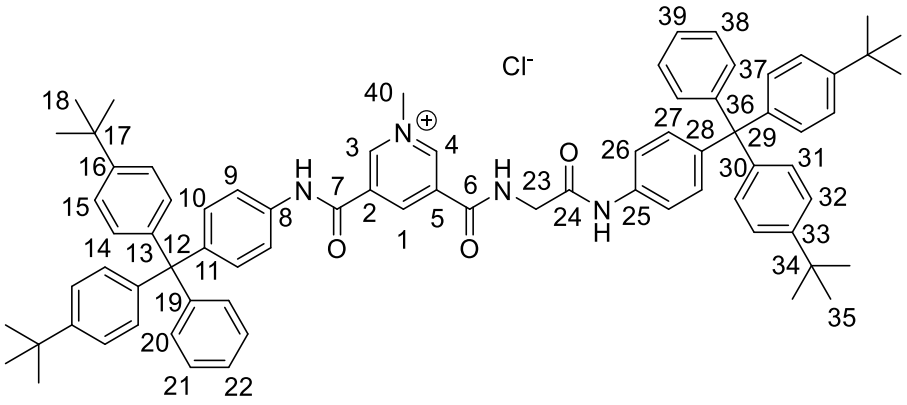

3.3 Bis-amine asymmetric macrocycle precursor

To a solution of bis-nitrile **3.15** (1.17 g, 2.74 mmol) in dry THF (10 mL), BH_3·THF (1 mol dm^{-3}, 14 mL, 14 mmol) was slowly added. The reaction mixture was heated to reflux for 1 h under an Ar, then quenched with MeOH. Concentrated $HCl_{(aq)}$ (5 mL) was added and the mixture was allowed to stir for a further 30 minutes at RT. The solvent was then removed *in vacuo* to leave a fluffy white solid which was then suspended in CH_2Cl_2 (50 mL) and 10% NaOH (50 mL), the biphasic mixture was stirred vigorously for 30 minutes. The organic layer was separated and washed with H_2O (2 × 100 mL) and dried over $MgSO_4$. The solvent was removed *in vacuo* to leave the product, an oily yellow solid (1.10 g, 92%).

^{1}H NMR (400 MHz, $CDCl_3$) δ: 7.14 (d, 2H, ^{3}J = 8.5 Hz, $C^{3}H$), 6.80 (d, 2H, ^{3}J = 8.5 Hz, $C^{4}H$), 6.75-6.77 (m, 4H, $C^{15/16}H$), 4.04 (t, 2H, ^{3}J = 4.9 Hz, $C^{6}H$), 4.00 (t, 2H, ^{3}J = 4.9 Hz, $C^{13}H$), 3.86 (t, 2H, ^{3}J = 5.2 Hz,

$C^{18}H$), 3.80-3.73 (m, 4H, CH_2O), 3.72 (s, 2H, C^1H), 3.58-3.68 (m, 8H, CH_2O), 3.07 (t, 2H, ^3J = 5.2 Hz, $C^{19}H$).

$^{13}C\{^1H\}$ NMR (100 MHz, $CDCl_3$) δ: 157.7 (C^5), 153.2, 153.1 ($C^{14,17}$), 135.6 (C^2), 128.6 (C^3), 115.7 (C^4), 115.4 , 114.7 ($C^{15,16}$), 70.8, 70.8, 70.8, 70.7, 69.9, 69.8 (6 × CH_2O), 68.1 (C^{13}), 67.5 (C^4), 45.9 (C^1), 41.7 (C^{19}). (1 × CH_2O missing – coincidental)

HRMS (ESI): *m/z*: 457.2330 $[M+Na]^+$, $C_{23}H34N_2O_6$ requires 457.2309.

IR υ_{max}: 3480 (m, NH_2 2920 (s, CH_2), 2867 (s, CH_2), 1611 (m, Ar1), 1507 (m, Ar).

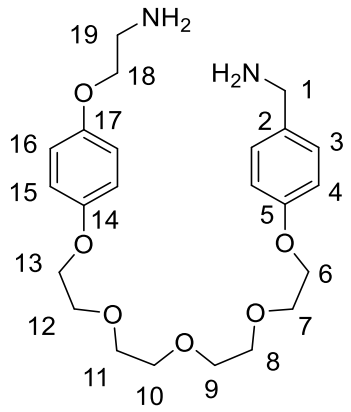

3.4 Mechanically Chiral Catenane Chloride Salt

To pyridinium macrocycle **3.17** (126 mg, 0.178 mmol) in dry CH_2Cl_2 (15 mL) bis-amine **3.3** (77 mg, 0.178 mmol) was added and the solution stirred for 30 minutes. NEt_3 (0.07 mL, 53 mg, 0.525 mmol) was added, followed by the dropwise addition of isophthaloyl chloride (43 mg, 0.21 mmol) in dry CH_2Cl_2 (10 mL). The solution was stirred for 1 h, then washed with 10% $HCl_{(aq)}$ (20 mL) and water (2 × 20 mL), then dried over $MgSO_4$ and the solvent removed *in vacuo*. The residue was purified by column chromatography (silica, 96:4 CH_2Cl_2:MeOH) followed by preparative TLC (96:4 CH_2Cl_2:MeOH) to afford the product as a yellows solid contaminated with some small amounts of impurities (15 mg, 7%).

^1H NMR (400 MHz, 1:1 $CDCl_3$:CD_3OD) δ: 8.87 (s, 1H, $C^{x/y}H$), 8.86 (s, 1H, $C^{x/y}H$), 8.40 (s, 1H, C^vH), 8.14 (dt, 1H, ^3J = 8.0 Hz, ^4J = 1.4 Hz, $C^{24/26}H$), 8.06 (dt, 1H, ^3J = 8.0 Hz, ^4J = 1.4 Hz, $C^{24/26}H$), 7.68 (t,

1H, ^{3}J = 8.0 Hz) 7.73 (d, 2H, ^{3}J = 8.6 Hz, ArH), 6.74 (d, 2H, ^{3}J = 9.2 Hz, ArH), 6.72 (d, 2H, ^{3}J = 9.3 Hz, ArH), 6.49 (d, 2H, ^{3}J = 8.9 Hz, ArH), 6.49 (d, 2H, ^{3}J = 8.9 Hz, ArH), 6.30 (d, 4H, ^{3}J = 8.3 Hz, ArH), 4.53 (q, 3H, ^{3}J = 11.3 Hz, NCH_3), 4.50 (d, 1H, ^{3}J = 15 Hz, NCH_2), 3.96-4.15 (m, 11H, OCH_2, NCH_2), 3.44-3.88 (m, 32 H, OCH_2).

HRMS (ESI): *m/z*: 1144.5128 $[M]^+$, $C_{62}H_{74}N_5O_{16}$ requires 1144.5125.

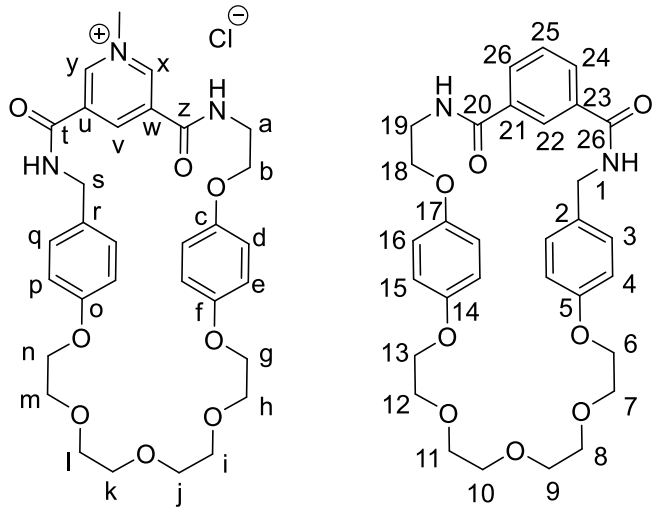

3.4-a Mechanically Chiral Catenane (1*S*)-(+)-10-camphorsulfonate Salt

Mechanically chiral catenane **3.4** (15 mg, 0.013 mmol) was dissolved in CH_2Cl_2 (10 mL) and then washed with 0.1 mol dm^{-3} ammonium (1*S*)-(+)-10-camphorsulfonate (8 × 5 mL), then water (10 mL). The solvent was removed *in vacuo* to afford a yellow solid (14 mg, 78 %).

^{1}H NMR (400 MHz, 1:1 $CDCl_3$:CD_3OD) δ: 8.87 (s, 1H, $C^{24/25}H$), 8.79 (d, 1H, $C^{24/25}H$) 8.63 (t, br, 1H, $C^{22}H$), 8.37 (s, 1H, $C^{v}H$) 8.14 (t, 1H, $C^{x,z}H$), 7.68 (s, 1H, $C^{y}H$), 7.27 (d, 1H, ArH), 6.72-6.90 (m, 6H, ArH), 6.49 (d, 1H, ArH), 6.27-6.32 (m, 2H, ArH), 4.47-4.56 (m, 2H,), 4.28 (d, 1H), 3.40-4.20 (m, 35H), 2.84 (d, 1H,), 2.67 (t, 1H) 2.36 (1dt, 1H), 2.00-2.12 (m, 3H), 1.91 (d, 1H), 1.65-1.74 (m, 2H), 1.42 (td, 2H), 1.13 (s, 3H), 0.88 (s, 3H).*

*Some peaks not assigned as it is almost impossible to make a reasonably accurate assignment.

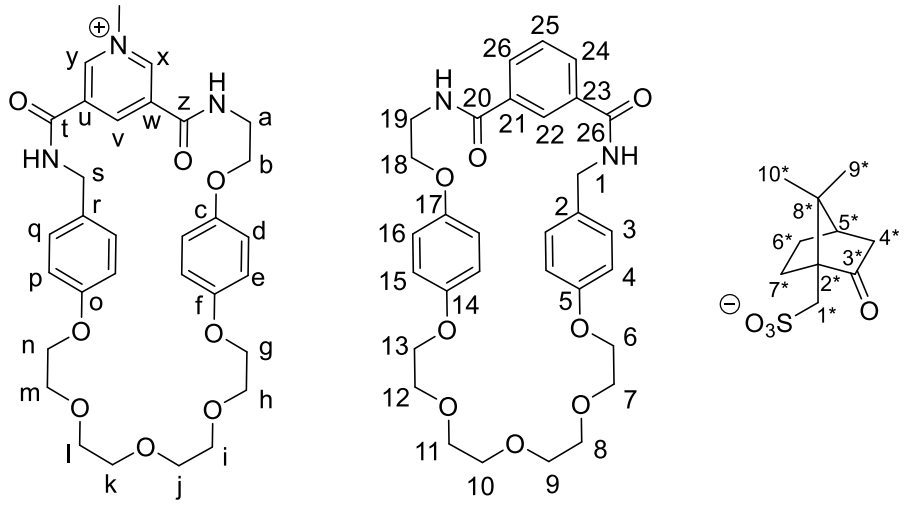

3.5 Dimethyl pyridine-3,5-dicarboxylate[8]

To pyridine-3,5- dicarboxylic acid (2.50 g, 15 mmol) in methanol (10 mL), conc. H_2SO_4 was added carefully and the mixture was heated to reflux for 16 h. The mixture was poured over ice and conc. NH_4OH was added carefully until the solution was strongly basic. The solution was washed with Et_2O (3 × 50 mL), the organic layers were combined to yield the product as an off-white solid (2.92 g, 75%)

^{1}H NMR (400 MHz, $CDCl_3$) δ: 9.39 (d, 2H, ^4J = 2.1 Hz, C^3H), 8.90 (t, 1H, ^4J = 2.1 Hz, C^1H), 4.01 (s, 6H, C^5H).

$^{13}C\{^1H\}$ NMR (100 MHz, $CDCl_3$) δ: 164.8 (C^4), 154.1 (C^3), 138.2 (C^1), 126.1 (C^2), 52.73 (C^5).

HRMS (ESI): *m/z*: 196.0596 $[M+H]^+$, $C_9H_9N_1O_4$ requires 196.0604.

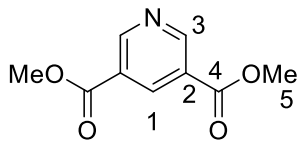

The obtained data is consistent with literature values.

3.6 5-(Methyloxycarbonyl)nicotinic acid[8]

Dimethyl ester **3.5** (2.14 g, 11.0 mmol) was dissolved in a solution of 0.1 M KOH in MeOH (122 mL) and stirred for 16 h at RT. The solvent was removed *in vacuo* and the resulting solid dissolved

in water (85 mL) and washed with Et_2O (3 × 85 mL) and the organic layers discarded. The aqueous layer was neutralised with 10% citric acid and the product was isolated as a white solid by vacuum filtration (1.55 g, 72%).

^{1}H NMR (400 MHz, $CDCl_3$) δ: 9.26 (d, 1H, ^4J = 2.1 Hz, C^3H), 9.25 (d, 1H, ^4J = 2.1 Hz, C^4H), 8.64 (t, 1H, ^4J = 2.1 Hz, C^1H), 4.01 (s, 3H, C^7H).

^{13}C{^{1}H} NMR (100 MHz, $CDCl_3$) δ:165.9 (C^8), 165.0 (C^6), 154.3, 153.6 ($C^{3,4}$), 137.6 (C^1), 127.4 (C^2), 126.1(C^5), 53.2 (C^7).

HRMS (ESI): *m/z*: 182.0446 $[M+H]^+$, $C_8H_2N_1O_4$ requires 182.0448.

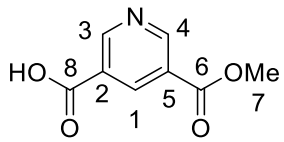

The obtained data is consistent with literature values.

3.7 Methyl 5-(3-glycine methyl ester) nicotinate

Monoester **3.6** (1 g, 5.52 mmol) was suspended in dry CH_2Cl_2 (25 mL), to which oxalyl chloride (0.47 mL, 0.70 g, 5.52 mmol) and a drop of dry DMF (cat) was added. The reaction mixture was stirred under Ar until all solids were dissolved. The solvent and excess oxalyl chloride was removed by distillation. The resulting acid chloride was dissolved in dry CH_2Cl_2 (50 mL), triethylamine (2.30 mL, 1.67 g, 16.6 mmol) and then glycine methyl ester hydrochloride (0.83 g, 6.62 mmol) were added and the mixture was stirred for 1 h under Ar. The resulting solution washed with 1 M $HCl_{(aq)}$ (2 × 50 mL) and the aqueous layers combined and neutralised with sat. $NaHCO_{3\,(aq)}$ and washed with CH_2Cl_2 (3 × 50 mL). The organic layers were combined, dried with $MgSO_4$ and the solvent was removed *in vacuo* to leave a brown solid. The solid was then purified by flash chromatography (silica, 98:2 CH_2Cl_2:MeOH) to give the product as a white solid (0.46 g, 33%).

R_f = 0.34 (98:2 CH_2Cl_2:MeOH)

Mp = 113-114 °C

^{1}H NMR (400 MHz, $CDCl_3$) δ: 9.34 (d, 1H, ^{4}J = 2.1 Hz, $C^{4}H$), 9.26 (d, 1H, ^{4}J = 2.1 Hz, $C^{3}H$), 8.72 (t, 1H, ^{4}J = 2.1 Hz, $C^{2}H$), 7.06 (t, 1H, ^{3}J = 5.0 Hz, $C^{8}NH$), 4.30 (d, 2H, ^{3}J = 5.0 Hz, $C^{9}H$), 4.00 (s, 3H, $C^{7}H$), 3.83 (s, 3H, $C^{11}H$).

$^{13}C\{^{1}H\}$ NMR (100 MHz, $CDCl_3$) δ:170.0 (C^{10}), 164.8 (C^{6}), 164.6 (C^{8}), 153.0 (C^{4}), 151.8 (C^{3}), 136.0 (C^{1}), 129.3 (C^{2}), 126.0 (C^{5}), 52.8 (C^{7}), 52.7 (C^{11}), 41.8 (C^{9}).

HRMS (ESI): *m/z*: 275.0629 $[M+Na]^+$, $C_{11}H_{12}N_2O_5$ requires 275.0638.

IR υ_{max}: 3259 (m, CONH), 3062 (m, CONH), 2959 (s, CH_2), 2852 (m, OCH_3), 1726 (s, CONH), 1682 (s, CONH), 1604 (s, Py), 1559 (s, CONH).

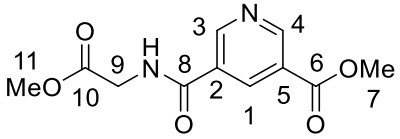

3.9 Methyl 5-(3-(bis(4-*tert*-butylphenyl)(phenyl)methyl)phenylcarbomyl)nicotinate[9]

Monoester **3.6** (0.40 g, 2.23 mmol) was suspended in dry CH_2Cl_2 (25 mL), to which oxalyl chloride (0.19 mL, 0.28 g, 2.23 mmol) and a drop of dry DMF (cat) was added. The reaction mixture was stirred under Ar until all solids were dissolved, the solvent and excess oxalyl chloride were then removed by distillation. The resulting acid chloride was dissolved in dry CH_2Cl_2 (25 mL), triethylamine (0.46 mL, 0.33 g, 3.30 mmol) and then amine **2.25** (1.00 g, 2.23 mmol) were added and the mixture was stirred for 1 h under Ar. The solution was washed with 1M $HCl_{(aq)}$ (2 × 50 mL) sat. $NaCO_{3(aq)}$ (2 × 50 mL) and water (2 × 50 mL), dried with $MgSO_4$ and the solvent removed *in vacuo*. The solid was then purified by flash chromatography (silica, 3:1 petrol 40-60:EtOAc) to give the product as a white solid (0.77 g, 57%).

R_f = 0.36 (3:1 petrol 40-60:EtOAc)

^{1}H NMR (300 MHz, $CDCl_3$) δ: 9.35 (d, 1H, ^{4}J = 2.1 Hz, $C^{3}H$), 9.31 (d, 1H, ^{4}J = 2.1 Hz, $C^{4}H$), 8.76 (t, 1H, ^{4}J = 2.1 Hz, $C^{1}H$), 8.04 (s br, 1H, $C^{8}NH$), 7.55 (d, 2H, ^{3}J = 8.8 Hz, $C^{10}H$), 7.17-7.31 (m, 11H, ArH), 7.13 (dt, 4H, ^{3}J = 13.4 Hz, ^{4}J = 2.8 Hz, ArH), 4.01 (s, 3H, $C^{7}H$), 1.32 (s, 18H, $C^{19}H$).

$^{13}C\{^{1}H\}$ NMR (75 MHz, $CDCl_3$) δ: 164.9 (C^{8}), 162.6 (C^{6}), 153.0 (C^{3}), 151.8 (C^{4}), 148.6, 147.0, 144.4, 143.5 (4 × ArC) 135.9 (C^{1}), 134.9, 132.0, 131.1, 130.7, 127.4, 126.1, 125.8, 124.3, 119.3 (9 × ArC), 63.8 (C^{13}), 52.8 (C^{7}), 34.3 (C^{18}), 31.4 (C^{19}), (1 × ArC missing – coincidental).

HRMS (ESI): *m/z*: 611.3250 $[M+H]^+$, $C_{41}H_{42}N_2O_3$ requires 611.3268.

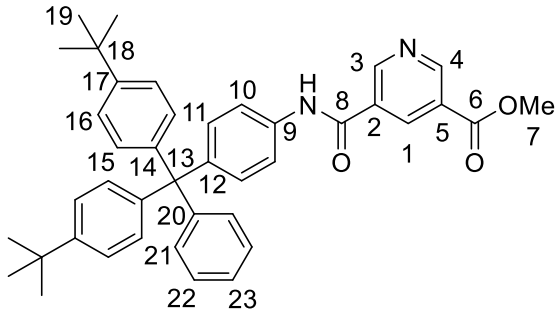

The data is consistent with the literature values.

3.10 5-(4-(Bis(4-*tert*-butylphenyl)(phenyl)methyl)phenylcarbamoyl)nicotinic acid[9]

To ester **3.9** (714 mg) in THF (10 mL) and water (10 mL) KOH (90 mg, 1.6 mmol) was added and the solution allowed to stir for 16 h. The solution was neutralised with 10% citric acid and washed with CH_2Cl_2 (3 × 30 mL). The organic layers were combined and dried with $MgSO_4$ and the solvent removed *in vacuo* to leave the product as an orange solid (586 mg, 84%).

^{1}H NMR (400 MHz, d_6 - acetone) δ: 9.97 (s br, 1H, $C^{6}O_2H$), 9.36 (d, 1H, ^{4}J = 2.1 Hz, $C^{4}H$), 9.29 (d, 1H, ^{4}J = 2.1 Hz, $C^{3}H$), 8.82 (t, 1H, ^{4}J = 2.1 Hz, $C^{1}H$), 8.00 (s br, 1H, $C^{8}NH$), 7.78 (dt, 2H, ^{3}J = 8.8 Hz, ^{4}J = 2.0 Hz, $C^{9}H$), 7.15-7.37 (m, 16H, ArH), 1.32(s, 18H, $C^{18}H$),

$^{13}C\{^{1}H\}$ NMR (100 MHz, d_6 - acetone) δ: 165.1 (C^{7}), 16.30 (C^{6}), 152.7 (C^{4}), 152.4 (C^{3}), 148.4, 147.2, 144.0, 143.1, 136.8, 135.8 (C^{1}), 131.2, 130.9, 130.8, 130.6, 127.4, 126.1, 125.8, 124.3, 119.2 (C^{9}), 63.8 (C^{12}), 34.0 (C^{17}), 30.8 (C^{18}).

HRMS (ESI): *m/z*: 597.3099 $[M+H]^+$, $C_{40}H_{40}N_2O_3$ requires 597.3112.

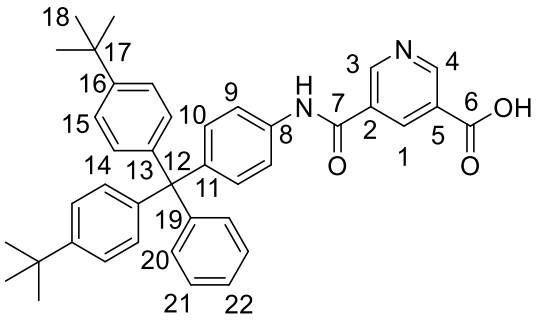

The data is consistent with literature values.

3.11 N^3-((Bis(4-*tert*-butylphenyl)(phenyl)methyl)phenyl-glycine)-N^5-((Bis(4-*tert*-butylphenyl)(phenyl)methyl)phenyl pyridine-3,5-dicarboxamide

Carboxylic acid **10** (270 mg, 0.452 mmol) was suspended in dry CH_2Cl_2 (20 mL), to which oxalyl chloride (0.04 mL, 57 mg, 0.452mmol) and a drop of dry DMF (cat) was added. The reaction mixture was stirred under Ar until all solids were dissolved, the solvent and excess oxalyl chloride were then removed by distillation. The resulting acid chloride was redissolved in dry CH_2Cl_2 (30 mL), triethylamine (0.09 mL, 69 mg, 0.678 mmol) and then amine **2.28** (227 mg, 2.23 mmol) were added and the mixture was stirred for 1 h under Ar. The solution was washed with 1 mol dm^{-3} $HCl_{(aq)}$ (2 × 25 mL) 1M $NaOH_{(aq)}$ (2 × 25 mL) and water (2 × 25 mL), dried with $MgSO_4$ and the solvent removed *in vacuo*. The solid was then purified by flash chromatography (silica, 98:2 CH_2Cl_2:MeOH) to give the product as a yellow solid (224 mg, 46%).

R_f = 0.30 (98:2 CH_2Cl_2:MeOH)

Mp = 220-222 °C

^{1}H NMR (400 MHz, d_6 - acetone) δ: 9.94 (s, 1H, C^2NH), 9.48 (s, 1H, C^6NH), 9.25 (d, 1H, ^4J = 2.1 Hz, $C^{3/4}$H), 9.22 (d, 1H, ^4J = 2.1 Hz, $C^{3/4}$H), 8.76 (t, 1H, ^4J = 2.1 Hz, C^1H), 8.57 (t, br, 1H, ^3J = 5.7 Hz, C^6NH), 7.77 (d, 1H, ^3J = 8.9 Hz, C^9H), 7.55 (d, 1H, ^3J = 8.9 Hz, C^{26}H), 7.11-7.37 (m, 30H, ArH), 4.29 (d, 2H, ^4J = 5.7 Hz, C^{23}H), 1.342 (s, 9H, $C^{18/35}$H), 1.32 (s, 9H, $C^{18/35}$H).

$^{13}C\{^{1}H\}$ NMR (100 MHz, d_6 - acetone) δ: 167.4 (C^{24}), 165.1 (C^{7}), 163.3 (C^{3}), 151.1, 150.8 ($C^{3,4}$), 148.4, 148.4, 147.2, 144.0, 143.0, 142.4, 236.8, 136.7 (8 × ArC), 133.8 (C^{1}), 131.2, 131.2, 130.9, 130.8, 130.6, 130.6, 130.5, 129.3, 127.5, 127.4, 125.8, 125.8, 124.3, 124.3 (14 xArC), 119.1, 118.4 ($C^{9, 26}$), 63.8, 63.7 ($C^{12,29}$), 43.8 (C^{23}), 34.0, 34.0 ($C^{34,17}$), 30.7 ($C^{18, 35}$) (2 × ArC and 1 × CH_3 missing – coincidental).

HRMS (ESI): *m/z*: 1083.6153 $[M+H]^+$, $C_{75}H_{78}N_4O_3$ requires 1083.6147.

IR υ_{max}: 3318 (m, CONH), 3055 (m, CONH), 2956 (m, CH_3/CH_2), 2905 (m, CH_3/CH_2), 2867 (m, CH_3/CH_2), 1655 (s, CONH), 1599 (s, py), 1507 (s, Ar).

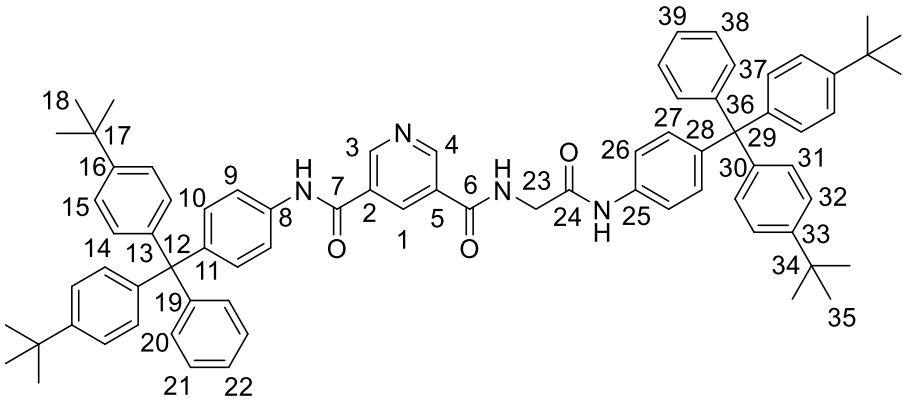

3.12 Tetraethylene glycol monotosylate[10]

To NaOH (0.81 g, 20.3 mmol) in water (4.5 mL), THF (4.5 mL) and tetraethylene glycol (26.4 mL, 152 mmol) were added and the resulting solution was cooled to 0 ºC. A solution of *p*-toluenesulfonyl chloride (2.49 g, 13.1 mmol) in THF (15 mL) was added slowly over 15 minutes, the mixture was allowed to stir for 2 h at 0 ºC, when it was then poured over ice water. The organic layer was separated and the aqueous layer was washed with CH_2Cl_2 (3 × 30 mL). The organic layers were combined and washed with water (3 × 30 mL), dried with $MgSO_4$ and the solvent removed *in vacuo* to leave the product as a colourless oil (3.66 g, 80%).

^{1}H NMR (400 MHz, $CDCl_3$) δ: 7.81 (d, 2H, ^{3}J = 8.2 Hz, $C^{4}H$), 7.36 (d, 2H, ^{3}J = 8.2 Hz, $C^{3}H$), 4.18 (t, 2H, ^{3}J = 4.8 Hz, $C^{6}H$), 3.74-3.56 (m, 14H, OCH_2), 2.46 (s, 3H, $C^{1}H$).

$^{13}C\{^{1}H\}$ NMR (100 MHz, $CDCl_3$) δ: 144.8 (C^5), 133.0 (C^2), 129.8 (C^3), 128.0 (C^4), 72.5, 70.7, 70.7, 70.5, 70.3, 69.3(6 × OCH_2), 68.7 (C^6), 61.7 (C^{13}), 21.6 (C^1).

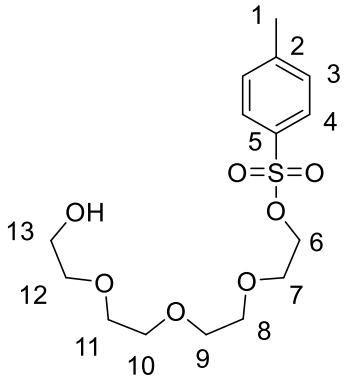

The obtained data is consistent with literature values.

3.13 Tetraethylene glycol mono-4-benzonitile

To compound **3.12** (3.66 g, 10.5 mmol) in dry CH_3CN (25 mL) K_2CO_3 (3.37 g, 26.3 mmol) then 4-hydroxybenzonitrile (1.88 g, 15.8 mmol) were added. The resulting mixture was heated to reflux for 48 h, under an Ar atmosphere, then allowed to cool. The suspension was filtered under suction and the solvent removed *in vacuo*. The resulting oil was dissolved in CH_2Cl_2 (50 mL) and washed with $NaOH_{(aq)}$ (1 mol dm^{-3}, 25 mL). The $NaOH_{(aq)}$ solution was washed with CH_2Cl_2 (2 × 25 mL) and the organic layers were combined, dried over $MgSO_4$ and the solvent removed *in vacuo* to leave the product as a colourless oil (2.89 g, 93%).

^{1}H NMR (400 MHz, $CDCl_3$) δ: 7.59 (dt, 2H, ^{3}J = 9.0 Hz, ^{3}J = 2.7 Hz, C^3H), 6.99 (dt, 2H, ^{3}J = 9.0 Hz, ^{3}J = 2.1 Hz, C^4H), 4.20 (t, 2H, ^{3}J = 4.7 Hz, C^6H), 3.89 (t, 2H, ^{3}J = 4.7Hz, C^7H), 3.66-3.77 (m, 12H, CH_2O), 3.62 (m, 2H, $C^{13}H$).

$^{13}C\{^{1}H\}$ NMR (100 MHz, $CDCl_3$) δ: 162.1 (C^5), 134.0 (C^3), 119.2 (C^1), 115.3 (C^4), 104.1 (C^2), 72.5, 70.9, 70.7, 70.6, 70.3 (5 × CH_2O), 69.4 (C^7), 67.7 (C^6), 61.7 (C^{12}).

HRMS (ESI): *m/z*: 318.1307 $[M+Na]^+$, $C_{15}H_{21}N_1O_5$ requires 318.1312.

IR υ_{max}: 3484 (s, OH) 2872, (s, OH), 2226 (s, CN), 1605 (m, Ar) 1508 (m, Ar).

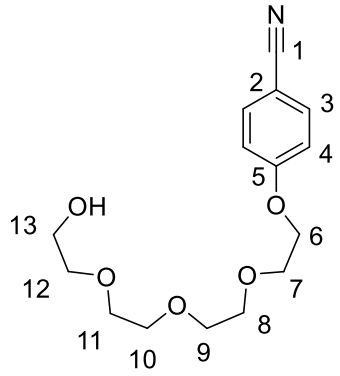

3.14 Tosylate of tetraethylene glycol 4-benzonitrile

To a solution compound **3.13** (2.80 g, 9.48 mmol) in dry CH_2Cl_2 (30 mL) cooled to 0 ^oC, NEt_3 (1.99 mL, 1.43 g, 10.42 mmol), DMAP (cat.) and *p*-toluenesulfonyl chloride (1.95 g, 10.2 mmol) was added. The reaction was stirred for 16 hours at RT, under an Ar atmosphere. CH_2Cl_2 (25 ml) and water (25 mL) were added and then the solution was neutralised with $HCl_{(aq)}$ (1 mol dm^{-3}). The organic layer was separated, washed with water (2 × 25 mL), brine (2 × 25 mL), dried with $MgSO_4$ and the solvent was removed *in vacuo* to give the product as a yellow oil (4.15 g, 97%)

^{1}H NMR (400 MHz, $CDCl_3$) δ: 7.84 (dt, 2H, ^3J = 8.4 Hz, ^4J = 1.7 Hz, $C^{15}H$), 7.58 (dt, 2H, ^3J = 9.0 Hz, ^4J = 2.1 Hz, C^3H), 7.35 (d, 2H, ^3J = 8.4 Hz, $C^{16}H$), 6.98 (dt, 2H, ^3J = 9.0 Hz, ^4J = 2.1 Hz, C^4H), 4.17 (t, 2H, ^3J = 4.7 Hz, C^6H), 4.16 (t, 2H, ^3J = 4.9 Hz, $C^{13}H$), 3.89 (t, 2H, ^3J = 4.7 Hz, C^7H), 3.64-3.75 (m, 6H, CH_2O), 2.45 (s, 3H, $C^{18}H$).

^{13}C{^{1}H} NMR (100 MHz, $CDCl_3$) δ: 162.1 (C^5), 144.8 (C^{14}), 134.0 (C^3), 133.0 (C^{17}), 129.8 (C^{16}), 128.0 (C^{15}), 119.2 (C^1), 115.4 (C^4), 104.0 (C^2), 70.9, 70.8, 70.7, 70.6 (4 × CH_2O), 69.4 (C^7), 69.2 (C^{13}), 67.8 (C^6), 21.6 (C^8).

HRMS (ESI): *m/z*: 472.1378 $[M+Na]^+$, $C_{22}H_{27}N_1O_7$ requires 472.1400.

IR υ_{max}: 2872 (s, br, CH_2), 2225 (s, CN), 1605 (m, Ar), 1508 (m, Ar).

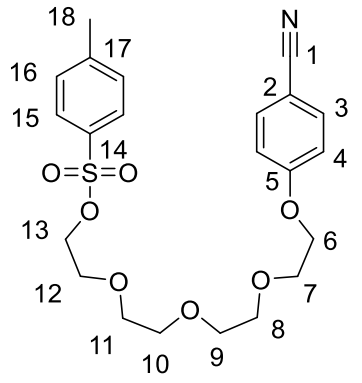

3.15 Bis-nitrile asymmetric macrocycle precursor

To compound **3.14** (3.97 g, 8.83 mmol) in dry CH_3CN (25 mL) K_2CO_3 (1.70 g, 13.3 mmol) and then compound **2.12** (1.32 g, 8.83 mmol) were added. The resulting mixture was heated to reflux for 48 h, under an Ar atmosphere, then allowed to cool. The suspension was filtered under suction and the solvent removed *in vacuo*. The resulting oil was dissolved in Et_2O and the precipitate removed by filtration and the solvent removed *in vacuo*. The resulting oil was then dissolved in CH_2Cl_2 and the precipitate removed by filtration and the solvent removed *in vacuo* to leave a brown oil (3.57 g, 94%) contaminated with a small amount of tosylate.

^{1}H NMR (400 MHz, $CDCl_3$) δ: 7.58 (dt, 2H, ^3J = 9.0 Hz, ^4J = 2.1 Hz, C^3H), 6.97 (d, 2H, ^3J = 9.0 Hz, C^4H), 6.94 (dt, 2H, ^3J = 9.4 Hz, ^4J = 2.9 Hz, $C^{15/16}H$), 6.89 (dt, 2H, ^3J = 9.4 Hz, ^4J = 2.9 Hz, $C^{15/16}H$), 4.73 (s, 2H, $C^{18}H$), 4.18 (t, 2H, ^3J = 4.7 Hz, C^6H), 4.09 (t, 2H, ^3J = 4.8 Hz,C^7H), 3.88 (t, 2H, ^3J = 4.7 Hz, C^7H), 3.85 (t, 2H, ^3J = 4.8 Hz, $C^{12}H$), 3.68-3.76 (m, 8H, CH_2O).

^{13}C{^{1}H} NMR (100 MHz, $CDCl_3$) δ: 162.1 (C^5), 154.8 (C^{17}), 150.8 (C^{14}), 134.0 (C^3), 119.2 (C^1), 116.7, 115.8 ($C^{4,5}$), 115.4 (C^{19}), 115.3 (C^4), 104.1 (C^2), 70.9, 70.8, 70.7 (3 × CH_2O), 69.8 (C^{12}), 69.4 (C^7), 68.0 (C^{13}), 67.8 (C^6), 54.8 (C^{18}).

HRMS (ESI): *m/z*: 449.1683 $[M+Na]^+$, $C_{23}H_{34}N_2O_6$ requires 449.1683.

IR υ_{max}: 2922 (s, CH_2), 2873 (s, CH_2) , 2224 (s, CN), 1605 (m, ArH), 1506 (m, ArH).

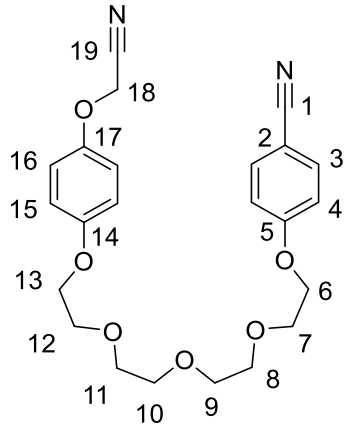

3.16 Neutral asymmetric isophthalamide macrocycle

Pyridinium axle **2.19** (330 mg, 0.801 mmol) was dissolved in dry CH_2Cl_2 (50ml) to which bis amine **3.3** (348 mg, 0.801 mmol) was added and the mixture was stirred for 30 minutes, at RT under Ar. NEt_3 (123 mg, 0.17 mL, 1.22mmol) was added and then isophthaloyl chloride (118 mg, 0.582 mmol) in CH_2Cl_2 (10 mL) was added dropwise and the reaction was left for 1 h, at RT under Ar. The mixture was washed with 10% $HCl_{(aq)}$ (2 × 25 mL) and then water (1 × 25 mL). The organic layer was dried with $MgSO_4$ and the solvent removed *in vacuo* to yield a yellow solid. The yellow solid was purified by column chromatography (silica, 99:1 to 98:2 CH_2Cl_2:MeOH) to obtain a white solid, contaminated with small amounts of pyridinium axle **2.19**. The solid was washed with ice cold MeOH to yield the product as a white solid (82 mg, 30%).

R_f = 0.30 (99:1 CH_2Cl_2:MeOH)

Mp = 164-165 °C

^{1}H NMR (400 MHz, 1:1 $CDCl_3$:CD_3OD) δ: 8.01 (dt, 1H, ^3J = 7.7 Hz, ^3J = 1.4Hz, $C^{24/26}H$), 7.97 (dt, 1H, ^3J = 7.7Hz, ^4J = 1.6 Hz, $C^{24/26}H$), 7.95 (s, 1H, $C^{22}H$), 7.49 (t, 1H, ^3J = 7.7 Hz, $C^{25}H$), 7.23 (t, 1H, ^3J = 8.6 Hz, C^3H), 6.87 (t, 1H, ^3J = 5.4 Hz, $C^{27}NH$), 6.82 (dt, 2H, ^3J = 6.7Hz, ^3J = 2.0 Hz, C^4H), 6.79-6.74 (m, 4H $C^{15/16}$), 6.68 (t, 1H, ^3J = 5.2 Hz, $C^{20}NH$), 4.55 (d, 2H, ^3J = 5.4 Hz, C^1H), 4.10 (t, 2H, ^3J = 5.1 Hz, CH_2O), 4.02-4.08 (m, 4H, CH_2O), 3.87 (t, 2H, ^3J = 4.8 Hz, CH_2O), 3.85-3.79 (m, 4H, CH_2O CH_2N), 3.69-3.77 (m, 4H, CH_2O).

$^{13}C\{^{1}H\}$ NMR (100 MHz, 1:1 $CDCl_3$:CD_3OD) δ: 167.0 ($C^{20/27}$), 166.6 ($C^{20/27}$), 158.3 (C^{5}), 153.3 ($C^{14/17}$), 152.6 ($C^{14/17}$), 134.5 ($C^{21/23}$), 134.4 ($C^{21/23}$), 131.0 ($C^{24/26}$), 130.8 ($C^{24/26}$), 130.1 (C^{2}), 129.3 (C^{25}), 129.3 (C^{23}), 115.7 ($C^{15/16}$), 115.4 ($C^{15/16}$), 114.8 (C^{4}), 70.9, 70.8, 70.8, 70.7, 69.7, 69.6, 68.2, 67.5, 67.0 (9 × OCH_2) 43.8 (C^{1}), 39.7 (C^{19}).

HRMS (ESI): *m/z*: 587.2355 $[M+Na]^+$, $C_{31}H_{36}N_2O_8$ requires 587.2364.

IR υ_{max}: 3331 (m, CONH), 3268 (m, CONH), 3060 (w, ArH), 2920 (m, CH_2), 2876 (m, CH_2), 1644 (s, CONH), 1544 (s, Ar), 1508 (s, Ar).

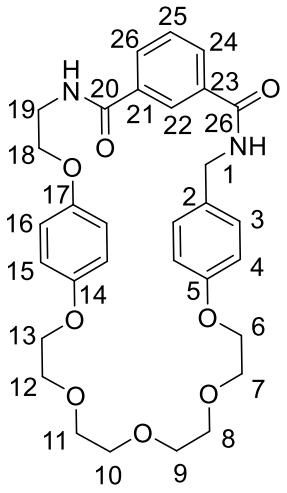

3.17 Pyridinium iodide macrocycle

Pyridinium macrocycle **3.18** (109 mg, 0.193 mmol) in $CHCl_3$ (5 mL) and MeI (2 mL) was refluxed for 16 h. The solvent was removed *in vacuo* to afford the iodide salt in quantitative yield as an orange solid, still contaminated with amounts of pyridinium template **2.19** (136 mg,).

^{1}H NMR (400 MHz, 1:1 $CDCl_3$:CD_3OD) δ: 9.43 (s, br, 1H $C^{22}H$), 9.28 (s, br, 2H, $C^{24,25}H$), 9.00 (t, br, 1H, ^{3}J = 5.4 Hz, $C^{20}NH$), 8.87 (t, br, 1H, ^{3}J = 5.2 Hz, $C^{26}NH$), 7.24 (d, 2H, ^{3}J = 8.4 Hz, $C^{17}H$), 6.79 (d, 2H, ^{3}J = 9.0 Hz, $C^{4/5}H$), 6.71 (d, 2H, ^{3}J = 8.4 Hz, $C^{16}H$), 6.67 (d, 2H, ^{3}J = 9.0 Hz, $C^{4/5}H$), 4.51 (s, 2H, $C^{19}H$), 4.49 (s, 3H, $C^{27}H$), 4.19 (t, 2H, ^{3}J = 4.7 Hz, $C^{2}H$), 3.89-3.96 (m, 4H, $C^{7,14}H$), 3.76-3.87 (m, 6H, $C^{1}H$, 2 × OCH_2), 3.75-3.72 (m, 4 × OCH_2).

$^{13}C\{^{1}H\}$ NMR (100 MHz, 1:1 $CDCl_3$:CD_3OD) δ: 158.0 (C^{15}), 152.9 ($C^{3/6}$), 152.8 ($C^{3/6}$), 147.0 (C^{22}), 140.7 ($C^{24,25}$), 134.1 ($C^{21,23}$), 129.6 (C^{17}), 129.5 (C^{18}), 115.5 ($C^{4/5}$), 115.2 ($C^{4/5}$), 114.4 (C^{16}), 70.5, 70.5, 70.5, 69.6 (6 × OCH_2, coincidental overlap), 68.0 ($C^{7/14}$), 67.6 ($C^{7/14}$), 66.3 (C^{2}), 48.9 (C^{27}), 43.5 (C^{19}), 40.5 (C^{1}).

(Absence of carbonyl carbon signals is attributed to dynamic behaviour of the macrocycle, resulting in weak and broad behaviour in both ^{1}H and $^{13}C\{^{1}H\}$ NMR spectra of peaks near the pyridinium moiety)

HRMS (ESI): *m/z*: 580.2658 $[M]^+$, $C_{31}H_{38}N_3O_8$ requires 580.2653.

IR υ_{max}: 3224 (m, CONH), 3058 (m, ArH), 2922 (m, CH_2), 2871 (s, OCH_2), 1662 (s, CONH), 1627 (w, Py), 1610 (w, Py), 1543 (s, ArH), 1508 (s, ArH)

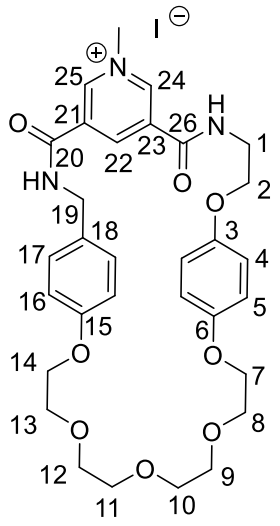

3.18 Asymmetric Pyridine Macrocycle

Pyridinium axle **2.19** (200 mg, 0.486 mmol) was dissolved in dry CH_2Cl_2 (20ml) to which bis amine **3.3** (211 mg, 0.486 mmol) was added and the mixture was stirred for 30 minutes. NEt_3 (242 mg, 0.34 mL, 2.40 mmol) was added and then isophthaloyl chloride (167 mg, 0.960 mmol) in CH_2Cl_2 (20 mL) was added dropwise and the reaction was left for 1 h. The mixture was washed with 10% citric acid (2 × 50 mL) and then water (1 × 50 mL). The organic layer was dried with $MgSO_4$ and the solvent removed *in vacuo* to yield a yellow solid. The yellow solid was purified by column

chromatography (silica, 95:5 CH_2Cl_2:MeOH) to obtain a yellow white solid, contaminated with small amounts of pyridinium axle **2.19**. The solid was purified twice more by column chromatography (silica, 97:3 CH_2Cl_2:MeOH) to afford a yellow solid contaminated with smaller amounts of pyridinium template **2.19** (125 mg, 30%).

R_f = 0.29 (97:3 CH_2Cl_2:MeOH)

^{1}H NMR (400 MHz, 1:1 $CDCl_3$:CD_3OD) δ: 9.11 (dd, 2H, ^3J = 12.5 Hz, ^4J = 2.1 Hz, $C^{24/25}$H), 8.51 (t, 1H, ^4J = 2.1 Hz, C^{22}H), 7.28 (d, 2H, ^3J = 8.6 Hz, C^{17}H), 6.81 (d, 2H, ^3J = 8.6 Hz, C^{16}H), 6.73-6.78 (m, 4H, $C^{4,5}$H), 4.51 (1H, s, C^{19}H), 3.98-4.06 (m, 4H, $C^{7,14}$H), 3.82-3.86 (m, 2H, C^{13}H), 3.77-3.81 (m, 4H, $C^{1,8}$H), 3.68-3.74 (m, 8H, 4 × OCH_2).

^{13}C{^{1}H} NMR (100 MHz, 1:1 $CDCl_3$:CD_3OD) δ: 166.0 ($C^{20/26}$), 165.4 ($C^{20/26}$), 158.1 (C^{15}), 153.0 ($C^{3/6}$), 153.0 ($C^{3/6}$), 150.9 ($C^{24/25}$), 150.9 ($C^{24/25}$), 133.4 (C^{22}), 130.2 (C^{18}), 129.8 ($C^{21/23}$), 129.8 ($C^{21/23}$), 129.2 (C^{17}), 115.4 ($C^{4/5}$), 115.3 ($C^{4/5}$), 70.6, 70.6, 70.5 (4 × OCH_2, coincidental overlap), 69.6 ($C^{8,13}$), 68.0 (C^{14}), 67.4 (C^7) 66.7 (C^2), 43.3 (C^{19}), 39.9 (C^1).

HRMS (ESI): *m/z*: 566.2498 $[M+H]^+$, $C_{30}H_{36}N_3O_8$ requires 566.2497.

IR υ_{max}: 3299 (m, CONH), 3058 (m, ArH), 2919 (s, CH_2), 2872 (s, OCH_2), 1642 (s, CONH), 1541 (s, ArH), 1508 (s, ArH).

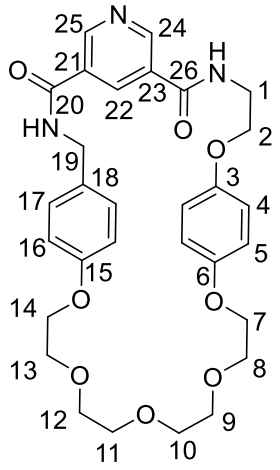

7.3.3. Experimental for Chapter 4

Compound **4.11** was kindly donated by Dr. Nicholas Evans.

4.6 1,3-Benzene Pyridyl Macrocycle

Method 1

DCC (130 mg, 0.630 mmol) and *N*-hydroxysuccinamide (73 mg, 0.630 mmol) were added to a solution of 2,6-Pyridine dicarboxylic acid (50.0 mg, 0.300 mmol) in dry MeCN (50 mL. The solution was stirred for 16 h at RT, under an Ar atmosphere. The reaction mixture was filtered by gravity and the solvent removed *in vacuo*, to leave a white solid. Bis-amine **2** dissolved in CH_2Cl_2 (200 mL) and the bis-*N*-hydroxysuccinamide ester dissolved in CH_2Cl_2 (200 mL), were added dropwise to NEt_3 (191 mg, 0.263 mL, 1.89 mmol) dissolved in CH_2Cl_2 (100 mL) at the same time at RT under an Ar atmosphere, the reaction was then stirred for 16h. The solvent volume was reduced to ¼ *in vacuo* and then washed with $HCl_{(aq)}$ (1 M, 100 mL) and NaOH (1 M, 100 mL), the organic layer was dried over $MgSO_4$ to leave a yellow solid. The solid was purified by column chromatography (silica, 99:1 CH_2Cl_2:MeOH) to obtain the product as a white solid, contaminated with DCC urea. The material was further purified by preparative TLC (197:3 CH_2Cl_2:MeOH), which removed some but not all of the DCC urea (34 mg, 22 %).

Method 2

2,6-Pyridine dicarboxylic acid (133 mg, 0.80 mmol) was dissolved in $SOCl_2$ (5 mL) with DMF (cat.), the solution was heated to reflux for 16h (using a condenser fitted with a $CaCl_2$ drying tube). The excess $SOCl_2$ was removed *in vacuo*, to leave the bis-acyl chloride, as a yellow solid. Bis-amine **2** dissolved in dry CH_2Cl_2 (200 mL) and the bis acyl-chloride dissolved in dry CH_2Cl_2 (200 mL), were added dropwise to NEt_3 (0.24 g, 0.33 mL, 2.4 mmol) dissolved in CH_2Cl_2 (200 mL) at the same time at RT under an Ar atmosphere, the reaction was then stirred for 16h. The solvent volume was reduced to ¼ *in vacuo* and then washed with $HCl_{(aq)}$ (1 M, 100 mL) and NaOH (1 M, 100 mL),

the organic layer was dried over $MgSO_4$ to leave a yellow solid. The solid was purified by column chromatography (silica, 99:1 CH_2Cl_2:MeOH) to give the product as a white solid (85 mg, 21 %).

Mp: 248-249 ^oC

^{1}H NMR (400 MHz, $CDCl_3$) δ: 8.21 (2H, t, ^3J = 5.9 Hz, $C^{11}NH$), 8.19 (2H, d, ^3J = 7.7 Hz, $C^{14}H$), 7.89 (1H, t, ^3J = 7.7 $C^{15}H$), 7.13-7.28 (12H, m, ArH), 4.56 (4H, d, ^3J = 6.0 Hz, $C^{11}H$), 4.49 (4H, s, C^6H),4.42 (4H, s, C^5H),

$^{13}C\{^1H\}$ NMR (100 MHz, $CDCl_3$) δ: 142.8 (C^{12}), 138.5, 136.8, 128.5, 128.4, 128.2, 128.1, 128.0, 127.5, 127.3, 127.2, 127.1 (11 × ArC), 72.0 ($C^{5,6}$), 46.3 (C^{11}).

IR υ_{max}: 3342 (m, br, CONH), 3293 (m, br, CONH), 3052 (w, ArH), 2851 (m, CH_2), 1677 (w, CON), 1653 (w, ArH), 1530 (w, ArH).

HRMS (ESI): *m/z*: 508.2216 $[M+H]^+$, $C_{31}H_{30}N_3O_4$ requires 508.2237.

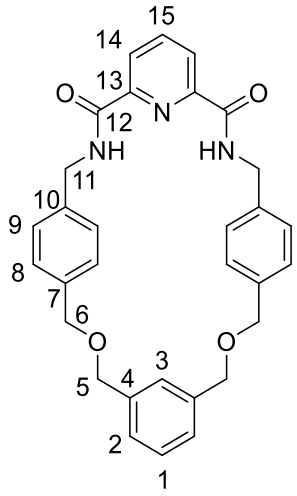

4.7 2,2-Diphenylethyl prop-2-yn-1-yl ether[11]

To 2,2-diphenylethanol (500 mg, 2.52 mmol) dissolved in dry THF (20 mL), NaH in mineral oil (60 %wt, 131 mg, 3.28 mmol) was added followed by 3-bromopropyne in toluene (80 %wt, 560 mg, 0.41 mL, 3.78 mmol). The reaction mixture was allowed to stir for 24 h at RT, under an Ar atmosphere. The reaction mixture was quenched with water and extracted with Et_2O (10 mL), the organic layer was dried over $MgSO_4$ and the solvent was removed *in vacuo* to leave a brown

solid. The solid was purified by column chromatography (silica, petrol and eluted with 95:5 petrol 40-60:EtOAc), with the product isolated as an off white waxy solid (456 mg, 77%)

^{1}H NMR (400 MHz, $CDCl_3$) δ: 7.15-7.34 (10H, m, $C^{1,2,3}H$), 4.31 (1H, t, ^{3}J = 7.4 Hz, $C^{5}H$), 4.17 (2H, d, ^{4}J = 2.4 Hz, $C^{7}H$), 4.08 (2H, d, ^{3}J = 7.4 Hz, $C^{6}H$), 2.43 (1H, t, ^{4}J = 2.4 Hz, $C^{9}H$).

$^{13}C\{^{1}H\}$ NMR (100 MHz, $CDCl_3$) δ: 141.9 (C^{4}), 128.5 (C^{2}), 128.3 (C^{1}), 126.6 (C^{3}), 79.6 (C^{8}), 74.6 (C^{6}), 72.9 (C^{9}), 58.3 (C^{7}), 50.9 (C^{5}).

IR υ_{max}: 3267 (s, C≡CH), 3065, (w, $COCH_2$), 3024 (w, br, ArH), 2892 (m, CH_2), 2864 (w, sp^3 CH), 2113 (w, C≡CH), 1597 (s, Ar), 1491 (m, Ar).

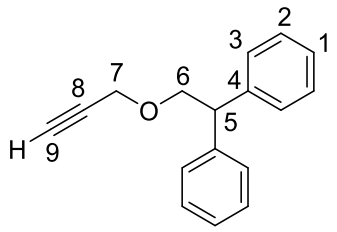

4.9 4,4-(Benzene-1,3-diylbis(methanediyloxymethanediyl)dibenzonitrile

NaH in mineral oil (60 %wt, 1.20 g, 29.0 mmol) was added to (1,3-benzene-diyl)dimethanol (2.00 g, 14.5 mmol) in dry THF (30 mL). Cyanobenzyl bromide (5.68 g, 28.96 mmol) was then added, the mixture stirred for 16 h, at RT under an Ar atmosphere. The reaction mixture was quenched with water and then extracted with CH_2Cl_2 (3 × 50 mL), dried over $MgSO_4$ and the solvent removed *in vacuo*, to leave a yellow solid. The solid was dry loaded onto a silica plug column, washed with petrol and then eluted with 50:50 petrol 40-60:EtOAc. The solvent was removed *in vacuo*, to leave the product, a yellow solid (4.14 g, 78%).

Mp: 74-76 ^{o}C

^{1}H NMR (400 MHz, $CDCl_3$) δ: 8.47 (4H, d, ^{3}J = 8.5 Hz, $C^{9}H$), 7.64 (4H, d, ^{3}J = 8.5 Hz, $C^{8}H$), 7.25-7.40 (4H, m, $C^{1,2,3}H$), 4.62 (4H, s, $C^{5}H$), 4.60 (4H, s, $C^{6}H$)

$^{13}C\{^{1}H\}$ NMR (100 MHz, $CDCl_3$) δ: 143.8 (C^7), 138.0 (C^9), 132.3, 128.8, 127.8, 127.3, 127.3 (6 × ArC), 118.8 (C^{11}), 72.6 (C^6), 71.3 (C^5),

IR υ_{max}: 3075 (w, ArH), 2853 (s, CH_2), 2223 (s, CN), 1610 (m, Ar), 1507 (m, Ar).

HRMS (ESI): *m/z*: 391.1417 $[M+Na]^+$, $C_{24}H_{20}N_2O_2$ requires 391.1423.

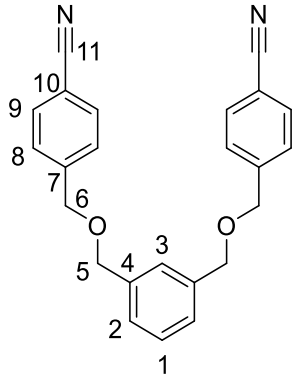

4.10 4,4-(Benzene-1,3-diylbis(methanediyloxymethanediyl))dibenzylamine

To a solution of bis-nitrile **4.9** (4.08 g, 11.1 mmol) in dry THF (40 mL), BH_3.THF (1 mol dm^{-3}, 44.0 mmol, 44.0 mL) was added dropwise. The reaction mixture was heated to reflux for 6 h under an Ar atmosphere. The reaction mixture was quenched with MeOH, concentrated $HCl_{(aq)}$ (10 mL) was added and the mixture was allowed to stir for a further 30 minutes at RT. The solvent was then removed *in vacuo* and the product was washed with cold methanol to leave a fluffy white solid. Half of the white solid was suspended in CH_2Cl_2 (200 mL) and 10% NaOH (200 mL). The biphasic mixture was stirred vigorously for 30 minutes, the organic layer was separated and washed with H_2O (2 × 100 mL) and dried over $MgSO_4$. The solvent was removed *in vacuo* to leave the product, an oily off white solid (2.10 g, 85%).

^{1}H NMR (400 MHz, $CDCl_3$) δ: 7.30-7.41 (12H, m, ArH), 4.58 (8H, s, $C^{5,6}H$), 3.89 (4H, s, $C^{11}H$).

$^{13}C\{^{1}H\}$ NMR (100 MHz, $CDCl_3$) δ: 142.9, 138.5, 136.8, 128.5, 128.2, 127.2, 127.1, 127.1 (8 × ArC), 72.0 ($C^{6,5}$), 46.3 (C^{11}).

IR υ_{max}: 3345 (m, br, NH_2), 3259 (m, br, NH_2), 2917 (m, CH_2), 2845 (s, CH_2), 1590 (m, NH_2), 1515 (s, Ar).

HRMS (ESI): *m/z*: 377.2207 $[M+H]^+$, $C_{24}H_{29}N_2O_2$ requires 377.2229.

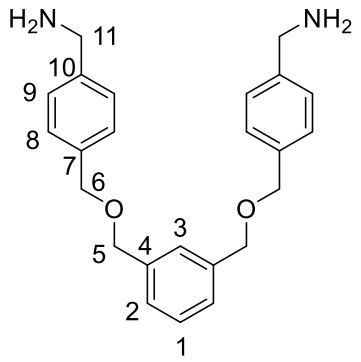

4.11 Pd templated pseudorotaxane

Macrocycle **4.6** (27 mg, 0.053 mmol) was dissolved in dry MeCN (1.5 mL) and dry CH_2Cl_2 (1.5 mL), to which $Pd(OAc)_2$ (12 mg, 0.053 mmol) was added and the solution stirred at RT for 2 h, under an Ar atmosphere. The solvent was removed *in vacuo* to give the Pd complexed macrocycle, a yellow solid. The Pd complexed macrocycle and bis azide axle **4.8** (18 mg, 0.053 mmol), were dissolved in dry CH_2Cl_2 (3 mL) and stirred at RT for 1 h, under an Ar atmosphere. The solvent was removed *in vacuo* to leave the product, a brown solid in a quantitative yield (54 mg).

^{1}H NMR (400 MHz, $CDCl_3$) δ: 10.28 (1H, s, C^3H), 9.21 (1H, t, ^3J = 4.9 Hz, C^4NH), 8.89 (1H, s, C^1H), 8.07 (1H, t, ^3J = 7.7 Hz, C^oH), 7.72 (2H, d, ^3J = 7.7 Hz, C^nH), 7.41 (1H, s, ^3J = 6.0 Hz, C^dH), 7.26 (1H, t, ^3J = 7.8 Hz, C^aH), 7.12 (2H, d, ^3J = 7.1 Hz, C^bH), 7.08 (4H, d, ^3J = 8.1 Hz, C^iH), 6.91 (1H, s, $C^{3'}H$), 6.76 (4H, d, ^3J = 8.1 Hz, C^hH), 5.91 (1H, t, ^3J = 5.4 Hz, $C^{4'}NH$), 5.22 (2H, d, ^3J = 14.9 Hz), 4.71 (2H, d, ^3J = 11.7 Hz), 4.52 (2H, d, ^3J = 11.5 Hz), 4.40 (2H, q, ^3J = 11.0 Hz) ($C^{e,f,k}H$), 3.42 (2H, q, ^3J = 6.1 Hz, C^5H), 3.15 (2H, t, ^3J = 6.7 Hz, C^7H), 2.97 (6H, m, $C^{5',e,f,k}H$), 1.69 (2H, q, ^3J = 6.7 Hz, C^6H), 1.50 (2H, q, ^3J = 7.0 Hz, $C^{6'}H$).

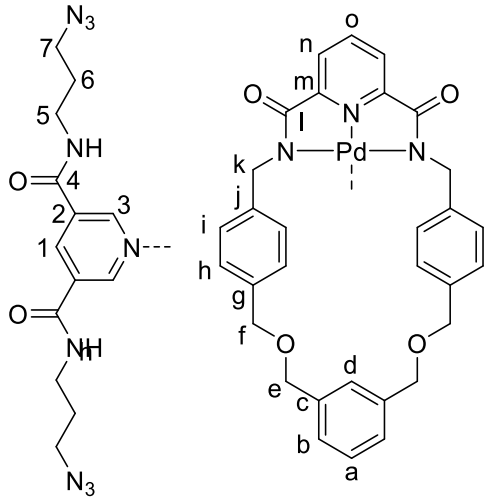

4.12 Polyether Pyridyl Macrocycle[12]

2,6-Pyridine dicarboxylic acid (226 mg, 1.35 mmol) was dissolved in $SOCl_2$ (5 mL) with DMF (cat.), the solution was heated to reflux for 16h (using a condenser fitted with a $CaCl_2$ drying tube). The excess $SOCl_2$ was removed *in vacuo*, to leave the bis-acyl chloride, as a yellow solid. Bis-amine **4.14** (0.47 g, 1.35 mmol) dissolved dry CH_2Cl_2 (250 mL) and the bis acyl-chloride dissolved in dry CH_2Cl_2 (250 mL), were added dropwise to NEt_3 (0.34 g, 0.47 mL, 3.4 mmol) dissolved in CH_2Cl_2 (300 mL) at the same time at RT under an Ar atmosphere, the reaction was then stirred for 16h. The solvent volume was reduced to ¼ *in vacuo* and then washed with $HCl_{(aq)}$ (1 M, 100 mL) and NaOH (1 M, 100 mL), the organic layer was dried over $MgSO_4$ to leave a yellow solid. The solid was purified by column chromatography (silica, 98:2 CH_2Cl_2:MeOH) to give the product as a white solid (92 mg, 14 %).

^{1}H NMR (400 MHz, $CDCl_3$) δ: 7.21 (2H, d, ^3J = 7.8 Hz, $C^{11}H$), 8.13 (2H, br s, C^8NH), 7.94 (1H, s, ^3J = 7.8 Hz, $C^{12}H$), 7.21, 7.13 (8H, d, ^3J = 8.1 Hz, $C^{5,6}H$), 4.56 (4H, d, ^3J = 5.4 Hz C^8H), 4.48 (4H, s, C^3H), 3.64 (8H, m, $C^{1,2}H$).

^{13}C{^{1}H} NMR (100 MHz, $CDCl_3$) δ: 163.3 (C^9), 148.6 (C^{10}), 139.4 (C^{12}), 139.7, 137.1 ($C^{4,7}$), 128.3, 127.6 ($C^{5,6}$), 125.1 (C^{11}), 72.9 (C^3), 70.8, 69.7 ($C^{1,2}$), 43.2 (C^8).

HRMS (ESI): *m/*z: 510.1802 $[M+Cl]^{+-}$, $C_{27}H_{29}N_3O_5$ requires 510.1801.

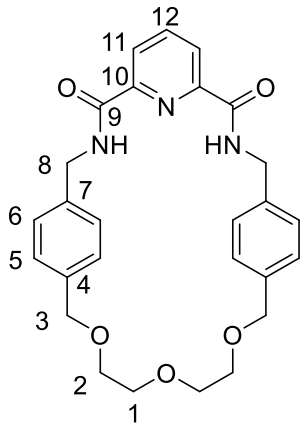

The obtained data is consistent with literature values.

4.13 4,4'-[Oxybis(ethane-2,1-diyloxymethanediyl)]dibenzonitrile[12]

NaH (0.73 g, 18.4 mmol, 60% dispersion in mineral oil) was added to diethylene glycol (0.72 mL, 0.81 g, 7.7 mmol) in dry THF (35 mL). Cyanobenzyl bromide (3.00 g, 15.3 mmol) was then added, the mixture stirred for 2 h, at RT under an Ar atmosphere. The reaction mixture was quenched with water and then extracted with CH_2Cl_2 (3 × 50 mL), dried over $MgSO_4$ and the solvent removed *in vacuo*, to leave a yellow solid. The solid was dry loaded onto a silica plug column, washed with petrol and then eluted with 50:50 petrol 40-60:EtOAc. The solvent was removed *in vacuo*, to leave the product, a colourless oil that solidifies to a waxy yellow solid (2.37 g, 92%).

^{1}H NMR (400 MHz, $CDCl_3$) δ: 7.64 (4H, dt, ^3J = 8.4 Hz, ^4J = 1.8 Hz, C^5H), 7.47 (4H, d, ^3J = 8.4 Hz, C^6H), 4.64 (4H, s, C^3H), 4.31 (8H, m, $C^{1,2}H$),

$^{13}C\{^1H\}$ NMR (100 MHz, $CDCl_3$) δ: 143.9 (C^4), 132.2 (C^2), 127.7 (C^1), 118.8 (C^3), 111.3 (C^8), 72.3 (C^3), 70.7, 70.1 ($C^{1,2}$).

HRMS (ESI): *m/z*: 359.1354 $[M+Na]^+$, $C_{20}H_{20}N_2O_3$ requires 259.1366.

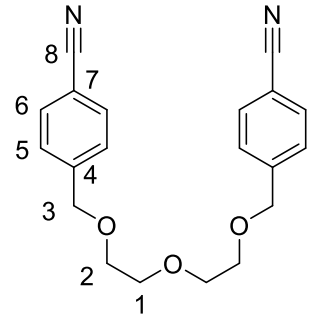

The data was consistent with literature values.

4.14 Polyether bis-amine[12]

To a solution of bis-nitrile **4.13** (2.19 g, 6.5 mmol) in dry THF (20 mL), BH_3.THF (1 mol dm^{-3}, 26.0 mmol, 26.0 mL) was added dropwise. The reaction mixture was heated to reflux for 6 h under an Ar atmosphere. The reaction mixture was quenched with MeOH, concentrated $HCl_{(aq)}$ (10 mL) was added and the mixture was allowed to stir for a further 30 minutes at RT. The solvent was then removed *in vacuo*. The resulting solid was suspended in CH_2Cl_2 (100 mL) and 10% NaOH (100 mL). The biphasic mixture was stirred vigorously for 30 minutes, the organic layer was separated and washed with H_2O (2 × 50 mL) and dried over $MgSO_4$. The solvent was removed *in vacuo* to leave the product, an oily off white solid (1.05 g, 46%).

^{1}H NMR (400 MHz, $CDCl_3$) δ: 7.21 (4H, m, $C^{5,6}H$), 4.48 (4H, s, C^3H), 3.77 (4H, s, C^8H), 3.58 (8H, m, $C^{1,2}H$), 1.97 (4H,s br, C^8NH).

^{13}C{^{1}H} NMR (100 MHz, $CDCl_3$) δ: 142.7, 136.8 ($C^{7,8}$), 128.1, 127.1 ($C^{5,6}$), 73.0 (C^3), 70.7, 69.4 ($C^{1,2}$), 46.3 (C^8).

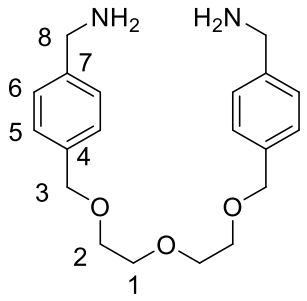

The obtained data is consistent with literature values.

4.19 Pd templated benzene pyridyl macrocycle pyridine complex

Macrocycle **4.6** (5 mg, 0.021 mmol) was dissolved in dry MeCN (0.5 mL) and dry CH_2Cl_2 (0.5 mL), to which $Pd(OAc)_2$ (2.9 mg, 0.021 mmol)was added and the solution stirred at RT for 2 h, under an Ar atmosphere. The solvent was removed *in vacuo* to give the Pd complexed macrocycle, a yellow solid. The Pd complexed macrocycle was dissolved in dry CH_2Cl_2 (1 mL) and one drop of pyridine was added. The mixture was stirred at RT for 1 h, under an Ar atmosphere. The solvent was removed *in vacuo* to leave the product, a brown solid (13 mg, 92 %)

^{1}H NMR (400 MHz, $CDCl_3$) δ: 8.55 (2H,br s, C^aH), 8.05 (1H, t, ^3J = 7.8 Hz, $C^{15}H$), 7.81 (2H, d, ^3J = 7.8 Hz, $C^{14}H$), 7.67 (1H, t, ^3J = 7.7 Hz, ^4J = 1.6 Hz, C^bH), 7.38 (1H, t, ^3J = 7.7 Hz, ^4J = 1.6 Hz, $C^{b'}H$), 7.30-7.13 (5H, m, ArH, PyH), 6.93 (4H, d, ^3J = 8.1 Hz, $C^{8,9}H$), 6.66 (4H, d, ^3J = 8.1 Hz, $C^{8,9}H$), 5.39 (2H, br S, $C^{11}H$), 4.48 (4H, S, C^6H), 4.36 (4H, S, C^5H), 3.13 (2H, br S, $C^{11'}H$).

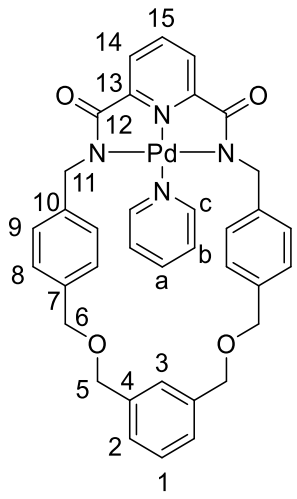

4.20 Pd templated polyether pyridyl macrocycle pyridine complex

Macrocycle **4.20** (10 mg, 0.021 mmol) was dissolved in dry MeCN (0.5 mL) and dry CH_2Cl_2 (0.5 mL), to which $Pd(OAc)_2$ (2.9 mg, 0.021 mmol)was added and the solution stirred at RT for 2 h, under an Ar atmosphere. The solvent was removed *in vacuo* to give the Pd complexed macrocycle, a yellow solid. The Pd complexed macrocycle was dissolved in dry CH_2Cl_2 (1 mL) and one drop of pyridine was added. The mixture was stirred at RT for 1 h, under an Ar atmosphere. The solvent was removed *in vacuo* to leave the product, a brown solid (13 mg, 92 %)

^{1}H NMR (400 MHz, $CDCl_3$) δ: 8.53 (1H,br s, $C^{a}H$), 8.05 (1H, t, ^{3}J = 7.8 Hz, $C^{12}H$), 7.80 (2H, d, ^{3}J = 7.8 Hz, $C^{12}H$), 7.61 (1H, t, ^{3}J = 7.6 Hz, ^{4}J = 1.7 Hz, $C^{b}H$), 7.36 (1H, t, ^{3}J = 7.6 Hz, ^{4}J = 1.7 Hz, $C^{b'}H$), 7.22 (1H, m, $C^{c}H$), 6.88 (4H, d, ^{3}J = 8.1 Hz, $C^{5,6}H$), 6.8 (1H, br, s, $C^{a'}H$), 6.61 (4H, d, ^{3}J = 8.1 Hz, $C^{5,6}H$), 4.33 (4H, S, $C^{3,8}H$), 4.27 (4H, br S, $C^{3,8}H$), 3.63-3.49 (8H, m, $C^{1,2}H$).

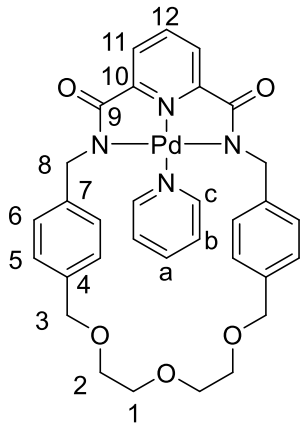

4.22 2,6-[(2,2,2-trifluoroethoxy)methyl]pyridine

NaH in mineral oil (60 %wt, 0.60 g, 15.0 mmol) was added to 2,6-pyridinedimethanol (0.82 g, 5.9 mmol) in dry THF (40 mL). 2,2-Trifluoroethyl tosylate **4.23** (3.40 g, 13.0 mmol) was then added, the mixture stirred for 16 h, at RT under an Ar atmosphere. The reaction mixture was quenched with water and then extracted with CH_2Cl_2 (3 × 50 mL), dried over $MgSO_4$ and the solvent removed *in vacuo*, to leave a colourless oil. The oil was purified by column chromatography (silica, 90:10 petrol 40-60:EtOAc, moving to 80:20 petrol 40-60:EtOAc) to give the product as a colourless oil (0.38 g, 21%).

^{1}H NMR (400 MHz, $CDCl_3$) δ: 7.80 (1H, t, ^{3}J = 7.8 Hz, $C^{6}H$), 7.42 (2H, d, ^{3}J = 7.8 Hz, $C^{5}H$), 4.80 (4H, s, $C^{4}H$), 3.98 (4H, q, $^{3}J_{HF}$ = 8.7 Hz, $C^{2}H$).

^{13}C{^{1}H} NMR (100 MHz, $CDCl_3$) δ: 156.5 (C^{4}), 137.8 (C^{6}), 123.9 ($^{1}J_{CF}$ = 279 Hz, C^{1}), 120.61 (C^{5}), 74.8 (C^{7}), 68.2 ($^{2}J_{CF}$ = 34.5 Hz, C^{2}).

^{19}F NMR (376 MHz, $CDCl_3$) δ: -73.88 (6F, t, $^{3}J_{HF}$ = 8.7 Hz, $C^{1}F$).

IR υ_{max}: 2939 (m, CH_2), 2845 (s, CH_2), 1597 (m, Py), 1580 (m, Py), 1274 (s, CF).

HRMS (ESI): *m/z*: 304.0767[M+H]$^+$, $C_{11}H_{12}NO_2F_6$ requires 304.0767.

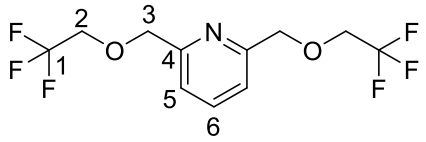

4.23 2,2,2-Trifluoroethyl tosylate[13]

To a solution of 2,2,2-trifluoroethanol (1.37 g, 1.00 mL, 13.7 mmol) in dry CH_2Cl_2 (50 mL) cooled to 0 ^oC, NEt_3 (2.90 mL, 2.10 g, 20.5 mmol), DMAP (cat.) and *p*-toluenesulfonyl chloride (2.87 g, 15.0 mmol) was added. The reaction was stirred for 16 hours at RT, under an Ar atmosphere. Water (25 mL) was added and then the solution was neutralised with $HCl_{(aq)}$ (1 M). The organic layer was separated, washed with water (2 × 25 mL), brine (2 × 25 mL), dried with $MgSO_4$ and the solvent was removed *in vacuo* to give the product as a white solid (3.05 g, 87%)

^{1}H NMR (400 MHz, $CDCl_3$) δ: 7.73 (2H, dt, ^3J = 8.3 Hz, ^4J = 1.7 Hz C^5H), 7.31 (2H, d, ^3J = 8.3 Hz, C^4H), 4.27 (2H, q, $^3J_{HF}$ = 7.9 Hz, C^2H), 2.39 (3H, s, C^7H).

^{13}C{^{1}H} NMR (100 MHz, $CDCl_3$) δ: 146.0 (C^6), 139.8 (C^3), 130.2 (C^4), 128.1 (C^5), 121.9 ($^1J_{CF}$ = 278 Hz, C^1), 64.6 ($^2J_{CF}$ = 31.5 Hz, C^2), 21.7 (C^7).

^{19}F NMR (376 MHz, $CDCl_3$) δ: -73.88 (3F, t, $^3J_{HF}$ = 7.9 Hz, C^1F).

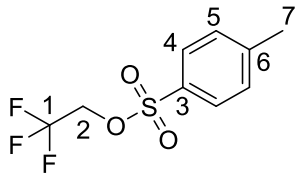

The obtained data is consistent with literature values.

4.25 2,6-Bis[(prop-2-yn-1yloxy)methyl]pyridine

NaH in mineral oil (60 %wt, 0.36 g, 9.0 mmol) was added to 2,6-pyridinedimethanol (0.50 g, 3.6 mmol) in dry THF (20 mL). propargayl bromide (1.18 g, 0.88 mL, 7.9 mmol) was then added, the mixture stirred for 4 h, at RT under an Ar atmosphere. The reaction mixture was quenched with

water and then extracted with CH_2Cl_2 (3 × 50 mL), dried over $MgSO_4$ and the solvent removed *in vacuo*, to leave a yellow oil. The oil was purified by column chromatography (silica, 90:10 petrol 40-60:EtOAc, moving to 80:20 petrol 40-60:EtOAc) to give the product as a yellow oil (0.60 g, 77 %).

^{1}H NMR (400 MHz, $CDCl_3$) δ: 7.74 (1H, t, ^3J = 7.7 Hz, C^1H), 7.39 (2H, d, ^3J = 7.7 Hz, C^2H), 4.74 (4H, s, C^4H), 4.31 (4H, d, ^4J = 2.5 Hz, C^5H), 2.49 (2H, t, ^4J = 2.4 Hz, C^7H).

$^{13}C\{^1H\}$ NMR (100 MHz, $CDCl_3$) δ: 157.2 (C^3), 137.4 (C^1), 120.4 (C^2), 79.3 (C^6), 74.9 (C^7), 72.5 (C^4), 58.1 (C^5).

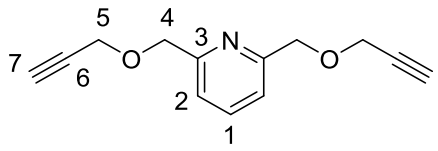

The data is consistent with literature values.

4.27 2,2-Diphenyl ethyl azide

To mesylate **4.28** in DMF (10 mL) NaN_3 (245 mg, 3.78 mmol) was added and the solution was heated to 80 °C for 72 h. Water (20 mL) was added and the solution was extracted with CH_2Cl_2 (3 × 20 mL), the organic layers were combined, dried with $MgSO_4$ to leave a colourless oil (186 mg, 65%).

^{1}H NMR (400 MHz, $CDCl_3$) δ: 7.23-7.40 (10H, m, ArH), 4.27 (1H, t, ^3J = 7.7 Hz, C^5H), 3.91 (2H, d, ^3J = 7.7 Hz, C^6H).

$^{13}C\{^1H\}$ NMR (100 MHz, $CDCl_3$) δ: 141.2 (C^4), 128.7, 128.0, 127.1 (3 × ArC), 55.5 (C^5), 50.7 (C^6).

IR υ_{max}: 3028 (w, ArH) 2928, (s, CH_2), 2890 (w, CH) 2090 (s, N_3) 1601 (m, Ar).

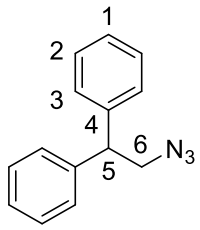

4.28 2,2-Diphenyl ethyl mesylate[14]

2,2-Diphenylethanol (250 mg, 1.26 mmol) in CH_2Cl_2 (10 mL) cooled to 0 °C, NEt_3 (191 mg, 0.26 mL, 1.89 mmol) was added followed by the dropwise addition of mesyl chloride (200 mg, 0.14 mL, 1.39 mmol) over 10 min. The reaction was stirred for a further 50 mins, then the solution was washed with $HCl_{(aq)}$ (1 M, 10 mL), saturated $Na_2CO_{3(aq)}$ (10 mL) and brine (2 × 10 mL). The solvent was removed *in vacuo* to leave a white solid (300 mg, 86%).

^{1}H NMR (400 MHz, $CDCl_3$) δ: 7.25-7.39 (10H, m, ArH), 4.77 (2H, d, ^3J = 7.5 Hz, C^6H), 4.46 (1H, t, ^3J = 7.5 Hz, C^5H), 2.77 (3H, s, C^7H).

The data is consistent with literature values.

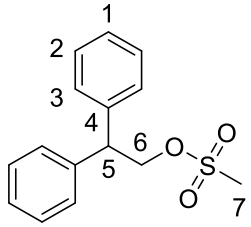

7.3.4. Experimental for Chapter 5

5.2 Rotationally asymmetric macrocycle

Bis-amine **5.9** (800 mg, 2.42 mmol) and pyridinium chloride template **2.19** (997 mg, 2.42 mmol) dissolved in dry CH_2Cl_2 (100 mL) and isophthaloyl chloride (590 mg, 2.90 mmol) dissolved in dry CH_2Cl_2 (100 mL), were added dropwise to NEt_3 (0.24 g, 0.33 mL, 2.4 mmol) dissolved in CH_2Cl_2 (100 mL) at the same time at RT under an Ar atmosphere, the reaction was then stirred for 1h. The solvent volume was reduced to ¼ *in vacuo* and then washed with $HCl_{(aq)}$ (1 mol dm^{-3}, 2 × 25 mL) and water (2 × 25 mL), the organic layer was dried over $MgSO_4$ to leave a yellow solid. The

solid was purified by column chromatography (silica, 80:20 EtOAc:CH_2Cl_2), the product was then triturated with EtOAc (3 × 2 mL) to give the product as a white solid (286 mg, 26 %).

Mp = 220-221 °C

^{1}H NMR (400 MHz, 1:1 $CDCl_3$:CD_3OD) δ: 8.02 (m, 2H, $C^{20/22}H$), 7.23 (t, 1H, ^4J = 1.5 Hz, $C^{18}H$), 7.58 (t, 1H, ^3J = 7.7 Hz, $C^{21}H$), 7.30 (s, 2H,$C^{12/13}H$), 7.25 (d, 2H, ^3J = 8.7 Hz, C^4H), 6.89 (d, 2H, ^3J = 8.7 Hz, C^3H), 4.53 (s, 2H, $C^{15}H$), 4.51 (s, 2H, $C^{10}H$), 4.47 (s, 2H, C^1H), 4.15-4.19 (m, 2H, C^6H), 3.81-3.84 (m, 2H, C^7H), 3.71-3.76 (m, 2H, C^8H), 3.59-3.62 (m, 2H, C^9H).

^{13}C{^{1}H} NMR (100 MHz, 1:1 $CDCl_3$:CD_3OD) δ: 167.9 (C^{16}), 167.8 (C^{23}), 158.5 (C^5), 137.4 (C^{11}), 137.1 (C^{14}), 134.5 ($C^{16/19}$), 134.3 ($C^{16/19}$), 131.0 ($C^{20/22}$), 130.9 ($C^{20/22}$), 130.0 (C^2), 129.6 (C^4), 129.1 (C^{21}), 128.6 ($C^{12/13}$), 128.1 ($C^{12/13}$), 124.6 (C^{18}), 115.0 (C^3), 73.6 (C^{10}), 70.7 (C^8), 69.4 (C^7), 69.3 (C^9), 67.8 (C^6), 43.8 (C^{15}), 43.7 (C^1).

HRMS (ESI): *m/z*: 459.1930 $[M-H]^-$, $C_{27}H_{28}N_2O_5$ requires 459.1930.

IR υ_{max}: 3260(s, br, CONH), 3070 (w, ArH), 2939 (m, CH_2), 2857 (m, OCH_2), 1638 (m, Ar).

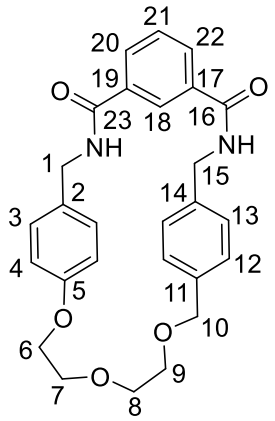

5.3 Hydrogen Bond Templated Mechanically Chiral Rotaxane

To macrocycle **5.2** (100 mg, 0.22 mmol) in CH_2Cl_2 (6 mL), 1.5 equivalents of azide **5.4** (111 mg, 0.33 mmol) was added and the solution gently heated until all components had dissolved. The solution was allowed to cool to room temperature, then cooled with ice. Alkyne **4.7** (77 mg, 0.33 mmol), diisopropylethylamine (0.06 mL, 46 mg, 0.36 mmol), 0.015 equivalents of $Cu(NCMe)_4BF_4$

(10 mg, 0.033 mmol) and 0.15 equivalents of TBTA (17 mg, 0.033 mmol) were added. The solution was allowed to stir for 16 hours and then CH_2Cl_2 (15 mL) was added. The solution was washed with $EDTA_{(aq)}$ (0.02 mol in 1 mol dm^{-3} NH_3, 10 mL) and water (2 × 10 mL). The organic layer was dried with $MgSO_4$ and the solvent removed *in vacuo* to leave a yellow solid, that was purified by column chromatography (silica, 99:1 to 98:2 $CHCl_3$:MeOH), to produce a colourless solid (100 mg, 44 %). Axle **5.10** was isolated as a by-product (95 mg, 50%)

Mp: 79-80 ^oC

R_f = 0.28 (98:2 $CHCl_3$:MeOH)

^{1}H NMR (400 MHz, $CDCl_3$) δ: 8.54 (s, 1H, $C^{18}H$), 8.33 (dt, 2H, ^3J = 7.8 Hz, ^4J = 1.3 Hz, $C^{20/22}H$), 8.09 (s, 2H, C^dH), 8.06 (s, 1H, C^aH), 7.64 (t, 1H, ^3J = 7.8Hz, $C^{21}H$), 7.18-7.31 (m, 11H, $C^{j/p/q/r}H$), 7.16 (t, br, 1H, ^3J = 3.7 Hz, $C^{16/23}NH$), 7.09 (t, br, 1H, ^3J = 4.3 Hz, $C^{16/23}NH$), 6.76 (d, 4H, ^3J = 7.9 Hz, $C^{3/13}H$), 6.65 (d, 2H, ^3J = 7.9 Hz, $C^{12}H$), 6.58 (t, br, 1H, ^3J = 4.5 Hz, C^fNH), 6.12 (d, 2H, ^3J = 7.9 Hz, C^4H), 4.70 (s, 2H, C^lH), 4.38-4.48 (m, 3H, $C^{1/10/15}H$), 4.15-4.36 (m, 6H, $C^{1/15/l/n}H$), 4.12 (d, 2H, ^3J = 7.3 Hz, C^mH), 3.68-4.02 (m, 8H, $C^{6/7/8/9}H$), 2.54-2.64 (m, 1H, C^gH), 2.41-2.49 (m, 1H, $C^{g'}H$), 1.95-2.10 (m, 2H, C^hH).

^{13}C{^{1}H} NMR (100 MHz, $CDCl_3$) δ: 166.0 ($C^{16,23}$), 165.8 ($C^{16/23}$), 163.7 (C^f), 157.6 (C^5), 145.4 (C^k), 142.0 (C^o), 137.5 (C^{11}), 135.6 (C^{14}), 135.1 (C^e), 133.8 ($C^{17/19}$), 133.5 ($C^{17/19}$), 132.1 ($C^{20/22}$), 131.4 ($^2J_{CF}$ = 30 Hz, C^B), 130.1 (C^{13}), 129.7 (C^{12}), 129.3 (C^{21}), 129.1 (C^2), 128.8 (C^3), 128.5 (C^p), 128.3 (br, C^d), 128.3 (C^q), 126.5 (C^r), 124.6 (br, C^a), 123.1 ($^1J_{CF}$ = 273 Hz, C^c), 123.0 (C^j), 122.7 (C^{18}), 113.5 (C^4), 74.3 (C^i), 74.0 (C^m), 70.6 (C^7), 70.3 (C^9), 70.2 (C^8), 66.6 (C^6), 64.7 (C^l), 51.0 (C^n), 48.1 (C^{10}), 44.9 ($C^{1/15}$), 44.8 ($C^{1/15}$), 38.3 (C^g), 28.1 (C^h).

^{19}F{^{1}H} NMR (376 MHz, $CDCl_3$) δ: -62.6 (s, 6F, C^cF_3)

IR υ_{max}: 3345 (m, br, CONH), 3026 (w, ArH), 2920 (w, CH_2), 2876 (m, OCH_2), 1646 (s, CONH), 1511 (s, Ar).

HRMS (ESI): *m/z*: 1037.4042 $[M+H]^+$, $C_{56}H_{54}N_6O_7F_6$ requires 1037.4031.

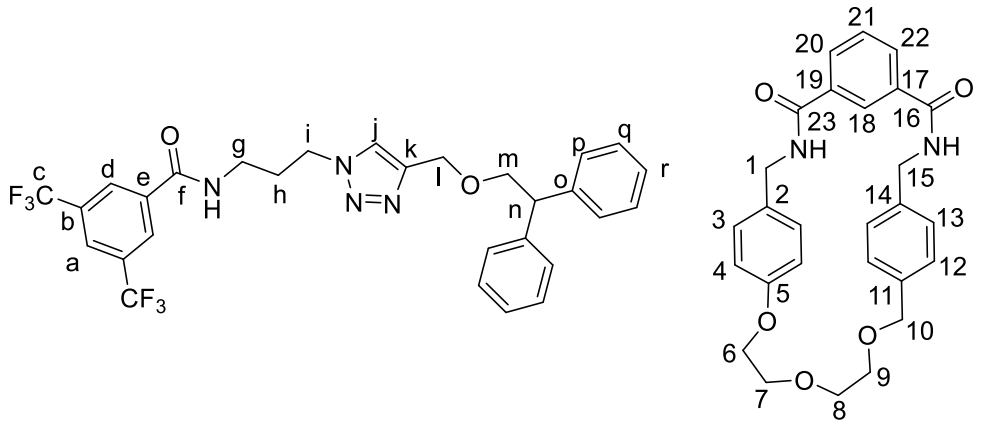

5.4 *N*-(3-azidopropyl)-3,5-trifluromethylbenzamide

To compound **5.5** (1.31 g, 3.47 mmol) in DMF (15 mL), NaN_3 (0.68 mg, 10.4 mmol) was added and the solution was heated to 80 °C for 72 h. Water (20 mL) was added and the solution was extracted with CH_2Cl_2 (3 × 30 mL), the organic layers were combined, dried with $MgSO_4$ and the solvent removed *in vacuo* to leave the product as a colourless oil (1.12 g, 94%).

^{1}H NMR (400 MHz, $CDCl_3$) δ: 8.24 (s, 2H, C^4H), 8.03 (s, 1H, C^1H), 6.62 (s, 1H, C^6NH), 3.63 (q, 2H, ^3J = 6.4 Hz, C^7H), 3.52 (t, 2H, ^3J = 6.4 Hz, C^9H), 1.97 (quintet, 2H, ^3J = 6.4 Hz, C^8H).

^{13}C{^{1}H} NMR (100 MHz, $CDCl_3$) δ: 164.7 (C^6), 136.4 (C^5), 132.3 (q, $^2J_{CF}$ = 34 Hz, C^2), 127.3 (C^4), 125.1 (q, $^4J_{CF}$ = 4 Hz, C^1), 122.9 (q, $^1J_{CF}$ = 273 Hz, C^2), 49.7 (C^7), 38.4 (C^8), 28.6 (C^9).

^{19}F{^{1}H} NMR (376 MHz, $CDCl_3$) δ: -62.9 (s, 6F, C^2F).

HRMS (ESI): *m/z*: 339.0685 $[M-H]^-$, $C_{12}H_{10}N_4OF_6$ requires 459.1930.

IR υ_{max}: 3301 (m, br, NH), 2943 (w, CH_2), 2877 (m, CH_2), 2096 (s, N_3), 1645 (s, CONH), 1551 (s, Ar).

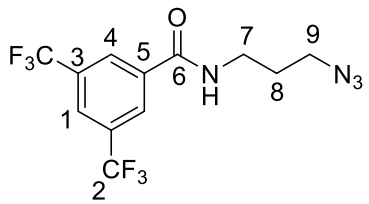

5.5 *N*-(3-bromopropyl)-3,5-trifluromethylbenzamide

3-Bromopropylamine hydrobromide (0.87 g, 3.62 mmol) was dissolved in dry CH_2Cl_2 (20 mL), NEt_3 (0.92 g, 1.26 mL, 9.05 mmol) then 3,5-bis(trifluoromethyl)benzoyl chloride (0.66 g, 0.25 mL, 6.6 mmol) were added. The reaction was stirred for 1h at RT, under an Ar atmosphere. The mixture was washed with $HCl_{(aq)}$ (1 mol dm^{-3}, 2 × 25 mL), $NaOH_{(aq)}$ (1 mol dm^{-3}, 2 × 25 mL) and water (25 mL) the organic layer was dried with $MgSO_4$. The solvent was removed *in vacuo* to leave the products as a waxy white solid (1.31 g, 96%).

^{1}H NMR (400 MHz, $CDCl_3$) δ: 8.24 (s, 2H, C^4H), 8.02 (s, 1H, C^1H), 6.69 (s, 1H, C^6NH), 3.69 (q, 2H, ^3J = 6.4 Hz, C^7H), 3.52 (t, 2H, ^3J = 6.4 Hz, C^9H), 2.27 (quintet, 2H, ^3J = 6.4 Hz, C^8H).

^{13}C{^{1}H} NMR (100 MHz, $CDCl_3$) δ: 164.9 (C^6), 136.6 (C^5), 132.3 (q, $^2J_{CF}$ = 34 Hz, C^2), 127.3 (C^4), 125.1 (q, $^4J_{CF}$ = 4 Hz, C^1), 122.9 (q, $^1J_{CF}$ = 273 Hz, C^2), 39.2 (C^7), 31.9 (C^8), 30.7 (C^9).

^{19}F{^{1}H} NMR (376 MHz, $CDCl_3$) δ: -62.9 (s, 6F, C^2F).

HRMS (ESI): *m/z*: 377.9889 $[M+Na]^+$, $C_{10}H_{12}NOF_6NaBr$ requires 377.9899.

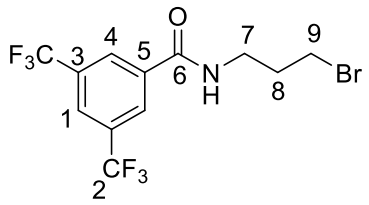

5.6 Diethylene glycol mono tosylate

To KOH (1.49 g, 26.7 mmol) in water (5 mL), THF (5 mL) and tetraethylene glycol (19 mL, 200 mmol) were added and the resulting solution was cooled to 0 ºC. A solution of *p*-toluenesulfonyl chloride (3.18 g, 16.6 mmol) in THF (20 mL) was added slowly over 15 minutes, the mixture was allowed to stir for 2 h at 0 °C, when it was then poured over ice water (50 mL). The organic layer was separated, and the aqueous layer was washed with CH_2Cl_2 (3 × 30 mL). The organic layers were combined, dried with $MgSO_4$ and the solvent removed *in vacuo* to leave the product as a colourless oil (3.48 g, 81%).

^{1}H NMR (400 MHz, $CDCl_3$) δ: 7.82 (dt, 2H, ^{3}J = 8.4 Hz, ^{4}J = 1.9 Hz, $C^{4}H$), 7.37 (d, 2H, ^{3}J = 8.4 Hz, $C^{3}H$), 4.21 (t, 2H, ^{3}J = 4.6 Hz, $C^{6}H$), 3.70-3.68 (m, 4H,$C^{7,8}H$), 3.54 (t, 2H, ^{3}J = 4.3 Hz $C^{9}H$), 2.47 (s, 3H, $C^{1}H$).

$^{13}C\{^{1}H\}$ NMR (100 MHz, $CDCl_3$) δ: 145.0 (C^{5}), 133.0 (C^{2}), 129.8 (C^{3}), 128.0 (C^{4}), 72.5 (C^{9}), 69.2 (C^{6}), 3.70, 3.68 ($C^{7,8}$), 21.6 (C^{1}).

IR υ_{max}: 3032 (w, ArH), 2920 (w, CH_3), 2877 (OCH_2), 1597 (m, Ar), 1351 (s, SO_2O).

HRMS (ESI): 283.0612 $[M+Na]^+$, $C_{11}H_{16}O_5SNa$ requires 283.0611.

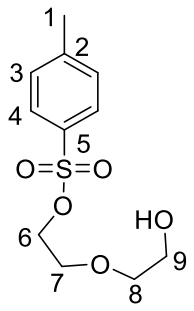

5.7 Diethylene glycol mono-4-benzonitile

To compound **5.6** (3.33 g, 12.8 mmol) in dry CH_3CN (50 mL) K_2CO_3 (3.98 g, 28.8 mmol) then 4-hydroxybenzonitrile (2.29 g, 19.2 mmol) were added. The resulting mixture was heated to reflux for 5 days, under an Ar atmosphere, then allowed to cool. The suspension was filtered under suction and the solvent removed *in vacuo*. The resulting oil was dissolved in CH_2Cl_2 (50 mL) then washed with $NaOH_{(aq)}$ (1 M, 25 mL), water (25 mL) and dried over $MgSO_4$ before the solvent was removed *in vacuo* to leave a colourless oil (2.00 g, 82%).

^{1}H NMR (400 MHz, $CDCl_3$) δ: 7.61 (dt, 2H, ^{3}J = 9.0 Hz, ^{4}J = 2.1 Hz, $C^{3}H$), 6.99 (dt, 2H, ^{3}J = 9.0 Hz, ^{3}J = 2.1 Hz, $C^{4}H$), 4.20 (t, 2H, ^{3}J = 4.6 Hz, $C^{6}H$), 3.91 (t, 2H, ^{3}J = 4.6 Hz, $C^{7}H$), 3.79 (t, 2H, ^{3}J = 4.5 Hz, $C^{8}H$), 3.69 (t, 2H, ^{3}J = 4.5 Hz, $C^{9}H$).

$^{13}C\{^{1}H\}$ NMR (100 MHz, $CDCl_3$) δ: 162.0 (C^{5}), 134.0 (C^{3}), 119.1 (C^{2}), 115.3 (C^{4}), 104.3 (C^{1}), 69.3 (C^{9}), 67.7 (C^{7}), 61.7 (C^{6}), 61.9 (C^{8}).

HRMS (ESI): *m/z*: 242.0589 $[M+Cl]^-$, $C_{11}H_{13}N_1O_3Cl$ requires 242.0589.

IR υ_{max}: 3494 (s, OH), 3047(w, ArH), 2933(w, CH_2), 2898 (m, OCH_2), 2857 (s, OH), 2227(s, CN), 1600 (s, Ar), 1576 (s, Ar).

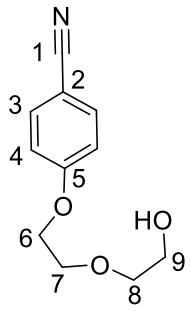

5.8 Bis-nitrile macrocycle precursor

NaH (60% in mineral oil, 0.49 g, 12.3 mmol) was added to compound **5.7** (2.00 g, 10.2 mmol) in dry THF (30 mL). Cyanobenzyl bromide (2.20 g, 11.2 mmol) was then added, the mixture stirred for 1 h, at RT under an Ar atmosphere. The reaction mixture was quenched with water (20 mL) and then extracted with CH_2Cl_2 (3 × 30 mL). The solution was dried over $MgSO_4$ and the solvent removed *in vacuo*, to leave a colourless oil. The solid was purified by column chromatography (silica, 4:1 to 3:1 petrol 40-60:EtOAc). The solvent was removed *in vacuo*, to leave the product, a waxy white solid (2.47 g, 75%).

Mp = 70-72 °C

^{1}H NMR (400 MHz, $CDCl_3$) δ: 7.64 (dt, 2H, ^3J = 8.5 Hz, ^4J = 1.5 Hz, $C^{13}H$), 7.59 (dt, 2H, ^3J = 9.0 Hz, ^4J = 2.1 Hz, C^3H), 7.47 (d, 2H, ^3J = 8.5 Hz, $C^{12}H$), 7.04 (dt, 2H, ^3J = 9.0 Hz, ^4J = 2.1 Hz, C^4H), 4.64 (s, 2H, $C^{10}H$), 4.21 (d, 2H, ^3J = 4.7 Hz, C^6H), 3.89-3.93 (m, 2H, C^7H), 3.76-3.80 (m, 2H, C^8H), 3.69-3.73 (m, 2H, C^9H).

^{13}C{^{1}H} NMR (100 MHz, $CDCl_3$) δ: 162.1 (C^5), 143.8 (C^{14}), 134.0 (C^3), 132.2 (C^{13}), 127.7 (C^{12}), 119.1 (C^1), 118.9 (C^{15}), 115.3 (C^4), 111.4 (C^{11}), 104.2 (C^5), 72.3 (C^{10}), 70.9 (C^8), 70.1 (C^9), 69.5 (C^7), 67.8 (C^6).

IR υ_{max}: 2930 (m, CH_2), 2898 (m, ArH), 2866 (w, OCH_2), 2223(s, CN), 1604 (s, Ar), 1505 (s, Ar)

HRMS (ESI): 345.1196 $[M+Na]^+$, $C_{19}H_{18}N_2O_3Na$ requires 345.1210.

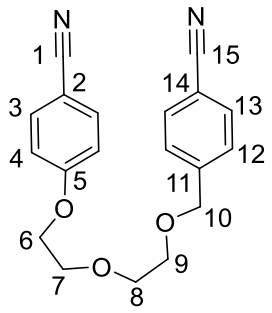

5.9 Bis-amine macrocycle precursor

To a solution of bis-nitrile **5.8** (1.26 g, 3.9 mmol) in dry THF (20 mL), BH_3.THF (1 mol dm^{-3}, 20.0 mmol, 20.0 mL) was added dropwise. The reaction mixture was heated to reflux for 3h under an Ar atmosphere. The reaction mixture was quenched with MeOH, then concentrated $HCl_{(aq)}$ (5 mL) was added and the mixture was allowed to stir for a further 10 minutes at RT. The solvent was then removed *in vacuo*. The resulting solid was dissolved in water (30 mL) and washed with CH_2Cl_2 (30 mL). The aqueous solution was retained and made basic with 10% NaOH. The aqueous solution was extracted with CH_2Cl_2 (3 × 30 mL) and dried over $MgSO_4$. The solvent was removed *in vacuo* to leave an off white solid. The solid was purified by column chromatography (silica, 93:4:2 CH_2Cl_2:MeOH:NEt_3) to give the product as a waxy white solid (0.80 g, 62 %).

^{1}H NMR (400 MHz, $CDCl_3$) δ: 7.27-7.36 (m, 4H, $C^{12,13}H$), 7.23 (d, 2H, ^3J = 8.7 Hz, C^3H), 6.91 (dt, 2H, ^3J = 8.7 Hz, ^4J = 2.1 Hz, C^4H), 4.58 (s, 2H, $C^{10}H$), 4.15 (t, 2H, ^3J = 4.9 Hz, C^6H), 3.86-3.89 (m, 4H, $C^{5,15}H$), 3.81 (s, 2H, C^1H), 3.74-3.78 (m, 2H, C^7H), 3.65-3.68 (m, 2H, C^9H).

^{13}C{^{1}H} NMR (100 MHz, $CDCl_3$) δ: 157.7 (C^5), 142.8 (C^{14}), 136.8 (C^{11}), 135.8 (C^2), 128.2 (C^3), 128.1 (C^{12}), 127.1 (C^{13}), 114.7 (C^4), 73.1 (C^{10}), 70.9 (C^7), 69.8 (C^8), 69.4 (C^9), 67.5 (C^6), 46.3 (C^{15}), 45.9 (C^1).

IR υ_{max}: 3340 (s, br, NH_2), 3027 (w, ArH), 2898 (m, CH_2), 2855 (m, OCH_2), 1608 (Ar), 1578 (s, Ar), 1508 (s, Ar).

HRMS (ESI): 353.1822 $[M+Na]^+$, $C_{19}H_{26}N_2O_3Na$ requires 353.1836.

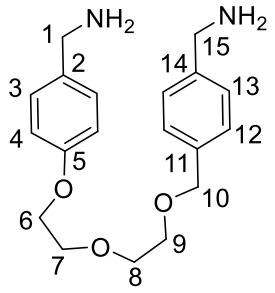

5.10 Asymmetric axle

Asymmetric axle **5.10** was isolated as a by-product from mechanically chiral rotaxane **5.3**.

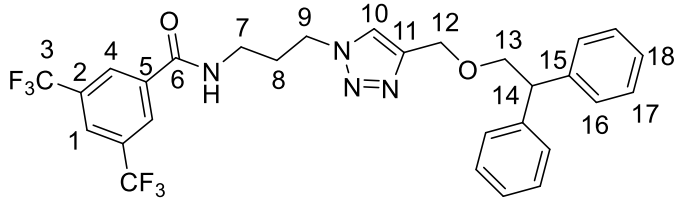

^{1}H NMR (400 MHz, $CDCl_3$) δ: 8.34 (s, 2H, C^4H), 8.01 (s, 1H, C^1H), 7.66 (t, 1H, ^3J = 5.8 Hz, C^6NH), 7.18-7.30 (m, 11H, ArH, $C^{10}H$), 4.61 (s, 2H, $C^{11}H$), 4.36 (t, 2H, ^3J = 6.7 Hz, C^9H), 4.27 (t, 2H, ^3J = 7.3 Hz, $C^{13}H$), 4.04 (d, 2H, ^3J = 7.3 Hz, $C^{13}H$), 3.48 (q, 2H, ^3J = 6.3 Hz, C^7H), 2.18 (quintet, 2H, ^3J = 6.6Hz, C^8H).

$^{13}C\{^1H\}$ NMR (100 MHz, $CDCl_3$) δ:164.9 (C^6), 145.5 (C^{11}), 141.9 (C^{15}), 136.3 (C^5), 132.1 (q, $^2J_{CF}$ = 33.9 Hz, C^2), 128.5 128.2 (2 × ArC), 127.6 (C^4), 126.6 (ArC), 124.9 (C^1), 123.0 (C^{10}), 123.0 (q, $^1J_{CF}$ = 273 Hz), 73.8 (C^{13}), 64.4 (C^{12}), 51.0 (C^{14}), 47.9 (C^9), 37.4 (C^7), 29.4 (C^8).

IR υ_{max}: 3297 (m, br CONH), 3084 (w, ArH), 3028 (w, ArH), 2935 (w, CH_2), 2866 (m, OCH_2), 1653 (s, CONH), 1545 (s, Ar).

HRMS (ESI): *m/z*: 577.2025 $[M+H]^+$, $C_{29}H_{26}N_4O_2F_6$ requires 577.2033.

5.11 Methylated Hydrogen Bond Templated Mechanically Chiral Rotaxane Iodide Salt

To rotaxane **5.3** (100 mg, 0.0965 mmol), MeI (5 mL) was added and the solution was heated to reflux for 16 h. The solvent was removed *in vacuo* to afford a yellow solid in quantitative yield (108 mg)

Mp = 197-199 °C

^{1}H NMR (400 MHz, $CDCl_3$) δ: 9.29 (s, 1H, $C^{j}H$), 8.42 (s, 1H, $C^{18}H$), 8.21 (s, 2H, $C^{d}H$), 8.19 (1H, d, ^{3}J = 7.9 Hz, $C^{20/22}H$), 8.17 (1H, d, ^{3}J = 7.9 Hz, $C^{20/22}H$), 8.07 (s, 1H, $C^{a}H$), 7.57 (t, 1H, ^{3}J = 7.9 Hz, $C^{21}H$), 7.41 (t, 1H, ^{3}J = 5.0 Hz, $C^{16/23}NH$), 7.34 (t, 1H, ^{3}J = 5.0 Hz, $C^{16/23}NH$), 7.19-7.33 (m, 10 H, ArH), 7.15 (t, 1H, ^{3}J = 5.1 Hz, $C^{f}NH$), 6.86 (d, 2H, ^{3}J = 8.0 Hz, $C^{13}H$), 6.80 (d, 2H, ^{3}J = 8.7 Hz, $C^{3}H$), 6.70 (d, 2H ^{3}J = 8.0 Hz, $C^{12}H$), 6.16 (d, 2H, ^{3}J = 8.7 Hz, $C^{4}H$), 4.81 (s, 2H, $C^{l}H$), 4.61 (dd, 1H, ^{2}J = 13.9 Hz, ^{3}J = 5.6 Hz, $C^{1/15}H$), 4.29-4.53 (m, 5H, OCH_2, $C^{n}H$), 4.07-4.25 (m, 6H, OCH_2, $C^{1/15}H$), 3.76-4.02 (m, 8H, OCH_2), 3.70 (s, 3H, $C^{s}H$), 2.61-2.71 (m, 2H, $C^{g}H$), 1.92 (2H, septet, ^{3}J = 9.8 Hz, $C^{h}H$).

^{13}C{^{1}H} NMR (100 MHz, $CDCl_3$) δ: 166.4 ($C^{16/23}$), 166.2 ($C^{16/23}$), 164.3 (C^{f}), 157.4 (C^{5}), 141.0 (ArC), 139.5 (C^{K}), 137.8, 135.8, 135.4, 134.4, 134.2, 131.6 (6 × ArC), 131.4 ($C^{20/22}$), 131.3 ($C^{20/22}$), 131.2 (ArC), 130.7 (C^{j}), 130.5 (q, $^{2}J_{CF}$ = 80 Hz, C^{b}), 130.0 (C^{3}), 129.7 (C^{12}), 129.5 (ArC), 129.2 (C^{18}), 128.9 (C^{13}), 128.7 (C^{d}), 128.1, 127.0 (2 × ArC), 124.6 (br, C^{a}), 123.9 (C^{18}), 123.1 (q, $^{1}J_{CF}$ = 273 Hz, C^{c}), 113.8 (C^{4}), 74.9, 74.1, 70.8, 70.4 (4 × OCH_2), 67.0 (C^{10}), 60.5 (C^{l}), 52.2 ($C^{1/15}$), 50.8 (C^{n}), 45.0 ($C^{1/15}$), 38.4 (C^{s}), 37.6 (C^{g}), 28.1 (C^{h}).

^{19}F{^{1}H} NMR (376 MHz, $CDCl_3$) δ: -62.5 (s, 6H, $C^{c}F_3$).

IR υ_{max}: 3112 (m, br CONH), 3054 (w, ArH), 3028 (w, ArH), 2922 (w, CH_3), 2870 (m, OCH_2), 1645 (s, CONH), 1511 (s, Ar).

HRMS (ESI): *m/z*: 1051.4203$[M]^+$, $C_{57}H_{57}N_6O_7F_6$ requires 1051.4187.

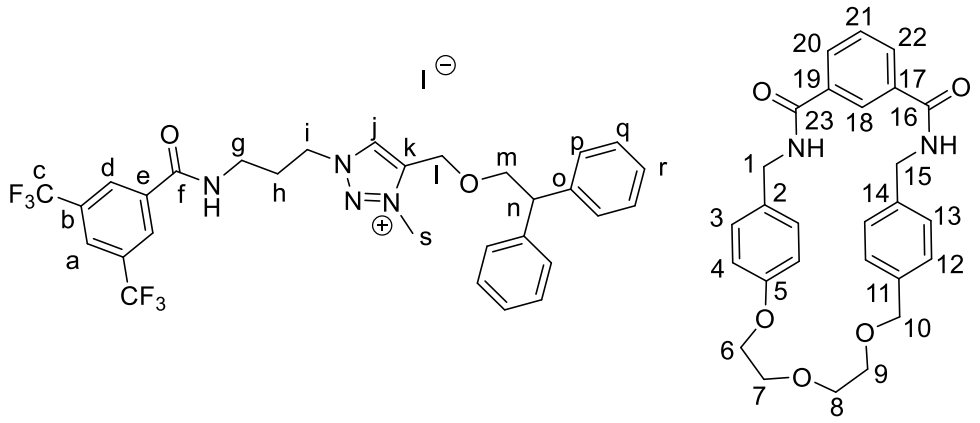

5.11-b Methylated Hydrogen Bond Templated Mechanically Chiral Rotaxane L-phenyl tartrate Salt

Mechanically chiral rotaxane **5.11** (25 mg, 0.0193 mmol) was dissolved in CH_2Cl_2 (20 mL), then washed with 0.1 mol dm^{-3} disodium L-phenyltartrate (8 × 4 mL) then water (2 × 4 mL). The solvent was removed *in vacuo* to afford a white solid (19 mg, 40 %).

^{1}H NMR (400 MHz, $CDCl_3$) δ: 8.94 (s, 2H, $C^{j}H$), 8.35 (s, 2H, ArH), 8.15 (d, 3H, ^3J = 7.5 Hz, ArH), 8.02-8.12 (m, 10H, ArH), 7.52 (t, 2H, ^3J = 7.1 Hz, $C^{21}H$), 7.40 (t, 4H, ^3J = 7.6 Hz, ArH), 7.19-7.32 (m, 22H, ArH), 6.77-6.85 (8H, m, $C^{3,13}H$), 6.67 (d, 4H, ^3J = 7.8 Hz $C^{4}H$), 6.11 (d, 4H, ^3J = 8.0 Hz , $C^{12}H$), 5.85 (s, 2H, $C^{6*}H$), 5.39 (s, 2H, $C^{6*'}H$), 4.26-4.83 (m, OCH_2, NCH_2,), 3.81-4.06 (m, 20H, OCH_2), 3.81 (s, 6H, $C^{s}H$), 3.64 (q, 4H, ^3J = 7.1 Hz, $C^{l}H$), 2.69-2.79 (m, 4H, $C^{g}H$), 1.82 (sextet, 4H, ^3J = 7.1 Hz $C^{h}H$).

*^{1}H NMR is extremely broad, thought to be due to be due to two rotaxanes binding to each L-phenyltartrate di-anion. Fewer than expected protons are detected due to water peak overlapping.

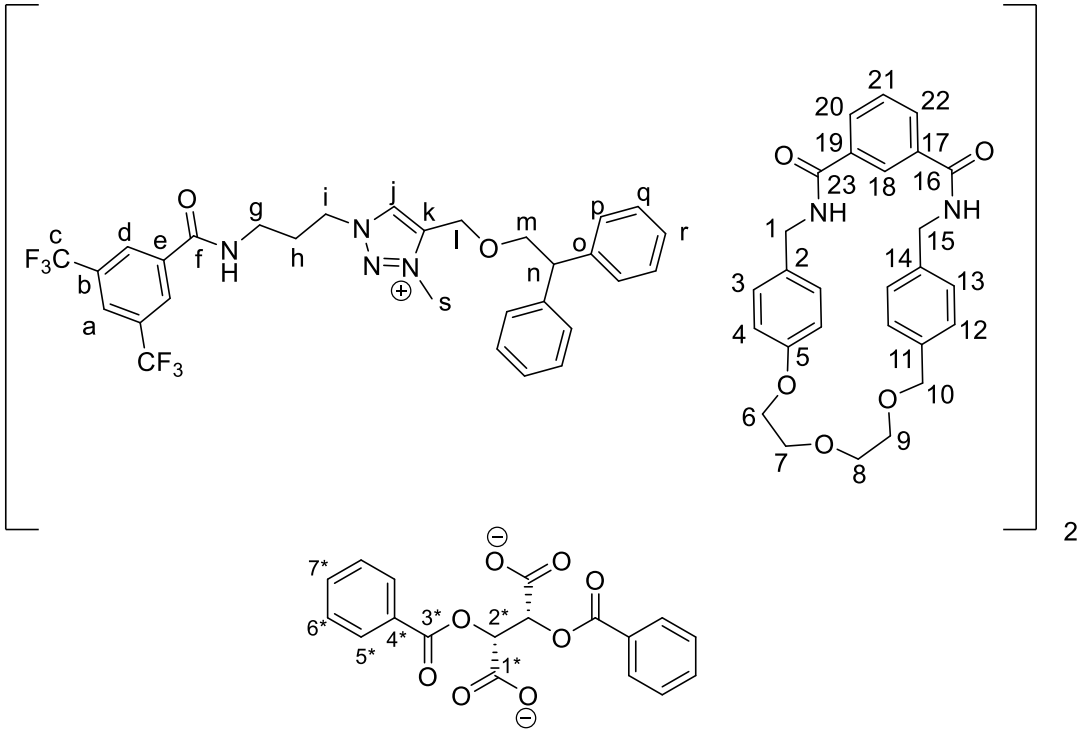

5.11-d Methylated Hydrogen Bond Templated Mechanically Chiral Rotaxane (*1R*)-(-)-10 Camphorsulfonate Salt

Mechanically chiral rotaxane **5.11** (25 mg, 0.0193 mmol) was dissolved in CH_2Cl_2 (10 mL), then washed with 0.1 mol dm^{-3} ammonium camphorsulfonate (8 × 5 mL) then water (2 × 5 mL). The solvent was removed *in vacuo* to afford a white solid (22mg, 71 %).

^{1}H NMR (400 MHz, $CDCl_3$) δ: 8.81 (s, 1H, $C^{j}H$), 8.40 (s, 1H, $C^{15/23}NH$), 8.32 (s, 1H, $C^{18}H$), 8.22 (s, 2H, $C^{d}H$), 8.06 (d, 2H, ^3J = 7.8 Hz, $C^{20/22}H$), 7.75 (s, br, 1H, $C^{f}NH$), 7.61 (t, 1H, ^3J = 7.8 Hz, $C^{21}H$), 7.56 (s, 1H, $C^{15/23}NH$), 7.18-7.32 (m, 10H, $C^{p,q,r}H$), 6.84 (dd, 2H, ^3J = 7.9 Hz, ^4J = 3.6 Hz, $C^{3}H$), 6.80 (dd, 2H, ^3J = 8.3 Hz, ^4J = 4.0 Hz, $C^{13}H$), 6.69 (d, 2H, ^3J = 7.8 Hz, $C^{4}H$), 6.13 (d, 2H, ^3J = 8.3 Hz, $C^{12}H$), 4.79 (s, 2H, $C^{l}H$), 4.51 (d, 1H, ^3J = 4.5 Hz, $C^{1/15}$), 4.44 (d, 1H, ^3J = 4.5 Hz, $C^{1/15}$), 4.34 (t, 1H, ^3J = 7.5 Hz, $C^{n}H$), 4.08-4.29 (m, 8H, $C^{1', 15', i, m}H$, OCH_2), 3.94-4.05 (m, 2H, $C^{10}H$), 3.78-3.91 (m, 6H, 3 × OCH_2), 3.76 (s, 3H, $C^{s}H$), 3.31 (d, 1H, ^2J = 14.8 Hz, CS-H), 2.88 (q, 2H, ^3J = 6.3 Hz, $C^{g}H$), 2.76 (d, 1H, ^3J = 14.8 Hz, CS-H) 2.57-2.66 (m, 1H, CS-H), 2.32 (dt, 2H, ^4J = 18.3 Hz, ^3J = 3.9 Hz, CS-H) 2.05 (t, 1H, CS-H), 1.93-2.03 (m, 1H, CS-H), 1.78-1.86 (m, 2H, $C^{h}H$), 1.57-1.65 (m, CS-H), 1.31-1.39 (m, 1H, CS-H), 1.09 (s, 3H, $C^{9*/10*}H$), 0.83 (s, 3H, $C^{9*/10*}H$).

*CS denotes camphorsulfonate protons

$^{19}F\{^{1}H\}$ NMR (376 MHz, $CDCl_3$) δ: -62.5 (s, 6H, C^cF_3).

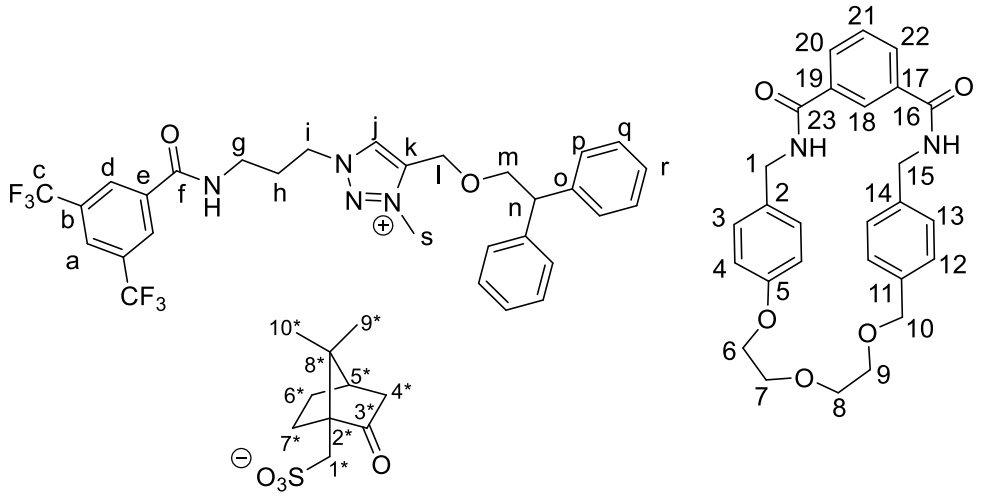

7.3.5. Experimental for Chapter 6

6.15 Diethylene glycol-isophthalamide macrocycle[12]

To bis-amine **4.14** (1.89 g, 5.48 mmol) and pyridinium template **2.19** (2.25 g, 5.48 mmol) in CH_2Cl_2 (60 mL) under an Ar atmosphere, NEt_3 (2.3 mL, 1.66 g, 16.45 mmol) was added, followed by the dropwise addition of solution of isophthaloyl chloride (1.34 g, 6.58 mmol) in CH_2Cl_2 (25 mL). The solution was stirred for 1h, then washed with 10 % HCl (50 mL) and water (2 × 50 mL) and dried with $MgSO_4$. The solvent was removed *in vacuo* to afford a yellow solid. The solid was purified using flash column chromatography (silica, 9:1 EtOAc:CH_2Cl_2) to afford a yellow solid contaminated with pyridinium template **2.19**, which was triturated with ice cold MeOH (5 mL) to afford the product as a white solid (344 mg, 16 %).

R_f = 0.35 (9:1 EtOAc:CH_2Cl_2)

^{1}H NMR (400 MHz, $CDCl_3$) δ: 7.98 (d, 2H, ^{3}J = 7.8 Hz, $C^{12}H$), 7.69 (br, s,1H, $C^{11}H$), 7.50 (t, 1H, ^{3}J = 7.8 Hz, $C^{13}H$), 7.23 (br, s, 8H, $C^{5,6}H$), 6.35 (br, s, 2H, $C^{9}NH$), 4.51 (d, 2H, ^{3}J = 5.4 Hz, $C^{9}H$), 4.43 (s, 2H, $C^{3}H$), 3.58-3.62 (m, 4H, $C^{1}H$), 3.51-3.54 (m, 4H, $C^{2}H$).

$^{13}C\{^{1}H\}$ NMR (100 MHz, $CDCl_3$) δ: 166.7 (C^{9}), 163.3 (C^{10}), 137.2 ($C^{7,15}$, coincidental), 131.0 (C^{12}), 129.5 (C^{13}), 128.7 ($C^{5,6}$), 128.5 ($C^{5,6}$), 123.4 (C^{11}), 72.9 (C^{3}), 70.6 ($C^{`1}$), 69.4 (C^{2}), 44.3 (C^{8}).

HRMS (ESI): *m/z*: $[M+Cl]^-$ = 509.1845, $C_{28}H_{30}N_2O_5Cl$ requires 509.1849.

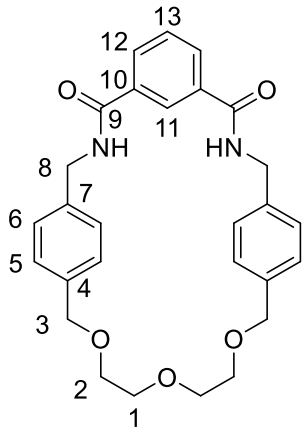

The data is consistent with literature values.

6.16 Fluorine Axle

To 2,2-diphenylethylamine (155 mg, 0.79 mL) in dry CH_2Cl_2, NEt_3 (119 mg, 0.17 mL, 1.19 mmol) was added followed by 2,3,4,5,6-pentafluorobenzyl chloride (200 mg, 0.13 mL, 0.87 mmol). The solution was stirred for 1 h, then further CH_2Cl_2 (10 mL) was added, the solution was then washed with HCl (1 mol dm^{-3}, 20 mL), NaOH (1 mol dm^{-3}, 20 mL) and then water (20 mL). The organic layer was then dried over $MgSO_4$ and the solvent removed *in vacuo* to afford the product as a white solid (299 mg, 97 %).

Mp: 116-121 ^{o}C

^{1}H NMR (400 MHz, $CDCl_3$) δ: 7.34-7.38 (m, 4H, ArH), 7.25-7.32 (m, 6H, ArH), 5.86 (br, s, 1H, $C^{5}NH$), 4.33 (t, 1H, ^{3}J = 8.0 Hz, $C^{7}H$), 4.14 (dd, 2H, ^{3}J = 8.0 Hz, ^{3}J = 5.8 Hz, $C^{6}H$).

$^{13}C\{^{1}H\}$ NMR (100 MHz, $CDCl_3$) δ: 157.4 (C^{5}), 141.2 (C^{8}), 128.9 (C^{10}), 128.0 (C^{9}), 127.1 (C^{11}), 50.3 (C^{7}), 44.6 (C^{6})*

*C^{1}-C^{4} are not detected due to extensive C-F coupling.

$^{19}F\{^{1}H\}$ NMR (400 MHz, $CDCl_3$) δ: -140.5--140.2 (m, 2F, C^2F), -150.4 (t, 1F, ^3J = 20.8 Hz, C^1F), -160.1--159.9 (m, 2F, C^3F).

IR υ_{max}: 3271 (m, br, CONH), 3086 (w, CONH), 3063 (w, CH), 3030 (w, CH_2), 1655 (s, CONH), 1556 (m, Ar).

HRMS (ESI): *m/z*: $[M+H]^+$ = 392.1059, $C_{21}H_{15}F_5NO$ requires 392.1068.

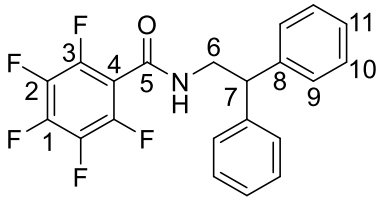

6.17 Fluorine thread

To amine **6.18** (253 mg, 1.57 mmol) in dry CH_2Cl_2 (10 mL), NEt_3 (82 mg, 0.11 mL, 0.81 mmol) followed by 2,3,4,5,6-pentafluorobenzyl chloride (151 mg, 0.09 mL, 0.76 mmol) were added. The solution was stirred for 1 h, then further CH_2Cl_2 (10 mL) was added, the solution was then washed with HCl (1 mol dm^{-3}, 20 mL), NaOH (1 mol dm^{-3}, 20 mL) and then water (20 mL). The organic layer was then dried over $MgSO_4$ and the solvent removed *in vacuo* to afford a white solid (391 mg, 70 %).

Mp: 118-120 ^oC

^{1}H NMR (400 MHz, $CDCl_3$) δ: 7.31 (dt, 2H, ^3J = 8.8 Hz, ^4J = 2.7 Hz, C^8H), 7.00 (dt, 2H, ^3J = 8.8 Hz, ^4J = 2.3 Hz, C^9H), 6.17 (br, s, 1H, C^5NH), 4.72 (d, 2H, ^3J = 5.8 Hz, C^6H), 4.62 (d, 2H, ^4J = 2.4 Hz, C^6H), 2.55 (t, 2H, ^4J = 2.4 Hz, C^6H).

$^{13}C\{^{1}H\}$ NMR (100 MHz, $CDCl_3$) δ: 157.3 (C^{10}), 129.7 (C^7), 129.2 (C^8), 115.3 (C^9), 78.4 (C^{12}), 75.7 (C^{13}), 55.9 (C^{11}), 43.9 (C^6).

*C^1-C^5 are not detected due to extensive C-F coupling.

$^{19}F\{^{1}H\}$ NMR (400 MHz, $CDCl_3$) δ: -140.3--140.2 (m, 2F, C^2F), -150.4 (t, 1F, ^3J = 20.8 Hz, C^1F), -159.9--159.8 (m, 2F, C^3F).

IR υ_{max}: 3316 (m, CCH), 3261 (m, br, CONH), 3034 (w, CH_2), 2928 (w, CH_2), 2868 (m, OCH_2), 2119 (w, CCH), 2063, 1886 (w, Ar), 1652(s, CONH), 1552 (s, CH_2),

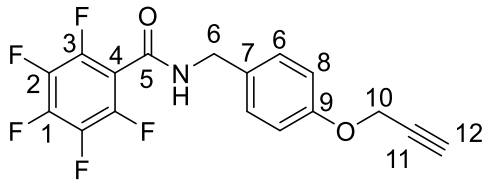

6.18 (4-(Prop-2-yn-1-yloxy)phenyl)methanamine[15]

$LiAlH_4$ (1.10 g, 28.9 mmol) was suspended in dry THF (25 mL), under an Ar atmosphere, then cooled to 0 °C. Compound **6.19** (1.12 g, 7.12 mmol) in dry THF (15 mL), was then added dropwise over 5 minutes. The reaction was stirred for 16 h, then quenched with aqueous NaOH (1 mol dm^{-3}) and then stirred for a further 30 minutes. The resulting suspension was filtered through sand, dried over $MgSO_4$ and the solvent removed *in vacuo*, to produce a yellow solid. The yellow solid was purified by flash chromatography (silica, 99:1 CH_2Cl_2:NEt_3) to produce the product as a yellow oil (0.67 g, 54%).

R_f = 0.33 (99:1 CH_2Cl_2:NEt_3)

^{1}H NMR (400 MHz, $CDCl_3$) δ: 7.27 (dt, 2H, ^3J = 9.0 Hz, ^4J = 2.6 Hz, C^6H), 6.97 (dt, 2H, ^3J = 9.0 Hz, ^4J = 2.4 Hz, C^5H), 4.70 (d, 2H, ^4J = 2.4 Hz, C^3H), 3.83 (s, 2H, C^8H), 2.53 (t, 1H, ^4J = 2.4 Hz, C^1H).

$^{13}C\{^{1}H\}$ NMR (100 MHz, $CDCl_3$) δ: 156.5 (C^4), 136.6 (C^7), 128.3 (C^6), 115.0 (C^5), 78.7 (C^2), 75.4 (C^1), 55.8 (C^3), 45.9 (C^8).

HRMS (ESI): *m/z*: $[M+H]^+$ = 158.0614, $C_{10}H_{12}NO_3$ requires 158.0600

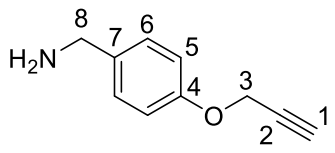

The data is consistent with literature values.

6.19 4-(Prop-2-yn-1-yloxy)benzonitrile[15]

To 4-hydroxybenzonitrile (4.97 g, 41.7 mmol) in dry CH_3CN (25 mL), K_2CO_3 (9.60 g, 69.5 mmol) and propargyl bromide (80% in toluene, 3.08 mL, 4.14 g, 27.8 mmol) were added. The resulting mixture was heated to reflux for 16 h, then allowed to cool. The suspension was filtered under suction and the solvent removed *in vacuo*. The resulting solid was dissolved in CH_2Cl_2 (50 mL) and washed with $NaOH_{(aq)}$ (1 mol dm^{-3}, 40 mL), then water (2 × 40 mL). The organic layer was dried over $MgSO_4$ and the solvent removed *in vacuo* to leave the product as a waxy white solid (3.64 g, 83%).

^{1}H NMR (400 MHz, $CDCl_3$) δ: 7.64 (dt, 2H, ^3J = 9.0 Hz, ^4J = 2.1 Hz, C^6H), 7.06 (dt, 2H, ^3J = 9.0 Hz, ^3J = 2.1 Hz, C^5H), 4.78 (d, 2H, ^4J = 2.4 Hz, C^3H), 2.59 (t, 1H, ^4J = 2.4 Hz, C^1H).

^{13}C{^{1}H} NMR (100 MHz, $CDCl_3$) δ: 160.7 (C^4), 134.0 (C^6), 119.0 (C^7), 115.7 (C^5), 105.0 (C^8), 77.3 (C^2), 76.6 (C^1), 56.0 (C^3).

HRMS (ESI): *m/z*: 158.0595 $[M+H]^+$, $C_{10}H_8NO^+$ requires 158.0600.

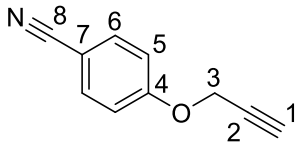

The data is consistent with literature values.

6.20 (Azidomethylene)dibenzene[16]

Bromodiphenylmethane (1.50 g, 6.06 mmol) and NaN_3 (1.18 g, 18.2 mmol) were dissolved in dry DMF (20 mL) and then heated to 80 °C for 72 h under an Ar atmosphere. Water (60 mL) was then added and the solution was extracted with EtOAc (5 × 30 mL). The combined organics were then washed with water (3 × 20 mL) then dried with $MgSO_4$. The solvent was removed *in vacuo* to afford the product as a colourless oil (0.77 g, 62 %).

^{1}H NMR (400 MHz, $CDCl_3$) δ: 7.30-7.42 (m, 10H, ArH), 7.54 (s, 1H, $C^{1}H$).

$^{13}C\{^{1}H\}$ NMR (100 MHz, $CDCl_3$) δ: 139.6 (C^{2}), 128.7 (C^{4}), 128.1 (C^{5}), 127.4 (C^{3}), 68.5 (C^{1}).

IR υ_{max}: 3062 (m, CH), 3028 (m, ArH), 2093 (s, N_3).

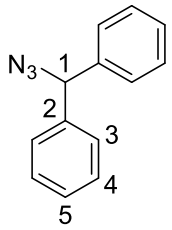

The data is consistent with literature values.

6.40 Eudesmic Acid Axle

Eudesmic acid (176 mg, 0.83 mmol) was suspended in $SOCl_2$, a catalytic amount of DMF (1 drop) was added and the suspension was refluxed for 1 h (using a condenser fitted with a $CaCl_2$ drying tube). Excess $SOCl_2$ was removed *in vacuo* and the resulting solid was dissolved in CH_2Cl_2 (10 mL). NEt_3 (119 mg, 0.17 mL, 1.19 mmol) was then added followed by 2,2-diphenylethylamine (155mg, 0.79 mmol). The solution was stirred for 1 h, then further CH_2Cl_2 (10 mL) was added, the solution was then washed with HCl (1 mol dm^{-3}, 20 mL), NaOH (1 mol dm^{-3}, 20 mL) and then water (20 mL). The organic layer was then dried over $MgSO_4$ and the solvent removed *in vacuo* to afford the product as a waxy white solid (297 mg, 96 %).

^{1}H NMR (400 MHz, $CDCl_3$) δ: 7.34-7.38 (m, 5H, ArH), 7.25-7.32 (m, 7H, ArH), 4.33 (t, 1H, $C^{7}NH$) 4.14 (dd, 2H, ^{3}J = 8.0 Hz, $C^{7}H$).

$^{13}C\{^{1}H\}$ NMR (100 MHz, $CDCl_3$) δ: 166.7 (C^{7}), 152.9 ($C^{2,3}$), 142.8 ($C^{2,3,10}$, coincidental), 128.6 ($C^{12,13}$), 128.1 (C^{11}), 126.5 ($C^{12,13}$), 125.2 (C^{6}), 106.8 (C^{5}), 60.9 (C^{1}), 56.2 (C^{4}), 52.2 (C^{9}), 47.0 (C^{8}).

IR υ_{max}: 3002 (w, CONH), 2952 (m, ArH), 2840 (m, OCH_3), 1714 (s, CONH), 1590 (w, CONH).

HRMS (ESI): *m/z*: not found, $C_{24}H_{25}NO_4$ requires 391.18.

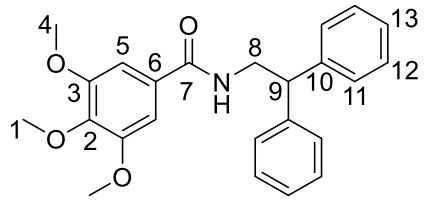

6.41 Eudesmic Acid Rotaxane

Attempt 1

Macrocycle **6.15** (20 mg, 0.042 mmol) and alkyne thread **6.42** (19 mg, 0.053 mmol) were dissolved in CH_2Cl_2 (5 mL) and stirred for 1 h under an inert Ar atmosphere. Azide **6.20** (11 mg, 0.053 mmol) $Cu(NCMe)_4BF_4$ (2 mg, 0.005 mmol), TBTA (3 mg, 0.005 mmol) and DIPEA (8 mg, 0.01 mL, 0.058 mmol) were added and the solution was stirred for 16 h. Further CH_2Cl_2 (10 mL) was added, then the solution was washed with EDTA in aqueous ammonia (0.02 mol dm^{-3}, 1 mol dm^{-3}, 10 mL) and water (2 × 10 mL). The solution was then dried with $MgSO_4$ and the solvent removed *in vacuo*. The material was then purified using flash column chromatography (silica, 8:2 to 3:7 CH_2Cl_2, EtOAc) to afford a foamy white solid (6 mg, 14 %)

Attempt 2

Macrocycle **6.15** (30 mg, 0.063 mmol) and alkyne thread **6.42** (129 mg, 0.364 mmol) were dissolved in CH_2Cl_2 (5 mL) and stirred for 1 h under an inert Ar atmosphere. Azide **6.20** (76 mg, 0.364 mmol) $Cu(NCMe)_4BF_4$ (11 mg, 0.036 mmol), TBTA (19 mg, 0.036 mmol) and DIPEA (77 mg, 0.08 mL, 0.437 mmol) were added and the solution was stirred for 16 h. Further CH_2Cl_2 (10 mL) was added, then the solution was washed with EDTA in aqueous ammonia (0.02 mol dm^{-3}, 1 mol dm^{-3}, 10 mL) and water (2 × 10 mL). The solution was then dried with $MgSO_4$ and the solvent removed *in vacuo*. The material was then purified using flash column chromatography (silica 98:2 CH_2Cl_2:MeOH) to the product as a foamy white solid (10 mg, 15 %).

Attempt 3

Macrocycle **6.15** (20 mg, 0.042 mmol) and alkyne thread **6.42** (86 mg, 0.243 mmol) were suspended in toluene (5 mL) and stirred for 1 h under an inert Ar atmosphere. Azide **6.20** (51 mg, 0.0243 mmol) $Cu(NCMe)_4BF_4$ (8 mg, 0.024 mmol), TBTA (13 mg, 0.024 mmol) and DIPEA (38 mg, 0.05 mL, 0.058 mmol) were added and the solution was stirred for 16 h, where it was found that the solution had gelated. To dissolve the gel, CH_2Cl_2 (20 mL) was added, then the solution was washed with EDTA in aqueous ammonia (0.02 mol dm^{-3}, 1 mol dm^{-3}, 10 mL) and water (2 × 10 mL). The solution was then dried with $MgSO_4$ and the solvent removed *in vacuo*. The material was then purified using flash column chromatography (silica, 99:1 to 98:2 CH_2Cl_2:MeOH) to afford the product as a foamy white solid (7 mg, 15 %).

Attempt 4

Macrocycle **6.15** (20 mg, 0.042 mmol) and alkyne thread **6.42** (86 mg, 0.243 mmol) were dissolved in a mixture of toluene (5 mL) and CH_2Cl_2 (2 mL) stirred for 1 h under an inert Ar atmosphere. Azide **6.20** (51 mg, 0.0243 mmol) $Cu(NCMe)_4BF_4$ (8 mg, 0.024 mmol), TBTA (13 mg, 0.024 mmol) and DIPEA (38 mg, 0.05 mL, 0.058 mmol) were added and the solution was stirred for 16 h, where it was found that the solution had gelated. To dissolve the gel, CH_2Cl_2 (10 mL) was added, then the solution was washed with EDTA in aqueous ammonia (0.02 mol dm^{-3}, 1 mol dm^{-3}, 10 mL) and water (2 × 10 mL). The solution was theb dried with $MgSO_4$ and the solvent removed *in vacuo*. The material was then purified using preparative TLC (silica, 98:2 CH_2Cl_2:MeOH) to afford the product as a foamy white solid (13 mg, 29 %).

Attempt 5

Macrocycle **6.15** (30 mg, 0.063 mmol) and alkyne thread **6.42** (129 mg, 0.364 mmol) were suspended in toluene (3 mL) and then heated to reflux for 1 h, under an inert Ar atmosphere. The solution was allowed to cool to room temperature, where a white precipitate was observed to form. The suspension was then heated until all solids had dissolved, then CH_2Cl_2 (1 mL) was

added, then the solution was allowed to cool to room temperature were a precipitate was again observed to form. The suspension was again heated until all solids had dissolved and further CH_2Cl_2 (1 mL) was added, the solution was allowed to cool to room temperature. Azide **6.20** (76 mg, 0.364 mmol) $Cu(NCMe)_4BF_4$ (11 mg, 0.036 mmol), TBTA (19 mg, 0.036 mmol) and DIPEA (77 mg, 0.08 mL, 0.437 mmol) were then added and the solution was stirred for 16 h, where it was found that the solution had gelated. To dissolve the gel, CH_2Cl_2 (10 mL) was added, then the solution was washed with EDTA in aqueous ammonia (0.02 mol dm^{-3}, 1 mol dm^{-3}, 10 mL) and water (2 × 10 mL). The solution was then dried with $MgSO_4$ and the solvent removed *in vacuo*. The material was then purified using preparative TLC (silica, 98:2 CH_2Cl_2:MeOH) to afford the product as a foamy white solid (19 mg, 29 %).

Attempt 6

Macrocycle **6.15** (60 mg, 0.126 mmol) and alkyne thread **6.42** (259 mg, 0.728 mmol) were suspended in toluene (4 mL) and then heated to reflux for 1 h, under an inert Ar atmosphere. The solution was allowed to cool slightly then CH_2Cl_2 was added. Once the solution had reached room temperature, azide **6.20** (152 mg, 0.728 mmol) $Cu(NCMe)_4BF_4$ (23 mg, 0.073 mmol), TBTA (39 mg, 0.073 mmol) and DIPEA (113 mg, 0.15 mL, 0.437 mmol) were added and the solution was stirred for 16 h, where it was found that the solution had gelated. To dissolve the gel, CH_2Cl_2 (30 mL) was added, then the solution was washed with EDTA in aqueous ammonia (0.02 mol dm^{-3}, 1 mol dm^{-3}, 20 mL) and water (2 × 120 mL). The solution was the dried with $MgSO_4$ and the solvent remove *in vacuo*. The material was then purified using flash column chromatography (silica, 99:1 to 98:2 CH_2Cl_2:MeOH) to afford the rotaxane as a waxy solid (60 mg, 46 %) and axle **6.43** as a waxy solid (366 mg, 89 %).

R_f = 0.21 (99:1 CH_2Cl_2:MeOH)

Mp: 74-76 ^oC

^{1}H NMR (400 MHz, $CDCl_3$) δ: 8.88 (s, 1H, $C^{11}H$), 8.35 (dd, 2H, ^{3}J =7.8 Hz, ^{4}J = 1.6 Hz, $C^{12}H$), 7.77 (t, br, 2H, ^{3}J = 4.5 Hz, $C^{8}NH$), 7.66 (t, 1H, ^{3}J = 7.8 Hz, $C^{13}H$), 7.54 (s, 1H, $C^{o}H$), 7.36-7.41 (m, 6H, ArH), 7.11 (s, 1H, $C^{p}H$), 6.79-6.91 (m, 10H, ArH), 6.75 (d, 4H, ^{3}J = 8.0 Hz, $C^{5}H$), 6.57 (t, 1H, ^{3}J = 5.3 Hz, $C^{g}NH$), 5.15 (s, 2H , $C^{m}H$), 4.63 (dd, 2H, ^{3}J = 14.6 Hz, ^{4}J = 4.5 Hz, $C^{8}H$), 4.49 (dd, 2H, ^{3}J = 14.6 Hz, ^{4}J = 4.5 Hz, $C^{8'}H$), 4.26 (d, 2H, ^{3}J = 10.4 Hz, $C^{3}H$), 4.16 (d, 4H, ^{3}J = 10.4 Hz, $C^{3'}H$), 3.99 (s, 3H, $C^{a}H$), 3.78 (s, 6H, $C^{d}H$), 3.55 (d, 2H, ^{3}J = 5.3 Hz, $C^{h}H$), 3.39-3.46 (m, 2H, $C^{1}H$), 3.31 (t, 4H, ^{3}J = 4.6 Hz, $C^{2}H$), 3.06-3.13 (m, 2H, $C^{1}H$).

^{13}C{^{1}H} NMR (100 MHz, $CDCl_3$) δ: 166.5 (C^{g}), 166.3 (C^{9}), 157.5 (C^{l}), 152.7 (C^{c}), 143.6 (C^{n}), 141.0 (C^{b}), 138.0 (C^{q}), 136.9 (C^{7}), 135.7 (C^{4}), 133.8 (C^{10}), 132.1 (C^{12}), 130.3 (C^{i}), 130.0 (C^{j}), 129.5 (C^{5}), 129.3 (C^{13}), 129.0 (C^{r}), 128.7 (C^{t}), 128.4 (C^{f}), 128.1 (C^{s}), 128.0 (C^{6}), 123.7 (C^{11}), 123.0 (C^{o}), 114.6 (C^{k}), 105.6 (C^{e}), 73.7 (C^{3}), 70.6 (C^{1}), 68.8 (C^{2}), 68.3 (C^{p}), 62.1 (C^{m}), 61.1 (C^{a}), 56.4 (C^{d}), 44.6 (C^{8}), 43.4 (C^{h}).

IR υ_{max}: 3134 (m, CONH), 3055 (w, ArH), 2920 (m, CH_2), 2870 (m, OCH_3/OCH_2), 1653 (s, Ar), 1578 (s, CONH), 1528 (s, Ar), 1511 (s, CONH).

HRMS (ESI): *m/z*: 1039.4614 $[M+H]^+$, $C_{61}H_{62}N_6O_4$ requires 1039.4600.

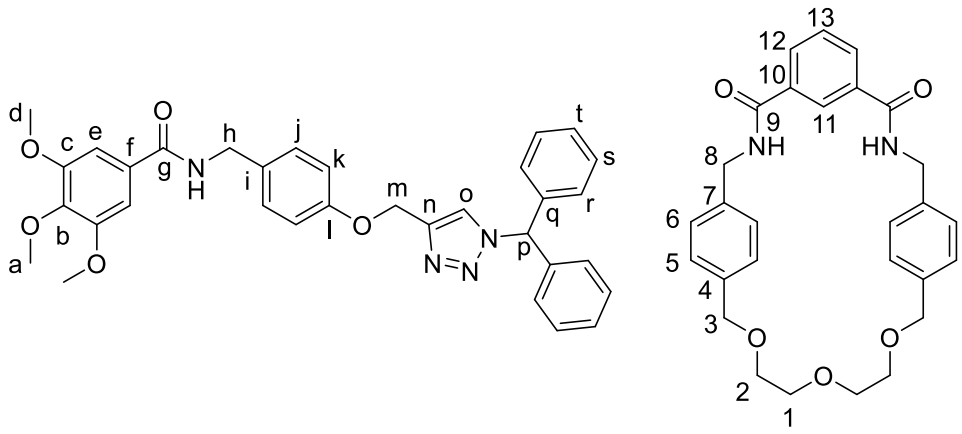

6.42 3,4,5-Trimethoxy-*N*-(4-(prop-2-yn-1-yloxy)benzyl)benzamide

Eudesmic acid (527 mg, 2.48 mmol) was dissolved in $SOCl_2$ (5 mL), DMF (cat.) was added and the solution was heated to reflux for 1h (using a condenser fitted with a $CaCl_2$ drying tube). The

excess $SOCl_2$ was removed *in vacuo* to leave an off-white solid. The acyl chloride was dissolved in dry CH_2Cl_2 (20 mL), NEt_3 (376 mg, 0.52 mL, 3.72 mmol) and amine **6.18** (400 mg, 2.48 mmol) were added, the reaction was stirred for 1h at RT, under an Ar atmosphere. The mixture was washed with $HCl_{(aq)}$ (1 M, 20 mL), NaOH (1 M, 20 mL) and water (20 mL), the organic layer was dried with $MgSO_4$ and the solvent was removed *in vacuo* to leave the product as a yellow solid (824 mg, 94%).

Mp: 130-131 ^oC

^{1}H NMR (400 MHz, $CDCl_3$) δ: 7.32 (d, 2H, ^3J = 8.7 Hz, $C^{10}H$), 7.03 (s, 2H, C^5H), 6.98 (dt, 2H, ^3J = 8.7 Hz, ^4J = 2.5 Hz, $C^{11}H$), 4.71 (t, 1H, ^3J = 5.2 Hz, C^7NH), 4.59 (d, 2H, ^4J = 2.4Hz, C^8H), 3.91 (s, 6H, C^4H), 3.89 (s, 3H, C^1H), 2.54 (t, 1H, ^3J = 2.4 Hz, $C^{15}H$).

^{13}C{^{1}H} NMR (100 MHz, $CDCl_3$) δ: 167.0 (C^7), 157.1 (C^{12}), 153.2 (C^3), 141.0 (C^2), 131.3 (C^9), 129.8 (C^6), 129.4 (C^{10}), 115.2 (C^{11}), 104.4 (C^5), 78.5 (C^{14}), 75.6 (C^{15}), 60.9 (C^1), 56.3 (C^4), 55.8 (C^{13}), 43.7 (C^8).

IR υ_{max}: 3260 (m, CONH), 2999 (w, ArH), 2953 (w, CH_2), 2838 (w, CONH), 2119 (s, CCH), 1627 (s, CONH), 1582 (s, Ar), 1536 (s, Ar).

HRMS (ESI): *m/z*: 378.1305 $[M+Na]^+$, $C_{20}H_{21}NO_5Na$ requires 378.1312.

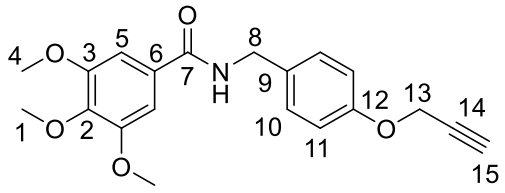

6.43 Eudesmic Acid Axle

Eudesmic Acid axle was isolated as a by-product from synthesis of eudesmic acid rotaxane **6.41** as a waxy solid (366 mg, 89 %).

R_f = 0.43 (99:1 CH_2Cl_2:NEt_3)

^{1}H NMR (400 MHz, $CDCl_3$) δ: 7.51 (s, 1H, $C^{o}H$), 7.35-7.41 (m, 6H, ArH), 7.29 (dt, 2H, ^{3}J = 8.7 Hz, ^{4}J =2.5 Hz, $C^{j}H$), 7.10-7.15 (m, 5H, ArH, $C^{p}H$), 7.04 (s, 2H, $C^{e}H$), 6.96 (dt, 2H, ^{3}J =8.7 Hz, , ^{4}J =2.5 Hz, $C^{k}H$), 6.46 (t, br, 1H, ^{3}J =5.5 Hz, $C^{g}NH$), 5.18 (s, 2H, $C^{m}H$), 4.58 (d, 2H, ^{3}J =5.5 Hz, $C^{h}H$), 3.89 (s, 9H, $C^{a,d}H$).

^{13}C{^{1}H} NMR (100 MHz, $CDCl_3$) δ: 167.0 (C^{g}), 157.8 (C^{l}), 153.2 (C^{c}), 143.8 (C^{n}), 141.0 (C^{b}), 138.0 (C^{q}), 131.0 (C^{i}), 129.9 (C^{f}), 129.3 (C^{j}), 129.0 (C^{s}), 128.7 (C^{t}), 128.1 (C^{r}), 112.9 (C^{o}), 115.1 (C^{k}), 104.4 (C^{e}), 68.3 (C^{p}), 62.2 (C^{m}), 60.9 (C^{a}), 56.3 (C^{d}), 43.6 (C^{h}).

IR υ_{max}: 3308 (m, CONH), 3063 (w, ArH), 2997 (w, CH_2), 2935 (w, CH_2), 2837(w, OCH_3), 1636 (s, CONH), 1582 (w, Ar), 1541 (w, Ar).

HRMS (ESI): *m/z*: $[M+Na]^+$ = 587.2251, $C_{24}H_{25}NO_4Na^+$ requires 587.2265.

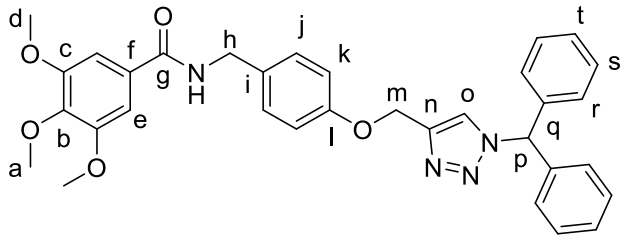

7.4. Titration Protocol

All ^{1}H NMR titrations were carried out on a Brucker Ultrashield 400 Plus spectrometer. To a solution of host (500 µL, 2.50 mmol dm^{-3}) at 298 K, a solution of guest (mmol dm^{-3}) was added. In quantitative titrations 0.2, 0.4, 0.6, 0.8, 1.0, 1.2, 1.4, 1.6, 1.8, 2.0, 2.5, 3.0, 4.0, 5.0, 7.0 and 10.0 equivalents of guest 1:1 $CDCl_3$:CD_3OD were added to a host (62.50 mmol dm^{-3}) in 1:1 $CDCl_3$:CD_3OD. The resulting data was analysed using winEQNMR2 to determine binding constants. The value of the observed chemical shift, host and guest concentrations, estimated chemical shift and binding stoichiometry were entered winEQNMR2 to produce a binding constant.

For qualitative titrations to a host (500 µL, 2.50 mmol dm^{-3} in CD_3OD, CD_3CN, $CDCl_3$ or *D_6*-benzene) equivalents of the guest species (62.50 mmol dm^{-3} mmol dm^{-3}in CD_3OD, CD_3CN, $CDCl_3$ or *D_6*-benzene) added were varied depending on the observed motion of the peaks observed in the ^{1}H NMR (^{19}F and ^{7}Li peaks were also monitored where appropriate). Equivalents of guest were added until no significant perturbation of host peaks could be observed.

7.5. Crystal Structure Data

Crystal Structure of Glycine Rotaxane 2.1 Cl

Crystals were grown by slow evaporation of a chloroform solution of rotaxane **2.1**. Sample acquired by Dr. Nathan Halcovitch.

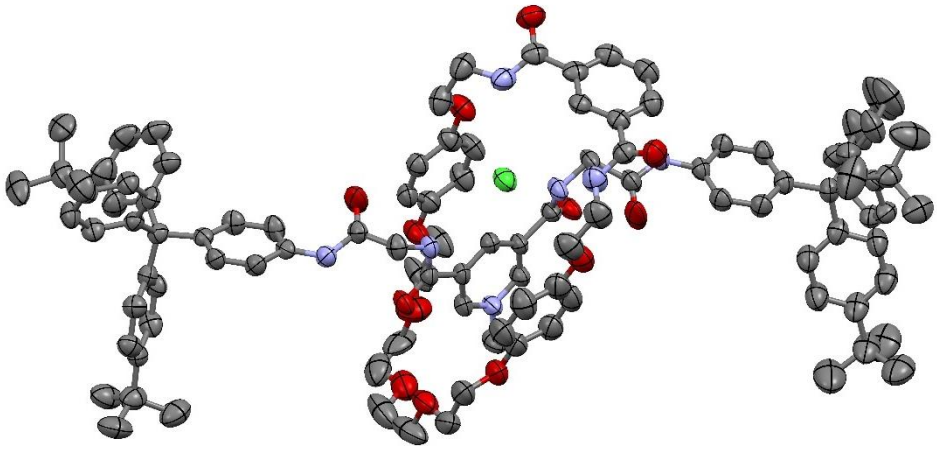

Figure 7.1 – X-ray structure of rotaxane 2.1 Cl. Thermal ellipsoids displayed at 80 % probability.

Compound reference	
Chemical formula	$C_{110}H_{120}Cl_1N_7O_{13}.CHCl_3$
Formula mass	1902.94
Crystal system	orthorhombic
a/Å	17.8288(3)
b/Å	41.6514(10)
c/Å	29.9468(7)
α/°	90
β/°	90
γ/°	90
Unit cell volume/ Å^3	22238.0
Temperature (K)	99.9
Space group	PBCN
Number of formulas per unit cell, Z	8
Number of reflections measured	91698
Number of independent reflections	21763
R_{int}	0.0593
Final *R1* values ($I > 2\sigma(I)$)	0.0777
Final *wR*(*F*2) values ($I > 2\sigma(I)$)	0.2281
Final *R1* values (all data)	0.0936
Final *wR*(*F*2) values (all data)	0.2426

Crystal Structure of Macrocycle 4.6

Crystals were grown by slow evaporation of an acetonitrile solution of macrocycle **4.6**. Sample acquired by Dr. Nathan Halcovitch.

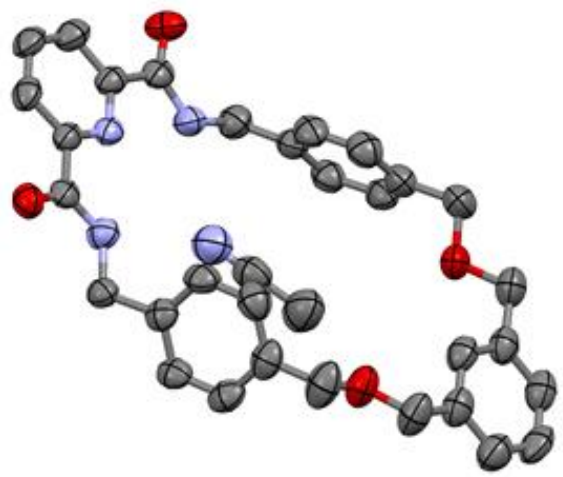

Figure 7.2 – X-ray structure of macrocycle 4.6 Thermal ellipsoids displayed at 95 % probability.

Compound reference	
Chemical formula	$C_{31}\ H_{29}\ N_3\ O_4.C_2\ H_3\ N$
Formula mass	548.62
Crystal system	orthorhombic
a/Å	5.66060(9)
b/Å	19.5450(4)
c/Å	25.9582(4)
α/°	90
β/°	90
γ/°	90
Unit cell volume/ Å^3	2871.92
Temperature (K)	294.57
Space group	P 2_1 2_1 2_1
Number of formulas per unit cell, Z	4
Number of reflections measured	14083
Number of independent reflections	5854
R_{int}	0.0437
Final *R1* values ($I > 2\sigma(I)$)	0.0474
Final *wR*(*F*2) values ($I > 2\sigma(I)$)	0.1148
Final *R1* values (all data)	0.0513
Final *wR*(*F*2) values (all data)	0.1174

Crystal Structure of attempted pseudorotaxane 4.17

Crystals were grown from slow evaporation of a chloroform solution of attempted pseudorotaxane **4.17**. Sample acquired by Dr. Nathan Halcovitch.

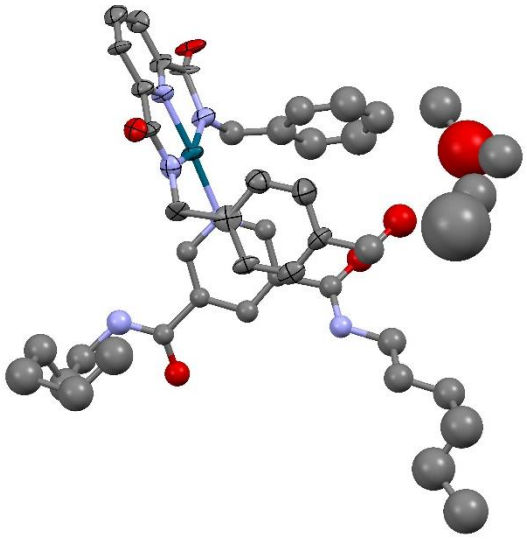

Figure 7.3 – Partial x-ray structure of rotaxane 4.17 Cl. Thermal ellipsoids displayed at 30 % probability.

Compound reference	
Chemical formula	$C_{60}H_{45}N_6O_6Pd$
Formula mass	1052.42
Crystal system	Orthorhombic
a/Å	14.9331(6)
b/Å	20.6946(6)
c/Å	31.8862(19)
α/°	90
β/°	90
γ/°	90
Unit cell volume/ Å^3	9853.9(8)
Temperature (K)	100.00
Space group	PBCN
Number of formulas per unit cell, Z	8
Number of reflections measured	19639
Number of independent reflections	5153
R_{int}	0.0478
Final *R1* values ($I > 2\sigma(I)$)	0.1478
Final *wR*(*F*2) values ($I > 2\sigma(I)$)	0.4385
Final *R1* values (all data)	0.1672
Final *wR*(*F*2) values (all data)	0.1672

7.6. References

[1] K.-Y. Ng, V. Felix, S. M. Santos, N. H. Rees and P. D. Beer, *Chem. Commun.* 2008, 1281-1283.

[2] L. M. Hancock, L. C. Gilday, S. Carvalho, P. J. Costa, V. Félix, C. J. Serpell, N. L. Kilah and P. D. Beer, *Chem. Eur. J.*, 2010, **16**, 13082–13094.

[3] D. Petrović and R. Brückner, *Org. Lett.*, 2011, **13**, 6524–6527.

[4] J. A. Wisner, P. D. Beer and M. G. B. Drew, *Angew. Chem. Int. Ed.* 2001, **40**, 3606-3609.

[5] L. C. Gilday, N. G. White and P. D. Beer, *Supramol. Chem.*, 2016, **28**, 62–83.

[6] H. W. Gibson, S.-H. Lee, P. T. Engen, P. Lecavalier, J. Sze, Y. X. Shen and M. Bheda, *J. Org. Chem*., 1993, **58**, 3748-3756.

[7] C. R. Allen, P. L. Richard, A. J. Ward, L. G. A. van de Water, A. F. Masters and T. Maschmeyer, *Tetrahedron Lett.*, 2006, **47**, 7367–7370.

[8] K. M. Broadus and S. R. Kass, *J. Am. Chem. Soc.*, 2000, **122**, 9014-9018.

[9] L. M. Hancock and P. D. Beer, *Chem. Commun.*, 2011, **47**, 6012-6014.

[10] M. D. Lankshear, I. M. Dudley, K.-M. Chan, A. R. Cowley, S. M. Santos, V. Felix and P. D. Beer, *Chem. Eur. J.*, 2008, **14**, 2248–2263.

[11] B. E. Fletcher, M. J. G. Peach and N. H. Evans, *Org. Biomol. Chem.*, 2017, **15**, 2797–2803.

[12] A. Vidonne and D. Philp, *Tetrahedron*, 2008, **64**, 8464–8475.

[13] S. C. Miller, *J. Org. Chem.*, 2010, **75**, 4632–4635.

[14] M. P. Stracke, G. Ebeling, R. Cataluña and J. Dupont, *Energy Fuels*, 2007, **3**, 1695-1698.

[15] R. Sekiya, Y. Uemura, H. Murakami and T. Haino, *Angew. Chem. Int. Ed.*, 2014, **53**, 5619–5623.

[16] J. H. Lee, S. Gupta, W. Jeong, Y. H. Rhee and J. Park, Angew. Chemie Int. Ed., 2012, 51, 10851–10855.